ACTA CHIMICA

ACADEMIAE SCIENTIARUM HUNGARICAE

TOMUS 89 FASCICULUS 1

AKADÉMIAI KIADÓ, BUDAPEST

1976

ACTA CHIM. (BUDAPEST) ACASA 2 89 1–100 (1976)

ACTA CHIMICA

A MAGYAR TUDOMÁNYOS AKADÉMIA KÉMIAI TUDOMÁNYOK OSZTÁLYÁNAK IDEGEN NYELVŰ KÖZLEMÉNYEI

Az Acta Chimica német, angol, francia és orosz nyelven közöl értekezéseket a kémiai tudományok köréből.

Az Acta Chimica változó terjedelmű füzetekben jelenik meg, egy-egy kötet négy füzetből áll. Évente átlag négy kötet jelenik meg.

A közlésre szánt kéziratok a szerkesztőség címére (1521 Bp., Műegyetem) küldendők.

Ugyanerre a címre küldendő minden szerkesztőségi levelezés. A szerkesztőség kéziratokat nem ad vissza.

Megrendelhető a belföld számára az „Akadémiai Kiadó"-nál (1363 Budapest, Pf. 24. Bankszámla 215 11488), a külföld számára pedig a „Kultúra" Könyv- és Hírlap Külkereskedelmi Vállalatnál (1389 Budapest 62, P.O.B. 149. Bankszámla: 218 10990) vagy annak külföldi képviseleteinél és bizományosainál.

Die Acta Chimica veröffentlichen Abhandlungen aus dem Bereich der chemischen Wissenschaften in deutscher, englischer, französischer und russischer Sprache.

Die Acta Chimica erscheinen in Heften wechselnden Umfanges. Vier Hefte bilden einen Band. Jährlich erscheinen 4 Bände.

Die zur Veröffentlichung bestimmten Manuskripte sind an folgende Adresse zu senden:

Acta Chimica
H-1521 Budapest

An die gleiche Anschrift ist auch jede für die Redaktion bestimmte Korrespondenz zu richten. Abonnementspreis pro Band: $ 32.00.

Bestellbar bei dem Buch- und Zeitungs-Außenhandels-Unternehmen »*Kultúra*« (1389 Budapest 62, P.O.B. 149. Bankkonto Nr. 218 10990) oder bei seinen Auslandsvertretungen und Kommissionären.

ACTA CHIMICA

ACADEMIAE SCIENTIARUM HUNGARICAE

TOMUS 89

AKADÉMIAI KIADÓ, BUDAPEST

1976

ACTA CHIMICA

TOMUS 89

Fasciculus 1 1973

Fasciculus 2 1973

Fasciculus 3 1973

Fasciculus 4 1973

INDEX

Acta Chimica Academiae Scientiarum Hungaricae, Tomus 89 (1), pp. 1–13 (1976)

APPLICATION OF WATER–ALCOHOL MIXTURES IN VAPOUR PRESSURE OSMOMETRY

J. SZABÓ-LAKATOS and I. LAKATOS

(Petroleum Engineering Research Laboratory of the Hungarian Academy of Sciences, Egyetemváros, Miskolc)

Received 12 January 1975

Water–methanol, water–ethanol and water–isopropanol mixtures were used in vapour pressure osmometry. It was found that with binary mixtures the slope of the analytical straight line obtained for water (molar resistance difference) can be increased, and the relative error of the method can be reduced to the desired value. A further advantage of the application of water–alcohol mixtures is that the tendency of the substance in question to dissociate can be detected, and the most probable molecular weight can be determined with an accuracy of 2—3 rel. %, even in the case of compounds which undergo dissociation (association) in water or aqueous medium. Although the measurements are disturbed by the slow establishment of the equilibrium of the liquid–vapour phase, this unfavourable effect can be eliminated with a longer measurement time and more frequent solvent exchange.

Introduction

Vapour pressure osmometry is one of the simplest and fastest means of determining the molecular weights of organic and inorganic substances. The only requirements of the analytical method are that the solvent and the solute under investigation should be compatible as regards the colligative properties, and that there should be a large difference between the vapour pressures of the two substances. In the case of organic substances these requirements can generally always be satisfied with pure solvents, and the practical role of the application of solvent mixtures is slight [1].

The situation is less favourable, however, when water is used as solvent. The difference between the vapour pressures of solute and solvent is normally not a problem, but the sensitivity and accuracy of the analytical method are the lowest in this case, while the dissociation, or possibly association of the water-soluble compounds in practice prevents exact determination of the molecular weight. This explains in part why no papers have as yet been published on the determination of the molecular weights of inorganic substances by vapour pressure osmometry. As regards its application in aqueous medium, only BURGE [2] has so far reported data in connection with the determination of the dissociation constants of compounds with known molecular weights.

The present experiments involve application of water–alcohol (water–methanol, water–ethanol and water–isopropanol) mixtures in vapour pressure

osmometry. A study was made of the relative accuracy of the analytical method, and the dynamics of establishment of the ΔR *vs.* t equilibrium. With water–ethanol mixtures as solvents, an investigation was carried out as to what possibilities exist for the vapour pressure osmometric determination of the molecular weights of substances which dissociate in water and aqueous solutions. Ascorbic acid, tartaric acid and succinic acid were used as model compounds.

Experimental

Measurements were made at 37 °C, with a Hewlett-Packard Model 302 vapour pressure osmometer. The thermistor beads used had hydrophilic surfaces for the study of aqueous solutions, and hydrophobic surfaces for organic solutions. The analytical straight lines were recorded with *n*-triacontane for organic solvents, and with saccharose for aqueous solutions and for water–alcohol mixtures. The solvents used (benzene, toluene, chloroform, carbon tetrachloride, *n*-hexane, methanol, ethanol, isopropanol) were Reanal products of the highest analytical purity. Doubly distilled water was employed to prepare the water–alcohol mixtures. The ascorbic, tartaric and succinic acids used to study the effect of dissociation were similarly of the highest analytical purity.

Study of the relative error of vapour pressure osmometry

The relation describing the basic principle of vapour pressure osmometry was derived by BONNAR *et al.* [3]; according to this, the resistance difference of thermistor beads holding a solvent drop in the vapour space of some solvent, and a solution drop formed from the solvent in question, is given by

$$\Delta R = \frac{RT^2}{k\Delta H}\left[\frac{M_{r,0}}{\varrho M_{r,A}} c_A - \left(\frac{1}{2}+\beta\right)\left(\frac{M_{r,0}}{M\varrho_{r,A}}\right)^2 c_A^2\right] \qquad (1)$$

For substances obeying the Raoult law, the molecular weight can be determined with sufficient accuracy if only the first term of the above expression is taken into account. In this case a plot of ΔR vs. c_A (generally with molar solutions) is linear.

For ready comparison of the analytical straight lines measured with a given calibration material but different solvents, these are plotted for *n*-hexane, chloroform, carbon tetrachloride, benzene, toluene and water in Fig. 1, while the slopes are listed in Table I.

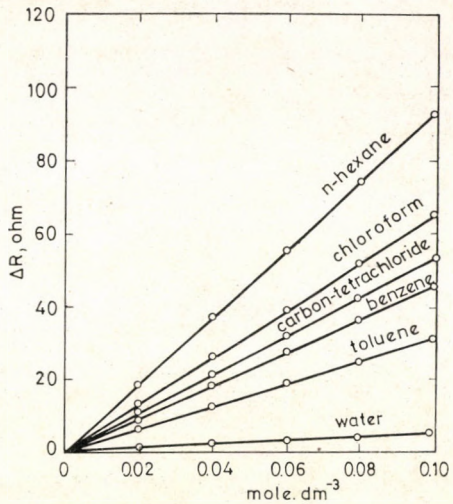

Fig. 1. Analytical straight lines at 37 °C in various solvents

Table I

Slopes of the analytical straight lines on the use of various solvents

Solvent	Molar resistance difference ohm · mole^{-1}
n-hexane	940
Chloroform	660
Carbon tetrachloride	552
Benzene	465
Toluene	336
Water	56

The formally defined slope $\Delta R/M_A$ gives the molar resistance difference, which characterizes the analytical method on the use of the solvent in question. The smallest division of the compensating potentiometer of the apparatus is 0.01 ohm (10^{-4} °C), but in an unfavourable case the standard deviation of the measurements may attain $\pm$0.1 ohm (10^{-3} °C). With the latter taken into consideration, the relative error of the analytical method is given in Table II for various solvents and molar solutions.

A partial explanation why vapour pressure osmometry has not become widespread in the study of inorganic substances is that the analytical straight

Table II

Relative error of vapour pressure osmometry on the application of various solvents

Concentration of solute mole · dm^{-3}	Relative error, %					
	n-hexane	chloroform	carbon tetrachloride	benzene	toluene	water
0.01	1.11	1.47	1.80	2.20	3.12	18.3
0.02	0.54	0.76	0.91	2.13	2.52	9.1
0.04	0.27	0.37	0.44	0.54	0.77	4.4
0.06	0.18	0.25	0.30	0.36	0.50	3.0
0.08	0.13	0.19	0.22	0.27	0.38	2.2
0.1	0.11	0.15	0.18	0.21	0.29	1.8

lines for aqueous solutions have low slopes, and the analytical method has a large relative error. In principle, this problem can be got over in two ways:

(a) increase of the concentration (absolute resistance difference) of the solute under investigation;

(b) increase of the slope (molar resistance difference) of the analytical straight line.

The fundamental relations of vapour pressure osmometry are valid for dilute solutions, and this limits the increase of the concentration, particularly for materials of high molecular weight. In our experience, the upper limit of concentrations of solutions is 10—15 g · dm^{-3}. In contrast, with aqueous solutions the small error obtained with organic solvents would be attainable only if measurements were made on solutions with concentrations about one order higher. There is thus no possibility to increase the sensitivity of the method as in (a) above.

Effect of water–alcohol mixtures on the slope of the analytical straight line

According to relation (1), the resistance (temperature) difference created by the given molar solution is directly proportional to the molecular weight of the solvent used, and inversely proportional to the heat of vaporization and density of the solvent. If the molar resistance difference can be increased *via* these factors in such a way that the colligative properties of the solute remain below 15 g · dm^{-3} for the water–alcohol mixtures in question, then a favourable result is to be expected from the application of the binary mixtures. Hydrophilic thermistor beads were used to determine the analytical straight

lines for solutions of saccharose in water–alcohol mixtures containing 20, 40 and 60 vol% methanol, ethanol and isopropanol. Those for water–ethanol mixtures are to be seen in Fig. 2.

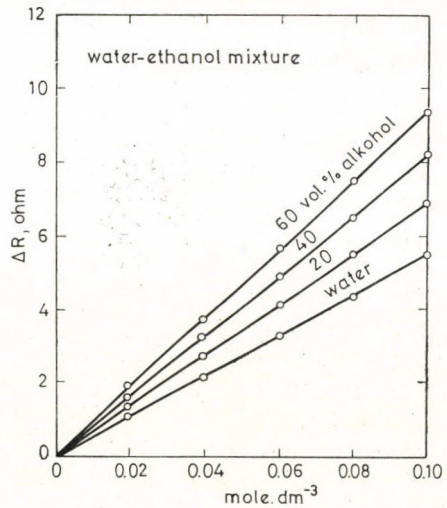

Fig. 2. Analytical straight lines in water–ethanol mixtures with various ethanol contents

Those for water–methanol and water–isopropanol mixtures are essentially similar. The slopes (molar resistance differences) of the lines were calculated, as was the relative error of the analytical method. These results are listed in Tables III and IV.

The experimental results lead to the following findings:

(a) The ΔR *vs.* M_A relation remains linear within the given concentration range, even when water–alcohol mixtures are used. (This is a practicable, but not inevitable requirement.)

Table III

Slopes of analytical straight lines on the appplication of various water–alcohol mixtures

Alcohol content vol.%	Molar resistance difference, ohm · mole^{-1}		
	methanol	ethanol	isopropanol
0	56	56	56
20	67	69	72
40	75	81	83
60	91	93	92

Table IV

Relative error of vapour pressure osmometry on the application of water–alcohol mixtures

Solvent	Alcohol concentration vol%	Relative error, % in saccharose solutions with concentrations of					
		0.01	0.02	0.04	0.06	0.08	0.1
		mole · dm^{-3}					
Water–methanol	20	15.4	7.7	3.8	2.6	1.9	1.5
	40	13.3	6.7	3.3	2.2	1.7	1.3
	60	11.8	5.7	2.9	1.9	1.4	1.1
Water–ethanol	20	14.5	7.2	3.6	2.4	1.8	1.5
	40	12.1	6.2	3.1	2.1	1.5	1.2
	60	10.7	5.4	2.6	1.8	1.3	1.0
Water–isopropanol	20	14.3	7.5	3.8	2.4	1.8	1.4
	40	12.0	6.2	3.0	2.0	1.5	1.2
	60	11.4	5.7	2.9	1.9	1.4	1.1

(b) The slopes of the analytical straight lines, *i.e.* the molar resistance difference, increase to a considerable extent.

(c) The relative error of the method decreases in accordance with the increase of the molar resistance difference.

As regards the analytical method, the use of water–alcohol mixtures leads to a favourable result overall; with their aid the slope of the analytical straight line can be increased, and the relative error of the method can be decreased. Although the molar resistance difference obtained for the binary water–alcohol mixtures is substantially lower than the values measured with *n*-hexane or chloroform, with 60 vol% alcohol-containing solvents the molecular weight and the dissociation or association equilibrium constants can be determined with an error of < 2 rel. %.

Study of the dynamics of the ΔR vs. t equilibrium

The processes taking place in the thermostated vapour space of the vapour pressure osmometer, and forming the basis of the measurement, were described in detail earlier [4, 5]. Here it is mentioned only that the variation in time of the resistance difference provides information on the mass transfer processes of the vapour–liquid phase, and on the dynamics of attainment of the equilibrium state.

The dynamics of establishment of the ΔR *vs.* t equilibrium were studied when water–alcohol mixtures were used. For solvents with various alcohol contents, the change in time of the resistance difference was measured with 0.02, 0.04, 0.06, 0.08 and 0.1 mole · dm^{-3} saccharose solutions. Figure 3 shows the ΔR *vs.* t curves for 0.1 mole · dm^{-3} saccharose in water–ethanol mixtures.

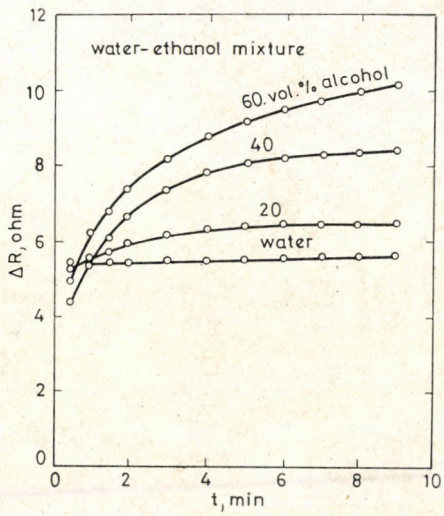

Fig. 3. Variation in time of the resistance difference in water–ethanol mixtures with various ethanol contents, with a saccharose concentration of 0.1 mole · dm^{-3}

It is clear that the equilibrium ΔR value is attained the more slowly, the higher the alcohol content of the mixture. The temperature difference of the two drops comes into equilibrium within the 10 min measurement time only in pure water and the mixture containing 20 vol% ethanol. In the solvent containing 60 vol% ethanol about 15 min is necessary for the resistance (temperature) difference proportional to the molecular weight to be established between the thermistor beads holding solvent and solution drops at the given saccharose concentration. The corresponding time for pure (one-component) solvents is 1—3 min.

Our experience to date indicates that the shapes of the ΔR *vs.* t curves always depend on the absolute value of the resistance difference. A study was therefore made of how the shapes depend on the solute concentration in various solvent mixtures. Figure 4 shows curves obtained for mixtures containing 40 vol% ethanol at saccharose concentrations of 0.04, 0.06, 0.08 and 0.10 mole · dm^{-3}.

These curves reveal that the greater the absolute value of the resistance difference determined by the concentration of the substance under examination

(or the lower the molecular weight of this substance in the case of the same weight concentration), the more difficult it is for thermal equilibrium to be established in the given system. Similar-shaped curves were obtained for water–methanol and water–isopropanol mixtures, with the difference that the time necessary for attainment of the equilibrium value was shorter for the former, and longer for the latter, than for water–ethanol.

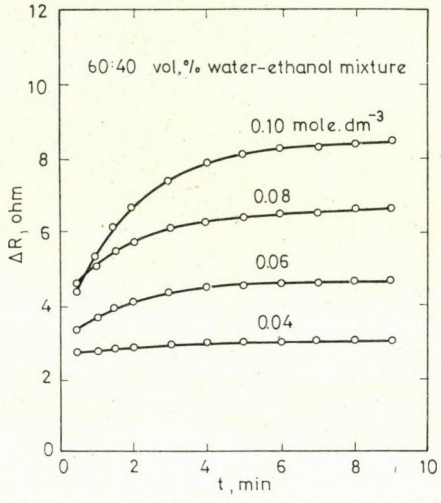

Fig. 4. Variation in time of the resistance difference in water–ethanol mixtures containing 40 vol% ethanol, with various saccharose concentrations

The shapes of the curves in Figs 3 and 4 indicate that a mass transfer process accompanied by a thermal effect occurs in the environment of the thermistor holding the solution drop, this delaying rapid establishment of the temperature difference for the liquid drops on the two thermistor beads. Excluding the possibility of chemical reaction, this mass transfer process, the rate of which is highest initially, can only be the vaporization of some component of the solution drop. Simultaneous vaporization of the solute is not possible, for the vapour pressure of saccharose is almost zero at the given temperature, while in the case of simultaneous vaporization of the solute the ΔR *vs.* t. curves tend to decrease exponentially [4].

The cause of the observed phenomenon is as follows. The thermostated vapour space of the apparatus, filled with vapour from the binary mixture, is prepared by putting a relatively large amount of solvent in the closed chamber of the vapour pressure osmometer. When water–alcohol mixtures are used, apart from the normal processes equilibrium is established between the liquid and vapour phases during the thermostating period. With water–alcohol mix-

tures containing 20—60 vol% alcohol, the alcohol content of the vapour phase is 40—80 mole%, compared to 10—50% in the liquid phase [6, 7]. Compared to the initial state, therefore, (when there is no vapour space above it) the composition of the liquid phase in the equilibrium state changes infinitesimally, but definitely. The concentration change is a function of the amount of solvent put in the osmometer, and the duration of the measurement.

For the above reasons, the alcohol concentration of a solution drop forming during the measurements is not the same as that of the liquid phase in the chamber. At any event, the difference between the two is sufficient for the sensitive electronic measuring system of the apparatus to detect and follow the double mass transfer process in the solution drop: passage of the solvent into vapour–liquid equilibrium (evaporation of a small amount of alcohol from the solution drop) and development of a temperature difference between the solvent and solution drops (mixed condensation). As regards their temperature effects, the two processes are opposing, and the recorded ΔR *vs.* t curves represent the resultant of the two.

Establishment of equilibrium for the solvent composition of the solution is a diffusion process. This explains why the time necessary to attain the equilibrium state is the longer

(a) the greater the difference of the equilibrium liquid and vapour phase compositions; and

(b) the lower the liquid and vapour phase diffusion rates of the alcohol. The data obtained suggest that the diffusion process in the cases of methanol and ethanol is fast enough not to extend the measurement time too much. The slow rise of the curves for isopropanol, however, is unfavourable as regards the analytical method.

The phenomena discussed above in connection with the shapes of the ΔR *vs.* t curves must be classified as unfavourable for analytical application of vapour pressure osmometry, for they increase the measurement time. However, the problems may be eliminated by more frequent solvent exchange, by careful pretreatment, and by using small solvent and solution drops. In contrast, there is the advantage that the error of the method can be limited to the desired value with binary water–alcohol mixtures.

Determination of molecular weight of dissociating compounds with the use of water–alcohol mixtures

The other great obstacle to the use of vapour pressure osmometry in aqueous medium is the fact that most water-soluble substances undergo dissociation (possibly association) in water. As a consequence of the colligative effect, the measured molecular weight is therefore less (or more) than the theoretical

value, and the error of the measurement depends on the value of the dissociation constant.

Since alcohols and the decrease of dilution are known to repress dissociation, such effects of water–alcohol mixtures were studied with the model compounds ascorbic, tartaric and succinic acids. Measurements were made on 0.02, 0.04, 0.08 and 0.10 mole · dm^{-3} solutions. The molecular weights found for ascorbic acid as a function of the alcohol content of the mixture are given in Fig. 5.

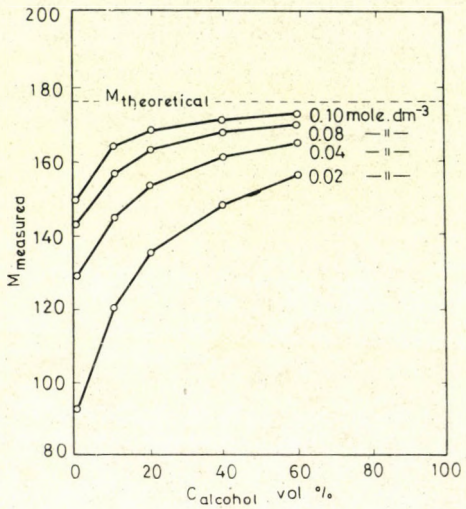

Fig. 5. Dependence of molecular weight measured for ascorbic acid on the alcohol content of the mixture and the concentration of the solute

It is readily seen that with the increase of the alcohol content and the concentration of the substance examined, the measured molecular weight better approximates to the theoretical value. It can also be observed that the slope decreases considerably with increase of the molar concentration. This is of importance primarily from a practical aspect, for the limiting value of the curves, *i.e.* the theoretical molecular weight can be extrapolated with the greatest certainty for the curve of lowest slope, though all curves have the same limiting value.

This common limiting value can be determined with mathematical approximation methods. In many cases, however, the extrapolation is simplified by plotting the measured molecular weight as a function of the logarithm of the alcohol content. In this case the experimental points for ascorbic acid, for instance, lie on a straight line (Fig. 6).

The intersection of the straight lines lies outside Fig. 6, showing that in very dilute solutions acids and bases undergo a certain dissociation even in

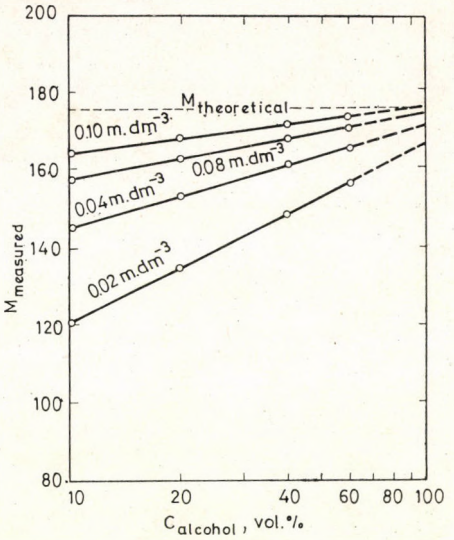

Fig. 6. Variation of the molecular weight measured for ascorbic acid as a function of the logarithm of the alcohol content of the mixture and the concentration of the solute

pure alcohol. The intersection is at 179, *i.e.* a difference of +1.7% from the theoretical value. The molecular weight extrapolated for an alcohol content of 100 vol%, however, is of acceptable accuracy except for the 0.02 and 0.04 mole · dm^{-3} solutions. As shown by the data in Table V, the practical requirements are also satisfied by the molecular weight measured directly in a mixture containing 40 vol% alcohol for a 0.10 mole · dm^{-3} solution.

Table V

Dependence of relative error on alcohol content of mixture and on dilution

Solvent	Alcohol concentration col%	Relative error, %					
		Ascorbic acid			Tartaric acid		Succinic acid
		0.02	0.04	0.08	0.10	0.10	0.10
		mole · dm^{-3}					
Water–ethanol mixture	0	−47.2	−26.8	−18.7	−15.3	−14.9	−10.3
	10	−31.8	−17.6	−10.8	− 6.8		
	20	−23.3	−13.1	− 7.4	− 4.5	− 9.9	− 5.2
	40	−15.9	− 8.5	− 4.5	− 2.8	− 5.8	− 1.2
	60	−11.2	− 6.2	− 3.4	− 1.7	− 2.8	+ 1.5
	100*	− 5.6	− 5.6	− 1.1	− 0.6		

* Extrapolated value

The tabulated data prove that in the determination of molecular weights of dissociating substances, increase of either the alcohol content of the mixture or the concentration of the examined substance has a favourable result. The two factors act in the same direction, and the considerable reduction of the error results from repression of the dissociation. At the same time, increase of the alcohol content leads to an increase in the molar resistance difference (slope of the analytical straight line), and increase of the concentration of the substance investigated increases the absolute resistance difference, *i.e.* it improves the accuracy of the method.

The results for tartaric and succinic acids by and large agree with those for ascorbic acid, but semi-logarithmic plotting of the points for tartaric acid did not give a straight line. This can presumably be explained by the stepwise dissociation, and the similarity of the dissociation constants. Difficulty in extrapolation and a further error arise if the substance in question has limited solubility in water–alcohol mixtures. A positive deviation from the theoretical molecular weight then results, and the method cannot be used. It must be noted, however, that molecular weights determined by extrapolation are not independent of the solvent–solute interaction, and within this of the properties of the alcohol and the substance (*e.g.* permittivity).

In connection with the accuracy of the analytical method, attention is drawn to the fact that the *relative error* arising from the subjective and constructional problems, which is typified by standard deviation in both positive and negative directions, must be sharply distinguished from the *dissociation* and *association errors*, which cause only negative *or* positive deviations, respectively. In every case these latter are accompanied by the relative error in the determination of ΔR.

In spite of its shortcomings, the method also has to following advantages:

(a) With its help, it can be established whether the substance examined dissociates in aqueous medium.

(b) If so, then the most probable molecular weight of the substance can be determined from the limiting value of the $M_{r,measd.}$ *vs.* $c_{alcohol}$ curves.

(c) The dissociation and association equilibria of compounds of known molecular weight can be studied with satisfactory accuracy in water–alcohol mixtures.

Apart from the examined and presented phenomena, the use of binary liquid mixtures in vapour pressure osmometry does not differ from the application of pure solvents.

Notations

c_A	concentration of solute	$g.dm^{-3}$
Δ_H	heat vaporization of solvent	$kcal.\ mole^{-1}$
M_A	concentration of solute	$mole.dm^{-3}$
$M_{r,0}$	molecular weight of solvent	
$M_{r,A}$	molecular weight of solute	
k	constant	
R	the gas constant	$kcal.kmole^{-1}.K^{-1}$
Δ_R	resistance difference	ohm
T	temperature	K
t	time	min
ϱ	density of solvent	$g.cm^{-3}$
β	Margules constant [3]	

REFERENCES

[1] Sakla, A., B., Badran, A. H., Sayed, N. A.: Acta Chim. (Budapest) **74,** 51 (1972)
[2] Burge, D. E.: J. Phys. chem. **67,** 2590 (1963)
[3] Bonnar, R. U., Dimbat, M., Stross, F. M.: Number Average Molecular Weights, Interscience, New York, 1958.
[4] Szabó-Lakatos, J., Lakatos, I.: Magyar Kém. Folyóirat **78,** 415 (1972)
[5] Szabó-Lakatos, J.: Kőolaj és Földgáz **6,** 214 (1973)
[6] Meranda, D., Furter, W. F.: AIChE J. **18,** 111 (1972)
[7] Roussau, R. W., Ashcraff, D. L., Schoenborn, E. M.: AIChE J. **18,** 825 (1972)

Julianna Szabó-Lakatos
István Lakatos
H-3515 Miskolc-Egyetemváros, PO Box 2.

Acta Chimica Academiae Scientiarum Hungaricae, Tomus 89 (1), pp. 15–21 (1976)

DETERMINATION OF HYDROGEN PEROXIDE AND INORGANIC PEROXO-MONOACIDS IN THE PRESENCE OF EACH OTHER

J. SCHNEIDER, L. NAGY and L. J. CSÁNYI

Research Group for Solution Kinetics of the Hungarian Academy of Sciences, József Attila University, Szeged)

Received April 10, 1975

At about pH 7 hydrogen peroxide is selectively decomposed by catalase in the presence of peroxo-monosulphuric and peroxo-monophosphoric acid. This observation can be exploited for analysis of system containing the mentioned substances. In an aliquot of the sample hydrogen peroxide is decomposed by catalase, and subsequently iodine liberated by the peroxo-monoacids is measured spectrophotometrically. In another sample, the total oxidizing capacity is determined in a similar way.

Several methods have been developed for the determination of hydrogen peroxide in the presence of peroxo-sulphuric acid. Volumetric methods are known for the determination of greater amounts of hydrogen peroxide [1—5]. However, they can be used only not below the semi-micro scale. For determinations on micro scale, two methods appear to be available. In one of them hydrogen peroxide is oxidized with cerium(IV) ions at a high concentration of sulphuric acid (which is necessary to suppress the induced reaction between peroxo-sulphuric acid and cerium(IV)), measuring the change in the absorbance of cerium(IV) [6]. Then in another sample the total oxidizing capacity is determined spectrophotometrically, with the use of iron(II) ions. In the other method, hydrogen peroxide is measured as peroxo-titanium(IV) complex by spectrophotometry, whereas the total oxidizing capacity is determined in another sample, similarly with the use of iron(II) ions [7]. The latter method has the advantage that hydrogen peroxide is complexed by titanium(IV) instantaneously, and this may serve as an efficient quenching in case of kinetic measurements. However, both methods have the drawback that the determinations of hydrogen peroxide and peroxo-sulphuric acid cannot be carried out at the same sensitivity due to differences in the absorbancies and thus the quantity of peroxo-sulphuric acid obtained as a difference is erroneous. In addition to that, the above-mentioned micro methods cannot be used for the analysis of samples containing hydrogen peroxide and peroxo-monophosphoric acid because both titanium(IV) and the formed iron(III) react with the phosphate ions which are inavoidable components in the samples to be analyzed. Therefore a new method is required to solve the problems indicated. On taking into account that the colours of the peroxo-complexes of other transition metals are not sufficiently intensive for the determination of hydrogen peroxide at an

adequate sensitivity, and that also these metal ions form complexes with phosphate ions, we attempted the determination of hydrogen peroxide as a mixed ligand peroxo-complex, with the use of a suitable chelating agent. These results will be reported elsewhere.

As another way of solving the above-mentioned problem we attempted the use of the technique suggested by VAN DER MEULEN [8]. This consists essentially in the removal of hydrogen peroxide from the system containing peroxo-disulphate by catalytic decomposition with osmium tetroxide. However, whereas under such conditions peroxo-disulphate remains in fact unaltered, peroxo-monosulphuric and peroxo-monophosphoric acid already undergo decomposition. According to our investigations the rate of decomposition of hydrogen peroxide catalysed by osmium tetroxide exhibits a maximum at pH 10.6, the autodecomposition of the peroxo-monoacids has a peak value where pH = pK. The pK value of peroxo-monosulphuric acid is 9.2 and that of peroxo-monophosphoric acid is 12.8.

It is known since long that hydrogen peroxide is decomposed by even minute amounts of catalase at a high rate and with remarkable selectivity. Thus, we carried out measurements to clear up the analytical applicability of the enzymatic removal. Catalase can be obtained relatively easily from various native raw materials, and is available also as a commercial product in solutions or in a lyophilized form. The dilute aqueous solution of the enzyme can be stored in a refrigerator for months without considerable change in the activity. Consequently, catalase appears to be suitable as an analytical reagent, too.

Catalase is known to be a hematoprotein of a molecular weight of about 250 000 containing four protoporphyrin groups in the molecule. The central iron(III) ions are planarly coordinated by the N atoms of the porphyrin ring. Below and above the plane, the protein is linked to one of the coordination sites 5 or 6 whereas water or hydrogen peroxide is linked to the other one. According to some authors [9] the activity of catalase to decompose hydrogen peroxide is independent of the pH in the pH range between 4—10 whereas other authors observed the maximum rate of decomposition at about pH 7 [10]. According to the preliminary investigations in unbuffered solutions as well as in the presence of Veronal buffer the rate of decomposition shows up a maximum at pH 7.3 with the only difference that the velocity was higher by about 15% than that observed in unbuffered medium (Fig. 1).

The absorption spectrum of the catalase solution with and without Veronal buffer is shown in Fig. 2 according to which there is a weak optical interaction at about 265 nm.

In the presence of peroxo derivatives catalase exhibits a peculiar behaviour. Peroxo-monosulphuric acid and peroxo-monophosphoric acid can be stored in a buffered solution at pH 7.3 for a longer period without any decomposition whereas peroxo-disulphate and to a smaller extent also peroxo-

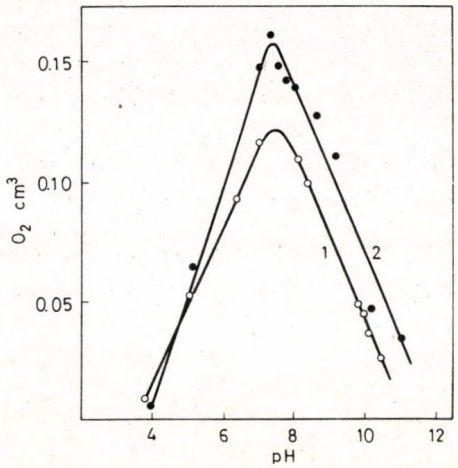

Fig. 1. Catalase activity at different pH values. Amount of oxygen evolved in 8 minutes (in normal cm^3); Hydrogen peroxide: 3.9×10^{-3} *M*. Catalase: 1×10^{-8}*M*. Curve 1: in unbuffered medium. Curve 2: in 0.01 *M* Veronal buffer

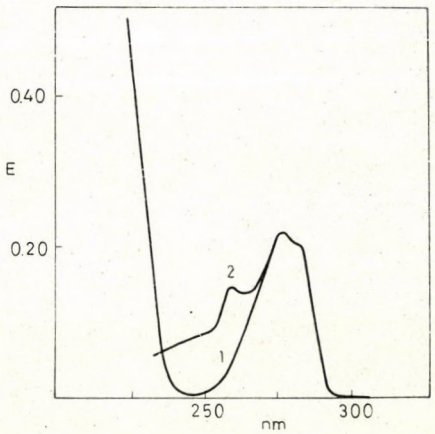

Fig. 2. Absorption spectra of 4.10^{-6} *M* catalase. Curve 1: in water. Curve 2: in a Veronal buffer, against a reference solution containing Veronal, light path: 0,2 cm.

diphosphate undergo decomposition. In contrast to the inorganic peroxo-monoacids also peroxo-benzoic acid suffers decomposition. According to our measurements no gas is evolved during the decomposition of peroxo-disulphate. — In a slightly acidic medium the concentration of peroxo-acids and the activity of catalase are decreased by the reaction between the peroxo-acids and catalase.

Based on observations mentioned above the following procedure is recommended for the simultaneous determination of hydrogen peroxide and inorganic peroxo-monoacids. Catalase solution is added to the sample to be analysed and the mixture allowed to stand in a neutral medium for a period needed for the decomposition of hydrogen peroxide. When the decomposition is completed the iodine liberated by the peroxo-acid is determined spectrophotometrically. In another sample the total oxidazing capacity is determined.

Reagents

0.2 *M* Na-Veronal
0.2 *M* HCl
10^{-6} *M* catalase, crystalline catalase preparation Reanal (produced from ox liver) dissolved in water
0.1 *M* potassium iodide (prepared freshly) solution
0.05 *M* acetic acid
0.1 *M* sodium monomolybdate

Procedure

Transfer 2 ml of the Na-Veronal, 2 ml of hydrochloric acid and 5 ml of catalase solution in a 25 ml volumetric flask. Then add the sample containing the peroxo-compounds to be analysed (the sum of concentration of peroxides must not exceed to 100 μM!). Allow the mixture to stand for 20—30 minutes, then adjust the pH to 3.4—3.8 with acetic acid, add 5 ml of potassium iodide solution. Having filled the volumetric flask allow to stand it for an hour and then measure the absorbance of the liberated iodine at 400 nm in a cell of adequate light path ($\varepsilon^{400} \approx 6400$ dm^3 · mole^{-1}cm^{-1}). On using a calibration curve for evaluation more accurate results can be obtained. Attention must be paid to the fact that acidification with acetic acid must precede the addition of potassium iodide since otherwise hypoiodite is formed which attacks the protein and thus the concentration of iodine is decreased.

Total oxidizing capacity is determined similarly but without adding catalase to the sample. Instead, 0.1 *M* sodium molybdate is added in order to accelerate the reduction of hydrogen peroxide by iodide ions. On measuring light absorption, also water can be applied in both cases as reference solution.

The data in Table I show that measurement is fairly reproducible. The standard deviation is $\delta = \pm 0.39$ μM, whereas the variation coefficient $\Delta\% = 0.74$.

Discussion

The peroxide-decomposing activity of catalase has its maximum value at about pH 7 (see Fig. 1). However, it appeared favourable to work at about pH 7 not only to ensure higher rates of decomposition but also because at lower pH values even the peroxo-monoacids are attacked by the enzyme. Since the pH changes with the progress of the decomposition of hydrogen peroxide, the use of a buffer is desirable. For this purpose we found Veronal to be quite adequate. In our opinion the acceleration of the rate of decomposition by about 15% in the medium buffered with Veronal in comparison to the rate in unbuffered medium is not due to certain activation of the enzyme induced by the buffering substance but simply to the alteration of the pH value during the decomposition

Table I

Hydrogen peroxide			Peroxo-acid		
Applied μM	Found μM	Residue %	Applied μM	Found μM	Deviation %
97.5	0.37	0.40	—	—	—
440.0	0.36	0.08	—	—	—
892.0	0.38	0.04	—	—	—
			Peroxo-monosulphuric acid		
—	—	—	28.0	27.0	−3.4
—	—	—	39.2	38.8	−1.0
—	—	—	78.4	78.4	0.0
—	—	—	117.6	119.0	+1.2
499.0	—	—	106.5	109.0	+2.0
499.0	—	—	530.0	523.0	−1.3
499.0	—	—	883.0	916.0	+3.5
100.2	—	—	540.0	546.0	+1.3
418.0	—	—	515.0	519.0	+0.8
736.0	—	—	515.0	519.0	+0.8
998.0	—	—	540.0	541.0	+0.3
			Peroxo-monophosphoric acid		
—	—	—	23.1	22.9	−1.0
—	—	—	32.2	22.9	−1.7
—	—	—	47.8	46.6	−2.5
—	—	—	70.4	70.7	+0.5
—	—	—	92.3	91.9	−0.5
—	—	—	138.6	138.0	−0.5
168.0	—	—	690.0	690.0	0.0
168.0	—	—	690.0	691.0	+0.1
168.0	—	—	690.0	684.0	−1.0
168.0	—	—	690.0	692.1	+0.2
168.0	—	—	690.0	690.2	0.0
168.0	—	—	690.0	697.0	+1.0
168.0	—	—	690.0	692.3	+0.2

Table I (continued)

			Standard deviation:		± 0.387 μM
			Variation coefficient:		0.741 %
			Peroxo-disulphuric acid		
—	—	—	91.2	78.7	—13.8
—	—	—	267.0	282.0	+ 5.5
—	—	—	430.0	348.0	—19.5
			Peroxo-benzoic acid		
—	—	—	45.6	37.0	—19.0
—	—	—	150.0	114.0	—24.0
—	—	—	242.3	223.0	— 8.0
—	—	—	350.0	280.1	—19.0

process in the absence of a buffer. Namely, the pH of the solution rises with the decrease of the concentration of hydrogen peroxide and this reduces the rate of decomposition. It can be seen in Fig. 2 that there a weak optical interaction: a small maximum appears at 253 nm between the enzyme and buffering substance. It is known that the catalase effect is decreased or even inhibited by strong Lewis bases by occupying one of the coordination sites 5 or 6, which is essential as regards of enzyme activity. Obviously, our method cannot be applied in the presence of substances of this type *e.g.* of cyanide.

In the behaviour of enzyme against various peroxo-compounds no regularities could be observed. On taking into account that inorganic peroxo-monoacids are both potentially and also kinetically strong oxidizing agents it is quite surprising that the enzyme does not suffer any alterations in their presence. Otherwise, however, the selectivity is very peculiar in that certain monosubstituted peroxo derivatives such as peroxo-monosulphuric acid and peroxo-monophosphoric acid are not whereas peroxo-benzoic acid is decomposed, to an appreciable extent by catalase. Actually, the latter behaviour could be expected on considering the behaviour of the alkyl hydroperoxides. — Peroxo-diacids are kinetically weaker oxidizing agents, and therefore their marked decomposition on the effect of catalase was quite unexpected. However, during their decomposition oxygen was formed only in a very minute quantity which points to the fact that the occurring decomposition reaction is not of the catalase type.

The suggested simple method offers over the procedures known up to the present the advantage that hydrogen peroxide and the peroxo-acids can be

determined with the same sensitivity. In addition to that, also the determination of peroxo-monophosphoric acid in the presence of hydrogen peroxide can be carried out by this method.

REFERENCES

[1] GLEU, K.: Z. anorg. Chem. **195,** 61 (1931)
[2] BERRY, A. J.: Analyst **58,** 464 (1933)
[3] MÜLLER, E., HOLDER, G.: Z. analyt. Chem. **84,** 410 (1931)
[4] CSÁNYI, L. J., SOLYMOSI, F.: Acta Chim. (Budapest) **13,** 257 (1958)
[5] CSÁNYI, L. J., SOLYMOSI, F.: Acta Chim. (Budapest) **17,** 89 (1958)
[6] MARIANO, M. H.: Anal. Chem. **40,** 1662 (1968)
[7] CSÁNYI, L. J.: Anal. Chem. **42,** 680 (1970)
[8] VAN DER MEULEN, J. H.: Rec. Trav. Chim. des Pay-Bas **58,** 553 (1939)
[9] KREMER, M. L.: Israel J. Chem. **9,** 321 (1971)
[10] DAMASCHKE, K., WINKELMANN, D.: Z. Naturforsch. **11b,** 85 (1956)

Jolán SCHNEIDER
László NAGY
László J. CSÁNYI
H-6720 Szeged, PO Box 440.

Acta Chimica Academiae Scientiarum Hungaricae, Tomus 89 (1), pp. 23—29 (1976)

MASS SPECTROMETRIC STUDIES ON $RSiH_3$ TYPE COMPOUNDS

G. INNORTA*, L. SZEPES and J. BOROSSAY**

**Istituto Chimico "G. Ciamician", Universita di Bologna, Bologna, Italy and **Department of General and Inorganic Chemistry, L. Eötvös University, Budapest*

Received December 28, 1974

The mass spectra of $EtSiH_3$, $PrSiH_3$ and $PhSiH_3$ are dominated by the fragment obtained by the loss of one and two a.m.u. The ionization potentials as well as the appearance potentials of abundant ions ($P\text{-}1^+$, $P\text{-}2^+$) have been determined and the ionic bond dissociation energies of Si–H bond are calculated. These data imply certain ionization mechanisms for alkyl- and arylsilanes. The problem of determining the D(Si–C) value on the basis of $AP(R^+)$ or $AP(SiH_3^+)$ is discussed, invoking Stevenson's rule. Approximate fragmentation mechanisms are proposed.

Introduction

Organosilicon compounds have been extensively studied by mass spectrometry and attention has been focused on energetic data used to obtain Si–H and Si–C bond dissociation energies [1—11]. However, energetic data are often in strong disagreement (see, *e.g.* the values reported for the ionization potential of Me_4Si) and few attempts have been made to clarify fragmentation processes by the study of metastable ion transitions and by energetic considerations. This point is of particular interest because organosilicon compounds may permit a further test of the quasiequilibrium theory of mass spectra, taking into account the great amount of work already done on analogous hydrocarbons.

In this study on $EtSiH_3$, $PrSiH_3$ and $PhSiH_3$ an attempt is made to clarify their ionization mechanism and fragmentation pathways as a first step to a QET calculation of their mass spectra.

Results and discussion

In Fig. 1 are presented the 50 eV mass spectra of $EtSiH_3$, $PrSiH_3$ and $PhSiH_3$ together with the corresponding spectra of carbon analogues. The main characteristics of the mass spectra are the following.

(1) In the silicon derivatives, fragment ions obtained by loss of one and two a.m.u. carry a large portion of the total ion current.

(2) Upon increasing the hydrocarbon chain, the similarity between the silicon and carbon derivatives becomes more evident; For example, in the case

of $EtSiH_3$ the base peak is $(P-2)^+$ while for propane it is $(P-15)^+$; however, for both $PrSiH_3$ and butane the base peak corresponds to $(P-15)^+$.

(3) The ion at $m/e = 31$, assigned as SiH_3^+ on the basis of its isotopic composition, is absent in the spectrum of $PhSiH_3$. In an attempt to clarify

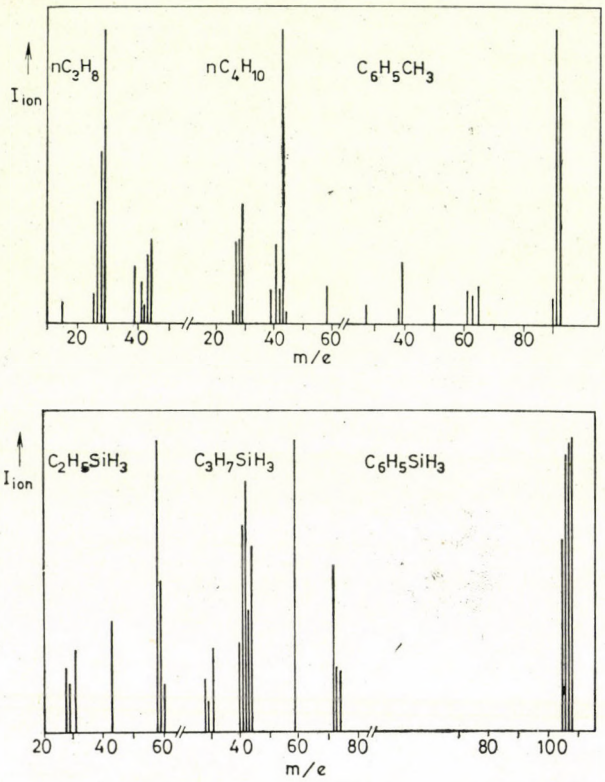

Fig. 1

the processes leading to the mass spectra of these compounds, we have determined the ionization potentials (I.P.) and appearance potentials (A.P.) of some interesting fragment ions. Moreover, in order to test the consistency of our experimental data with those found in the literature, we have measured also the I.P.'s of methyl substituted silanes. The I.P.'s (in eV) are given in Table I. From the data, it is evident that for the alkyl derivatives, the I.P.'s decrease with increasing electron releasing effect of the group(s) bonded to the Si atom.

This trend, together with the lower I.P. values relative to those of the corresponding carbon compounds suggests a charge localization on the silicon atom at least at the ionization threshold. This hypothesis is in contrast with that of STEELE *et al.* [10] who suggested an ionization from the alkyl groups.

Table I

Compound	Ionization potentials (eV)	
	This work	Literature
Me_2SiH_2	10.72	—
Me_3SiH	10.22	10.10*, 9.8[1]
Me_4Si	9.92**	
$EtSiH_3$	10.19	10.18 [10]
$PrSiH_3$	10.04	—
$PhSiH_3$	9.52	9.09[a]

* Adiabatic value by photoelectron spectroscopy; G. DISTEFANO, S. PIGNATARO, L. SZEPES, unpublished results.
** This value is in good agreement with the best data of the literature [2—7].
[a] Adiabatic value by photoelectron spectroscopy [13]

Some support to our hypothesis comes from the I.P. of $PhSiH_3$: the ionization potential of this compound is too low to be explained by the electronic effect of the aryl group on the silicon atom; an ionization from the aromatic ring is more likely.*

On the other hand the ionization potential of the phenylsilane is higher than that of the toluene showing that the substitution of a methyl by a silyl group causes an increase in the I.P. and not a decrease, as would be obvious from an ionization from the methyl or silyl group.

The appearance potentials are reported in Table II; these data were used to calculate the bond dissociation energies also shown in this Table; they allow to establish the nature of the neutrals of some fragmentation processes. The lower A.P. for the loss of two a.m.u. from the molecular ion (we have found the appropriate metastable ions which show that these are primary processes) clearly indicates that these fragmentations are accompained by the formation of hydrogen molecules. Assuming this mechanism, we can calculate $D(RSiH—H)^+$, also reported in Table II, from the following relationship:

$$A.P.\ (RSiH)^+ = I.P.(RSiH_3) + D(RSiH_2—H)^+ + D(RSiH—H)^+ - D(H—H)$$

It is also assumed that the two hydrogen atoms come from the silicon atom. There is no direct evidence for this assumption, but we should like to note that in the mass spectra of R_3SiH type compounds there are no ions formed by the loss of two a.m.u. from the molecular ion [16].

* This idea is supported by the photoelectron spectrum of phenylsilane whose first band, extending from 9.0 to 9.8 eV, has been assigned to the uppermost π levels of the benzene ring [3].

Table II

Compound	Ion A. P. (eV)	AP-IP (eV)	D(RSiH-H)$^+$(eV)
$EtSiH_3$	$EtSiH_2^+$ 11.38	1.19**	
	$EtSiH^+$ 10.69	0.50	3.38
$PrSiH_3$	$PrSiH_2^+$ 11.00	0.96**	
	$PrSiH^+$ 10.60	0.56	4.12
$PhSiH_3$	$PhSiH_2^+$ 11.60	2.08**	
	$PhSiH^+$ 11.32	1.80	4.24
$EtCH_3$ [15]	$EtCH_2^+$ 11.76	0.56*	$D(RCH-H)^+$
	$EtCH^+$ 12.20	1.00	4.96
		D(Si—C)	
$PrSiH_3$	$C_3H_7^+$ 11.0	3.20 eV =	
		73.6 kcal/mol	

* The suggested structure of this ion is $(CH_3^+CHCH_3)$; according to VESTAL [14], the activation energy for the loss of a terminal hydrogen is 1.14 eV.
** This value corresponds to $D(SiH_2-H)^+$

These data, when compared with those for propane, can be used to explain some features of the mass spectra. It is evident that the activation energy for the loss of H_2 is low with respect to both the analogous process in propane and the loss of a hydrogen atom; in addition, the bond dissociation energies listed in the last column of Table II show a higher value for propane. In this situation it is not surprising that the mass spectra of the silicon derivatives are dominated by fragments obtained by the loss of one and two a.m.u. In view of the rather similar Si–H and C–H bond dissociation energies (about 90 and 98 kcal/mol, respecitvely), it seems likely that the differences found in the activation energies (which in turn determine the differences in the mass spectra) could be ascribed to a preferential charge localization on the silicon atom for the alkyl derivatives.

In the case of phenylsilane the activation energies for the same processes are higher than those for the alkyl derivatives and, as a consequence, also the ionic bond dissociation energies show a trend which is not in contrast with the different ionization mechanism of this compound, suggested before. The positive charge localization on the benzene ring enhances the stability of the molecular ion and the Si–H bond energy is lowered less extensively in the ion (see Table II, column 4).

It would be obvious to determine the Si–C bond dissociation energy by measuring the A.P. of the SiH_3^+ or R^+ fragment ions. In all cases, except for the $C_3H_7^+$ ion, the ionization efficiency curves show a long tail which excludes an accurate A.P. determination. For $EtSiH_3$, the ions $C_2H_5^+$ and SiH_3^+ are

Table III

Reaction	I.P. of the corresponding radicals eV	Relative abundance I_f/I_t
$C_2H_5SiH_3^+ \rightarrow SiH_3^+ + C_2H_5\cdot$	8.32 [10]	9.6
$C_2H_5SiH_3^+ \rightarrow C_2H_5^+ + SiH_3\cdot$	8.78 [17]	$\geq$5.8
$C_3H_7SiH_3^+ \rightarrow SiH_3^+ + C_3H_7\cdot$	8.32 [10]	4.9
$C_3H_7SiH_3^+ \rightarrow C_3H_7^+ + SiH_3\cdot$	7.80 [17]	14.4

not suitable for this type of measurements because of two different reasons. According to Stevenson's rule, the $C_2H_5^+$ ion should be formed with a considerable amount of excess energy (see Table III); on the other hand, the SiH_3^+ ion can be formed also by secondary processes (see later, the metastable transitions). These two facts are responsible for the long tails observed in the ionization efficiency curves of these ions.

The low I.P. of the C_3H_7 radical indicates that the $C_3H_7^+$ ion from $PrSiH_3$ should be formed without excess energy, so its appearance potential has to provide a reasonable value to calculate the Si–C bond dissociation energy. In fact, the result (3.20 eV = 73.6 kcal/mol) is in good agreement with bond dissociation energy data for other $RSiH_3$ type compounds [10].

The relative abundances of the SiH_3^+ and R^+ ions are governed by the I.P. of the related radicals, showing that the mass spectra are strongly influenced by the activation energies of the various processes [18]. However, the mass spectrum of $PhSiH_3$ seems not to follow this pattern: one would expect a relatively intense SiH_3^+-fragment ion, owing to the high I.P. of the phenyl radical (9.89 eV). The very low intensity, or the absence of this ion, implies a very high activation energy for its formation, attributable to a strong $(p–d)_\pi$ effect which stabilizes the Si–C bond to a considerable extent. Evidence for such type of interaction comes also from photoelectron spectroscopy [13].

Table IV

Compound	m^*	Reaction	m(calcd.)
$C_2H_5SiH_3$	56.2	$C_2H_5{}^{28}SiH_3^+ \rightarrow C_2H_5{}^{28}SiH^+ + H_2$	56.07
	16.3	$C_2H_5{}^{28}SiH_2^+ \rightarrow {}^{28}SiH_3^+ + C_2H_4$	16.29
$C_3H_7SiH_3$	72.1	$C_3H_7{}^{28}SiH_3^+ \rightarrow C_3H_7{}^{28}SiH^+ + H_2$	70.06
	27.8	$C_3H_7{}^{28}SiH_2^+ \rightarrow {}^{28}SiCH_5^+ + C_2H_4$	27.74
	26.8	$C_3H_7{}^{28}SiH^+ \rightarrow {}^{28}SiCH_4^+ + C_2H_4$	26.80
	16.25	$C_2H_4{}^{28}SiH_3^+ \rightarrow {}^{28}SiH_3^+ + C_2H_4$	16.27
$C_6H_5SiH_3$	103.0	${}^{28}SiC_6H_7^+ \rightarrow {}^{28}SiC_6H_5^+ + H_2$	103.04

Table IV shows the metastable transitions found for the compounds studied. On the basis of energetic considerations and metastable transitions, we propose the following tentative fragmentation pathways:

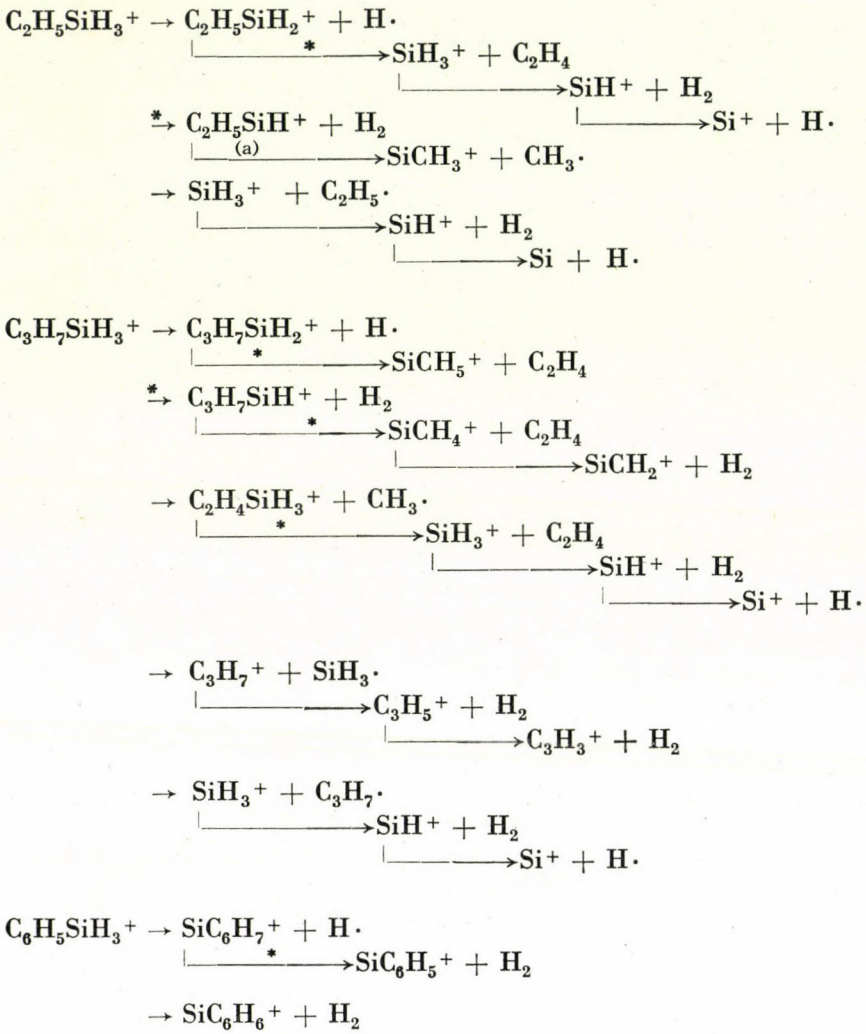

* Fragmentations proved by metastables.
(a) A.P.$(SiCH_3)^+$ = 12.12 eV; this relatively high value makes this mechanism probable.

It is important to note that the formation mechanism of the last fragment ions is rather uncertain[23]; a serious complicating factor is the strong randomization of hydrogen atoms [24].

Experimental

The measurements were performed with an Atlas CH4 spectrometer. The samples were introduced via a gas inlet system. At the normal operating temperature of the ion source (≈150 °C), there was no indication of thermal decomposition of the compounds. Ionization potentials have been determined by the methods of HONIG and LOSSING et al. [19, 20] and the appearance potentials by the WARREN method [21].

Xenon was introduced together with the sample to calibrate the electron energy. The reproducibility was ±0.1 eV.

Silanes were prepared by reduction of the corresponding chlorosilanes with $LiAlH_4$ in ether solution [22]. Purity was checked by g.l.c. and bulb to bulb destillation was made when necessary.

*

We thank the Ministero per gli Affari Esteri Italiano for a grant to L. Sz. The authors are grateful to Prof. A. FOFFANI and Dr. G. DISTEFANO for helpful discussions.

REFERENCES

[1] HOBROCK, B. G., KIESER, R. W.: J. Phys. Chem., **67,** 1283 (1963)
[2] HESS, G. G., LAMPE, F. W., SOMMER, L. H.: J. Amer. Chem. Soc., **87,** 5327 (1965)
[3] HESS, G. G., LAMPE, F. W., SOMMER, L. H.: J. Amer. Chem. Soc., **86,** 3174 (1964)
[4] HOBROCK, B. G., KIESER, R. W.: J. Phys. Chem., **65,** 2186 (1961)
[5] BAND, S. J., DAVIDSON, I. M. T., LAMBERT, C. A.: J. Chem. Soc. A., **2068** (1968)
[6] BAND, S. J., DAVIDSON, I. M. T., LAMBERT, C. A., STEPHENSON, T. L.: Chem. Commun. **723** (1967)
[7] LAPPERT, M. F., PEDLEY, J. B., SIMPSON, J., SPADLING, T. R.: J. Organometal. Chem., **29,** 195 (1971)
[8] DISTEFANO, G.: Inorg. Chem., **9,** 1919 (1970)
[9] POTZINGER, P., LAMPE, F. W.: J. Phys. Chem., **74,** 719 (1970)
[10] STEELE, W. C., NICHOLS, L. D., STONE, F. G. A.: J. Amer. Chem. Soc., **84,** 3599 (1962)
[11] BOROSSAY, J., CSÁKVÁRI, B., KNAUSZ, D., SZEPES, L.: Magyar Kém. Folyóirat, **77,** 539 (1971)
[12] CORNU, A., MASSOT, R.: Compilation of mass spectral data. Heyden and Son Ltd. 1966
[13] MCLEAN, R. A. N.: Can. J. Chem., **51,** 2089 (1973)
[14] VESTAL, M. L.: J. Chem. Phys., **43,** 1356 (1965)
[15] OMURA, I.: Bull. Chem. Soc. Japan, **34,** 1227 (1961)
[16] VAN DER KELEN, G. P., VOLDERS, H., VAN ONCKELEN, H., EECKHAUT, Z. Z.: Z. Anorg. Allgem. Chem., **338,** 106 (1965)
[17] TURNER, D. W.: Adv. Phys. Org. Chem., **4,** 31 (1966)
[18] INNORTA, G., TORRONI, S., PIGNATARO, S., MANCINI, V.: Org. Mass Spectr., **7,** 1399 (1973)
[19] HONIG, R. E.: J. Chem. Phys., **16,** 105 (1948)
[20] LOSSING, F. P., TICKNER, A. W., BRYCE, W. A.: J. Chem. Phys., **19,** 1254 (1951)
[21] WARREN, J. W.: Nature, **165,** 810 (1950)
[22] EABORN, C.: Organosilicon Compounds. Butterworth Scientific Publications, London 1960
[23] BOHLMAN, F., KÖPPEL, C., SCHWARZ, H.: Org. Mass Spectr., **9,** 622 (1974)
[24] UJSZÁSZY, K. *et al.*, unpublished results

G. INNORTA; Istituto Chimico "G. Ciamician", Universita di Bologna, Italy

József BOROSSAY
László SZEPES } H-1088 Budapest, Múzeum krt. 6—8.

Acta Chimica Academiae Scientiarum Hungaricae, Tomus 89 (1), pp. 31—44 (1976)

COMPLEX STUDY OF RANEY NICKEL SKELETON CATALYSTS, VII

NICKEL PARTICLE SIZE AND HYDROGEN CONTENT IN SKELETON CATALYSTS

A. TUNGLER, J. PETRÓ, T. MÁTHÉ, J. HEISZMAN, S. BÉKÁSSY and Z. CSŰRÖS

(Research Group for Organic Chemical Technology, Hungarian Academy of Sciences)

Received March 6, 1975

The magnetization of six different nickel skeleton catalysts has been measured after heat treatment at 100—400 °C, as a function of the field strength and temperature. A computer method was applied to calculate the saturation magnetization and the Curie temperature from these data. Changes in magnetization values have been compared with the results of thermodesorption and thermal analysis. Relationships were established between changes in the saturation magnetization of the catalysts and the type and quantity of desorbed hydrogen, on the one hand, and between the increase of the Curie temperature and the change in particle size of the catalyst, on the other hand. From these findings it has been concluded that the Curie temperature of ferromagnetic nickel in the skeleton catalysts is significantly lower, owing to the small particle size, than the Curie temperature of bulk nickel, and that the two types of hydrogen sorbed on nickel reduce the magnetization of the latter to different extents.

Introduction

As Raney nickel is a widely applied hydrogenation catalyst, its properties and structure have been extensively studied without, however, the emergence of a consistent opinion.

The catalytic properties of Raney nickel have been studied in liquid-phase and gas-phase hydrogenations [1–5]. Its surface area was measured using physical and chemisorption methods. Its hydrogen content was determined by means of miscellaneous chemical and physical methods. Its particle size has been determined by X-ray diffraction, its surface properties studied with the electron microscope, with electron microprobe analysis and electrochemically. Finally, the particle size distribution, hydrogen content and thermal stability of ferromagnetic and catalytically active nickel have been investigated by magnetic methods [6–13].

The majority of workers agree on the following points:

(i) Raney catalysts contain metallic nickel, nickel-aluminium alloy, aluminium hydroxides, water, alkali ions and hydrogen.

(ii) If only equilibrium alloy phases were contained in the initial alloy, the active nickel, according to most investigations, is ferromagnetic.

(iii) Part of the aluminium remaining in the catalyst is present as metal in the undecomposed nickel–aluminium alloy, while the other part is present

in the form of aluminium hydroxide. The undecomposed nickel–aluminium alloy is paramagnetic. The degree of hydration of the aluminium hydroxides is varying. The results of thermal analysis (1) indicate that in the case of extraction with NaOH, Raney nickel contains mainly hydrargillite.

(iv) Raney nickel contains large amounts of hydrogen (usually >10 cm^3/g). This is partly adsorbed on its surface, and partly adsorbed in the nickel lattice.

(v) During heat treatment of Raney nickel, on the one hand, sorbed hydrogen is removed (the quantity of the removed gas and the characteristic temperature of desorption can be determined by thermal desorption experiments [11, 12, 13], and on the other hand, metal crystallites in the catalyst aggregate under the effect of heat [14]. As a result of both processes, the magnetic properties of the catalyst will change [14].

The open question in this respect is how hydrogen desorption and increase in particle size affect the magnetic characteristics, namely the saturation magnetization and Curie temperature.

Data are available in the literature [14, 16—31] on the effect of hydrogen sorption on the saturation magnetization of nickel catalysts and on the effect of particle size on the saturation magnetization and Curie temperature.

According to these data, the magnetization of superparamagnetic nickel, at lower temperatures, linearly decreases with the quantity of sorbed hydrogen. No unequivocal relationship exists for ferromagnetic catalysts between the quantity of sorbed hydrogen and magnetic characteristics of the catalyst. Only the fact that magnetization decreases with hydrogen sorption could be established. From the dependence of the magnetization of supermagnetic catalysts on the field strength and temperature, the magnetic moment of nickel particles and hence their diameter can be calculated.

No unambiguous relationship between the magnetization and Curie temperature of catalysts containing ferromagnetic nickel particles in the transition range between superparamagnetic and ferromagnetic states, on the one hand, and particle size, on the other, has been found. MACNAB and ANDERSON [32] assert that the Curie temperature of catalysts containing 50 Å nickel particles cannot differ greatly from that of bulk nickel. They therefore attribute the measured, significantly lower values to the non-homogeneous solid solution of hydrogen and aluminium in nickel. This explanation is, however, doubtful since aluminium present in the catalyst is either aluminium hydroxide or metallic aluminium. The former does not affect the magnetization of nickel, as demonstrated by studies of catalysts on alumina support. Metallic aluminium, on the other hand, is present in the form of its nickel alloy, in undecomposed particles similar in composition to the initial alloy. For this reason, aluminium can act only on nickel in the alloy, in close contact with it, that is, it can only reduce the saturation magnetization and Curie temperature of this nickel, but

cannot affect separate ferromagnetic nickel particles in its vicinity. X-ray diffraction studies confirm that metallic aluminium cannot be detected in Raney nickel, only varying amounts of the nickel–aluminium alloy phase, depending on the extent of extraction.

The effect of hydrogen content in the catalyst on the magnetization of nickel has been elucidated. Its reducing effect on the Curie temperature has not been confirmed up to now.

A more probable explanation for the difference between the Curie temperatures of Raney nickel and bulk nickel assumes that a reduction of nickel particle size is accompanied by the lowering of the Curie temperature, and in heat treatment, as a result of particle aggregation, the Curie temperature of the catalyst tends towards the Curie temperature of bulk nickel [15, 16, 28, 33].

In another paper, MACNAB and ANDERSON [34] attempt to evaluate experimental results obtained with Raney nickel by assuming that the catalyst is superparamagnetic and the modified Langevin formula is valid. This assumption is based on nickel particles smaller than 300 Å being considered as independent Weiss domains, *i.e.* superparamagnetic. Thus, the 100 Å particles in Raney nickel are thought to belong to this class. This explanation, however, contradicts earlier findings [32], according to which, the Curie temperature of nickel particles larger than 50 Å is close that of bulk nickel, *i.e.* that such particles are ferromagnetic. In one of our earlier papers [33] we have pointed out the error caused if ferromagnetic nickel catalysts are considered superparamagnetic. Another source of error may arise from the fact that the saturation magnetization of one and the same nickel catalyst is different in the presence of hydrogen and in the gas-free state. Therefore particle sizes calculated from magnetic measurements on imperfectly degassed catalysts will not reflect the true particle size.

We have carried out studies on skeleton nickel catalysts belonging to different types. We followed the processes taking place during heat treatment of the catalysts by means of magnetic measurements, thermodesorption measurements, and thermal analysis. From the data obtained, conclusions were made on the structure of the active catalyst.

Experimental

A Faraday magnetic balance was used for magnetic measurements. The apparatus allows to vary the field strength in the range of 5 to 10 kOe and the temperature in the range of 25 to 450 °C. Hydrogen and/or argon can pass through the measuring chamber.

Sample weights were between 2 and 10 mg. The magnetic balance was calibrated with high-purity metallic nickel. The accuracy of the measurement was $\pm 1\%$.

The catalyst samples were treated in the chamber of the magnetic balance at increasing temperatures, in argon flow. After each treatment, magnetization as a function of field strength and temperature was measured at the temperature of the heat treatment and at lower temperatures.

A computer procedure was used to calculate the saturation magnetization and Curie temperature characterizing the equilibrium state established after heat treatment [33]. The essence of this procedure consists in using the formula valid for ferromagnetic substances

$$\sigma/\sigma_\infty = \tanh \frac{\sigma/\sigma_\infty + H/W\varrho\sigma_\infty}{T/\Theta} \tag{1}$$

and a modified variant of the procedure of HOOKE and JEEVES [35].

In the formula, σ is the magnetization at the given temperature and field strength, σ_∞ the saturation magnetization at $T = 0$ K (in emu $g^{-1}cm^3$), H is the field strength (O_e), W the ferromagnetic constant, ϱ the density of nickel ($g\,cm^{-3}$), T the absolute temperature (K), and Θ the Curie temperature (K).

Thermodesorption studies were carried out in an apparatus fitted with a catalytic combustion chamber detector. A linear temperature program at a rate of 8 °C/min was applied and experiments were carried out in an argon flow. (The apparatus was calibrated with accurately measured hydrogen. The amount of desorbed hydrogen was determined from the peak area of the detector signal). The temperature corresponding to the peak maximum was accepted as the temperature characterizing the desorption of the given type of hydrogen.

Thermal analysis was carried out with a Derivatograph (system PAULIK–PAULIK–ERDEY, manufactured by MOM). Catalyst samples of about 1g were dehydrated before an analysis with alcohol. The alcohol was then evaporated in the chamber of the instrument, in an argon flow at ambient temperature, thereby preventing oxidation of the catalyst by air in the course of introducing the sample into the instrument. DTA, DTG and TG curves were recorded in argon at a heating rate of 5 °C/min.

It should be remarked that thermomagnetic analysis served to characterize the equilibrium state established in the course of heat treatment, as opposed to thermodesorption and thermal analysis recording non-equilibrium changes taking place at steadily rising temperatures. This may cause some deviation in the values of characteristic temperatures. Nonetheless, we think that the results obtained in these measurements may be compared.

Catalysts

One of the samples was a commercial Raney nickel manufactured by Chinoin, Budapest. The other samples were prepared from 50—50 wt. % nickel–aluminium alloy, 35—65 wt. % nickel–zinc alloy and 50—50 wt. % nickel–silicon alloy. The particle size was <60 μm for all alloys.

The commercial sample, marked CH, is made from a Ni—Al alloy containing 48 wt. % nickel, by extraction at 50 °C with 15 wt. % NaOH.

The catalyst marked RI was prepared from the 50—50 wt. % Ni–Al alloy by extraction at 90—100 °C with 25 wt. % NaOH.

The catalysts marked R2 and R3 were also prepared from this alloy, using a special procedure [36]. These catalysts are so-called high-activity skeleton catalysts.

The catalysts marked H and E skeleton catalysts with reduced pyrophoric properties. They were prepared from the above-mentioned Ni–Zn and Ni–Si alloys by partial extraction with NaOH [37].

After extraction with alkali, all catalysts were washed with distilled water and stored under water. Measurements were performed at least one week after the catalysts had been prepared.

Results

The Ni–Al, Ni–Zn and Ni–Si alloys used as starting materials were paramagnetic and contained no ferromagnetic contaminations. The results of thermomagnetic analysis for the different catalysts are presented in Figs 1—6. All samples were heat-treated similarly, in steps of 50 °C, between 100 and 400 °C. The magnetization was measured first at 25 °C before heat treatment, and subsequently, after heat treatment, at the temperature of the treatment and at successively lower temperature in steps of 50 °C. The field strength was in the range of 5 to 10 kOe.

From magnetization, field strength and temperature data, using Eq. (1), the saturation magnetization exprolated to O K, σ_∞ belonging to the equilibrium state (corresponding to the temperature of heat treatment), and the Curie temperature, Θ, were computed. The results are presented in Figs 1—6 as a function of temperature of heat treatment.

The figures indicate that for all catalysts prepared from the Ni–Al alloy, the value of σ_∞ changes mainly in the 25—100 °C and 200—300 °C ranges. The Curie temperature increases between 100 and 200 °C, and decreases by about 20 to 40 °C between 250 and 300 °C.

With the catalyst prepared from the Ni–Zn alloy, the decrease of the Curie temperature takes place already at lower temperatures (150—200 °C).

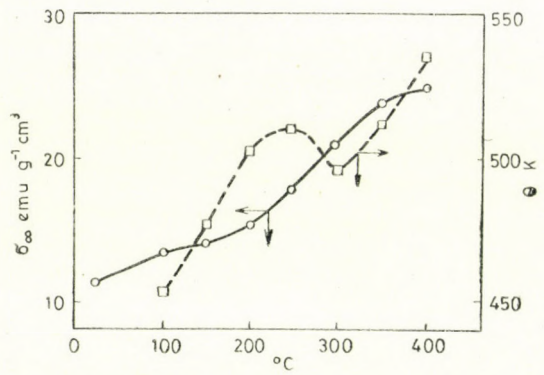

Fig. 1. Saturation magnetization and Curie temperature *vs.* temperature of heat treatment. Catalyst CH ○——○ σ_∞ □——□ Θ

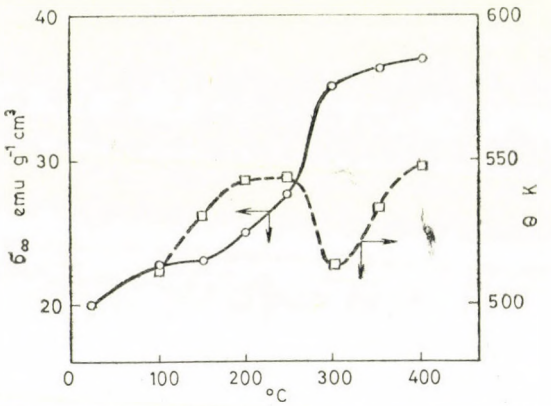

Fig. 2. Saturation magnetization and Curie temperature *vs.* temperature of heat treatment. Catalyst RI ○——○ σ_∞ □——□ Θ

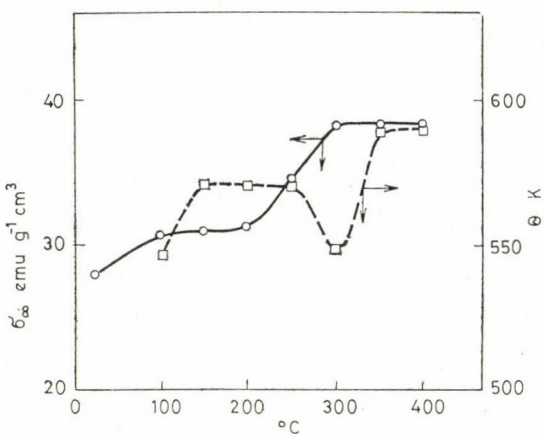

Fig. 3. Saturation magnetization and Curie temperature *vs.* temperature of heat treatment. Catalyst R2 ○——○ σ_∞ □——□ Θ

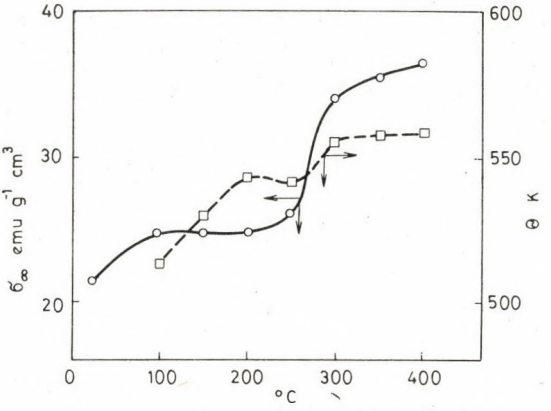

Fig. 4. Saturation magnetization and Curie temperature *vs.* temperature of heat treatment. Catalyst R3 ○——○ σ_∞ □——□ Θ

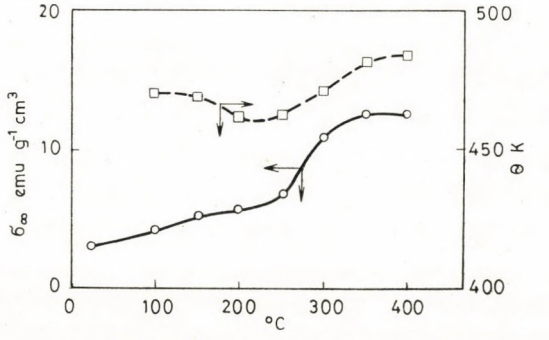

Fig. 5. Saturation magnetization and Curie temperature *vs.* temperature of heat treatment. Catalyst H ○——○ σ_∞ □——□ Θ

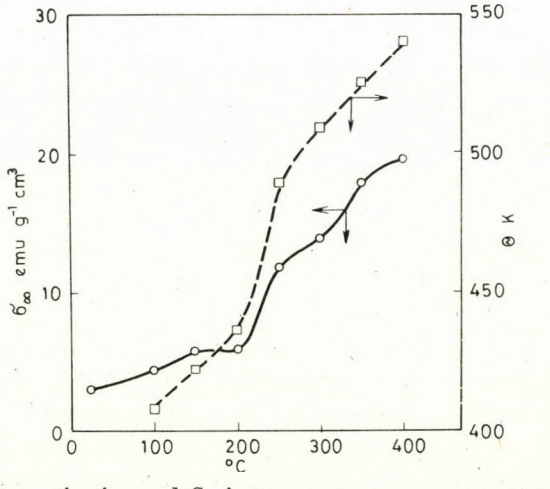

Fig. 6. Saturation magnetization and Curie temperature *vs.* temperature of heat treatment. Catalyst E ○——○ σ_∞ □——□ Θ

With the catalyst prepared from the Ni–Si alloy, the values of both σ_∞ and Θ increase monotonically with the temperature of heat treatment.

The thermodesorption diagram for the skeleton catalyst CH is presented in Fig. 7. The curves obtained with the other catalysts are similar in shape, so that only the diagram for catalyst CH is shown by way of a typical example.

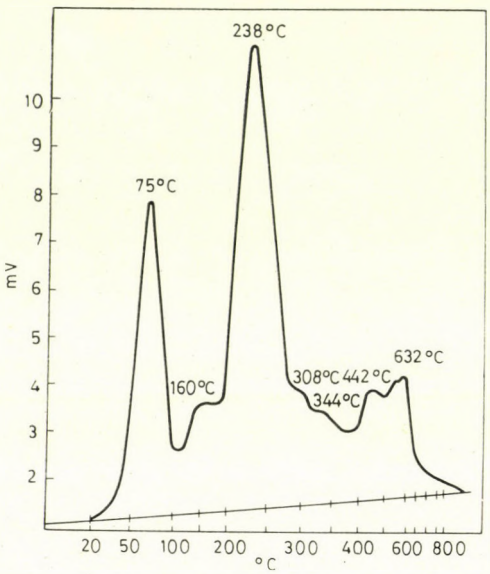

Fig. 7. Thermodesorption measured on catalyst CH. Quantity of desorbed hydrogen (dectector signal) *vs.* temperature

The quantities and types of the desorbed hydrogen and the characteristic temperatures of desorption are listed in Table I. With the exception of catalyst E, two types of hydrogen are desorbed from each catalyst, one with lower bond strength at a temperature around 100 °C, and one with higher bond strength at a temperature close to 250 °C.

Hydrogen desorbed at temperature above 400 °C is negligible as compared to the former. Apparently this is not adsorbed hydrogen, but is presumably formed in the reaction of H_2O released from aluminium and Zn hydroxides with the residual aluminium, Zn and nickel.

The results of thermal analysis are presented in Figs 8—10. Catalyst RI prepared from the Ni–Al alloy (Fig. 8) loses the water bound in aluminium hydroxides in the 200—300 °C range. The characteristic temperature of water loss is 250 °C, indicating that aluminium hydroxides are present in the form of hydrargillite. The magnetic analysis of this catalyst revealed a sharp rise in magnetization and a decrease of the Curie temperature around 250 °C, and

Table I

Thermodesorption of hydrogen

Catalyst	Characteristic peak temperature (°C)	Desorbed hydrogen (cm^3/g catalyst)	Total desorbed hydrogen (cm^3/g catalyst)
CH	80	14	
	257	44,3	58,3
RI	95	25	
	230	47	72
R2	118	18	
	200	32	50
R3	150	35	
	268	28	63
H	90	0.56	
	287	0.7	1.26
E	65	28	28

thermodesorption measurements demonstrated that substantial amounts of hydrogen are desorbed at this temperature. The DTA curve also indicates the endothermic loss of water.

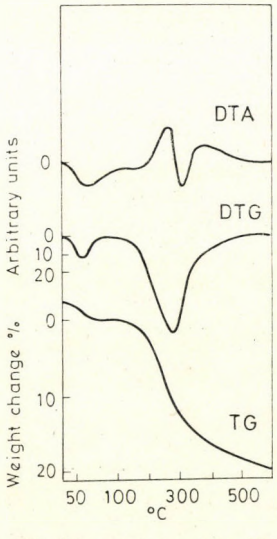

Fig. 8. Derivatogram of catalyst RI. Change in weight (TG), rate of change in weight (DTG and change in enthalpy (DTA) *vs.* temperature

Catalyst H prepared from the Ni–Zn alloy (Fig. 9) loses water between 150 and 200 °C. (A similar process was observed with zinc hydroxide prepared from pure zinc by dissolution in alkali.) With catalyst H, the agreement between thermomagnetic and thermal analyses was again apparent, since the decrease of its Curie temperature takes place in the above temperature range.

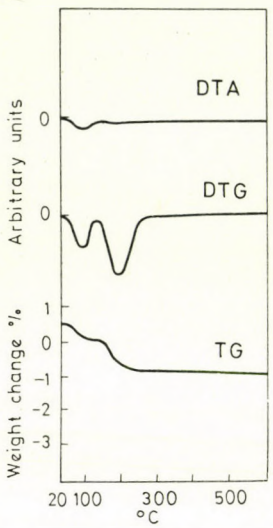

Fig. 9. Derivatogram of catalyst H. Change in weight (TG), rate of change in weight DTG) and change in enthalpy (DTA) *vs.* temperature

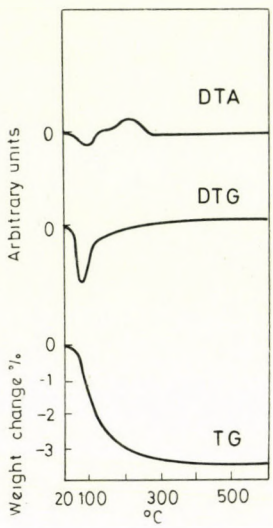

Fig. 10. Derivatogram of catalyst E. Change in weight (TG), rate of change in weight (DTG) and change in enthalpy (DTA) *vs.* temperature

Dehydration of catalyst E prepared from the Ni–Si alloy starts already above 50 °C (Fig. 10) and the sample weight decreases monotonically with rising temperature. Hydrogen desorption also proceeds at a low temperature, around 65 °C. In good agreement with this finding, the magnetization and Curie temperature also increase monotonically with temperature.

A comparison of the desorbed quantities of the two types of hydrogen with the change in saturation magnetization taking place in the approximate temperature ranges of desorption (Table II) shows that hydrogen desorbed at the lower temperature causes an average change of $\sim$0.22 in the number of Bohr magnetons per hydrogen atom, while the corresponding value for the desorption at the higher temperature is $\sim$0.55.

In this respect, catalyst H prepared from the Ni–Zn alloy behaves differently, because its magnetization — in view of its ferromagnetic nickel content — specifically increases to a multiple of its original value in the course of heat treatment. This is presumably not exclusively attributable to hydrogen desorption.

Table II

Relationship between changes in magnetization and the quantities of desorbed hydrogen

Catalyst	Temperature range (°C)	$\Delta\sigma_\infty$ (emu $g^{-1}cm^3$)	Desorbed hydrogen (cm^3/g catalyst)	μ_B/H atom*
CH	50—120	1.4	14	0,20
	150—400	10.8	44.3	0.49
RI	25—120	2.8	25	0.22
	150—350	13.5	47	0.58
R2	25—150	3.0	18	0.33
	175—300	7.0	32	0.44
R3	25—180	3.5	35	0.20
	200—350	10.5	28	0.76
H	25—200	2.6	0.56	9.4
	230—350	6.2	0.7	18
E	25—200	3.0	28	0.22

* μ_B = number of Bohr magnetons

Discussion

The interpretation of magnetic analysis results is difficult with Raney catalysts, owing to the complex, multi-constituent systems involved. This is the reason why we attempted to follow the changes taking place in the catalyst as a result of heat treatment simultaneously by several different techniques.

The results indicate that the state of the catalysts can be characterized by their saturation magnetization and their Curie temperature. The deviation of these values from these observed after heat treatment and from those of bulk nickel may, on the one hand, serve as a measure for the quantity and type of hydrogen sorbed on the catalyst and, on the other hand, will characterize the particle size and its changes upon heat treatment.

It may be seen from the data in Table II that changes in saturation magnetization for certain temperature ranges are in good agreement with the quantity of desorbed hydrogen: the change in saturation magnetization taking place as the result of the desorption of unit amounts of hydrogen is similar for the different catalyst types. These data indicate that the type of hydrogen desorbed at the lower temperature exerts a smaller effect on magnetization since it is more loosely bound to nickel.

The significant difference between the saturation magnetization of catalysts treated at 400 °C (*i.e.* containing only negligible amounts of sorbed hydrogen) and that of bulk metallic nickel may presumably be associated with the significant amounts of undecomposed Ni–Al, Ni–Zn and Ni–Si alloys and hydrated Al, Zn and Si hydroxides, contained in the catalysts, so that the percentage of ferromagnetic substance is lower.

Our results indicate that the Curie temperature of the catalysts is in close relationship with the particle size. Reliable X-ray diffraction measurements [14] have demonstrated a particle size increase from 93 to 150 Å in Raney nickel catalysts treated at increasing temperatures (25—600 °C). Our measurements indicate that the Curie temperature of the catalysts treated at increasing temperatures tends towards the Curie temperature of bulk nickel, but does not reach it in either case. It appears therefore that even after heat treatment at 400 °C, the catalysts are in a finely dispersed state, as also shown by the diffraction patterns. A further proof for polydisperse fine particles is that — in agreement with data in the literature [32] — we also found a close to linear relationship between magnetization and temperature in the vicinity of the Curie temperature of bulk nickel.

The finding that the Curie temperature of all catalysts prepared by alkaline extraction from Ni–Al alloys decreases upon heat treatment between 250 and 300 °C is surprising. This decrease took place with the catalyst prepared from the Ni–Zn alloy between 150 and 200 °C, while no such phenomenon was observed with the catalyst prepared from the Ni–Si alloy.

The TG curves indicate that in these temperature ranges the catalysts lose water, *i.e.* aluminium and zinc hydroxides contained in the catalyst are decomposed and transformed. Also, substantial amounts of hydrogen are desorbed. The decrease of the Curie temperature indicates a decrease in the size of nickel particles. It seems probable that this is due to sintering caused by water loss from the gel-like, semicrystalline aluminium and zinc hydroxides which have a stabilizing effect on the structure and can be regarded, in a manner, as supports, but lose their cohesive effect on nickel particles when they lose water. This may lead to a change in the spongy structure of nickel and to a decrease in its particle size. Hydrogen desorption will enhance these processes.

The fact that no decrease of the Curie temperature was observed with the catalyst prepared from the Ni–Si alloy whose TG curve points to a continuous loss of water above 50 °C may serve as indirect evidence for the correctness of the above assumption.

Summarizing the results of thermomagnetic analysis, thermodesorption measurements and thermal analysis, the following statements can be made:

(i) The major constituent of Raney-type catalysts is finely dispersed, ferromagnetic nickel containing sorbed hydrogen. The Curie temperature of the catalyst is substantially lower (by more than 80 °C) than that of bulk nickel.

The increase of the Curie temperature (*i.e.* its approach to that of bulk nickel) with increasing temperatures of heat treatment indicates that the Curie temperature is in close relationship with the size of the catalyst particle.

(ii) The interaction of hydrogen desorbed at different temperatures with the catalyst differs significantly, as demonstrated by magnetic data: the average change in magnetization is 0.22 Bohr magnetons per hydrogen atom for the type of hydrogen bound more weakly, and 0.55 Bohr magnetons per hydrogen atom for that bound with greater strength. Thus, the quantity and nature of the hydrogen desorbed from the catalyst has a significant effect on the saturation magnetization of the catalyst.

(iii) A decrease of the Curie temperature takes place after heat treatment at 250—300 °C in the case of catalysts prepared from the Ni–Al alloy, and at 150—200 °C in the case of the catalyst prepared from the Ni–Zn alloy. These temperature ranges coincide with the temperatures of water loss in aluminium and zinc hydroxides and hydrogen desorption. From this phenomenon we conclude that residual hydroxides have a stabilizing effect on the structure so that when they become dehydrated, the size of nickel particles in the catalyst will decrease and the particle will disintegrate.

REFERENCES

[1] Csűrös, Z., Petró, J., Kálmán, V., Erdey, L., Paulik, F.: Magyar Kém. Folyóirat **70,** 337 (1964)
[2] Kokes, R. J., Emmet, P. H.: J. Amer. Chem. Soc. **81,** 5032 (1959)
[3] Mars, P., Scholten, J. J. F., Zwietering, P.: Actes Cong. Inter. Catal. 2e, (Paris 1960) **1,** 1245 (1961)
[4] Smith, H. A., Chadwell, A. J., Kirolis, S. S.: J. Phys. chem. **59,** 820 (1955)
[5] Kokes, R. J., Emmet, P. H.: J. Amer. Chem. Soc. **82,** 4497 (1960)
[6] Aubry, J.: Diss. University of Grenoble (1941)
[7] Robertson, S. D., Anderson, R. B.: J. Catal. **23,** 286 (1971)
[8] Freel, J., Robertson, S. D., Anderson, R. B.: J. Catal. **18,** 243 (1970)
[9] Freel, J., Pieters, W. J. M., Anderson, R. B.: J. Catal. **14,** 247 (1969), **16,** 281 (1970)
[10] Robertson, S. D., Freel, J., Anderson, R. B.: J. Catal. **24,** 130 (1972)
[11] Krejci, M., Janicek, M.: Chemicke Listy **60,** 83 (1966)
[12] Zapletal, V., Kolomaznik, K., Saukup, J., Ruzicka, V.: Chemicke Listy **62,** 210 (1968)
[13] Saukup, J., Zapletal, V., Kolomaznik, K., Ruzicka, V.: Coll. Czechoslovak Chem. Comm. **34,** 1444 (1969)
[14] Fouilloux, P., Martin, G. A., Renouprez, A. J., Moraweck, B., Imelik, B., Prettre, M.: J. Catal. **25,** 212 (1972)
[15] Tungler, A., Petró, J., Máthé, T., Csűrös, Z.: Magyar Kém. Folyóirat **78,** 434 (1972)
[16] Selwood, P. W.: Magnetochemistry. New York, Interscience, 1956. 2nd ed 374
[17] Selwood, P. W., Adler, S., Phillips, T. R.: J. Amer. Chem. Soc. **76,** 2281 (1954)
[18] Selwood, P. W.: J. Amer. Chem. Soc. **78,** 249 (1956)
[19] Trzebiatowski, W.: Catalysis and Chemical Kinetics. New York, Academic Press, 1960 p. 187.
[20] Broeder, J. J., Van Reijen, L. L., Sachtler, W. M.: Z. für Elektrochemie **60,** 838 (1956)
[21] Umemura, K.: Nippon Kagaku Zasshi **81,** 1793 (1960)
[22] Shishida, S.: Nippon Kagaku Zasshi **81,** 679 (1960)
[23] Selwood, P. W.: J. Amer. Chem. Soc. **79,** 3346 (1957)
[24] Martin, G., Gibert, R.: Comptes Rendus **256,** 4889 (1963)
[25] Hahn, A.: Ann. Phys. **7, 11,** 7—8, 277 (1963)
[26] Klein, M., Smith, R.: Physics Rew. **81,** 379 (1951)

[27] CRITTENDEN, E. C., HOFFMAN, R. W.: Rev. mod. Physics **25,** 310, 1953
[28] ABELEDO, C. R., SELWOOD, P. W.: J. Appl. Phys. **32,** 229 (1961)
[29] DIETZ, R. E., SELWOOD, P. W.: J. Chem. Phys. **35,** 1,270 (1961)
[30] GENS, J. W., NOBEL, A. P., ZWIETERING, P.: J. Catal. **1,** 8 (1962)
[31] REINEN, D., SELWOOD, P. W.: J. Catal. **2,** 109 (1963)
[32] MACNAB, J. I., ANDERSON, R. B.: J. Catal. **29,** 328 (1973)
[33] TUNGLER, A., PETRÓ, J., MÁTHÉ, T., CSŰRÖS, Z., LUGOSI, K.: Acta Chim. (Budapest) **79,** 289 (1973)
[34] MACNAB, J. I., ANDERSON, R. B.: J. Catal. **29,** 338 (1973)
[35] HOOKE, R., JEEVES, T. A., JACM **8,** 212 (1961)
[36] Hungarian Patent 162 281.
[37] US Patent 3 691 103.

Antal TUNGLER
József PETRÓ
Tibor MÁTHÉ
József HEISZMAN
Sándor BÉKÁSSY
Zoltán CSŰRÖS

H-1111 Budapest, Műegyetem rkp. 3.

Acta Chimica Academiae Scientiarum Hungaricae, Tomus 89 (1), pp. 45—53 (1976)

ON α-DIOXIMINE COMPLEXES OF TRANSITION METALS, LI

THE DINITRO-BIS-(PROPOXIMATO)-COBALT(III) COMPLEX AND ITS AQUATION KINETICS

Cs. VÁRHELYI, Z. FINTA, A. BENKŐ and Sz. MIHÁLYCSA

(Faculty of Chemistry, Babes-Bolyai University, Cluj-Napoca, Romania)

Received May 5, 1975

The new $[Co(Propox \cdot H)_2(NO_2)_2]^-$ complex ion was obtained by a substitution reaction from $[Co(NO_2)_6]^{3-}$ with methylisopropylglyoxime (propoxime = Propox · H_2). A series of new salts of this anion has been prepared by double decomposition reactions. The IR spectrum was recorded and discussed. The aquation kinetics of $[Co(Propox \cdot H)_2(NO_2)_2]$ were studied in a wide range of pH and the kinetic parameters compared with those of the analogous dimethylglyoxime derivative.

The symmetric 3,4-hexanedione dioxime (diethylglyoxime) and five asymmetric 2,3- and 1,2-hexanedione dioximes have been obtained and characterized by UV spectra [1—4]. These isomeric dioximes form chelates of the type $[M(diox \cdot H)_2]$ and $[M(diox \cdot H)_2XY]$, respectively, with M(II): Ni, Pd, Co, Cu, Fe, Pt and M(III): Co, Rh, Ir. The coordination chemistry of these chelating agents was hardly investigated.

In a previous paper [5] the formation of some complex acids of the type $H[Co(Propox \cdot H)_2X_2]$ with X=Cl, Br, I has been studied.

We have observed that propoxime reacts readily with $Na_3[Co(NO_2)_6]$ in a warm aqueous alcoholic solution:

$$Na_3[Co(NO_2)_6] + 2\ Propox \cdot H_2 = Na\ [Co(Propox \cdot H)_2\ (NO_2)_2] + \\ + 2NaNO_2 + 2HNO_2 \qquad (1$$

The aqueous solution of the sodium salt precipitates Ag^+, Tl^+, Cu^+, Hg_2^{2+} and Cs^+ and the diacido-tetramine type complex cations $[M(amine)_4X_2]^+$ (M = = Co and Cr).

Neither the hexamine and monoacido-pentamine type complexes of cobalt and chromium (*e.g.* $[M(NH_3)_6]^{3+}$, $[M(en)_3]^{3+}$, $[M(NH_3)_5X]^{2+}$), nor the di- and trivalent transition metal ions (*e.g.* Zn(II), Cd(II), Co(II), Ni(II), Fe(III), Cr(III)) form well-defined compounds with $[Co(Propox \cdot H)_2(NO_2)_2]^-$. Like other $[Co(diox \cdot H)_2X_2]^-$ type anions, this complex readily forms $[Co(diox.H)_2\ (amine)_2] \cdot [Co(Propox \cdot H)_2(NO_2)_2]$ type binary salts. The syntheses and analyses for 8 compounds of this type are summarized in Table II.

Table I

New derivatives of the complex acid $H[Co(Propox \cdot H)_2(NO_2)_2]$ with metals and cobalt(III)-amines

No.	Formula	Mol.wt. Calcd.	Yield (%)	Appearance	Analysis(%)		
					Calcd.		Found
1.	$Tl[Co(Propox \cdot H)_2(NO_2)_2]$	641.6	10	Long, thin yellow needles	Co N	9.18 13.10	9.02 12.75
2.	$Ag[Co(Propox \cdot H)_2(NO_2)_2]$	544.9	80	Yellow micro-crystals	Co	10.82	10.64
3.	$Cs[Co(Propox \cdot H)_2(NO_2)_2]$	570.2	40	Square, yellow prisms	Co N	10.33 14.73	10.15 14.35
4.	$Hg_2[Co(Propox \cdot H)_2(NO_2)_2]_2$	1275.7	85	Yellow micro-crystals	Co	9.25	9.14
5.	trans-$[Co(en)_2Cl_2]$ · $[Co(Propox \cdot H)_2(NO_2)_2]$	686.9	40	Green-yellow plates	Co	17.15	17.02
6.	trans-$[Co(en)_2Br_2]$ · $[Co(Propox \cdot H)_2(NO_2)_2]$	775.8	50	Hexagonal, green-yellow plates	Co	15.18	15.07
7.	trans-$[Co(pn)_2Cl_2]$. $[Co(Propox \cdot H)_2(NO_2)_2]$	715.2	50	Green-yellow prisms	Co N	16.48 19.59	16.20 19.20
8.	$[Co(pyridine)_4Cl_2]$ · $[Co(Propox \cdot H)_2(NO_2)_2]$	883.1	70	Yellow micro-crystals	Co N	13.34 15.86	13.28 15.60

The salts $[Co(diox \cdot H)_2(amine)_2] \cdot [Co(Propox \cdot H)_2(NO_2)_2]$ and $[Co(Propox \cdot H)_2(amine)_2] \cdot [Co(diox \cdot H)_2(NO_2)_2]$, which can be obtained *via* analogous routes, are coordination isomers. They differ to a small extent in their solubility, colour and crystal form.

We observed that in conc. aqueous solutions, in the presence of sulfuric acid, $[Co(Propox \cdot H)_2(NO_2)_2]^-$ loses a NO_2 group and $[Co(Propox \cdot H)_2(NO_2)(H_2O)]$ is precipitated. This nitro-aqua nonelectrolyte undergoes a number of anation reactions with Cl^-, Br^-, I^-, NCS^-, $NCSe^-$, N_3^-, resulting in the formation of $[Co(Propox \cdot H)_2(NO_2)X]^-$ type complexes. In excess KCN or Na_2SO_3, coordinated NO_2 is also substituted.

The $[Co(Propox \cdot H)_2(NO_2)X]^-$ and $[Co(Propox \cdot H)_2(CN)_2]^-$ complex ions can be isolated as binary salts. The tervalent $[Co(Propox \cdot H)_2(SO_3)_2]^{3-}$ ion can be separated as $[Co(NH_3)_6] \cdot [Co(Propox \cdot H)_2(SO_3)_2] \cdot 6H_2O$, $[Co(en)_3]$. $[Co(Propox \cdot H)_2(SO_3)_2] \cdot 6H_2O$ or $[Co(NH_3)_5(H_2O)] \cdot [Co(Propox \cdot H)_2(SO_3)_2] \cdot 6H_2O$.

The IR spectrum of $K[Co(Propox \cdot H)_2(NO_2)_2]$ shows the presence of strong intramolecular O–H . . O hydrogen bridges, similarly to the analogous dimethylglyoxime derivative. [$^{\nu}$O–H 2300—2400 cm^{-1}(w), $^{\varrho}$O–H . . O 1700—

Table II

New binary salts of the type $[Co(DH)_2(amine)_2]\,[Co(Propox \cdot H)_2(NO_2)_2]$

No.	Formula	Mol. wt. Calcd.	Yield %	Appearance	Analysis %	
					Calcd.	Found
1.	$[Co(DH)_2(NH_3)_2] \cdot R$	760.2	60	Yellow micro-crystals	Co 15.50 NH_3 4.48	15.60 4.36
2.	$[Co(DH)_2(aniline)_2] \cdot R$	912.3	70	Brown dendrites	Co 12.91 N 18.42	12.84 18.20
3.	$[Co(DH)_2(p\text{-toluidine})_2] \cdot R$	940.3	75	Brown regular prisms	Co 12.53	12.40
4.	$[Co(DH)_2(pyridine)_2] \cdot R$	884.3	80	Yellow-brown needles	Co 13.32	13.29
5.	$[Co(DH)_2(m\text{-toluidine})_2] \cdot R$	940.3	70	Brown prisms	Co 12.53 N 17.86	12.28 17.60
6.	$[Co(DH)_2(p\text{-phenetidine})_2] \cdot R$	1000.28	80	Red-brown prisms	Co 11.70 N 16.80	11.86 16.64
7.	$[Co(DH)_2(o\text{-anisidine})_2] \cdot R$	944.3	75	Yellow-brown needles	Co 12.48	12.50
8.	$[Co(DH)_2(p\text{-Br-aniline})_2] \cdot R$	1070	85	Brown plates	Co 11.01 N 15.70	11.20 15.40

$R = [Co(Propox \cdot H)_2(NO_2)_2]$

1770 cm^{-1}(w)]. These hydrogen bridges stabilize the coplanar $Co(Propox \cdot H)_2$ ring system, *i.e.* the trans geometric configuration of the dinitrocomplex and, therefore, ligand exchange reactions occur with retention of configuration.

The $\nu C{=}N$ stretching, vibrations of the coordinated oxime group have been found at 1575 cm^{-1} (s). This band is situated at 1640 cm^{-1} (m) in the case of the free, non-coordinated propoxime.

The $\nu N{-}O$ and $\nu N{-}OH$ stretching vibrations of coordinated propoxime appear at 1245 cm^{-1} (s) and 1120 cm^{-1} (m). In the case of the analogous dimethylglyoxime derivative, $K[Co(DH)_2(NO_2)_2]$, they were found at 1240 cm^{-1} and 1090 cm^{-1} as very strong, sharp bands. The $\nu C{-}H$, ϱCH_3 and ϱCH_2 vibrations appear at 2990 (m), 2960 (m), 1470 (m) and 1360—80 cm^{-1}. The latter two bands are overlapped by the strong $\nu N{-}O$ stretching vibrations of the coordinated NO_2 groups. These vibrations [$\nu_{as}N{-}O$ (nitro): 1418—1430 cm^{-1}(s), $\nu_s N{-}O$(nitro): 1330 cm^{-1}(s), and the $\varrho O{-}N{-}O$ deformational vibration, 824—830 cm^{-1}, and $\varrho_w(NO_2)$: 620—630 cm^{-1}(w)] appear approximately at the same frequencies as in the case of other nitrocobalt(III) complexes. The presence of the strong $\nu_s N{-}O$ absorption band at 1330 cm^{-1} and the absence of a strong

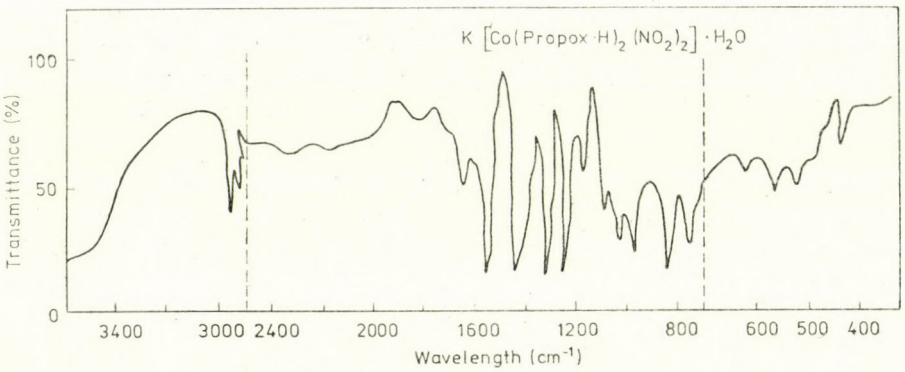

Fig. 1. IR spectrum of $K[Co(Propox \cdot H)_2(NO_2)_2] \cdot H_2O$

$^{\nu}_{s}N{-}O$ (nitrito) band at 1030—1050 cm^{-1} point to a $Co{-}NO_2$ bonding through the nitrogen atom.

In aqueous solutions $[Co(Propox \cdot H)_2(NO_2)_2]^-$ undergoes an aquation reaction, leading to the liberation of NO_2^- ions. The kinetics of this reaction was followed at different temperatures, in a wide pH range. In both acidic and alkaline media, apparent first order reactions were observed. The rate constants (k_{exp}) of these reactions are presented in Table III.

The pH dependence of the aquation rate is very similar to that observed in the case of the analogous $[Co(DH)_2(NO_2)_2]^-$ ion (DH_2 stands for dimethylglyoxime) studied in our previous papers [10, 11]. According to our previous data, the influence of the pH on the aquation rate is a result of the protolytic pre-equilibria established between some conjugate species of the complex studied, and of the parallel aquation of these species at different rates.

Thus, in acidic solutions the following pre-equilibrium occurs:

$$[Co(Propox \cdot H_2)(Propox \cdot H)(NO_2H)(NO_2)]^+ \underset{k_1}{\rightleftharpoons} [Co(Propox \cdot H_2)(Propox \cdot H)(NO_2)_2] + H^+ \quad (1)$$

whereas in alkaline media the deprotonation of the coordinated dioxime takes place:

$$[Co(Propox \cdot H)_2(NO_2)_2]^- \underset{k_1}{\rightleftharpoons} K_2[Co(Propox \cdot H)(Propox)(NO_2)_2]^{2-} + H^+ \quad (2)$$

K_1 and K_2 are the acidity constants of the corresponding species. In acidic solutions the aquation of the conjugate acid is faster, whereas in basic media the conjugate base is more reactive. Since the aquation of the complexes $[Co(Propox \cdot H_2)(Propox \cdot H)(NO_2)_2]$ and $[Co(Propox \cdot H)_2(NO_2)_2]^-$ can be neglected as compared with that of their conjugate species, the individual first order rate constant of $[Co(Propox \cdot H_2)(Propox \cdot H)(NO_2H)NO_2)]^+$ (k_1) and $[Co(Propox.H)(Propox)(NO_2)_2]^{2-}$ (k_2), and the corresponding-acidity constants

Table III

Overall first order rate constants (k_{exp}) of the aquation of $[Co(Propox \cdot H)_2(NO_2)_2]^-$ at $\mu = 1.0$ M, at different temperatures and pH values

$[H^+]\times10^2$ (M)	$k_{exp}\times10^5(s^{-1})$			
	18 °C	20 °C	23 °C	25 °C
2	1.48	1.82	2.20	2.88
3	2.00	2.50	3.13	3.94
4	2.54	3.04	3.82	5.05
5	2.91	3.64	4.48	5.81
7	3.57	4.46	5.71	7.25
10	4.24	5.32	6.94	9.01
15	5.13	6.49	8.62	11.1
20	5.59	7.19	9.52	12.3
30	6.25	8.13	11.4	14.7
40	6.85	8.40	11.9	15.2

$[OH^-]\times10^2$ (M)	$k_{exp}\times10^5(s^{-1})$			
	35 °C	40.5 °C	45 °C	50 °C
0.4	1.33	2.08	2.83	3.79
0.8	2.21	3.13	4.85	7.58
1.2	2.70	4.26	6.21	9.01
1.6	3.07	4.93	7.14	11.8
2.0	3.40	5.62	9.17	13.5
3.0	3.76	6.33	10.0	14.7
4.0	4.39	6.94	11.7	17.8
6.0	4.44	7.98	12.8	20.3
10.0	4.75	—	14.7	—

K_1 and K_2 can be graphically derived from the k_{exp} values determined at different pH's (Fig. 2), by using the following relations [11, 12]

$$\frac{1}{k_{exp}} = \frac{K_1}{k_1}\frac{1}{[H^+]} + \frac{k_1}{1} \tag{3}$$

and

$$\frac{1}{k_{exp}} = \frac{K_w}{K_2 k_2}\frac{1}{[OH^-]} + \frac{1}{k_2} \tag{4}$$

The values calculated by the least squares method are given in Table III.

In order to compare the results with those obtained for the analogous dimethylglyoxime derivative, in Table IV we have summarized the acidity constants and the kinetic parameters of the species studied.

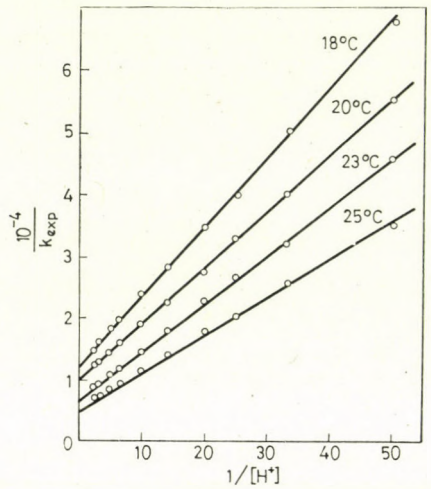

Fig. 2. Graphical determination of k_1 and k_2

Table IV

Acidity constants and individual aquation rate constants of several conjugate species of $[Co(Propox \cdot H)_2(NO_2)_2]^-$, *at different temperatures and* $\mu = 1.0$ *M*

t(°C)	$K_1 \times 10^2$	$K_2 \times 10^{12}$	$k_1 \times 10^4(s^{-1})$	$k_2 \times 10^4(s^{-1})$
18	9.14	—	0.822	—
20	9.56	—	1.05	—
23	12.1	—	1.55	—
25	11.7	—	1.96	—
35	—	1.77	—	0.541
40.5	—	1.80	—	1.05
45	—	1.86	—	1.83
50	—	2.00	—	3.13

According to these data, the nature of the coordinated dioxime exerts only a weak influence on the acidity and the kinetic behaviour of the complexes studied, as has been found in the case of other analogous compounds with various dioximes [12, 13].

The deprotonation of the coordinated dioxime occurs more easily in the case of the propoxime, probably because of the stronger inductive effect of the isopropyl group as compared with that of the methyl group in the coordi-

nated dimethylglyoxime molecule. On the other hand, the substitution rate of the NO_2 group in the deprotonated species $[Co(diox{\cdot}H)\,(diox)(NO_2)_2]^{2-}$ is lower in the case of the propoxime derivative. This also can be explained by the stronger inductive effect of the isopropyl group, which leads to an increase of the electron density on the central atom, thus favouring π-electron transfer to the NO_2 group. The more pronounced π-character of the Co–NO_2 bond in the propoxime derivative is also in agreement with the higher acidity of the protonated NO_2 group in this complex.

Table V

Acidity constants and kinetic parameters of various conjugate species of $[Co(diox \cdot H)_2(NO_2)_2]^-$ *type complexes*

Complex	$K_1\times10^2$ (25 °C)	$K_2\times10^{12}$ (35 °C)	$k_1\times10^4$, s^{-1} (25 °C)	$k_2\times10^4$, s^{-1} (35 °C)	ΔH (kcal/mol)	ΔS (e.u.)	Ref.
$[Co(Propox \cdot H_2)(Propox \cdot H)(NO_2)(NO_2H)]^+$	11.7	—	1.96	—	20.9±0.3	−5.2	—
$[Co(DH_2)(DH)(NO_2)(NO_2H)]^+$	7.23	—	2.23	—	20.9±0.6	−4.9	[10]
$[Co(Propox \cdot H)(Propox)(NO_2)_2]^{2-}$	—	1.77	—	0.541	22.6±0.3	−4.8	—
$[Co(DH)(D)(NO_2)_2]^{2-}$	—	6.56	—	1.22	22.1±0.4	−4.7	[11]

(DH_2 = dimethylglyoxime)

The aquation rate as well as the activation parameters of the species with coordinated NO_2H are practically equal, thus it is essentially the Co–NO_2 σ-bond that is responsible for the observed differences between the aquation rates of the two deprotonated complexes, since these differences disappear when the π-character of the Co–NO_2 bond is diminished by protonation.

No unequivocal conclusions can be drawn about the mechanism of the reactions studied. On the basis of the above considerations a dissociative pathway may be assumed, similarly to the case of a large number of complexes of this type. The clearly negative activation entropy values, however, do not agree with this assumption. It seems more likely that the mechanism of these reactions is of an intermediate type, in which both the breaking of the Co–NO_2 bond and the formation of the Co–OH_2 bond play a considerable role in the transition state. A similar kinetic behaviour has been observed in the case of other analogous $[Co(diox{\cdot}H)_2XY]$ complexes with π-acceptor ligands [14, 15] in the *trans* position.

Experimental

Synthesis of methylisopropylglyoxime (propoxime)

The isonitrozation of methylisobutylketone (Austranal) with ethyl nitrite, under cooling, in the presence of HCl leads to the formation of the monoxime: $CH_3—C=O—C(=N—OH)—CH(CH_3)_2$ (m.p. 74 °C). Upon treating the monoxime with an excess of hydroxylamine hydrochloride in sodium acetate buffer solution, the methylisopropylglyoxime separates in sparkling irregular plates. Yield: 60—70% (m.p. 158 °C)

Na $[Co(Propox \cdot H)_2(NO_2)_2] \cdot H_2O$ 20.2 $Na_3[Co(NO_2)_6]$ (50 mmol) dissolved in 100 ml water was mixed with 13.5 g propoxime (100 mmol) in 100 ml 50% ethanol. The mixture was kept on a warm water bath for 1—2 hrs. Nitrogen oxide evolved and a brown solution formed. An excess of solide $NaNO_3$ was added and after 1—2 hrs the crystalline natrium salt was filtered and washed with a small amount of ice-cooled water. Trigonal, sparkling brown-yellow prisms.

$Co(C_6H_{11}N_2O_2)_2(NO_2)_2 \cdot NaH_2O$ (478.2)

Calcd. Co 12.32; N 17.56; H_2O 3.76. Found Co 12.20; N 17.40; H_2O 3.50%.

K$[Co(Propox \cdot H)_2(NO_2)_2]$ 5 g $Na[Co(Propox \cdot H)_2(NO_2)_2]$ in 30—40 ml water was treated with 10 g KNO_2. The potassium salt precipitates as brown yellow prisms.

Analysis: Calcd. Co 12.36; N 17.63. Found Co 12.66; N 17.83%.

Synthesis of Me(I) $[Co(Propox \cdot H_2)(NO_2)_2]$ and $[Me(III)(amine)_4X_2]$

$[Co(Propox \cdot H)_2(NO_2)_2]$. 10 mmol $MeNO_3$, or 5 mmol of the corresponding diacidotetraamine salt in 50—100 ml water was treated with 5 mmol $Na[Co(Propox \cdot H)_2(NO_2)_2]$ in 40—60 ml water. The precipitated crystalline products were filtered after 1/2—1 hr, washed with a small amount of water and dried in air.

Synthesis of $[Co(DH)_2(amine)_2] \cdot [Co(Propox \cdot H)_2(NO_2)_2]$ binary salts

5 mmole of $[Co(DH)_2(amine)_2]$ acetate (DH_2 = dimethylglyoxime in 50—100 ml 50% alcohol was treated with 5 mmol $Na[Co(Propox \cdot H)_2(NO_2)_2]$ in 25—30 ml water. The characteristic crystalline precipitates were filtered after 1/2—1 hr, washed and dried as above.

Analyses. Cobalt was determined complexometrically, using Murexide as indicator. Organic ligands were destroyed by heating with conc. sulfuric acid and a few crystals of KNO_3. Nitrogen was determined by the micro-Dumas method.

Kinetic measurements. The concentration of the liberated NO_2^- was determined colorimetrically by means of the Griess—Ilosvay diazotization [16, 17]. Weighed samples of $K[Co(Propox.H)_2(NO_2)_2]$ (10^{-3} mol) were dissolved in pre-heated solutions containing the required amounts of $HClO_4$ (or NaOH) and $NaNO_3$ for obtaining constant ionic strength of $\mu = 1M$. In acidic media, 2.5×10^{-2} mol/l sulfanilic acid was also added to the solutions to prevent decomposition of the liberated HNO_2. Samples of 1—2 ml were withdrawn from time to time and added to a mixture of 2 ml 2×10^{-2} *M*, sulphanilic acid and 2 ml 2×10^{-2} *M* α-naphthylamine in 0.5% acetic acid. The mixture was kept at room temperature for 10 min to allow completion of the diazotization reaction, then it was diluted to 50 ml with a saturated borax solution. After 2 min the absorbance of the solutions was measured at 420 nm.

REFERENCES

[1] Banks, C. V., Anderson, S.: J. Inorg. Chem., **2,** 112 (1963)
[2] Heilmann, R., Baret, P.: Compt. rend. hébd. Sci., **C 267,** 579 (1968)
[3] Borello, E., Colombo, M.: Gazz. chim. ital., **87,** 615 (1957)
[4] Millone, M., Borello, E., Ambrosio, C.: J. Inorg. Nuclear Chem. **8,** 496 (1958)
[5] Várhelyi, Cs., Finta, Z., Benkő, A., Binder, A.: Monatshefte, **105,** 490 (1974)
[6] Nakahara, A.: Bull. Chem. Soc. Japan, **28,** 473 (1955)
[7] Blinc, R., Hadzi, D.: J. Chem. Soc., **4536** (1958)
[8] Beattie, I. R., Tyrrell, H. J. V.: J. Chem. Soc., **2849** (1956)
[9] Penkand, R. B., Lane, T. J., Quagliano, J. V.: J. Amer. Chem. Soc., **78,** 887 (1956)
[10] Zsakó, J., Finta, Z., Várhelyi, Cs.: Proc. 3rd Symposium on Coord. Chem., Debrecen, Hungary, 1970, Vol. I. p. 333

[11] ZSAKÓ, J., FINTA, Z., VÁRHELYI, Cs.: J. Inorg. Nuclear Chem., **34**, 2887 (1972)
[12] FINTA, Z., ZSAKÓ, J., VÁRHELYI, Cs.: Rev. Roumaine Chim., **16**, 1731 (1971)
[13] VÁRHELYI, Cs., ZSAKÓ, J., FINTA, Z.: J. Inorg. Nuclear Chem., **34**, 2583 (1972)
[14] FINTA, Z., VÁRHELYI, Cs.: Acta Chim. (Budapest) **83**, 281 (1974)
[15] FINTA, Z., VÁRHELYI, Cs., DAKÓ, E.: J. Inorg. Nuclear Chem. (In press)
[16] GRIESS, P.: Ber. dtsch. chem. Ges., **12**, 428 (1879)
[17] ILOSVAY, L.: Bull. Soc. chim. France, **2**, 347 (1889)
[18] PILKINGTON, K. A., STAPLES, P. J.: J. Inorg. Nuclear Chem., **29**, 1029 (1967)

Csaba VÁRHELYI
Zoltán FINTA
András BENKŐ
Szilveszter MIHÁLYCSA

Cluj-Napoca, str. Arany János 11, Romania.

Acta Chimica Academiae Scientiarum Hungaricae, Tomus 89 (1), pp. 55—60 (1976)

THIOUREA DERIVATIVES IN THE MORPHINE GROUP, I

R. Bognár, Gy. Gaál, P. Kerekes, G. Horváth and E. Szikszai

(Department of Organic Chemistry, Kossuth Lajos University, Debrecen)

Received March 12, 1975

Normorphine, norcodeine and nordihydrocodeine were allowed to react with various isothiocyanates to obtain the corresponding thiourea derivatives; the following compounds have been prepared: N-[N-benzylthiocarbamino]-normophine (**IV**); N-[N-cyclohexylthiocarbamino]-normorphine (**V**); N-[N-methylthiocarbamino]-norcodeine (**VI**); N-[N-phenylthiocarbamino]-norcodeine (**VII**); N-[N-benzylthiocarbamino]-norcodeine (**VIII**); N-[N-cyclohexylthiocarbamino]-norcodeine (**IX**); N-[N-2,3,4,6-tetraacetyl-β-D-glucosylthiocarbamino]-norcodeine (**X**); N-[N-methylthiocarbamino]-nordihydrocodeine(**XI**); N-[N-phenylthiocarbamino]-nordihydrocodeine(**XII**); N-[N-benzylthiocarbamino]-nordihydrocodeine(**XII**); N-[N-benzylthiocarbamino]-nordihydrocodeine (**XIII**); N-[N-cyclohexylthiocarbamino]-nordihydrocodeine(**XIV**); N-[N-2,3,4,6-tetraacetyl-β-D-glucosylthiocarbamino]-nordihydrocodeine (**XV**); N-[N-adamantylthiocarbamino]-nordihydrocodeine (**XVI**).

It is well known that isothiocyanates react with primary or secondary amines to give thiourea derivatives. The synthesis of several thiourea compounds has been reported by us earlier [1—3].

In the group of morphine alkaloids, Braun [4] prepared two thiourea derivatives by melting normorphine and norcodeine with phenyl isothiocyanate.

In the course of our experiments the corresponding thiourea derivatives have been synthesized from normorphine (**I**) with benzyl- and cyclohexyl isothiocyanate; from norcodeine (**II**) with methyl-, phenyl-, benzyl-, cyclohexyl- and tetraacetyl-β-D-glucosyl isothiocyanate; and from nordihydrocodeine (**III**) with methyl-, phenyl-, benzyl-, cyclohexyl-, adamantyl- and tetraacetyl-β-D-glucosyl isothiocyanate.

The reactions were effected in dry ethanol or chloroform solutions. The progress of the reaction was checked by thin-layer chromatography.

The compound prepared from norcodeine with phenyl mustard oil according to Braun [4] and the product obtained by reaction in solution were identical on the basis of their physical characteristics.

The structures of the compounds are supported by IR spectroscopy and elementary analyses.

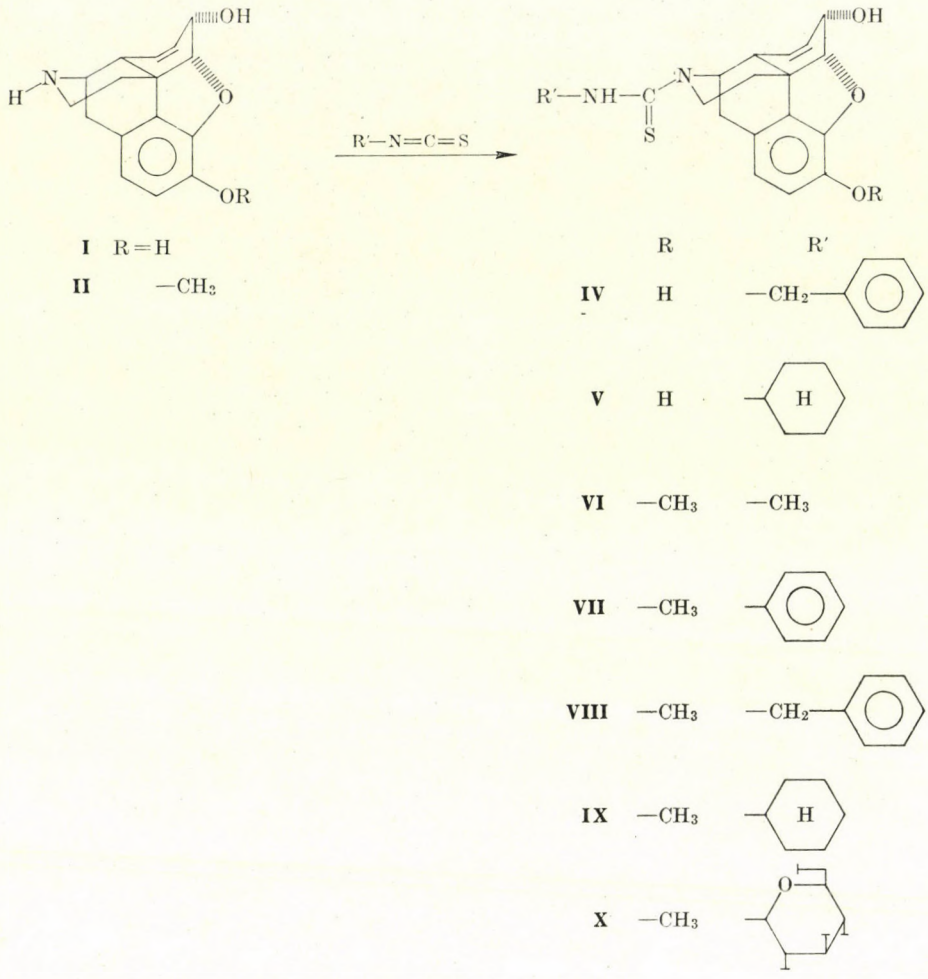

Fig. 1

Experimental

M.p.'s are uncorrected.

The IR spectra were recorded in KBr pellets with UNICAM SP. 200 G spectrophotometer.

The progress of the reaction was followed by thin-layer chromatography (Silicagel layer; benzene : methanol (8 : 2) solvent system; detection with Dragendorff's reagent and iodine vapour).

Column chromatography (Silicagel, benzene : methanol (8 : 2) was used for the purification of the products).

Among the components to be separated the R_f value of the mustard oils is the highest, so that these were eluted first from the column. The R_f values of the thiourea compounds are also considerably higher than those of the nor-compounds, thus they can be readily separated The nor-compounds either remain at the start line, or have very low R_f values.

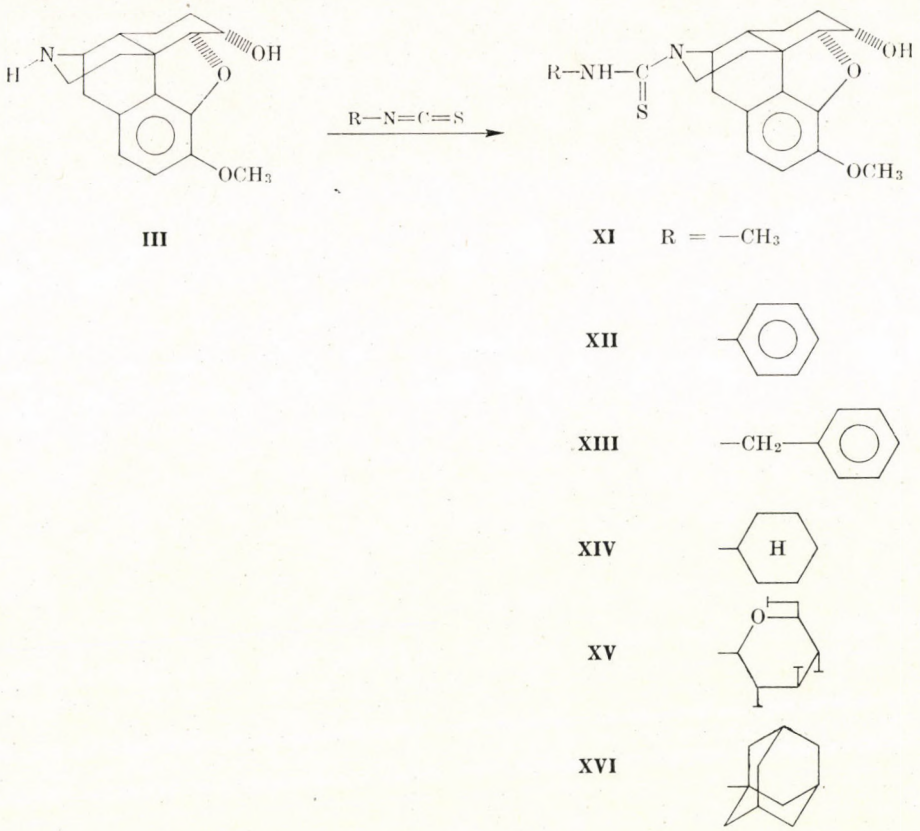

III XI R = —CH_3

XII

XIII —CH_2—

XIV H

XV O

XVI

Fig. 2

N-[N-Benzylthiocarbamino]-normorphine (IV)

Benzyl isothiocyanate (1.05 g; 0.007 mole) was dissolved in dry ethanol (100 ml) and normorphine (1.9 g; 0.007 mole) was suspended in the solution. The mixture was stirred for 20 hrs. at room temperature, filtered, clarified, evaporated and purified on the column. The fraction containing the product was evaporated and the residue washed repeatedly with ether to obtain a white, amorphus substance (0.5 g. 17%), m.p. 129—130 °C.

$C_{24}H_{24}N_2O_3S$ (420.3). Calcd. N 6.66; S 7.61. Found N 6.50; S 7.61%.

IR: $\nu_{\text{thioureide I}}$ 1530 cm^{-1}; $\nu_{\text{thioureide II}}$ 1275 cm^{-1}.

N-[N-Cyclohexylthiocarbamino]-normorphine (V)

Cyclohexyl isothiocyanate (1 g; 0.007 mole) was dissolved in dry ethanol (100 ml) and normorphine (1.9 g; 0.007 mole) was added to the solution. After 30 hrs of stirring at room temperature, the extent of conversion did not change any longer. Processing was the same as described above. A slightly yellowish, amorphous substance (0.75 g; 27%) was obtained, m.p. 115—116 °C.

$C_{23}H_{28}N_2O_3S$ (412.3). Calcd. N 6.79; S 7.76. Found N 6.44; S 7.68%.

IR* $\nu_{\text{thioureide I}}$ 1525 cm^{-1}; $\nu_{\text{thioureide II}}$ 1272 cm^{-1}.

* In the IR spectrum, a band (1690—1672 cm^{-1}) indicative of urethane impurity wa also present.

N-[N-Methylthiocarbamino]-norcodeine (VI)

Norcodeine (1 g; 0.0035 mole) and methyl mustard oil (0.25 g; 0.0035 mole) were dissolved in chloroform (30 ml). After standing for a day at room temperature, the mixture was evaporated, the residue washed with ether and separated on a column. The thiourea solution eluted from the column was evaporated, washed with ether, to obtain a white, powdery substance (0.95 g; 77%), which was found homogeneous in thin-layer chromatography, m.p. 169—171 °C.

$C_{19}H_{22}N_2O_3S$ (358.3). Calcd. N 7.81; S 8.95. Found N 7.84; S 8.84%.

IR: $\nu_{\text{thioureide I}}$ 1537 cm^{-1}; $\nu_{\text{thioureide II}}$ 1278 cm^{-1}.

N-[N-Phenylthiocarbamino]-norcodeine (VII)

(a) According to BRAUN [4]: Norcodeine (0.5 g; 0.0017 mole) and phenyl mustard oil (0,47 g; 0.0035 mole) were mixed and heated for 30 min. on steam bath. The mixture agglomerated to a solid mass, which was broken up, suspended in alcohol (25 ml) and boiled for 40 min. The white, powdery substance was recovered by filtration. It was found homogeneous in thin-layer chromatography. Yield: 0.5 g (70%), m.p. 201—202 °C.

$C_{24}H_{24}N_2O_3S$ (420.3). Calcd. N 6.61; S 7.63. Found N 6.50; S 7.50%.

IR: ν_{NH} 3300—3340 cm^{-1}; $\nu_{\text{thioureide I}}$ 1529 cm^{-1}; $\nu_{\text{thioureide II}}$ 1224 cm^{-1}.

(b) In solution: Norcodeine (0.3 g; 0.001 mole) and phenyl mustard oil (0.13 g; 0.001 mole) were dissolved in chloroform (10 ml). The next day, the product was found homogeneous in thin-layer chromatography. The mixture was evaporated and washed repeatedly with ether to obtain a white, amorphous substance (0.38 g; 95%). m.p. 201—202 °C.

$C_{24}H_{24}N_2O_3S$ (420.3). Calcd. N 6.61; S 7.63. Found N 6.54; S 7.61%.

IR: ν_{NH} 3300—3340 cm^{-1}; $\nu_{\text{thioureide I}}$ 1529 cm^{-1}; $\nu_{\text{thioureide II}}$ 1224 cm^{-1}.

N-[N-Benzylthiocarbamino]-norcodeine (VIII)

Norcodeine (1 g; 0.0035 mole) and benzyl mustard oil (0.5 g; 0.0035 mole) were dissolved in chloroform (70 ml). After 2 days of standing, the conversion was found to be complete. The solution was evaporated, purified on a column, evaporated again and washed with ether. A slightly yellowish, amorphous product (1.4 g; 93%) was obtained, m.p. 101—102 °C.

$C_{25}H_{26}N_2O_3S$ (434.33). Calcd. N 6.44; S 7.37. Found N 6.42; S 7.45%.

IR: $\nu_{\text{thioureide I}}$ 1530 cm^{-1}; $\nu_{\text{thioureide II}}$ 1247 cm^{-1}.

N-[N-Cyclohexylthiocarbamino]-norcodeine (IX)

Norcodeine (0.5 g; 0.0017 mole) and cyclohexyl mustard oil (0.25 g; 0.0017 mole) were dissolved in chloroform (20 ml). After 1 day of standing, thin-layer chromatography showed the presence of a homogeneous product. The mixture was evaporated and the residue washed with ether. A slightly yellowish amorphous substance (0.7 g; 99%) was obtained, m.p. 100—103 °C.

$C_{23}H_{30}N_2O_3S$ (426.3). Calcd. N 6.56; S 7.56. Found N 6.55; S 7.51%.

IR*: $\nu_{\text{thioureide I}}$ 1525 cm^{-1}; $\nu_{\text{thioureide II}}$ 1273 cm^{-1}.

N-[N-2,3,4,6-Tetraacetyl-β-D-glucosylthiocarbamino]-norcodeine (X)

Norcodeine (0.25 g; 0.0008 mole) and 2,3,4,6-tetraacetyl-β-D-glucosylisothiocyanate (0.4 g; 0.0008 mole) were dissolved in chloroform (10 ml). The next day thin-layer chromatography showed the presence of a homogeneous product. The mixture was evaporated and the residue washed with ether to obtain the white, powdery thiourea compound (0.5 g; 93%), m.p. 113—115 °C.

$C_{32}H_{38}O_{12}N_2S$ (672.33). Calcd. S 4.76; CH_3CO 25.58. Found S 4.72; CH_3CO 25.01%.

IR: ν_{NH} 3405 cm^{-1}; ν_{OH} 3460 cm^{-1}; $\nu_{\text{thioureide I}}$ 1540 cm^{-1}.

* The IR spectrum also had a band (1638—1603 cm^{-1}) indicative of urethane impurity.

N-[N-Methylthiocarbamino]-nordihydrocodeine (XI)

Nordihydrocodeine (1 g; 0.0035 mole) and methyl mustard oil (0.25 g; 0 0035 mole) were dissolved in chloroform (30 ml). After 2 days of standing, the spot of the starting material was still visible in the thin-layer chromatogram, yet no further conversion occurred. The mixture was evaporated, the residue washed with ether and separated on a column. An amorphous substance with pearly lustre was obtained (0.6 g; 48%), which was homogeneous in thin-layer chromatography; m.p. 107—108 °C.

$C_{19}H_{24}N_2O_3S$ (360.3). Calcd. N 7.77; S 8.88. Found N 7.63; S 8.70%

IR: $\nu_{\text{thioureide I}}$ 1530 cm^{-1}; $\nu_{\text{thioureide II}}$ 1274 cm^{-1}.

N-[N-Phenylthiocarbamino]-nordihydrocodeine (XII)

Nordihydrocodeine (0.5 g; 0.0017 mole) and phenyl mustard oil (0,23 g; 0.0017 mole) were dissolved in chloroform (10 ml). Conversion was complete by the next day. The mixture was processed as described above to obtain the thiourea derivative as a white, amorphous substance (0.7 g; 98%), m.p. 180—181 °C.

$C_{24}H_{26}N_2O_3S$ (422.3). Calcd. N 6.63; S 7.57. Found N 6.43; N 7.44%.

IR: ν_{NH} 3328 cm^{-1}; $\nu_{\text{thioureide I}}$ 1524 cm^{-1}; $\nu_{\text{thioureide II}}$ 1267 cm^{-1}.

N-[N-Benzylthiocarbamino]-nordihydrocodeine (XIII)

Nordihydrocodeine (1.5 g; 0.0052 mole) and benzyl mustard oil (0.77 g; 0.005 mole) were dissolved in chloroform (30 ml). After two days of standing, the starting materials were almost completely converted. The mixture was evaporated and separated on a column. Thin-layer chromatography showed the homogeneity of the white, powdery product (0.9 g; 41%), m.p. 111—113 °C.

$C_{24}H_{28}N_2O_3S$ (436.3). Calcd. N 6.41; S 7.33. Found N 6.10; S 7.28%.

IR: $\nu_{\text{thioureide I}}$ 1530 cm^{-1}; $\nu_{\text{thioureide II}}$ 1272 cm^{-1}.

N-[N-Cyclohexylthiocarbamino]-nordihydrocodeine (XIV)

Nordihydrocodeine (1 g; 0.0035 mole) and cyclohexyl mustard oil (0.5 g; 0.0035 mole) were dissolved in chloroform (30 ml). Conversion was complete by the next day. The mixture was processed in the usual way. The product eluted from the column was a homogeneous, slightly yellowish powdery substance (1.4 g; 95%), m.p. 81—82 °C.

$C_{24}H_{32}N_2O_3S$ (428.3). Calcd. N 6.52; S 7.45. Found N 6.44; S 7.40%.

IR*: $\nu_{\text{thioureide I}}$ 1525 cm^{-1}; $\nu_{\text{thioureide II}}$ 1271 cm^{-1}.

N-[N-2,3,4,6-Tetraacetyl-β-D-glucosylthiocarbamino]-nordihydrocodeine (XV)

Nordihydrocodeine (0.25 g; 0.0008 mole) and 2,3,4,6-tetraacetyl-β-D-glucosyl isothiocyanate (0.4 g; 0.0008 mole) were dissolved in chloroform (10 ml). Standing overnight was sufficient to attain complete conversion. Processed in the way described, the product was a white, amorphous substance (0.4 g; 75%), m.p. 118—121 °C.

$C_{32}H_{40}N_2O_{12}S$ (674.33). Calcd. S 4.74; CH_3CO 25.50. Found S 4.84; CH_3CO 25.23%.

IR: $\nu_{\text{thioureide I}}$ 1540 cm^{-1}.

N-[N-Adamantylthiocarbamino]-nordihydrocodeine (XVI)

Adamantyl isothiocyanate (0.5 g; 0.0014 mole) and nordihydrocodeine (0.2 g; 0.0014 mole) were dissolved in abs. ethanol (30 ml). After 30 hrs of boiling, no further conversion was observed. The white, crystalline substance after evaporation was recrystallised from ethanol to obtain 0.5 g (74%) of **XVI** m.p. 173—175 °C.

$C_{28}H_{35}N_2O_3S$ (484.3). Calcd. S 6.62; N 5.79. Found S 6.56; N 5.71%.

IR: ν_{NH} 3416 cm^{-1}; ν_{OH} 3593 cm^{-1}; $\nu_{\text{thioureide I}}$1529 cm^{-1}; $\nu_{\text{thioureide II}}$ 1260 cm^{-1}.

* The IR spectrum also had a band (1694 cm^{-1}) indicative of urethane impurity.

REFERENCES

[1] BOGNÁR, R., TŐKÉS, A. L., RÁKOSI, M.: Acta Chim. (Budapest) **58,** 195 (1968)
[2] GYÖRGYDEÁK, Z., SKWARSKI, D., BOGNÁR, R.: Acta Chim. (Budapest) **79,** 449 (1973)
[3] BOGNÁR, R., MAKLEIT, S., MILE, T., RADICS, L.: Monatsh. **103,** 143 (1972)
[4] BRAUN, J. V.: Ber. **47,** 2312 (1914)

Rezső BOGNÁR
György GAÁL
Péter KEREKES
Géza HORVÁTH
Eszter SZIKSZAI

H-4010, Debrecen. Institute of Organic Chemistry
Kossuth Lajos University

Acta Chimica Academiae Scientiarum Hungaricae, Tomus 89 (1), pp. 61—84 (1976)

STEREOCHEMICAL STUDIES, XXVI* ACID AMIDES OF POTENTIAL PHARMACOLOGICAL ACTIVITY, II**

THE SYNTHESIS OF *CIS*- AND *TRANS*-2-AMINO-1-CYCLOPENTANE-, 1-CYCLOHEXANE- AND 1-CYCLOHEPTANECARBOXAMIDE DERIVATIVES

G. BERNÁTH, L. GERA***, GY. GÖNDÖS, I. PÁNOVICS and Z. ECSERY+

(Institute of Organic Chemistry, Attila József University, Szeged and +Chemical and Pharmaceutical Works, Chinoin, Budapest)

Received April 16, 1975

Starting with *cis* and *trans*-2-amino-1-cyclopentanecarboxylic acid (**2a**, **3a**), *cis*- and *trans*-2-amino-1-cyclohexanecarboxylic acid (**2b**, **3b**), and with *trans*-2-amino-1-cycloheptanecarboxylic acid (**3c**), a great number of N-substituted *cis*- and *trans*-2-amino-1-cycloalkanecarboxamides (**16**, **17a—17ee**, **18**, **19a—19h**, **20a** and **20b**) have been synthesized for pharmacological testing. Further, some N-substituted *cis*- and *trans*-2-formylamino-1-cyclohexanecarboxamides (**22a—22f**, **23**) N-substituted *cis*-2-acetylamino-1-cyclohexanecarboxamides (**27a—27f**), and N-substituted *trans*-2-acetylamino-1-cyclohexanecarboxamides (**28a—28e**) have been prepared.

Introduction

For stereochemical studies we have prepared a number of *cis*- and *trans*-2-aminomethylcyclopentanol- [1, 2], *cis*- and *trans*-2-aminomethylcyclohexanol- [3—5], *cis*- and *trans*-2-aminomethylcycloheptanol-[6], and related derivatives [7]. Since many compounds with acid amide structure are known to possess hypnotic, anticonvulsive, antidepressant, hypotensive, or other valuable pharmacological effects [8, 9], we have prepared the N-acyl derivatives of the mentioned alicyclic 1,3-amino alcohols and their analogues, for pharmacological testing. This work was motivated by the circumstance that while the N-alkyl- and N-dialkyl-derivatives of aminomethylcyclohexane and of related compounds substituted in the skeleton are widely studied analgetics [10], the corresponding N-acyl derivatives have not been investigated.

It has been found [11—13] that the N-cycloalkyl acid amides prepared by us [14] exert a definite tranquillizing effect upon the central nervous system and their therapeutic ratio is high.

* Part XXV: JANCKE, H., ENGELHARDT, G. BERNÁTH, G., GÖNDÖS, GY., TICHÝ, M.: J. prakt. Chem.; **317**, 1005 (1975)

** As Part I of this series is regarded: BERNÁTH, G., CSÓKÁSI, E., HEVÉR, J., GERA, L., KOVÁCS, K.: Acta Chim. (Budapest) **70**, 271 (1971)

*** This paper includes a substantial part of the Doctoral Thesis (Szeged, 1974) o f L. GERA.

As a continuation of this work, it was obvious to synthesize also the amide type derivatives of our stereochemical model substances, *i.e.* of *cis*- and *trans*-2-amino-1-cyclohexanecarboxylic acid (**2b**, **3b**) and their analogues with cyclopentane and cycloheptane skeleton (**2a**, **3a**, **3c**). By the pharmacological testing of a great number of structurally analogous compounds differing in the ring size, the majority of them being stereochemically homogeneous, we hoped to gain insight into the relationship between chemical fine structure and pharmacological effects.

Close analogues of the type of compound **1** synthesized by us, are described as intermediates in a patent specification published not long ago [15], where the target compounds, *i.e.* the 2-anilino- and 2-anilinomethyl-1-cycloalkylamine derivatives were found to have diuretic and antidiabetic effects.

An analogous aromatic carboxylic acid derivative, *o*-[3-trifluoromethyl-(phenylamino)] benzoic acid (flufenamic acid) is a potent antiphlogistic drug [16, 17].

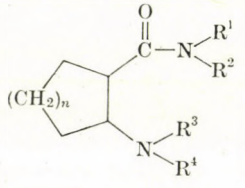

1

n = 1, 2, 3

R^1, R^2, R^3 = H, alkyl, aralkyl or aryl

R^4 = H or acyl

Fig. 1

A further incentive to the synthesis of compounds of type **1** was found in the circumstance that our work aiming at the preparation and study of the conformations of condensed heterocycles with two heteroatoms [6, 18—20] prompted the synthesis of 4a,5,6,7,8,8a-hexahydroquinazolin-4(3*H*)-ones and related derivatives. The aromatic analogues of these compounds have been very thoroughly studied [21] from both the chemical and pharmacological points of view. 2-Methyl-3-(*o*-tolyl)quinazol-4(3*H*)-one, Methaqualone, prepared by Indian authors [22] is a valuable non-barbiturate hypnotic agent.

Based on the analogy of the generally used methods [21] for the preparation of quinazolones, *i.e.* the aromatic analogues, it seemed reasonable to attempt the preparation of the hitherto hardly studied [23], stereochemically homogeneous hydrogenated derivatives by cyclization of the 2-acylamino-1-

cyclohexanecarboxamides (**1**: R^1, R^3 = H; R^2 = H, alkyl, aralkyl, aryl; R^4 = acyl).

It may be worth mentioning that the metabolic product of Methaqualone discharged by the organism is the corresponding 2-nitro acid amide, *i.e.* 2-nitrobenzo-*o*-toluidide. The study of the acid amide type metabolites of the related quinazolones is in the foreground also in these days [23].

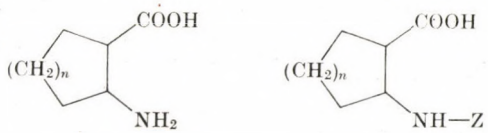

2: *cis* **4**: *cis*

3: *trans* **5**: *trans*

a: $n = 1$; *b*: $n = 2$; *c*: $n = 3$

$$Z = -\overset{\overset{O}{\|}}{C}-O-CH_2-C_6H_5$$

Fig. 2

The relationship transcending formal analogy prompted us to study 2-amino-N-cycloalkyl-1-carboxamides in parallel with hexahydroquinazolones. In this paper the synthesis of compounds of type **1** will be discussed (**1**: R^1 = H; R^2 = alkyl, aralkyl, or aryl; R^3 = H, R^4 = H, acyl). Details of the work on the synthesis of further analogues (**1**: R^1 = H, alkyl, aralkyl; R^2 = alkyl, aralkyl, aryl; R^3 = H, alkyl, aralkyl, aryl, acyl; R^4 = H, alkyl) and of hydrogenated quinazolones derived from them [24—26] will be published later.

Results and discussion

Since one of the aims of this work was the synthesis of model substances for the study of the relationship between chemical fine structure and pharmacological action, we endeavoured to produce stereochemically homogeneous compounds. In a synthesis of compounds of type **1**, SZMUSKOVICZ supposed [15] that the reduction of enamines, prepared from ethyl-2-oxo-1-cyclohexanecarboxylates with amines, gave *cis* derivatives but the stereohomogeneity of the compounds, as they were only intermediates, was not proved. He isomerized the *cis* isomers with potassium-*t*-butoxide into the corresponding *trans* derivatives, which were converted — again without evidence for stereochemical homogeneity — into the required end-products.

Earlier we have shown [35] that catalytic reduction of the imino derivative, easily prepared from ethyl-2-oxo-1-cyclohexanecarboxylate with ammonium hydroxide, always yields a mixture of ethyl-*cis*-, and ethyl-*trans*-2-amino-1-cyclohexanecarboxylates. It is also known that the isomerization of alicyclic 1,2-disubstituted systems leads to an equilibrium which assures the presence chiefly, but not exclusively, of the *trans* isomer [36]. Therefore we thought it useful to synthesize the alicyclic N-substituted 2-amino-1-carboxamides (**1**) by starting with stereochemically homogeneus *cis*- and *trans*-2-amino-1-carboxylic acids (**2**, **3**). The syntheses of these β-amino acids are described in earlier communications [2, 4, 6].

For the preparation of N-substituted *cis*- and *trans*-2-amino-1-cycloalkanecarboxamides (**1**), the methods usually employed in peptide chemistry were applied. The alicyclic β-amino acids (**2**, **3**) were treated with benzyl chloroformate [27] and the resulting 2-carbobenzoxyamino-1-carboxylic acid derivatives (**4**, **5**) [2-(Z-amino)-1-carboxylic acids; Z = carbobenzoxy] were made to react with the corresponding amines in the presence of dicyclohexylcarbodiimide (DDC) as the condensing agent. The desired reactions proceeded, in general, to give satisfactory yields. However, the attempted reactions with butylamine and 2-(*m*,*p*-dimethoxyphenyl)ethylamine led only to the formation of the salts; no acid amide was obtained.

Besides the required *cis*-2-(Z-amino)-1-cyclohexane-*p*-chlorocarboxanilide (**11n**), the N-acyl-N,N'-dicyclohexylurea derivatives (**6**) were also produced when *cis*-2-(Z-amino)-1-cyclohexanecarboxylic acid (**4b**) was allowed to react with *p*-chloroaniline in tetrahydrofurane. Similar side-reactions are known in peptide syntheses [28, 29]. The N-acylurea derivative (**6**) is obtained by O→N acyl migration from the addition product (**7**) primarily formed.

Owing to these side-reactions, the mixed anhydride method [30] proved more suitable for the preparation of the 2-amino-1-carboxamides. The Z-amino

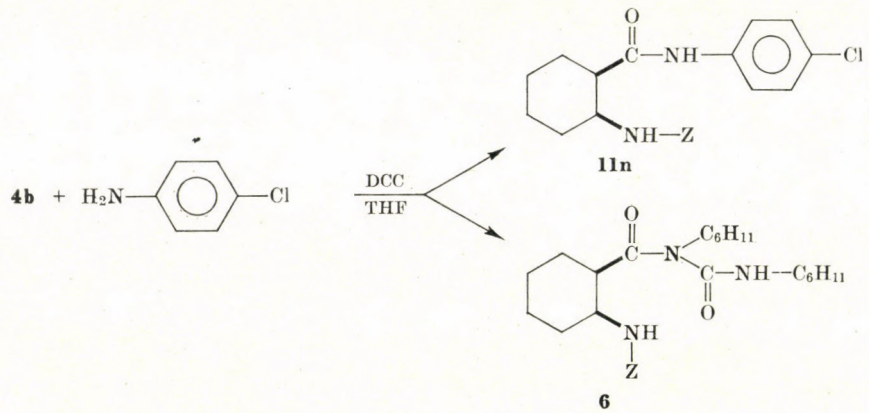

Fig. 3

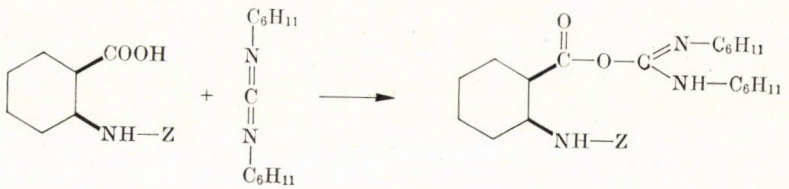

4b **7**

Fig. 4

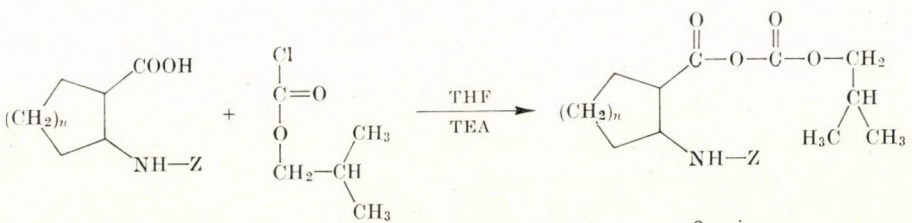

4: *cis*
5: *trans*

a: $n=1$; *b*: $n=2$; *c*: $n=3$

8: *cis*
9: *trans*

Fig. 5

acids (**4, 5**) were treated in tetrahydrofurane, in the presence of triethylamine, with isobutyl chloroformate, and the resulting mixed anhydride (**8, 9**) was allowed to react with the corresponding amines at —10 °C. The yields of N-substituted *cis*- and *trans*-2-carbobenzoxyamino-1-cyclopentanecarboxamides (**10a, 10b, 12a, 12b**), *cis*- and *trans*-2-carbobenzoxyamino-1-cyclohexanecarboxamides (**11a-ü, 13a-g**) and *trans*-2-carbobenzoxyamino-1-cycloheptanecarboxamides (**14a, 14b**) were between 60 and 80%. As by-products, some carbamic acid esters (**15**) also formed in these reactions [31, 32]. With secondary amines (diethylamine, N-methyl-benzylamine) and with cyclic secondary amines (piperidine, morpholine) the formation of carbamic acid esters was prevailing. Thus the mixed anhydride method proved unsuitable for the synthesis of derivatives disubstituted on the amide nitrogen.

The undesired preponderance of carbamic acid ester formation when using secondary and cyclic amines can be interpreted as a consequence of steric hindrance during carboxamide formation.

The protecting Z-grup of the compounds **10—14** (Tables I—III) was removed by treatment with hydrogen bromide in glacial acetic acid [33]. Hydrogenolysis wiht palladium-charcoal [27, 34] proved to be unsuitable. The method actually used had the advantage of directly yielding the hydrogen bromide salts of the 2-amino-1-carboxamides **16—20** for pharmacological testing. In some cases (hygroscopic substances, difficulties in purification) the base

Table I

Melting points and analysis data of N-substituted cis-2-carbobenzoxyamino-1-cyclohexanecarboxamides **(11a—11ii)**

Compound	R	Formula Molecular weight	M.p., °C Solvent	Analysis, % Calculated Found			Yield, %
				C	H	N	
11a	H	$C_{15}H_{20}O_3N_2$ 276.34	148—149 ethanol	65.20 65.00	7.30 7.49	10.14 9.70	61.23
11b	$-CH_3$	$C_{16}H_{22}O_3N_2$ 290.36	137—138 ethanol	66.18 66.26	7.64 7.62	9.65 9.74	65.17
11c	$-CH_2(CH_2)_2CH_3$	$C_{19}H_{28}O_3N_2$ 332.45	101—103 ethanol	68.64 67.76	8.49 8.58	8.43 8.31	65.25
11d	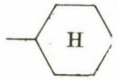	$C_{21}H_{30}O_3N_2$ 358.48	164—165 ethanol	70.36 70.00	8.44 8.20	7.82 7.45	70.17
11e	$-C_6H_5$	$C_{21}H_{24}O_3N_2$ 354.44	172—173 ethanol	71.58 71.52	6.87 6.92	7.94 7.79	72.20
11f	$-C_6H_4CH_3(o)$	$C_{22}H_{26}O_3N_2$ 366.46	169—171 ethanol	72.10 72.42	7.15 7.31	7.64 7.54	71.15
11g	$-C_6H_4CH_3(m)$	$C_{22}H_{26}O_3N_2$ 366.46	186—188 ethanol	72.10 71.97	7.15 6.98	7.64 7.38	70.27
11h	$-C_6H_4CH_3(p)$	$C_{22}H_{26}O_3N_2$ 366.46	178—179 ethanol	72.10 72.10	7.15 7.18	7.64 7.40	72.35
11i	$-C_6H_2(CH_3)_3(o,o',p)$	$C_{24}H_{30}O_3N_2$ 394.52	198—201 dioxane	73.07 73.23	7.67 7.67	7.10 7.21	62.51
11j	$-C_6H_3CH_3(o)Cl(m)$	$C_{22}H_{25}O_3N_2Cl$ 400.91	214—215 dioxane	65.91 65.99	6.27 6.35	6.99 7.09	61.12
11k	$-C_6H_4F(m)$	$C_{21}H_{23}O_3N_2F$ 370.43	187—188 ethanol	68.10 68.30	6.26 6.29	7.56 7.55	65.07
11l	$-C_6H_4Cl(o)$	$C_{21}H_{23}O_3N_2Cl$ 386.88	175—177 ethanol	65,20 65.69	5.99 6.18	7.24 7.61	74.20

11m	$-C_6H_4Cl(m)$	$C_{21}H_{23}O_3N_2Cl$ 386.88	197—199 ethanol	65.20 65.36	5.99 6.16	7.24 7.06	73.15
11n*	$-C_6H_4Cl(p)$	$C_{21}H_{23}O_3N_2Cl$ 386.88	179—180 ethanol	65.20 65.41	5.99 5.59	7.24 7.57	54.03
11o	$-C_6H_3Cl_2(o, m)$	$C_{21}H_{22}O_3N_2Cl_2$ 421.33	195—197 dioxane	59.87 59.60	5.26 4.94	6.65 6.56	60.15
11p	$-C_6H_3Cl(o)Br(m)$	$C_{21}H_{22}O_3N_2ClBr$ 465.78	172—174 ethanol	54.19 54.31	4.76 4.64	6.01 6.31	60.27
11r	$-C_6H_4Br(p)$	$C_{21}H_{23}O_3N_2Br$ 431.34	184—185 ethanol	58.48 58.24	5.38 5.43	6.50 6.23	79.25
11q	$-C_6H_4CF_3(m)$	$C_{22}H_{23}O_3N_2F_3$ 420.43	167—169 ethanol	62.85 62.42	5.52 5.45	6.66 6.61	64.38
11s	$-C_6H_4OCH_3(p)$	$C_{22}H_{26}O_4N_2$ 382.46	170—172 ethanol	69.08 69.07	6.85 6.94	7.32 7.09	63.10
11t	$-C_6H_3OCH_3(o)Cl(m)$	$C_{22}H_{25}O_4N_2Cl$ 416.91	158—160 ethanol	63.38 63.42	6.05 5.81	6.72 6.99	63.37
11u	$-C_6H_4OC_2H_5(p)$	$C_{23}H_{28}O_4N_2$ 396.49	165—167 ethanol	69.67 69.27	7.21 7.10	7.07 6.78	62.15
11v	$-C_6H_4(COCH_3)(p)$	$C_{23}H_{26}O_4N_2$ 394.47	196—198 dioxane	70.02 69.89	6.64 6.68	7.10 7.11	68.39
11w	$-C_6H_4(NHCOCH_3)(p)$	$C_{23}H_{27}O_4N_3$ 409.49	233—236 dimethyl- formamide	67.46 67.80	6.65 7.00	10.26 10.33	70.15
11x	$-C_6H_4NO_2(p)$	$C_{21}H_{23}O_5N_3$ 397.42	200—202 dioxane	63.46 63.17	5.83 5.66	10.58 10.66	47.31
11y	$-CH_2C_6H_5$	$C_{22}H_{26}O_3N_2$ 366.46	125—127 ethanol	72.10 71.80	7.15 7.34	7.64 7.20	69.36
11z	$-CH_2C_6H_4Cl(p)$	$C_{22}H_{25}O_3N_2Cl$ 400.91	160—161 ethanol	65.91 66.47	6.29 6.25	6.99 6.83	68.70
11aa	$-CH_2C_6H_4OCH_3(p)$	$C_{23}H_{28}O_4N_2$ 396.49	140—142 ethanol	69.67 69.77	7.12 7.00	7.07 7.05	65.30
11bb	$-CH_2CH_2C_6H_5$	$C_{23}H_{28}O_3N_2$ 380.49	154—155 ethanol	72.60 72.69	7.42 7.38	7.36 6.72	68.45

Table I (continued)

Compound	R	Formula Molecular weight	M.p., °C Solvent	Analysis, % Calculated Found			Yield, %
				C	H	N	
11cc	$-CH_2CH_2C_6H_3(OCH_3)_2(m,p)$	$C_{25}H_{32}O_5N_2$ 440.54	137—139 ethanol	68.17 67.95	7.32 7.45	6.36 6.26	65.40
11dd	$-CH_2CH_2C_6H_4(SO_2NH_2)(p)$						
11ee	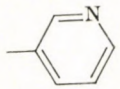	$C_{23}H_{29}O_5N_3S$ 459.97	155—157 ethanol	60.11 59.70	6.36 6.41	9.14 9.19	71.20
11ff	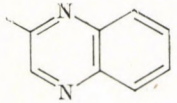	$C_{20}H_{23}O_3N_3$ 353.42	173—174 ethanol	67.97 68.43	6.56 6.62	11.89 11.53	70.15
		$C_{23}H_{26}O_3N_4$ 406.49	195—197 dioxane	67.96 68.18	6.45 6.05	13.79 13.51	49.57
11gg	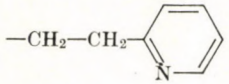	$C_{22}H_{27}O_3N_3$ 381.48	142—143 ethanol	69.27 68.90	7.13 7.52	11.01 10.90	67.15
11hh	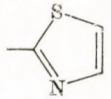	$C_{18}H_{21}O_3N_3S$ 359.45	187—189 ethanol	60.14 60.10	5.89 6.01	11.69 11.40	68.30
11ii	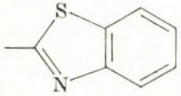	$C_{22}H_{25}O_3N_3S$ 411.53	205—208 benzene	64.21 64.24	6.21 5.92	10.21 10.13	55.20

* Compound **11n** was prepared by the dicyclohexylcarbodiimide method.

Table II

Melting points and analysis data of N-substituted trans-2-(carbobenzoxyamino)-1-cyclohexanecarboxamides **(13a—13g)**

Compound	R	Formula Molecular weight	M.p., °C Solvent	Analysis. % Calculated Found			Yield, %
				C	H	N	
13a	$-CH_2(CH_2)_2CH_3$	$C_{19}H_{28}O_3N_2$ 332.45	187—189 ethanol	68.46 69.19	8.49 8.84	8.43 8.92	61.13
13b	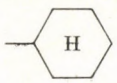	$C_{21}H_{30}O_3N_2$ 358.48	239—241 ethanol	70.36 70.41	8.44 8.63	7.82 7.61	61.35
13c	$-C_6H_4CH_3(p)$	$C_{22}H_{26}O_3N_2$ 366.46	228—230 dioxane	72.10 72.32	7.15 7.27	7.64 7.37	68.27
13d	$-C_6H_4Cl(p)$	$C_{21}H_{23}O_3N_2Cl$ 386.88	242—244 ethanol	65.20 64.80	5.99 6.00	7.24 7.38	71.10
13e	$-C_6H_4Br(p)$	$C_{21}H_{23}O_3N_2Br$ 431.34	251—253 methanol	58.48 58.88	5.38 5.91	6.50 6.44	70.17
13f	$-CH_2C_6H_5$	$C_{22}H_{26}O_3N_2$ 366.46	223—225 ethanol	72.10 71.60	7.15 7.42	7.64 7.36	61.20
13g	$-CH_2CH_2C_6H_5$	$C_{23}H_{28}O_3N_2$ 380.49	185—187 ethanol	72.60 72.90	7.42 7.47	7.36 7.56	63.30

Table III

Melting points and analysis data of N-substituted cis- and trans-2-(carbobenzoxyamino)-1-cyclopentanecarboxamides **(10a, 10b, 12a, 12b)**, *and -1-cycloheptanecarboxamides* **(14a, 14b)**

Compound	R	Configuration	Formula Molecular weight	M.p.,°C Solvent	Analysis, % Calculated Found			Yield, %
					C	H	N	
10a	$-C_6H_4CH_3(p)$	*cis*	$C_{21}H_{24}O_3N_2$ 352.44	176—178 ethanol	71.58 71.44	6.87 6.84	7.95 8.19	71.53
10b	$-C_6H_4Cl(p)$	*cis*	$C_{20}H_{21}ON_2Cl$ 377.84	178—180 ethanol	64.42 63.64	5.68 5.71	5.51 5.50	70.21
12a	$-C_6H_4CH_3(p)$	*trans*	$C_{21}H_{24}O_3N_2$ 352.44	181—183 methanol	71.58 71.81	6.87 6.59	7.95 7.95	68.61
12b	$-C_6H_4Cl(p)$	*trans*	$C_{20}H_{21}O_3N_2Cl$ 377.85	198—200 methanol	64.42 64.68	5.68 5.75	7.51 7.99	65.74
14a	$-C_6H_4CH_3(p)$	*trans*	$C_{23}H_{28}O_3N_2$ 380.47	206—207 methanol	72.60 72.56	7.42 7.44	7.36 7.45	71.32
14b	$-C_6H_4Cl(p)$	*trans*	$C_{22}H_{25}O_3N_2Cl$ 400.87	217—218 methanol	65.90 65.30	6.28 6.23	6.98 6.90	68.95

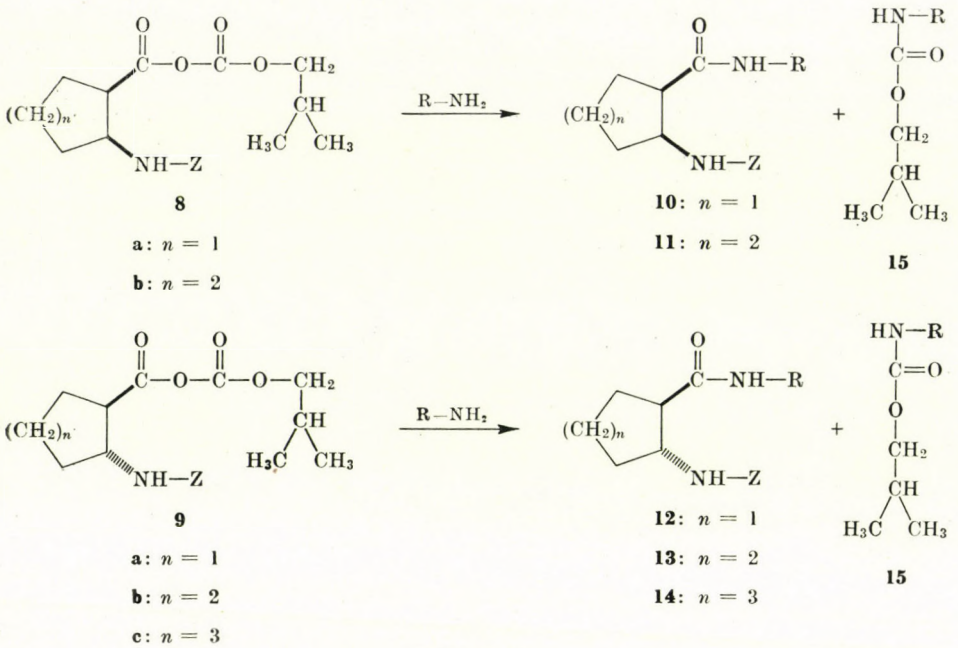

8

a: $n = 1$

b: $n = 2$

10: $n = 1$

11: $n = 2$

15

9

a: $n = 1$

b: $n = 2$

c: $n = 3$

12: $n = 1$

13: $n = 2$

14: $n = 3$

15

Fig. 6

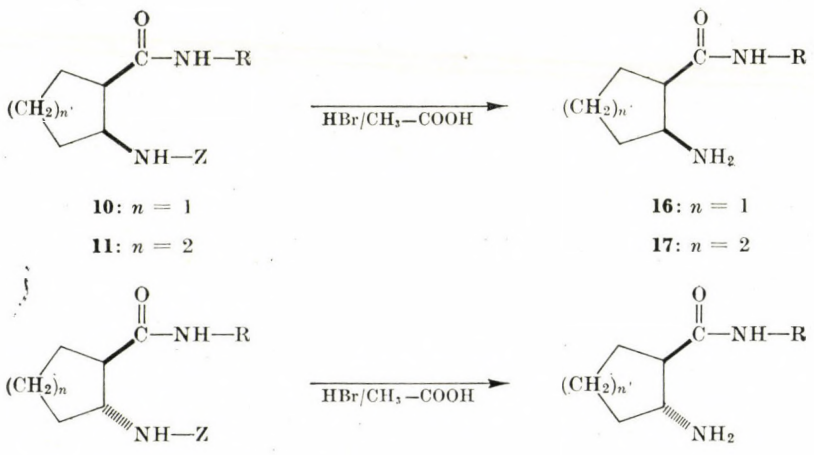

10: $n = 1$

11: $n = 2$

16: $n = 1$

17: $n = 2$

12: $n = 1$

13: $n = 2$

14: $n = 3$

18: $n = 1$

19: $n = 2$

20: $n = 3$

Fig. 7

was liberated by means of Varion-AD anion-exchange resin. Liberation of the base with sodium hydrogen carbonate was feasible only form the pure salts. Tables IV and V give a survey of the *cis*- and *trans*-2-amino-1-cyclohexanecarboxamide derivatives.

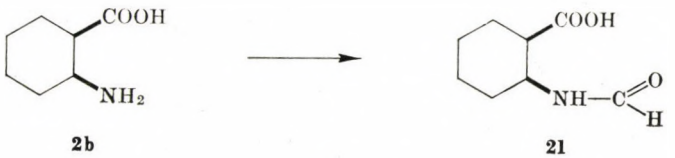

2b **21**

Fig. 8

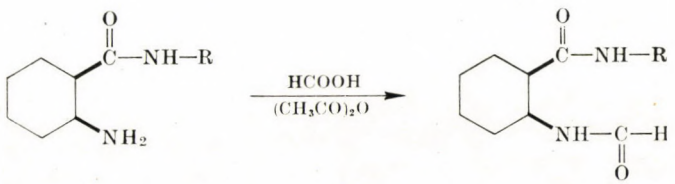

17 **22**

Fig. 9

Some N-acyl derivatives of the *cis*-2-amino-1-cyclohexanecarboxamides were also prepared. Formylation of *cis*-2-amino-1-cyclohexanecarboxylic acid (**2b**) was effected in the usual way [37], with a mixture of formic acid and acetic acid anhydride. However, the mixed anhydride method [30] failed in the attempted conversion of *cis*-2-formylamino-1-cyclohexanecarboxylic acid (**21**) into 2-formylamino-1-carboxamide derivatives, therefore we had to use the longer route, *i.e.* formylation of the appropriate N-substituted *cis*-2-amino-1-cyclohexanecarboxamides. We wish to note here that 2-formylamino-1-cyclohexanecarboxylic acid had been prepared earlier by Le Bel *et al.* [38] who obtained the parent acid, *i.e.* 2-amino-1-cyclohexanecarboxylic acid, by the catalytic hydrogenation of anthranilic acid, and found the melting point of the formyl derivative prepared therefrom to be 200—201 °C. In contrast to this, compound **21** prepared by us from stereochemically homogeneous *cis*-2-amino-1-cyclohexanecarboxylic acid (**2b**) had m.p. 206—208 °C, suggesting that the catalytic reduction of anthranilic acid had not produced **2b** in stereochemically homogeneous form.

Cis-2-acetylamino-1-cyclopentanecarboxylic acid (**24**) and the homologous *cis*- and *trans*-cyclohexane derivatives (**25, 26**) were synthesized by the usual acetylation procedure [39], from the corresponding, stereochemically homogeneous amino acids **2a**, **2b** and **3b**.

Table IV

Melting points and analysis data of N-substituted cis-2-amino-1-cyclohexanecarboxamides* **(17a—17ee)**

Compound	R	Form*	Formula Molecular weight	M.p.,°C Solvent	Analysis, % Calculated Found			Yield, %
					C	H	N	
17a**	H	α	$C_7H_{14}ON_2$ 142.20	125—126 ethyl acetate	59.13 59.15	9.95 10.33	19.70 19.51	68.73
17b	$-CH_2(CH_2)_2CH_3$	α	$C_{11}H_{22}ON_2$ 198.31	39—42 benzene–petroleum ether	66.63 65.99	11.18 10.82	14.13 14.01	54.17
17c	$-CH_2(CH_2)_2CH_3$	β	$C_{11}H_{23}ON_2Cl$ 234.77	142—144 ethanol–ether	56.27 55.80	9.88 10.19	11.98 11.78	51.27
17d	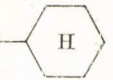	γ	$C_{13}H_{25}ON_2Br$ 305.27	204—207 (d.) ethanol–ether	51.14 51.67	8.25 8.49	9.18 9.53	61.05
17e	$-C_6H_5$	α	$C_{13}H_{18}ON_2$ 218.30	143—144 ethanol	71.53 72.11	8.31 8.33	12.83 12.03	68.27
17f	$-C_6H_5$	β	$C_{13}H_{19}ON_2Br$ 299.22	188—191 (d.) ethanol	52.19 51.73	6.40 6.21	9.36 9.18	71.02
17g	$-C_6H_4CH_3(o)$	α	$C_{14}H_{20}ON_2$ 232.33	92—93 ether	72.39 72.34	8.68 8.54	12.06 11.52	71.21
17h	$-C_6H_4CH_3(m)$	α	$C_{14}H_{20}ON_2$ 232.33	130—133 benzene	72.39 72.95	8.68 8.56	12.06 11.62	67.10
17i	$-C_6H_4CH_3(p)$	α	$C_{14}H_{20}ON_2$ 232.33	144—147 benzene	72.38 72.31	8.68 8.85	12.06 12.21	85.25
17i	$-C_6H_4CH_3(p)$	β	$C_{14}H_{21}ON_2Br$ 313.25	200—203 ethanol	53.69 53.77	6.76 7.08	8.95 8.71	78.15
17j	$-C_6H_2(CH_3)_3(o, o', p)$	β	$C_{16}H_{25}ON_2Br$ 341.30	275—277 ethanol	56.31 55.75	7.38 7.17	8.21 7.92	61.27

17k	$-C_6H_3CH_3(o)Cl(m)$	β	$C_{14}H_{20}ON_2ClBr$ 347.69	244–247 ethanol	48.37 48.64	5.80 5.58	8.06 7.92	60.29
17l	$-C_6H_4F(m)$	β	$C_{13}H_{18}ON_2BrF$ 313.25	207–210 (d.) ethanol	49.22 48.92	5.72 5.77	8.83 8.79	63.17
17m	$-C_6H_4Cl(o)$	β	$C_{13}H_{18}ON_2ClBr$ 333.66	168–170 ethanol	46.79 46.39	5.44 5.75	8.40 8.30	77.51
17n	$-C_6H_4Cl(m)$	α	$C_{13}H_{17}ON_2Cl$ 252.75	121–123 benzene	61.77 61.85	6.78 6.67	11.09 10.90	69.31
17o	$-C_6H_4Cl(p)$	α	$C_{13}H_{17}ON_2Cl$ 252.75	121–123 ethanol	61.77 61.75	6.78 6.90	11.09 11.10	79.31
17p	$-C_6H_4Cl(p)$	β	$C_{13}H_{18}ON_2ClBr$ 333.66	197–200 ethanol	46.79 47.20	5.44 5.80	8.40 8.19	82.31
17r	$-C_6H_4Br(p)$	α	$C_{13}H_{17}ON_2Br$ 297.30	140–142 ethanol	52.52 52.02	5.77 5.81	9.43 9.59	75.17
17q	$-C_6H_4CF_3(m)$	β	$C_{14}H_{18}ON_2BrF_3$ 367.22	169–172 ethanol	45.80 45.53	4.98 5.13	7.64 7.95	62.27
17s***	$-C_6H_4OCH_3(p)$	α	$C_{14}H_{20}O_2N_2$ 248.83	102–103 ether	67.72 67.98	8.12 8.45	11.28 11.51	65.25
17t	$-C_6H_4OCH_3(p)$	β	$C_{14}H_{21}O_2N_2Br$ 329.25	135–138 ethanol–ether	51.07 51.16	6.43 6.80	8.51 8.40	70.27
17u	$-C_6H_4OC_2H_5(p)$	α	$C_{15}H_{22}O_2N_2$ 262.36	95–96 benzene	68.66 68.91	8.45 8.88	10.68 10.56	65.31
17v	$-C_6H_4OC_2H_5(p)$	β	$C_{15}H_{23}O_2N_2Br$ 343.27	122–126 ethanol	52.48 51.91	6.78 7.41	8.16 7.91	68.71
17w	$-CH_2C_6H_5$	α	$C_{14}H_{20}ON_2$ 232.33	55–57 ethanol–ether	72.38 72.03	8.68 8.53	12.06 11.54	71.21
17x	$-CH_2C_6H_4Cl(p)$	α	$C_{14}H_{19}ON_2Cl$ 266.77	60–62 ethanol–ether	63.03 63.40	7.18 7.31	10.50 10.86	73.23
17y	$-CH_2C_6H_4OCH_3(p)$	β	$C_{15}H_{23}O_2N_2Br$ 343.27	194–196 ethanol	52.48 52.70	6.75 6.88	8.08 8.38	68.31
17z	$-CH_2CH_2C_6H_5$	α	$C_{15}H_{22}ON_2$ 246.36	86–88 ethanol–ether	73.12 73.24	9.00 8.81	11.37 11.86	69.45

Table IV (continued)

Compound	R	Form*	Formula Molecular weight	M.p., °C Solvent	Analysis,% Calculated Found			Yield, %
					C	H	N	
17aa	$-CH_2CH_2C_6H_3(OCH_3)_2(m,p)$	α	$C_{17}H_{26}O_3N_2$ 306.41	69—71 ethanol–ether	66.64 66.25	8.55 8.81	9.14 9.42	70.15
17bb	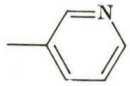	α	$C_{12}H_{17}ON_3$ 219.29	131—133 ethanol–ether	65.72 65.87	7.81 7.60	8.04 8.17	63.21
17cc	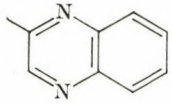	α	$C_{15}H_{19}ON_4$ 271.34	165—167 benzene	66.41 66.64	7.06 6.63	20.64 20.37	51.20
17dd	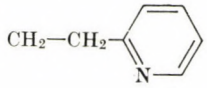	α	$C_{14}H_{21}ON_3$ 247.34	60—62 ethanol–ether	67.99 68.40	8.56 8.71	16.99 16.69	55.30
17ee	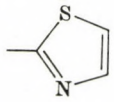	α	$C_{10}H_{15}ON_3S$ 225.31	156—158 ethanol	53.31 53.58	6.98 6.98	18.27 18.27	69.87

Notes: * α = base, β = HBr, γ = HCl; ** The lit. m.p. of **17a** is 124 °C [45]; *** The lit. m.p. of **17s** is 99—100 °C [15].

Table V

Melting points and analysis data of N-substituted trans-2-amino-1-cyclohexanecarboxamides **(19a—19h)**

Compound	R	Form*	Formula Molecular weight	M.p., °C Solvent	Analysis, % Calculated Found			Yield, %
					C	H	N	
19a	$-CH_2(CH_2)_2CH_3$	α	$C_{11}H_{22}ON_2$ 198.31	72—75 ethanol–ether	66.63 66.49	11.18 11.40	14.13 13.42	49.11
19b	$-C_6H_4CH_3(p)$	α	$C_{14}H_{20}ON_2$ 232.33	140—141 ethanol	72.39 72.67	8.68 8.75	12.06 11.37	65.15
19c	$-C_6H_4CH_3(p)$	β	$C_{14}H_{21}ON_2Br$ 313.25	206—209 ethanol	53.69 54.20	6.76 6.79	8.95 8.70	78.27
19d	$-C_6H_4Cl(p)$	α	$C_{13}H_{17}ON_2Cl$ 252.75	161—163 ethanol	61.77 64.41	6.78 7.05	11.09 11.73	65.25
19e	$-C_6H_4Cl(p)$	β	$C_{13}H_{18}ON_2ClBr$ 333.66	228—230 ethanol	46.79 46.43	5.44 5.41	8.40 8.12	77.21
19f	$-C_6H_4Br(p)$	β	$C_{13}H_{18}ON_2Br_2$ 378.12	255—257 ethanol	41.30 41.14	4.80 4.39	7.41 7.44	70.03
19g	$-CH_2CH_2C_6H_5$	α	$C_{15}H_{22}ON_2$ 246.36	98—101 ethanol	73.12 72.83	9.00 9.21	11.37 11.12	60.21
19h	$-CH_2CH_2C_6H_3(OCH_3)_2(m,p)$	α	$C_{17}H_{26}O_3N_2$ 306.41	120—122 ethanol–ether	66.64 66.31	8.55 8.39	9.14 9.04	65.11

*α = base, β = HBr

The attempted GRIMMEL-type phosphorous trichloride reaction [40] with amines **25** and **26** did not afford the expected hexahydroquinazolone derivatives (**29**) but gave the N-substituted *cis*- and *trans*-2-acetylamino-1-cyclohexanecarboxamides **27** and **28**. In the course of the reaction of *cis*-2-acetylamino-1-cyclohexanecarboxylic acid (**25**) with amines, small amounts (4—5%) of N-substituted *trans*-2-acetylamino-1-cyclohexanecarboxamides (**28**) were also formed. The *cis* and *trans* isomers could be separated by fractional crystallization.

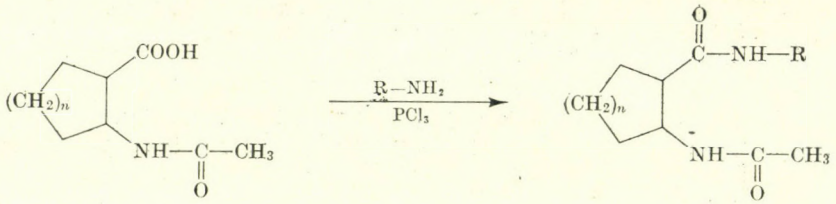

24: $n = 1$, *cis*

25: $n = 2$, *cis*

26: $n = 2$, *trans*

27: $n = 2$, *cis*

28: $n = 2$, *trans*

Fig. 10

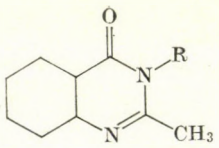

29

Fig. 11

It may appear surprising that the GRIMMEL-type reaction of **25** and **26** did not give the expected hexahydroquinazolones as it is well known that the most various N-acyl-anthranilic acid derivatives yield by this reaction quinazolines in very good yields.

The synthesis of hexahydroquinazolones was achieved in another way [41]. The discussion of this method and the synthesis of the 2-alkyl-, 2-aralkyl- and 2-arylderivatives of the compounds described in this paper, will be given in a subsequent publication [42].

Among the compounds mentioned, several *cis*-2-amino-1-cyclohexanecarboxamide derivatives show a narcosis potentiating effect. Most potent are the compounds **17i**, **17l**, **17q** (R = C_6H_4X; X = *p*-CH_3, *m*-F, *m*-CF_3). A dose of these (50 mg/kg, given orally) protracts, by a factor of about 5, the sleep induced in mice by a dose (40 mg/kg, *i.v.*) of venobarbital. Interestingly, this effect is much smaller, or altogether missing, with the corresponding *trans* isomers.

A number of these compounds have antipyretic and/or analgetic effects. This antipyretic effect is pronounced again with the *cis*-2-amino-1-cyclohexanecarboxamide derivatives; the corresponding *trans* isomers, *e.g.* **17r** and **19f**, R = $C_6H_4Br(p)$, are ineffective.

The N-acyl derivatives of alicyclic β-amino acids (**24**—**26**) and the *cis*- or *trans*-2-acylamino-1-cyclohexanecarboxamides (**22**, **23**, **27**, **28**) possess no appreciable antiphlogistic or antipyretic action.

The compounds described in this paper form the subject of a patent application [43]. Detailed pharmacological results will be published elsewhere [44].

Experimental

Cis-2-carbobenzoxyamino-1-cyclohexanecarboxylic acid (4b)

Cis-2-amino-1-cyclohexanecarboxylic acid (**2b**) (14.32 g; 0.10 mole) was dissolved, with stirring in a 2*N* solution of sodium hydroxide (0.10 mole). The solution was cooled to 0 °C in a salt-ice bath, then benzyl chloroformate (18.77 g; 0.11 mole) and of sodium hydroxide (4.00 g; 0.10 mole, in the form of a 2*N* solution) were added parallel, by drops, during 30 min.; care was taken that the reaction mixture should remain always slightly alkaline. Stirring was continued at 0 °C for 1 hr., and for further 4 hrs at room temperature. The excess benzyl chloroformate was then removed from the mixture by extraction with ether. The aqueous phase was cooled in ice and acidified to pH 2 with a 1 : 1 solution of hydrochloric acid. The precipitate, *cis*-2-carbobenzoxyamino-1-cyclohexanecarboxylic acid (**4b**) was filtered off and washed with cold water. Recrystallization from ethanol yielded a white crystalline substance (23.70 g; 85.5%), m.p. 127—129 °C.

$C_{15}H_{19}O_4N$ (277,32). Calcd. C 64.97; H 6.91; N 5.05. Found C 64.86; H 7.01; N 5.08%.

Trans-2-carbobenzoxyamino-1-cyclohexanecarboxylic acid (5b)

This compound was prepared, in the way described for the *cis* isomer **4b**, from *trans*-2-amino-1-cyclohexanecarboxylic acid (**3b**). Recrystallization from methanol gave white crystals, m.p. 145—147 °C; yield 93.04%.

$C_{15}H_{19}O_4N$ (277.32). Calcd. C 64.97; H 6.91; N 5.05. Found C 65.15; H 7.09; N 4.99%.

Cis- and *trans*-2-carbobenzoxyamino-1-cyclopentanecarboxylic acid (4a, 5a)

These acids were prepared, in the way described for compound **4b**, from *cis*- and *trans*-2-amino-1-cyclopentanecarboxylic acid (**2a** and **3a**, respectively). In the synthesis of *cis*-2-carbobenzoxyamino-1-cyclopentanecarboxylic acid (**4a**), the product of acidification with hydrochloric acid separated as a viscous oil; this was extracted with ethyl acetate and the solution dried over sodium sulfate. Evaporation of the ethyl acetate left a product which was used without further purification for the synthesis of derivatives.

Trans-2-carbobenzoxyamino-1-cyclopentanecarboxylic acid (**5a**) was recrystallized from ethanol, m.p. 149—151 °C, yield 87.35%.

$C_{14}H_{17}O_4N$ (263.30). Calcd. C 63.86; H 6.51; H 5.32. Found C 66.76; H 6.71; N 5.36%.

Trans-2-carbobenzoxyamino-1-cycloheptanecarboxylic acid (5c)

This was prepared, in the way described for compound **4b**, from *trans*-2-amino-1-cycloheptanecarboxylic acid (**3c**). Recrystallization from ethanol gave the acid **5c**, m.p. 132—133 °C; yield 78.23%.

$C_{16}H_{21}O_4N$ (219.34). Calcd. C 65.95; H 7.77; N 4.81. Found C 66.14; H 7.39; N 4.22%.

Cis-2-carbobenzoxyamino-1-cyclohexane-*p*-chlorocarboxanilide (**11n**)

Cis-2-carbobenzoxyamino-1-cyclohexanecarboxylic acid (**4b**) (41.6 g; 0.15 mole), dicyclohexylcarbodiimide (30.50 g; 0.15 mole) were placed in anhydrous tetrahydrofurane (420 ml), and the mixture was allowed to stand at room temperature for one day. The N,N'-dicyclohexylurea which separated was then removed by filtration. Evaporation of tetrahydrofurane left a yellowish white, sticky mass which crystallized on the addition of ether (80 ml) and standing. The crystals were collected on a glass filter. TLC (silica gel, benzene ethanol 9 : 1, detection with iodine vapour) showed two spots. Recrystallization from ethanol (500 ml) gave *cis*-2-carbobenzoxyamino-1-cyclohexane-*p*-chlorocarboxanilide as white crystals (31.35 g), m.p. 177—179 °C; yield 54.03%.

$C_{21}H_{23}O_3N_2Cl$ (386.88). Calcd. C 65.20; H 5.99; N 7.24. Found C 65.04; H 5.59; N 7.57%.

Evaporation of the mother liquor to about 100 ml gave, after cooling, N-(*cis*-2-carbobenzoxyamino-1-cyclohexylcarbonyl)-N,N'-dicyclohexylurea (**6**) (15.25 g; yield 21.82%) as white crystalline powder; m.p. 113—115 °C (from ethanol).

$C_{28}H_{41}O_4N_4$ (483.66). Calcd. C 69.63; H 8.54; N 8.69. Found C 69.22; H 8.65; N 8.65%.

N-substituted *cis*- and *trans*-2-carbobenzoxyamino-1-cyclohexanecarboxamides (**11a—11ii, 13a—13g**)

0.02 mole of *cis*- or *trans*-2-carbobenzoxyamino-1-cyclohexanecarboxylic acid (**4b** and **5b**, respectively) was dissolved in pure tetrahydrofurane (70 ml) and this solution was cooled to —10 °C in a salt-ice bath. With vigorous stirring, triethylamine (0.02 mole) and isobutyl chloroformate (0.02 mole) were added; after stirring for another 2—3 minutes, the amine (0.02 mole) dissolved in pure tetrahydrofurane (20 ml) and cooled to —10 °C was added dropwise into the reaction mixture. Stirring at salt—ice temperature was continued for another 5 hrs, then the mixture was allowed to stand overnight at room temperature. The tetrahydrofurane was evaporated and, in order to remove the unreacted amine component, the residue was shaken for 20 min. with an aqueous mixture of an organic solvent chosen for this purpose (petroleum ether, ether or benzene). The crystalline substance thus obtained was collected on a glass filter, then shaken for 5 min. in a chilled 10% solution of sodium hydroxide (0.02 mole). The product was filtered off washed with water until neutral, dried and recrystallized. The data of the N-substituted *cis*- and *trans*-2-carbobenzoxylamino-1-cyclohexanecarboxamides (**11a—11ii, 13a—13g**) thus prepared are collected in Tables I and II.

Synthesis of N-substituted *cis*- and *trans*-2-(carbobenzoxyamino)-1-cyclopentanecarboxamides (**10a, 10b, 12a, 12b**)

These cyclopentane derivatives were synthesized as described for the corresponding cyclohexanecarboxamides (**11a—ii, 13a—g**), from *cis*- and *trans*-2-carbobenzoxyamino-1-cyclopentanecarboxylic acid (**4a** and **5a**) respectively. The derivatives prepared are listed in Table III.

Synthesis of N-substituted *trans*-2-carbobenzoxyamino-1-cycloheptanecarboxanilides (**14a, 14b**)

These compounds were prepared as described for compounds **11a—ii** and **13a—g**, from *trans*-2-carbobenzoxyamino-1-cycloheptanecarboxylic acid (**5c**). The derivatives obtained are listed in Table III.

Cis-2-amino-1-cyclopentane-*p*-methylcarboxanilide hydrobromide (**16**)

This compound was synthesized from *cis*-2-carbobenzoxyamino-1-cyclopentane-*p*-methylcarboxanilide (**10a**) according to the method used for the synthesis of *trans*-2-amino-1-cyclopentane-*p*-methylcarboxanilide hydrobromide (**18**). Recrystallization from ethanol gave **16**, m.p. 236—238 °C, yield 72.0%.

$C_{13}H_{19}ON_2Br$ (299.22). Calcd. C 52.19; H 6.40. Found C 52.15; H 6.71%.

N-substituted *cis*- and *trans*-2-amino-1-cyclohexanecarboxamides (**17a—17ee, 19a—19h**)

Four to five equivalents of hydrogen bromide, 20% solution in glacial acetic acid, was added to the N-substituted *cis*- or *trans*-2-carbobenzoxyamino-1-cyclohexanecarboxamides (**11a—11ii, 13a—13g**). Upon admixture with dry ether, the N-substituted *cis*- or *trans*-2-

amino-1-cyclohexanecarboxamide hydrobromides separated, usually as oily liquids which crystallized on rubbing with a glass rod. The N-substituted *cis*- or *trans*-2-amino-1-cyclohexanecarboxamides were liberated from the crystalline hydrobromides by treatment with a 10% solution of sodium hydrogen carbonate.

When the hydrobromides could not be obtained in crystalline form, the bases were liberated by means of Varion-AD ion-exchange resin. Characteristic data of the derivatives prepared are shown in Tables IV and V.

Trans-2-amino-1-cyclopentane-*p*-methylcarboxanilide hydrobromide (18)

Four to five equivalents of hydrogen bromide, as 20% solution in glacial acetic acid, was added to *trans*-2-carbobenzoxyamino-1-cyclopentane-*p*-methylcarboxanilide (**12a**) and the mixture was allowed to stand 50 min. at room temperature. On the addition of dry ether *trans*-2-amino-1-cyclopentane-*p*-methylcarboxanilide hydrobromide (**18**, R = $C_6H_4CH_3(p)$ separated in crystalline form. Recrystallization from ethanol—ether gave white crystals, m.p. 195—198 °C, yield 62.15%.

$C_{13}H_{19}N_2Br$ (299.22). Calcd. C 52.19; H 6.40; N 9.36. Found C 52.26; H 6.18; N 9.53%.

N-substituted *trans*-2-amino-1-cycloheptanecarboxanilides (20a, 20b)

These compounds were prepared in the same way as the N-substituted *cis*- or *trans*-2-amino-1-cyclohexanecarboxamides (**11a**—**11ii**, **13a**—**13g**), from *trans*-2-carbobenzoxyamino-1-cycloheptanecarboxanilides (**14a**, **14b**).

Trans-2-amino-1-cycloheptane-*p*-methylcarboxanilide hydrobromide (20a)

Recrystallized from ethanol, **20a** had m.p. 159—160 °C; yield 56.29%.

$C_{15}H_{23}ON_2Br$ (327.27). Calcd. C 55.05; H 7.08; N 8.55. Found C 54.76; H 6.96; N 8.40%.

Trans-2-amino-1-cycloheptane-*p*-chlorocarboxanilide hydrobromide (20b)

Recrystallized from ethanol, **20a** had m.p. 162—163 °C; yield 47.32%.

$C_{14}H_{20}ON_2ClBr$ (347.67). Calcd. C 48.34; H 5.75; N 8.05. Found C 48.48; H 5.56; N 8.37%.

Cis-2-formylamino-1-cyclohexanecarboxylic acid (21)

A mixture of *cis*-2-amino-1-cyclohexanecarboxylic acid (**2a**) (4.30 g; 0.03 mole), 98—100% formic acid (5.52 g; 0.12 mole) and acetic acid anhydride (12.35 g; 0.12 mole) was warmed at 35—40 °C for 1.5 hr. The suspension became homogeneous and a few minutes later the separation of *cis*-2-formylamino-1-cyclohexanecarboxylic acid (**21**) began. The reaction mixture was kept at +4 °C for one day, whereupon 3.80 g of white crystals separated. Recrystallization from methanol gave 3.30 g (64.2%) of the product, m.p. 206—208 °C (lit. [38] m.p. 201—202 °C).

$C_8H_{13}O_3N$ (171.20). Calcd. C 56.13; H 7.65; N 8.18. Found C 56.33; H 7.76; N 7.72%.

Cis-2-acetylamino-1-cyclopentanecarboxylic acid (24)

Following the method used for the synthesis of *cis*-2-acetylamino-1-cyclohexanecarboxylic acid (**25**), from *cis*-2-amino-1-cyclopentanecarboxylic acid (**2a**) (12.92 g; 0.10 mole) we obtained 11.35 g (66.30%) of compound crystallizable from ether, m.p. 79—81 °C.

$C_8H_{13}O_3N$ (171.20). Calcd. C 56.13; H 7.65; N 8.18. Found C 55.95; H 7.64; N 8.27%.

Cis-2-acetylamino-1-cyclohexanecarboxylic acid (25)

In a three-necked flask equipped with a stirrer and condenser, *cis*-2-aminocyclohexanecarboxylic acid (**2b**) (14.32 g; 0.10 mole) was dissolved in water (60 ml) and, with vigorous stirring, in one portion, acetic acid anhydride (25.52 g; 0.25 mole) was added. The mixture got very warm. Stirring was continued for 60 min. then the mixture was allowed to stand overnight at +4 °C. The crystals which separated were collected by filtration, and recrystallized from ethanol, to obtain *cis*-2-acetylamino-1-cyclohexanecarboxylic acid (**25**) (10.92 g; 58.96%) as a white crystalline powder, m.p. 149—151 °C. Evaporation of the acid mother liquor and recrystallization of the residue gave a further crop (3.52 g; 19.01%) of compound **25**.

$C_9H_{15}O_3N$ (185.22). Calcd. C 58.37; H 8.16; N 7.56. Found C 58.25; H 8.34; N 7.37%.

Table VI

Melting points and analysis data of N-substituted cis- and trans-2-(formylamino)-1-cyclohexanecarboxamides **(22a—22f, 23)**

Compound	R	Configuration	Formula Molecular weight	M.p., °C Solvent	Analysis,% Calculated Found			Yield, %
					C	H	N	
22a	$-CH_2(CH_2)_2CH_3$	*cis*	$C_{12}H_{22}O_2N_2$ 226.32	127—129 ethanol	63.69 63.46	9.88 10.03	12.38 12.28	71.30
22b*	$-C_6H_4Cl(p)$	*cis*	$C_{14}H_{17}O_2N_2Cl$ 280.76	230—232 ethanol	59.89 60.10	6.10 6.38	9.98 9.81	52.91
22c	$-C_6H_4Br(p)$	*cis*	$C_{14}H_{17}O_2N_2Br$ 325.21	243—245 methanol	51.81 51.69	5.27 5.45	8.62 9.05	78.27
22d	$-C_6H_4OC_2H_5(p)$	*cis*	$C_{16}H_{22}O_3N_2$ 290.36	183—185 methanol	66.18 65.95	7.64 7.53	9.65 9.89	75.17
22e	$-CH_2CH_2C_6H_3(OCH_3)_2(m,\ p)$	*cis*	$C_{18}H_{26}O_4N_2$ 334.42	167—169 ethanol	64.65 64.47	7.84 7.97	8.38 8.34	68.13
22f	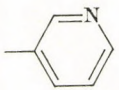	*cis*	$C_{13}H_{17}O_2N_3$ 247.30	217—219 ethanol	63.14 62.87	6.93 6.93	16.99 16.91	65.27
23	$-C_6H_4Cl(p)$	*trans*	$C_{14}H_{17}O_2N_2Cl$ 280.76	262—264 ethanol	59.89 60.22	6.10 6.37	9.98 9.95	60.27

* Compounds **22b** and **23** were prepared by refluxing *cis*- and *trans*-2-amino-1-cyclohexane-*p*-chlorocarboxanilide with triethylorthoformate [37].

Table VII

Melting points and analysis data of N-substituted cis-2-acetylamino-1-cyclohexanecarboxamides **(27a—27f)**

Compound	R	Formula Molecular weight	M.p., °C Solvent	Analysis,% Calculated Found			Yield, %
				C	H	N	
27a	$-CH_2(CH_2)_2CH_3$	$C_{13}H_{24}O_2N_2$ 240.35	133—135 chloroform–ether	64.95 64.64	10.06 10.02	11.65 11.37	55.73
27b	$-C_6H_5$	$C_{15}H_{20}O_2N_2$ 260.34	211—213 ethanol	69.22 69.27	7.75 7.82	10.76 11.50	70.30
27c	$-C_6H_4Cl(p)$	$C_{15}H_{19}O_2N_2Cl$ 294.78	234—236 ethanol	61.12 61.60	6.50 6.30	9.50 9.86	44.70
27d	$-C_6H_4Br(p)$	$C_{15}H_{19}O_2N_2Br$ 339.24	237—238 ethanol	53.11 52.89	5.65 5.47	8.26 8.50	68.30
27e	$-CH_2C_6H_5$	$C_{16}H_{22}O_2N_2$ 274.36	191—192 ethanol	70.04 69.29	8.08 8.19	10.21 10.21	71.30
27f	$-CH_2CH_2C_6H_3(OCH_3)_2(m,p)$	$C_{19}H_{28}O_4N_2$ 348.45	166—168 ethanol	65.48 64.87	8.10 7.67	8.04 7.94	68.20

Table VIII

Melting points and analysis data of N-substituted trans-2-acetylamino-1-cyclohexanecarboxamides **(28a—28e)**

Compound	R	Formula Molecular weight	M.p., °C Solvent	Analysis, % Calculated Found			Yield, %
				C	H	N	
28a	$-CH_2(CH_2)_2CH_3$	$C_{13}H_{24}O_2N_2$ 240.35	218—222 ethanol	64.95 64.68	10.06 10.20	11.65 11.19	59.30
28b*	$-C_6H_5$	$C_{15}H_{20}O_2N_2$ 260.34	266—268 ethanol	69.22 69.60	7.75 8.03	11.65 10.70	5.15
28c	$-C_6H_4Cl(p)$	$C_{15}H_{19}O_2N_2Cl$ 294.78	283—285 ethanol	61.12 60.93	6.50 6.60	9.50 9.25	85.51
28d	$-C_6H_4Br(p)$	$C_{15}H_{19}O_2N_2Br$ 339.24	289—290 methanol	53.11 52.93	5.56 5.75	8.26 8.32	74.20
28e	$-CH_2CH_2C_6H_3(OCH_3)_2(m, p)$	$C_{19}H_{28}O_4N_2$ 348.45	198—200 ethanol	65.48 64.98	8.10 8.33	8.04 8.85	69.15

*This is a by-product recovered by fractional crystallization from the synthesis of *cis*-2-acetylamino-1-cyclohexanecarboxanilide **(27b)**, made on the analogy of Grimmel's quinazoline synthesis [40], using *cis*-2-acetylamino-1-cyclohexanecarboxylic acid **(25)** and aniline.

Trans-2-acetylamino-1-cyclohexanecarboxylic acid (26)

According to the method used for the synthesis of the *cis* isomer (**25**), *trans*-2-amino-1-cyclohexanecarboxylic acid (**3b**) (14.36 g; 0.10 mole) gave compound **26** as white, glistening crystals (14.36 g; 77.54%); recrystallized from ethanol, m.p. 206—208 °C.

$C_9H_{15}O_3N$ (185.22). Calcd. C 58.37; H 8.16; N 7.56. Found C 58.57; H 8.41; N 7.58%.

Synthesis of N-substituted *cis*-2-formylamino-1-cyclohexanecarboxamides (22a, 22c—22f)

The appropriate N-substituted *cis*- or *trans*-2-amino-1-cyclohexanecarboxamides (**17b**, **17r**, **17u**, **17aa** or **17bb**) (0.02 mole) was dissolved in 98—100% formic acid (0.12 mole) and acetic anhydride (0.12 mole) was added to the solution. The mixture was warmed at 35—40 °C for 1.5—2 hrs. The white, crystalline product was filtered off and recrystallized from a suitable solvent (table VI) until constant m.p. was attained. Table VI gives a survey of the compounds obtained.

Synthesis of N-substituted *cis*- and *trans*-2-acetylamino-1-cyclohexanecarboxamides (27a—27f, 28a—28e)

1.0 mole of *cis*- or *trans*-2-acetylamino-1-cyclohexanecarboxylic acid (**25** or **26**) was suspended in dry toluene, and to this suspension 1.0 mole of the amine, dissolved in anhydrous toluene, was added in one portion. The mixture was shaken vigorously, and 0.33 mole of phosphorus trichloride, dissolved in dry toluene, was added to it. The mixture was then refluxed for 2 hrs. The solution was decanted and allowed to stand at +4 °C for one day. The crystals which separated were collected on a glass filter and recrystallized, each from the solvent indicated in Tables VII and VIII, until constant m.p. was attained.

*

The authors thank the Chemical and Pharmaceutical works CHINOIN, Budapest, for financial assistance. Thanks are due Prof. Z. Mészáros, Budapest, and to Prof. K. Kovács, Szeged for their interest in this work, to Prof. P. Sohár (Pharmaceutical Research Institute, Budapest) for the IR and NMR spectra, to Drs. L. Leszkovszky and L. Tardos, Budapest, for the pharmacological tests, to Mrs. K. Lakos, Mrs. G. Bartók, and Mrs. É. Gács for the great number of microanalyses, and to Miss A. Polyák for technical assistance.

REFERENCES

[1] Bernáth, G., Láng, K. L., Göndös, Gy., Márai, P., Kovács, K.: Tetrahedron Letters **1968,** 4441
[2] Bernáth, G., Láng, K. L., Göndös, Gy., Márai, P., Kovács, K.: Acta Chim. (Budapest) **74,** 479 (1972)
[3] Bernáth, G., Kovács, K., Láng, K. L.: Tetrahedron Letters **1968,** 2713
[4] Bernáth, G., Kovács, K., Láng, K. L.: Acta Chim. (Budapest) **65,** 347 (1970)
[5] Bernáth, G., Láng, K. L., Kovács, K.: Acta Phys. et Chem. Szeged **18,** 227 (1972)
[6] Bernáth, G., Göndös, Gy., Kovács, K., Sohár, P.: Tetrahedron **29,** 981 (1973)
[7] Bernáth, G., Göndös, Gy., Láng, K. L., Márai, P., Kovács, K.: Acta Phys. et Chem. Szeged **17,** 161 (1971)
[8] Vargha, L., Kasztreiner, E., Borsy, J., Dumbovich, B.: Hung. Pat. 151 581 (July 1, 1965)
[9] Toldy, L., Borsy, J., Fekete, M., Dumbovich, B., Hung. Pat. 150 956 (July 1, 1964)
[10] Lee, J., Ziering, A., Berger, L., Heineman, S. D.: Jubilee Vol. Emil Barell **1964,** 246; C. A. **41,** 6246 (1947)
[11] Bernáth, G., Kovács, K., Pálosi, E., Görög, P., Szporny, L.: Hung. Pat. 156 542 (May 1, 1970)
[12] Bernáth, G., Kovács, K., Pálosi, É., Görög, P., Szporny, L.: Austrian Pat. 286 959 (January 11, 1971)
[13] Bernáth, G., Kovács, K., Pálosi, É., Görög, P., Szporny, L.: Swiss Pat. 505 786 (May 28, 1971)
[14] Bernáth, G., Csókási, E., Hevér, I., Gera, L., Kovács, K.: Acta Chim. (Budapest), **70,** 271 (1971)

[15] SZMUSZKOVICZ, J.: U. S. Pat. 3 510 492 (May 5, 1970); C. A. **73,** 35233a (1970)
[16] WINDER, C. V., SERRANO, S., JONES, E. M., PCHEE, M. L.: Arthr. and Rheum. **6,** 36 (1963)
[17] BOWMAN, R. E., BRUNT, K. D., GOLDFREY, K. E., KRUSZYNSKA, L., REYNOLDS, A. A., THRIFT, R. I., WAITE, D., WILLIAMSON, W. R. N.: J. Chem. Soc. Perkin I **1973,** 1
[18] BERNÁTH, G., LÁNG, K. L., KOVÁCS, K., RADICS, L.: Acta Chim. (Budapest) **73,** 81 (1972)
[19] SOHÁR, P., BERNÁTH, G.: Organic Magnetic Resonance **5,** 159 (973)
[20] BERNÁTH, G., GÖNDÖS, GY., GERA, L., TÖRÖK, M., KOVÁCS, K., SOHÁR, P.: Acta Phys. et Chem. Szeged **19,** 147 (1973)
[21] ARMAREGO, W. L. F.: Quinazolines. In the series entitled "Fused Pyrimidines" (ed. Weissberger, A.) Part I, Interscience Publ., New York, 1967
[22] KACKER, I. K., ZAHEER, S. H.: Indian J. Chem. Soc. **28,** 344 (1951)
[23] GUNN, B. C., STEVENS, M. F. G.: J. Chem. Soc. Perkin I **1973,** 1682
[24] GERA, L.: Ph. D. Thesis (Attila József University, Szeged, 1974)
[25] BERNÁTH, G., ECSERY, Z., GERA, L., GÖNDÖS, GY.: Lecture presented at the session of the Organic and Pharmaceutical Chemistry Section of the Hungarian Chemical Society, May 31, 1974
[26] BERNÁTH, G., GÖNDÖS, GY., GERA, L., ECSERY, Z., TARDOS, L : Hungarian Patent Application, 1975
[27] BERGMANN, M , ZERVAS, L.: Ber. **65,** 1192 (1932)
[28] KLAUSNER, Y. S., BODANSZKY, M.: Synthesis **1972,** 453
[29] FENWICK, G. R.: Chem. and Ind. **1973,** 636
[30] WIELAND, T., KERN, W., SEHRING, R.: Ann. **569,** 117 (1950)
[31] EMERY, A. R., GOLD, V.: J. Chem. Soc. **1950,** 1443
[32] WIELAND, T., HEINKE, B., VOGELER, K., MORIMOTO, H.: Ann. **655,** 189 (1962)
[33] BEN-ISHAI, D., BERGER, A.: J. Biol. Chem. **17,** 1564 (1952)
[34] FLETCHER, G. A., YOUNG, G. T.: J. Chem. Soc. Perkin I **1972,** 1867
[35] BERNÁTH, G., KOVÁCS, K., LÁNG, K. L.: Acta Chim. (Budapest) **64,** 183 (1970)
[36] ZIMMERMAN, H. E., ENGLISH, J.: J. Am. Chem. Soc. **75,** 2367 (1953)
[37] ARMAREGO, W. L. F., KOBAYASHI, T.: J. Chem. Soc. (C) **1971,** 238
[38] LEBEL, N. A., POST, M. E., WHANG, J. J.: J. Am. Chem. Soc. **86,** 3759 (1964)
[39] VOGEL, A. J.: Practical Organic Chemistry, 3rd ed., p. 909. Longmans, London, 1961
[40] GRIMMEL, H. W., GUENTHER, A., MORGAN, J. F.: J. Am. Chem. Soc. **68,** 542 (1946)
[41] G. BERNÁTH *et al:* Results to be published later
[42] G. BERNÁTH *et al.:* Results to be published later
[43] BERNÁTH, G., GERA, L., GÖNDÖS, GY., KOVÁCS, K., ECSERY, Z., TARDOS, L.: Hungarian Patent Application, 1975
[44] TARDOS, L., LESZKOVSZKY, L.: Results to be published later
[45] ARMAREGO, W. L. F., KOBAYASHI, T.: J. Chem. Soc. (C) **1969** 1635

Gábor BERNÁTH
Lajos GERA
György GÖNDÖS
István PÁNOVICS
H-6720 Szeged, Dóm tér 8.

Zoltán ECSERY; H-1045 Budapest, Tó u. 1—5.

Acta Chimica Academiae Scientiarum Hungaricae, Tomus 89 (1), pp. 85—89 (1976)

ALKALOIDS CONTAINING THE INDOLO[2,3-c]-QUINAZOLINO[3,2-a]PYRIDINE SKELETON, IV*

THE MASS SPECTRA OF RUTECARPINE, EVODIAMINE AND 3,14-DIHYDRORUTECARPINE

J. TAMÁS*, Gy. BUJTÁS*, K. HORVÁTH-DÓRA** and O. CLAUDER**

*(*Central Research Institute for Chemistry of the Hungarian Academy of Sciences, Budapest, and **Institute of Organic Chemistry, Faculty of Pharmaceutical Sciences, Semmelweis Medical University, Budapest)*

Received April 17, 1975

The electron bombardment mass spectra of rutecarpine, evodiamine and 3,14-dihydrorutecarpine are reported. As shown by the investigations, the molecular ion of the latter compound undergoes a skeleton rearrangement prior to fragmentation.

The mass spectrometric behaviour of rutecarpine and evodiamine, the two longest known alkaloids with indolopyridoquinazoline skeleton, has not been investigated so far. However, the characteristic mass spectral data of some new members of this group have been published; such compounds are paraensine (**I**) [2], euxylophorine-c (**IIa**) and its dihydro-derivative (**IIb**) [4], as well as hydroxyrutecarpine (**III**) [5], isolated by DANIELI *et al.* [1—5] from Euxylophora paraänsis Hub., a plant of the Rutaceae family.

In our previous papers [6, 7] we reported the synthesis of 3,14-dihydrorutecarpine (**VI**) from which rutecarpine (**IV**) and evodiamine (**V**) can readily be obtained.

In the present paper we report the mass spectrometric behaviour of these three compounds.

The 70 eV mass spectra of compounds **IV**—**VI** are shown in Fig. 1.

The molecular skeleton of *rutecarpine* (**IV**), similarly to that of compound **IIa** [4] and **III** [5], is very stable against electron bombardment. The only significant fragmentation process is the loss of a hydrogen atom from the molecular ion. The high frequency of this process can be explained by the splitting of one of the protons in β-position to the N_b nitrogen and by the development of a stable immonium ion structure, extending the conjugation. Also a competing loss of CO can be observed, which is accompanied by ring contraction (formation of the m/e 259 ion). The ions of m/e 143 and 129, having similarly low intensities, can be attributed to the two types of fragmentation of ring C shown in Fig. 1a.

* Part III: Acta Chim. (Budapest), **84**, 93 (1975)

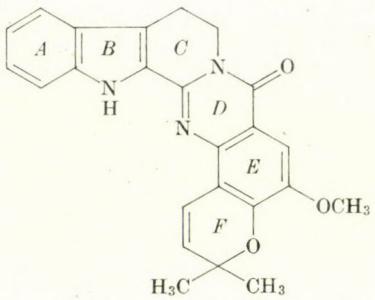

I

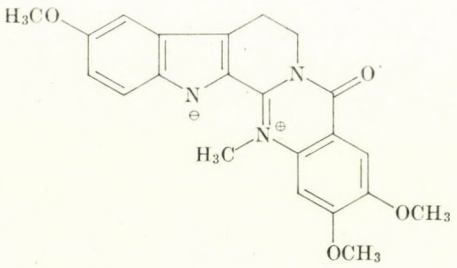

IIa

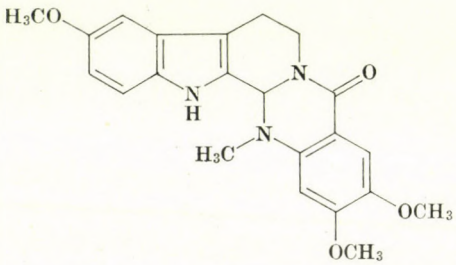

IIb

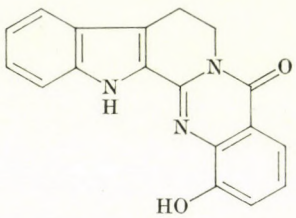

III

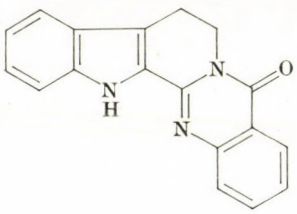

IV

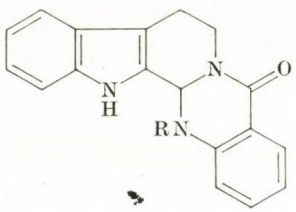

R = CH_3 V

R = H VI

In the case of *evodiamine* (**V**) the molecular ion is less stable, owing to the disappearance of the continuous conjugation system; nevertheless, it gives the most intense peak of the spectrum. Immonium ion formation consisting of the loss of one hydrogen atom is significant, yet, as it is usual, in the case of compounds with tetrahydro-β-carboline skeleton [8], mainly the splitting off of the 3-H atom must be expected. The principal fragmentation process of compound **V** is the α-splitting of the skeleton (see Fig. 1b) which is partly a retro-Diels-Alder reaction leading to ion of m/e 170, and partly involves H migration, affording the ion 169 and its complementary ion of m/e 134. Also the formation of ions 143 attributable to the cleavage of ring C can be observed. The ion types

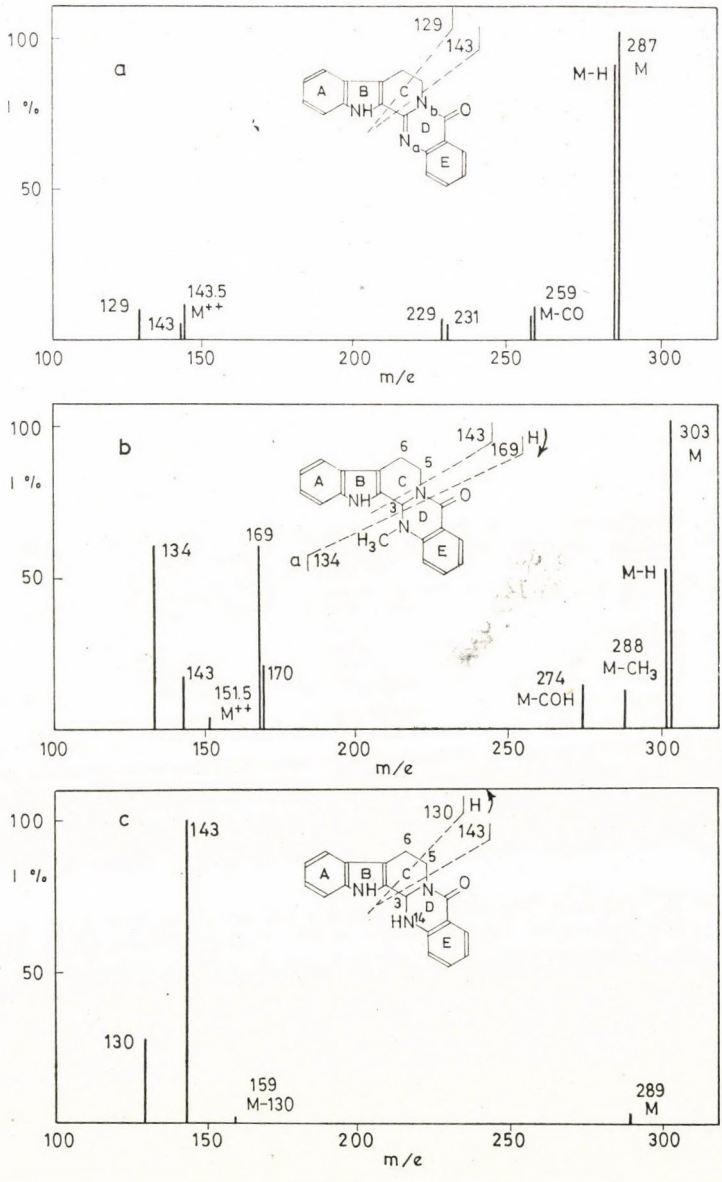

Fig. 1. 70 eV mass spectra of compounds **IV, V, VI**

corresponding to these processes also appear in the spectrum of compound **IIb** [4].

In contrast to the compounds mentioned above, *3,14 dihydrorutecarpine* **(VI)** exhibits a surprising behaviour on electron bombardment. The stability of the molecular ion is very low, and the main fragmentation route is the

splitting of ring C (formation of ions 130 and 143). The *a*-splitting which has been found to be the main splitting process for compound **V** having an identical skeleton, does not occur at all in compound **VI**. On the basis of this unexpected behaviour, we presume that the molecular ion of **VI** undergoes the following molecular rearrangement:

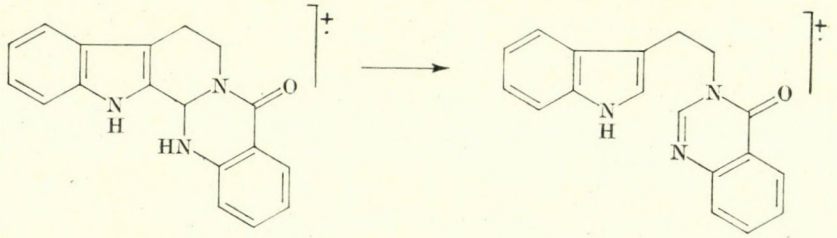

A B

This presumption is supported by the predominance of the formation of the ions of *m/e* 143 and 130, which is readily explained if structure B is present; these ions can also be observed during the fragmentation of N-substituted triptamines [9]. The ion 143 can be formed from structure B by means of H migration, through a four- or six-membered cyclic transition state, and the fragments produced correspond to stable molecules:

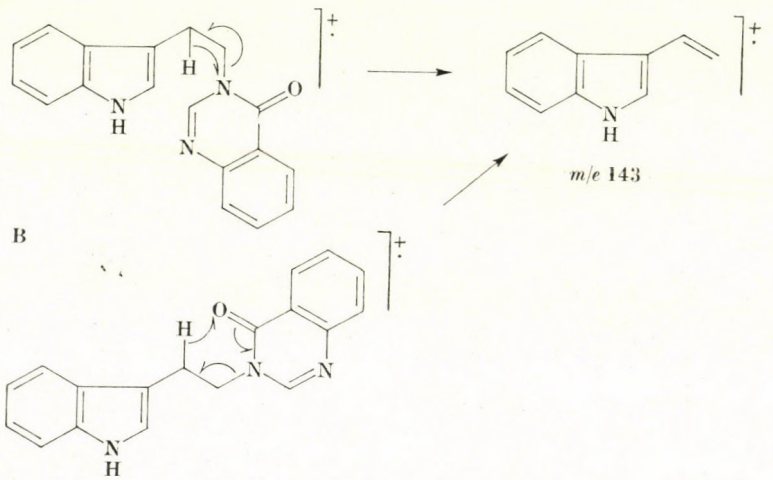

The ion of *m/e* 130 can be derived by the homolytic splitting (*β*-splitting) of the C_5–C_6 bond. The A → B conversion of the molecular ion of **VI** and the suggested mechanism of their further decomposition route are also supported by investigations with compound labelled by deuterium: on replacing the active protons of compound **VI** by deuterium, the molecular weight is increased by two units, and in the labelled spectrum the deuterium content in the ions of *m/e* 143 and 130 is completely identical with that in the molecular ion.

Experimental

The mass spectra were obtained with an MS-902 spectrometer. The exact mass of the main ion peaks was determined at high resolution with an accuracy of ± 2 ppm.

Samples were introduced by direct insertion. The temperature of the ion chamber was 150 °C, the ionizing electron energy being 70 eV.

The preparation, physical constants and spectroscopic (UV, IR) data of compounds rutecarpine (**IV**), evodiamine (**V**) and 3,14-dihydrorutecarpine (**VI**) are described in a preceding paper [7].

Compound **VI** labelled with deuterium was prepared by dissolving it in D_2O + DCl.

REFERENCES

[1] Canonica, L., Danieli, B., Manitto, P., Russo, G., Ferrari, G.: Tetrahedron Letters **47**, 4865 (1968)
[2] Danieli, B., Manitto, P., Ronchetti, F., Russo, G., Ferrari, G.: Experientia **28**, 249 (1972)
[3] Danieli, B., Manitto, P., Ronchetti, F., Russo, G., Ferrari, G.: Phytochem. **11**, 1833 (1972)
[4] Danieli, B., Palmisano, G., Russo, G., Ferrari, G.: Phytochem. **12**, 2521 (1973)
[5] Danieli, B., Palmisano, G., Rainoldi, G., Russo, G.: Phytochem. **13**, 1603 (1974)
[6] Clauder, O., Horváth-Dóra, K.: Acta Chim. (Budapest) **72**, 221 (1972)
[7] Horváth-Dóra, K., Clauder, O.: Acta Chim. (Budapest) **84**, 93 (1975)
[8] Budzikiewicz, H., Djerassi, C., Williams, D. H.: Structure Elucidations of Natural Products by Mass Spectrometry. Vol. 1, p. 77, Holden-Day, Inc., San Francisco, 1964.
[9] Tamás, J.: Unpublished data

József Tamás
György Bujtás } H-1088, Budapest, Puskin u. 11—13.

Klára Horváth-Dóra
Ottó Clauder } H-1092, Budapest, Hőgyes E. u. 7.

Acta Chimica Academiae Scientiarum Hungaricae, Tomus 89 (1), pp. 91—100 (1976)

THE TAUTOMERISM AND ISOMERISM OF ENAMINES RELATED TO ACRYLIC ACID

J. FRANK, P. DVORTSÁK, G. HORVÁTH, Z. MÉSZÁROS and G. TÓTH*

*(Chemical and Pharmaceutical Works, Chinoin, Budapest, and *Ruhr University, Bochum, Germany)*

Received June 26, 1975

The tautomerism of acrylic esters and acrylonitriles was studied by PMR spectroscopy. The existence of the isomers *Z* and *E* was established and their relative ratio determined. By measuring the coalescence temperature, the activation free enthalpy of the isomerization was determined.

In the course of the synthesis of therapeutically useful 4-hydroxyquinoline derivatives, the final products were obtained by making use of some intermediates related to acrylic acid.

In his early work CLAISEN [1] described the condensation reaction of aniline and ethyl ethoxymethylenemalonate (abbreviated in the literature as EMME) to yield ethyl α-ethoxycarbonyl-β-anilinoacrylate. Thereafter this reaction has found the most widespread application for the preparation of intermediates of various 4-hydroxyquinolines [2, 3, 4, 5].

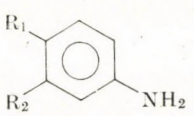

1

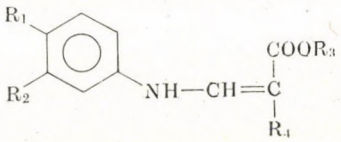

2

The condensation reaction of aromatic amines (1) with EMME, *i.e.* the synthesis of the compounds **2a—g** was effected by boiling the components in absolute ethanol, or gasoline. By allowing the anilines **1h—k** to react with ethyl α-cyano-β-ethoxyacrylate (abbreviated in the literature as EMCE) in the above solvents, compounds **2h—k** were obtained in nearly quantitative yields. Compound **2l** was prepared by the reaction of aniline with ethyl formylsuccinate [6]. The compounds synthesized are summarized in Table I.

* Present adress: Institute of Organic Chemistry, Semmelweis Medical University, Pharmaceutical Faculty, Budapest

Table I

Compounds of type 2

R_1	R_2		R_3	R_4	Ref.
a	H	H	C_2H_5	$COOC_2H_5$	[3]
b	OH	C_2H_5O	C_2H_5	$COOC_2H_5$	
c	CH_3COO	C_2H_5O	C_2H_5	$COOC_2H_5$	
d	$C_{10}H_{21}O$	C_2H_5O	C_2H_5	$COOC_2H_5$	[10]
e	$O-CH_2-O$		C_2H_5	$COOC_2H_5$	[7]
f	$O-CH_2-O$		C_4H_9	$COOC_4H_9$	
g	$O-CH_2-O$		$C_6H_5CH_2$	$COOCH_2-C_6H_5$	
h	H	H	C_2H_5	CN	[8]
i	OH	C_2H_5O	C_2H_5	CN	
j	$C_{10}H_{21}O$	C_2H_5O	C_2H_5	CN	[10]
k	$O-CH_2-O$		C_2H_5	CN	[9]
l	H	H	C_2H_5	$CH_2COOC_2H_5$	[6]

Results and discussion

The compounds of type **2** can exist in the enamine or ketimine tautomeric form. According to the literature, in secondary amines which are conjugated with a keto-, or ester- or nitrile function, the tautomeric equilibrium is predominantly shifted towards the enamine form [11, 12]. In agreement with this, also in compounds **2a**—**l** the enamine tautomeric form is prevailing, as shown by the IR and NMR spectra, resembling each other to a large extent. As a model, compound **2e** was studied in detail. In its NMR spectrum the N*H* signal appears as a doublet ($\delta = 11.1$, $J = 13$ Hz). The signal of the vinyl proton can be found at $\delta = 8.46$, similarly split to a doublet. Upon the addition of D_2O the former band disappears, while the olefinic proton becomes a singlet, showing that the proton exchanged has been in the N*H* group, located in *vicinal* position to the olefinic =CH. The NH band, appearing at 3260 cm^{-1} in the IR spectrum similarly proves the predominant character of the amine tautomeric form.

During the investigation of conjugated enamines it has been established that as a consequence of extended conjugation, these compounds can be considered, in good approximation, as planar molecules [13]. As a result, the UV absorption maximum above 300 nm in the spectrum of these derivatives appears with a very high intensity ($\varepsilon > 10^4$) [13] (see Experimental).

By temperature-dependent NMR studies it has been shown that rotation is hindered not only around the C=C double bond, but also about the N—C

bond [13—18]. Furthermore, DABROWSKI *et al.* gave evidence for the hindered character of the rotation about the =C—CO bond in enamino-carbonyl derivatives, and also detected the presence of s-*cis* and s-*trans* isomers [13]. The latter rotation requires the lowest activation energy, while hindrance of the rotation around the =C—NH bond is more definite, and that about the —C=C bond is strongest. SHVO and SHANAN-ATIDI [13] as well as DAHLQUIST [20] found the rotation barrier (ΔG^*) of the C=C bond in 1-dimethylamino-1-methyl-2-cyanocarbomethoxyethylene to be 14.8 kcal/mole, while for the C—N bond they gave the corresponding value as 10.8 and 12.9 kcal/mole, respectively. On the basis of what has been said above, the appearance of the following conformers can be expected (not considering the carbonyl s-*cis* and s-*trans* isomers):

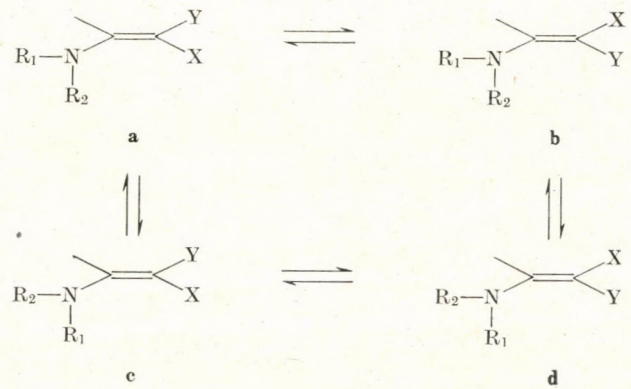

The conformers (*a*—*d*) are diastereomers; they differ energetically, and consequently their population is also different. If X=Y (*e.g.* in **2a**—**c**), the conformers (*a*—*b*) and (*c*—*d*), respectively, are "degenerated isomers" (topomers), as X and Y are, from the point of view of the rotation, nonequivalent. A rotation about the C=C bond means here the exchange of the diastereotopic groups [21].

The main purpose of the present work was to study the isomerization of the type $Z \rightleftharpoons E$, arising from rotation about the C=C bond.

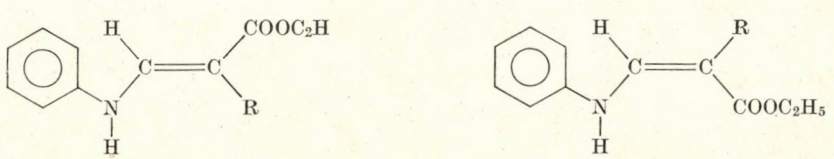

The high value of the coupling constant ($J_{NH,CH}$ = 13 Hz) suggests that, as a result of steric factors, the equilibrium of the conformers produced in the

Table II

Compound	Solvent	*E*		*Z*		Ratio *E*/*Z**
		CH	NH	CH	NH	
2h	$CDCl_3$	8.46(d)	8.7(d)	7.96(d)	10.7(d)	40 : 60
	$CDCl_3D_2O$	8.46(s)	—	7.96(s)	—	40 : 60
	$C_6D_5—NO_2$	8.32(d)	8.95(d)	7.98(d)	10.61(d)	40 : 60
2k	$CDCl_3$	8.40(d)	8.6(d)	7.71(d)	10.8(d)	50 : 50
	$CDCl_3D_2O$	8.40(s)	—	7.71(s)	—	50 : 50
	$C_6D_5—NO_2$	8.28(d)	8.91(d)	7.90(d)	10.74(d)	50 : 50
		$CH_2—COOC_2H_5$		$CH_2—COOC_2H_5$		
2i	$CDCl_3$	3.46(s)		—		—
	$CDCl_3D_2O$	3.46(s)		3.22(s)		30 : 70**
	$C_6D_5—NO_2$	3.61(s)		3.32(s)		95 : 5

* Immediately after dissolution
** After standing for one day
The measurements were carried out at room temperature; the ratio *E*/*Z* does not in each case equal the composition in thermodynamical equilibrium (the latter is shown in Table III).

rotation about the N—C= bond is predominantly shifted towards the conformer containing the phenyl group in *trans* position related to C=C.

The relative ratio of the isomers $Z \rightleftharpoons E$ was determined by means of their NMR spectra. The data are summarized in Table II, in which only the most characteristic proton signals are shown for the isomerization model compounds studied.

In the isomer *Z*, in each case an intramolecular hydrogen bond is formed. Accordingly, the process of exchange of the N*H* against deuterium requires several days at room temperature, while the N*H* in isomer *E* is exchanged immediately.

Since the N*H* signal chelated with the carbonyl group appears at a higher δ value than that of the free, N*H* among others this fact also offers a way to differentiate between the isomers *Z* and *E* by NMR spectroscopy.

The isomerism can be best observed on the $CH_2—COOC_2H_5$ signal of compound **2l**; the *E*/*Z* ratio can also be determined here. The assignment based upon the N*H* proton could easily be done, as isomer *E* of compound **2l** could be isolated and studied in pure form. In deuterochloroform solution the C*H*$_2$ signal of this isomer appears at $\delta = 3.46$, while the N*H* signal at 7.7 ppm. Upon standing a couple of hours at room temperature, the substance in solution changes into a mixture of the isomers, and the singlet of the $CH_2—COOC_2H_5$ group

characteristic of isomer *Z* appears at $\delta = 3.22$, and the N*H* band at 10.0 ppm. As the assignment of the signals is in this manner unambiguous, only the data characteristic of $CH_2-COOC_2H_5$ are shown in the Table.

The ratio of the geometrical isomers of compound **2l** measured immediately after dissolution undergoes a change with time. Upon standing at room temperature for three hours in chloroform solution the amount of the originally pure isomer *E* is decreased to 60%, and after 3 days the equilibrium is already shifted towards isomer *Z*, the isomer ratio being 75 : 25.

The isomerization $Z \rightarrow E$ of the enamines was studied on the compounds **2a, e, h, k, l** as well as on the N-methyl derivative of **2h** [3]. The IR spectra of the studied compounds, recorded in KBr pellets, support the results on the existence and transformations of the isomers. In the spectra several $\nu C=O$ bands could be observed, from among which the low frequency value of that appearing at 1685 cm^{-1} arises from the hydrogen bond in isomer *Z*, while the $\nu C=O$ (ester) band of the isomer *E* is, in types **2a—g**, at 1720 cm^{-1}. In compounds **2h—k** it appears at about 1710 cm^{-1}, and in **2l** at 1712; the band appearing at 1745 cm^{-1} in the case of the latter compound can be attributed to the $\nu C=O$ vibration of the non-conjugated ester group. (For the detailed, exact data see Experimental.)

When the temperature was raised gradually up to 220 °C during the recording of the spectrum, the band characteristic of isomer *E* became gradually weaker, while the band characteristic of *Z* grew stronger.

In the temperature-dependent NMR measurements it has been observed that the bands separately characteristic of *Z* and *E* coalesce above a certain temperature value (T_c), corresponding to the fact that the isomerization became unhindered. From the above effect the activation enthalpy of the isomerization can be determined on the basis of the Eyring correlation [22]. The results of the measurements are contained in Table III.

Isomerization around the non-conjugated C=C double bond is at room temperature mostly hindered, as a result of the great activation free enthalpy ($\Delta G^* = 25-65$ kcal/mole). In the case of olefins with extended conjugation, where on one side of the double bond electron-withdrawing, and on the other

Table III

Compound	Signal evaluated	Hz	T_c °C	Kcal/mole	Solvent	Ratio *E/Z*
2a	$-OCH_2-CH_3$	3.3	88	19.8	$C_6D_5-NO_2$	x
e	$-OCH_2-CH_3$	4.1	86	19.5	$C_6D_5-NO_2$	x
h	$-OCH_2-CH_3$	6.5	162	23.4	$C_6D_5-NO_2$	40 : 60
k	$-OCH_2-CH_3$	7.0	161	23.3	$C_6D_5-NO_2$	25 : 75
l	$-CH_2COOC_2H_5$		200	25.0	$C_6D_5-NO_2$	70 : 30

side electron-releasing substituents are located, the activation free enthalpy may be decreased to such an extent ($\Delta G^* = 5-25$ kcal/mole), that the investigation of the rotation by DNMR becomes possible [18].

The isomerization $Z \rightleftharpoons E$ of the enamines can proceed in two ways. It is possible that it takes place *via* the ketimine tautomeric form, although this form could not be detected experimentally, since components being present at stationary concentrations of less than 1%, cannot be detected by the method applied. The other possibility consists of rotation around the C=C bond. The isomerization $Z \rightleftharpoons E$ will take the reaction route which requires less energy.

If the isomerization $Z \rightleftharpoons E$ proceeds *via* tautomerization, strong proton catalysis can be expected. It has been shown that the isomerization, *e.g.* of enamines and ketenaminals is strongly catalyzed by traces of acid or water in the solvent [17, 23, 24]. Proton catalysis was also observed in the isomerizations of the enamines studied in this work. Addition of a catalytic amount of CF_3COOH to the $CDCl_3$ solution increased the rate of isomerization to about the double, and in nitrobenzene it resulted in a significant decrease in the coalescence temperature T_c. Based on this evidence it can be suggested that in protic medium the isomerization proceeds predominantly *via* tautomerization.

For the purpose of studying the non-catalyzed thermal rotation about the C=C bond, excluding the possibility of tautomerization, ethyl α-cyano-β-(N-methyl)-anilinoacrylate (**3**) was synthetized. This compound had been studied by Shvo [13], and similarly to our results they concluded that by introducing the $N-CH_3$ group, the equilibrium $Z \rightleftharpoons E$ is shifted to such a large extent that the isomerization $Z \rightleftharpoons E$ can no longer be studied.

Another way of avoiding tautomerization is to use an aprotic solvent. For this purpose the measurements were carried out in pure nitrobenzene containing no trace of water or acid. In this case the isomerization takes its course by rotation around the C=C bond, *via* a dipolar transition state (B), the formation of which

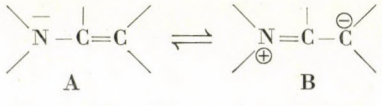

A B

is influenced by the electron-releasing or electron-attracting properties of the attached substituents.

Among the obtained data it is striking that upon replacing the ester group by nitrile, the activation free enthalpy increases, in spite of the fact that $\sigma_{CN} < \sigma_{COOCH_3}$. According to Shvo [13], however, both the ground and the excited states should be taken into consideration, and in this manner the mesomeric part of σ is of decisive importance, thus $\sigma_{mCH} < \sigma_{mCOOCH_3}$.

On this basis it can also be understood that in the case of the ester side chain extended by a methylene group (**21**) the activation free enthalpy is significantly increased, because $\sigma_{CH_2COOC_2H_5} < \sigma_{CN}$.

In this case of compound **21** the thermodynamically less stable isomer *E* could be isolated in pure form, though a mixture of the isomers (*E* : *Z* = 36:64) was formed in the reaction. Isomer *Z* can be separated by fractional crystallization, and as a consequence of the large value of ΔG^* no isomerization occurs after precipitation of the crystals.

Experimental

The UV spectra were obtained with a Unicam SP 800, the IR spectra with a Zeiss UR 20 and the NMR spectra with a Perkin-Elmer R12, VARIAN NV-14 and a JEOL C 60-HL spectrometer. The IR spectra were recorded, also at high temperatures, in KBr pellets. In the NMR measurements tetramethylsilane was used as standard, the values of the chemical shifts are given on the δ scale. Preparative layer chromatography was carried out on 0.25 mm Kieselgel G (Merck) adsorbent layers on microplates of the size 4×7.5 cm. The spots were detected by using iodine vapour or Draggendorff's reagent.

Preparation of α-ethoxycarbonyl-β-anilinoacrylic esters (2a—g)

Ethyl α-ethoxycarbonyl-β-anilinoacrylate (2a) [3]

M.p. 50—52 °C

UV (ethanol): λ_{max} 313 and 289 nm.

IR (KBr): νNH 3200; νC=O 1700; νC=C 1652; νC=C(ar) 1605, 1590, 1512; νC—O—C 1280, 1260, 1040 cm^{-1}.

NMR ($CDCl_3$): 11.02 (1, d, N*H*); 8.48 (1, d, =C*H*); 7.4—6.9 (5, m, Ar—*H*); 4.28 (2, q, OCH_2); 4.23 (2, q, OCH_2); 1.36 (3, t, CH_3); 1.32 (3, t, CH_3).

Ethyl α-ethoxycarbonyl-β-(3-ethoxy-4-hydroxyanilino)-acrylate (2b)

A mixture of 4-hydroxy-3-ethoxyaniline (15.31 g; 0.10 mole) and EMME (26.01 g; 0.12 mole) was heated on a water bath for 1 hr. After dilution with gasoline (30 ml) the solution was refluxed for additional 2 hrs. The material which precipitated upon cooling was separated by filtration. A sand-coloured substance (27.78 g; 86%) was obtained, m.p. 80 °C.

$C_{16}H_{21}NO_6$ (323.347). Calcd. C 59.43; H 6.54; N 4.33. Found C 59.57; H 6.61; N 4.30%.

UV (ethanol) : λ_{max} 334 and 227 nm.

IR (KBr): νOH 3550; νNH 3270; νC=O 1720 and 1665; νC=C 1630; νC—O—C 1260 and 1160 cm^{-1}.

NMR ($CDCl_3$): 11.0 (1, d, N*H*, J = 14 Hz); 8.48 (1, d, =C*H*, J = 14 Hz); 7.1—6.5 (3, m, ar-*H*); 6.0 (1, broad, O*H*); 4.6—3.9 (6, q, OCH_2); 1.6—1.2 (9, t, CH_3).

Ethyl α-ethoxycarbonyl-β-(3-ethoxy-4-acetoxyanilino)-acrylate (2c)

4-Acetoxy-3-ethoxy-aniline (58.56 g; 0.30 mole) was allowed to react with EMME (80.40 g; 0.33 mole) in boiling ethyl acetate (45 ml) for 3 hrs. The product crystallized upon cooling; the white substance was filtered off and washed with absolute alcohol to obtain a white substance (98.22 g; 89.6%). m.p. 115 °C

$C_{18}H_{23}NO_6$ (365.380). Calcd. C 59.17; H 6.34; N 3.83. Found C 59.90; H 6.60; N 4.01%.

IR (KBr): νNH 3250; νC=O (acyl) 1770; νC=O (ester) 1720 and 1670; νC=C 1630; νC—O—C 1260, 1235 and 1170 cm^{-1}.

NMR ($CDCl_3$): 11.1 (1, d, N*H*, J = 13 Hz); 8.51 (1, d, =C*H*, J = 13 Hz); 7.8—7.1 (3, m, ar-*H*); 4.6—3.8 (6, q, OCH_2); 2.3 (3, s, CH_3CO); 1.6—1.2 (9, t, CH_3).

Ethyl α-ethoxycarbonyl-β-(3-ethoxy-4-decyloxyanilino)-acrylate (2d) [10]

M.p. 46 °C.

UV (ethanol): λ_{max} 330 nm.

IR (KBr): νNH 3280; νC=O 1720, 1702, 1675; νC=C 1631; νC=C (ar) 1600, 1530, 1472; νC—O—C 1260, 1238, 1044 cm^{-1}.

NMR ($CDCl_3$): 12.0 (1, d, N*H*, J = 14 Hz); 8.51 (1, d, =C*H*, J = 14 Hz); 7.1—6.6 (3, m, ar-*H*); 4.6—3.9 (8, m, OCH_2); 2.0—0.8 (28, m, aliphatic *H*).

Ethyl α-ethoxycarbonyl-β-(3'4-methylenedioxyanilino)acrylate (2e) [7]

M.p. 109—111 °C.

UV (ethanol): λ_{max} 332 and 222 nm.

IR (KBr): νNH 3260; νC=O 1717, 1695; νC=C 1650; νC=C (ar) 1610, 1520; νC—O—C 1280, 1240 and 1040 cm^{-1}.

NMR ($CDCl_3$): 11.5 (1, d, N*H*, J = 13 Hz); 8.43 (1, d, =C*H*, J = 13 Hz); 6.9—6.3 (3, m, ar-*H*); 6.03 (2, s, O—CH_2—O); 4.29 (2, q, OCH_2); 4.16 (2, q, OCH_2); 1.36 (3, t, CH_3); 1.30 (3, t, CH_3).

Butyl α-butoxycarbonyl-β-(3,4-methylenedioxyanilino)-acrylate (2f)

A mixture of 3,4-methylenedioxyaniline, (13.71 g; 0.1 mole) dibutyl ethoxymethylenemalonate (34.04 g; 0.1 mole) and butanol (6 ml) was boiled for 30 min. The crystals which precipitated upon cooling were filtered off and washed with cold alcohol. A slightly coloured product (26.89 g; 74%), m.p. 58—60 °C, was obtained.

$C_{19}H_{25}NO_6$ (363.414). Calcd. C 62.80; H 6.93; N 3.85. Found C 62.27; H 6.81; H 3.82%.

UV (ethanol): λ_{max} 333 nm.

IR (KBr): νNH 3270; νC=O 1700; νC=C 1650; νC=C (ar) 1610, 1522, 1476; νC—O—C 1250, 1040 cm^{-1}.

NMR ($CDCl_3$): 12.0 (1, d, N*H*, J = 13 Hz); 8.49 (1, d, =C*H*, J = 13 Hz); 7.0—6.5 (3, m, ar-*H*); 6.04 (2, s, O—CH_2—O); 4.29 and 4.24 (4, t, OCH_2); 2.0—0.8 (14, m, aliphatic *H*).

Benzyl α-benzyloxycarbonyl-β-(3,4-methylenedioxyanilino)-acrylate (2g)

3,4-Methylenedioxyaniline (13.71 g; 0.1 mole) was dissolved in benzyl alcohol (15 ml) and dibenzyl ethoxymethylenemalonate (34.04 g; 0.1 mole) was added to the solution. After termination of the exothermic reaction, upon cooling, a crystalline substance precipitated. After a few hours the cooled suspension was filtered and the product washed with alcohol to obtain a white crystalline material 23.8 g; 55.2%, 121—122 °C.

$C_{25}H_{21}NO_6$ (431.449). Calcd. C 69.60; H 4.90; N 3.25. Found C 69.23; H 4.79; N 3.22%.

UV (ethanol): λ_{max} 335 nm.

IR (KBr): νNH 3266; νC=O 1695; νC=C 1640; νC=C (ar) 1610, 1512; νC—O—C 1280, 1235, 1046 cm^{-1}.

NMR ($CDCl_3$): 11.0 (1, d, N*H*, J = 14 Hz); 8.48 (1, d, =C*H*, J = 14 Hz); 7.5—6.5 (13, m, ar-*H*); 5.98 (2, s, O—CH_2—O); 5.33 and 5.29 (4, s, OCH_2).

Preparation of ethyl α-cyano-β-anilinoacrylates (2h-k)

Ethyl α-cyano-β-anilinoacrylate (2h)

M.p. 109 °C.

UV (ethanol): λ_{max} 318 nm.

IR (KBr): νNH 3210; νCN 2222; νC=O 1708, 1677; νC=C 1636; νC=C (ar) 1605, 1592, 1500; νC—O—C 1258, 1038 cm^{-1}.

NMR ($CDCl_3$): isomer *Z*: 10.7 (1, d, N*H*, J = 14 Hz); 7.96 (1, d, =C*H*, J = 14 Hz); isomer *E*: 8.70 (1, d, N*H*, J = 14 Hz); 8.46 (1, d, =C*H*, J = 14 Hz); 7.7—7.0 (5, m, ar-*H*); 4.35 (2, q, OCH_2); 1.36 (3, t, CH_3).

Ethyl α-cyano-β-(3-ethoxy-4-hydroxyanilino)-acrylate (2i)

A mixture of 3-ethoxy-4-hydroxyaniline (3.06 g; 0.02 mole) and EMCE (3.72 g; 0.022 mole) was molten in gasoline (30 ml) and heated on a boiling water bath for 3 hrs. During the reaction the originally brown oily phase disintegrated to give a light coloured solid. Filtration gave the product (5.5 g; 99%), m.p. 129—130 °C.

$C_{14}H_{16}N_2O_4$ (276.294). Calcd. C 60.85; H 5.84; N 10.14. Found C 60.70; H 5.98; N 10.42%.

Ethyl α-cyano-β-(3-ethoxy-4-decyloxyanilino)-acrylate (2j) [10]

M.p. 112—113 °C.

UV (ethanol): λ_{max} 334 and 258 nm.

IR (KBr): νNH 3230; νCN 2226; νC=O 1718, 1680; νC=C 1654; νC=C (ar) 1605, 1537, 1478; νC—O—C 1240, 1042 cm^{-1}.

NMR ($CDCl_3$): 10.8 (1, d, N*H*, J = 13 Hz); 7.82 (1, d, =C*H*, J = 13 Hz); 7.1—6.5 (3, m, ar-*H*); 4.5—3.8 (6, m, OCH_2); 2.0—0.7 (25, m, aliphatic *H*).

Ethyl α-cyano-β-(3,4-methylenedioxyanilino)-acrylate (2k)

M.p. 158 °C.

UV (ethanol): λ_{max} 332 and 257 nm.

IR (KBr): νNH 3222; νCN 2216; νC=O 1709, 1684; νC=C 1653; νC=C (ar) 1510, 1478; νC—O—C 1248, 1040 cm^{-1}.

NMR ($CDCl_3$): isomer *Z*: 10.8 (1, d, N*H*, J = 13 Hz); 7.71 (1, d, =C*H*, J = 13 Hz); isomer *E*: 8.60 (1, d, N*H*, J = 14 Hz); 8.40 (1, d, =C*H*, J = 14 Hz); 7.0—6.5 (3, m, ar-*H*); 6.06 (2, s, O—CH_2—O); 4.22 (2, q, OCH_2); 1.37 and 1.34 (3, t, CH_3).

Ethyl 3-anilino-β-ethoxycarbonylvinylacetate (2l)

A mixture of aniline (37.24 g; 0.4 mole) and diethyl formylsuccinate (80.82 g; 0.4 mole) was boiled in benzene (400 ml) for 3 hrs in a flask equipped with an automatic water separator. The mixture of water and benzene, obtained as the distillate, was removed. The yellow solution was evaporated to dryness in vacuum and the remaining orange coloured oil was crystallized by cooling and rubbing, to obtain an apricot-yellow, sticky material (108.4 g; 98.3%), consisting of a mixture of the isomers *Z* and *E*. Recrystallization from acetone or dry alcohol gave snow-white crystals melting at 100 °C (lit. [6] m.p. 102 °C), representing isomer *E*. In this manner one of the geometrical isomers was isolated in a homogeneous, pure form, as proved unambiguously by the NMR spectrum and TLC examination (one spot, developed in the solvent mixture benzene: methanol = 4 : 1).

UV (ethanol): λ_{max} 314 nm.

IR (KBr): νNH 3355; νC=O 1715 and 1685; νC=C 1656; νC=C (ar) 1610 and 1510; νC—O—C 1250 cm^{-1}.

NMR (CCl_4): isomer *Z*: 10.0 (1, d, N*H*, J = 12 Hz); 7.30 (1, d, =C*H*, J = 12 Hz); 3.22 (2, s, CH_3); isomer *E*: 8.11 (1, d, =C*H*, J = 14 Hz); 7.70 (1, d, N*H*, J = 14 Hz); 3.46 (2, s, CH_2); 7.6—6.8 (5, m, ar-*H*); 4.5—4.0 (4, m, OCH_2); 1.5—1.1 (6, m, CH_3).

Ethyl α-cyano-β-(N-methylanilino)-acrylate (3)

N-methylaniline (1.07 g; 0.01 mole) was dissolved in dry alcohol (5 ml), and EMCE (1.85 g; 0.011 mole) was added. The mixture was refluxed for 3 hrs. The solvent was evaporated, the residue dissolved in acetone and the product precipitated by the addition of petroleum ether and cooling, to obtain a yellow substance (0.8 g; 34.8%), m.p. 98 °C.

Recrystallization from an ethyl acetate-petroleum ether raised the melting point to 105 °C.

$C_{13}H_{14}N_2O_2$ (230.267). Calcd. C 67.81; H 6.13; N 12.16. Found C 67.39; H 6.09; N 12.26%.

UV (ethanol): λ_{max} 299 nm.

IR (KBr): νCN 2210; νC=O 1710; νC—O—C 1245 cm^{-1}.

NMR (CD_3OD): 8.15 (1, s, =C*H*); 7.7—7.3 (5, m, ar-*H*); 4.26 (2, q, OCH_2); 3.77 (3, s N—CH_3); 1.30 (3, t, CH_3).

REFERENCES

[1] Claisen, L.: Ann. **297,** 75 (1897)

[2] Schofield, K., Simpson, J. C.: J. Chem. Soc. **1946,** 1033

[3] Duffin, G. F., Kendall, J. D.: J. Chem. Soc. **1948,** 893

[4] Price, C. C., Roberts, R. M.: J. Am. Chem. Soc. **68,** 1204 (1946)

[5] Riegel, B., Lappin, G. R., Adelson, B. H., Jackson, R. I., Albisetti, C. J., Dodson, R. M., Baker, R. H.: J. Am. Chem. Soc. **68,** 1264 (1946)

[6] Carriere, M. E.: Ann. de Chim. **17** (9), 38 (1922)

[7] Kaminsky, D., Meltzer, R. I.: J. Med. Chem. **11,** 160 (1968)

[8] (*a*) Price, C. C., Leonard, N. J., Herbrandson, H. F.: J. Am. Chem. Soc. **68,** 1251 (1946) (*b*) Snyder, H. R., Jones, R. E.: J. Am. Chem. Soc. **68,** 1253 (1946)

[9] Okumura, K., Adachi, T., Tomie, M., Kondo, K., Inoue, J.: J. Chem. Soc. **1972,** 173

[10] Davis, M., Parnell, E. W., Sharp, B. W., Warburton, D.: Hung. Pat. 155,695. (Priority date: 12. 5. 1967; published: 25. 11. 1968)

11] LAMANT, M., GUIGNARD, A., RIOBÉ, O.: Bull. Soc. Chim. France **1964,** 1606
12] COOK, A. G.: "Enamines", p. 343. Marcel Dekker, New York and London, 1969.
13] SHVO, Y., SHANAN-ATIDI, H.: J. Am. Chem. Soc. **91,** 6683, 6689 (1969)
14] SHVO, Y., TAYLOR, E. C., BARTULIN, J.: Tetrahedron Letters **1967** (34), 3259
15] SHVO, Y., BELSKY, I.: Tetrahedron **25,** 4649 (1969)
16] WENNERBECK, I., SANDSTRÖM, J.: Org. Magn. Resonance **4,** 783 (1972)
[17] KALINOWSKY, H. O., KESSLER, H.: Topics in Stereochem. **7,** 295 (1972)
[18] BÁRCZAI-BEKE, B., DÖRNYEI, G., TÓTH, G., SZÁNTAY, CS.: Tetrahedron **29,** 4153 (1973)
[19] DABROWSKI, J., KANIENSKA-TRELA, K., KOZERSKI, L.: Org. Magn. Resonance **6,** 499 (1974)
[20] DAHLQUIST, K. I.: Acta Chem. Scand. **24,** 1941 (1970)
[21] MISLOW, K., RABAN, M.: Topics in Stereochem. **1,** 1 (1967)
[22] GUTOWSKY, H. S., HOLM, C. H.: J. Chem. Phys. **25,** 1228 (1956)
[23] HERBIG, K., HUISGEN, R., HUBER, H.: Chem. Ber. **99,** 2546 (1966)
[24] KESSLER, H.: Chem. Ber. **103,** 973 (1970)

Judit FRANK
Péter DVORTSÁK
Gábor HORVÁTH
Zoltán MÉSZÁROS
H-1045, Budapest, Tó u. 1—5.

Gábor TÓTH; H-1092, Budapest, Hőgyes Endre u. 7.

INDEX

ANALYTICAL CHEMISTRY

PHYSICAL AND INORGANIC CHEMISTRY

ORGANIC CHEMISTRY

Printed in Hungary

A kiadásért felel az Akadémiai Kiadó igazgatója — Műszaki szerkesztő: Zacsik Annamária

A kézirat nyomdába érkezett: 1976. I. 30. — Terjedelem: 9,10 (A/5) ív, 54 ábra

76.2657 Akadémiai Nyomda, Budapest — Felelős vezető: Bernát György

ACTA CHIMICA

ТОМ 89—ВЫП. 1

РЕЗЮМЕ

Применение смесей воды со спиртом в осмометрии упругости паров

Ю. САБО-ЛАКАТОШ и И. ЛАКАТОШ

На основе экспериментальных данных, полученных при использовании смесей воды с метанолом, воды с этанолом и воды с изопропанолом в осмометрии упругости паров, были сделаны следующие заключения.

1. Наклон аналитической прямой для воды, полученный в бинарных смесях (изменение полярного сопротивления), может быть увеличен и относительная погрешность метода может быть уменьшена до желаемой величины.

2. Дальнейшим преимуществом при использовании смесей вода-спирт является то, что может быть определена способность к диссоциации изучаемого вещества, а также наиболее вероятный молекулярный вес (с точностью до 2—3 относительных процентов) веществ, претерпевающих диссоциацию (ассоциацию) в воде или водных средах.

3. Было установлено, что хотя медленное установление фазового равновесия жидкость-пар мешает измерениям, однако, такого рода помехи могут быть устранены увеличением продолжительности измерений, более частой сменой растворителей.

Определение перекиси водорода и неорганических пероксомонокислот при их совместном присутствии

И. ШНЕЙДЕР, Л. НАДЬ и Л. Й. ЧАНИ

Было найдено, что около pH = 7 катализа селективно расщепляет перекись водорода, в присутствии пероксо-моносерной кислоты или пероксо-монофосфорной кислоты. Это поведение может быть использовано при определении перекиси водорода и пероксомонокислот, присутствующих совместно. Перекись водорода, в одном из образцов анализируемого вещества, расщепляют с помощью катализы, а после этого pH раствора доводится до 4 и выделяющийся за счет пероксо-монокислот свободный йод измеряют спектрофотометрически. В другом же образце подобным образом определяют всю окисляющую способность.

Масс-спектрометрическое исследование соединений типа $XSiH_3$

Г. ИННОРТА, Л. СЕПЕШ и Й. БОРОШАИ

Были исследованы соединения $EtSiH_3$, $PrSiH_3$, $PhSiH_3$. В снятых спектрах доминируют фрагменты, полученные потерей одного или двух а. м. е. Были определены потенциалы ионизации также как и потенциалы появления доминирующих ионов ($P\text{-}1^+$, $P\text{-}2^+$) и были рассчитаны энергии диссоциации ионной связи Si—H. Эти данные получены при использовании механизмов ионизации для алкил и арил-силанов. Проблема определения величины D(Si—C) на основе $AP(s^+)$ или $AP(SiH_3^+)$ обсуждается, принимая во внимание правило Стивенсона. Предлагаются приближенные механизмы фрагментации.

Комплексное исследование никелевых скелетных катализаторов, VII

Распределение никеля и содержание водорода на скелетных катализаторах

А. ТУНГЛЕР, Й. ПЕТРО, Т. МАТЕ, Й. ХЕЙСМАН, Ш. БЕКАШИ и З. ЧЮРЁШ

Намагничиваемость шести различных никелевых скелетных катализаторов была измерена в зависимости от силы поля и температуры. Образцы предварительно подвергались термообработке при 100—400°С. Отсюда с помощью расчетного метода на ЭВМ были определены насыщенная намагничиваемость и температура Кюри. Изменение магнитных величин сравнивалось с результатами термодесорбционных и дериватографических исследований. Была определена зависимость, с одной стороны, между изменением насыщенной намагничиваемости и «качеством» и количеством десорбированного H_2, а с другой стороны, между увеличением температуры Кюри и изменением размеров частиц катализатора. Отсюда можно заключить, что температура Кюри ферромагнитного никеля, находящегося на скелетных катализаторах, вследствие малых размеров частиц, значительно меньше для компактного никеля, а также что две формы водорода, сорбированного на никеле, в различных степенях уменьшают намагничиваемость никеля.

Комплексы переходных металлов с α-диоксиимином, LI

Комплекс динитро-бис-пропоксимато-кобальта(III) и кинетика его аквотизации

Ч. ВАРХЕИ, З. ФИНТА, А. БЕНКЁ и С. МИХАЛЬЧА

Новый комплексный ион $[Co(Пропокс.H)_2(NO_2)_2]^-$ был получен реакцией замещения с метализопропилглиоксимом («пропоксим» - Пропокс.H_2) из $[Co(NO_2)_6]^{-3}$. Ряд новых солей этого аниона был приготовлен реакциями двойного разложения. ИК спектр этого соединения был снят и обсуждается. Кинетика аквотизации $[Co(Пропокс.H)_2(NO_2)_2]^-$ была исследована в широком интервале pH и полученные кинетические параметры сравнивались с аналогичными им параметрами для диметилглиоксима.

Тиокарбамидные производные в морфиновом ряду, I

Р. БОГНАР, ДЬ. ГААЛ, П. КЕРЕКЕШ, Г. ХОРВАТ и Е. СИКСАИ

Из норморфина, норкодеина и нордигидрокодеина с помощью различных изотиоцианатов были получены следующие тиокарбамидные производные:
N-[N-бензилтиокарбамино]-норморфин (IV),
N-[N-циклогексилтиокарбамино]-норморфин (V),
N-[N-фенилтиокарбамино]-норкодеин (VI),
N-[N-метилтиокарбамино]-норкодеин (VII),
N-[N-бензилтиокарбамино]-норкодеин (VIII),
N-[N-циклогексилтиокарбамино]-норкодеин (IX),
N-[N-2,3,4,6-тетраацетил-β-D-глюкозилтиокарбамино]-норкодеин (X),
N-[N-метилтиокарбамино]-нордигидрокодеин (XI),
N-[N-фенилтиокарбамино]-нордигидрокодеин (XII),
N-[N-бензилтиокарбамино]-нордигидрокодеин (XIII),
N-[N-циклогексилтиокарбамино]-нордигидрокодеин (XIV),
N-[N-2,3,4,6-тетраацетил-β-D-глюкозилтиокарбамино]-нордигидрокодеин (XV) и
N-[N-адамантилтиокарбамино]-нордигидрокодеин (XVI).

Стереохимические исследования, XXVII

Синтез потенциальных фармаконов типа амидов кислот, III
Получение производных цис- и транс-2-амино-1-циклопентан, 1-циклогексан и 1-циклогептанкарбоксимидов

Г. БЕРНАТ, Л. ГЕРА, ДЬ. ГЁНДЁШ и И. ПАНОВИЧ

Исходя из *цис-* и *транс*-2-амино-1-циклопентанкарбоновых кислот (2а, 3а), *цис-* и *транс*-2-амино-1-циклогексанкарбоновых кислот (2в, 3в), а также *транс*-2-амино-1-циклогептановой кислоты (3с), были синтезированы для фармакологических исследований многочисленные N-замещенные *цис-* и *транс*-2-амино-1-циклоалканкарбоксамиды (16, 17а—е, 18, 19а—h, 20а, b). Были получены также некоторые N-замещенные *цис-* и *транс*-2-(формиламино)-1-циклогексанкарбоксамиды (22а—f, 23), N-замещенные *цис*-2-(ацетиламино)-1-циклогексанкарбоксамиды (27а—f) и N-замещенные *транс*-2-(ацетиламино)-1-циклогексанкарбоксамиды (28а—е).

Алкалоиды со скелетом индоло[2,3-с)хиназолино[3,2-а)пиридина, IV

Масс-спектр рутекарпина, эводиамина и 3,14-дигидрорутекарпина

И. ТАМАШ, ДЬ. БУЙТАШ, К. ХОРВАТ-ДОРА и О. КЛАУДЕР

Приводится масс-спектр рутекарпина, эводиамина и 3,14-дигидрорутекарпина. На основе исследований было найдено, что перед фрагментацией молекулярный ион последнего соединения претерпевает перегруппировку в скелете.

О таутомерии и изомеризации энаминов акриловой кислоты

Й. ФРАНК, П. ДВОРТШАК, Г. ХОРВАТ, З. МЕСАРОШ и Г. ТОТ

Таутомерия акриловых эфиров и акрилонитрилов была исследована с помощью ЯМР спектроскопии. Было определено существование изомеров Z и E и было определено их соотношение. Измерением температуры коалесценции была определена свободная энтальпия активации изомеризации.

The Acta Chimica publish papers on chemistry, in English, German, French and Russian.

The Acta Chimica appear in volumes consisting of four parts of varying size, 4 volumes being published a year.

Manuscripts should be addressed to

Acta Chimica
H-1521 Budapest, Hungary

Correspondence with the editors should be sent to the same address.

The rate of subscription in $ 32.00 a volume.

Orders may be placed with "*Kultúra*" Foreign Trade Company for Books and Newspapers (1389 Budapest 62, P.O.B. 149. Account No. 218 10990) or with representatives abroad.

Les Acta Chimica paraissent en français, allemand, anglais et russe et publient des mémoires du domaine des sciences chimiques.

Les Acta Chimica sont publiés sous forme de fascicules. Quatre fascicules seront réunis en un volume (4 volumes par an).

On est prié d'envoyer les manuscrits destinés à la rédaction à l'adresse suivante:

Acta Chimica
H-1521 Budapest, Hungary

Toute correspondance doit être envoyée à cette même adresse.

Le prix de l'abonnement est de $ 32,00 par volume.

On peut s'abonner à l'Entreprise pour le Commerce Extérieur de Livres et Journaux «*Kultúra*» (1389 Budapest 62, P.O.B. 149. Compte-courant No. 218 10990) ou à l'étranger chez tous les représentants ou dépositaires.

«*Acta Chimica*» издают трактаты из области химической науки на русском, французском, английском и немецком языках.

«*Acta Chimica*» выходят отдельными выпусками разного объема. 4 выпуска составляют один том. 4 тома публикуются в год.

Предназначенные для публикации рукописи следует направлять по адресу:

Acta Chimica
H-1521 Budapest, BHP

По этому же адресу направлять всякую корреспонденцию для редакции.

Подписная цена — $ 32,00 за том.

Заказы принимает предприятие по внешней торговле книг и газет «*Kultúra*» (1389 Budapest 62, P.O.B. 149. Текущий счет № 218 10990) или его заграничные представительства и уполномоченные.

Reviews of the Hungarian Academy of Sciences are obtainable at the following addresses:

AUSTRALIA

C. B. D. Library and Subscription Service
Box 4886, G. P. O.
Sydney N. S. W. 2001

Cosmos Bookshop
145 Acland St.
St. Kilda 3182

AUSTRIA

Globus
Höchstädtplatz 3
A–1200 Wien XX

BELGIUM

Office International de Librairie
30 Avenue Marnix
1050–Bruxelles

Du Monde Entier
162 Rue du Midi
1000–Bruxelles

BULGARIA

Hemus
Bulvar Ruski 6
Sofia

CANADA

Pannonia Books
P. O. Box 1017
Postal Station "B"
Toronto, Ont. M5T 2T8

CHINA

C N P I C O R
Periodical Department
P. O. Box 50
Peking

CZECHOSLOVAKIA

Mad'arská Kultura
Národní třída 22
115 66 Praha

PNS Dovoz tisku
Vinohradská 46
Praha 2

PNS Dovoz tlače
Bratislava 2

DENMARK

Ejnar Munksgaard
Nörregade 6
DK–1165 Copenhagen K

FINLAND

Akateeminen Kirjakauppa
P. O. Box 128
SF–00101 Helsinki 10

FRANCE

Office International de Documentation et Librairie
48 Rue Gay-Lussac
Paris 5

Librairie Lavoisier
11 Rue Lavoisier
Paris 8

Europeriodiques S. A.
31 Avenue de Versailles
78170 La Celle St. Cloud

GERMAN DEMOCRATIC REPUBLIC

Haus der Ungarischen Kultur
Karl-Liebknecht-Strasse 9
DDR–102 Berlin

Deutsche Post
Zeitungsvertriebsamt
Strasse der Pariser Kommüne 3–4
DDR-104 Berlin

GERMAN FEDERAL REPUBLIC

Kunst und Wissen
Erich Bieber
Postfach 46
7 Stuttgart S

GREAT BRITAIN

Blackwell's Periodicals
P. O. Box 40
Hythe Bridge Street
Oxford OX1 2EU

Collet's Holdings Ltd.
Denington Estate
London Road
Wellingborough Northants NN8 2QT

Bumpus Haldane and Maxwell Ltd.
5 Fitzroy Square
London W1P 5AH

Dawson and Sons Ltd.
Cannon House
Park Farm Road
Folkestone, Kent

HOLLAND

Swets and Zeitlinger
Heereweg 347b
Lisse

Martinus Nijhoff
Lange Voorhout 9
The Hague

INDIA

Hind Book House
66 Babar Road
New Delhi 1

India Book House
Subscription Agency
249 Dr. D. N. Road
Bombay 1

ITALY

Santo Vanasia
Via M. Macchi 71
20124 Milano

Libreria Commissionaria Sansoni
Via Lamarmora 45
50121 Firenze

JAPAN

Kinokuniya Book-Store Co. Ltd.
826 Tsunohazu 1-chome
Shinjuku-ku
Tokyo 160–91

Maruzen and Co. Ltd.
P. O. Box 5050
Tokyo International 100–31

Nauka Ltd.–Export Department
2–2 Kanda
Jinbocho
Chiyoda-ku
Tokyo 101

KOREA

Chulpanmul
Phenjan

NORWAY

Tanum-Cammermeyer
Karl Johansgatan 41–43
Oslo 1

POLAND

Węgierski Instytut Kultury
Marszałkowska 80
Warszawa

BKWZ Ruch
ul. Wronia 23
00–840 Warszawa

ROUMANIA

D. E. P.
Bucureşti

Romlibri
Str. Biserica Amzei 7
Bucureşti

SOVIET UNION

Soyuzpechaty – Import
Moscow
and the post offices in each town

Mezhdunarodnaya Kniga
Moscow G–200

SWEDEN

Almqvist and Wiksell
Gamla Brogatan 26
S–101 20 Stockholm

A. B. Nordiska Bokhandeln
Kunsigatan 4
101 10 Stockholm 1 Fack

SWITZERLAND

Karger Libri AG.
Arnold-Böcklin-Str. 25
4000 Basel 11

USA

F. W. Faxon Co. Inc.
15 Southwest Park
Westwood, Mass. 02090

Stechert-Hafner Inc.
Serials Fulfillment
P. O. Box 900
Riverside N. J. 08075

Fam Book Service
69 Fifth Avenue
New York N. Y. 10003

Maxwell Scientific International Inc.
Fairview Park
Elmsford N. Y. 10523

Read More Publications Inc.
140 Cedar Street
New York N. Y. 10006

VIETNAM

Xunhasaba
32, Hai Ba Trung
Hanoi

YUGOSLAVIA

Jugoslovenska Knjiga
Terazije 27
Beograd

Forum
Vojvode Mišića 1
21000 Novi Sad

ACTA CHIMICA

ACADEMIAE SCIENTIARUM HUNGARICAE

TOMUS 89 FASCICULUS 2

AKADÉMIAI KIADÓ, BUDAPEST
1976

ACTA CHIM. (BUDAPEST) ACASA 2 89 (2) 101–186 (1976)

ACTA CHIMICA

A MAGYAR TUDOMÁNYOS AKADÉMIA KÉMIAI TUDOMÁNYOK OSZTÁLYÁNAK IDEGEN NYELVŰ KÖZLEMÉNYEI

SZERKESZTI

LENGYEL BÉLA

TECHNIKAI SZERKESZTŐK

DEÁK GYULA és HARASZTHY-PAPP MELINDA

Az Acta Chimica német, angol, francia és orosz nyelven közöl értekezéseket a kémiai tudományok köréből.

Az Acta Chimica változó terjedelmű füzetekben jelenik meg, egy-egy kötet négy füzetből áll. Évente átlag négy kötet jelenik meg.

A közlésre szánt kéziratok a szerkesztőség címére (1521 Bp., Műegyetem) küldendők. Ugyanerre a címre küldendő minden szerkesztőségi levelezés. A szerkesztőség kéziratokat nem ad vissza.

Megrendelhető a belföld számára az „Akadémiai Kiadó"-nál (1363 Budapest, Pf. 24. Bankszámla 215 11488), a külföld számára pedig a „Kultúra" Könyv- és Hírlap Külkereskedelmi Vállalatnál (1389 Budapest 62, P.O.B. 149. Bankszámla: 218 10990) vagy annak külföldi képviseleteinél és bizományosainál.

Die Acta Chimica veröffentlichen Abhandlungen aus dem Bereich der chemischen Wissenschaften in deutscher, englischer, französischer und russischer Sprache.

Die Acta Chimica erscheinen in Heften wechselnden Umfanges. Vier Hefte bilden einen Band. Jährlich erscheinen 4 Bände.

Die zur Veröffentlichung bestimmten Manuskripte sind an folgende Adresse zu senden:

Acta Chimica
H-1521 Budapest

An die gleiche Anschrift ist auch jede für die Redaktion bestimmte Korrespondenz zu richten. Abonnementspreis pro Band: $ 32.00.

Bestellbar bei dem Buch- und Zeitungs-Außenhandels-Unternehmen »*Kultúra*« (1389 Budapest 62, P.O.B. 149. Bankkonto Nr. 218 10990) oder bei seinen Auslandsvertretungen und Kommissionären.

Acta Chimica Academiae Scientiarum Hungaricae, Tomus 89 (2), pp. 101—122 (1976)

PREPARATION AND MASS SPECTROMETRY OF MOLYBDENUM AND TUNGSTEN OXYBROMIDES AND TUNGSTEN BROMIDES

O. KAPOSI*, T. DEUTSCH**, A. POPOVIĆ*** and J. PEZDIĆ***

*(*Department of Physical Chemistry and Radiology, Eötvös L. University, Budapest*
***Chinoin Works for Pharmaceutical and Chemical Products, Budapest*
****Jozef Stefan Institute, Ljubljana, Yugoslavia)*

Received February 20, 1975

MoO_2Br_2, WO_2Br_2, $WOBr_4$, WBr_4 and W_2Br_6 were prepared by the bromination of the respective metals or metal oxides and studied mass-spectrometrically. The mass-spectrometric fragmentation of these compounds was determined, the appearance potentials of the ionic species present in higher relative amounts was measured and their heats of formation calculated. Some ions were observed whose composition could be interpreted from the solid phase structure of these compounds. Ions originating from the cluster compound W_2Br_6 were detected in high relative intensities. Some thermochemical and thermostatic parameters of the compounds under investigation were calculated from the experimental appearance and ionization potentials.

I. Introduction

The increasing technological importance of molybdenum and tungsten [1, 2] lends special importance to the study of systems composed of these metals and halogens. The theoretically calculated high-temperature parameters of these compounds were first surveyed by BREWER *et al.* [3]. Because of the lack of the necessary experiments, their approximate thermodynamic data are still used in the literature [4, 5].

Since the discovery of the halogen incandescent lamps [6, 7, 8] the practical importance of the tungsten–halogen and tungsten–halogen–oxygen systems [9, 10, 11] has increased dramatically. The halogen concentration needed for the operation of these lamps can be ensured by the introduction of gaseous halogens into the vapour space of the lamp or by the pyrolysis of halogenated hydrocarbons within the lamp [12, 13, 14]. The chemical transport reactions taking place in halogen lamps, the composition of the gas phase and the heterogeneous equilibria between the tungsten filament and the gas phase [15, 16, 17, 18] are calculated, owing to the lack of adequate experimental data, either from BREWER's [3] or the JANAF Tables [19] or from the theoretically calculated data of NEUMAN [20, 21]. Only lately has some experimental work been published on the kinetics of these systems [22, 23, 24, 25, 26] and on the thermodynamics of tungsten halides, and oxyhalides. These publications will be referred to in the discussion of the experimental results.

In this paper we shall describe the results of a mass-spectrometric investigation of the bromination products of molybdenum and tungsten oxides and metallic tungsten. These experimental data supplement the high-temperature chemical [27] and mass-spectrometric [28, 29] parameters of molybdenum and tungsten oxyhalides determined in the last few years. The mass-spectrometric studies on tungsten bromides are the first experiments in this field by the given technique.

II. Experimental

II.1. Instruments

A mass spectrometer equipped with a Knudsen-type effusion cell, built in the Jozef Stefan Institute (Ljubljana), was employed. In this form the spectrometer was suitable for measurements at high temperatures [30], *i.e.* it could be used for the determination of the heats of sublimation and of other thermodynamic parameters of the oxybromides and bromides under investigation. These data are of fundamental importance also for the modelling of halogen-filled incandescent lamps [31]. The mass spectrometer had a Nier geometry, single focussing and a resolution of about 800. Two oil diffusion pumps provided a vacuum of 10^{-7} Torr in the ion source. The joint containing the ion source and the vaporization cell could be baked to 250—300 °C to reduce the background. The Knudsen effusion cell [32] made of tungsten had an orifice of about 0.3 mm and was heated by a tungsten resistance wire; its temperature around 100 °C was measured by a CrNi–AlNi thermocouple with an accuracy of ± 0.5 °C. The instrument was equipped with a Faraday-type collector and an electron multiplier. The spectra were recorded by a Speedomax Type G recorder.

The ionization efficiency curves were recorded in the usual manner [33], using neon for calibration. The ion accelerating potential was measured with a digital voltmeter (Fluke Type 8300 A) with an accuracy of ± 0.01 V. The curves of ionization efficiency were evaluated by the electron energy distribution difference method (EDD), as worked out by WINTERS *et al.* [34].

The mass scale was calibrated in the known manner with perfluorokerosene. In case of ions of very high mass numbers (such as *e.g.* $W_2Br_6^+$) the spectra were recorded also with the double-focussing CEC-21-110 C mass spectrometer; this permitted to identify with absolute certainty the various peaks by means of the isotope distribution calculated from the peak heights and by the accurate determination of the mass number based on the peak-matching method [35].

Since the oxybromides and bromides under investigation are highly sensitive to humidity [36], all operations with these compounds were performed in a dry-box under nitrogen.

II.2. Preparation of the compounds

2/a *Preparation of molybdenum bromide.* For the preparation of MoO_2Br_2 [36, 37, 38], the following reaction was utilized:

$$Mo + 2\,MoO_3 + 3\,Br_2 \rightarrow 3\,MoO_2Br_2 \qquad (1)$$

The reaction was performed in the apparatus shown in Fig. 1.

The Ar carrier gas entered the reaction space 4 through drying column *1* filled with dehydrated $Mg(ClO_4)_2$ at a rate measured by rotameter *2*, through a system of valves either through the thermostated (40 °C) storage vessel for Br_2 *3* (during the reaction) or through a side-branch (during the preliminary flushing of the equipment). About 8 g of the stoichiometric mixture of the metal with the metal oxide was placed into quartz boat *5* which was introduced into the reaction space through a pipe which could be closed. To remove the last traces of water, the entire system was carefully heated and the temperature of the reactor tube kept at 300 °C by means of tube furnace *6* for 1 to 2 hrs while the flow of Ar was main-

tained. At the start of the reaction Ar was allowed to flow through the Br_2 storage vessel from where the gas mixture entered the reaction space. The gas carrying the unreacted Br_2 flowed through absorber *8* into the pressure-compensating vessel. The bulk of the products of the transport reaction was collected in vessel *9* which had a neck and could be sealed. The products condensing in the cooler surfaces of the apparatus fell, when gentle knocking was applied to the wall, into the collecting vessel. The pressure of the gas mixture was measured before and after the reactor with manometers *10*.

The part of the apparatus between the rotameter to the adsorber was made of quartz. The quartz—quartz parts were joined by teflon tubing. The temperature of the reaction tube, measured between the lining of the oven and the reactor tube was 230—250 °C. The

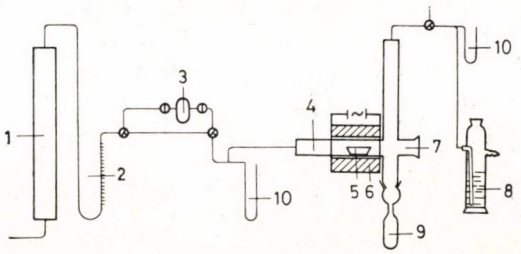

Fig. 1. Apparatus for the production of MoO_2Br_2

flow rate of the carrier gas was 12—15 hrs, its pressure 790—810 Torr. Under these conditions MoO_2Br_2 was formed at a rate of about 10 g/hr. The product consisted of brown, flat, lustrous crystals which hydrolized in air with the formation of HBr. The qualities of the materials were: Br_2, analytical grade (Merck), MoO_3, analytical grade (UCB, Bruxelles), Mo powder (Tungsram, Budapest).

2/b *Preparation of tungsten oxybromides.* The two most important tungsten oxybromides, WO_2Br_2 and $WOBr_4$ have been described [39]. Essentially, two methods are known for the preparation of WO_2Br_2 : 1/bromination of WO_2, that is, of $W + WO_3$ [40, 41] when the following reactions take place atl ower temperatures (200—250 °C):

$$WO_2 + Br_2 = WO_2Br_2 \tag{2}$$

$$W + 2\,WO_3 + 3\,Br_2 = 3\,WO_2Br_2 \tag{3}$$

At higher temperatures the reaction between the components on the left-hand side of Eq. (3) proceeds according to Eq. (6).

The other method involves the reaction of WO_3 with CBr_4 in a high pressure tube reactor at 20 to 30 atm and 440—490 °C [40, 42].

Since beside (4), reaction (5)

$$2\,WO_3 + CBr_4 = 2\,WO_2Br_2 + CO_2 \tag{4}$$

$$WO_3 + CBr_4 = WOBr_4 + CO_2 \tag{5}$$

may also take place, the WO_2Br_2 needed for the experiments was prepared by the bromination of WO_2.

Because of the high sensitivity of tungsten oxybromides to humidity, water was removed from the bromine reagent and from the reaction space most carefully by means of evacuation which is a far more reliable method than the one applied in the case of MoO_2Br_2 when moisture was removed by the carrier gas. The chemical transport reaction took place in the quartz reactor tube shown in Fig. 2.

The tungsten oxide (Tungsram, Budapest) was placed into section *3*, the reactor evacuated to 10^{-6} Torr and kept at this pressure for several hours, while the tube with the WO_2 was heated by a Bunsen burner to remove the last traces of moisture. From analytical grade bromine (Merck) the traces of moisture were removed by distillation at −18 °C so that one branch of an appropriately shaped, closed flask containing the Br_2 to be purified was kept at the temperature of the eutectic mixture of ice–salt–water, while the other branch was

immersed into a Dewar flask filled with liquid air into which the bromine distilled over and solidified. After several repetitions of this operation, bromine was diluted from P_2O_5 into container *1* of the reactor tube (Fig. 1), by immersing the container into liquid air and keeping the flask with the purified Br_2 at room temperature. When somewhat more than the necessary amount of bromine for the reaction had solidified, the reaction tube was evacuated and sealed at point *a*. Then section *3* containing the WO_2 was placed between *c* and *d* into the tube furnace in whose middle section the temperature was 250 °C. In the reaction space containing the WO_2, a constant flow of Br_2 was ensured by keeping containers *1* and *5* alternately at the temperature of liquid air and at room temperature. After a few hours of the alternating flow

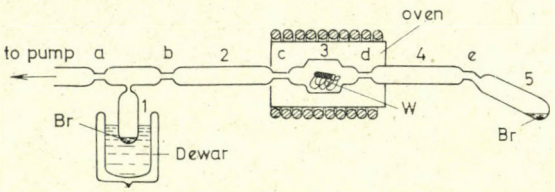

Fi. 2. Apparatus for the bromination of tungsten and tungsten oxides

of Br_2 a sufficient amount of orange WO_2Br_2 crystals for the experiments precipitated on the cooler walls of sections *2* and *4*. Next, the total amount of bromine in *1* was made to solidify and the reaction tube sealed at its neck. The reaction product was sublimed at 100—150 ° into section *5* of the tube and the latter sealed at point *e*. The ampoule was opened and the Knudsen cell filled under nitrogen in the dry box.

$WOBr_4$ was prepared similarly to WO_2Br_2 according to reaction (5) [40] or by the bromination of a mixture of W powder and WO_3 [41, 43, 44] according to the following reaction:

$$2\ W + WO_3 + 6\ Br_2 = 3\ WOBr_4 \qquad (6)$$

However, according to other authors, beside $WOBr_4$, oxybromides of lower valencies are formed simultaneously [45]. At temperatures above 500 °C $WOBr_4$ is formed also by the decomposition of WO_2Br_2

$$2\ WO_2Br_2 = WO_3 + WOBr_4 \qquad (7)$$

As will be shown later, in agreement with previous observations [47], if tungsten contains some oxides, the products of its bromination at high temperatures include $WOBr_4$.

The apparatus shown in Fig. 2 was also employed for the preparation of $WOBr_4$, but in this case reaction space *3* was filled with tungsten wool on which WO_3 powder was sprinkled (both W and the WO_3 powder were products of Tungsram, Budapest), thereby ensuring a large surface for the heterogeneous reaction. Otherwise the procedure was the same as before with the sole difference that the reaction space was heated to 400 °C. By the end of the transport reaction, dark brown $WOBr_4$ precipitated in the form of needle-shaped crystals on the cooler parts of the tube (sections *2* and *4*).

2/c *Bromination of tungsten.* It has been demonstrated by other authors [46] that when metallic tungsten is brominated in the absence of moisture and oxygen, the composition of the tungsten bromides formed will be determined primarily, by the temperature of the reaction space. When bromination is performed in a stream of nitrogen at lower temperatures, WBr_6 will be the main product [40, 49], while at 450—500 °C the reaction proceeds almost quantitatively in the direction of WBr_5 formation [40, 47, 49]. Above 200 °C WBr_6 is reversibly converted into WBr_5. [40]. Reduction of WBr_5 with W or Al by the temperature gradient method leads to WBr_4 [50, 54]. A compound of even lower oxidation state, WBr_3, can be prepared from WBr_2 by bromination at 50 °C. The WBr_3 formed in this way decomposes slowly at 80 °C into WBr_2, Br_2 and WBr_5 [51]. WBr_2 can be prepared either by the disproportionation of WBr_4 or by brominating W at a 'sufficiently high' temperature in a manner similar to the preparation of WI_2 [52]. In some of the procedures described for the W + Br_2 reaction the conditions are not strictly defined; under the same or very similar conditions different reaction products were obtained by different authors. An accurate assessment of the facts is further complicated by the circumstance that the identification of the compounds formed has not always been convincingly reliable, since in the majority of cases it was performed only

by the determination of the W : Br ratio by means of classical analysis. The possibility of the formation of tungsten bromides of an intermediate oxidation state adds to the complexity of the problem [48, 53].

Thus, it is not possible to prepare pure, homogeneous tungsten bromide by the bromination of the metal. There are, however, roundabout ways, *e.g.* for the production of WBr_6 *via* the reaction $W(CO)_6 + Br_2$ [40]. In our present work we have undertaken a mass-spectrometric study of the products formed at a relatively high temperature (600 °C) upon the bromination of tungsten with or without a carrier gas.

For the bromination of tungsten in a carrier gas the apparatus shown in Fig. 1 was used. In this case about 5 g of tungsten wool was placed into the boat and moisture was removed as described in the paragraph on the bromination of $Mo + MoO_3$. The temperature of the reaction space was kept at 600 °C. After about 10 min, when the bromination of the surface oxide layer of tungsten could be considered as completed, the process was interrupted and the products which had precipitated on the cooler walls of the apparatus were sublimed into the collecting vessel by immersion of the latter into liquid air while the other parts of the apparatus were heated with a Bunsen burner. The product formed upon continued bromination was collected in another flask. The conditions (except the temperature) were the same as those employed in the bromination of $Mo + MoO_3$. After 3 hrs about 3 g of the tungsten wool had reacted forming a dark brown crystalline product.

Tungsten was next brominated in vacuum by the method described in the paragraph on the preparation of tungsten oxybromides (Fig. 2). To remove all the oxide traces, prior to bromination the tungsten wool has treated in a hydrogen stream at 900 °C for 2 hrs. During bromination the temperature of the tube furnace in the middle of the reaction space was 600 °C and 200 °C at the two ends. The reaction products sublimed into tube sections *2* and *4*. The reaction involved the distillation of bromine approximately ten times from container *1* into container *5* and back, after which the bulk of the tungsten wool (about 5 g) seemed to have reacted. The black crystalline end-product was sublimed in an electric oven (where the temperature in the middle was 250 °C) into section *2* of the sealed reaction tube, so that the reaction tube was gradually pushed forward in the tube furnace while section *2* was cooled.

III. Results and discussion

III.1. *Mass spectrum of* MoO_2Br_2

The gas pressure needed for the recording of the mass spectrum was ensured in the ion source by the evaporation of the material under investigation from the Knudsen cell. The relative intensities of the ions formed by the collision of the gas molecules produced by the evaporation of MoO_2Br_2 with electrons are given in Table I. We have listed only those ions whose quantity relative to $MoO_2Br_2^+$ is more than 1%.

The recorded isotope peaks of the $MoO_2Br_2^+$ molecular ion in the mass spectrum are shown in Fig. 3 as a function of the mass number. There is a good agreement between the isotope ratios calculated from the peak heights and the theoretically calculated values (Table VII).

The appearance potentials shown in Table I were contained by recording and evaluating the ionization efficiency curves. Employing WINTERS' evaluation method [34], $\Delta I_{MoO_2Br_2}$ (where ΔI is the difference in ion currents measured at two successive accelerating potentials) was plotted vs. the uncorrected electron energy (Fig. 4). The ionization potential value obtained for MoO_2Br_2 was in good agreement with the published data [28]; for the appearance potential of the other fragments there are no data in the literature.

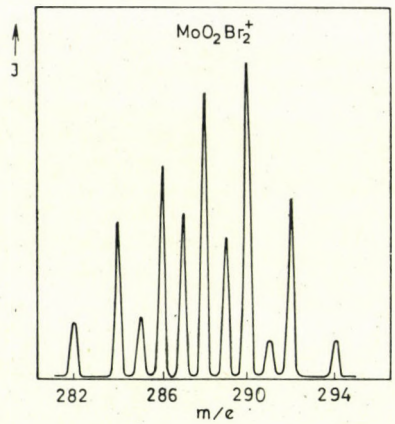

Fig. 3. Heights of the isotpe peaks (I) of $MoO_2Br_{2I}^+$ *vs.* the mass number (m/e)

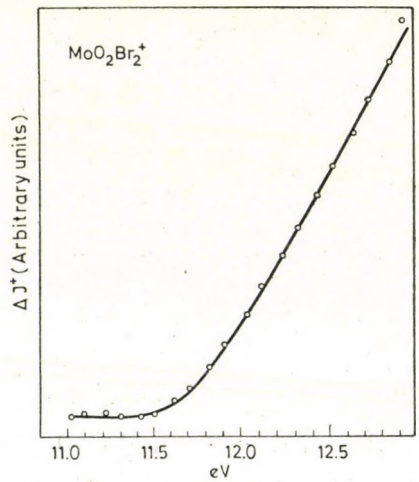

Fig. 4. Ionization efficiency of $MoO_2Br_2^+$ *vs.* the uncorrected electron energy

In the case of MoO_2Br_2 the intensities of the fragments, as measured by us, are similar to the experimental data of BARRACLOUGH [56], while SINGLETON observed a less extensive fragmentation [29]. Besides the ions resulting from the fragmentation of MoO_2Br_2 we have also detected the ions MoO_4Br^+ and MoO_3Br^+. The appearance of these ions can be interpreted in terms of the crystal structure of MoO_2Br_2. According to the IR spectra of these compounds [56], MoO_2Br_2 and WO_2Br_2 have structures composed of MO_4Br_2 (where M=Mo or W) octahedra linked by O atoms. This oxygen-bridged structure characterizes also the dimeric molecules in the gas phase [56]; BARRACLOUGH has found peaks of fairly high intensities, corresponding to these ions in the mass spectrum of MoO_2Br_2. We have detected the ions $Mo_2O_4Br_2^+$ and $Mo_2O_4Br^+$

Table I

Mass spectrum of MoO_2Br_2
Temperature of the Knudsen cell 320 K

m/e	Ion	(1)	(2)	Probable process		(3)
288	$MoO_2Br_2^+$	100	11.0 ± 0.2	$MoO_2Br_2 \rightarrow$	$MoO_2Br_2^+$	126
272	$MoOBr_2^+$	4.7			$MoOBr_2^+ + O$	
256	$MoBr_2^+$	3.3			$MoBr_2^+ + 2O$	
240	MoO_4Br^+	3.6				
224	MoO_3Br^+	1.1				
208	MoO_2Br^+	58.4	13.4 ± 0.2	$MoO_2Br_2 \rightarrow$	$MoO_2Br_2^+ + Br$	154
192	$MoOBr^+$	22.5	19.6 ± 0.3		$MoOBr^+ + O + Br$	238
176	$MoBr^+$	10.1	26.1 ± 0.5		$MoBr^+ + 2O + Br$	328
128	MoO_2^+	14.5	16.0 ± 0.3		$MoO_2^+ + 2Br$	187
112	MoO^+	18.0	22.9 ± 0.4		$MoO^+ + O + 2Br$	314
96	Mo^+	12.5	(16 ± 0.5)	$(MoO_2Br_2 -$	$Mo^+ + Br_2 + O_2$	231)
160	Br_2^+	1.0				
81	HBr^+	9.6				
80	Br^+	19.20				

(1) Relative intensity, electron energy 40 eV
(2) Appearance potential (eV)
(3) Heat of ion formation (kcal/mol)
ΔH_f^0 ($MoO_2Br_{2(g)}$) = −127.3 kcal/mol [38]
ΔH_f^0 (Br) = 26.7 kcal/mol [54]
ΔH_f^0 (O) = 59.0 kcal /mol [55]

only in very low (less than 1%) intensities. The appearance of HBr^+ in the spectra indicates some hydrolysis, which may have occurred during the transfer of the Knudsen cell from the dry box to the mass spectrometer and its evacuation 5×10^{-7} torr.

III.2. *Mass spectrum of WO_2Br_2*

Part of the mass spectrum of WO_2Br_2 with the two most intense peaks is shown in Fig. 5. There is a good agreement between the isotope distributions calculated theoretically and obtained from the heights of the peaks (Table VII). The shape of the peaks of fragments containing odd and even numbers of bromine atoms (Fig. 5) is very characteristic of tungsten bromides and facilitates their identification.

Table II lists the fragment ions formed from WO_2Br_2 at a higher relative intensity than 1%. The appearance potentials of the ions were determined from the ionization efficiency curves of the more intense fragments. The ionization efficiency curve of $WO_2Br_2^+$ and WO_2Br^+ is shown in Fig. 6.

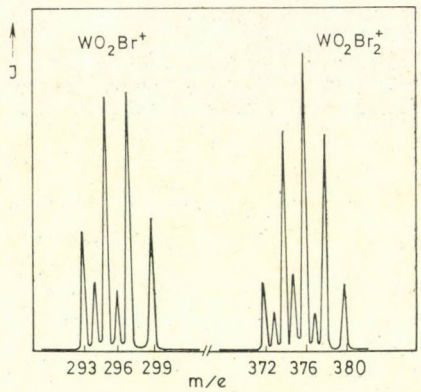

Fig. 5. Part of the spectrum of WO_2Br_2. Height of the isotope peaks of $WO_2Br_2^+$ and WO_2Br^+ *vs.* the mass number

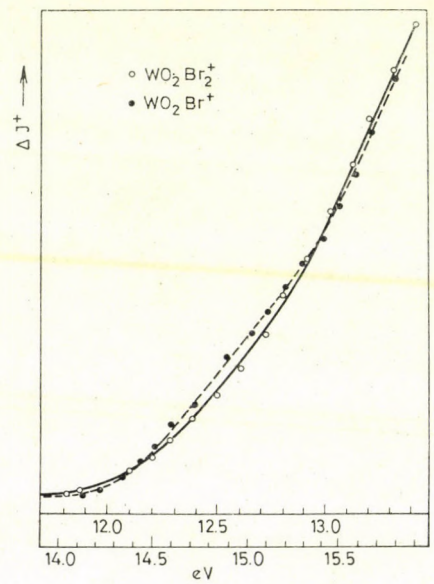

Fig. 6. Ionization efficiency of $WO_2Br_2^+$ and WO_2Br^+ *vs.* the uncorrected electron energy

Like in the case of MoO_2Br_2, we have observed more extensive fragmentation than other authors [56, 57]. A direct comparison is difficult because of the different conditions under which the spectra have been recorded (temperature of the sample, electron energy). In addition to the ions in the Table II $WO_3Br_2^+$ and WO_3Br^+ were detected in intensities below 1% and $W_2O_4Br_2^+$ in even lower quantities. All these facts suggest a crystal structure such as already mentioned in the case of MoO_2Br_2. The appearance of the ditungstenic ions can be explained by the following process:

$$2\ WO_2Br_{2(s)} \rightarrow W_2O_4Br_{2(g)} + Br_{2(g)} \qquad (8)$$

Table II

Mass spectrum of WO_2Br_2
Temperature of the Knudsen cell 300 K

m/e	Ion	(1)	(2)	Probable process	(3)
376	$WO_2Br_2^+$	100	11.4 ± 0.2	$WO_2Br_2 \rightarrow WO_2Br_2^+$	128
360	$WOBr_2$	6		$WOBr_2^+ + O$	
344	WBr_2^+	11.6		$WBr_2^+ + 2O$	
297	WO_2Br^+	88	$13\,6 \pm 0.2$	$WO_2Br^+ + Br$	145
281	$WOBr^+$	36.7	19.8 ± 0.3	$WOBr^+ + O$	228
265	WBr^+	20.2	25.7 ± 0.5	$WBr^+ + 2O + Br$	305
216	WO_2^+-	17.0	15.8 ± 0.5	$WO_2^+ + 2Br$	168
200	WO^+	24.0	21.3 ± 0.5	$WO + 2Br + O$	236
184	W^+	10.4		$W^+ + 2Br + 2O$	
160	Br_2^+	1.6			
81	HBr^+	3.2			
80	Br^+	13.6			

(1) Relative intensity, electron energy 40 eV
(2) Appearance potential (eV)
(3) Heat of ion formation (kcal/mol)
$\Delta H_f^0 (WO_2Br_{2(g)}) = -141.3$ kcal/mol [41]

This reaction may take place during the preparation of WO_2Br_2 or during its evaporation. This latter pathway is confirmed by the appearance of Br_2^+ ions in the spectrum. Since according to the assumed decomposition mechanism, based on electron collision, no Br_2 is formed, the bulk of Br_2^+ must originate partly from reaction (8) and partly from the ionization of Br_2 formed by thermal dissociation at the cathode of the ion source at 2400 K. The low pressure during measurement favours the formation of ditungsten compounds by reaction (8). These experiments seem to indicate that molecules of the formula MO_2X_2 (where M = W or Mo) are evaporated mainly as MO_2X_2 molecules, with a minor part in the form of MO_4X_2, offering a direct proof of the octahedral structure, or, depending upon the experimental conditions (pressure, temperature) as $M_2O_4X_2$ molecules. This last process is accompanied by the formation of halogen vapour.

It appears from Tables I and II that the ionization potentials of MoO_2Br_2 and WO_2Br_2 due to electron collision are almost the same. Taking into consideration SINGLETON's results [29], it appears that the ionization potentials of the dioxy-dihalides of the elements in group VI/B depend only slightly upon the nature of the central metal atom.

III. 3. *Mass spectrum of $WOBr_4$*

It appears from the low resolution spectrum of $WOBr_4$ (Table III) that the intensity of the parent ion is only about 1% of the intensity of the $WOBr_3^+$ base peak. This low intensity is related to the d^0 structure [28]. The relative intensity distribution of the ions is similar to that reported earlier [29, 57]. In contrast to the dioxy-dibromides, the intensity of Br_2^+ is high, amounting in SINGLETON's measurements [29] to about 33% of that of the base peak.

Table III

Mass spectrum of $WOBr_4$
Temperature of the Knudsen cell 400 K

(m/e	Ion	(1)	(2)	Probable process	(3)
520	$WOBr_4^+$	1.2		$WOBr_4 \rightarrow WOBr_4^+$	
504	WBr_4^+	0.5		$WBr_4^+ + O$	
441	$WOBr_3^+$	100	10.5 ± 0.2	$WOBr_3^+ + Br$	103
425	WBr_3^+	7.5	17.9 ± 0.4	$WBr_3^+ + O + Br$	215
360	$WOBr_2^+$	39.2	14.5 ± 0.2	$WOBr_2^+ + 2Br$	170
344	WBr_2^+	16.4	20.9 ± 0.4	$WBr_2^+ + O + 2Br$	283
281	$WOBr^+$	14.7	18.3 ± 0.5	$WOBr^+ + 3Br$	230
265	WBr^+	12.8	26.1 ± 0.5	$WBr^+ + O + 3Br$	349
200	WO^+	5.9		$WO^+ + 4Br$	
184	W^+	7.0			
160	Br_2^+	17.0			
81	HBr^+	5.3			
80	Br^+	23.7			

(1) Relative intensity, electron energy 40 eV
(2) Appearance potential (eV)
(3) Heat of ion formation (kcal/mol)
$\Delta H^0_f(WOBr_{4(g)}) = -11.2$ kcal/mol [41]

The relative intensities of the isotope peaks of $WOBr_3^+$ *vs.* the mass number are shown in Fig. 7. In this case too the isotope ratios calculated from the Figure 7 are similar to those obtained by theoretical calculation (Table VII). The values of the appearance potentials obtained from the ionization efficiency curve (for $WOBr_3^+$, see Fig. 8) are in good agreement with GUPTA's results [57], except for the appearance potential of WBr_2^+. The assumed decomposition processes fail to explain the high Br_2^+ intensity. According to the experiments aimed at the clarification of the structure of $WOBr_4$ [58] in the solid state this last compound consists of chains of WBr_4 groups joined by oxygen bridges, thus, like in the case of WO_2Br_2 [56], di-

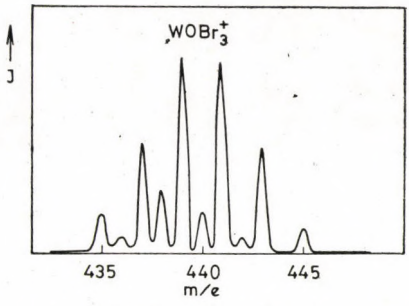

Fig. 7. Height of the base peak of $WOBr_4$ and of the isotope peaks of $WOBr_3^+$ *vs.* the mass number

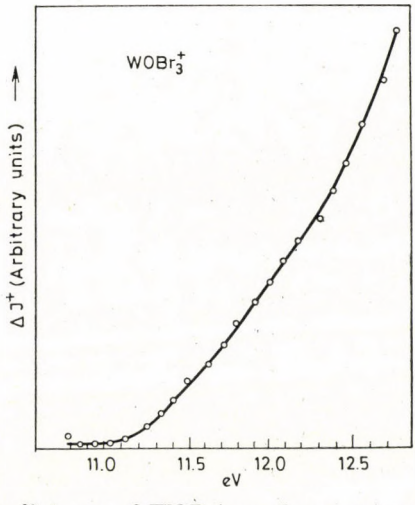

Fig. 8. Ionization efficiency of $WOBr_3^+$ *vs.* the uncorrected electron energy

tungsten compounds and Br_2 might be formed. (In fact, we were able to detect W_2Br_6 with the high resolution mass spectrometer in a relatively high intensity among the bromination products of tungsten.)

In addition, one should take into account thermal dissociation at the cathode of the source.

III. 4. *Mass spectrometric analysis of the bromination products of tungsten*

The spectra of the products of the transport reaction $W + Br_2$ in Ar as carrier gas were recorded by a high resolution mass spectrometer and the relative intensities calculated from the spectra were expressed in per cent of the total ion current (Table IV). It appears from the Table that beside the fragments of tungsten bromides, considerable quantities of ions originating from tungsten oxybromides are formed, which means that the presence of

Table IV

Mass spectra of the bromination products of tungsten
(Bromination in Ar stream, temperature of the ion source 373 K)

m/e	Ions formed, electron energy 40 eV	Relative intensity in % of total ion current
584	WBr_5^+	0.5
536	$WO_2Br_4^+$	0.1
428	$W_2Br_2^+$	0.2
520	$WOBr_4^+$	0.1
504	WBr_4^+	13.5
457	$WO_2Br_3^+$	0.4
448	W_2Br^+	0.1
441	$WOBr_3^+$	16.3
425	WBr_3^+	6.4
392	$WO_3Br_2^+$	1.6
376	$WO_2Br_2^+$	1.1
360	$WOBr_2^+$	8.2
344	WBr_2^+	9.8
312	WO_3Br^+	0.6
297	WO_2Br^+	0.5
281	$WOBr^+$	5.1
265	WBr^+	9.3
216	WO_2^+	0.2
200	WO^+	3.3
184	W^+	7.3
160	Br_2^+	6.5
81	HBr^+	0.7
80	Br^+	7.1

small amounts of oxygen during the reaction, or that is the bromination of insufficiently deoxydized tungsten, will lead to the formation of oxybromides. Of course, manipulation of the products might promote the tungsten bromide → tungsten oxybromide transformation. Nevertheless, comparison with the products of bromination in vacuum (when the end-product was treated and analyzed in exactly the same way) shows that the relatively large oxybromide contamination must be due to the conditions of preparation. In the present case (Table IV) the $I_{WBr_4^+}/I_{WOBr_3^+}$ ratio at the beginning of analysis was about 0.8 then increased after treatment at 100 °C for one hour to roughly 10, while heating for a few hours in vacuum (in the mass spectrometer) led to evaporation of the total amount of tungsten oxybromides,

leaving a residue, in whose mass spectrum, dimeric tungsten bromides of higher mass numbers occur in small quantities together with small amounts of WBr_5^+ and significant amounts of WBr_4^+ and their fragments. This indicates that the vapour pressure of the oxybromides formed as by-products at the temperature of measurements considerably higher than that of the corresponding bromides, consequently, the intensive oxybromide peaks represent in fact relatively low concentrations of the contaminants.

The data in Table IV further show that under the given conditions of bromination the main by-product is $WOBr_4$ (high $WOBr_3^+$ peak and high peaks of its fragments) and less WO_2Br_2 is formed (the peaks of $WO_2Br_2^+$ and its fragments are less intensive). The appearance of $WO_2Br_4^+$ ions and of its fragments ($WO_2Br_3^+$) is a result of the structure of $WOBr_4$ [58].

The results of bromination experiments in Ar as carrier gas show that in the case of halogen lamps, whose conditions of operation are similar to the conditions of this reaction, first of all the formation of tungsten oxybromides must be expected. This assumption is supported by the values of the free enthalpies of these compounds calculated on the basis of theoretical considerations by NEUMANN and KNATZ [20, 59], which show that in these systems the formation of oxybromides is accompanied by a far greater decrease in free enthalpy than is the formation of tungsten bromides.

When tungsten is brominated without carrier gas, as a result of the removal of oxides in high vacuum prior to the reaction, the mass spectrum indicates the formation of tungsten bromides almost completely free of oxybromides. The appearance of a small amount of oxybromide fragments at the beginning of recording ($I_{WBr_4^+}/I_{WOBr_3^+} \sim 10$) is due to some hydrolysis in the Knudsen cell. After treatment for 1 hr at 400 K the ions originating from the oxybromide fragments disappear from the mass spectrum. WBr_5^+ was the monotungsten bromide of the highest mass number and the most intensive peak pertained to WBr_4^+. The ratio $I_{WBr_4^+}/I_{WBr_5^+}$ was about 20. This ratio did not increase when the temperature of the cell was raised to 800 °K, and heat treatment caused a gradual decrease in the intensity of WBr_5^+ until, after 2 to 3 hrs, the entire amount of WBr_5 sublimed, as indicated by its presence in a relatively small quantity in the reaction product. The ditungsten bromides were present in readily measurable quantities with the highest mass number corresponding to $W_2Br_6^+$. Besides the fragments of WBr_2^+ and $W_2Br_6^+$, intensive peaks corresponding to Br^+ and Br_2^+ and less intensive peaks of HBr^+ ions also appeared. At the beginning of evaporation the relative ion currents calculated from the heights of the peaks were:

$$I_{WBr_4^+}/I_{Br} \sim 0.5; \quad I_{WBr_4^+}/I_{Br_2^+} \sim 12.5$$

$$I_{WBr_4^+}/I_{HBr^+} \sim 30$$

After the sublimation of the oxybromide and WBr_5 a product spectrum showing both WBr_4 and W_2Br_6 was recorded (Tables V and VI).

Table V

Mass spectrum of WBr_4
Temperature of the Knudsen cell 800 K

m/e	Ion	(1)	(2)	Probable process	(3)
504	WBr_4^+	44.3	8.2 ± 0.2	$WBr_4 \rightarrow WBr_4^+$	166
425	WBr_3^+	100.0	11.2 ± 0.2	$WBr_3^+ + Br$	208
344	WBr_2^+	50.3	15.1 ± 0.3	$WBr_2^+ + 2Br$	271
265	WBr^+	65.4	19.4 ± 0.3	$WBr^+ + 3Br$	343
184	W^+	85.0	23.2 ± 0.5	$W^+ + 4Br$	401

(1) Relative intensity, electron energy 30 eV
(2) Appearance potential (eV)
(3) Heat of ion formation (kcal/mol)
$\Delta H_f^0 (WBr_{4(s)}) = -58.6$ kcal/mol [21]
$\Delta H_{subl} (WBr_4) = 37.0$ kcal/mol [31]

Table VI

Mass spectrum of W_2Br_6
Temperature of the Knudsen cell 800 K

m/e	Ion	(1)	(2)	Probable process	(3)
848	$W_2Br_6^+$	54	9.0 ± 0.2	$W_2Br_6 \rightarrow W_2Br_6^+$	154
768	$W_2Br_5^+$	100	11.0 ± 0.2	$W_2Br_5^+ + Br$	174
688	$W_2Br_4^+$	31.4	15.2 ± 0.3	$W_2Br_4^+ + 2Br$	242
608	$W_2Br_3^+$	43.8	19.5 ± 0.3	$W_2Br_3^+ + 3Br$	314
528	$W_2Br_2^+$	20.4		$W_2Br^+ + 5Br$	
448	W_2Br^+	13.1		$W_2^+ + 6Br$	
368	W_2^+	6			

(1) Relative intensity, electron energy 30 eV
(2) Appearance potential (eV)
(3) Heat of ion formation (kcal/mol)
$\Delta H_f^0 (W_2Br_{6(g)}) = -53.5$ kcal/mol [31]

The intensity ratio of the base peaks is

$$I_{WBr_4^+}/I_{W_2Br_6} \sim 2.5$$

The mass spectra of the ions WBr_4^+ and $W_2Br_6^+$ recorded by means of the double-focussing mass-spectrometer are shown in Figs 9 and 10.

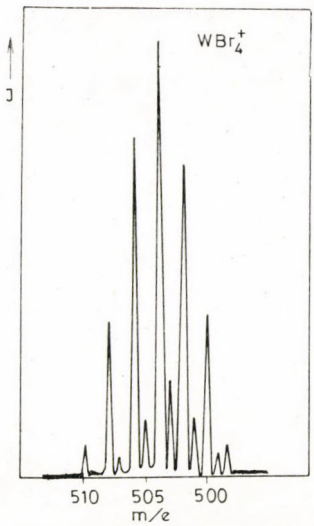

Fig. 9. Height of the isotope peaks of WBr_4^+ *vs.* the mass number

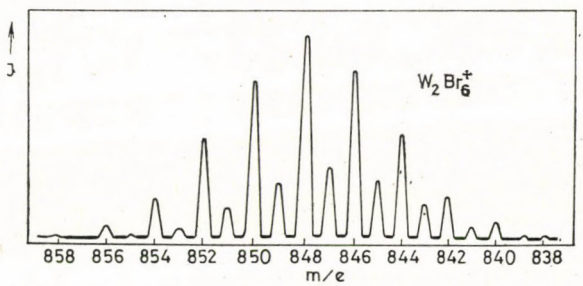

Fig. 10. Mass spectrum of the molecular peaks of $W_2Br_6^+$ recorded by means of the high resolution mass-spectrometer

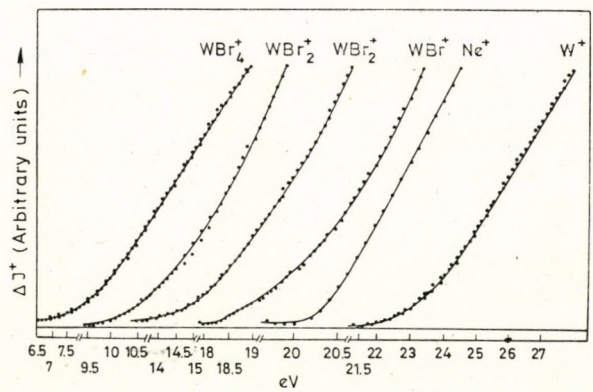

Fig. 11. Ionization efficiency of WBr_4^+ and its fragments *vs.* the uncorrected electron energy

There is a fairly good agreement between the isotope ratios calculated theoretically and obtained from the heights of the peaks (Table VII). Figures 11 and 12 are the ionization efficiency curves of WBr_4^+ and $W_2Br_6^+$ and its fragments, respectively. It appears from these curves that molecular ions of lower mass numbers than WBr_4 and W_2Br_6 can be disregarded in the calculations, *i.e.* no tungsten compounds of lower oxidation state than WBr_4 are formed in significant quantities during the bromination of tungsten.

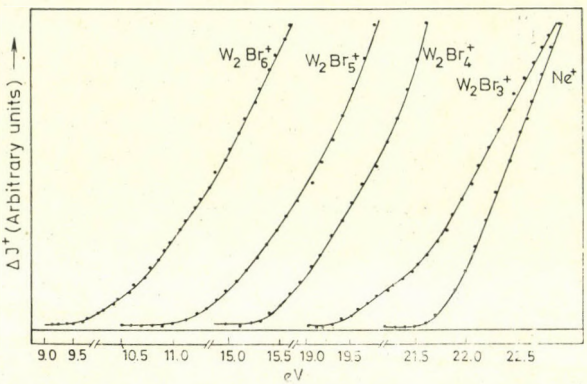

Fig. 12. Ionization efficiency of $W_2Br_6^+$ and its fragments *vs.* the uncorrected electron energy

The appearance potential of Br_2 was determined to give a value of 10.9 ± 0.2 eV. This is in good agreement with the value reported for $IP(Br_2^+)$ [33], confirming that Br_2 originates from a chemical reaction (9) rather than from fragmentation due to electron collisions, since the latter would produce a far higher $AP(Br_2^+)$ value. The low values of $IP(WBr_4^+)$ (8.2eV) and $IP(W_2Br_6^+)$ (9.0 eV) unambiguously show the presence of molecular ions, *i.e.* tungsten bromides of higher mass numbers, which produce the above ions *via* fragmentation, but could not have been present in any significant quantity at the time of recording.

Literature data [4, 40, 48] suggest that the bromination of tungsten at 450—500 °C leads to WBr_5, which is reduced by tungsten to WBr_4 under the effect of the temperature gradient. In our experiments performed without carrier gas at a temperature gradient of 600—200 °C (the temperature in the middle of the reaction space was 600 °C and 200 °C at both ends) in vacuum, in the presence of a large excess of W wool, the reaction

$$WBr_5 \xrightarrow{W} WBr_4$$

was almost quantitative. In addition, there is a possibility of disproportionation of the primarily formed WBr_5, since the conditions of high vacuum favour this process [60]. This proves that WBr_4^+ is not a fragment of WBr_5^+ and that

Table VII

Relative amounts of some intensive isotope peaks in per cent of the most intensive isotope peak, theoretically calculated and determined experimentally from the observed peak heights

Compound	m/e	Calculated	Experimental
MoO_2Br_2	284	52.0	50.6
	286	66.0	66.6
	288	90.0	90.7
	290	100.0	100.0
	292	58.2	57.2
WO_2Br_2	372	23,4	23,8
	372	72.3	73.4
	376	100.0	100.0
	378	75.1	74.6
	380	24.1	23.5
$WOBr_3^+$	437	55.1	54.5
	439	98.7	98.7
	441	100.0	100.0
	443	56.5	57.0
WBr_4	500	34.6	36.0
	502	77.6	76.2
	504	100.0	100.0
	506	78.5	77.5
	508	35.1	35.6
W_2Br_6	844	53.2	51.9
	846	86.0	84.8
	848	100.0	100.0
	850	83.7	82.3
	852	51.0	50.5

WBr_5^+ appears in a very low intensity only, furthermore, after heat treatment in vacuum it disappears completely from the spectrum.

The appearance of cluster compounds containing metal-metal bonds also support the formation of WBr_4. The formation of such compounds has been observed with tungsten compounds of the oxidation state of four or lower, but never in the case of tungsten of higher valency [61, 62]. RINKE and SCHAFFER [63] were the first to detect such dimers with metal-metal bonds in tungsten halides in the form of W_2Cl_6 by means of mass spectrometry, but only from WCl_4 and not from WCl_5.

Our experiments provide unequivocal evidence for the existence of the cluster compound W_2Br_6 containing a metal-metal bond.

We have not detected $W_3Br_9^+$ ions or its fragments, which would have indicated the presence of trinuclear clusters. We have assumed that W_2Br_6 is formed in the reaction

$$2\ WBr_{4(s)} \rightarrow W_2Br_{6(s)} + Br_{2(g)} \tag{9}$$

This concept is supported by the appearance of Br_2 in the spectrum, formed *via* a chemical reaction. The thermodynamic parameters of this reaction were determined mass-spectrometrically from the temperature dependence of the partial pressure of Br_2 [31]. It follows from Eq. (9) that decreasing pressure will shift the reaction in the direction of the upper arrow, resulting in the appearance of dimeric ions in higher intensities upon bromination without carrier gas. In our experience higher temperatures of the evaporator also favour the formation of W_2Br_6. In tungsten bromides of lower oxidation state, polymeric tungsten bromides have also been observed [64], such as the polymer of WBr_2, *viz.* W_6Br_2 which, when treated with liquid bromine at various temperatures, is transformed into a series of compounds containing the cluster nucleus W_6Br_8 with an apparent valency of 2.33 for tungsten. We also observed a conversion of these compounds in vacuum accompanied by the evolution of Br_2.

III. 5. *Calculation of thermostatic parameters from the experimentally determined ionization and appearance potentials*

The heats of formation of ions shown in Tables I, II, III, V and VI were calculated in the following manner: in the general case a fragmentation reaction due to electron collision proceeds as follows:

$$R_1R_2 + e \rightarrow R_1^+ + R_2 + 2e \tag{10}$$

For this reaction the following correlation is valid:

$$AP(R_1^+) = \Delta H_r = \Delta H_f(R_1^+) + \Delta H_f(R_2) - \Delta H_f(R_1R_2) \tag{11}$$

where AP is the appearance potential, ΔH_r the heat of the reaction and ΔH_f the corresponding heat of formation.

From the appearance potentials and heats of ion formation shown in the Tables conclusions can be drawn on the strength of the various bonds in the ions, assuming that the ions are formed without excess energy [33].

In the general case the decomposition of the molecular ion can be modelled by means of the following reaction

$$R_1R_2^+ \rightarrow R_1^+ + R_2 \tag{12}$$

$$D = AP(R_1^+) - IP(R_1R_2^+) = \Delta H_f(R_1^+) + \Delta H(R_2) - \Delta H_f(R_1R_2^+) \tag{13}$$

where D is the bond dissociation energy, IP and AP are the ionization and appearance potentials, respectively, and ΔH_f are the corresponding heats of formation. For instance from the reaction

$$MoO_2Br_2^+ \rightarrow MoO_2^+ \rightarrow 2Br$$

$$1/2\ D(MoO_2 - Br_2) = 57.5\ \text{kcal/mol}.$$

We calculated the bond strengths of individual Br and O atoms in the various ions and since these showed no significant differences for ions of various compositions but containing the same atoms, we took the average bond energy of the given atom in the ions. The results are summarized in Table VII.

The assumption that the bond strengths of the individual atoms are equal in the ions, regardless of the oxidation state of the central atom, that is, *e.g.*

$$D(WBr_3^+ - Br) = \frac{1}{2} D(WBr_2^+ - Br_2) = \frac{1}{3} D(WBr^+ - Br_3) = \frac{1}{4} D(W^+ - Br_4)$$

is only a rough approximation [33, 65], though sufficient (as confirmed by the data in Table VIII) for the comparison of the average bond strengths of identical atoms in ions formed from various compounds by electron collision.

Table VIII

Average bond strengths in various ions

Ion	Bond	kcal/mol
$MoO_2Br_2^+$	MoO_2Br^+–Br	56.3
	$MoOBr_2^+$–O	146.0
$WO_2Br_2^+$	WO_2Br^+–Br	50.6
	$WOBr_2^+$–O	139.0
$WOBr_3^+$	$WOBr_2^+$–Br	87.0
	WBr_3^+–O	173.6
WBr_4^+	WBr_3^+–Br	86.0
$W_2Br_6^+$	$W_2Br_5^+$–Br	80.6

In addition, since in many cases there is a fairly good agreement between the average bond strengths in ions and in neutral molecules [33], it is possible to estimate from the data in Table VIII the bond strengths of Br and O atoms in the corresponding neutral molecules too.

In order to calculate the average bond strength referred to one Br atom in the neutral WBr_4 molecule it is necessary to known the ionization potential of W and its appearance potential in the spectrum of WBr_4. The value of $IP(W^+)$ is 8.0 eV [33] and $AP(W^+) = 23.1$ eV (Table V). The calculation is performed as follows:

$$WBr_{4(g)} \rightarrow W^+ + 4\ Br_{(g)} \tag{14}$$

$$AP(W^+) = IP(W^+) + 4\ D(W—Br) \tag{15}$$

$$23.1 = 8.0 + 4\ D(W—Br) \tag{16}$$

$$D(W—Br) = 3.8\ eV = 87.4\ kcal/mol$$

For $1/4\ D(W^+—Br_4)$, 86.0 kcal/mol is obtained. The very good agreement between the two values confirms the validity of our earlier assumption.

Finally, from the values of the ionization and appearance potentials, with the exception of $WOBr_4^+$ whose ionization potential could not be calculated because of its low intensity, we determined the activation energies ($\Delta H^{\ddagger}$) of the decomposition of the molecular ions [33]. In the general case the decomposition of a molecular ion can be written as

$$X^+ \rightarrow Y^+ + Z \tag{17}$$

The sum of the activation energy and that heat of this reaction is

$$AP(Y^+) - IP(X^+) = \Delta H_{exp} \tag{18}$$

where $AP(Y^+)$ is the appearance potential of the ion Y^+ in the mass spectrum of X and $IP(X^+)$ is the ionization potential of X^+, while the heat of the reaction ΔH_R can be expressed as

$$\Delta H_r = \Delta H_f(Y^+) + \Delta H_f(Z) - \Delta H_f(X^+) \tag{19}$$

Hence, the activation energy of reaction (17) is

$$\Delta H^{\ddagger} = \Delta H_{calc} - \Delta H_R \tag{20}$$

The results are summarized in Table IX. It appears that in the case of the molecular ions of molybdenum and tungsten oxybromides and tungsten bromides the activation energy of the decomposition accompanied by the formation of Br atoms is zero or a very low positive value.

Table IX

Activation energy of the decomposition of molecular ions

Process	$\Delta H^{\ddagger}$ (kcal/mol)
$MoO_2Br_2^+ \rightarrow MoO_2Br^+ + Br$	1.2
$WO_2Br_2^+ \rightarrow WO_2Br^+ + Br$	4.4
$WBr_4^+ \rightarrow WBr_3^+ + Br$	0
$W_2Br_6^+ \rightarrow W_2Br_5^+ + Br$	1

The mass spectra of MoO_2Br_2, WoO_2Br_2, $WOBr_4$, WBr_4 and W_2Br_6 have furnished some additional, previously lacking data for inorganic mass spectrometry. The experimental data permit conclusions with respect to the evaporation of these compounds and the calculation of thermodynamic parameters from the values of the ionization and appearance potentials. The Knudsen effusion mass spectrometry has provided some important additional thermodynamic data. The results of these experiments will be reported elsewhere. [31]

*

The authors wish to thank Professor J. MARSEL, Head, Department of Mass Spectrometry, Jozef Stefan Institute (Ljubljana, Yugoslavia) for the material and moral support of this research. Our thanks are due to Dr. V. KRAMER, Jozef Stefan Institute, for the recording of the high resolution spectra, and to Mr. J. HODÁCS, Research Department, Tungsram, Ltd., Budapest, for help in the preparative work.

REFERENCES

[1] NORTHCOTT, L.: Metallurgy of the Rarer Metals. No. 5. Molybdenum. Butterworths, London 1956
[2] RIECK, G. D.: Tungsten and its Compounds. Pergamon Press, Oxford 1967
[3] BREWER, L., BROMLEY, L. A., GILLES, LOFGREN N. L.: The Chemistry and Metallurgy of Miscellaneous Materials. Ed. L. L. Quill, McGraw-Hill, New York 1950
[4] FERGUSSON, J. E.: Halide Chemistry of Chromium, Molybdenum and Tungsten in Halogen Chemistry, 3. Ed. V. Gutmann, Academic Press, London, New York 1967
[5] CANTERFORD, J. H., COLTON, R.: Halides of the Second and Third Row, Transition Metals. Wiley, London 1968
[6] ZUBLER, E. G., MOSBY, F. A.: Ill. Eng., **54,** 734 (1959)
[7] T'JAMPENS, G. R., VAN DER WEIJER, M. H. A.: Phillips Techn. Rev., **27,** 165 (1966)
[8] MOSBY, F. A., SCHUPP, L. J., STEIMER, G. G., ZUBLER, G.: Ill. Eng., **62,** 198 (1967)
[9] TILLACK, J., ECKERLIN, P., DETTINGMAYER, J. H.: Angew. Chem., **78,** 4512 (1966)
[10] RABENAU, A.: Angew. Chem., **79,** 43 (1967)
[11] SCHAFER, H.: Chemische Transportreaktionen. Symposium Reinstoffe in Wissenschaft und Technik. Dresden 1970
[12] KAPOSI, O., RIEDEL, M., DEUTSCH, T.: Acta Chim., (Budapest) **81,** 43 (1974)
[13] DEUTSCH, T.: Thesis, Eötvös L. University, Budapest 1973
[14] KAPOSI, O., RIEDEL, M., SÁNCHEZ, R. G.: Magy. Kém. Foly., **80,** 419 (1974)
[15] KOPELMAN, B., VAN DER WORMER, K. A.: Ill. Eng., **63,** 176 (1968)
[16] KOPELMAN, B., VAN DER WORMER, K. A.: Ill. Eng., **64,** 230 (1969)
[17] YANNOPOULOS, N., PEBLER, A.: J. Appl. Phys., **42,** No. 2, 258 (1971)
[18] HANGOS, I., DEUTSCH, T.: Kém. Közl., **37,** 459 (1972)
[19] Janaf Thermochemical Tables and Addenda I—III. Dow Chemical Corp., Middland, Michigan 1965—68
[20] NEUMANN, G. M., KNATZ, W.: Naturforsch. **26a,** 863 (1971)

[21] NEUMANN, G. M.: Z. Metallkunde, **64**, 26, 117, 193, 279, 444 (1973)
[22] ZUBLER, E. G.: J. Phys. Chem., **74**, 2479 (1970)
[23] NEUMANN, G. M., MÜLLER, U.: J. Less-Common Metals, **26**, 391 (1972)
[24] ZUBLER, E. G.: J. Phys. Chem., **76**, 320 (1972)
[25] ROSNER, D. E., ALLENDORF, H. D.: J. Phys. Chem., **75**, 308 (1971)
[26] ABBOTT, P. C., STICKNEY, R. E.: J. Phys. Chem., **76**, 2930 (1972)
[27] ROSNER, D. E.: Ann. Rev. Materials Science, **2**, 573 (1972)
[28] LINSEN HSIA NGAI, STAFFORD, F. E.: Gaseous Oxohalides, Hydroxides and Complex Oxides of Group III and Transition Elements. Advances in High Temperature Chemistry. V/3. Academic Press, New York 1971
[29] SINGLETON, D. L.: Dissertation, Northwestern University 1971
[30] DROWART, J.: Mass Spectrometry and High Temperature Chemistry. Mass Spectrometry. Ed. J. Marsel. Ljubljana 1971
[31] KAPOSI, O. *et al.:* To be published
[32] MARGRAVE, J. L.: The Characterization of High Temperature Vapors. Wiley, New York 1967
[33] FIELD, F. H., FRANKLIN, J. L.: Electron Impact Phenomena. Academic Press, New York 1970
[34] WINTERS, R. E., COLLINS, J. H., COURCHENE, W. L.: J. Chem. Phys., **45**, 1971 (1966)
[35] ROBOZ, J.: Mass Spectrometry. Wiley, New York 1968
[36] COLTON, R., TOMKINS, J. B.: Austr. J. Chem., **18**, 447 (1965)
[37] GMELIN's Handbuch der Anorganischen Chemie. Molybdän, **53**, Verlag Chemia, 1935
[38] OPPERMANN, H.: Z. Anorg. Allg. Chem., **379**, 362 (1970)
[39] ROSCOE, H. E.: J. Liebigs Ann. Chem., **162**, 349 (1872)
[40] SHCHUKAREV, A. S., KOKOVIN, G. A.: Russ. J. Inorg. Chem., **9**, 1303, 1565 (1964)
[41] OPPERMANN, H., STÖVER, G.: Z. anorg. allg. Chem., **383**, 14 (1971)
[42] POURAND, M., CHAIGNEAU, M.: Compt. Rend., **249**, 2568 (1959)
[43] HESS, H., HARTUNG, H.: Z. anorg. allg. Chem., **344**, 157 (1966)
[44] COLTON, R., TOMKINS, J. B.: Austr. J. Chem., **21**, 1975 (1968)
[45] TILLACK, J., KAISER, R.: Angew. Chem. Int. Ed., 7142, 294 (1968)
[46] KOKOVIN, G. A.: Russ. J. Inorg. Chem., **12**, 7 (1967)
[47] COLTON, R., TOMKINS, J. B.: Austr. J. Chem., **19**, 759 (1966)
[48] SHCHUKAREV, A. S., NOVIKOV, G. J., KOKOVIN, G. A.: Russ. J. Inorg. Chem., **4**, 2185 (1959)
[49] MCCARLEY, R. E., BROWN, T. M.: Inorg. Chem., **3**, 1232 (1964)
[50] HILDEBRAND, D. L., KRAMER, W. R., MCDONALD, R. A., STULL, D. R.: J. Amer. Chem. Soc., **80**, 4129 (1958)
[51] MCCARLEY, R. E., BROWN, T. M.: J. Amer. Chem. Soc., **84**, 3216 (1962)
[52] SCHAFER, H., SCHNERING, H. G., TILLACK, J., KUHNEN, F., WÖHRLE, H., BAUMANN, H.: Z. anorg. allg. Chem., **353**, 281 (1967)
[53] JOLLY, W. Z.: Preparative Inorganic Reactions, J. Wiley Interscience, New York 1971
[54] SIEPMANN, R., SCHAFER, H.: Naturwissenschaften, **52**, 344 (1965)
[55] WEAST, R. C.: Handbook of Chemistry and Physics. 51st ed., 1970—71
[56] BARRACLOUGH, C. G., STALS, J.: Aust. J. Chem., **19**, 741 (1966)
[57] GUPTA, S. K.: J. Phys. Chem., **75**, 112 (1971)
[58] HESS, H., HARTUNG, H.: Z. anorg. allg. Chem., **344**, 157 (1966)
[59] NEUMANN, G. M., KNATZ, W.: Z. Naturforsch., **26a**, 1046 (1971)
[60] ROBINSON, B. H., FERGUSSON, J. E., WILKINS, C. J.: Unpublished results
[61] FERGUSSON, J. E.: Metal–Metal-Bonded Halogen Compounds of the Transition Metals. W. L. JOLLY: Preparative Inorganic Reactions, **7**, Wiley Interscience, New York 1971
[62] BAIRD, M. C.: Metal–Metal-Bonds in Transition Metal Compounds. Progress in Inorganic Chemistry **9**, Wiley Interscience, New York 1968
[63] RINKE, K., SCHAFER, A.: Angew. Chem., **79**, 650 (1967)
[64] SCHAFER, H., SIEPMANN, R.: Z. anorg. allgem. Chem., **357**, 273, 289 (1968)
[65] MARGRAVE, J. L.: Mass Spectrometry in Inorganic Chemistry. Am. Chem. Soc. Publication, New York 1968

Olivér KAPOSI; H-1088 Budapest, Puskin utca 11—13.
Tibor DEUTSCH; H-1045 Budapest, Tó u. 1—5.
Arkady POPOVIĆ, Joze PEZDIĆ } Ljubljana, Yugoslavia Jamova 39.

Acta Chimica Academiae Scientiarum Hungaricae, Tomus 89 (2), pp. 123—136 (1976)

KINETICS OF ETHANE DEHYDROGENATION ON α-Cr_2O_3 CATALYST, I

THE RATE-DETERMINING STEP

P. KŐNIG and P. TÉTÉNYI

(Institute of Isotopes of the Hungarian Academy of Sciences, Budapest)

Received April 17, 1975

Dehydrogenation of ethane has been studied on α-chromia catalyst, in a circulation reactor, between 0 and 4 kN m^{-2} pressures and in the temperature range between 430 and 580 °C. Several chemical processes take place on the catalyst under these conditions; in addition to gaseous products (H_2, C_2H_4 ,CH_4) surface deposits are also formed; the composition of the latter depends on the activity of the catalyst and the temperature. By appropriate pretreatment and regeneration of the catalysts, it was possible to perform kinetic experiments on catalysts of practically constant activity. The temperature dependence of the initial rate of dehydrogenation, the kinetic isotope effect and the relative rates of dehydrogenation and D–H exchange indicate that the rate of ethane dehydrogenation is limited by the surface reaction.

Introduction

The dehydrogenation of hydrocarbons on catalysts containing chromia is of considerable interest from both theoretical and industrial viewpoints. In spite of the large amount of experimental data available, there is no uniform opinion concerning the kinetics of the reactions. Corresponding to practical requirements, kinetic experiments have been limited to dehydrogenation of C_4 hydrocarbons [1—8] and cyclohexane [9—16].

DODD and WATSON suggested a so-called 'dual-site' mechanism for butane dehydrogenation with the surface reaction as the rate-determining step [1]. On the other hand, BALANDIN put forward a 'single site' mechanism; he believed that the rate-determining step was the associative adsorption of butane [2, 3]. The work of CARRÀ and FORNI [8] supports the former opinion. Applying the method of stoichiometric numbers to his own [4, 5] and BALANDIN's results, HAPPEL has come to conclusions which differ from both concepts mentioned. Investigating the dehydrogenation of isobutane by the same method, he has found a single rate-determining step, which is the associative chemisorption of the hydrocarbon [7].

The rate-determining step of the three-step dehydrogenation of cyclohexane [15] is also the adsorption of cyclohexane but there is no uniform opinion whether this adsorption is associative [13, 14] or dissociative [16]; there were also arguments about the form of the rate equation [8—13].

The catalysts for the kinetic experiments mentioned were different: partly α-chromia, partly alumina-supported chromia of various origins and compositions. The preparation and pretreatment of the catalysts used by different authors show large variations, which may have contributed to the lack of a common kinetic picture. The chemisorption and catalytic properties of α-chromia are dependent to a high degree on the method of preparation — first of all on the conditions of heat treatment [17, 18] and of the activation in hydrogen [19] as well as on the amount of residual water in the catalyst [20]. For supported catalysts, an additional uncertainty may be caused by the fact that pretreatment and activation lead to the formation of a solid solution phase whose composition and dispersity may be different [21]. The catalytic activity of these is determined by their — various — chromium contents [22, 23]. The presence of alkali and alkaline earth metals — which cannot be avoided in industrial catalysts — leads to other complications [24, 25].

Considering all these, it seemed expedient to study the catalytic dehydrogenation of hydrocarbons choosing a model reaction as simple as possible, a reproducible catalyst and reproducible reaction conditions. Although the equilibrium conversion of the simplest hydrocarbon that can be dehydrogenated (ethane) is extremely low in the practicable temperature region [26], the experimental difficulties due to this fact are compensated by the small number of possible side reactions. Similarly, the knowledge of the structure and surface properties of α-chromia [19, 27, 28] which can be prepared in a way producing a uniform structure may compensate the experimental drawback caused by the relatively rapid deactivation of this catalyst [21].

Experimental

Apparatus

Experiments were carried out in a glass circulation apparatus described elsewhere [29], having a volume of 204.3 cm^3. The temperature of the quartz reaction vessel was maintained with an accuracy of ± 0.5 °C by means of an electrical oven connected to a thyristor control unit.

Analysis

Sampling was done using an evacuable sampling stopcock 0.34 cm^3 in volume, installed into the gas circuit. Upon turning the stopcock, the sample was flushed by a nitrogen stream (flow rate 0.8 $cm^3\ s^{-1}$) into a chromatographic column (length: 2 m, I.D. 5 mm) containing activated SiO_2 (Carlo Erba 510/1100). The column temperature was 125 °C. Two detectors, a katharometer and a flame ionization detector, were connected in series after the column. The smallest amounts to be measured with a fair reproducibility were: 5.25×10^{-10} mol of hydrogen and 4.53×10^{-12} mol of ethane. Calibration was done by pressure measurement, using an absolute manometer; the combined average error of sampling and analysis was $\pm 1.6\%$ on the F.I.D. and $\pm 2.0\%$ on the katharometer. Retention times for the components in routine kinetic analyses were as follows: H_2 48 s; CH_4 58 s; C_2H_6 125 s; C_2H_4 185 s.

The analysis of deuterated hydrocarbons was performed on a DuPont 21490 B mass spectrometer, from the corresponding fraction of the mixture separated on the chromatographic column. Spectrum evaluation was done by a multiple regression computer program, using an ICT 1905 machine [30].

Catalyst

The catalyst was prepared by thermal decomposition of $(NH_4)_2Cr_2O_7$ ("Reanal", p.a. grade) in a thin layer; the product was dehydrated in air at 680 °C for 6 hrs. Both DTA and X-ray diffraction showed that the product was entirely crystalline α-Cr(III)oxide. Its IR absorption spectrum corresponded to that reported by MARSHALL *et al.* [31]. Its specific surface was 16.2 $m^2\ g^{-1}$ (determined on a Sartorius microbalance using the BET method, with N_2 as adsorbent).

Materials

Hydrogen: Cylinder hydrogen was deoxygenated and dehydrated by passing through a Pd/SiO_2 catalyst then cooling it in a liquid nitrogen trap. It was collected in a vessel and passed through a Pd/Ag membrane before use.

Oxygen: $KMnO_4$ (p.a. "Merck") was thermally decomposed, then the gas condensed into a liquid nitrogen trap and distilled.

Ethane: FLUKA pss. grade (ethane 98%, impurities: ethylene, propane, propylene), purified as follows: a "finger" (I.D. 3 cm, length 25 cm) was filled with activated SiO_2 and evacuated; then ethane was frozen into this vessel. After slow distillation, the middle fraction (between 25 and 75%) contained less impurities than 0.1 ppm.

Ethylene: FLUKA pss. grade, purified like ethane.

Deuteroethane: "Isocommerz", Dresden. C_2D_6 content 92%, the rest mainly C_2D_5H, and traces of less deuterated ethane species.

Experimental

0.02—0.1 g catalyst of 0.1—0.2 mm particle size was placed into the upward branch of a U-shaped quartz reactor tube between quartz wool plugs, slightly pressed, in order to avoid "channeling". Preparation and regeneration was carried out as follows.

The catalyst was maintained at 600 °C in an atmosphere of oxygen pressure 7 kN m^{-2} for 3 hrs; CO_2 and H_2O produced were frozen in a trap with liquid nitrogen. Afterwards it was pumped out at the same temperature for 6—8 hrs (final pressure 10^{-3} N m^{-2}). The catalyst was then activated in hydrogen (7 kN m^{-2}) at 480 °C for 3 hrs with the water produced frozen out, then it was pumped out until final pressure reached the value mentioned (3—4 hrs).

The reaction mixture was prepared in the mixing chamber by introducing components of given pressure: its exact composition was determined in the chromatograph after homogenization for 10—15 min. This was followed by passing the circulating mixture through the catalyst chamber; the gas composition was followed by sampling at 5 min intervals. The evaluation of the chromatograms was performed by measuring peak heights since a statistical comparison of all practicable methods showed this to be the most accurate. A carbon and hydrogen balance was calculated for each run on the ICT 1905 computer, using corresponding time—peak height—reaction temperature—room temperature data as input values, together with chromatographic factors checked before each run and considering the temperature gradient in the apparatus as well as the error caused by sampling. The average error of such balances for the empty reactor was ±0.5%. The output of the balance — that is the distribution of the total quantity of the reaction mixture among the various chemical species — served as the basis for calculating the reaction rate while the deficit made it possible to determine the amount and composition of deposits formed on the catalyst.

Results

Temperature and pressure limits of the experiments

The temperature for 50% equilibrium conversion of ethane dehydrogenation is 720 °C [32]. Chromia catalysts, however, suffer intense ageing in a reducing atmosphere above 580 °C and this process becomes irreversible above 650 °C [33]. Consequently, reproducible measurements can only be performed below 580 °C. Considering, furthermore, that the effect of the

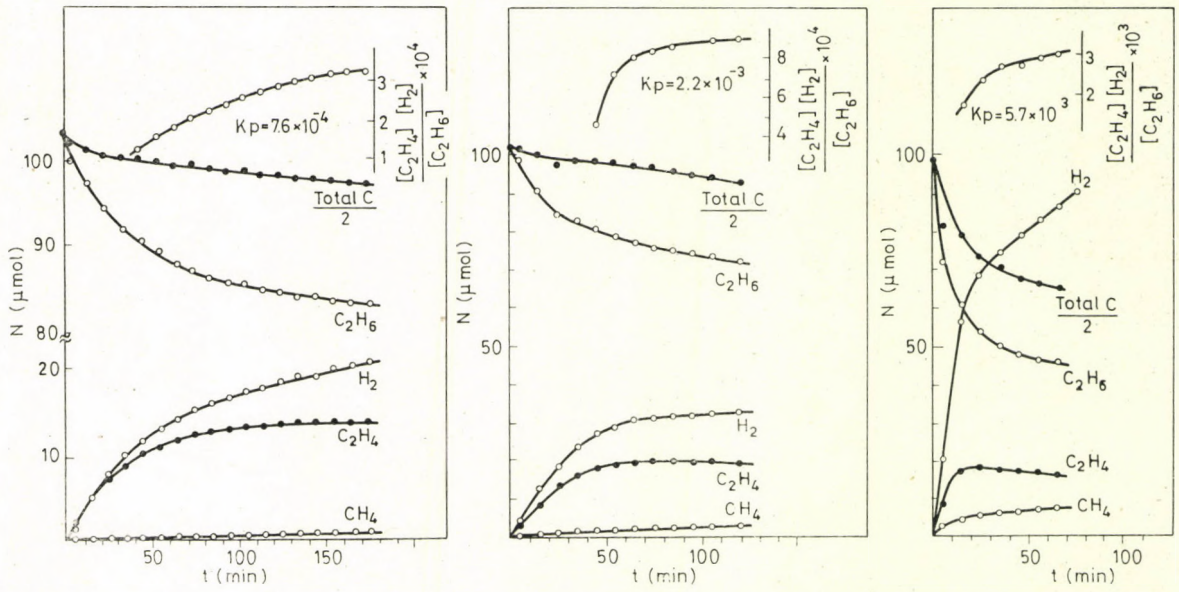

Fig. 1. Composition of the reaction mixture and the value of the apparent equilibrium constant for ethane dehydrogenation on α-Cr_2O_3. Catalyst weight: 0.125 g, $P_{ethane} = 1.30 \pm 0.03$ kN m^{-2}; *a*: t = 450 °C; *b*: t = 488 °C; *c*: *t* = 525 °C

reverse reaction can only be avoided if the conversion is below 10% of the equilibrium value, the equilibrium data permit to calculate the temperature and pressure range in which the experimental results can be readily evaluated. On the basis of the experimental error, the lowest conversion to be evaluated is 1.5% (that is, the equilibrium conversion should exceed 15%) and this may be realized above 450 °C and below 4 kN m^{-2}. Thus, kinetic experiments were carried out between 450 and 580 °C and in the pressure range of 0—4 kN m^{-2}.

Product distribution

Figure 1 shows the transformation of ethane on a freshly activated catalyst at different temperatures. The data indicate that the overall process must consist of several reactions. In addition to dehydrogenation, hydrogenolysis and a third, hydrogen-producing process also take place, since ethylene

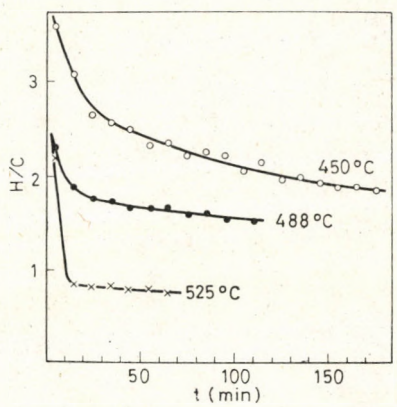

Fig. 2. Variation of the composition of the deposit for ethane dehydrogenation on α-Cr_2O

and hydrogen are not formed in a stoichiometric ratio. The latter two side reactions occur also in the quasi-steady-state region, where dehydrogenation and hydrogenation are approximately in equilibrium. Therefore, as shown in the figure, the apparent equilibrium constant is lower than the value given in the literature [26].

No other product could be found in the gas phase, thus the deficit of the material balance must be connected with deposits on the catalyst surface. Its composition, as calculated from the mass balance (Fig. 2), was near to that of ethane, (H/C = 3) in the initial stages, but as the reaction proceeded, it contained less and less hydrogen.

The rates of competing processes can be evaluated from selectivity values calculated from initial reaction rates (Table I).

Table I

*Selectivity values for different transformation of ethane**

	450 °C	488 °C	525 °C
C_2H_4	0.76	0.77	0.46
CH_4	0.004	0.015	0.071
dep.	0.23	0.21	0.47

* Selectivity: $\alpha_i = \frac{r_i^0/\nu_i}{\sum_{i=1}^{n} r_i^0/\nu_i}$ where r_i^0 is the initial reaction rate; ν_i the stoichiometric coefficient of the reaction; n the number of reactions

Catalytic activity

As expected from the high selectivity of deposit formation (α_{dep}), the catalyst becomes poisoned during dehydrogenation. On evacuating the reaction vessel after reaction, the catalytic activity decreases to a fraction of its initial value and even a prolonged activation procedure cannot restore its original level. It can be concluded, however, from Figure 1 that deposit formation depends in a reverse sense on hydrogen coverage of the surface. Evacuation removes mobile hydrogen species from the surface and this, in turn, may promote further loss of hydrogen from immobile deposits, producing "coke" which cannot be removed by evacuation. Indeed, if the reaction is terminated by introducing hydrogen in a large excess with simultaneous freezing out of the hydrocarbons, a considerable activity can be restored.

Figure 3 shows the decrease of the catalytic activity measured at 450 °C caused by identical amounts of ethane (1 kN m^{-2}) reacting for periods of various duration. The catalyst was regenerated in a great excess (10 kN m^{-2}) of hydrogen at the reaction temperature for 1 hr. Disregarding the initial rapid decay, the catalytic activity decreased in proportion to the reaction time, with the selectivity unchanged. An oxygen treatment of the catalyst after about 30 hrs of operation produced considerable amounts of carbon dioxide, but the catalytic activity increased only slightly. This indicates that the activity change observed may be analogous to the activity decrease of Cr_2O_3/Al_2O_3 catalysts in a reducing atmosphere [33]. This latter was attributed — at least partly — to the growth of Cr_2O_3 crystallites, corresponding to the decrease of the surface area in the case of α-chromia. It was possible to determine the BET surface of the catalyst 'in situ' in the reaction chamber using methane as the adsorbate at —196 °C and applying the F.I.D. as the pressure gauge. Taking the surface requirement of the methane molecule to be equal to 1.64×10^{-19} m^2 [34], the surface areas obtained were about 20% less than

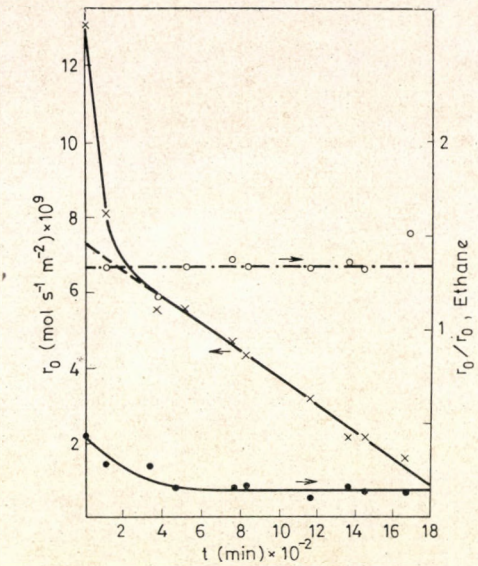

Fig. 3. Rate of formation of ethylene (×), methane (●) and hydrogen (○) (the latter two related to the former) as a function of the duration of reaction from catalyst activation.
Catalyst: 0.043 g α-chromia, $t = 450$ °C,
$P_{\text{ethane}} = 1.0$ kN m^{-2}

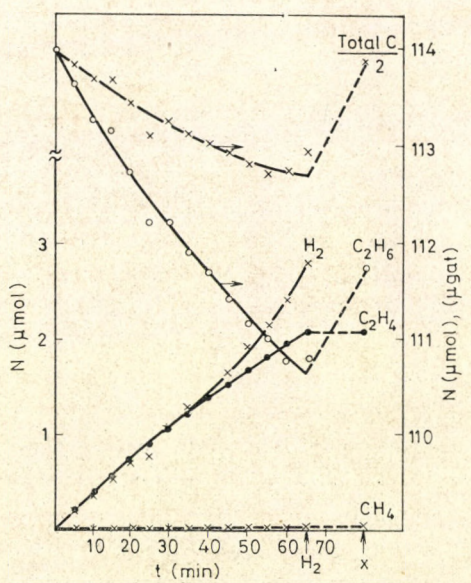

Fig. 4. Variation of the composition of the reaction mixture for ethane dehydrogenation on stabilized α-Cr_2O_3.
Catalyst: 0.0689 g (1.12 m^2), $t = 527$ °C,
$P = 1.19$ kN m^{-2} ethane

those determined by N_2/BET, but these values were reproducible within $\pm 2\%$. On keeping the catalyst in hydrogen for about 500 hrs, the catalytic activity decreased by about two orders of magnitude but the surface remained the same within the limits of experimental error.

On repeating several times the catalyst pretreatment described in the Experimental section, the activity decreased by about two orders of magnitude as compared with the fresh sample, but the rate of further deactivation became very low. *E.g.* after repeating a cycle consisting of one hour's reaction (525 °C, 1 kN m^{-2} ethane) and 20 minute's regeneration (525 °C, 10 kN m^{-2} H_2) five times, the catalytic activity remained constant within the limits of experimental error. Figure 4 shows the product distribution obtained on a catalyst stabilized in this way. It can be seen that dehydrogenation is accompanied by a strong deposit formation, the H/C ratio characteristic of this latter being close to 3. Upon terminating the reaction after 65 min and treating the catalyst with 10 kN m^{-2} hydrogen at the reaction temperature, the analysis of the trapped hydrocarbons showed that residues were adsorbed almost entirely in the form of C_2 deposits, as indicated by their desorption as ethane (data denoted by X in the figure).

Further experiments have been performed on this stabilized catalyst sample (0.0689 g → 1.12 m^2); it was regenerated after each experiment in the way described above.

Temperature dependence of the reaction rates

Deposit formation as well as non-stoichiometric hydrogen formation lead to the conclusion that no simple expression can be expected to describe the actual pressure of the components as a function of time. Figure 4 shows, however, that ethylene formation can be characterized by a monotonic function, thus the initial reaction rate can presumably be determined by extrapolating some simple function to zero time. Figure 5 shows the derivative of the ethylene amount *vs.* time plot of Fig. 4. The derivation was carried out according to WHITACKER and PICKFORD [35] by performing a numerical derivation for the first five points of the integral curve and repeating this procedure for the 2nd—6th, 3rd—7th, 4th—8th etc. points. This procedure gives the derivative of a quadratic function fitted to these five points according to the method of least squares. The error of the middle (third) points is always the lowest; the Figure shows these third points for each group of five points, except for the first and last two points. The points shown are, with a good approximation, on a straight line. The first two points have been neglected in the extrapolation to zero partly owing to the larger error mentioned, and partly due to the disturbing effect of adsorption.

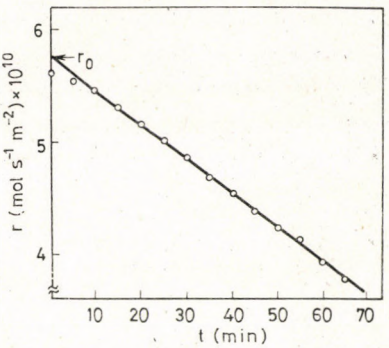

Fig. 5. Variation of the rate of ethylene formation during the reaction

The Arrhenius plot of the initial reaction rates is shown in Fig. 6. The apparent energy of activation has been calculated by the method of weighted least squares [36]; its value is

$$E = 148.4 \pm 6.5 \text{ kJ mol}^{-1}$$

The statistical weights have been calculated from the following equation:

$$w_T = \frac{r_T^2}{s^2(r_T)}$$

where r_T denotes the initial rate at temperature T, and $s_2(r_T)$ its mean quadratic spread.

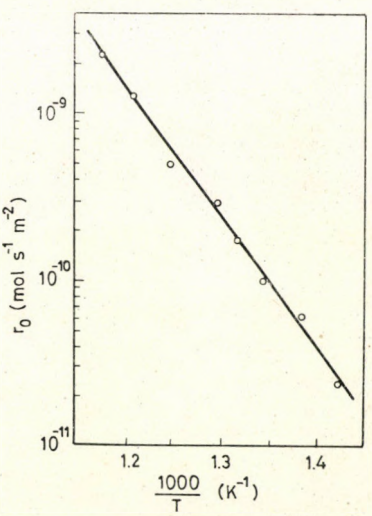

Fig. 6. Arrhenius plot of the initial rates of ethylene formation. Catalyst: 0.0689 g, $P_{\text{ethane}} = 1.04 \pm 0.03$ kN m^{-2}

The latter value can be determined from the error of numerical derivation in the calculation of the initial rates [35].

The regression coefficient of the Arrhenius plot for the temperature range suitable for kinetic experiments ($T = 430-580$ °C) is $r = -0.98$, indicating the independence of the activation energy of the temperature.

Kinetic isotope effect and H–D exchange

Determination of the kinetic isotope effect can provide valuable data for recognizing the nature of the rate-limiting step. The reaction rates of C_2H_6 and C_2D_6 dehydrogenation at 450 °C are significantly different (Table II).

Table II

Kinetic isotope effect in the dehydrogenation of ethane and deuteroethane

	Pressure (kN m^{-2})		$r^0 \times 10^{11}$ (mol s^{-1} m^{-2})	η
	C_2H_6	C_2D_6		
I	1.30		6.73	3.06
		1.32	2.20	
II		1.25	2.18	2.63
	1.26		5.73	
Average:				2.85

By dehydrogenating perdeuteroethane in the presence of protium and by analyzing the product samples mass-spectrometrically, it is possible to study dehydrogenation and hydrogen–deuterium exchange simultaneously (Fig. 7). Clearly, dehydrogenation is accompanied by an intense exchange whose rate is higher than that of dehydrogenation on both ends of the kinetic temperature range. The protium content of the initial deuteroethane can be found entirely in molecules of C_2D_5H at the actual maximum conversion of 2%.

Discussion

Experimental evidence has been obtained that the reaction of ethane on α-Cr_2O_3 has a transient and a quasi-steady-state region (Fig. 1). The transient region can be characterized by rapid formation of ethylene and hydrogen:

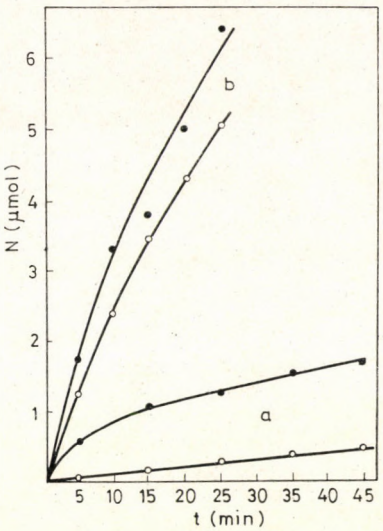

Fig. 7. Deuterium–hydrogen exchange (○) and deuteroethylene production (×) for deuteroethane as a function of reaction time at *(a)* 450 °C; *(b)* 550 °C. Calalyst: 0.0689 g, $P_{C_2D_6} = 1.32 \pm 0.03$ kN m^{-2}; $p_{H_2} = 2.05 \pm 0.05$ kN m^{-2}

the ethylene concentration has a maximum and slowly decreases in the steady-state region. Ethane dehydrogenation is accompanied in both regions by ethane hydrogenolysis and the formation of hydrogen-deficient deposits. This latter process results in hydrogen formation, exceeding the stoichiometric amount. This excess hydrogen shifts the equilibrium backwards. This fact might have been the reason of why the ethylene concentration has a maximum but in this case the mass effect ratio should approximate the equilibrium constant from the upper side. Actually, the opposite has been observed, indicating that ethylene or a surface species being in equilibrium with ethylene must be the precursor of the deposits.

When evaluating the composition of deposits, it must be remembered that it was deduced from the deficit of the carbon and hydrogen balance but this deficit contains also reversibly chemisorbed hydrogen and hydrocarbon. In other words, surface deposits must be more hydrogen-deficient — especially at lower temperatures — than it seems from Fig. 2.

Both deposit formation and the change of its composition as well as methane formation are the most rapid in the initial stage of the transient region (a few minutes) when the catalyst surface has a relatively low coverage. This indicates that chemisorbed hydrogen must hinder deposit formation. This is also supported by the fact that deposits corresponding to low conversion can be removed from the surface *via* hydrogenation as methane or ethane (Fig. 4) and further by the decrease of the dehydrogenation selectivity with increasing temperature, that is, with lower hydrogen coverages.

As a working hypothesis, the following facts can be stated about the reactions of ethane on α-Cr_2O_3.

Ethane molecules chemisorbed on the catalyst surface gradually lose hydrogen, leading to H/C values down to unity, depending on the temperature and hydrogen content of the catalyst. Some of the intermediate stages of this process is accompanied by C–C bond rupture. Two products of this reaction sequence may appear in the gas phase after desorption and/or hydrogen uptake: methane and ethylene. The process of interest for us is ethane dehydrogenation into ethylene; this occurs in the transient stage of the reaction and, presumably, consists of several elementary steps. The question arises of whether any of these is rate-determining and if so, which.

The apparent energy of activation is nearly independent of the temperature in the temperature range spreading over 150°. The regression coefficient of the Arrhenius plot is very close to unity, and this — in spite of the well-known insensitivity of the exponential function — suggests that a single rate-determining step exists*.

The numerical value of the kinetic isotope effect is $\eta = 2.85$ at 450 °C; according to EYRING and CAGLE, the theoretical maximum at this temperature is $\eta_{max} = 3.5$ [37]. As the actual value is close to the maximum, the rate-determining step may be the rupture of a C–H bond in the activated complex. YUNG-FANG YU YAO has reached the same conclusion for ethane oxidation on α-chromia [38], for which the kinetic isotope effect is as high as $\eta = 2.22$.

The process of ethane dehydrogenation involves the cleavage of 2 C–H bonds. According to generally accepted views, hydrocarbon chemisorption is dissociative [15, 16, 18], thus the rupture of the first C–H bond occurs during chemisorption. The problem whether dissociative adsorption or the subsequent surface reaction involving C–H bond splitting is rate-determining can be approached by comparing the rates of dehydrogenation and hydrogen–deuterium exchange for the given hydrocarbon. Assuming that dissociative chemisorption is an indispensable precondition of H–D exchange (and this assumption is in correspondence with our present knowledge), no exchange should be observed at low conversions, *i.e.* for negligible rates of the reverse reaction, if dissociative chemisorption were rate-determining. In the opposite case, the rate of exchange should exceed by several orders of magnitude that of dehydrogenation. Although exchange can be observed throughout the whole range and its rate is always higher than that of dehydrogenation (*cf.* Fig. 7), it cannot be concluded from these rates only that the surface reaction is rate-determining. This contradiction can, however, be resolved by con-

* In the opposite case a sum of rate constants appears in the rate expression and, on a logarithmic scale, this approaches a straight line only if the activation energy of one of the steps is much higher than those of the others. Since the rates of elementary processes in question are commensurable, the probability of this is very low.

sidering that since molecules reacting on the surface must have been chemisorbed previously, the rate of the surface reaction should be compared with the combined rates of surface reaction *and* exchange; on the other hand, exchange involves more elementary steps with finite rates, thus its overall rate is necessarily lower than that of chemisorption.

These elementary steps mentioned are: desorption of the exchanged hydrocarbon and surface migration of H and D. The deuterium eliminated from the starting hydrocarbon (for technical reasons, the reverse exchange was studied in our case) should change its place with a hydrogen atom from the gas phase; this latter then combines with the hydrocarbon residue and the resulting C_2D_5H may then leave the surface. Since CONNER and KOKES have shown by a very convincing experiment that "the sites of chemisorption are discrete and non-interacting" on oxides of zinc and chromium (and, presumably, on most oxides), unlike on metals, the migration process must be very slow [39]. Thus, the rate of exchange must be assumed to be much lower than that of dissociative chemisorption, since the most probable reaction of chemisorbed molecules is their recombination with their original deuterium atoms and subsequent desorption.

Considering these, it may be concluded that the rate-determining step of ethane dehydrogenation on α-Cr_2O_3 must be, in all probability, the surface reaction subsequent to dissociative chemisorption.

REFERENCES

[1] DODD, R. H., WATSON, K. M.: Trans. Am. Inst. Chem. Engrs., **42**, 263 (1946)
[2] BALANDIN, A. A.: Advances in Catalysis, **10**, 96 (1958)
[3] TYURYAEV, I. Ya.: Russian Chem. Rev. **35**, 59 (1966)
[4] HAPPEL, I., BLANCK, H., HAMILL, T. D.: Ind. Eng. Chem., Fundam., **5**, 289 (1966)
[5] ATKINS, R. S., HAPPEL, I.: Intern. Symp. on the Mechanism and Kinetics of Complex Catalytic Reactions. Moscow, 1968, Paper No. 4.
[6] HAPPEL, I., ATKINS, R. S., TANAKA, K.: J. Res. Inst. Catal., Hokkaido Univ., **17**, 197 (1969)
[7] HAPPEL, I., KAMHOLZ, K., WALSH, D., STRANGIO, V.: Ind. Eng. Chem., Fundam, **12**, 263 (1973)
[8] CARRÀ, S., FORNI, L., VINTANI, C.: J. Catal., **9**, 154 (1967)
[9] BALANDIN, A. A., ISSAGULYANTS, G. V.: Dokl. Akad. Nauk SSSR, **63**, 261 (1948)
[10] BALANDIN, A. A., ROSHDESTVENSKAYA, I. D.: Zh. Fiz. Khim., **34**, 1336 (1960)
[11] FLID, R. M., KAGAN, M. Ya.: Zh. Fiz. Khim., **24**, 1409 (1950)
[12] MASLYANSKY, G. N., BURSIAN, N. R.: Zh. Obshch. Khim., **28**, 2663 (1958)
[13] HADSHI-KASUMOV, V. S., KIPERMAN, S. L., ISSAGULYANTS, G. N., BALANDIN, A. A.: Kinet. Katal., **7**, 273 (1966)
[14] HADSHI-KASUMOV, V. S., KIPERMAN, S. L., ISSAGULYANTS, G. V., BALANDIN, A. A.: Kinet. Katal., **8**, 609 (1967)
[15] CARRÀ, S., UGO, R., ZANDERIGHI. L.: Inorg. Chim. Acta, **3**, 55 (1959)
[16] VAN REIJEN, L. L., SACHTLER, W, M. H., COSSEE, P., BROUWER, D. M.: Proc. Third Int. Congr. Catal., Vol. II, p. 829. North-Holland Amsterdam 1965
[17] BIELANSKI, A., DEREN, I., HABER, J.: Zesz. Nauk. Akad. Gorn.-Hutn., **247**, 129 (1969)
[18] BURWELL, R. L., READ, F. J., TAYLOR, K. C., HALLER, G. L.: Z. Phys. Chem. NF, **64**, 18 (1969)
[19] BURWELL, R. L., HALLER, G. L., TAYLOR, K. C., READ, F. J.: Advances in Catalysis, **20**, 2 (1969)

[20] LYUBARSKY, F. D.: Usp. Khim., **27,** 316 (1958)
[21] MARCILLY, Ch., DELMON, B.: J. Catal., **24,** 336 (1972)
[22] PEPE, F., STONE, F. S.: Catalysis, Ed. Hightower, J. W., 2—137. North-Holland Amsterdam 1973
[23] STONE, F. S., VICKERMAN, J. C.: Z. Naturforsch., **24a,** 1415 (1969)
[24] TRAYNARD, P., MASSON, J., DELMON, B.: Bull. Soc. Chim., 2652 (1973)
[25] TRAYNARD, P., MASSON, J., DELMON, B.: Bull. Soc. Chim., 2892 (1973)
[26] FREY, F. E., HUPPKE, W. F.: Ind. Eng. Chem., **25,** 54 (1933)
[27] DEREN, J., HABER, J.: Ceramika, **13,** 5 (1969)
[28] UMA, R., KURIACOSE, J. C.: Indian Chem. Mfr., **8,** 11 (1970)
[29] GUCZI, L., TÉTÉNYI, P.: Acta Chim. Acad. Sci. Hung., **51,** 275 (1967)
[30] KÁLMÁN, J., EMŐDY, Z., KŐNIG, P., SOMLAI, L.: Magyar Kém. Lapja, 30, 623 (1975)
[31] MARSHALL, R., MITRA, S. S., GIELISSI, P. J., RENALL, J. N., MANSUR, L. C.: J. Chem. Phys., **43,** 2893 (1965)
[32] KEARBY, K. K.: in Catalysis, Ed. Emmett, P. H., Vol. III, p. 455. Rheinhold, New York 1955
[33] BREMER, H., MUCHE, J., WILDE, M.: Z. anorg. allg. Chem., **407,** 40 (1974)
[34] MC. CLENNAN, A. L., HAMSBERGER, H. F.: J. Colloid Interface Sci., **23,** 577 (1967)
[35] WHITACKER, S., PIGFORD, R. L.: Ind. Eng. Chem., **52,** 185 (1960)
[36] MARGERISON, D.: The Treatment of Experimental Data, in "Comprehensive Chemical Kinetics", Ed. Bamford, C. H., Tipper, C. F. H., Vol. 1, p. 404. Elsevier, Amsterdam 1969
[37] EYRING, H., CAGLE, W.: J. Phys. Chem., **56,** 889 (1952)
[38] YUNG-FANG YU YAO: J. Catal., **28,** 139 (1973)
[39] CONNER, W. C., KOKES, R. J.: J. Phys. Chem., **73,** 2436 (1969)

Péter KŐNIG
Pál TÉTÉNYI
H-1525 Budapest 114, P.O.B. 77.

Acta Chimica Academiae Scientiarum Hungaricae, Tomus 89 (2), pp. 137—150 (1976)

KINETICS OF ETHANE DEHYDROGENATION ON α-Cr_2O_3 CATALYST, II

THE RATE EQUATION

P. KŐNIG and P. TÉTÉNYI

(Institute of Isotopes of the Hungarian Academy of Sciences, Budapest)

Received July 3, 1975

The kinetics of ethane dehydrogenation has been investigated in a circulation reactor, in the temperature range of 450—580 °C and in the pressure range of 0—4 kN m^{-2}. Initial reaction rates determined gas chromatographically have been compared with the appropriate HOUGEN–WATSON rate equations by nonlinear parameter estimation on a digital computer. The kinetic equation found to be most probable statistically, its sorption and rate constants, as well as the values of activation energy, sorption enthalpy and entropy determined on their basis support the "dual site" mechanism of dehydrogenation with the modification that the two catalytic centers in question are not identical.

Introduction

In a preceding publication, on the basis of a many-sided investigation of ethane dehydrogenation, it had been established that the rate of dehydrogenation — in all probability — is limited by a single step on an appropriately stabilized catalyst with a reproducible activity, this step being the surface reaction. This fact permits the application of the HOUGEN—WATSON concept well proved in kinetic experience [1]. In the present paper, an attempt is made to determine the HOUGEN—WATSON equation by computer fitting to our experimental kinetic data and, at the same time, to calculate its reaction rate and sorption equilibrium constants. These data may provide valuable help in elucidating the mechanism of dehydrogenation disputed until now.

Experimental

Procedure

The experimental procedure has been described in detail in the first part of the series. Experiments to be discussed hereafter have been carried out on the same stabilized catalyst sample (0.0689 g → 1.12 m^2 α-Cr_2O_3).

The fact that, before stabilization, the reaction rate exceeded by about two orders of magnitude that observed in the present series, made it unnecessary to investigate whether diffusion may play any role.

The activity of catalysts has been checked periodically by control experiments. The activity decrease during the whole series of experiments was as low as 22%, with unchanged catalyst surface. For better comparison, the initial rates measured have been referred to the activity level found at the beginning of the series.

Calculations

The most probable kinetic equation and its constants have been determined on the basis of initial rates (r_0) and their average error (s_r) calculated as described in Part I. The parameters φ of the equation ensuring the best fit to n experimental points have been determined by the method of weighted least squares, by searching for the minimum of the target function

$$S(\varphi) = \sum_{i=1}^{n} w_i(r_{0i} - r_i(\varphi))^2 \tag{1}$$

Here $w_i = 1/s_{ri}^2$ denotes the statistical weight; $r_i(\varphi)$ the i-th initial rate calculated by using the actual value of parameters φ.

The computer program applied is a modification of the method of FLETCHER and POWELL [2] described earlier in detail [3, 4]. This program gives also the error limits $\pm\delta\varphi$ of the optimal parameters $\hat{\varphi}$ at the minimum $S(\hat{\varphi})$ of target function (1). These are given at a 95% confidence level. The calculations have been carried out on an ICT 1905 computer.

Results

Initial reaction rate as a function of ethane partial pressure

The results are shown in Fig. 1. If the surface reaction is indeed the rate-determining step, the experimental data are described by one of the following two expressions:

$$r_0 = \frac{kb_E p_E}{(1 + b_E p_E)^2} \quad \text{I}$$

$$r_0 = \frac{kb_E p_E}{1 + b_E p_E} \quad \text{II} \tag{2}$$

depending on whether or not C–H bond rupture requires an adjacent free active site left by an ethane molecule*. Optimization was carried out for the

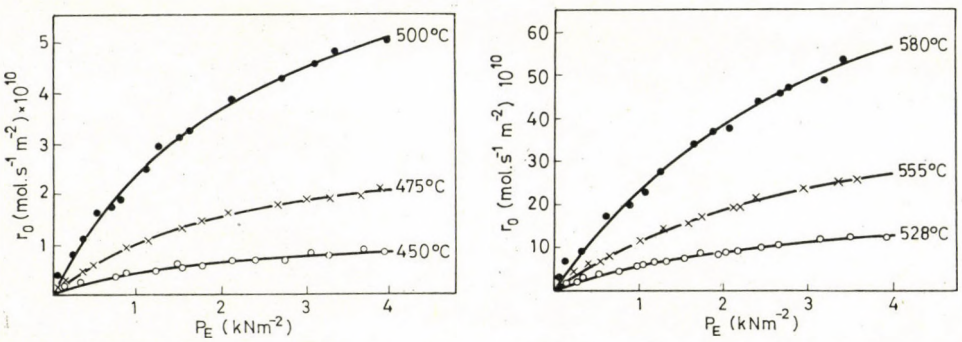

Fig. 1. Initial rates as a function of ethane partial pressure

* The symbol r_0 is related to 1 m^2 catalyst surface, thus the dimension of both r_0 and k is [mol s^{-1} m^{-2}].

experimental $r_0 = f(p_E)$ data obtained at temperatures 450, 528 and 580 °C; the resulting optimal parameters and the value of the residual sum of quadratic errors are as given in Table I.

Table I

Best parameters and residual quadratic errors for the optimization of the experimental results according to two alternative mechanisms

t (°C)	k (mol s^{-1})		$m^{-2}) \times 10^{10}$		b_E (m^2 N^{-1}) $\times 10^4$		$S(\hat{\varphi})$	
	I		II		I	II	I	II
450	3.53	± 0.24	1.20	± 0.28	1.58 ± 0.29	5.5 ± 1.1	0.1620	0.01106
528	55.7	± 6.2	22.2	± 2.6	1.26 ± 0.22	3.36 ± 0.64	1.473	1.061
580	292	± 37	114	± 17	0.94 ± 0.21	2.57 ± 0.65	27.16	21.60

Approximations according to Equation II give in all cases lower errors than those according to Equation I, but the difference is not sufficient to favour the former using the usual statistical method, *i.e.* SNEDECOR's F-test [5].

Energies of activation and ethane sorption enthalpies calculated from the two types of rate constants and sorption equilibrium coefficients according to the ARRHENIUS equation using the method of least squares are as follows:

$$\text{I: } E = 176.3 \pm 2.0 \text{ kJ mol}^{-1};\ \Delta H = -20.0 \pm 4.7 \text{ kJ mol}^{-1}$$

$$\text{II: } E = 179.6 \pm 0.1 \text{ kJ mol}^{-1};\ \Delta H = -30.6 \pm 0.3 \text{ kJ mol}^{-1}$$

These values are rather close to each other, but the confidence level of those calculated with Equation II is by about an order of magnitude better, indicating a closer fitting of Equation II to the ARRHENIUS equation.

The apparent energy of activation calculated from the expression

$$E' = E + \Delta H$$

is $E' = 156$ kJ mol^{-1} for Equation I and $E' = 149$ kJ mol^{-1} for Equation II. The apparent energy of activation determined in an independent series of experiments (Part I: $E' = 148.4 \pm 6.5$ kJ mol^{-1}) agrees within the limits of experimental error with the second result only.

These results are already in favour of Equation II over Equation I; it can be decided, however, only after careful further studies whether this expression gives indeed a sufficient agreement with the experimental data.

The theoretical function may be regarded as "well-fitted" to the experimental points if the estimated standard deviation of the fit is about the same as the average error of the experimental points, and further, if the spread

of the latter gives a random distribution around the theoretical function. The first requirement can be investigated by means of the F-test already mentioned; this gives a reasonable result in our case. The distribution of experimental points can be best characterized by the analysis of the residuals [6, 7]. The "residuals" are defined as the differences between measured and calculated values of the dependent variable. By dividing this quantity by the variance estimate (this procedure is called standardization) a probability variable (q) can be obtained, the expectation value of which is 0 and the variance is 1 [4]. This has been plotted as a function of the independent variable in our case the partial pressure of ethane (Fig. 2). As can be seen, the standard-

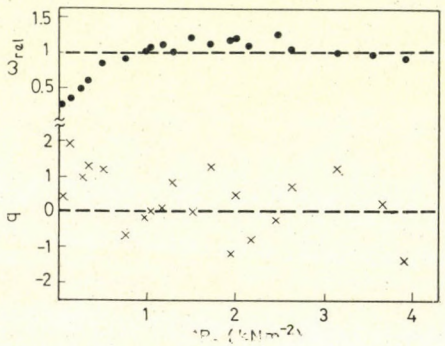

Fig. 2. Standardized residuals *(q)* and relative weights of experimental points *(w_{rel})* as a function of ethane partial pressure, at 528 °C

ized "residuals" show no definite direction of deviation, the experimental points are randomly distributed around the theoretical function *($q = 0$)*, except for those related to the lowest pressures. On the basis of the relative statistical weights shown in the Figure, one can also see that these latter points have but a small influence on the result.

Table II

Optimal values for reaction rate constants and ethane equilibrium sorption constants

t (°C)	k (mol s^{-1} m^{-2}) $\times 10^{10}$	b_E (m^2 N^{-1}) $\times 10^4$
450	1.20 ± 0.28	5.5 ±1.1
475	3.28 ± 0.64	4.50 ± 0.69
500	8.38 ± 0.91	3.97 ± 0.51
528	22.2 ± 2.6	3.36 ± 0.64
555	52.6 ± 9.8	2.77 ± 0.78
580	114 ±17	2.57 ± 0.65

It can thus be concluded that rate equation II represents a satisfactory expression for the dependence of initial rate on the ethane partial pressure. The optimum constants determined on this basis are summarized in Table II; the theoretical curves calculated with these are represented by the continuous lines in Figure 1. The agreement with experimental data is very good at each temperature.

Initial reaction rate as a function of hydrogen partial pressure

Using identical amounts of ethane ($p_E = 2.19 \pm 0.03$ kN m^{-2}) and hydrogen pressures varying between 0 and 4 kN m^{-2}, the effect of hydrogen partial pressure could be studied on the initial rate of ethane dehydrogenation. Results are shown in Fig. 3.

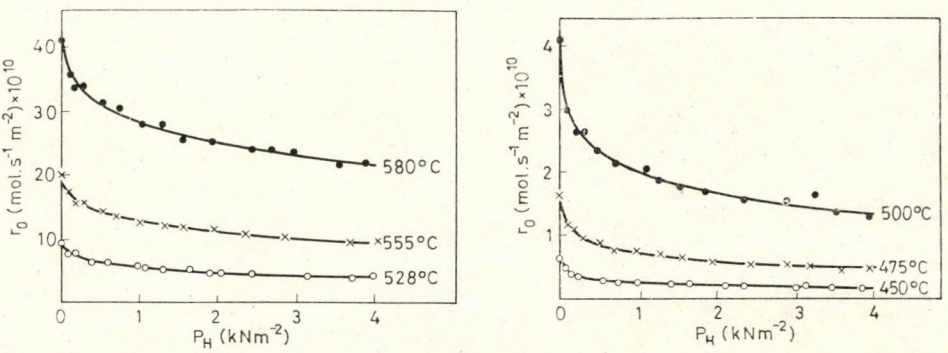

Fig. 3. Initial rates as a function of hydrogen partial pressure

In agreement with the HOUGEN—WATSON concept applied so far and considering also the dependence of the reaction rate on ethane partial pressure, the following equations can be proposed for the process in question, depending on the fact whether the active sites for ethane and hydrogen chemisorption are identical *(a)* or different *(b)*:

$$r_0 = \frac{kb_E p_E}{1 + b_E p_E + b_H p_H} \quad (a)$$

I

$$r_0 = \frac{kb_E p_E}{(1 + b_E p_E)(1 + b_H p_H)} \quad (b) \qquad (3)$$

$$r_0 = \frac{kb_E p_E}{1 + b_E p_E + \sqrt{b_H p_H}} \quad (a)$$

II

$$r_0 = \frac{kb_E p_E}{(1 + b_E p_E)(1 + \sqrt{b_H p_H})} \quad (b)$$

For the equations in Group I, associative, for those in Group II, dissociative hydrogen chemisorption was assumed. In order to simplify the calculations, these two groups can be combined into the following formulas:

$$\begin{aligned} \text{I:}\quad & r_0 = k_1/(k_2 + b_H p_H) \\ \text{II:}\quad & r_0 = k_1/(k_2 + \sqrt{b_H p_H}) \end{aligned} \tag{4}$$

where the meaning of k_1 and k_2 is:

for Group *(a)*: $k_1 = k b_E p_E$; $k_2 = 1 + b_E p_E$;

Group *(b)*: $k_1 = k b_E p_E/(1 + b_E p_E)$; $k_2 = 1$

Table III

Optimal parameters and residual quadratic errors for the optimization of the experimental results according to two alternative mechanisms

t (°C)	$k_1 \times 10^{10}$		k_2	
	I	II	I	II
450	2.89±0.84	0.664±0.034	4.9 ±1.8	0.981±0.057
528	7.9 ±1.3	8.07 ±0.69	0.91±0.17	0.83 ±0.23
580	30.1 ±3.4	39.00 ±0.87	0.83±0.11	0.91 ±0.19
	b_E ($m^2\ N^{-1}$) $\times 10^4$		$S(\hat{\varphi})$	
	I	II	I	II
450	83.9 ±3.1	30.10 ±0.62	1.93×10^{-2}	5.04×10^{-3}
528	4.5±1.2	3.49± 0.67	1.373	0.4094
580	1.67±0.34	1.59 ±0.10	40.27	5.248

Optimizing these two expressions for the experimental points determined at 450, 528 and 580 °C, the parameters shown in Table 3 are obtained. It can be seen from the residual sums of quadratic errors shown in Table III, that Model II is a better approximation for the experimental results, which can also be verified by the F-test. The value of k_2 is close to unity, independently of the temperature, indicating the validity of Model II/b. A fixed value of k_2 and optimization according to the expression

$$r_0 = \frac{k_1}{1 + \sqrt{b_H p_H}} \tag{5}$$

results in a minor change in the values of k_1 and b_H but the residual sum of

squares remains constant, confirming that the reason why k_2 was not equal to unity was that it has a low grade correlation with the other parameters.

Optimization of all parameters according to expression (5) results in the curves shown by continuous lines in Fig. 3. The closeness of fit has been investigated as indicated in the previous section; this gave diagram II in Fig. 4, where experimental points show a random distribution around the theoretical curve. For comparison, the same series of experiments has also been processed

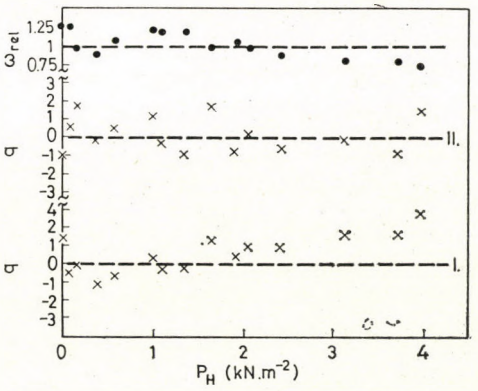

Fig. 4. Standardized residuals *(q)* and relative weights of experimental points (w_{rel}) as a function of hydrogen partial pressure, at 528 °C

according to expression I resulting in diagram I in Fig. 4. Here, experimental values for low pressures lie below, those for high pressures above the $q = 0$ line.

The optimum parameters of Eq. (5) are listed in Table IV. The third column contains the reaction rate constants calculated from k_1 values using the values of b_E as shown in Table II, by means of Eq. (4) Group *(b)*. Since these are in good agreement with the rate constants calculated from the previous series of experiments, this provides additional support for the correctness of Equation II/*b*.

Table IV

Optimal values for reaction rate constants and hydrogen equilibrium sorption constants

t (°C)	$k_1 \times 10^{10}$	k (mol s^{-1} m^{-2}) $\times 10^{10}$	b_H (m^2 N^{-1}) $\times 10^4$
450	0.677±0.038	1.235±0.070	31.3 ±8.4
475	1.64 ±0.13	3.30 ±0.026	17.4 ±4.2
500	4.05 ±0.24	8.72 ±0.51	9.7 ±2.4
528	9.68 ±0.38	22.97 ±0.91	5.0 ±1.3
555	19.5 ±1.1	51.7 ±2.8	3.04±0.63
580	41.3 ±1.9	114.8 ±5.2	1.85±0.37

Initial reaction rate as a function of ethylene partial pressure

On admixing various amounts of ethylene to ethane of a pressure of 1.01 ± 0.03 kN m^{-2}, and reacting this mixture as before, the initial rate remained unchanged up to a certain ethylene concentration. This is illustrated by Fig. 5. This finding indicates that ethylene is either not chemisorbed on the active sites of dehydrogenation in the presence of ethane, or its chemisorption is so slow that it does not influence the initial reaction rate. If the latter case were valid, assuming that the rate of ethylene chemisorption is com-

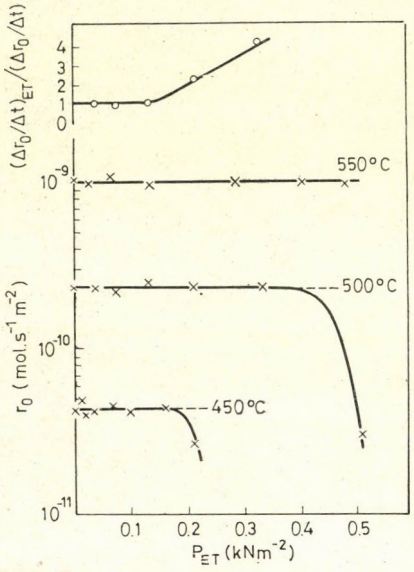

Fig. 5. Initial rates and relative variations of initial rates as a function of ethylene partial pressure

mensurable with that of dehydrogenation, the rate of dehydrogenation ought to decrease more rapidly with increasing reaction time in the presence of added ethylene than without it. Figure 5 contains also the ratios of the slopes of straight lines serving for the determination of initial rates (*cf.* Part I, Fig. 5) at 500 °C

$$\frac{(\Delta r_0/\Delta t)_{Et}}{(\Delta r_0/\Delta t)}$$

with various amounts of ethylene added (numerator), and without it (denominator), respectively. The time dependence of the rate of ethane dehydrogenation is indeed independent of the presence of ethylene up to a partial pressure of 0.2 kN m^{-2}, but above this value the reverse reaction *i.e.* ethylene hydrogenation is not negligible and the reaction rate decreases faster in the presence of ethylene with higher rates of deposit formation and hydrogen evolution.

Table V

Average values of initial rates and reaction rate constants calculated from them for ethane dehydrogenation in the presence of ethylene

t (°C)	$\bar{r}_0$ (mol s^{-1} m^{-2})$\times 10^{10}$	k (mol s^{-1} m^{-2})$\times 10^{10}$
450	0.44±0.10	1.24±0.28
500	2.43±0.35	8.3 ±1.2
550	10.0 ±1.3	44.2 ±5.5

Table V contains reaction rate constants calculated from the average of initial dehydrogenation rates in the presence of ethylene with the appropriate values of b_E using Eq. (2)II. Since the reaction rate has been calculated from the increase in the amount of ethylene, these results are much less accurate than those obtained so far, nevertheless, the rate constants are in good agreement with the corresponding data of Tables II and IV.

The most probable rate equation

From the analysis of the influence of the reactants on the reaction rate it could be established that the most probable kinetic equation for ethane dehydrogenation at low pressures is

$$r = \frac{kb_E p_E}{(1 + b_E p_E)\left(1 + \sqrt{b_H p_H}\right)} \tag{6}$$

This has been selected from the possible equations (2) and (3) mainly on the basis of statistical considerations. It is possible, however, to prove the correctness of Eq. (6) experimentally, omitting statistical parameter estimation from the procedure.

If a series of paired experiments with different amounts of ethane is carried out where a constant amount of hydrogen is always added to one member of the pair, the ratio of the initial rates will be independent of ethane partial pressure only in the case of validity of Eq. (6). This can be visualized on the basis of the following considerations.

Let us denote the reaction rate in the presence of hydrogen by r_0:

$$r_0 = \frac{kb_E p_E}{(1 + b_E p_E)\left(1 + \sqrt{b_H p_H}\right)}$$

and that in the absence of hydrogen by r_0':

$$r_0' = \frac{kb_E p_E'}{1 + b_E p_E'}$$

If $p_E = p'_E$, then

$$\frac{r'_0}{r_0} = 1 + \sqrt{b_H p_H} = \text{const} \quad (p_H = \text{const}) \tag{7}$$

Applying the same considerations to the other reaction rates it is obvious that none of the other equations suggested:

$$r_0 = \frac{k b_E p_E}{1 + b_E p_E + \sqrt{b_H p_H}}$$

$$r_0 = \frac{k b_E p_E}{(1 + b_E p_E + \sqrt{b_H p_H})^2} \tag{8}$$

permit the independence of the ratio r'_0/r_0 of the partial pressure of ethane p_E.

Results are shown in Table VI. The temperature was 500 °C, the amount of hydrogen added 1.50 ± 0.03 kN m^{-2}. The value of b_H calculated from the mean value of r'_0/r_0 (7) was:

$$b_H = (9.97 \pm 1.12) \times 10^{-4} \text{ m}^2 \text{ N}^{-1}$$

which is in good agreement with the corresponding result in Table IV.

Table VI

Reaction rates in the presence (r_0) and absence (r'_0) of a given amount of hydrogen, and their ratios

p_{Et}(kNm^{-2})	$r_0 \times 10^{10}$	$r'_0 \times 10^{10}$	r'_0/r_0
0.57	0.64	1.50	2.34
1.22	1.23	2.75	2.24
2.14	1.60	4.15	2.59
2.39	1.96	3.80	1.94
2.92	2.13	4.29	2.01
3.19	2.11	4.69	2.23
3.60	2.23	4.94	2.22
Average			2.224±0.068

The ARRHENIUS plots for the rate constants and sorption equilibrium constants determined using different methods are shown in Fig. 6. The constants of the plots were determined as described in Part I, by the method of weighted linear least squares. The kinetic and thermodynamic constants calculated from these are as follows:

Energy of activation:	E	$= 178.4 \pm 0.6$ kJ mol^{-1}
Preexponential factor:	k_0	$= 947 \pm 85$ mol s^{-1} m^{-2}
Sorption enthalpy of ethane:	ΔH	$= -30.3 \pm 1.4$ kJ mol^{-1}
Sorption entropy of ethane:	ΔS	$= -104.5 \pm 1.7$ mol^{-1} K^{-1}
Sorption enthalpy of hydrogen:	ΔH	$= -111.8 \pm 0.9$ kJ mol^{-1}
Sorption entropy of hydrogen:	ΔS	$= -202.5 \pm 1.2$ J mol^{-1} K^{-1}

The value of the apparent energy of activation determined earlier *(E')* is in good agreement with the sum of the true energy of activation and the sorption enthalpy of ethane:

$$E'_{exp} = 148.4 \pm 6.5 \text{ kJ mol}^{-1};$$

$$E' = E + \Delta H = 148.1 \pm 2.0 \text{ kJ mol}^{-1}$$

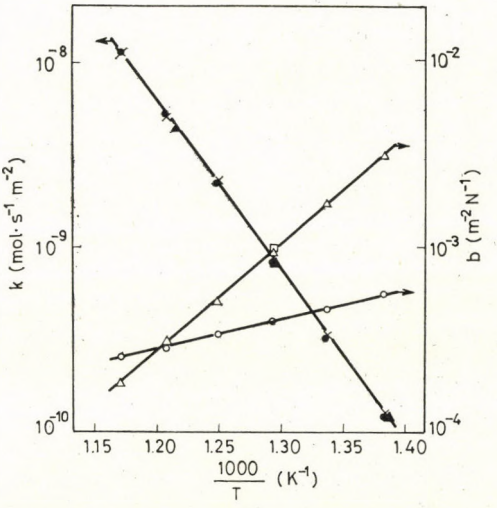

Fig. 6. Arrhenius plots for rate constants and sorption equilibrium constants of ethane *(b_E)* and hydrogen *(b_H)*. × ○ Calculated from dependence on ethane partial pressure; ● △ calculated from dependence on hydrogen partial pressure; ▲ calculated from dependence on ethylene partial pressure; □ calculated from the relative decrease of rate caused by hydrogen cf. Eq. (7)

Discussion

Equation (6) characterizing the kinetics of ethane dehydrogenation seems to support the "dual site" mechanism of dehydrogenation. Its classical interpretation suggested two, chemically identical active sites for the breaking of the C–H bond in the rate-determining step, thus, the kinetics was approximated with Eq. (8) [8].

Our results show, however, that two, chemically different active sites participate in the breaking of the bond in question, the surface coverage

of one of them is determined by the partial pressure of the hydrocarbon, that of the other one by the partial pressure of hydrogen. (It has to be noted that different active sites do not mean necessarily different surface ions, they may represent different co-ordination states of the same type of ion.) The chemical nature of these active sites can, however, be derived only by indirect evidence, by comparing the chemisorption properties of chromia described in the literature and our own results.

Ethane chemisorption on α-Cr_2O_3 is a heterolytic process [9]; the alkyl carbanion is bonded to a Cr^{3+} ion by a σ-bond similarly to the well-known organic chromium compounds [10], whereas hydrogen is linked to one of the neighbouring O^{2-} ions.

Different types of hydrogen chemisorption are possible [11]. BURWELL et al. suggests heterolytic chemisorption [12], this is supported by the IR spectrum of hydrogen chemisorbed on ZnO evidencing the presence of O–H and Zn–H bonds [13]. On the other hand, SIEGEL assumed a homolytic hydrogen chemisorption, at least at higher temperatures, mainly on the basis of analogies with homogeneous catalysis. This would involve the bonding of both hydrogen atoms to the same surface chromium atom with trigonal or tetragonal co-ordination [14]. The heat of hydrogen chemisorption on α-Cr_2O_3 determined in a static system was found to be $\Delta H = -113$ kJ mol^{-1} [15], in good agreement with our kinetic result.

On the basis of the probable mechanism of hydrogen and ethane chemisorption outlined above, and considering the sorption enthalpies determined, the energies of the bonds formed can be estimated: $Q_{H-H} = 2\,Q_{H-K} + \Delta H_H = 435.4$ kJ mol^{-1} [17] for the energy of the H–H bond. Thus, the average energy of the catalyst–hydrogen bond would be $Q_{H-K} = 273.6$ kJ mol^{-1}. On the basis of ethane chemisorption: $Q_{C-H} = Q_{C-K} + Q'_{H-K} + \Delta H_E = 410.7$ kJ mol^{-1} [16] for the energy of the C_2H_5–H bond.

Assuming the bond energy of hydrogen originating from hydrogen chemisorption, *i.e.* $Q'_{H-K} = Q_{H-K}$, we obtain for the average energy of the catalyst–carbon bond: $Q_{C-K} = 167.4$ kJ mol^{-1}.

Only one literature data has been found for the energy of the Cr–C bond [18] according to which the dissociation energy of chromium acetylide per single bond is 222 ± 21 kJ mol^{-1}. As the bond in the acetylide is to some extent ionic, this value is presumably much higher than that of the chromium–carbon σ-bond, thus, the assumption that the carbon atom of the chemisorbed ethane is bonded to chromium ion through a σ-bond, does not seem contradictory, even compared with the estimated value of Q_{C-K}.

Hydrogen can be bound to either a Cr^{3+} or an O^{2-} ion of Cr_2O_3. The energy of the Cr–H bond is 276.8 kJ mol^{-1} [19], that of O–H bond 427.9 kJ mol^{-1} [20]. The Q_{H-K} value found by us is closer to the former one. Although considerations of this type contain several factors of uncertainty, both this agree-

ment and the square root dependence of the reaction rate on hydrogen partial pressure support SIEGEL's homolytic mechanism for hydrogen chemisorption.

On the basis of the sorption entropy values a rough estimation of the localization of chemisorbed hydrogen and ethane can be made [21]. In these calculations the minor contributions of the configurational and vibrational terms to the sorption entropy are neglected.

The change in entropy for the dissociative chemisorption of hydrogen at 800 K, assuming the loss of all translational and one rotational degrees of freedom is equal to:

$$\Delta S = -138.1 - 39.8 = -177.9 \text{ J mol}^{-1} \text{ K}^{-1}$$

The experimental value was $\Delta S = -202.5$ J mol^{-1} K^{-1} indicating localized hydrogen chemisorption, suggested by KOKES [13].

The entropy change for dissociative ethane chemisorption assuming the loss of all translational and one rotational degrees of freedom (with respect to the rotation about the axis perpendicular to the C–C bond) would be:

$$\Delta S = -180.5 - 57.5 = -238.0 \text{ J mol}^{-1} \text{ K}^{-1}$$

which is considerably higher than the experimental value of -104.5 J mol^{-1} K^{-1}. Delocalization of the chemisorbed ethyl radical (*i.e.* if it were a two-dimensional ideal gas) would decrease the calculated entropy change by 98.0 J mol^{-1} K^{-1}. Thus, agreement between calculated and experimental values can only be achieved if it is assumed that carbonaceous fragments formed during ethane chemisorption are to some extent delocalized.

The other product of dehydrogenation, ethylene, does not hinder the reaction. The rate decrease observed at higher pressures can be attributed to intense deposit formation involving the abrupt growth of hydrogen partial pressure exerting a kinetic inhibition even during the initial reaction period and bringing about detectable ethylene hydrogenation.

These phenomena are in agreement with the picture on ethylene chemisorption involving a loose π-complex type chemisorption on a co-ordinatively unsaturated Cr^{3+} ion [13, 15], which makes it obvious why it does not inhibit ethane dehydrogenation. In the presence of hydrogen, however, the formation of alkyl radicals with hydrogen uptake is more favourable, this radical will then be bonded to a Cr^{3+} through a σ-bond [12, 13, 15]. It has been shown in Part I that alkyl radicals are precursors of deposit formation which, in turn, gives rise to even more hydrogen. This autocatalytic process may be responsible for the abrupt decrease of dehydrogenation activity above a certain ethylene concentration.

REFERENCES

[1] HOUGEN, O. A., WATSON, K. M.: Chemical Process Principles, Part III. p. 917. John Wiley and Sons, New York 1962
[2] FLETCHER, R.: Communications of the ACM, **9,** 686 (1966)
[3] FEJES, P., KŐNIG, P.: Acta Chim. (Budapest) **71,** 217 (1972)
[4] KŐNIG, P., FEJES, P.: Acta Chim. (Budapest) **84,** 141 (1975)
[5] WILLIAMS, E. I.: Regression Analysis, Chap. 5. John Wiley, New York 1959
[6] ANSCOMBE, F. I., TUKEY, I. W.: Technometrics, **5,** 141 (1963)
[7] BOX, G. E. P.: Ann. N. Y. Acad. Sci., **86,** 792 (1960)
[8] CARRÀ, S., FORNI, L., VINTANI, C.: J. Catal., **9,** 154 (1967)
[9] BURWELL, R. L. Jr., LITTLEWOOD, A. B., CARDEW, M., PASS, G., STODDART, C. T. H.: J. Amer. Chem. Soc., **82,** 6272 (1960)
[10] COATES, G. E., GREEN, M. L. H., WADE, K.: Organometallic compounds. Vol. II, Methuen, London 1968
[11] SELWOOD, P. W.: J. Amer. Chem. Soc., **92,** 39 (1970)
[12] BURWELL, R. L., Jr., READ, J. F., TAYLOR, K. C., HALLER, G. L.: Z. Phys. Chem. N. F., **64,** 18 (1969)
[13] KOKES, R. J.: in "Catalysis", Ed. Hightower, J. W., Vol. 1, A-1. North-Holland, New York 1973
[14] SIEGEL, S.: J. Catal., **30,** 139 (1973)
[15] BURWELL, R. L. Jr., HALLER, G. L., TAYLOR, K. C., READ, J. F.: Advances in Catalysis, **20,** 2 (1969)
[16] TLUSKO, V. P., MEDVEDEVA, V. A.: Termicheskie konstanty veshchestv. VINITI, Moscow 1970
[17] MORTIMER, C. T.: Reaction Heats and Bond Strengths. Pergamon, Oxford 1962
[18] KOHL, F. J., STEARNS, C. A.: J. Phys. Chem., **74,** 2714 (1970)
[19] GAYDON, A.: Dissociation Energies and Spectra of Diatomic Molecules. 37 Ed., Chapman and Hall, London 1968
[20] KONDRATYEV, V. N.: Energii razryva svyazei. Nauka, Moscow 1974
[21] KEMBALL, C.: Advances in Catalysis, **2,** 233 (1950)

Péter KŐNIG
Pál TÉTÉNYI
H-1525 Budapest 114, P.O.B. 77.

Acta Chimica Academiae Scientiarum Hungaricae, Tomus 89 (2), pp. 151—160 (1976)

COMPLEX STUDY OF RANEY NICKEL SKELETON CATALYSTS, VIII

STUDY OF THE EFFECT OF HEAT-TREATMENT ON RANEY NICKEL BY MAGNETIC, ELECTROCHEMICAL AND THERMODESORPTION METHODS

A. TUNGLER, J. PETRÓ, T. MÁTHÉ, J. HEISZMAN, F. BUELLA and Z. CSŰRÖS

(Department of Organic Chemical Technology, Technical University, Budapest)

Received May 25, 1975

Raney nickel catalyst samples heat-treated in argon at increasing temperatures were subjected to thermomagnetic, thermal desorption and electrochemical examinations, — activity and surface measurements, while thermomagnetic analysis and thermal desorption measurements were carried out on samples polarized electrochemically to various extents. The results of electrochemical hydrogen content determination were compared with the results of thermal desorption and magnetic measurements, and a study was made of the effect of heat-treatment on the catalysts.

It was found that the change taking place in Raney nickel above 200° is fundamental: the hydrogen content, the surface, the magnetization and the Curie temperature decrease, and the catalytic activity is eliminated.

In the electrochemically treated samples, nickel with a coarser structure is formed when the aluminium is dissolved out. The Raney nickel can be polarized by about 150 mV without oxidation.

There is a correlation between the hydrogen contents determined electrochemically and by thermal desorption. In sample 3, heat-treated at a higher temperature, a desorbing hydrogen species appears at $>350°$.

A number of procedures have been developed for determination of the hydrogen content or the hydrogen content *vs.* electrochemical potential relation of Raney Ni catalysts [1]. The essence of these is that the catalyst is suspended in the electrolyte and polarized during stirring. However, the results are made uncertain by the high contact resistance between the particles and the electrode. STURM and RICHTER [2] have elaborated an electrochemical procedure applicable to ferromagnetic catalysts (*e.g.* Raney Ni, Fe, Co), the essence of which is that the catalyst is attached to the electrode by a magnetic force, and thus the duration and strength of contact of the electrode and the catalyst particles can be regulated and the contact resistance can be eliminated. In this way it is possible to determine the double layer capacity of the catalyst, the exchange current per unit weight, and the potential *vs.* hydrogen content (charge amount) relation.

If Raney nickel is connected as anode in alkaline solution, H^+ ions leave the catalyst, *i.e.* the hydrogen content of the catalyst decreases. The amount of hydrogen oxidized can be determined from the quantity of charge passing (if oxidation of the catalyst and impurities can be excluded). First to be oxidized electrochemically is the hydrogen sorbed on the surface. The rate of this oxidation is higher than the rate of hydrogen diffusion from the

interior of the catalyst to the surface, and therefore the surface becomes poorer in hydrogen and below a certain surface hydrogen content, *i.e.* electrochemical potential, oxidation of the metal begins too.

Raney nickel always contains undecomposed aluminium alloy, oxidation of which also disturbs determination of the hydrogen content. STURM and RICHTER [2] first remove the aluminium by alternating positive and negative polarization, and begin oxidation of the hydrogen after this, by waiting for establishment of the hydrogen equilibrium between the surface and the interior of the catalyst grains before every new polarization.

The Pourbaix diagram of nickel shows that in the case of positive polarization in alkaline solution (pH >12) nickel is thermodynamically unstable. In contrast, STURM and RICHTER [2] demonstrated that after oxidation of the aluminium, Raney nickel is reversibly polarizable in the range 0—200 mV, *i.e.* in this potential interval the catalyst can be regarded as practically stable. Since neither the literature [2] nor our own (see Fig. 4) charge curves of Raney nickel exhibit a break indicative of complete oxidation of the sorbed hydrogen (in the vicinity of 200 mV and above this, nickel and hydrogen are probably oxidized together), the total sorbed hydrogen cannot be determined by the method of recording the charging curve. For this reason, the hydrogen content to be determined in Raney nickel by the electrochemical method was arbitrarily characterized by the amount of charge necessary for polarization of the catalyst from 0 mV to 150 mV.

In this series of papers, we have so far reported on thermodesorption, thermomagnetic and thermogravimetric studies of skeleton catalysts prepared in different ways. It is generally characteristic for these that they can be used to follow changes resulting in catalysts on heat-treatment.

The aims of the present experiments were to compare the results on the electrochemical determination of hydrogen content with magnetic and thermodesorption measurements, and to study the effect of heat-treatment on catalyst samples obtained at the individual temperatures of heat-treatment.

Experimental

The base catalyst was obtained by a special procedure from an alloy containing 50 wt.% Ni and 50 wt.% Al [10]; this is known as 'high-activity' Raney Ni (sample 1). The base catalyst stored under abs. alcohol was treated for 2 hrs in an argon atmosphere at temperatures of 25, 100, 150, 200, 250, 320 and 400 °C in the apparatus to be seen in Fig. 1, and the heat-treated samples (samples 2—7) were then again placed under absolute alcohol, to eliminate contact with air. The catalysts were heated to the temperature of heat treatment at a rate of at most 2 °C/min, for on faster heating a reaction accompanied by rapid evolution of gas occurs at temperatures above 100 °C.

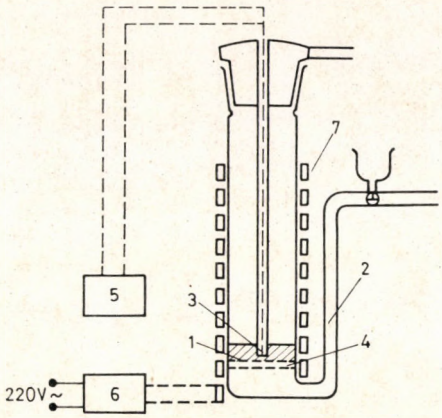

Fig. 1. Apparatus for heat-treatment of catalyst samples.
1. Catalyst, 2. gas inlet tube, 3. thermocouple, 4. glass filter, 5. temperature readout, 6. temperature regulator, 7. heating strip

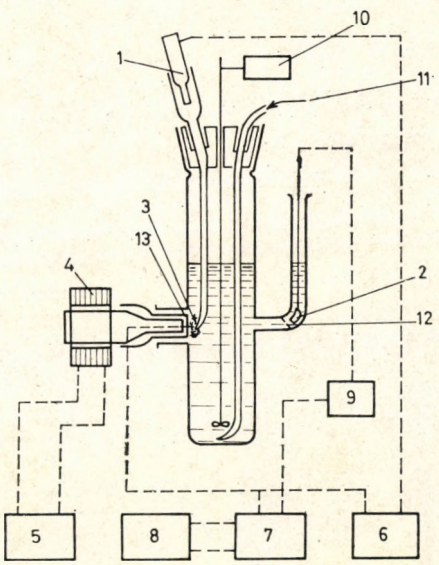

Fig. 2. Apparatus for electrochemical investigations. 1. Calomel electrode, 2. platinum auxiliary electrode, 3. platinum electrode, 4. electromagnet, 5. stabilized D. C. supply unit, 6. electrometer, 7. pole changer, 8. stabilized D. C. supply unit, 9. ammeter, 10. stirrer and stirrer motor, 11. gas inlet tube, 12. glass filter, 13. catalyst

Electrochemical investigations were carried out in the apparatus shown in Fig. 2.

Its main parts are the measuring cell with electrodes and a gas inlet, the electrometer, an ammeter, the magnet and its supply unit, with a stirring motor and a gas-supply system (H_2 and Ar bottles, pneumatic supply units, differential manometers, deoxo contact).

The measuring cell is a cylindrical vessel of about 600 ml. The magnet reaches to the outer side of the Pt sheet electrode welded into the wall of the cell. About 2 mm from the inner side of the Pt electrode is the Luggin capillary, which is filled with saturated KCl agar-agar and provides conduction to the saturated calomel electrode. The polarizing Pt electrode is in a side-arm closed by a glass filter, to inhibit mixing of the gases formed on polarization.

In the 6 *N* NaOH solution serving as electrolyte, the e.m.f. between the Raney Ni catalyst saturated with hydrogen and the calomel electrode was 1100 $\pm$ 2 mV. The potentials of the catalysts were calculated from the measured e.m.f., and were always referred to the hydrogen-saturated catalyst, *i.e.* to the hydrogen electrode.

The polarizing current was led through a pole changer with a stabilized supply unit to the electrodes, and measured with an ammeter with an accuracy of $\pm$1 mA. The e.m.f. between the catalyst electrode and the calomel was measured with an electrometer with an accuracy of $\pm$1 mV. H_2 and/or Ar could be led into the electrolyte through the gas inlet tube below the mixing head.

In every case the catalyst sample weighed 0.15—0.20 g (the weight was determined by drying after the measurement) and covered the surface of the Pt electrode uniformly. The e.m.f. was measured by connecting the current of the magnet during constant stirring of the electrolyte; the catalyst adhered to the electrode, the electrometer reading was taken, and the exciting current of the magnet was switched off. This operation was repeated a number of times, until the difference between two consecutive readings was less than 1 mV.

The aluminium remaining in the catalyst on preparation was removed by electrolytic dissolution, the catalyst held on the electrode first being polarized by 200 mV in the positive direction (anodically), and then by 200 mV from the initial value in the negative direction (cathodically), and next being mixed in the electrolyte. This operation was repeated until the amounts of charge passed up to the same potential difference in the two directions agreed within $\pm$10% (5—6 cycles). On the final cathodic polarization the catalyst was saturated with hydrogen electrolytically.

On recording of the hydrogen content *vs.* potential curve the dissolved hydrogen was first expelled from the solution with argon, and a charge of 1—3 Cb was then passed through the catalyst (the current was about 150 mA). The e.m.f. was next measured, the catalyst being stirred in the electrolyte between measurements. The equilibrium potential of the catalyst was plotted as a function of the amount of charge passed.* Anodic polarization was con-

* The amount of charge passed was calculated as the product of the polarizing current and the polarization time.

tinued until the equilibrium potential of the catalyst differed from that of the one saturated with hydrogen by 140—150 mV. The catalysts were subsequently saturated with gaseous hydrogen and the polarization curve was again recorded. Faraday's law was used to calculate the electrochemically oxidizable hydrogen content of the catalyst from the amount of charge passed up to a potential of 150 mV and from the weight of the catalyst.

Catalyst samples were also prepared which were freed from hydrogen electrochemically (samples 11—15, from sample 11) only aluminium being leached out.

The hydrogenating activities of the heat-treated samples were determined at atmospheric pressure and room temperature, and their specific surfaces were measured by the physical adsorption of nitrogen. Further, the hydrogen contents of all the samples (including the electrochemically oxidized ones) were determined by thermodesorption, and thermomagnetic analysis was performed. The experimental conditions and the method of evaluating the experimental data were reported in earlier papers in this series [3—9].

Results

The results obtained in the various investigations are listed in Table I. The saturation magnetizations of the catalysts are given for the states before (σ_{25}) and after (σ_{400}) thermomagnetic analysis, together with the Curie temperatures for the states after heat treatment at 100 (Θ_{100}) and 400 °C (Θ_{400}). It can be seen from the measured magnetic data that the samples heat-treated at 250 and 320 °C differ fundamentally from the others: their saturation magnetizations (σ_{400}) and Curie temperatures (Θ_{400}) measured after heat treatment at 400 °C are smaller than those of samples heat-treated at either lower or higher temperatures. Figure 3 shows plots of the $\Delta\sigma$ and $\Delta\Theta$ values

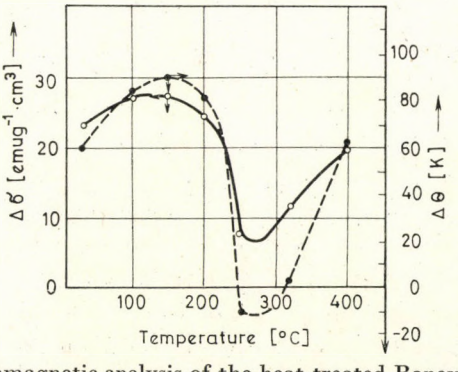

Fig. 3. Results of thermomagnetic analysis of the heat-treated Raney nickel samples. Changes in magnetization ($\Delta\sigma$) and Curie temperature ($\Delta\Theta$) as functions of the temperature of thermal pre-treatment

Table 1

Results on heat-treated and electrochemically

Catalyst No.	Heat-treatment temp. °C	Magnetic parameters				Electrochemical parameters			Catalytic activity eugenol nitrobenzene	
		σ 25	σ 400	Θ 100	Θ 400	potential (mV)	ml H_2/g pol. 1.	cat. pol. 2.	ml H_2/ml	cat/min
1	2	3				4			5	
1.	25	18.5	41.7	470	532	55	56	39	35	21
2.	100	13.5	41.3	451	538	77	51	34	24	2
3.	150	12.0	39.6	450	542	85	47	24	22	2
4.	200	16.2	40.8	472	554	120	15	23	23	3
5.	250	13.8	21.7	486	477	146	8	13	0	0
6.	320	17.0	28.6	465	470	135	9	13	0	0
7.	400	16.8	36.8	470	534	139	10	16	0	0
11.	—	20.4	37.7	508	598	0		45	—	—
12.	—	24.9	39.1	523	596	75		39	—	—
13.	—	20.5	36.7	508	600	119		24	—	—
14.	—	16.6	35.8	488	593	139		0	—	—
15.	—	20.7	36.7	501	577	160		0	—	—

* There is no sharp maximum, and thus the temperature values are only approximate

(*i.e.* $\sigma_{400}-\sigma_{25}$ and $\Theta_{400}-\Theta_{100}$) for samples 1—7 as functions of the temperature of the preliminary heat treatment.

There is no significant difference between the magnetic data of the anodically polarized samples; the nearly identical saturation magnetization values (σ_{400}) after heat treatment at 400 °C confirmed that the ferromagnetic nickel contents of the catalysts did not change, *i.e.* it was not oxidized electrochemically.

The electrochemical measurements led to the determination of the potentials of the individual catalyst samples before the aluminium was leached out, and then their hydrogen contents, in the electrochemically saturated state (polarization 1) and the state saturated with gaseous hydrogen (polarization 2). The charge amount *vs.* potential relation for the base catalyst is shown in Fig. 4 (curves of a similar nature were obtained for the other catalysts, and this is therefore presented as a typical example). In the case of the electrochemically pretreated samples (11—15), the potential is the value up to which polarization was carried out after removal of aluminium, while the hydrogen content was the value read from the polarization curve of the base catalyst (Fig. 4).

oxidized Raney nickel catalysts

Specific surface (m^2/g) treated at 100 °C	Thermodesorption results Amount of hydrogen (mlg), temp. of desorption peak max. (° C)							Magnetic moment μ_B/H atom		
	H_1		H_2		H_3		sum	H_1	H_2	H_3
	ml/g	°C	ml/g	°C	ml/g	°C*				
6	7							8		
132	34	60	41	201	—	—	75	0.21	0.75	—
113	10	54	19	186	17	350	46	0.32	1.6	2.4
85	7	73	13	181	9	430	29	0.68	0.95	—
120	8	62	23	233	6	580	37	0.31	0.98	—
5	1	73	5	231	5	(400)	11	—	1.1	—
20	2	90	8	242	3	480	13	—	—	—
72	1	85	6	238	3	(400)	10	—	—	—
—	14	62	5	265	—	—	19			
—	1	76	10	289	—	—	11			
—	2.5	88	—	—	—	—	2.5			
—	—	—	—	—	—	—	—			
—										

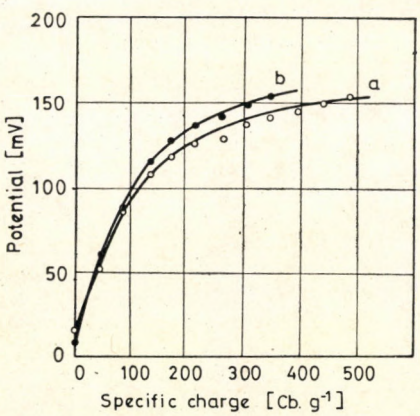

Fig. 4. Charge passed *vs.* potential for Raney nickel.
a) Polarization (polarization 1) in state saturated with hydrogen electrochemically, *b)* polarization (polarization 2) in state saturated with gaseous hydrogen

Activity measurements indicated that catalysts heat-treated at temperatures above 200 °C are inactive.

The results of specific surface and thermodesorption hydrogen content measurements can be seen in the sixth and seventh columns of Table I. In

addition to the total hydrogen content, the amounts desorbed at the three different temperatures are also given, together with the temperatures corresponding to the maximum rate of desorption.

The last column of the Table contains the values of the 'magnetic moment per H atom', characteristic of the bond strengths of the hydrogen species, calculated from the amount of hydrogen desorbed and from the increase in saturation magnetization in the approximate temperature interval of desorption.

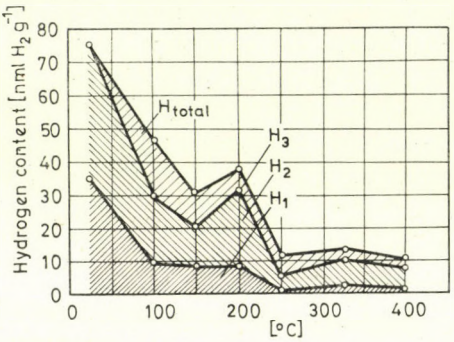

Fig. 5. Hydrogen contents of heat-treated Raney nickel samples, determined by thermodesorption, as a function of the temperature of heat-treatment

Figure 5 shows the hydrogen content determined by thermodesorption, against the temperature of heat treatment of the catalyst; the amounts of the three types of hydrogen with different bond strengths, and also their sum, are all plotted separately.

Discussion

In a general evaluation of these experiments it must be emphasized that systematic differences were observed on comparison of the results obtained in the course of a continuous increase of temperature and results referring to samples heat-treated at the given temperature and then covered with alcohol again: equilibrium may be restorted on standing in heat-treated samples returned to alcohol, while in measurements made with continuous temperature increase the samples come into a new state within a very short time.

On the basis of the data obtained by the various measurements, it is clear that Raney nickel undergoes a decisive change above 200 °C (see Ref. [9]); the magnetic parameters (σ and Θ) (Fig. 3), the specific surface and the hydrogen content determined electrochemically and by thermodesorption decrease, and there is no longer any catalytic activity in room temperature reactions.

As indicated by the sharp decrease of $\Delta\sigma$ and $\Delta\Theta$ between 200 and 250 °C, this change means a transformation in the structure of the skeleton nickel, and an appreciable fall in the hydrogen content; there is a close correlation between these two factors.

Surprisingly, the Curie temperatures and saturation magnetizations of samples once heat-treated at 250 and 320 °C do not change at higher temperature and on repeated heat treatment (Fig. 3), indicating that the first heat treatment has stabilized an intermediate state.

According to the magnetic data for the electrochemically oxidized samples, when the aluminium is leached out, the resulting nickel has a coarser structure (Θ larger than that of the base catalyst) (Table I, column 3/3, samples 11—15); further, nickel is not oxidized during the electrochemical polarization in the examined interval of about 150 mV (σ_{400} is nearly the same for samples 11—15), and thus the total charge passed was consumed in the oxidation of the sorbed hydrogen.

The catalytic activities can be brought into parallel with the hydrogen content and the specific surface area, *i.e.* the atmospheric hydrogenating activity at room temperature is bound to a certain surface area and structure, and to the sorbed hydrogen content.

The potentials measured before the catalysts are freed from aluminium (Table I, column 4/1) approximately characterize the hydrogen contents of the samples, *i.e.* the more the potential differs from that of the hydrogen electrode, the lower the hydrogen content.

The hydrogen contents determined electrochemically and by thermodesorption are in correlation, and nearly agree for samples heat-treated at higher temperatures.

The thermodesorption results indicate that a desorbing at higher temperatures (>350 °C) hydrogen species appears in all of the heat-treated samples. At room temperature this hydrogen species can be found in the catalysts only after storage for several months. The two hydrogen species desorbing at 50—100 and at 180—250 °C, respectively, are to be found in all the samples, which permits the conclusion that the hydrogen remaining in the heat-treated samples re-immersed in abs. alcohol (from which samples one or both of these hydrogen species have been desorbed) is distributed between these two forms, *i.e.* the individual hydrogen species may transform into one another.

The tendencies of the temperature of the hydrogen desorption peak maxima and the increase of the Bohr magneton number per hydrogen atom desorbed (μB/H atom) show that heat treatment at increasing temperatures leads to changes in the catalysts, such that the bond strengths of the residual hydrogen species increase.

REFERENCES

[1] STURM, F. v.: Electrochemische Stromerzeugung, pp. 85—90. Verlag Chemie, Weinheim 1969
[2] STURM, F. v., RICHTER, G.: Electrochim. Acta, **10,** 1169 (1965)
[3] HEISZMAN, J., PAYER, K., BÉKÁSSY, S., PETRÓ, J.: Magy. Kém. Folyóirat, **80,** 411 (1974)
[4] HEISZMAN, J., PETRÓ, J., TUNGLER, A., MÁTHÉ, T., CSŰRÖS, Z.: Magy. Kém. Folyóirat, **80,** 560 (1974)
[6] TUNGLER, A., BÉKÁSSY, S., PETRÓ, J.: Magy. Kém. Folyóirat, **80,** 566 (1974)
[7] BÉKÁSSY, S., LIPTAY, Gy., PETRÓ, J.: Magy. Kém. Folyóirat, **81,** 26 (1975)
[8] BÉKÁSSY, S., PETRÓ, J., KRISTÁK, E., CSANÁDI, A., KÁLMÁN, A.: Magy. Kém. Folyóirat 82, 40 (1976)
[9] TUNGLER, A., PETRÓ, J., HEISZMAN, J., MÁTHÉ, T., BÉKÁSSY, S., CSŰRÖS, Z.: Magy. Kém. Folyóirat, 82. 11, (1976)
[10] Hungarian patent 162, 281

Antal TUNGLER
József PETRÓ
Tibor MÁTHÉ
József HEISZMAN
Ferenc BUELLA
Zoltán CSŰRÖS

H-1111 Budapest, Műegyetem rkp. 3.

Acta Chimica Academiae Scientiarum Hungaricae, Tomus 89 (2), pp. 161—172 (1976)

SYNTHESIS OF TRIHYDROXYALKYLTETRAHYDROISOQUINOLINE DERIVATIVES

G. DÖRNYEI* and Cs. SZÁNTAY

(Chinoin Pharmaceutical and Chemical Works, Budapest and Department of Organic Chemistry, Technical University, Budapest)*

Received April 12, 1975

Starting with D-tartaric acid, 1-trihydroxypropyltetrahydroisoquinoline derivatives, readily soluble in water, have been synthesized. The absolute configurations of the compounds having three chiral centres have been elucidated.

The favourable pharmacological action of tetrahydroisoquinoline derivatives substituted on C-1 has been known for a long time [1]. It is also known that an increase of the water-solubility of the compounds — especially if independent of the pH-value of the medium — has usually a positive influence on the pharmacological effect.

In the following we report the synthesis of new tetrahydroisoquinoline derivatives substituted in the C-1 position by a 1,2,3-trihydroxypropyl group (**1a, b**).

These compounds have been synthesized in the way shown in Scheme 1.

O,O-Diacetyl-D-tartaric anhydride (**2**) prepared by the acylation of D-tartaric acid was subjected to methanolysis, and the product was treated with thionyl chloride to obtain the half-ester chloride **3** [2]. This compound can be used to acylate the appropriate 3,4-dialkoxyphenylethylamine (**4**) to give the acid amide (**5**). The acid amide **5** can also be prepared in a simpler way and almost in quantitative yield, if the acylation is carried out directly with the anhydride **2**, and the resulting amide-carboxylic acid (**6**) is methylated with diazomethane.

Bischler—Napieralski ring closure of the amide **5** afforded the dihydroisoquinoline derivative **7** only in the presence of phosphorus pentachloride in methylene chloride [3]; compound **8** was obtained on methanolic deacetylation. Both compounds are stable as salts; liberation of the base is presumably accompanied by an undesired elimination in the side chain.

It seemed therefore advisable to carry out the hydrogenation of the C=N double bond of the dihydroisoquinoline derivatives in acidic medium. Reduction of the dihydroisoquinoline hydrochloride (**8**) with sodium borohydride in acetic acid, or by catalytic hydrogenation, yielded the tetrahydroisoquinoline hydrochloride (**9**). When basic medium was applied in the course of the reduction or work up, pyrrolo [2,1-a] isoquinoline derivatives (**10** or **11**) having a five-membered lactam ring could be isolated. The reaction of the

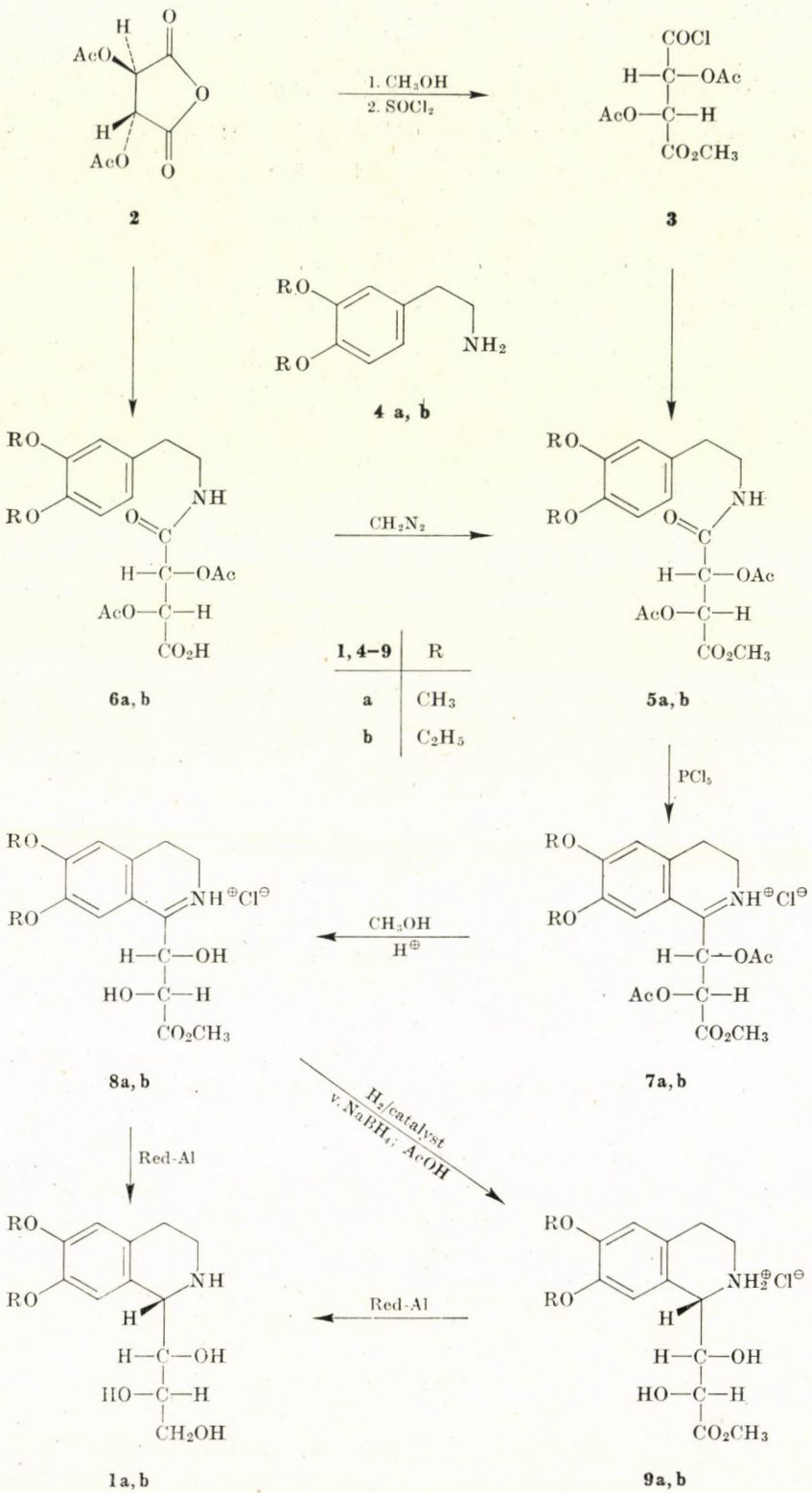

2 **3** **4 a, b** **6a, b** **5a, b** **8a, b** **7a, b** **1a, b** **9a, b**

Scheme 1

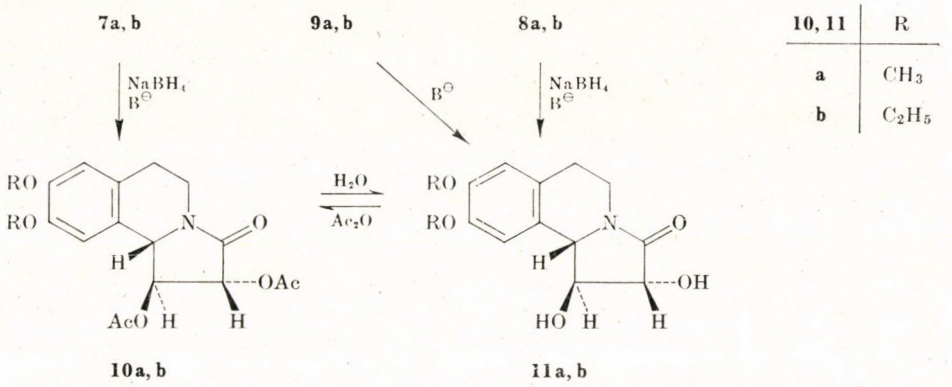

10, 11	R
a	CH_3
b	C_2H_5

Scheme 2

hydrochloride **9** with sodium bis-(2-methoxyethoxy) aluminium hydride (Red-Al) in benzene or toluene afforded the end-product (**1**).

The reaction sequence **8** → **9** → **1** can also be achieved in one step by the direct reduction of the hydrochloride **8** with Red-Al.

The structures of **1a** and **1b** have been unequivocally proved by their NMR and MS spectra, as well as by the elementary analysis and spectroscopic investigation of their tetraacetyl derivatives.

In giving the exact stereochemical structure of **1**, the absolute configurations of C1' and C2' in the side chain are certainly known from the stereochemistry of the starting D-tartaric acid.

In the determination of the absolute configuration of the chiral C-1 atom, the CD curve of the trihydroxypropyltetrahydroisoquinoline derivative **1b** (see Fig. 1) is of assistance.

The negative Cotton effect (^1L_b-band) observed at about 285 nm proves the $-M$ helicity of ring B [4]. According to data given in the literature [5], in the case of tetrahydroisoquinolines substituted on C1, the conformer having a substituent in *quasi-axial* position is always preferred. On this basis, the steric structure of the chiral second sphere responsible for the Cotton effect appearing at 285 nm and that of the C1 substituent are shown in Fig. 2. Thus the absolute configuration of the C1 atom is *S*. As the conditions of symmetry in compound **1a** having dimethoxy substituents in the aromatic ring are identical with those of the ethoxy homologue, it is highly probable that the steric arrangements of **1a** and **1b** are identical, *i.e.* 1(*S*), 1'(*S*), 2'(*S*). Owing to the correlations between the compounds, the absolute configuration at C1 in **1** and **9**, and at C10b in **10** and **11** is the same. Consequently, an evaluation of the NMR spectra of the diacetyl-lactam **10b** (and **10a**) gave valuable data for the elucidation of the steric structure of all compounds (Fig. 3). Peaks 1—7 (3 protons) could be assigned with the aid of the spectrum of the compound having deuterium at carbon atom 10b (Fig. 4). In the latter spectrum

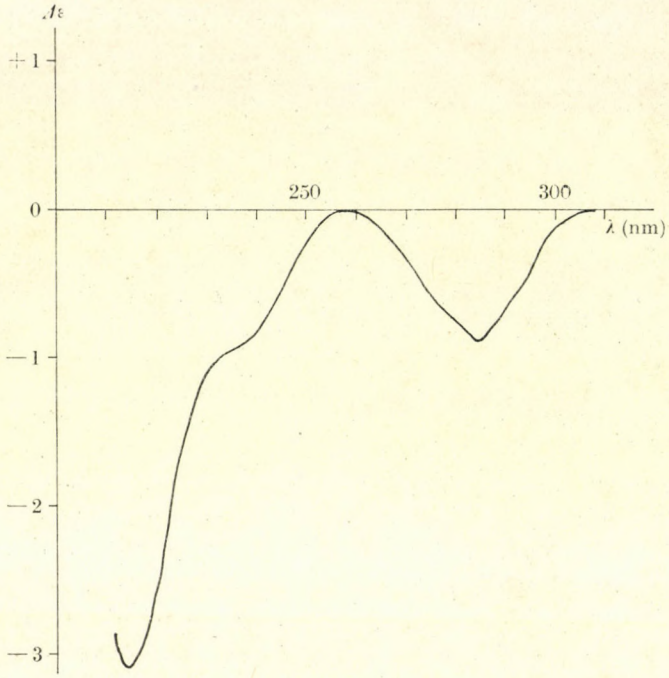

Fig. 1. CD curve of **1b** in methanol

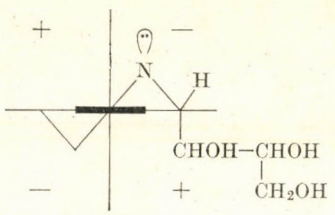

M-helicity

Fig. 2. Projection of compound **1**

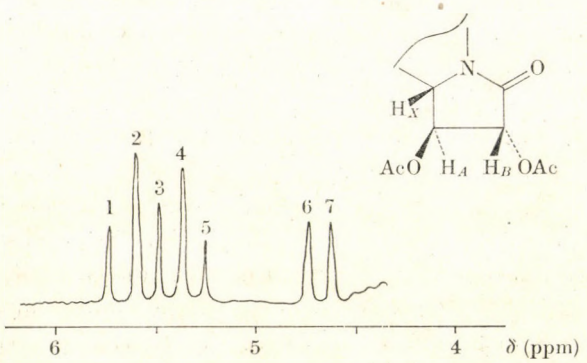

Fig. 3. Part of the NMR spectrum of **10b** (DMSO-d_6)

the H_A and H_B protons give an AB system ($J_{AB} = 7.5$; $\delta H_A = 5.38$; $\delta H_B = 5.64$).

The seven peaks appearing in the spectrum of **10b** at δ 4.5—6 can be assigned by assuming that two peaks due to the H_B proton (1,2; 1H) remain unchanged during the D → H exchange, whereas the peaks attributable to H_A are further split by the 10b proton ($\delta H_X = 4.79$; d, 1H, $J_{AX} = 7.5$ Hz; peaks 6 and 7), where the coupling constant happens to be the same; this results in the asymmetric triplet also of 1H intensity (peaks 3, 4 and 5).

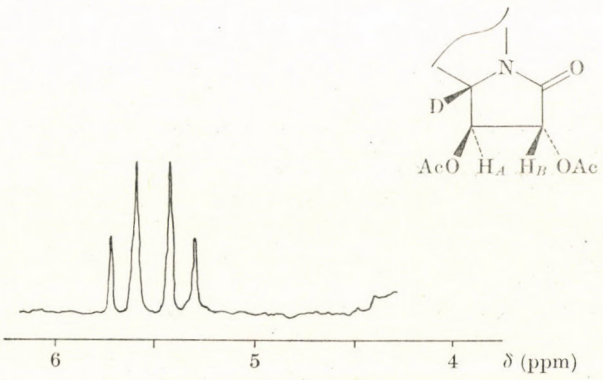

Fig. 4. Part of the NMR spectrum of 10b-deutero-10b (DMSO-d_6)

The coupling constants J_{AB} and J_{AX} give unambiguous evidence for the β-orientation of the hydrogen atom attached to carbon atom 10b, *i.e.* for the *S*-configuration of the chiral centre, since the dihedral angles (10b(*S*): C—H_X/C—H_A ~ 150°, C—H_A/C—H_b ~ 150°; 10b(*R*): C—H_X/C—H_A ~ 30°, C—H_A/C—H_B ~ 90°) measured on the Dreiding model of the stereoisomers 10b(*S*) and 10b(*R*) forming a rather rigid ring system, are in good agreement with the coupling constants of the X—AB system in the former case.

Although the direct conversion of **8** to **1** is less stereoselective than the indirect way (**8** → **9** → **1**), according to our experiments, the former gives the compounds **1** having 1(*S*), 1'(*S*), 2'(*S*) absolute configuration in higher yields, as they can be readily separated from the 1(*R*) stereoisomer by crystallization.

The pharmacological investigation of the resulting compounds **1a** and **1b**, which are excellently soluble in water, is in progress.

Experimental

The IR spectra were recorded in KBr or in a solution with a Spectronom 2000 and a Perkin–Elmer 221 spectrophotometer. The NMR spectra were obtained with a Perkin–Elmer R12 (60 MHz) spectrometer; the chemical shifts (δ) are given in ppm; TMS was used as internal standard. The mass spectra (MS) were obtained with an AEI MS 902 instrument (70 eV;

temperature of the ion source 150 °C; direct insertion). The CD curve was measured with a JASCO J30 dichrograph in methanol solution ($c = 10^{-3}$ mole/l) in a 1-mm cell at room temperature.

The course of the reactions was checked by qualitative thin-layer chromatography TLC). Inactive silica gel (Kieselgel GF_{254}; Merck) was used as the adsorbent. The following developing solvent systems were employed:

System A: benzene–methanol 5 : 1
System B: saturation with NH_4OH for 5 min, CH_2Cl_2–methanol 12 : 1
System C: CH_2Cl_2–methanol 5 : 1
System D: benzene–ethyl acetate 1 : 1
System E: saturation with NH_4OH for 5 min, CH_2Cl_2–methanol 6 : 1

The chromatograms were evaluated under a UV lamp ($\lambda = 254$ nm), and by visualizing the spots in iodine vapour.

1. 2(R), 3(R)-Diacetoxy-3-(N-3,4-dialkoxyphenyl-ethylcarbamoyl)propionic acid (6)

A solution of **2** (21.6 g; 100 mmoles) in methylene chloride (200 ml) was placed in a flask equipped with a dropping funnel and reflux condenser, and a solution of **4** (100 mmoles) in methylene chloride (60 ml) was added at a rate to maintain gentle boiling of the reaction mixture. It was then allowed to stand at room temperature for 1 hr, then in a refrigerator overnight; the precipitated crystals were filtered off.

The 3,4-*dimethoxyphenyl derivative* (**6a**) was obtained as colourless crystals (36.8 g; 93%), m. p. 220 °C (d.).

$C_{18}H_{23}NO_9$ (397.37). Calcd. C 54.40; H 5.83; N 3.53. Found C 54.46; H 5.93; N 3.70%.
IR (KBr): 1760 (C=O ester); 1735 (C=O acid); 1640 (C=O amide); 3370 cm^{-1} (NH).

The colourless crystals of the 3,4-*diethoxyphenyl* derivative (**6b**) (38.6 g; 91%) melt at 180—181 °C.

$C_{20}H_{27}NO_9$ (425.42). Calcd. C 56.46; H 6.40; N 3.29. Found C 56.39; H 6.48; N 3.48%.
IR (KBr): 1755 (C=O ester), 1740 (C=O acid,) 1635 (C=O amide), 3370 cm^{-1} (NH).

2. Methyl [2(R), 3(R)-diacetoxy-3-(N-3,4-dialkoxyphenylethylcarbamoyl)]propionate (5)

2.1. *Synthesis of the* 3,4-*dimethoxyphenylethyl derivative* (**5a**)

2.1.1. The propionic acid derivative **6a** (11.91 g; 30 mmoles) was dissolved in a mixture of methanol (140 ml) and methylene chloride (190 ml) and diazomethane in ether was added with stirring at room temperature, until the reaction was complete (TLC system A: R_f**6a** 0.1; R_f**5a**: 0.52). The reaction mixture was evaporated to dryness in vacuum. The remaining oil, on treatment with a mixture of ether and hexane, yielded a colourless crystalline product (12.00 g; 97%), m. p. 81—83 °C.

$C_{19}H_{25}NO_9$ (411.40). Calcd. C 55.47; H 6.13; N 3.40. Found C 55.70; H 6.34; N 3.55%.
IR (KBr): 1750 (1765 sh., C=O esters); 1675 (C=O amide); 3370, 3400 cm^{-1} (NH).
IR ($CHCl_3$): 1770 (C=O esters); 1700 (C=O amide).
NMR ($CDCl_3$): 2.10 and 2.14 s, (3H (each), CH_3—CO); 2.80 (m, 2H, Ph—CH_2—); 3.55 (m, 2H, —CH_2—NHCO); 3.79 (s, 3H, CO_2CH_3); 3.91 and 3.94 (s, 3H (each), OCH_3); 5.70 and 5.82 (AB system, 1H (each); $J = 2.5$; >CH—OAC); 6.30 (1H, broad, NH); 6.85—6.89 (3H, aromatic protons).

2.1.2. Acylation with acid chloride **3**. O,O-Diacetyl-D-tartaric acid semi-chloride half-ester (**3**) was obtained according to the method described in the literature [2] in a yield of 52%, calculated for D-tartaric acid. The latter compound (5.33 g; 20 mmoles) was dissolved in ether (300 ml) and a solution of **4a** (7.24 g; 40 mmoles) in ether (100 ml) was added under stirring and ice-cooling; the evolution of heat was observed. After stirring for 1 hr water (100 ml) and methylene chloride (50 ml) were added. The mixture was shaken in a separatory funnel, then the organic layer was washed with water (2×50 ml), dried ($MgSO_4$) and the solvent evaporated. The residue was recrystallized from a mixture of ether and hexane. The resulting **5a** (5.35 g; 65%) proved to be identical in every respect (m. p., IR, NMR, TLC) with the product obtained in Experiment 2.1.1.

2.2. *Synthesis of the* 3,4-*diethoxyphenylethyl derivative* (**5b**)

2.2.1. The propionic acid derivative **6b** (12.75 g; 30 mmoles) was suspended in a mixture of ether (200 ml) and methanol (5 ml). The procedure of methylation with diazomethane was the same as for **6a** (Experiment 2.1.1.) (TLC system A, R_f**6b**: 0.1; R_f**5b**: 0.53). At the end of the reaction the suspension cleared up, then the ester **5b** started to crystallize. The precipitation was promoted by adding hexane (100 ml). After filtration and drying, the colourless crystals of **5b** (11.83 g; 90%) 104—105 °C, $[\alpha]_D^{25}$–11° (c = 1, methanol).

$C_{21}H_{29}NO_9$ (439.45). Calcd. C 57.39; H 6.65; N 3.19. Found C 57.55; H 6.67; N 3.18%.

IR (KBr): 1765, 1750 (C=O ester); 1695 (C=O chelated ester); 1660 (C=O amide); 3420, 3270 and 3090 cm^{-1} (NH asymm.).

IR ($CHCl_3$): 1770 (C=O esters); 1700 cm^{-1} (C=O amide).

NMR ($CDCl_3$): 1.44 (t, 6H, J = 7, OCH_2-CH_3); 2.06 and 2.09 (s, 3H (each), CH_3-CO); 2.74 (t, 2H, J = 7, $-CH_2-CH_2-NH$); 3.53 (q, 2H, J = 7, CH_2-CH_2-NH); 5.64, 5.76 (2H, J_{AB} = 2.5 Hz, H—C—O); 6.28 (1H, broad, NH); 6.78—6.82 (3H, aromatic protons).

2.2.2. The acylation of **4b** (8.36 g; 40 mmoles) with acid chloride **3** (5.33 g; 20 mmoles) was effected according to Experiment 2.1.2. Compound **5b** obtained in this way (6.05 g; 70%) was identical in every respect with the product described in 2.2.1.

3. Cyclization with PCl_5

3.1. *Methyl* [2*(R)*, 3*(S)*-*dihydroxy*-3-*(*6,7-*dimethoxy*-3,4-*dihydroisoquinoline*-1-*yl)*]*propionate*(**8a**)

Phosphorus pentachloride (12 g; 58 mmoles) was dissolved in methylene chloride (90 ml) with stirring and heating. Stirring was maintained and the mixture cooled (precipitation of fine crystals); then the amide ester **5a** (12.33 g; 30 mmoles) in methylene chloride (100 ml) was added at a temperature of 5—10 °C.

After the reaction mixture had become homogeneous, it was allowed to stand overnight in a refrigerator. The reaction **5a** → **7a** could be followed by TLC (System B, R_f**5a**: 0.60; R_f**7a**: 0.50). The majority of the solvent was evaporated in vacuum, methanol (100 ml) was cautiously added to the residue, and the mixture was refluxed for 30 min. After deacetylation (TLC system B, R_f**7a**: 0.50; R_f**8a**: 0.42), ether was added to the luke-warm solution until crystallization started. Filtration gave the colourless crystals of the hydrochloride of **8a** (9.53 g; 87%), which decomposed at 162—163 °C; $[\alpha]_D^{25}$–58° (c = 1, methanol).

$C_{15}H_{20}NO_6Cl \cdot 1/2\ CH_3OH$ (361.73). Calcd. C 51.46; H 6.13; N 3.87. Found C 51.78; H 6.29; N 4.03%.

IR (KBr): 1735 (C=O); 1675 (C=$\overset{\oplus}{N}$); 1570, 1615 cm^{-1} (arom.).

NMR (CD_3OD): 3.10 (s, 1,5H, CH_3OH); 3.60, 3.70, 3.77 (9H, OCH_3); 4.23 (d, 1H $\overset{\oplus}{N}$=C—CH—OH); 5.60 (m, 1H >C=$\overset{\oplus}{N}$(H)—C—H "peri"); 6.90 (s, 1H, C5–H); 7.18 (s, 1H, C8—H).

If the methanolic treatment after the ring closure was omitted and the oil was repeatedly precipitated from the reaction mixture with ether, the oily diacetoxy compound **7a** could finally be transformed into a solid foam (10.2 g; 79%).

IR (KBr): 1750 (broad C=O); 1650 (>C=$\overset{\oplus}{N}$); 1555, 1610 (arom.); 1205 cm^{-1} ($CH_3-CO-O-C$).

3.2. *Methyl* [2*(R)*, 3*(S)*-*dihydroxy*-3-*(*6,7-*diethoxy*-3,4-*dihydroisoquinoline*-1-*yl)*]*propionate*(**8b**)

The cyclization of the amide ester **5b** (13.17 g; 30 mmoles) was carried out as described in Experiment 3.1. The crystals of the hydrochloride of **8b** (8.95 g; 80%), precipitated from a mixture of methanol and ether, decomposed at 174.5—175 °C; $[\alpha]_D^{25}$–70° (c = 1, methanol).

$C_{17}H_{24}NO_6Cl$ (373.82). Calcd. C 54.62; H 6.47; N 3.75; Cl 9.50. Found C 54.87; H 6.85; N 3.76; Cl 9.51%.

IR (KBr): 1730 (C=O); 1670 (C=$\overset{\oplus}{N}$<); 1565, 1615 cm^{-1} (arom.).

NMR (CD_3OD): 1.42 and 1.45 (2×t, 6H, J = 7, CH_3-CH_2-O); 3.96 (s, 3H, OCH_3); 4.22 (q, 4H, J = 7; CH_3-CH_2-O-); 4.60 (d, 1H, $\overset{\oplus}{N}$=C—CH—OH); 5.79 (m, 1H, >C=$\overset{\oplus}{N}$H—CH "peri"); 7.11 (s, 1H, C5—H); 7.31 (s, 1H, C8—H).

MS (*m/e*, %): 337 (M—HCl, 3); 320 (1); 278 (2); 249 (93); 248 (50); 247 (17); 234 (33); 220 (100); 206 (30); 204 (11); 194 (30); 192 (17).

If the deacetylation step was omitted, the hydrochloride of **7b** could be obtained as a foam (11.4 g; 83%).

IR (KBr): 1760 (C=O); 1655 (C=$\overset{\oplus}{N}$<); 1560, 1605 (arom.); 1200 cm^{-1} (CH_3—CO—O—C).

4. Reduction of the dihydroisoquinoline 8 to the tetrahydro derivative 9

4.1. *Methyl[2(R),3(S)-dihydroxy-3-(6,7-dimethoxytetrahydroisoquinoline-1(S)-yl)]propionate* (9a)

4.1.1. The dihydroisoquinoline **8a** (1.08 g; 3 mmoles) was dissolved in methanol (30 ml) containing 1 ml of 1*N* methanolic HCl, and the mixture was hydrogenated at room temperature and atmospheric pressure in the presence of palladium-on-carbon (0.8 g). The reduction was completed in about 3 hrs (hydrogen absorbed 77 ml, theoretical: 72 ml). The solution was evaporated to dryness and the residue (1.02 g; 100%) was recrystallized from a mixture of methanol and methylene chloride. The colourless crystals of the hydrochloride of **9a** decomposed at 186—187 °C, then solidified and melted again at 243—245 °C.

$C_{15}H_{22}NO_6Cl$ (347.80). Calcd. C 51.80; H 6.38; N 4.03; Cl 10.20. Found C 51.58; H 6.15; N 4.07; Cl 10.17%.

IR (KBr): 1730 (C=O); 1605 (arom.); 3000—3400 cm^{-1} (broad, OH).

NMR (DMSO-d_6): 3.64 (s, 3H, CO_2CH_3); 3.73 (s, 6H, OCH_3); 4.12 (broad, 1H, C3—OH); 4.65 (broad, 3H, C2—OH, >*CH*—OH); 6.86 (s, 1H C5'—H; 6.98 (s, 1H, C8'—H).

NMR (DMSO-d_6+D_2O): The signal at 4.12 ppm disappeared and the intensity of the group at 4.56 diminished to two.

MS (*m/e*, %): the fragmentation was the same as observed with compound **11a**, indicating a quick lactam ring closure reaction of the ester under the conditions of measurement (*cf.* Experiment 5.1.2.).

4.1.2. The dihydro compound **8a** (0.36 g; 1 mmole) was dissolved in a mixture of methylene chloride (8 ml) and acetic acid (1 ml), and reduced with $NaBH_4$ (50 mg; about 1 mmole) at 5 °C. The reaction was followed by TLC (System C, R_f**8a**: 0.58; R_f**9a**: 0.33). The reaction mixture was evaporated to dryness and the residue purified by chromatography using solvent system C on a Kieselgel 60 (0.063—0.200 mm) column. The fractions containing the product **9a** were combined, evaporated to dryness and the residue was recrystallized from a mixture of methylene chloride and methanol. The resulting crystalline product (0.184 g; 53%) proved to be identical in all respects (m. p., TLC, NMR) with the tetrahydroisoquinoline hydrochloride **9a** prepared in Experiment 4.1.1.

4.2. *Methyl[2(R),3(S)-dihydroxy-3-(6,7-diethoxytetrahydroisoquinoline-1(S)-yl)]propionate* (9b)

4.2.1. The dihydroisoquinoline hydrochloride **8b** (1.12 g; 3 mmoles) was reduced catalytically as described in Experiment 4.1.1. The hydrochloride **9b** was obtained as colourless microcrystals (1.12 g; 100%) after rubbing with ether, m. p. 170—171 °C (d); $[\alpha]_D^{25}$ + 60° (*c* = 1, methanol).

$C_{17}H_{26}NO_6Cl$ (375.85). Calcd. C 54.32; H 6.97; N 3.73; Cl 9.43. Found C 54.04; H 6.79; N 3.91; Cl 9.90%.

IR (KBr): 1750 (C=O); 1620 (arom.); 3200—3500 cm^{-1} (>$\overset{\oplus}{N}H_2$; OH).

NMR (CD_3OD + $CDCl_3$): 1.41 (t, 6H, *J* = 6; CH_3—CH_2—O); 3.09 (2H, Ph—CH_2—); 3.34 (2H, >$\overset{\oplus}{N}$—CH_2—); 3.78 (s, 3H, CH_3O); 4.10 (4H, —CH_2—O—); 4.60 (6H, broad, OH, NH_2, >*CH*—OH); 6.83 (2H, broad, aromatic protons.).

4.2.2. The dihydro derivative **8b** (0.37 g; 1 mmole) was reduced with sodium borohydride according to Experiment 4.1.2. The resulting hydrochloride **9b** was in every respect (TLC, m. p., IR, NMR) identical with the product described in Experiment 4.2.1.

5. Synthesis of pyrrolo[2,1-a]isoquinoline derivatives

5.1. *1(S), 2(R)-Dihydroxy*-8,9-*dimethoxy*-1,2,3,5,6,10*b(S)-hexahydropyrrolo*[2,1-*a*]*isoquinoline*-3-*one* (**11a**)

5.1.1. The dihydroisoquinoline hydrochloride **8a** (0.362 g; 1 mmole) was dissolved in methanol (8 ml) and reduced with sodium borohydride (*cf.* Experiment 4.1.2.). After the reaction had been completed, water (10 ml) and 2*N* NH_4OH (0.6 ml) were added to the solution (pH 10) containing mainly **9a**. The solution was allowed to stand overnight, then concentrated. The precipitated crystalline product was filtered off and washed with water. The colourless crystals of lactam **11a** (0.19 g; 68%) had m. p. 243—245 °C. R_f (System C) 0.64.

$C_{14}H_{17}NO_5$ (279.29). Calcd. C 60.20; H 6.14; N 5.02. Found C 59.96; H 6.13; N 4.89%.

IR (KBr): 1695 (C=O 5-membered lactam ring); 1605 (arom.); 3260 and 3380 cm^{-1} (OH).

NMR (DMSO-d_6): 3.92 (s, 6H, OCH_3); 4.10—4.62 (m, 3H, C*H*OH and Ph—C*H*—N); 5.85 (d, 1H, J = 6, C1—OH); 6.31 (d, 1H, J = 6, C2—OH); 6.96 (s, 1H, C7—H); 7.26 (s, 1H C10—H).

NMR (DMSO-d_6 + 3 drops of D_2O): The two doublets at 5.85 and 6.31 disappeared.

MS (*m/e;* %): 279 (M^+, 87); 262(40); 250(29); 248(4); 192(100); 191(96); 176(41); 92(8); 77(10).

5.1.2. The tetrahydroisoquinoline hydrochloride **9a** (0.35 g; 1 mmole) was dissolved in a mixture of water (8 ml) and methanol (2 ml). The solution was filtered and 2*N* NH_4OH solution (0.6 ml) was added. The mixture was allowed to stand at room temperature for 1 hr, then in a refrigerator for 10 hrs. The precipitated crystals were filtered off. The resulting lactam **11a** (0.20 g; 72%) was in all respects identical with the product obtained from Experiment 5.1.1.

5.1.3. The diacetyl-lactam **10a** (0.36 g; 1 mmole) was dissolved in warm methanol (5 ml) and 2*N* aqueous hydrochlorid acid (5 ml) or 2*N* sodium hydroxide (5 ml) was added to the boiling solution. After refluxing for 10 min., the solution was neutralized, and the greatest part of the methanol was evaporated. The crystals obtained on cooling were filtered off, washed with water and dried. The resulting dihydroxylactam **11a** (0.14—0.17 g; 50—60%) was in all respects identical with the products prepared according to Experiments 5.1.1. and 5.1.2.

5.2. *1(S), 2(R)-Diacetoxy*-8,9-*dimethoxy*-1,2,3,5,6,10*b(S)-hexahydropyrrolo*[2,1-*a*]*isoquinoline* 3-*one* (**10a**)

5.2.1. The diacetoxydihydroisoquinoline hydrochloride **7a** (0.430 g; 1 mmole) was dissolved in methanol (10 ml) and reduced with sodium borohydride. The reaction could be followed by TLC (System C, R_f**7a**: 0.63). After the spot of the starting material had disappeared, the solvent was evaporated and the residue extracted with a system of benzene and 0.1*N* aqueous NH_4OH solution. The benzene solution was washed until it became neutral, dried ($MgSO_4$), and evaporated to dryness. The residue was treated with warm ether, the crystals which precipitated were filtered off. The colourless crystals of **10a** (0.197 g; 52.5%) had m. p. 175 °C (R_f**10a**: 0.76, System C).

$C_{18}H_{21}NO_7$ (363.36). Calcd. C 59.50; H 5.83; N 3.86. Found C 59.66; H 5.90; N 3.74%.

IR (KBr): 1740 (C=O acetyl); 1710 (C=O lactam); 1615 cm^{-1} (arom.).

NMR ($CDCl_3$): 2.12 and 2.22 (s, 3H (each), CH_3—CO); 3.83 and 3.88 (s, 3H (each), CH_3O); 4.38 (m, 1H, C5—$H_{equat.}$ "peri"); 4.80 (d, 1H, J = 7.5, C10b—H); 5.43 (t, 1H, J_{AB} = = 7.5; J_{AX} = 7.5, C1—H); 5.69 (d, 1H, AB syst., J_{AB} = 7.5, C2—H); 6.70 (s, 1H, C7—H); 6.76 (s, 1H, C10—H).

MS (*m/e*, %): 363(M^+, 7); 320(0.5); 303(66); 261(100); 246(16); 244(52); 192(45); 191(9); 190(7); 176(13); 43(51).

5.2.2. The dihydroxylactam **11a** (0.19 g; 0.68 mmole) was stirred in a mixture of acetic anhydride (5 ml) and pyridine (0.1 ml) at 60 °C. After the material had dissolved, this temperature was maintained for 10 hrs, then the light brown solution was poured into a mixture of ice-water (20 ml) and methanol (1 ml). A few hours later the crystals of **10a** were filtered off and dried. The resulting product (0.181 g; 73%) was in all respects identical with the diacetoxy-lactam (**10a**) obtained in Experiment 5.2.1.

5.3. *1(S),2(R)-dihydroxy*-8,9-*diethoxy*-1,2,3,5,6,10*b(S)-hexahydropyrrolo*[2,1-*a*]*isoquinoline*-3-*one* (**11b**)

5.3.1. The dihydroisoquinoline hydrochloride **8b** (0.374 g; 1 mmole) in methanol (8 ml) was reduced according to Experiment 5.1.1. with sodium borohydride. The lactam **11b** precipitated

as colourless crystals from the slightly basic solution (0.194 g; 63%), m. p. 195—196 °C; R_f (System C): 0.66.

$C_{16}H_{21}NO_5$ (307.34). Calcd. C 62.52; H 6.88; N 4.56. Found C 62.35; H 6.78; N 4.60%.

IR(KBr): 1680 (C=O lactam); 1620 (arom.); 3230 and 3430 cm^{-1} (OH).

NMR (DMSO-d_6): 1.26 (t, 6H, $J = 7$, CH_3-CH_2O); 3.96 (q, 4H, $J = 7$, CH_3-CH_2-O); 4.26 (d, 1H, $J = 7$, C10b—H); 5.60 (d, 1H, $J = 7$, C1—OH); 6.05 (d, 1H, $J = 7$, C2—OH); 6.72 (s, 1H, C7—H); 7.03 (s, 1H, C10—H).

NMR (DMSO-d_6 + D_2O): The signals of OH at 5.60 and 6.05 are missing from the spectrum. If the reaction was carried out with sodium borodeuteride, no peak appeared at 4.26 ppm in the NMR spectrum.

MS (*m/e*, %): 307 (M^+, 78); 290 (24); 278 (27); 262 (4); 250 (3); 220 (87); 219 (100); 204 (4); 198 (7); 192 (9); 191 (14); 190 (21); 162 (36); 163 (12).

5.3.2. The tetrahydroisoquinoline hydrochloride **9b** (0.376 g; 1 mmole) was transformed to lactam **11b** according to Experiment 5.1.2. The resulting material (0.173 g; 57%) proved to be identical in every respect with the compound described in Experiment 5.3.1.

5.3.3. When the diacetyllactam **10b** (0.391 g; 1 mmole) was deacetylated according to Experiment 5.1.3., (50—60%), the dihydroxylactam **11b** was obtained, the product being identical in all respects with the compounds described in Experiments 5.3.1. and 5.3.2.

5.4. *1(S),2(R)-Diacetoxy-8,9-diethoxy-1,2,3,5,6,10b(S)-hexahydropyrrolo[2,1-a]isoquinoline-3-one* (**10b**)

5.4.1. The diacetoxydihydroisoquinoline hydrochloride **7b** (0.458 g; 1 mmole) was converted to diacetoxylactam according to Experiment 5.2.1. (TLC system C, R_f**7b**: 0.73, R_f**10b**: 0.86). The colourless crystals of **10b** (0.192 g; 49%) decomposed at 163—163.5 °C, $[\alpha]_D^{25} + 120°$ (*c* = 2, methanol).

$C_{20}H_{25}NO_7$ (391.41). Calcd. C 61.37; H 6.44; N 3.58. Found C 61.60; H 6.42; N 3.73%.

IR (KBr): 1740 (C=O ester); 1715 (C=O lactam); 1615 (arom.); 1230 cm^{-1} ($CH_3-\overset{\overset{O}{\|}}{C}-O-C$).

NMR($CDCl_3$): 1.40 and 1.42 (2×t, 3H (each), $J = 7$; CH_3-CH_2-O); 2.10 (s, 3H, $Cl-O-\overset{\overset{O}{\|}}{C}-CH_3$); 2.18 (s, 3H, $C2-O-\overset{\overset{O}{\|}}{C}-CH_3$); 2.6—2.9 (m, 2H, C6—$H_2$); 3.10 (m, 1H, C5—$H_{ax}$); 3.99 and 4.03 (2×q, 2H (each), $J = 7$, CH_3-CH_2-O); 4.30 (m, 1H, C5—$H_{equat.}$ "peri"); 4.67 (d, 1H, $J = 7.5$, C10b—H); 5.38 (asymm. t, 1H, $J_{AB} = 7.5$, $J_{AX} = 7.5$ Cl—H); 5.64 (d of an AB system, $J_{AB} = 7.5$, 1H, C2—H); 6.68 (s, 1H, C7—H); 6.75 (s, 1H, C10—H).

When the reduction was carried out with sodium borodeuteride, the derivative having deuterium on the C-10b atom was obtained. The doublet at 4.67 ppm was missing and the signal system between 5.3 and 5.72 ppm simplified to an AB system.

5.4.2. The dihydroxylactam **11b** (0.200 g; 0.65 mmole) was acetylated as described in Experiment 5.2.2. The resulting diacetoxylactam (**10b**) (0.220 mg; 86%) was in every respect identical with the compound obtained in Experiment 5.4.1.

6. Synthesis of 1-trihydroxypropyltetrahydroisoquinoline derivatives (1)

6.1. *1(S)-[1'(S), 2'(S), 3'-Trihydroxypropyl]-6,7-dimethoxy-1,2,3,4-tetrahydroisoquinoline* (**1a**)

6.1.1. The dihydroisoquinoline hydrochloride **8a** (3.62 g; 10 mmoles) was suspended with stirring in a mixture of benzene (20 ml) and toluene (4 ml). A 70% benzene solution of sodium bis-(methoxyethoxy)aluminium hydride (Red-Al) (30 ml; 75 mmoles) was added to the reaction mixture while the temperature was maintained under 25 °C. The resulting solution was heated to 80 °C and stirred for 2 hrs. After cooling to room temperature, conc. HCl (60 ml) and distilled water (120 ml) were added to the reaction mixture. The two phases were separated and the aqueous acid phase was washed with benzene (50 ml). The mixture was made alkaline (pH > 11) with 1*N* NaOH under efficient cooling, and extracted with methylene chloride (4×100 ml). The organic layer was dried ($MgSO_4$), toluene was added (20 ml) to it, then the solvent was cautiously evaporated until the precipitation of crystals started, which was promoted by the addition of ether. The colourless crystals of **1a** that separated from the *1(R)*-epimer (1.7 g; 60%) had m. p. 169—170 °C.

$[\alpha]_D^{25}$ + 63° (c = 2, H_2O). TLC (System E), R_f *1(R)*: 0.32; R_f **1a**: 0.46.
IR(KBr): 1610 (arom.); 3240 and 3500 cm^{-1} (broad OH).
NMR ($CDCl_3$ + 3 drops of CD_3OD): 3.85 and 3.87 (s, 3H (each), OCH_3): 3.80—4.60 (9H, NH, >CH—OH, $-CH_2OH$, C1—H); 6.68 (s, 1H, C5—H), 6.72 (s, 1H, C8—H).

MS (*m/e;* %): 283 (M^+; 0.1); 282 (0.1); 266 (0.1); 265 (0.1); 252 (0.4); 222 (0.7); 221 (0.6); 220 (0.7); 192 (100); 177 (4); 176 (9).

The trihydroxypropyl derivative **1a** was acetylated with acetic anhydride in the presence of pyridine. The colourless crystals of the tetraacetyl derivative (89%) had m. p. 125—126 °C (methanol–ether–hexane).

$C_{29}H_{29}NO_9$ (451.46). Calcd. C 58.53; H 6.47 N 3.10. Found C 58.26; H 6.56; N 3.07%.

IR (KBr): 1740 (C=O ester); 1650 (C=O amide); 1610 (arom.); 1220, 1250 cm^{-1} (CH_3COO-C).

NMR ($CDCl_3$): 2.02, 2.04, 2.14 and 2.20 (s, 3H (each), CH_3-CO); 3.90 (s, 6H, OCH_3); 3.70—4.50 (3H, C3—H_2, C1—H); 5.20—6.00 (4H, CH—OAc, $-CH_2OAc$); 6.68 (s, 1H, C5—H); 6.78 (s, 1H, C8—H).

6.1.2. The tetrahydroisoquinoline hydrochloride **9a** (0.348 g; 1 mmole) was reduced with Red-Al (70%) in a mixture of benzene (5 ml) and toluene (1 ml). The reaction and work-up were carried out as described in Experiment 6.1.1. The resulting **1a** (0.140 g; 49%) proved to be identical in every respect with the product described in Experiment 6.1.1.

6.2. *1(S)*-[1'*(S)*, 2'*(S)*, 3'-*Trihydroxypropyl*]-6,7-*diethoxy*-1,2,3,4-*tetrahydroisoquinoline* (**1b**)

6.2.1. The dihydroisoquinoline hydrochloride **8b** (3.73 g; 10 mmoles) was reduced with Red-Al according to Experiment 6.1.1. The trihydroxypropyl derivative **1b** could be separated from the reaction mixture containing about 10% of the **1b**-*1(R)*-epimer by recrystallization (methylene chloride, toluene and ether) to obtain 1.40—1.90 g (45—61%), m. p. 109—110 °C. TLC (System E), R_f*1(R)*-epimer: 0.35; R_f**1b**: 0.41. $[\alpha]_D^{25}$ + 69° (*c* = 2, H_2O).

IR (KBr): 1615 (arom.); 3300–3450 cm^{-1} (broad OH).

NMR ($CDCl_3$): 1.40 and 1.44 (2×t, 6H, *J* = 7, CH_3-CH_2O); 2.70—3.30 (4H, C3— and C4—H_2); 3.50—4.50 (13H, $-CH_2O-$, >CH—O—, OH, NH, C1—H); 6.62 (s, 1H, C5—H); 6.68 (s, 1H, C8—H).

CD (ethanol): see Fig. 1.

MS (*m/e;* %): 311 (M^+, 0.1); 310 (0.3); 293 (0.1); 280 (0.4); 250 (0.6); 249 (0.6); 248 (0.4); 247 (0.4); 246 (0.3); 233 (0.9); 220 (100); 192 (10); 190 (3.5); 176 (5); 164 (6); 163 (6); 162 (7); 147 (4); 134 (4).

The trihydroxypropyl derivative **1b** was acetylated with acetic anhydride in the presence of pyridine. The colourless crystals of the tetraacetyl derivative (96%) had m. p. 127.5—129 °C.

$C_{24}H_{33}NO_9$ (479.51). Calcd. C 60.11; H 6.94; N 2.92. Found C 60.29; H 6.82; N 2.96%.

IR (KBr): 1740 (C=O ester); 1640 (C=O amide); 1605 (arom.); 1210 cm^{-1} ($CH_3-CO-O-C$).

NMR ($CDCl_3$): 1.41 (t, 6H, *J*=7, CH_3-CH_2O); 1.98 (6H, CH_3COCH_2- and CH_3CON<); 2.06 and 2.14 (s, 3H (each), CH_3COCH); 2.86 (2H, C4—H_2); 3.75 (2H, C3—H_2); 4.04 (q, 4H, *J* = 7, CH_3-CH_2-O-); 5.10—5.80 (4H, >CH—OAc and $-CH_2OAc$); 6.58 (s, 1H, C5—H); 6.70 (s, 1H, C8—H).

6.2.2. The tetrahydroisoquinoline hydrochloride **9b** (0.376 g; 1 mmole) was reduced with Red-Al (70%, 2.5*N*) in a mixture of benzene (5 ml) and toluene (1 ml). The reaction and work-up were carried out as described in Experiment 6.1.1. The resulting trihydroxypropyl derivative **1b** (0.120 g; 38.5%) proved to be identical in all respects with the derivative obtained in Experiment 6.2.1.

*

The authors thank Dr. P. KOLONITS and his co-workers for recording the IR and NMR spectra, Mrs. Dr. BALOGH—I. BATTA and the members of her microanalytical group for the analyses. Thanks are also due to Dr. J. TAMÁS for recording the MS spectra, as well as to

Dr. M. KAJTÁR for obtaining the CD curves. In the experimental work Mrs. S. KRAKOWICZER gave valuable help.

The authors also thank the Chinoin Pharmaceutical and Chemical Works, Budapest, for their interest in, and financial support of this work.

REFERENCES

[1] *a)* RETI, L.: "Simple Isoquinoline Alkaloids" in "The Alkaloids", Vol. IV, p. 19. Ed. Manske, R. F. H. and Holmes, H. L., Academic Press, New York 1954
b) BURGER, A.: "The Benzylisoquinoline Alkaloids" *ibid.*, pp. 44, 57
c) BEKE, D., SZÁNTAY, Cs.: Magyar Kém. Foly., **63,** 67 (1957); Acta Chim. Acad. Sci. Hung., **14,** 325 (1958)
[2] LUCAS, H. J., BAUMGARTEN, W.: J. Am. Chem. Soc., **63,** 1655 (1941)
[3] BEKE, D., SZÁNTAY, Cs.: Acta Chim. Acad. Sci. Hung., **12,** 286 (1957); Magyar Kém. Foly. **62,** 247 (1956)
[4] SNATZKE, G., KAJTÁR, M., WERNER-ZAMOJSKA, F.: Tetrahedron **28,** 281 (1972)
[5] *a)* SNATZKE, G., WOLLENBERG, G., HRBEK, J., SANTAVY, F., BLAHA, K., KLYNE, W., SWAN, R. J.: Tetrahedron **25,** 5059 (1969)
b) CRABBÉ, P.: "Recent Applications of ORD and CD" in "Topics in Stereochemistry", Vol. 1, pp. 150 and 171. Ed. Allinger, N. L. and Eliel, E. L., Interscience Publishers, New York, London, Sydney 1967, and references cited therein.

Gábor DÖRNYEI
Csaba SZÁNTAY
H-1111 Budapest, Gellért tér 4.

Acta Chimica Academiae Scientiarum Hungaricae, Tomus 89 (2), pp. 173—179 (1976)

CONVERSIONS OF TOSYL AND MESYL DERIVATIVES IN THE MORPHINE GROUP, XV*

NUCLEOPHILIC SUBSTITUTION REACTIONS OF PSEUDOCODEINE TOSYLATE**

S. MAKLEIT, G. SOMOGYI and R. BOGNÁR

(Department of Organic Chemistry, Kossuth L. University, Debrecen)

Received June 11, 1975

Pseudocodeine tosylate unknown up to now have been prepared and their nucleophilic substitution reactions studied. The structures of the products indicate that two types (A and B) of compounds are formed depending on the nature of the anion. The compounds with C-6-iso structure, are most probably formed by S_Ni' reaction whereas the formation of the C-8-pseudo compounds is more likely to follow S_Ni mechanism with retention.

These statements are based on studies of the comparative solvolysis of codeine tosylate and pseudocodeine tosylate, and on a kinetic examination of the reaction between pseudocodeine tosylate and piperidine.

In the course of the preparation of 6-O-tosyl and 6-O-mesyl derivatives of the morphine group (morphine, codeine, 14-hydroxycodeine and their dihydro derivatives) and theoretical studies on their nucleophilic substitution reactions, several new morphine derivatives modified in ring C were prepared which had been previously unknown, or could only be prepared in a more complicated way. In addition to theoretical results, several new compounds of pharmaceutical importance were obtained. In the course of these investigations the structure of Pschorr's "bis-thio derivatives" was elucidated and the mechanism of their formation was assumed to involve probably S_Ni reaction with retention, occurring between the alcoholic potassium sulfide and bromocodide or bromomorphide having a pseudocodeine structure [1]. Further extension of these studies, as well as the confirmation of the above mentioned hypothetic mechanism required the preparation of pseudocodeine tosylate unknown up to now, and a detailed investigation of its nucleophilic substitution reactions.

The synthesis of the tosyl ester (**II**) of pseudocodeine (**I**) [2], obtainable from α-chlorocodide, could readily be achieved by the general preparation method of tosyl esters (tosyl chloride, pyridine).

In studying the nucleophilic substitution reactions of pseudocodeine tosylate, the following considerations should be taken into account. STORK [3] assumed that the Δ^6 systems (pseudo compounds) are more stable than the

* Part XIV: S. MAKLEIT, S. BERÉNYI, R. BOGNÁR: Acta Chim., (Budapest), (in press) and Magyar Kém. Foly., **81**, 449 (1975)

** 3-Methoxy-4,5 α-epoxy-6,7-didehydro-8β-tosyloxy-17-methylmorphinan

Δ^7 compounds in this case. Our quantum chemical calculations [4] regarding morphine alkaloids confirmed STORK's assumption quantitatively, as shown by the energy contents of several C-6- (Δ^7) and C-8- (Δ^6; pseudo) substituted compound pairs, calculated taking into account the 'core-repulsion potential' (E_{rep}) values, too. Owing to its geometric properties, the morphine molecule is not sterically hindered on the 'iso' side, where the tosyloxy group is also situated in *pseudoequatorial* position in the case of pseudocodeine tosylate, thus its S_N2 type reaction is sterically hindered. On the other hand, its position is sterically favourable for S_N2' reactions, on the basis of the so-called '*cis*' rule that can be considered generally valid. Such reactions are, however, energetically unfavourable with respect to the facts mentioned above. This is also supported by the experimental data reported by STORK [3] who obtained 8-piperidocodide in 73% yield on refluxing α-chlorocodide with piperidine in benzene solution for 6 hours. In contrast with this, when β-chlorocodide having a pseudocodeine structure was refluxed with piperidine in benzene for 238 hours, 6-piperidocodide was obtained in 50% yield only. It should be pointed out that, according to the investigations of STORK and CLARKE [3], codeine tosylate and α-chlorocodide react with piperidine in reactions of type S_N2 and S_N2', respectively.

The following reactions were accomplished using pseudocodeine tosylate as the starting material (Fig. 1).

The conditions and yields for the individual reactions are given below. (Data for the similar reactions of codeine tosylate are given in parentheses).

IIIa: LiCl, acetone, boiling point, 25 hrs, 16.3%; (4 hrs, 60% [3]).
IIIb: $[(Bu)_4N]F$, acetonitrile, boiling point, 29 hrs, 10.2%; (4 hrs, 48.2% [6]).
IIIc: Piperidine, benzene, 127 hrs, boiling point, 64.9%; (36 hrs, boiling point [3]).
IVa: LiBr, acetone, boiling point, 19 hrs, 52.3% (2.5 hrs, 98% [3]).
IVb: NaI, acetone, boiling point, 19 hrs, 25.9% (2.5 hrs, 43% [3]).
IVc: KSCN, acetone, boiling point, 16.5 hrs, 15.3%; (2.5 hrs, 48.7% [7]).
IVd: NaN_3, DMF, 100 °C, 8 hrs, 30.2%; (4 hrs, 65% [8]).
IVe: $KSCOCH_3$, DMF, 100 °C, 8 hrs, 10.7%; (5 hrs, 57.3% [9]).

According to the data, the reaction of pseudocodeine tosylate with the various negatively charged nucleophilic reagents does not yield different products like codeine tosylate; however, more vigorous reaction conditions must be applied and the yields are also lower. Thus the use of pseudocodeine tosylate offers no advantage as compared with codeine tosylate, and these reactions do not represent a real extension of the scope of our previous work.

However, with respect to the structure of the compounds isolated, studies on the mechanism of the reactions seemed promising. In view of the previous experiences, there are two theoretical possibilities for the mechanism of both

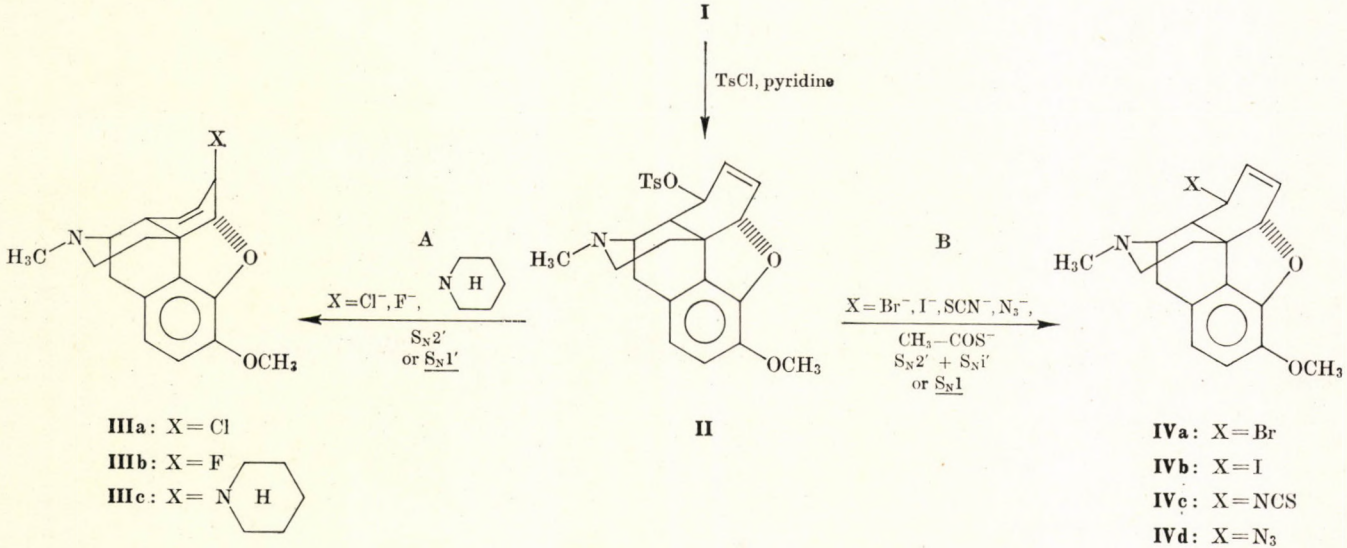
I
TsCl, pyridine
TsO
H3C
N
O
OCH3
A
X=Cl⁻, F⁻,
SN2′
or SN1′
B
X=Br⁻, I⁻, SCN⁻, N3⁻,
CH3—COS⁻
SN2′ + SNi′
or SN1
X
III a: X=Cl
III b: X=F
III c: X=
II
IV a: X=Br
IV b: X=I
IV c: X=NCS
IV d: X=N3
IV e: X=SCOCH3

reactions, having direction A or B (Fig. 1). The reactions going in direction A and yielding a product with C-6 iso structure may occur by either S_N1' or S_N2' mechanism. On the other hand, the mechanism of reactions with direction B, resulting in compounds of C-8 pseudo structure, is either S_N1 accompanied by retention, or a combination of S_N2' and S_Ni'.

This problem was studied by the following experiments. First of all, the comparative solvolysis of codeine tosylate and pseudocodeine tosylate was examined (Table I). As indicated by the data, both compounds undergo solvolysis in a first-order reaction in the system absolute acetic acid and potassium acetate, in accordance with the literature data reported for tosyl esters formed with secondary hydroxyl groups [10]. However, the solvolysis of pseudocodeine tosylate always takes place more slowly than that of codeine tosylate though the actual rate naturally depends on the temperature applied; the difference is also revealed by the activation free energy and the activation free entropy values (Table I).

Table I

Kinetic data of the comparative solvolysis of codeine tosylate and pseudocodeine tosylate

Temp., °C	CTs conc., mole/l	KOAc conc., mole/l	k, min^{-1}	Error, %	ψCTs conc., mole/l	KOAc conc., mole/l	k, min^{-1}	Error, %
50±0.1	0.01	0.01	$1.241 \cdot 10^{-3}$		0.01	0.01	$3.924 \cdot 10^{-4}$	
			$1.236 \cdot 10^{-3}$				$3.732 \cdot 10^{-4}$	
60±0.1	0.01	0.01	$3.350 \cdot 10^{-3}$		0.01	0.01	$1.071 \cdot 10^{-3}$	
			$3.346 \cdot 10^{-3}$				$1.065 \cdot 10^{-3}$	
	0.01	0.02	$1.309 \cdot 10^{-2}$	+3.96	0.01	0.02	$3.997 \cdot 10^{-3}$	−10.6
	0.02	0.02	$1.276 \cdot 10^{-2}$	+0.79	0.02	0.02	$4.722 \cdot 10^{-3}$	+ 5.56
70±0.1	0.01	0.005	$1.141 \cdot 10^{-2}$	−9.52	0.01	0.005	$4.716 \cdot 10^{-3}$	+ 5.43
	0.01	0.01	$1.240 \cdot 10^{-2}$	−1.58	0.01	0.01	$4.320 \cdot 10^{-3}$	− 3.40
	0.01	0.025	$1.347 \cdot 10^{-2}$	+6.34	0.01	0.025	$4.612 \cdot 10^{-3}$	+ 3.10
80±0.1	0.01	0.01	$2.578 \cdot 10^{-2}$		0.01	0.01	$1.134 \cdot 10^{-2}$	
			$2.609 \cdot 10^{-2}$				$1.143 \cdot 10^{-2}$	

$\Delta E^{\ddagger}$ = 23.9 Kcal/mole $\Delta E^{\ddagger}$ = 27.91 Kcal/mole
$\Delta S^{\ddagger}$ = −0.1 cal $mole^{-1}$ $degree^{-1}$ $\Delta S^{\ddagger}$ = 9.5 cal $mole^{-1}$ $degree^{-1}$
CTs = Codeine tosylate ψCTs = Pseudocodeine tosylate

STORK and CLARKE [3] studied the kinetics of the interaction of codeine tosylate and piperidine, and found it to be an S_N2 reaction, since the product was a

C-6 iso derivative. We thought important to examine the kinetics of the analogous reaction of pseudocodeine tosylate. The results are summarized in Table II. On this basis, the reaction follows first-order kinetics, being of either S_N1 or S_N1' type. In order to decide the actual type, the reaction of pseudocodeine tosylate with piperidine had to be investigated preparatively, too. In this reaction the product was unambiguously 6-piperidocodide (IIIc), thus the reaction mechanism must be S_N1'.

Table II

Kinetic data for the reaction of pseudocodeine tosylate with piperidine

Temperature °C	ψCTs conc., mole/l	Pip. conc., mole/l	k, sec^{-1}	Error, %
120±0.1	0.01005	0.01988	$1.636 \cdot 10^{-4}$	−6.08
	0.00857	0.01940	$1.784 \cdot 10^{-4}$	+2.41
	0.01000	0.03952	$1.684 \cdot 10^{-4}$	−3.32
	0.00863	0.03920	$1.865 \cdot 10^{-4}$	+7.05

ψCTs = Pseudocodeine tosylate
Pip = Piperidine.

On the basis of the evidence obtained up to now, the reactions going in direction A very probably occur by S_N1' mechanism, whereas S_N1 reactions with retention are more likely in direction B.

Experimental

M.p.'s were determined in open capillaries, and were uncorrected. The purity of the compounds was checked by thin-layer chromatography (Silicagel G, benzene–methanol 8 : 2, Dragendorff reagent).

Pseudocodeine tosylate(II)

Pseudocodeine [2] (5 g; 0.0167 mole), obtainable from α-chlorocodide (I), was dissolved in absolute pyridine (20 ml) in a three-necked flask equipped with a stirrer reflux condenser and dropping funnel. The solution was cooled to 0 — —5 °C in an ice-salt cooling bath, and a solution of *p*-toluenesulfonic acid chloride (3.5 g; 0.0184 mole) in absolute pyridine (20 ml) was added dropwise, with stirring. After having completed the addition, the reaction mixture was stirred for 2 hrs at this temperature, then cooling and stirring was stopped, and the solution was allowed to stand at room temperature for 24 hrs. The reaction mixture was poured into water (500 ml), saturated with sodium hydrogen carbonate and extracted with 3×150 ml of ether. The combined ethereal extract was washed with water (2×100 ml), dried over $MgSO_4$, filtered, and the filtrate evaporated to dryness in vacuum. The residual syrup was crystallized from a mixture of ether and petroleum ether to obtain white or slightly pink crystals (5.8 g; 76.5%), m. p. 108—110 °C, $\nu_{S=O}$ 1366 cm^{-1}. $C_{25}H_{27}O_5NS$. Calcd. S 7.08. Found S 6.62, 6.69%.

6-Deoxy-6-chloroisocodeine (IIIa)

Pseudocodeine tosylate (II) (0.5 g; 0.0011 mole) was allowed to react with dry lithium chloride (0.18 g; 0.004 mole) in absolute acetone (20 ml) at the boiling point for 25 hrs, according to Ref. [3], to obtain 0.08 g (16.3%) of the product, m. p. 152—154 °C (lit. [2] m. p. 152—153 °C).

6-Deoxy-6-fluoroisocodeine (IIIb)

Pseudocodeine tosylate (II) (0.5 g; 0.0011 mole) was allowed to react with tetrabutylammonium fluoride (1.57 g; 0.006 mole) in dry acetonitrile (20 ml) at the boiling point for 29 hrs, according to Ref. [6], to obtain 33.95 mg (10.2%) of the product, m. p. 145—146 °C (lit. [6] m. p. 145—146 °C).

6-Deoxy-6-piperidocodeine (IIIc)

Pseudocodeine tosylate (II) (1 g; 0.0022 mole) was allowed to react with piperidine (3 ml; 0.03 mole) in benzene (37 ml) at the boiling point for 127 hrs., according to Ref. [3], to obtain 0.55 g (64.9%) of the product. Picrate, m. p. 240—241 °C (lit. [3] m. p. 240—241 °C).

8-Deoxy-8-bromopseudocodeine (IVa)

Pseudocodeine tosylate (II) (0.95 g; 0.0021 mole) was allowed to react with lithium bromide (1.25 g; 0.014 mole) in absolute acetone (20 ml) at the boiling point for 19 hrs, according to Ref. [3], to obtain 0.42 g (52.3%) of the product, m. p. 154—156 °C (lit. [3] m. p. 155—156 °C).

8-Deoxy-8-iodopseudocodeine (IVb)

Pseudocodeine tosylate (II) (0.95 g; 0.0021 mole) was allowed to react with sodium iodide (0.32 g; 0.0033 mole) in absolute acetone (50 ml) at the boiling point for 19 hrs, according to Ref. [3], to obtain 0.2 g (25.9%) of the product, m. p. 158—159 °C (lit. [3] m. p. 161 °C).

8-Deoxy-8-isothiocyanatopseudocodeine (IVc)

Pseudocodeine tosylate (II) (1 g; 0.0022 mole) was allowed to react with potassium thiocyanate (0.42 g; 0.0042 mole) in absolute acetone (20 ml) at the boiling point for 16.5 hrs, according to Ref. [7], to obtain 0.1 g (15.3%) of the product, m. p. 110—112 °C (lit. [7] m. p. 110—111 °C).

8-Deoxy-8-azidopseudocodeine (IVd)

Pseudocodeine tosylate (II) (0.5 g; 0.001 mole) was allowed to react with sodium azide (0.1 g; 0.017 mole) in dimethylformamide (15 ml) at 100 °C for 8 hrs., according to Ref. [8], to obtain 0.105 g (30.2%) of the product, m. p. 137—138 °C (lit. [8] m. p. 137—138 °C).

8-Deoxy-8-acetylthiopseudocodeine (IVe)

Pseudocodeine tosylate (II) (0.95 g; 0.0021 mole) was allowed to react with potassium thioacetate (0.61 g; 0.0042 mole) in absolute dimethylformamide (10 ml) at 100 °C for 8 hrs, according to Ref. [9]. The crude product was dissolved in a 9 : 1 mixture of benzene and methanol and purified on a Silicagel G column by eluting it with the same solvent mixture, then crystallized from absolute ether; 0.08 g (10.7%) of the product was obtained, m. p. 137—138 °C (lit. [9] m. p. 137—138 °C).

Kinetic measurements

(a) Comparative solvolysis of codeine tosylate [11] and pseudocodeine tosylate (II)

Codeine tosylate and pseudocodeine tosylate were dissolved separately, together with anhydrous potassium acetate, in absolute glacial acetic acid; then 6 ml aliquots were transferred into ampoules of 10 ml volume. Eight samples were taken in each case. The ampoules were

sealed and placed in an ultrathermostat. Simultaneously, 5 ml of the stock solution was titrated with 0.02*N* perchloric acid in absolute glacial acetic acid in the presence of Bromophenol Blue indicator. This titration yielded the 0 minute concentration of codeine tosylate and pseudocodeine tosylate, respectively. (Blank tests were carried out before each run.) The progress of the reaction was followed by means of the above titration, assaying 5 ml portions of the solution in the ampoules removed from the thermostat at different times and placed into an ice bath to stop the reaction. The reaction time was chosen such as to accomplish the last titration at about 60% conversion.

The k values were determined graphically.

(b) Reaction of pseudocodeine tosylate with piperidine in absolute toluene

The measurement was carried out in the same way as above, but the progress of the reaction was monitored by titrating with 0.02*N* hydrochloric acid solution in the presence of phenolphthalein indicator.

*

The authors' thanks are due to the Natural Science Department I of the Hungarian Academy of Sciences and to the Alkaloida Chemical Works, Tiszavasvári, Hungary, for supporting this research.

Thanks are expressed to Dr. K. HARSÁNYI (Chinoin Chemical Works, Budapest) for valuable scientific discussions.

REFERENCES

[1] MAKLEIT, S., BOGNÁR, R., MILE, T., RADICS, L.: Acta Chim. Acad. Sci. Hung., **66,** 455 (1970); Magyar Kém. Foly., **76,** 464 (1970)
[2] SMALL, L. F.: Chemistry of the Opium Alkaloids, pp. 221, 223—4. Government Printing Office, Washington 1932
[3] STORK, G., CLARKE, F. H.: J. Am. Chem. Soc., **78,** 4619 (1956)
[4] DINYA, Z., MAKLEIT, S., BOGNÁR, R., JÉKEL, P.: Acta Chim., (Budapest) **71,** 125 (1972) DINYA, Z., MAKLEIT, S., BOGNÁR, R.: Kémiai Közl., **39,** 141 (1973)
[5] DINYA, Z.: Doctoral Thesis, Debrecen, Hungary, 1972
[6] BOGNÁR, R., MAKLEIT, S., RADICS, L.: Acta Chim. Acad. Sci. Hung., **67,** 63 (1971)
[7] BOGNÁR, R., MAKLEIT, S., MILE, T., RADICS, L.: Mh. Chem., **103,** 143 (1972); Magyar Kém. Foly., **78,** 163 (1972)
[8] BOGNÁR, R., MAKLEIT, S., MILE, T.: Acta Chim. Acad.Sci. Hung., **59,** 379 (1969); Magyar Kém. Foly., **74,** 525 (1968)
[9] BOGNÁR, R., MAKLEIT, S., MILE, T., RADICS, L.: Acta Chim. Acad. Sci. Hung., **64,** 273 (1970); Magyar Kém. Foly., **76,** 102 (1970)
[10] PRITZKOW, W., SCHÖPPLER, K. H.: Ber., **95,** 834 (1962)
[11] KARRER, P., WIDMARK, G.: Helv. Chim. Acta **34,** 34 (1951)

Sándor MAKLEIT
Gábor SOMOGYI
Rezső BOGNÁR

KLTE Szerves Kémiai Intézet H-4010, Debrecen.

RECENSIONES

R. AMMON and W. DIRSCHERL: *Vitamine, Vol. III*

Georg Thieme Verlag, Stuttgart 1974

The book gives a comprehensive view of our present knowledge of vitamins. The first edition, published under the editorship of Professors AMMON and DIRSCHERL in 1937, has become a widely applied, most popular handbook, in fact, the best in the field.

After a considerable elapse of time, following the third edition of Vols I ("Fermente", 1959) and II ("Hormone", 1960), the section on vitamins has finally appeared in an enlarged edition of a two-volume book (Vol. III, 1—2). In the long run, however, this delay of a decade-and-a-half proved to be very useful for it allowed the inclusion of the most recent knowledge acquired in the rapidly developing field of biochemical and biological sciences. Comprising the work of more than 20 authors, "Vitamine", Vol. III, Part I, summarizes in over approx. 1000 pages our present knowledge of important biochemical substances in the following arrangement:

anti-vitamins; the significance of vitamins in therapeutics and nourishment; Vitamin A, Vitamin D (Calciferol), Vitamin E (Tocopherol), Vitamin K, Vitamins F (essential fatty acids), alpha-lipoic acid, ubiquinones, Vitamins B_1 and B_2 (Riboflavin), further Vitamins B, (pyridoxine, pantothenic acid and other coenzyme components; anti-pellagra vitamin nicotinic acid and nicotinic acid amide), biotin, the group of folic acids, choline, myo-inositol, Vitamin C (ascorbic acid) and bioflavonoids ("Vitamin P").

As is immediately evident from the list of contents, compounds such as lipoic acid and collin, which have gained significance most recently, have been assigned a separate chapter and treated in detail.

Substances with controversial vitamin properties, *e.g.*, essential fatty acids and bioflavonoids have also been widely discussed and presented in a comprehensive study, giving a practical guide to their analytical treatment as well.

A further merit of this enlarged edition is that, in addition to offering a comprehensive review, it discusses in detail the specific properties of vitamins and compounds with vitamin-like effects, their interactions and relationships with enzymes and hormones. It is, above all, this biological-biochemical approach that renders this lengthy publication so important and invaluable.

The book is well readable, gives an outline of the historical background and treats under one cover biosynthesis and the elucidation of chemical structure and mechanism. The data are clearly presented in 109 figures and 155 tables. Another great asset of the book is the detailed discussion of the therapeutic aspects, helpful for researchers working both in specialized fields and on adjoining topics.

Part 2 (Vol. III, Part 2), dealing with the properties of Vitamins B_{12} and related corrinoids over 350 pages, with 66 figures and 57 tables, was published in 1975. The special role and significance of the Vitamin-complex B_{12} has been described by professor FRIEDRICH in a similarly intriguing style, with special stress laid on specific features.

J. HOLLÓ

J. SCHURZ: *Physikalische Chemie der Hochpolymeren* (Eine Einführung)

Springer Verlag, Berlin, Heidelberg, New York 1974, 196 Seiten

Das Buch ist für Studenten der Chemie und Physik gedacht, die die höheren Jahrgänge der Universität besuchen. Das Buch beschreibt die wichtigsten Prinzipien, Gesetze und Methoden der physikalischen Chemie von hochmolekularen Stoffen. Der erste Teil beschäftigt sich mit den Eigenschaften der gelösten, der zweite mit denen der festen Makromoleküle. Die wichtigsten Abschnitte des Buches beschäftigen sich mit den folgenden Themen:

I. Gelöste Makromoleküle

Molekulargewicht und Molekulargewichtsverteilung der Makromoleküle. Grundlegende Charakteristika der gelösten Makromoleküle. Thermodynamik der Lösungen, Lösungsmittel-Typen vom Gesichtspunkt der Thermodynamik, chemisches Potential und Aktivität, Mischungs-Enthalpie, Mischungs-Entropie, Mischungs-Entropie bei Polymeren, Mischungswärme. Die Flory-Hugginssche Theorie, Wechselwirkungs-Konstante. Kolligative Eigenschaften, osmotischer Druck. Abweichung vom idealen Zustand, Viralkoeffizient. (Hier fehlt unter den modernen Methoden die Dampfdruck-Osmometrie.)

Phasentrennung in polymeren Lösungen. Mehrkomponentensysteme. Fraktionierte Präzipitation. (Hier fehlt die Gelpermeations-Chromatographie.) Konformation, Kettenendglied-Abstände in Lösungen.

Rheologie verdünnter Lösungen, Viskositätsfunktionen, Bestimmung der Grenzviskositätszahl. Molekulargewichtsbestimmung aus der Grenzviskositätszahl.

Strömungsdoppelbrechung. Viskosität der Polyelektrolyte und der geladenen Teile.

Transporterscheinungen. Diffusion, Sedimentation, Elektrophorese. Die Streuung von Licht- und Röntgenstrahlen. Kleinwinkel-Röntgenstreuung. Streuung des sichtbaren Lichtes. Kritische Opaleszenz.

Infrarot- und Ultraviolett-Spektroskopie.

Optische Rotationsdispersion und Zirkulardichroismus. Kernmagnetische Resonanz-Spektroskopie. Elektronenspinresonanz-Spektroskopie.

II. Makromoleküle in festem Zustand

Kristallinität. Röntgen-Strukturanalyse. Kristalline Teilchengröße. Orientation. Röntgenanalyse der großen Perioden.

Optische Doppelbrechung.

Morphologie der Polymere: Kristallite, Sphärolite, Kettenfaltung (hier fehlt die elektronenmikroskopische Untersuchungsmethode der Polymeren).

Messung der Kristallinität mit Infrarot- und NMR-Spektroskopie.

Schmelzpunkt.

Kristallisationskinetik. Glaszustand, Umwandlungspunkt zweiter Ordnung.

Gummielastischer Zustand und seine thermodynamischen Beziehungen.

Phasenübergänge und mesomorphe Zustände. Thermoanalyse.

Thermomechanische Kurven. Lineare Viskoelastizität. Viskoelastische Modelle. Mechanische Spektroskopie. Festigkeit und Reißprozesse.

In der Zusammenstellung der Abschnitt vereinigte der Verfasser mit glücklicher Hand das für die Studenten wichtigste Material mit den neuesten Literaturangaben. Natürlich widerspiegelt die Auswahl die individuellen Interessenkreise des Verfassers, was sich vor allem auf die Untersuchung der gelösten Makromoleküle bezieht. Dieser Tatsache ist es zuzuschreiben, daß der Beschreibung des Verhaltens von Lösungen 122 Seiten gewidmet sind, während die feste Phase, bloß auf 66 Seiten behandelt wird. Die Kleinwinkel Röntgenstreuung wird bei festen Polymeren eben nur erwähnt, während die kleinwinklige Lichtstreuung der festen Polymere gar nicht behandelt wird.

Außer den bereits erwähnten Ausnahmen enthält das Buch sämtliche Kenntnisse, die ein absolvierender Chemiker, Chemieingenieur bzw. Physiker über die physikalische Chemie der Makromoleküle benötigt. Das Buch kann jedoch als erste Referenzquelle mit gutem Nutzen auch von Diplomierten verwendet werden, die in der Industrie oder auf anderen Forschungsgebieten arbeiten, umsomehr, als die Referenzen gut zusammengestellt sind, so daß die einschlägige Literatur der einzelnen Themen leicht zu finden ist.

G. BODOR

D. DOBOS: *Electrochemical Data*

Akadémiai Kiadó, Budapest 1975. (Pp. 339)

Following the intentions of the prematurely deceased Author, this is a modern, English version of an earlier, very successful edition in Hungarian, augmented and revised according to the SI system of units, since then officially introduced. As a handbook, this is a valuable and detailed collection of data. The individual chapters contain the necessary fundamentals. Chapter 1: fundamental physical constants, conversion tables of the SI units, relative atomic masses, the most important electrochemical equations and formula as well as series of data suggested as suitable for application Chapter 2: conductivity, transference numbers, diffusion coefficients, thermodynamic data, relative permittivities, relaxation times for various electrolyte solutions and ions at various temperatures; Chapter 3: equilibrium data, activity coefficients, solubility products, pH-values; Chapter 4: data of indicators, measurement of pH, buffer solutions, dielectric measurements; Chapter 5: electrode potentials, electromotive forces, diffusion potentials, galvanic cells and storage batteries; Chapter 6: coulometric, electrogravimetric, polarographic data, deposition potentials, decomposition voltages important in instrumental analyses; Chapter 7: electrokinetic data, and finally (in Chapter 8) titles of the more important monographs and handbooks on electrochemical theory and analysis, on electroplating, corrosion, industrial electrochemistry, electrochemical engineering, primary electrochemical supply units, storage batteries, fuel cells and electrochemical calculations.

This book would have been even more useful and up-to-date if in the course of its edition, besides the consistent use of the SI system also that of the new electrochemical nomenclature and definitions had been observed since in many aspects the latter diverge from the usual concerning both the names of individual quantities (*e.g.* specific conductance instead of conductivity, specific molar conductance instead of equivalent conductivity, ionic molar conductance instead of relative mobility, etc.) and their definitions (between absolute and relative activity; use of the corresponding composition variable instead of the word concentration — if not expressed as c — since concentration c is but one of the composition variables, *viz.* the composition expressed in units of the mol/dm^3, etc.).

This book is the result of very careful work, well arranged and most serviceable. In spite of the remarks made, there is no doubt that it satisfies the needs envisaged and attains the goals set; it justifies the claim in its sub-title, *viz.* that it is a "Handbook for Electrochemists in Industry and Universities".

E. BERECZ

Mössbauer-Spectroscopy

Ed. Uli Gonser (5th Volume of the series "Topics in Applied Physics")
Springer Verlag, Berlin, Heidelberg, New York 1975

This book (241 pp., 96 figures) consists of six chapters written by U. GONSER, P. GÜTLICH, R. W. GRANT, C. E. JOHNSON, S. S. HAFNER and F. E. FUJITA.

Considering the 25—30 monographs published till now in English on Mössbauer spectroscopy, this book does not seem to aim at the theroetical foundations of the method. Its purpose is the discussion of the newer fields of application. Besides this, it summarizes the physical fundamentals necessary for understanding the results presented, and also the applications that rank already as classical in this field. The book does not assume special preparatory studies on the part of its readers: it can be used both as an introduction into, or as a monograph on Mössbauer spectroscopy.

In the first chapter (51 p., 17 figures, 5 tables, and 41 numbered correlations) U. GONSER illustrates, on the basis of 105 references, how the Mössbauer effect has expanded into Mössbauer spectroscopy and, as aptly noted, into a gold mine for researchers. The era before the detection of the Mössbauer effect, the detection of the effect and the specific features of a Mössbauer spectrum are discussed in a very concise manner (intensity and line-width, the isomer shift due to hyperfine interactions, magnetic and quadrupole splitting). The presentation with the help of illustrative figures and with well devised comprehensive tables enhances understanding; the final equations (discussed but not derived) add exactitude. After the dis-

cussion of perturbation effects consequent upon hyperfine interactions, and after that of relativistic effects, the principal questions of the method are analyzed; besides transmission, also scattering technique and Mössbauer polarimetry are dealt with. Finally, on two examples, the application of the method to the measurement of biological movements is demonstrated.

In the second chapter (43 p., 12 figures, 6 tables, and 81 references) P. GÜTLICH discusses the chemical applications of Mössbauer spectroscopy. This is one of the best parts of the book, perhaps also because chemical science offers the most extensive and richest field of application. (This seems to be so since most of the physicists who work on Mössbauer spectroscopy have some chemical problem as the subject of their studies.) Briefly, yet touching every important aspect, the physical fundamentals of the parameters of Mössbauer spectra are summarized. There is some overlap with Chapter 1 as the most important hyperfine interactions are discussed twice, *e.g.* Equations 1.28 and 2.29, as well as 1.30 and 2.25 are the same. It should be noted, however, that neither chapter mentions the fact that 1.30, *i.e.* 2.25, will be the eigenvalue of the Hamiltonian only if $\frac{3}{2}$. Subsequently, P. GÜTLICH illustrates with carefully selected examples the more important applications of Mössbauer spectroscopy in chemistry, primarily in the chemistry of complexes.

In the third chapter (40 pp. 21 figures, 26 numbered equations and 67 references) R. W. GRANT gives a good review of the study of magnetic phenomena by means of Mössbauer spectroscopy. After the analysis of the magnetic hyperfine structure of ^{57}Fe, the interaction of the magnetic and electric interactions is discussed in its essentials, and the determination of the sign of the magnetic field is shown. In connect with the study of magnetic characteristics, the determination of the temperatures and types magnetic ordering of by Mössbauer spectroscopy and of the local distribution as well as its application for phase analysis and the study of phase transitions are explained. With the help of suitable examples (colinear structure of $Ca_2Fe_2O_5$, noncolinear structure of FeOCl, spin arrangement in $ErFe_2O_5$) the applicability of the Mössbauer effect in the study of magnetic structures is also analyzed and demonstrated.

In the fourth chapter (28 pp., 16 figures, 4 tables, 29 references), by C. E. JOHNSON, some biological applications of the method are described. First an evaluation of the spectral parameters is given with regard to information to be gathered concerning the chemical bonding, local structure and symmetry of biological compounds. This is followed by results achieved in the field of iron-containing proteins. For nonproteins the spectral parameters of low spin ferro-HbO_2 and -HbCO are compared with those of high spin ferro-Hb as well as the parameters of low spin ferri-HiCN, -HiN_3, -HiOH with there of ferri-HiF and -HiH_2O. Mössbauer studies on ironsulfur proteins, on rubredoxins which contain one iron, plant ferredoxins which contain two iron atoms, and proteins which contain 4 and 8 iron atoms are also mentioned. As a prospective field of application medical research is indicated.

Nearly every known method of structural analysis has been utilized in the study of samples of lunar rock. Mössbauer spectroscopy is eminently suitable for the elucidation of the oxidation state, chemical surroundings, electronic structure and the crystal structure of the matrix of Mössbauer atoms (chiefly of iron) in lunar samples. In the fifth chapter (43 p., 11 figures, 5 tables) S. S. HAFNER reviews 52 papers, a great part of these dealing with the analysis of lunar samples of American lunar searches and expeditions.

F. E. FUJITA, author of the sixth chapter (36 p., 19 figures, 13 equations, 67 references) summarizes the application of Mössbauer spectroscopy in the field of metallurgy and metal physics. The evaluation of spectral parameters with regard to qualitative and quantitative analysis in metallurgical studies, and the statistical calculation of atomic arrangements in alloys, are discussed first, then the examination of the various metallographic phases of carbon steels, as a group of interstitial alloys (with martensitic transformations in a separate subchapter) is described. Concerning substitutional alloys, data on arrangement and separation are given, then invar alloys are described in a somewhat greater detail. At the end of the chapter, measurements for the determination of texture, oxidation, diffusion and defect structure are briefly mentioned.

A. VÉRTES
E. KUZMANN

C. J. KEATTCH and D. DOLLIMORE: *An Introduction to Thermogravimetry*

2nd edition, Heyden and Son, London 1975

The literature about thermal analysis has again been enriched with a new monograph. This second edition of "An Introduction to Thermogravimetry" by C. J. KEATTCH and D. DOLLIMORE, is about three times the size of the first. Arranged in ten chapters, on 164 pages, it deals with theoretical and practical aspects of thermogravimetry, from fundamental problems of measurement to a presentation of the theory of kinetic calculations now widely applied. Other thermoanalytical methods which are often used together with thermogravimetry are also briefly used.

The concluding part, about one fourth of the book, summarizes the fields of application, separately treating inorganic, organic and mineral substances.

The principal virtue of this book is its conciseness: every problem is presented in its essentials only. At the same time, the nearly 400 references substantially facilitate a more detailed study for those who wish to gain deeper insight in to any particular aspect of this topic. The book is a useful help for the beginner as well as for the analyst already versed in thermogravimetry.

J. PAULIK

Thermal Analysis. Proceedings of the Fourth International Conference on Thermal Analysis. Volumes 1, 2 and 3.

Edited by I. Buzás, Akadémiai Kiadó, Budapest 1975

The International Confederation for Thermal Analysis (ICTA) organizes a conference every three years. The steadily growing importance of this field of science is shown by the fact that whereas only abstracts were published of the papers presented at the Aberdeen conference (1965) the proceedings of the conference at Worchester (1968) filled two volumes, and the 180 papers read at the third conference, Davos 1971, were printed in three volumes. About 600 participants from 30 countries were present at the conference in Budapest, July 8—13, 1974, and the 277 papers presented there occupy about 3000 printed pages arranged in three massive volumes. These proceedings contain the full text of every paper, in the form of articles for a journal, complete with references.

In the volumes the arrangement accords with the division of the conference into six sections. Thus the subject matter is ordered as follows.

Volume 1:	Theory
	Inorganic Chemistry
Volume 2:	Organic, and Macromolecular Chemistry
	Earth Sciences
Volume 3:	Applied Sciences
	Methods and Instrumentation

The papers presented clearly show the wide range and diverse applications of the various methods of thermal analysis and demonstrate that these are very important complementary methods of scientific research.

A table of contents and an author index in each volume help orientation in this extensive subject matter. Published by Akadémiai Kiadó within a year after the conference, this work is carefully edited and beautifully printed.

G. LIPTAY

INDEX

PHYSICAL AND IN ORGANIC CHEMISTRY

ORGANIC CHEMISTRY

Printed in Hungary

A kiadásért felel az Akadémiai Kiadó igazgatója. Műszaki szerkesztő: Zacsik Annamária
A kézirat nyomdába érkezett: 1976. I. 30. — Terjedelem: 7,7 (Al5) ív, 39 ábra

76.2745 Akadémiai Nyomda, Budapest — Felelős vezető: Bernát György

ACTA CHIMICA

ТОМ 89—ВЫП. 2

РЕЗЮМЕ

Получение и масс-спектрометрическое исследование оксибромидов молибдена и вольфрама и бромидов вольфрама

О. КАПОШИ, Т. ДЁЙТЧ, А. ПОПОВИЧ и Й. ПЕЗДЁЧ

Бромированием металлов и окислов металлов были получены и исследованы масс-спектрометрически следующие соединения: MoO_2Br_2, WO_2Br_2, $WOBr_4$, WBr_4 и W_2Br_6. Была определена масс-спектрометрическая фрагментация этих соединений, были измерены потенциалы появления ионов в области повышенных относительных интенсивностей и были рассчитаны их теплоты образования. Наблюдались также и такие ионы, состав которых объяснялся на основе структуры этих соединений в твердой фазе. В области высоких относительных интенсивностей, среди прочих ионных частиц, удалось детектировать ионы, образующиеся из кластеров W_2Br_6. Исходя из полученных величин потенциалов появления, были рассчитаны некоторые термохимические и термостатические данные.

Кинетика дегидрировании этана над катализатором α—Cr_2O_3, I

Лимитирующая стадия реакции

П. КЁНИГ и П. ТЭТЭНИ

Была изучена реакция дегидрирования этана над катализатором $\alpha-Cr_2O_3$ в циркуляционном реакторе при давлении 0—4 к Н. м$^{-2}$ и температуре 430—580°С. При таких условиях на катализаторе протекают различные химические превращения; помимо образования газообразных продуктов реакции (H_2, C_2H_4, CH_4) наблюдается также образование поверхностных отложений, состав которых зависит от активности катализатора и температуры реакции. При изучении кинетики реакции путем соответствующей обработки и восстановления катализатора удалось обеспечить почти постоянную активность катализатора. На основании зависимости начальных скоростей реакции дегидрования от температуры и на основании данных кинетического изотопного эффекта, и сопоставления скоростей D—H обмена можно предположить, что лимитирующей стадией реакции дегидрирования этана является реакция на поверхности катализатора.

Превращения тозиловых и мезиловых производных в ряду морфина, .

Синтез тозилата псевдокодеина и изучение его нуклеофильных реакций

Ш. МАКЛЕЙТ, Г. ШОМОДИ и Р. БОГНАР

Было получено новое соединение — тозилат псевдокодеина и были исследованы его некоторые реакции нуклеофильного замещения. На основе структуры продуктов, зависящей от анионов, были получены два материала A и B. Для образования C-6-изосоединений наиболее вероятным является механизм S_N1,' а в случае C-8-псевдосоединений — механизм S_N1 с сохранением конфигурации. Эти заключения основаны на сравнительном сольволизе тозилата кодеина и тозилата псевдокодеина и на кинетическом исследовании реакции тозилата псевдокодеина с пиперидином.

ACTA CHIMICA

ТОМ 89—ВЫП. 2

РЕЗЮМЕ

Получение и масс-спектрометрическое исследование оксибромидов молибдена и вольфрама и бромидов вольфрама

О. КАПОШИ, Т. ДЁЙТЧ, А. ПОПОВИЧ и Й. ПЕЗДЁЧ

Бромированием металлов и окислов металлов были получены и исследованы масс-спектрометрически следующие соединения: MoO_2Br_2, WO_2Br_2, $WOBr_4$, WBr_4 и W_2Br_6. Была определена масс-спектрометрическая фрагментация этих соединений, были измерены потенциалы появления ионов в области повышенных относительных интенсивностей и были рассчитаны их теплоты образования. Наблюдались также и такие ионы, состав которых объяснялся на основе структуры этих соединений в твердой фазе. В области высоких относительных интенсивностей, среди прочих ионных частиц, удалось детектировать ионы, образующиеся из кластеров W_2Br_6. Исходя из полученных величин потенциалов появления, были рассчитаны некоторые термохимические и термостатические данные.

Кинетика дегидрировании этана над катализатором α—Cr_2O_3, I

Лимитирующая стадия реакции

П. КЁНИГ и П. ТЭТЭНИ

Была изучена реакция дегидрирования этана над катализатором α—Cr_2O_3 в циркуляционном реакторе при давлении 0—4 к Н. $м^{-2}$ и температуре 430—580°С. При таких условиях на катализаторе протекают различные химические превращения; помимо образования газообразных продуктов реакции (H_2, C_2H_4, CH_4) наблюдается также образование поверхностных отложений, состав которых зависит от активности катализатора и температуры реакции. При изучении кинетики реакции путем соответствующей обработки и восстановления катализатора удалось обеспечить почти постоянную активность катализатора. На основании зависимости начальных скоростей реакции дегидрования от температуры и на основании данных кинетического изотопного эффекта, и сопоставления скоростей D—H обмена можно предположить, что лимитирующей стадией реакции дегидрирования этана является реакция на поверхности катализатора.

Кинетика дегидрирования этана на катализаторе α—Cr_2O_3, II

Уравнение скорости

П. КЁНИГ и П. ТЕТЕНИ

Изучена кинетика реакции дегидрирования этана в интервале температур 450—580 °С и давлений 0—4 кн.м$^{-2}$.

Нелинейным методом оценки параметров — применяя ЭВМ — расчитанные значения начальных скоростей реакции были сопоставлены с кинетическими уравнениями Хюгена—Уатсона, применяемыми для данной реакции.

Методами математической статистики получено наиболее адекватное уравнение скорости дегидрирования. Константы скорости и константы равновесной адсорбции данного уравнения скорости и расчитанные значения энергии активации и энтальпии адсорбции подтверждают что реакция дегидрирования протекает по двухцентровому механизму, причем предполагаемые каталитически активные центры отличаются друг от друга.

Комплексное исследование никелевых скелетных катализаторов, VIII

Исследование влияния термообработки на никель Ренея с помощью магнитного, электрохимического и термодесорбционного методов

А. ТУНГЛЕР, Й. ПЕТРО, Т. МАТЭ, Й. ХЕЙСМАН, Ф. БУЭЛЛА и З. ЧЮРЁШ

На образцах катализатора никеля Ренея, подвергнутых термообработке в условиях повышенной температуры и в аргоне, были проведены термомагнитные, термодесорбционные и электрохимические измерения, измерения активности и величины поверхности, термомагнитный анализ образцов, электрохимически поляризованных в различной степени, а также термодесорбционные исследования. Сравнивались результаты электрохимического определения содержания водорода с термодесорбционными и магнитными измерениями; было исследовано влияние термообработки на катализаторы.

Было установлено, что изменения, протекающие на никеле Ренея выше 200°, являются генеральными: уменьшаются содержание водорода, величина поверхности, намагничиваемость, температура Кюри и исчезает каталитическая активность.

В образцах, обработанных электрохимически, за счет растворения алюминия образуется никель с гораздо более грубой поверхностью. Никель Ренея может быть поляризован на 150 мв без окисления.

Содержания водорода, определенные электрохимически и термодесорбцией, находятся в корреляции. В образце 3, подверженном термообработке при более высокой температуре, при более высоких температурах (< 350°) появляется новый тип десорбированного водорода.

Синтез производных тригидроксиалкил изохинолина

Г. ДЁРНЕИ и Ч. САНТАИ

Исходя из D-виннокаменной кислоты были синтезированы хорошо растворимые производные 1-тригидроксипропил-тетрагидроизохинолина. Была выяснена абсолютная конфигурация соединений, обладающих тремя хиральными центрами.

Превращения тозиловых и мезиловых производных в

Синтез тозилата псевдокодеина и изучение его нукл

Ш. МАКЛЕЙТ, Г. ШОМОДИ и Р. БОГНАР

Было получено новое соединение — тозилат псевдокодеина и
некоторые реакции нуклеофильного замещения. На основе структур
щей от анионов, были получены два материала А и В. Для образован
наиболее вероятным является механизм S_N1,' а в случае С-8-псевдосое
S_N1 с сохранением конфигурации. Эти заключения основаны на сравн
тозилата кодеина и тозилата псевдокодеина и на кинетическом ис
тозилата псевдокодеина с пиперидином.

The Acta Chimica publish papers on chemistry, in English, German, French and Russian.

The Acta Chimica appear in volumes consisting of four parts of varying size, 4 volumes being published a year.

Manuscripts should be addressed to

Acta Chimica
H-1521 Budapest, Hungary

Correspondence with the editors should be sent to the same address.

The rate of subscription in $ 32.00 a volume.

Orders may be placed with "*Kultúra*" Foreign Trade Company for Books and Newspapers (1389 Budapest 62, P.O.B. 149. Account No. 218 10990) or with representatives abroad.

Les Acta Chimica paraissent en français, allemand, anglais et russe et publient des mémoires du domaine des sciences chimiques.

Les Acta Chimica sont publiés sous forme de fascicules. Quatre fascicules seront réunis en un volume (4 volumes par an).

On est prié d'envoyer les manuscrits destinés à la rédaction à l'adresse suivante:

Acta Chimica
H-1521 Budapest, Hungary

Toute correspondance doit être envoyée à cette même adresse.

Le prix de l'abonnement est de $ 32,00 par volume.

On peut s'abonner à l'Entreprise pour le Commerce Extérieur de Livres et Journaux «*Kultúra*» (1389 Budapest 62, P.O.B. 149. Compte-courant No. 218 10990) ou à l'étranger chez tous les représentants ou dépositaires.

«*Acta Chimica*» издают трактаты из области химической науки на русском, французском, английском и немецком языках.

«*Acta Chimica*» выходят отдельными выпусками разного объема. 4 выпуска составляют один том. 4 тома публикуются в год.

Предназначенные для публикации рукописи следует направлять по адресу:

Acta Chimica
H-1521 Budapest, BHP

По этому же адресу направлять всякую корреспонденцию для редакции.

Подписная цена — $ 32,00 за том.

Заказы принимает предприятие по внешней торговле книг и газет «*Kultúra*» (1389 Budapest 62, P.O.B. 149. Текущий счет № 218 10990) или его заграничные представительства и уполномоченные.

Reviews of the Hungarian Academy of Sciences are obtainable at the following addresses:

AUSTRALIA

C. B. D. Library and Subscription Service
Box 4886, G. P. O.
Sydney N. S. W. 2001

Cosmos Bookshop
145 Acland St.
St. Kilda 3182

AUSTRIA

Globus
Höchstädtplatz 3
A–1200 Wien XX

BELGIUM

Office International de Librairie
30 Avenue Marnix
1050–Bruxelles

Du Monde Entier
162 Rue du Midi
1000–Bruxelles

BULGARIA

Hemus
Bulvar Ruski 6
Sofia

CANADA

Pannonia Books
P. O. Box 1017
Postal Station "B"
Toronto, Ont. M5T 2T8

CHINA

CNPICOR
Periodical Department
P. O. Box 50
Peking

CZECHOSLOVAKIA

Mad'arská Kultura
Národní třída 22
115 66 Praha

PNS Dovoz tisku
Vinohradská 46
Praha 2

PNS Dovoz tlače
Bratislava 2

DENMARK

Ejnar Munksgaard
Nörregade 6
DK–1165 Copenhagen K

FINLAND

Akateeminen Kirjakauppa
P. O. Box 128
SF–00101 Helsinki 10

FRANCE

Office International de Documentation et Librairie
48 Rue Gay-Lussac
Paris 5

Librairie Lavoisier
11 Rue Lavoisier
Paris 8

Europeriodiques S. A.
31 Avenue de Versailles
78170 La Celle St. Cloud

GERMAN DEMOCRATIC REPUBLIC

Haus der Ungarischen Kultur
Karl-Liebknecht-Strasse 9
DDR–102 Berlin

Deutsche Post
Zeitungsvertriebsamt
Strasse der Pariser Kommüne 3–4
DDR-104 Berlin

GERMAN FEDERAL REPUBLIC

Kunst und Wissen
Erich Bieber
Postfach 46
7 Stuttgart S

GREAT BRITAIN

Blackwell's Periodicals
P. O. Box 40
Hythe Bridge Street
Oxford OX1 2EU

Collet's Holdings Ltd.
Denington Estate
London Road
Wellingborough Northants NN8 2QT

Bumpus Haldane and Maxwell Ltd.
5 Fitzroy Square
London W1P 5AH

Dawson and Sons Ltd.
Cannon House
Park Farm Road
Folkestone, Kent

HOLLAND

Swets and Zeitlinger
Heereweg 347b
Lisse

Martinus Nijhoff
Lange Voorhout 9
The Hague

INDIA

Hind Book House
66 Babar Road
New Delhi 1

India Book House
Subscription Agency
249 Dr. D. N. Road
Bombay 1

ITALY

Santo Vanasia
Via M. Macchi 71
20124 Milano

Libreria Commissionaria Sansoni
Via Lamarmora 45
50121 Firenze

JAPAN

Kinokuniya Book-Store Co. Ltd.
826 Tsunohazu 1-chome
Shinjuku-ku
Tokyo 160–91

Maruzen and Co. Ltd.
P. O. Box 5050
Tokyo International 100–31

Nauka Ltd.–Export Department
2–2 Kanda
Jinbocho
Chiyoda-ku
Tokyo 101

KOREA

Chulpanmul
Phenjan

NORWAY

Tanum-Cammermeyer
Karl Johansgatan 41–43
Oslo 1

POLAND

Węgierski Instytut Kultury
Marszalkowska 80
Warszawa

BKWZ Ruch
ul. Wronia 23
00–840 Warszawa

ROUMANIA

D. E. P.
Bucureşti

Romlibri
Str. Biserica Amzei 7
Bucureşti

SOVIET UNION

Soyuzpechaty – Import
Moscow
and the post offices in each town

Mezhdunarodnaya Kniga
Moscow G–200

SWEDEN

Almqvist and Wiksell
Gamla Brogatan 26
S–101 20 Stockholm

A. B. Nordiska Bokhandeln
Kunstgatan 4
101 10 Stockholm 1 Fack

SWITZERLAND

Karger Libri AG.
Arnold-Böcklin-Str. 25
4000 Basel 11

USA

F. W. Faxon Co. Inc.
15 Southwest Park
Westwood, Mass. 02090

Stechert-Hafner Inc.
Serials Fulfillment
P. O. Box 900
Riverside N. J. 08075

Fam Book Service
69 Fifth Avenue
New York N. Y. 10003

Maxwell Scientific International Inc.
Fairview Park
Elmsford N. Y. 10523

Read More Publications Inc.
140 Cedar Street
New York N. Y. 10006

VIETNAM

Xunhasaba
32, Hai Ba Trung
Hanoi

YUGOSLAVIA

Jugoslovenska Knjiga
Terazije 27
Beograd

Forum
Vojvode Mišića 1
21000 Novi Sad

ACTA CHIMICA

ACADEMIAE SCIENTIARUM HUNGARICAE

TOMUS 89 FASCICULUS 3

AKADÉMIAI KIADÓ, BUDAPEST

1976

ACTA CHIM. (BUDAPEST) ACASA 2 89 (3) 187–287 (1976)

ACTA CHIMICA

A MAGYAR TUDOMÁNYOS AKADÉMIA KÉMIAI TUDOMÁNYOK OSZTÁLYÁNAK IDEGEN NYELVŰ KÖZLEMÉNYEI

Az Acta Chimica német, angol, francia és orosz nyelven közöl értekezéseket a kémiai tudományok köréből.

Az Acta Chimica változó terjedelmű füzetekben jelenik meg, egy-egy kötet négy füzetből áll. Évente átlag négy kötet jelenik meg.

A közlésre szánt kéziratok a szerkesztőség címére (1521 Bp., Műegyetem) küldendők. Ugyanerre a címre küldendő minden szerkesztőségi levelezés. A szerkesztőség kéziratokat nem ad vissza.

Megrendelhető a belföld számára az Akadémiai Kiadónál (1363 Budapest, pf. 24. Bankszámla 215 11488), a külföld számára pedig a Kultúra Könyv- és Hírlap-Külkereskedelmi Vállalatnál (1389 Budapest 62, pf. 149. Bankszámla: 218 10990) vagy külföldi képviseleteinél és bizományosainál.

Die Acta Chimica veröffentlichen Abhandlungen aus dem Bereich der chemischen Wissenschaften in deutscher, englischer, französischer und russischer Sprache.

Die Acta Chimica erscheinen in Heften wechselnden Umfanges. Vier Hefte bilden einen Band. Jährlich erscheinen 4 Bände.

Die zur Veröffentlichung bestimmten Manuskripte sind an folgende Adresse zu senden:

Acta Chimica
H-1521 Budapest

An die gleiche Anschrift ist auch jede für die Redaktion bestimmte Korrespondenz zu richten. Abonnementpreis pro Band: $ 32.00.

Bestellbar bei dem Buch- und Zeitungs-Außenhandels-Unternehmen »*Kultúra*« (1389 Budapest 62, P. O. B. 149. Bankkonto Nr. 218 10990) oder bei seinen Auslandsvertretungen und Kommissionären.

Acta Chimica Academiae Scientiarum Hungaricae, Tomus 89 (3), pp. 187—202 (1976)

MÓR KORACH

1888—1975

Kossuth-prize winner and member of the Hungarian Academy of Sciences, internationally recognized authority on chemical technology, distinguished scientist and indefatigable teacher, great humanist and polyhistor, the Nestor of the Chemical Section of our Academy, Mór KORACH passed from among us.

Mór KORACH was born on the 8th February, 1888, in Miskolc. He received his secondary education in Fiume, and proceeded therefrom to Budapest where, at the József Technical University he graduated as a chemical engineer, in 1911. Already as a university student he took part in revolutionary activities and was, for three years, vice-president of the Galilei Circle; that was the time he wrote his first paper about the legal proceedings against Galilei. In the course of his military service he realized that the Habsburg monarchy was preparing for war, therefore he refused to take the officers' oath of allegiance. In the autumn of 1912 he emigrated to Italy. First he worked at the University of Padova, as an assistant to the socialist professor PANEBIANCO, in the Mineralogical Institute. From Padova he went to Faenza where, at that time, under the auspices of the International Museum of Ceramics, the preliminary steps for the founding of the first Italian higher technical school and research establishment of ceramic sciences were in progress. In this Mór KORACH participated as the head of the research laboratory and of the technological section of the school and, in the rank of director, remained there for ten years, as the head of the research laboratory. In this period he designed and constructed the first Italian ceramics pilot plant, and also designed and put in operation the first electric ceramic oven. At the same time he continued his studies in physics and mathematics as a pupil of RIGHI, ENRIQUEZ and BURGATTI, but did German philology as well, and also obtained his diploma at the end of these studies.

After World War I he resumed relations with his family and friends in Hungary and, having acquired Italian nationality, he could be of help to the fugitives of the 1919 Hungarian Soviet Republic. He succeded in saving Aladár KOMJÁT from the presecution of the white terrorists. The help and protection he extended to the comrades fled from Hungary to Italy drew the attention

of the Italian police, later that of the fascists, to KORACH's activities, this attention being shown by repeated house-raids and corporeal attack upon his person. These attacks did not cease even after Mór KORACH had become, in 1924, professor at the University of Bologna, and later the head of its department for chemical industrial machinery.

His researches in the field of the science of ceramics began at Faenza, and continued in every branch of this science. Following his master, Vince WARTHA, the guiding thread of KORACH's work remained the consistent endeavour to introduce the scientific method into industrial practice. At that time this was trail-blazing work in Italian university tuition as well as in research. Thus close personal connections with industrial product personnel were established, and Mór KORACH became technical consultant to several factories; he designed and supervised the operation of several, at that time modern, industrial kilns and manufacturing plants.

His first researches dealt with the colouring techniques for Cassius Purple and Persian glazes in the domain of fine ceramics, but were soon extended to include rough ceramics too. As early as 1921 he began a systematic study of Italian raw materials of the ceramics industry and their utilization; this work he continued persistently. In this domain his results, being industrial secrets, could only be published in a small part. The formulation of Persian glazes for earthenware he worked out on the occasion of the renaissance of Rhodian faience industry, to be utilized by the earthenware manufacturing plant designed and built by him in 1932, and still at work today, in continuation of the Rhodian tradition.

Mór KORACH published two papers on the role of alkaline earth oxides in ceramics; the first appeared in the Proceedings of the International Chemical Congress at Palermo, in 1926. Outstanding among his subsequent researches on Italian ceramic raw materials were those relevant to the china clay deposits in Sardinia, which induced a country-wide exploration of ceramic raw materials in Italy, and his work on the application of Piedmont steatites in the manufacture of a new type of cordierite soft porcelain; furthermore, the production of high-frequency insulating materials.

In 1925, Mór KORACH was invited to the newly established chair of chemical machinery at the University of Bologna. At that time also this was a pioneering job, because this was the first university faculty that trained mechanical engineers specifically for the chemical industry and, as BERL's fundamental handbook on chemical machinery had not yet been published, his lectures had to be based on practice and publications in the various journals. 1928 witnessed to the publication of his first Italian textbook on the technology of ceramics manufacture.

In addition to his studies and technological work on ceramics, he worked for some time on the problems of cement manufacture; in this field puzzolane

cements and calcination were his chief concerns. Together with his pupil, Dr. RANDACCIO, he worked out, in experiments continued over five years, a method for the regeneration of used lubricating oils; this method also found use in industrial practice.

In 1938, Mór KORACH fled to Western Europe where he worked as an industrial consultant. During World War II he lived in Italy and took part in the activities of the resistance, the so-called Liberation Movement. He was found out and imprisoned. As a prisoner in the San Vittore gaol at Milano, he joined the Italian Communist Party at the beginning of 1945.

In the summer of 1952, at the call of the Hungarian government and with the consent of the Italian Communist Party, Mór KORACH finally returned to Hungary. As of the 1st March, 1953, the Cabinet nominated him for the directorship of the Central Research Institute of Building Materials, to be founded. Besides this, he was given several jobs. In February 1954, he was made a member of the Technical Council of the Ministry of Housing; in May of the same year he was elected a member of the Chief Council for Building Sciences, Department of Technical Sciences of the Hungarian Academy of Sciences. On the 6th October 1955, the vice-president of the Cabinet appointed him member of the Technical Development Council.

Besides his research and science organization work, he again took part in higher education. From August 1956 on he was professor at the Chemical Machinery and Agricultural Industries Department of the Faculty for Mechanical Engineering of the Technical University of Budapest. On the 5th of June, 1957, the Government appointed him a member of the Scientific Council of Higher Education; also in this capacity he did much active work. On the 19th July of the same year, he became a permanent member of the Expert Committee of Building Materials of the Ministry of Housing. As taking effect on the 1st September in the same year, the Minister of Education transferred him from the Mechanical Engineering Faculty to the Chemical Engineering Faculty of the Technical University, to act, in secondary employment as the head of the Department of Chemical Technology.

On the 11th November, 1957, he gave up his directorship at the Central Research Institute of Building Materials and became scientific adviser to the Minister of Housing. On the 2nd May, 1958, he transferred from the Ministry of Housing to the Department of Chemical Technology of the Technical University of Budapest, but was re-affirmed in his position, in secondary employment, as a scientific adviser to the Minister of Housing. Besides his zealous and successful activities as a professor, Mór KORACH organized one of the first research institutes for chemical technology in Middle Europe, to the directorship of which he was appointed by the president of the Hungarian Academy of Sciences on the 25th February 1960. He deserves high credit for the development and outlining the scope of this institute. On the 1st March, 1962, the

Government appointed him a member of the National Council of Technological Development. In 1963 he retired as a professor, and retained the directorship of the research institute, which he served as a scientific adviser till his death.

His scientific work in Hungary comprised, first of all, the field of chemical technology and industrial chemistry. The recognition of several general rules of chemical technology, *e.g.* that of the scaling-up effect and cost parameters, the initiating of process-theoremes and, in this domain, chiefly the utilization of the graph theory for the systematization of chemical technological processes are associated with his name. He repeatedly studied mathematical methods with a view to their applicability in technological sciences. He deserves credit for the modernization of higher technical education, especially in the training of chemical engineers. It is owing to him that the curriculum for general chemical technology was elaborated. He insisted that the engineering aspects in the training of chemical engineers be emphasized. He did much for the carrying into effect training by technological work in pilot plant, and for the use of audio-visual methods. For years he studied some problems of heating techniques in industrial chemistry; he was especially interested in continuous furnaces, where he introduced sandwich-burning which is now practised the world over.

Mór KORACH became private docent of the science of chemical apparatus and machinery still in Italy. In 1920 he was awarded the gold medal of the International Museum of Ceramics; in 1925 he was elected fellow of the Inspectorate of the International Museum of Ceramics at Faenza. In Hungary, in 1952, he became doctor of the technical sciences; in 1956, a corresponding member and in 1958 an ordinary member of the Hungarian Academy of Sciences. He was very active and did many-sided work in the Academy; in recognition of this he was awarded the Gold Medal in 1969.

In 1958 he was honoured with a Kossuth prize II Class, and the decoration Red Flag of Labour. In November 1958, as the leading member of the Galilei Circle he was presented with its memorial leaf at the fiftieth anniversary of its foundation; in March 1959 he was presented with the memorial leaf of the Veterans of the Hungarian Soviet Republic. In 1961 he received the gold diploma, in 1971 the diamond diploma, of the Technical University of Budapest. In December 1953, the Presidential Council awarded him the Order of Labour, and in 1968, the gold class of this Order. From the Central Committee of the Hungarian Socialist Workers' Party he received a memorial leaf in 1965, in recognition of his services to the people. In April 1967, he was awarded a gold medal for his work in the field of the silicate industry. In 1970 he was honoured by the Jubilee Memorial Plaque of Liberation, and the Jubilee Plaque of the City of Veszprém.

His outstanding results in the field of chemical technology and the silicate industry were acknowledged by a doctorate honoris causa conferred upon him by the Technical University of Budapest, on the 3rd November 1967.

This high honour was bestoved upon him by the Leningrad Technological Institute, in 1968; in the same year the Science Policy Foundation, London, elected him an honorary member. In 1971 he became Hungarian Councillor of the Centre of Logical and Comparative Sciences at Bologna, and an honorary member of the international Academy of Ceramics at Genova; the Bolognese Academy of Sciences elected him a corresponding member in 1972; in the same year he became a honorary member of the Italian Ceramical Society at Bologna. The diploma conferring on him the Freedom of the City of Faenza was presented to Mór KORACH in 1975, during his last illness.

Besides his academical and scientific activities, Mór KORACH did much work in the Federation of Technical and Scientific Societies. He was for years president, and then honorary president till his death, of the Society of Silicate Science and Industry; of the Club of Engineers of Fifty Years' Standing; and of the METESZ Club of the Science of Sciences.

Academician Mór KORACH was an outstanding personality not only in the field of chemical technology and organisation of scientific endeavours, but produced lasting work also in the domain of literature and painting. He wrote 24 short stories, 10 prose poems, 49 tales, 10 dialogues, one play, 12 polemical papers, 8 literary essays, and two on aesthetics. His first collection of stories, entitled "Il figliuol prodigo" appeared in 1933, the second, entitled "Il volto umano di Claudio Vasari" in 1961. He studied esperanto as a means of scientific communication. His portrait of Vince WARTHA hangs in the gallery of the Technical University of Budapest.

The wide scope of his life work is reflected by the bibliography here appended, and by the literary products mentioned, but in addition he is the author of 10 popular scientific papers, 37 communications on economics and politics and 5 illustrated political papers. He wrote 28 critical articles and reviews, and did 24 translations.

It is with a heavy heart that we part from a very gifted, many-sided personality of our Academy. His many accomplishments and results, the guidance in his life, and his scientific legacy give us strength for our further endeavours to achieve progress both in science and higher education.

With reverence we shall keep him in our remembrance!

Károly POLINSZKY

MÓR KORACH'S PUBLICATIONS

A Galilei-pör
Világ, Budapest, 20th Nov., 1910.

Appunti al 'Geidrovolante'
Il Resto del Carlino, Bologna, 18th Sept., 1917.

Un nuovo apparecchio d'aviazione e i getti dei fluidi entro i fluidi
Il Monitore Tecnico, **24** (1918.) No. 5. p. 34–39.

L'opera d'un decennio
Faenza, Bollettino del Museo Internazionale delle Ceramiche di Faenza, **7** (1919.)

La maiolica di Faenza ed il suo rinnovamento
Le Vie d'Italia, **4** (1920.) No. 2.

Metodi di Studio Microscopici nella Ceramica
Faenza. Bollettino del Museo Internazionale delle Ceramiche di Faenza, **8** (1920.) fasc. 3–4. p. 93–95.

Dati statistici relativi all'industria delle ceramiche (laterizi esclusi) in Italia
Faenza. Bollettino del Museo Internazionale delle Ceramiche di Faenza, **8** (1920.) fasc. 1–2. p. 40–46.

Sulla porpora di Cassio
Faenza. Bollettino del Museo Internazionale delle Ceramiche di Faenza, **9** (1921.)

Sulla temperatura delle formaci di maiolica a fiarma diritta
Faenza. Bollettino del Museo Internazionale delle Ceramiche di Faenza, **9** (1921.) fasc. 2. p. 43–46., fasc. 3. p. 69–72.

Ancora sui metodi di studio microscopici nella ceramica
Faenza. Bollettino del Museo Internazionale delle Ceramiche di Faenza, **9** (1921.) fasc. 3. p. 72.

Recenti ricerche sulle paste di ceramica
Faenza. Bollettino del Museo Internazionale delle Ceramiche di Faenza, **9** (1921.) fasc. 4. p. 101–104.

L'Istituto di ceramica francese
Faenza. Bollettino del Museo Internazionale delle Ceramiche di Faenza, **10** (1922.) fasc. 1. p. 17.

Gli industriali di ceramica inglesi e l'arte
Faenza. Bollettino del Museo Internazionale delle Ceramiche di Faenza, **10** (1922.) fasc. 1. p. 17.

Sui forni continui a galleria e sul Sistema Herda
Faenza, Bollettino del Museo Internazionale delle Ceramiche di Faenza, **10** (1922.) fasc. 1. p. 18–23.

Sul Concetto di rendimento termico di formace, e su alcuni...
Faenza. Bollettino del Museo Internazionale delle Ceramiche di Faenza, **10** (1922.) fasc. 3–4. p. 151–160.
(ua.)
Laterizi ed Affini, **1** (1923.) No. 12. [6 pages]

Relazione del direttore ing. Maurizio KORACH sull' attività evolta negli anni 1920–1926. Laboratorio sperimentale di ricerche termiche e fisico-chimiche applicate alla ceramica. Regia Scuola di Ceramica in Faenza, **12** (1926.) p. 1–10.

Decomposizione del calcare negli impasti. Atti II. Congr. Nazionale Chimica Pura e Applicata. Palermo, 1926.

Lezioni di impianti chimici. Tenute negli anni 1925–26 e 1926–27 all' Università di Bologna. Università, Bologna, 1927.

Forno elettrico per la cottura delle ceramiche
Corriere dei Ceramisti, **9** (1928.) No. 1. p. 1–6.

Elementi di tecnologia ceramica I–III. Ed. del Museo delle Ceramiche in Faenza. Tip. F. Lega. 1928.

Il problema dei silicati in Italia
Le Industrie dei Silicati, **7** (1929.) No. 1. p. 3–7.

Industria Ceramica. Manuale dell'Ingegnere 'Colombo'. Milano, Ed. Hoepli, 1929. p. 51–58.

Lezioni di impianti chimici. [2. ed.] Università, Bologna, 1929–30.

Forno elettrico per la cottura della ceramica
Faenza. Bollettino del Museo Internazionale delle Ceramiche di Faenza, **17** (1929.) fasc. 1. p. 22–28.
Faenza. Bollettino del Museo Internazionale delle Ceramiche di Faenza, **17** (1929.) fasc. 2. p. 48–52.

I caolini e le terre refrattarie della Sardegna. Roma, Tip. Camera Deputati, 1931. p. 47.

Ancora i problemi dei refrattari nazionali
L'Industria del Vetro e della Ceramica, **3** (1932).

Rigenerazione degli olii usati col procedimento [Maurizio] KORACH–[Carlo] RANDACCIO
Giornale di Chimica Industriale ed Applicata, **14** (1932.) No. 5. p. 228–252.

Assagi e laboratori d'assaggi per l'industria ceramica
L'Industria del Vetro e della Ceramica, **3** (1932.) fasc. 6.

Esperienze sull' effetto degli ossidi alcalino-terrosi negli impasti ceramici
L'Industria del Vetro e della Ceramica, **4** (1933.) fasc. 7. p. 10.

La porcellana italiana senza vernice. [Primo] 1° Congresso Internazionale del vetro e della ceramica, sett. 1933.

La porcellana italiana senza vernice. Teramo, Tip. La Fiorita, 1933.

Una nuova porcellana per isolatori
L'Elettrotecnica, **21** (1934.) No. 5. p. 1–8.

Industria Ceramica. Manuele dell' Ingegnere 'Colombo'. [66–70. ed.] Milano, Ed. Hoepli, 1939.

La "Sacra Famiglia" di Carlantonio Grue di Castelli
Faenza. Bollettino del Museo Internazionale delle Ceramiche di Faenza, **23** (1947.) fasc. 3. 7. pages.

Definizione tecnologica del termine "ceramica"
Faenza, Bollettino del Museo Internazionale delle Ceramiche di Faenza, **25** (1949.) fasc. 4–6. p. 118–134.

Che accade al telescopio di M[onte] Palomar?
Coelum, **19** (1949.) No. 5–6. p. 1–4.

Sulla cottura a fiamma nella ceramica. Atti del Convegno per il Commercio Estero della Ceramica, Vicenza, 10 Settembre 1950. Vicenza, 1950. p. 32–34.

A dolgozók tömegeiben teremtő energia szabadult fel
Újítók Lapja, **2** (1950.) No. 21. p. 5.

Del concetto di "rendimento termico" dei forni
L'Industria della Ceramica e Silicati, — (1951.) No. 3. 2 pages.

Herend és a kerámiai iparművészet problémája a népi demokráciában
Építőanyag, **5** (1953.) No. 1. p. 16–20.

A tudomány és a termelés szocialista kapcsolatai.
MTA Társadalmi-Történeti Tudományok Osztályának Közleményei, **3** (1953.) No. 3–4. p. 434–436.

Az alagútkemence és a szendvics gyorségetés
Építőanyag, **5** (1953.) No. 8–9. p. 262.

Válasz MATTYASOVSZKY Lászlónak és BRÉDA Gyulának.
Építőanyag, **6** (1954.) No. 1. p. 10–11.

A hazai kutatás problémája.
Magyar Technika, **9** (1954.) No. 11. p. 646–650.

A műszaki tudományok szerepe a tudományok osztályozásában.
Akadémiai Értesítő, **61** (1954.) No. 506. 281—294.

Bevezetés VÁNDOR József: „A hatványtörvények és jelentőségük a műszaki tudományban" c. munkájához.
Tudományos Közlemények. Építőanyagipari Központi Kutató Intézet. (Építésügyi Minisztérium Műszaki Főosztálya.) 1954. No. 1. p. 3—9.

Üvegolvasztás szulfátvízüveg segítségével. Építésügyi Kiadó, Budapest. 1954. No. 2. 66 pages. Építőanyagipari Központi Kutató Intézet. Report. No. 8.

Az építőanyagipari kutatás feladata és módszerei
Építőanyag, **7** (1955.) No. 1. p. 2—6.

Théorie du four-tunnel et cuisson rapide "Sandwich". I. P. Essais sur modèles de fours-tunnel théoriques.
Acta Technica Academiae Scientiarum Hungaricae, **11** (1955.) fasc. 1—2. p. 161—184.

Szilikátiparunk helyzetéről
Műszaki Élet, **10** (1955.) No. 9. p. 11—17.

Az alagútkemence elmélete és a "szendvicsgyorségetés"
Magyar Energiagazdaság, **8** (1955.) No. 7. p. 246—257.

Cottura in forni sandwich e in forni a galleria normale [Co-author: G. Silipandril]
La Ceramica, **10** (1955.) No. 8. p. 48—57.

Műszaki felsőoktatásunk kérdéseihez
Műszaki Élet, **10** (1955.) No. 16. p. 9—13.

Társadalmi forradalom és műszaki forradalom
Újítók Lapja, **7** (1955.) No. 21. p. 3—4.

Fémkohászat és szilikátkohászat
Műszaki Élet, **10** (1955.) No. 24. p. 1—4.

Die Technologie der Kervit-Platten-Herstellung
Silikattechnik, **6** (1955.) No. 12. p. 521—528.

Prodotti Ceramici. Manuale C. FERRI: "Guida dei principali prodotti chimici". Bologna, Ed. ZANICHELLI, 1955. p. 197—211.

Industria Ceramica. Manuale Colombo. [80. Ed.] Milano, Ed. Hoepli, 1955. p. 1336—1346.

Az új technika alkalmazása a szilikátiparban
Építőanyag, **8** (1956.) No. 1. p. 3—6.

VÁNDOR József [Necrology.]
Magyar Kémikusok Lapja, **11** (1956.) No. 2. p. 50—52.

Theorie und Technologie der Kervit-Platten-Herstellung
Acta Technica Academiae Scientiarum Hungaricae, **14** (1956.) fasc. 3—4. p. 439—462.

Mit jelent számunkra WARTHA Vince?
Természet és Társadalom, **95** (1956.) No. 4. p. 215—217. p.

A matematika szerepe a technológiai (gyakorlati) tudományokban.
Tudományos Közlemények. Építőanyagipari Központi Kutató Intézet. 1956. 2. p. 1—15.

Teorija i tehnologija proizvodsztva keramicseszkoj plitki metodom Litja.
Keramika, (1957.) No. 2.

Essais sur modèles de fours-tunnel théoriques. (Beograd, 1957.) Conférence Mondiale de l'Énergie. 11. session partielle. B. Section, 16. rapport.

A technológia módszertana
Magyar Tudomány, **2** (1957.) No. 5—6. p. 205—229.

The problem of technical teaching
Tudományos Munkások Világszövetségének V. Közgyűlése (World Federation of Scientific Workers), Helsinki, 1957.

On methodological problems of technology
Periodica Polytechnica. Chemical Engineering. **2** (1958.) No. 3. p. 145—171.

Az építőanyagok "forradalma"
Magyar Tudomány, **3** (1958.) 8—9. sz. p. 343—349.

A vegyészmérnökképzés helyzete és kérdései
Felsőoktatási Szemle, **7** (1958.) 5. sz. p. 277—282.

Az égetés hőgazdasága az alagútkemencében
Építőanyag, **10** (1958.) 1—2. sz. p. 1—5.

La Révolution Sociale et Culturelle Hongroise d'après la guerre et les événements d'Octobre 1956
Comprendre. Revue de la Société Européenne de Culture. **19** (1958.) p. 133—141.

Egy mérnök a forradalomban
Műszaki Élet, **14** (1959.) 28th May.

Théorie du four-tunnel et cuisson rapide "Sandwich". II. P. Essais sur modèles théoriques de fours-tunnel de types normal et sandwich.
Acta Technica Academiae Scientiarum Hungaricae, Bp., **25** (1959.) fasc. 1—2. p. 25—62. [the same] Budapesti Műszaki Egyetem Vízgépek Tanszékének Közleményei, No. 47. 1959.

Über Maßstabeffekt in der chemischen Technologie
Acta Technica Academiae Scientiarum Hungaricae, Bp., **25** (1959.) fasc. 3. p. 345—358.

A hazai technológia-oktatás problémái
Magyar Kémikusok Lapja, **14** (1959.) No. 11. p. 421—424.

A léptékhatás a kémiai technológiában.
MTA Kémiai Tudományok Osztályának Közleményei, **11** (1959.) No. 2. p. 205—215.

Kémiai technológia I. 1. füzet. Bevezetés a kémiai technológiába. Kőszénipar. Kőolaj és földgázipar. Metallurgia. Felsőokt. Jegyzetell. V., Budapest., 1960. 274 pages. [Co-authors: Ackermann L., Jécsai L., etc.]

Kémiai technológia I. 2. füzet. Víz, kerámiai anyagok. Építőipari kötőanyagok és üvegek. Szerves szerkezeti anyagok. Atomreaktor fűtőanyagok technológiája. Felsőokt. Jegyzetell. V., Budapest., 1960. 169 pages. Co-authors: Ackermann L., Déri, M. etc.]

Kémiai technológia. Felsőokt. Jegyzetell. V. Budapest., 1960. 91 pages. [Co-operative.]

A szervetlen kémiai technológia a felszabadulás után.
MTA Kémiai Tudományok Osztályának Közleményei, **14** (1960.) No. 2. p. 201—204.

A magyar kémiai technológiai iskola elvei.
Veszprémi Vegyipari Egyetem Közleményei, **4** (1960.) p. 227—242.

Kémiai technológia feladatok. Editor: T. Téri 2. revised ed. Felsőokt. Jegyzetell. V., Budapest., 1960. 91 pages. [Co-authors: Ackermann L., Szebényii., Vajta L.]

Szerves szerkezeti anyagok technológiája. Felsőokt. Jegyzetell. V., Budapest., 1960. 49 pages. [Co-author: Menyhárt, J.]

Kémiai technológia I. 2. Ábrafüzet. Felsőokt. Jegyzetell. V., Budapest., 1960. 18 pages.

Einige Probleme der physikalischen Maß- und Einheitssysteme. Felsőokt. Jegyzetell. V., Budapest 1961. 13 pages. Co-authors: Seitz K., Sasvári Gy.]

Prüfung ungarischer Flugaschen. (Die Flugasche als Rohstoff.)
Periodica Polytechnica. Chemical Engineering. **5** (1961.) No. 4. p. 341—356. [Co-authors: Déri M., Sasvári Gy., Moldvai Á., Práger I., Ackermann L., Szebényi I.]

Műszaki tudományok. [Key-word] Új Magyar Lexikon, 5. Ed. Akadémiai K., Budapest 1961. p. 84.

Világviszonylatban is kiemelkedő teljesítmény a II. Nemzetközi Tudományos Filmfesztivál. Filmfesztivál. (Proceedings of the 2nd International Scientific Film Festival.) Gépipari Tudományos Egyesület, Budpest No. 4. sz.

Kémiai technológia. 1. füzet. Ábrafüzet. SÜTŐ J., SZEBÉNYI I. Tankönyvkiadó, Felsőokt. Jegyzetell. V., Budapest 1961. 55 pages.

Kémiai technológia I. 2. füzet. Ábrafüzet a víz, kerámiai anyagok, építőipari kötőanyagok, szerves szerkezeti anyagok, atomreaktor fűtőanyagok technológiájához. Tankönyvkiadó, Felsőokt. Jegyzetell. V., Budapest 1961. 18 pages.

Kémiai technológiai feladatok. Tankönyvkiadó, Budapest 1961. 79 [Co-authors: ACKERMANN L., SZEBÉNYI I., VAJTA L.]

Közlekedéskari kémiai technológia. Útmutató. Tankönyvkiadó, Felsőokt. Jegyzetell. V., Budapest 1961. 37 [Co-author: PRÁGER I.]

Kémiai technológiai útmutató. Tankönyvkiadó, Felsőokt. Jegyzetell. V., Budapest 1961. 34 Co-author [SZEBÉNYI I.]

A kémiai technológia mint tudomány.
A Budapesti Műszaki Egyetem 1961. évi Tudományos Évkönyve, Tankönyvkiadó, Budapest 1961. p. 186—200.

Rol' matematiki v tehnologicseszkih naukah.
Transactions of the Hungarian Institute of Building Material Research, **1** (1961.) p. 19—52.

Beszámoló az 1959. évi IUPAC Kongresszusról.
MTA Kémiai Tudományok Osztályának Közleményei, **15** (1961.) No. 2. p. 227—236.

L'extension de la notion de modèle et ses applications thermotechniques.
Acta Technica Academiae Scientiarum Hungaricae, **33** (1961.) fasc. 3—4. p. 351—357.

Théorie du four-tunnel et cuisson rapide "sandwich". 3. P.
Acta Technica Academiae Scientiarum Hungaricae, **33** (1961.) p. 327—350.

Hőenergiagazdálkodás az alagútkemencében.
Ipari Energiagazdálkodás, **2** (1961). No. 3. p. 49—52.

A Magyar Tudományos Akadémia Kémiai Technológiai Bizottságának Műszaki Kémiai Ankétja. (Presidential opening address.)
MTA Kémiai Tudományok Osztályának Közleményei, **15** (1961.) No. 1. p. 77—90

Az oktatási reform és a vegyészmérnökképzés elvi kérdései
Magyar Tudomány, **6** (1961.) 3. No. 3. p. 153—159.

A kémiai technológia egyik fejlődéstörvényéről
MTA Kémiai Tudományok Osztályának Közleményei, **16** (1961.) No. 2. p. 163—173.

Porszénhamufajták technológiai vizsgálata. [Co-author SASVÁRI GY.]
Építőanyag, **13** (1961.) No. 4. p. 134—140.

A szilikáttechnológia perspektívái.
Építőanyag, **13** [1961.] p. 439—441.

Une loi du dévéloppement de la technologie chimique
Chimie et Industrie [Suppl. "Génie Chimique"], **86** (1961.) No. 5. p. 132—137.

Az atomkérdésről
A Budapesti Műszaki Egyetem Vegyészmérnöki Karának Tudományos Évkönyve, Tankönyvkiadó, Budapest 1962. p. 167—177.

Általános kémiai technológia I—II. Tankönyvkiadó, Budapest 1962. 266 pages. Ed. SIKLÓS P., SÜTŐ J.)

Kémiai technológiai útmutató és vizsgálati módszerek. Tankönyvkiadó, Budapest 1962. 69 pages. [Co-authors: SZEBÉNYI I., ACKERMANN L.]

Kémiai technológiai gyakorlatok. Tankönyvkiadó, Bp., 1962. 35 pages. [Co-authors: ACKERMANN L., KISS L., MOSER M.]

Aktuelle Fragen der Silikatwissenschaft und Perspektiven der Silikattechnologie
Silikattechnik, **13** (1962.) No. 2. p. 43—44.

Die Trocknung in der Keramik
Acta Technica Academiae Scientiarum Hungaricae, **39** (1962.) fasc. 1—2. p. 195—214. [Co-author: SASVÁRI Gy.]

Aprított halmazok elosztása
Építőanyag, **14** (1962.) No. 3. p. 81—86.

Kerámiai kromatográfia
Építőanyag, **14** (1962.) No. 4. p. 121—128. [Co-author: MOLDVAI Á.]

A kémiai technológia egyik fejlődési törvénye. Magyar Kémikusok Egyesülete, Budapest, Aug. 23—25. 1962.

Sandwich-Schnellbrennen und Wirtschaftlichkeit der Tunnelöfen
Berichte der Deutschen Keramischen Gesellschaft, **39** (1962.) No. 12. p. 583—589.

Die Prüfung ungarischer Flugaschen. Kalkgebundene Flugaschenkörper.
Periodica Polytechnica. Chemical Engineering. **6** (1962.) p. 21—34. [Co-authors: DÉRI M., SASVÁRI Gy., PRÁGER I. etc.]

Grain Size Distribution of Crushed Products.
Proceedings of the 6. Conference on the Silicate Industry. Akadémiai K., Budapest 1963. p. 221—230.

Ceramic Chromatography
Proceedings of the 6. Conference on the Silicate Industry. Akadémiai K., Budape 1963. p. 231—243. [Co-author: MOLDVAI Á.]

Behaviour of silicon carbide in the burning space
Acta Chimica Academiae Scientiarum Hungaricae, **35** (1963.) fasc. 3. p. 321—350. [Co-author: MENYHÁRT M.]

Keramicseszkaja hromatografija
Acta Chimica Akademiae Scientiarum Hungaricae, **37** (1963.) fasc. 3. p. 261—278. [Co-author: MOLDVAI Á.]

A köznyelv és a műszaki tudományos nyelvek kapcsolata
Hungara Esperantisto, [**3**] (1963.) No. 7. p. 4—5.

Verbilligung des Brandes durch "Sandwich"-Tunnelöfen
Ziegelindustrie, **13** (1963.) p. 485—487.

Általános kémiai technológia. III. rész. Az alapanyagok kémiai technológiája. 2. (Ed. BUCSY I.) Tankönyvkiadó, Budapest, 1963. 143 pages.

Kémiai technológia. Tankönyvkiadó, Budapest 1963. 218 pages. [Co-authors: BUCSY I., KESZTHELYI K., SZEBÉNYI I., WIENER G.]

Kemencék. Tankönyvkiadó, Budapest, 1963.

A méréstan néhány ismeretelméleti kérdése
Magyar Filozófiai Szemle, **7** (1963.) No. 2. 177—198.

Problemi e prospettive della ceramica vicentina
Vicenza Economica, 1963. No. 1. p. 11—14.

A műszaki tudományos film nemzetközi jelentősége.
Filmfesztivál. (Proceedings of the 3rd International Stientific Film Festival.) Gépipari Tudományos Egyesület, Budapest, 1964. No. 1. p. 1.

Gaetano BALLARDINI
La Ceramica, 1964. No. 9. p. 62.

Művelet, folyamat, eljárás
Intenzív Vegyipari Eljárások Konferenciája, Kecskemét, oct. 22—24. 1964.

A porcelángyorségetés tanulmányozása modellezéssel. 1964.

Über die dimensionslosen Kennzahlen der industriellen Erwärmung
Acta Chimica Academiae Scientiarum Hungaricae, **40** (1964.) fasc. 3. p. 357—366. [Co-author: SASVÁRI Gy.]

Általános kémiai technológia. I—II. rész. Az általános kémiai technológia alapjai. Tankönyvkiadó, Budapest 1964. 275 pages. [SIKLÓS P., SÜTŐ J.]

Általános kémiai technológia. III. Tankönyvkiadó, Budapest 1964. 152 pages. [Co-author: BUCSY I.]

Kémiai technológiai feladatok. 2. Ed. Tankönyvkiadó, Budapest 1964. 79 pages. [Co-authors: ACKERMANN L., SZEBÉNYI I., VAJTA L.]

Az Építőanyagipari Központi Kutatóintézet tízéves tudományos működése. Előszó. Építésügyi Minisztérium Dokumentációs Iroda, Budapest 1964. p. 5—8.

The Science of Industry. The Science of Science Society in the Technological Age. Ed. by Maurice GOLDSMITH and Alan MACKAY. Souvenir Press, London—Toronto, 1964. p. 179—194.
[the same.] Hosey University Press, Japan, 1965. p. 249—267.
[2.] Penguin Books, Ltd. Pelican Book, London, 1966.
[3.] Nauka o nauke. (Szbornik sztatej) Izd. Progressz, Moscow, 1966. p. 217—235. [the same] Ed. by SIMON and SCHUSTER, New York, 1966.

Gaetano Ballardini
Faenza. Bollettino del Museo Internazionale delle Ceramiche di Faenza, **50** (1964.) fasc. 4—5. p. 103—109.

Porózus kerámiai testek előállítása kromatográfiai kísérletek céljára
Építőanyag, **17** (1965.) No. 1. p. 1—6.

Introductory addresses.
Proceedings of the 7. Conference on the Silicate Industry. Akadémiai K., Budapest 1965. p. 13—22.

A vegyipar fejlesztésének legfontosabb feltétele a nagyméretű műszaki jellegű vegyipari kutatómunka.
Újítók Lapja, **17** (1965.) 11. sz. p. 7.

A rhodoszi fajánszok kerámiai színezékeiről.
Kolorisztikai Értesítő, **7** (1965.) No. 7—8. sz. p. 222—224.

Systématisation du génie chimique. Congrès International de Chimie Industrielle, Beograd. Sept. 1963.
22—29. Recueil des Conférences Plenières, Beograd, 1965. p. 81—87.

A Műszaki Kémiai Kutató Intézet 5 éve és a magyar műszaki kémiai kutatás.
MTA Kémiai Tudományok Osztályának Közleményei, **24** (1965.) No. 2. p. 159—172.

Verteilung von Zerkleinerungshaufen
Silikattechnik, **16** (1965.) No. 1. p. 12—16.

Zakljucsitel'nüj otcset. [A KGST 8. sz. szilikátipari témájának zárójelentése.] Bp., 1965. [1966.] 155 pages.

A műszaki kémiai kutatás helyzete és eredményei Magyarországon.
Magyar Tudomány, **10** (1965.) No. 10. p. 645—653.

Die Wechselwirkung zwischen Chemie und Maschinenbau-, Chemie- und Elektroingenieurswissenschaften.
Periodica Polytechnica. Chemical Engineering. **9** (1965.) No. 4. p. 263—274.

Baustoffe der Zukunft?
Technische Gemeinschaft, **13** (1965.) No. 12. p. 24—26.

My observation on the economic and cultural development of moderately advanced countries.
Tudományos Munkások Világszövetségének Szimpoziuma, Sept. 20—23. 1965. (Symposium of the World Federation of Scientific Workers), p. 1—3. p.

Process, Flow, Method. Conference on some aspects of physical chemistry. II. General section. Budapest, 1966. p. 1—13.

Résultats d'expériences aérodynamiques sur modèles de fours tunnel.
Acta of the World Power Conference, Tokio, Oct. 16—20. 1966. Section III/A. p. 1—11.

Kémiai technológiai feladatok. 3. Revised ed. Tankönyvkiadó, 1966. 119 pages. [Co-authors: ACKERMANN L., SZEBÉNYI I., VAJTA L.]

Megjegyzések a "Science of Science" vitához
Magyar Tudomány, **11** (1966.) No. 10. p. 632—639.

Some principles of flow engineering
Acta Chimica Academiae Scientiarum Hungaricae, **50** (1966.) [Jubilee issue.] p. 457—470.

I maggiori problemi dell'estetica ceramica-Faenza
Faenza. Bollettino del Museo Internazionale delle Ceramiche di Faenza, **52** (1966.) fasc. 4—5—6. p. 75—82.

Újabb kerámiai kromatográfiai kísérletek
Kolorisztikai Értesítő, **9** (1967.) No. 3—4. p. 50—62. [Co-author: MOLDVAI Á.]

A tudomány tudománya
Élet és Tudomány, **22** (1967.) máj. 5. p. 843—845. [Co-author: SZÁNTÓ L.]

Un antico documento sulla porcellana cinese in Europa
Faenza. Bollettino del Museo Internazionale delle Ceramiche di Faenza, Faenza, **53** (1967.) fasc. 2—3—4—5.

Technological research and technical development
Scientific World, **11** (1967.) No. 4. p. 16—20.

A kutatás módszertana a technológiában. Bevezetés az ipari kutatómunkába. Budapest, 1967. (Editors: GILLEMOT L., MÉSZÁROS S.) (Mérnöki Továbbképző Intézet előadássorozata. 4572. sz.) Chapter 11. p. 235—263.

WARTHA Vince. [Bevezetés MÓRA László: WARTHA Vince a hazai kémiai technológia megalapítója (1844—1914.) c. könyvéhez. Budapesti Műszaki Egyetem Központi Könyvtára Műszaki Tudománytörténeti Kiadványok. 15 .sz.] Tankönyvkiadó, Budapest., 1967. p. 7—9.

La scienza dell'industria
Sapere, Milano, (1967.) No. 12.

Kémiai technológia. Revised ed. Tankönyvkiadó, Budapest., 1967. 204 lap. [Co-author: BUCSY I.]

A "Science of Science" meghatározása.
Magyar Tudomány, **13** (1968.) No. 1. p. 40—42.

Vincenzo WARTHA fondatore della technologia scientifica ungherese.
Faenza. Bollettino del Museo Internazionale delle Ceramiche di Faenza, **54** (1968.) fasc. 1. p. 9—13.

Kémiai technológiai folyamatok gráf-elméleti leképzése
Kémiai Közlemények, **29** (1968.) No. 3. p. 263—290. [Co-author: HASKÓ L.]

Teoreticseszkie osznovü himicseszkoj tehnologii
Akademia Nauk U.S.S.R., Moscow, **2** (1968.) No. 3. p. 346—364. [Co-author: HASKÓ L.]

Un effet thermique des fours-tunnel
Acta Technica Academiae Scientiarum Hungaricae, **61** (1968.) fasc. 1—2. p. 137—154.

Az alagútkemencék egy hőtechnikai effektusáról
Építőanyag, **20** (1968.) p. 245—252.

On a heat engineering effect of continuous kilns
Proceedings of the 9. Conference on the Silicate Industry, Budapest., Akadémiai K., 1968. p. 77—93.

Feuerfeste Stoffe in der keramischen Chromatografie
Silikattechnik, **19** (1968.) No. 10. p. 312—313 [Co-author: MOLDVAI Á.]

Wartha Vince
Építőanyag, **20** (1968.) No. 11. p. 409—411.

A Műszaki Kémiai Kutató Intézet perspektívája.
Évi kutatások. MTA Műszaki Kémiai Kutató Intézet. Veszprém—Budapest., 1968. p. 1—5.

A technológia törvényeiről
Évi kutatások. MTA Műszaki Kémiai Kutató Intézet. Veszprém—Budapest., 1968. p. 6—14.

Kémiai technológia. Revised ed. Tankönyvkiadó, Budapest., 1968. 198 pages. [Co-author: BUCSY I.]

A kerámia esztétikája
Valóság, **12** (1969.) No. 1. p. 56—61.

1968. évi tudományos munkásságom összefoglalása
Évi kutatások. MTA Műszaki Kémiai Kutató Intézet. Veszprém—Budapest., 1969. p. 19—21.

Az alagútkemencék egy hőtechnikai effektusáról.
Évi kutatások. MTA Műszaki Kémiai Kutató Intézet. Veszprém—Budapest., 1969. p. 22—30. [Co-author: FÜLÖP J.]

Mire emlékeztet a Tanácsköztársaság?
Felsőoktatási Szemle, **18** (1969.) No. 3. p. 129—136.

[Rev.] RÉNYI Alfréd: Dialógusok a matematikáról. Akadémiai K., Budapest., 1966. 156 pages and Levelek a valószínűségről. Akadémiai K. Bp., 1967. 103 lap.
Magyar Tudomány, **14** (1969.) No. 5. p. 324—327.

[Rev.] Gerecs Árpád: Einführung in die chemische Technologie. Tankönyvkiadó Budapest., 1968. 583 pages.
Periodica Polytechnica. Chemical Engineering. **13** (1969.) No. 3. p. 281—282.

A műszaki kémia általános terminológiája.
Évi kutatások. MTA Műszaki Kémiai Kutató Intézet. Veszprém—Budapest., 1970. p. 5—29. [Co-author: POLINSZKY K.]

Programozott oktatás vagy öntevékeny, de irányított tanulás?
Természet Világa, **14** (1970.) No. 3. p. 131—132.

A magyar szilikátipar fejlődése a felszabadulás óta.
Műszaki Élet, **25** (1970.) No. 7. p. 4.

Nuovi sviluppi nella cottura ceramica ed il ruolo di Faenza in tale camp
Ceramica Informazione, 1970. No. 5. p. 179—186.

Atti del 1° convegno sulle moderne techn. cer. Faenza, May. 28—29. 1970. Necrology.

HEVESI Gyula. [Necrology.]
Magyar Tudomány, **15** (1970.) No. 7—8. p. 570—575.

Progressi nella cottura ceramica
Ceramica Informazione, 1970. No. 7.

Man's biological ballance imperilled
Ossolineum — Special issue of "Zagadnienia Naukoznawstwa". Polish Acad. o Sci. Press, Warsaw, 1970. p. 133—141.

A kerámiai égetés újabb fejlődése
Építőanyag, **22** (1970.) No. 11. p. 401—408.

La cuisson rapide: problèmes et avenir
L'Industrie Céramique, 1970. No. 634. p. 827—828.

Bevezető. VAJTA László—SZEBÉNYI Imre: Kémiai technológia (gépészmérnökhallgatók számára.) Tankönyvkiadó, Budapest., 1970. p. 7—12.

Kerámiai kromatográfia
Kromatográfiás Vándorgyűlés Előadásai. 1. Eger, Oct. 4—7. 1971. Magyar Kémikusok Egyesülete és a Magyar Tudományos Akadémia Kromatográfiai Munkabizottsága. Budapest., 1971. p. 41—44. [Co-author: SPAAPAI J.]

Veszélyben az ember biológiai egyensúlya
Tudománytani Szemelvények, **1** (1971.) p. 27—37.

A Magyar Tudományok Tudománya Csoport történetéhez
Tudománytani Szemelvények, **1** (1971.) p. 39—41.

Ötven év után. Művészet és közérthetőség. Editor: SZERDAHELYI I. Akadémiai K., Budapest., 1972. 125. p.

Development of petroleum refining technologies in graph theoretical representation. 1. Distillation.
Acta Chimica (Budapest), **72** (1972.) fasc. 1. p. 77—91. [Co-author: HASKÓ L.]

Egy dinamikus rendszerekre vonatkozó ismeretelméleti feltevés
Magyar Tudomány, **17** (1972.) No. 3. p. 142—154.

John Desmond BERNAL emlékezete
Tudománytani Szemelvények, **3** (1972.) p. 5—6.

A Tudományok Tudománya Kör mint a Galilei Kör utóda
Tudománytani Szemelvények, (1973.) p. 1—11.

Preface. PACZOLAY Gyula: Tudományok és rendszerek. Tudományterületek közös törvényszerűségei. Akadémiai K., Bp., 1973. p. 9—11.

WARTHA Vince. (A múlt magyar tudósai.) Akadémiai K., Budapest., 1974. 227 pages, [Co-author: MÓRA L.]

Adatok a kerámia lemezek kromatográfiás célra történő alkalmazásához.
Kromatográfiás Vándorgyűlés Előadásai. 4. Győr, 28. Oct.—1. Nov., 1974. Magyar Kémikusok Egyesülete és a Magyar Tudományos Akadémia Kromatográfiai Munkabizottsága. Budapest., 1974. p. 23—30. [Co-authors: SZABÓ P., SALLAI J., SZOTYORY L.]

Kémiai technológiai feladatok. 4. Revised ed. Budapest., Tankönyvkiadó, 1974. 141 pages. [Co-authors: ACKERMANN L., SZEBÉNYI I., VAJTA L.]

Kémiai technológiai rendszerek gráfelméleti vizsgálata. Budapest., Akadémiai K., 1975. 135 pages. [Co-author: HASKÓ L.]

Development of petroleum refining technologies in graph theoretical representation. 2. Manufacture of Otto engine fuel.
Acta Chimica (Budapest), **88** (1976.) fasc. 1. p. 97—113. [Co-author: HASKÓ L.]

Modern algebrai és topológiai módszerek alkalmazása műszaki kémiai rendszerek szerkezetvizsgálatára. [In English] Budapest., Akadémiai K. In preparation. [Co-authors: BLICKLE T., SEITZ K.]

Acta Chimica Academiae Scientiarum Hungaricae, Tomus 89 (3), pp. 203—208 (1976)

CONTRIBUTIONS TO THE KINETICS OF THE REACTION OF DICHLOROGALLANE AND ETHYL IODIDE, I

A. MESZTICZKY, D. KNAUSZ, B. CSÁKVÁRI and J. EMMER

(Department of General and Inorganic Chemistry, L. Eötvös University, Budapest)

Received April 6, 1975

The reduction reaction of ethyl iodide with dichlorogallane has been investigated, using one of the reactants (ethyl iodide) as a solvent. The progress of the reaction has been followed by measuring the volume of ethane formed during the reaction. The activation energy of the reaction is -6.5 ± 1 kcal, the enthalpy of activation -6.8 ± 1 kcal and the entropy of activation -101 ± 4 cal/K. Conclusions concerning the presumed mechanism of the reaction have been drawn according to these data.

We have established in our preliminary communication [1] that ethyl halides are reduced by dichlorogallane to ethane. The objective of the present work has been the kinetic investigation of the reaction between dichlorogallane and ethyl iodide.

The reaction $GaHCl_2 + C_2H_5I = GaCl_2I + C_2H_6$ can be studied in a relatively simple way by measuring the volume of the ethane evolved. The reaction is carried out expediently in a liquid phase. Quite a number of experiments were made in order to find an adequate solvent for this reaction. The difficulty of the problem was that dichlorogallane is only poorly soluble in apolar solvents, and thus its concentration can be varied in solvent of this type only in a very narrow range. It is, however, known from literature [2] that dichlorogallane forms stable complexes with polar solvents (alcohols, ethers, amines etc.) whereas an undesired side-reaction occurs with higher hydrocarbons, particularly with aromatic hydrocarbons. Therefore, instead of using a separate solvent, ethyl iodide — one of the reactants — was used as a solvent. This necessarily implied that in the initial stage of the reaction the dissolution run parallel to the reduction reaction. However, the results were not affected markedly by this fact since the dissolution was completed within 1—2 seconds.

Experimental

The preparation and purification of dichlorogallane and the analysis of the products have been described in our preliminary communication [1]. On starting from gallium (of 99.99% purity), it was converted with elementary chlorine into gallium trichloride and the product purified by sublimation. A partial reduction was carried out with trimethyl silane, and trimethyl chlorosilane was removed from the formed dichlorogallane by vacuum distillation. Since both gallium trihalides and dichlorogallane are highly sensitive to atmospheric oxygen

and to air humidity, the procedures of preparation and purification, and the reaction were carried out in an atmosphere of high purity (99.99% by volume) nitrogen. The reaction was carried out in the apparatus shown in Fig. 1.

The temperature of the dichlorogallane crystals prepared previously in reaction flask "A" kept in a nitrogen atmosphere and of ethyl iodide liberated from iodine and placed in dropping funnel "B" was adjusted to the desired temperature with the use of thermostat "D" packed with dry ice. The reaction was started by the addition of ethyl iodide to dichlorogallane. The reaction mixture was shaken continuously. The volume of the ethane evolved was measured in gas burette "E" attached to the reaction flask. During the measurement, the pressure of the gas was continuously made equal to the atmospheric pressure with the use of levelling flask "F". The time of addition of ethyl iodide was chosen as the starting time of the reaction.

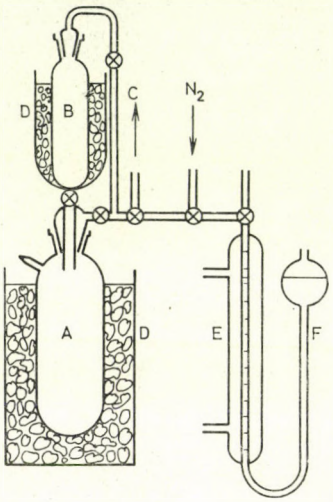

Fig. 1. Diagram of the apparatus used for the preparation of $GaHCl_2$ and for carrying out the reaction. A: reaction flask, B: dropping funnel, C: attachment to the vacuum pump, D: condenser packed with dry ice, E: gas burette, F: suction flask

Our measurements were carried out in the temperature range between —25 °C and —40 °C at various concentrations of dichlorogallane (from 0.1 to 1.0 *M*). Under such conditions the reaction proceeds with well measurable rates.

Evaluation of the results of measurements

Since during the measurement the reaction was followed by varying the quantity of a single component, the determination of the order of the reaction required particular care. Therefore, the order of the reaction was calculated from the data of experiments carried out at the same temperature at various concentrations of dichlorogallane. This resulted in an average value of 2.1 ± 0.2. Subsequently, it was examined whether the same order is obtained in experiments where the temperature is varied. In fact, the order of reaction was found to be 2.0 ± 0.2 on the basis of experiments carried out at various temperatures as nearly identical concentrations of dichlorogallane. The reac-

tion is second order in respect of dichlorogallane and the reaction is pseudo zero order in respect of ethyl iodide, the latter being in an about 20-fold excess.

Since the reaction is of second order in respect of dichlorogallane and that the volume of the ethane evolved has been measured, the following rate equation can be described.

$$\frac{\partial V}{\partial t} = k' (V_\infty - V)^2 \tag{1}$$

where V_∞ is the volume of ethane at the completion of the reaction,
V the volume of ethane evolved during time t,
$k' = k \cdot V_M^{m-1}$
k rate constant expressed in units of concentration,
V_M mole volume at the temperature at which the gas volume has been measured,
t time needed for the evolution of volume V of ethane.

On integration of equation (1) we obtain

$$V = \frac{V_\infty^2 \cdot k' \cdot t}{1 + V_\infty \cdot k' \cdot t} \tag{2}$$

The algebraic transformation of equation (2) affords

$$\frac{1}{V} = \frac{1}{V_\infty} + \frac{1}{V_\infty^2 \cdot k'} \cdot \frac{1}{t} \tag{3}$$

On plotting the values of $\frac{1}{V}$ against $\frac{1}{t}$ on the basis of Eq. (3), V_∞ and k' can be determined (see Fig. 2).

In several cases V_∞ was determined also experimentally, by measuring the volume of the ethane evolved after long reaction periods (of several hours). V_∞ measured experimentally and that calculated on the basis of Eq. (3), showed a rather good agreement:

$$\frac{V_\infty \text{ (extrapolated)}}{V_\infty \text{ (experimental)}} \approx 1.05$$

The value of V_∞ can be determined also from the initial weight of gallium. However, these values are not reliable because the losses occurring during the purification of gallium trichloride and the preparation of dichlorogallane cannot be taken into account.

The k' values calculated on the basis of Eq. (3) are presented in Table I.

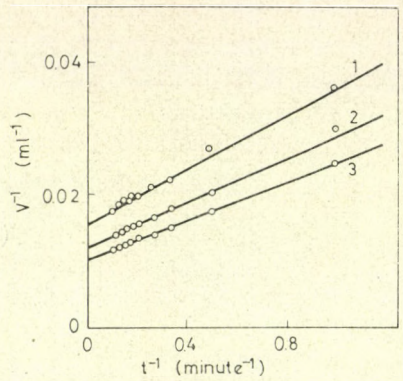

Fig. 2. Determination of V_∞ and k'. T=248 °K.
Number of curve 1 2 3
Concentration of:
$GaHCl_2$, M 0.5025 0.7708 0.9283

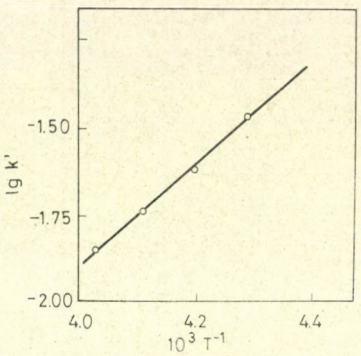

Fig. 3. Determination of the activation energy of the reaction by means of the temperature dependence of the rate constant
$E^{\neq} = -6.5 \pm 1$ kcal/mole

Table I

Temperature, °C	Concentration of $GaHCl_2$ M	k'	k'_{mean}
	0.5025	0.01642	
−25	0.7708	0.01436	0.0146
	0.9282	0.01310	
	0.1984	0.0188	
−30	0.2115	0.0168	0.0182
	0.2190	0.0189	
	0.1942	0.0275	
−35	0.2920	0.0222	0.0239
	0.5183	0.0220	
	0.1257	0.0365	
−40	0.2125	0.0294	0.0336
	0.2177	0.0245	

The activation energy of the reaction can be calculated from the temperature depencence of the rate constant (Fig. 3).

By using the relationship

$$\lg \frac{k}{T} \frac{H\,\Delta^{\neq}}{2.303 \times RT} + \frac{\Delta S^{\neq}}{2.303 \times R} + \lg \frac{k^*}{h}$$

— where $\Delta H^{\neq}$ is the enthalpy of activation, $\Delta S^{\neq}$ the entropy of activation, R the universal gas constant, k^* the Boltzmann constant, h the Planck constant, k the rate constant and T the absolute temperature, — the enthalpy of activation and the entropy of activation of the reaction were calculated, plotting the relationship $\lg \frac{k'}{T}$ *vs* $\frac{1}{T}$. (Fig. 4)

The negative activation energy and the highly negative entropy of activation allow the conclusion that probably a complex formation preequilibrium is involved in the path of the reaction.

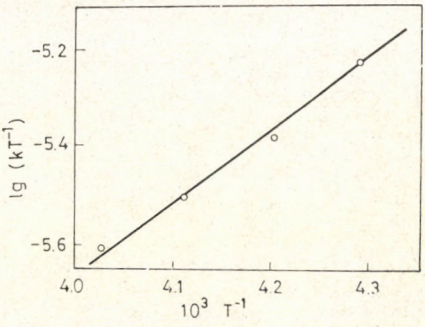

Fig. 4. Determination of the enthalpy of activation and of the entropy of activation
$\Delta H^{\neq} = -6.8 \pm 1$ kcal $\Delta S^{\neq} = -101 \pm 4$ cal/°K

Mechanism of the reaction

Since the reaction is second order in respect of dichlorogallane and that the activation energy and the entropy of activation of the reaction are negative the following mechanisms can be presumed:

1.

$$(GaHCl_2)_2 \underset{k_2}{\overset{k_1}{\rightleftharpoons}} 2\,GaHCl_2 \qquad \text{I}$$

$$(GaHCl_2)_2 + 2\,C_2H_5I \underset{k_4}{\overset{k_3}{\rightleftharpoons}} (GaCl_2H)_2 \cdot 2\,C_2H_5I \qquad \text{II}$$

$$(GaHCl_2)_2 \cdot 2\,C_2H_5I \xrightarrow{k} (GaHCl_2)_2 + 2\,C_2H_6 \qquad \text{III}$$

On assuming that all the equilibria are rapid and they are shifted in the direction of dimer formation and complex formation *i.e.* $k \ll k_3$, k_4 $k_2 \ll k_1$ and $k_3 \gg k_4$, the following equation can be derived for the rate of evolution of ethane, with the use of the method of quasi-steady states:

$$\frac{\partial[C_2H_6]}{\partial t} = k \cdot \frac{k_3}{k_4} \cdot \frac{k_2}{k_1} [C_2H_5I]^2 [GaHCl_2]^2$$

2. $$(GaHCl_2)_2 \underset{k_2'}{\overset{k_1'}{\rightleftharpoons}} 2\,GaHCl_2 \qquad IV$$

$$GaHCl_2 + C_2H_5I \underset{k_4'}{\overset{k_3'}{\rightleftharpoons}} GaHCl_2 \cdot C_2H_5I \qquad V$$

$$GaHCl_2 \cdot C_2H_5I + GaHCl_2 \xrightarrow{k'} GaHCl_2 + GaCl_2I + C_2H_6 \qquad VI$$

Conditions: $k_1' \gg k_2'$ $k_3' \gg k_4'$ and $k' \ll k_3'$, k_4', consequently, $[(GaHCl_2)_2] \approx 0$.

Using the method of quasi-steady states, the following equation is obtained for the rate of evolution of ethane

$$\frac{\partial[C_2H_6]}{\partial t} = k' \frac{k_3'}{k_4'} [C_2H_5I] [GaHCl_2]^2.$$

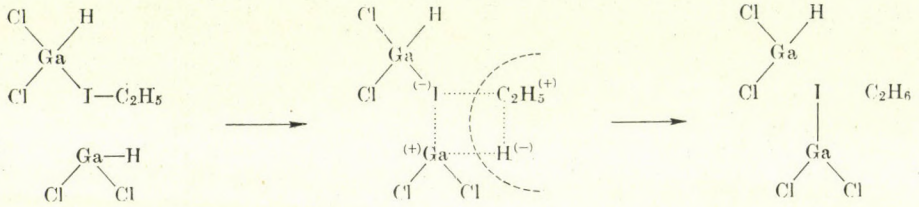

Fig. 5. The charge transfer complex presumably formed during the reaction

Both relationships derived from the two types of conditions represent rate equations that are second order in respect of dichlorogallane, quite in accordance with the fact that the values obtained for the activation energy and for the entropy of activation were negative. However, the mechanism described in point 1 is in contrast to the data of literature [2, 3, 4] according to which the dimers $(GaCl_3)_2$ and $(GaHCl_2)_2$ are split to monomers on complex formation. The reaction described by equation VI may be interpreted by the formation of a charge transfer complex (see Fig. 5).

REFERENCES

[1] Csákvári, B., Jenei, S., Knausz, D., Meszticzky, A.: Acta Chim. Acad. Sci. Hung. **59**, 225 (1969)
[2] Greenwood, N. N.: The Chemistry of Gallium. Advances in Inorganic Chemistry and Radiochemistry. Vol. 5
[3] Ali, S. M., Brever, F. M., Chadwick, J., Garton, G.: J. Inorg. and Nuclear Chem. **9**, 124 (1959)
[4] Greenwood, N. N., Worral, I. J.: J. Inorg. and Nuclear Chem. **3**, 357 (1957)

Aranka Meszticzky
Dezső Knausz
Béla Csákvári
János Emmer

H-1088 Budapest, Múzeum körút 6—8.

Acta Chimica Academiae Scientiarum Hungaricae, Tomus 89 (3), pp. 209—214 (1976)

ANTIMONY(III) COMPLEXES OF SCHIFF BASES DERIVED FROM BENZALDEHYDE AND AMINOALCOHOLS

O. P. SINGH* and J. P. TANDON

(Chemical Laboratories, R. B. S. College, Agra and University of Rajasthan, Jaipur–302 004, India)

Received April 17, 1975

In revised form September 20, 1975

The synthesis of antimony(III) Schiff base complexes of various co-ordination numbers is reported. The syntheses have been performed by interacting antimony(III) isopropoxide with monofunctional bidentate Schiff bases, having the general formula $C_6H_5CH{=}NROH$ (where R is $-(CH_2)_2-$, $-CH_2-\underset{\displaystyle CH_3}{\underset{|}{CH}}-$ and $-(CH_2)_3-$), in different stoichiometries. The reactions at mole ratios of 1:1, 1:2 and 1:3 yield $Sb(OPr^i)_2(SB)$, $Sb(OPr^i)(SB)_2$ and $Sb(SB)_3$ type derivatives, respectively (where SBH is the monofunctional bidentate Schiff base). In the resulting derivatives, the central metal atom appears to be in tetra-, penta- and hexacoordinate environment, respectively as indicated by the monomeric nature of the compounds in boiling benzene. The infrared spectra of these derivatives have been recorded and tentative assignments are made.

Introduction

During the last decade, alkoxides of Sb(III) and Sb(V) as well as their derivatives with a variety of ligands have been described [1—4]. Recently, the reactions of antimony(III) ethoxide with glycols [5] and oximes [6] have been described. In the present work antimony(III) Schiff base complexes of the types $Sb(OPr^i)_2SB$, $Sb(OPr^i)(SB)_2$ and $Sb(SB)_3$ have been synthesized by the reaction of antimony(III) isopropoxide with monofunctional bidentate Schiff bases (**I**) obtained by the condensation of benzaldehyde with aminoalcohols such as 2-aminoethanol-1, 1-aminopropanol-2 and 3-aminopropanol-1 in 1 : 1, 1 : 2 and 1 : 3 mole ratios.

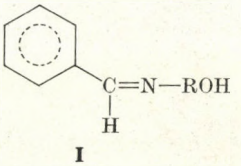

I

where R = $-(CH_2)-_2$, $-CH_2-\underset{\displaystyle CH_3}{\underset{|}{CH}}-$ and $-(CH_2)_3-$

* Chemistry Department, R. B. S. College, Agra, India.

Experimental

Materials and methods

The reactions were carried out under strictly anhydrous conditions. Isopropanol (BDH) was dried over sodium wire and then fractionated over aluminium isopropoxide. Benzene (BDH) was dried in the same manner, followed by azeotropic fractionation in the presence of ethanol. Antimon isopropoxide was prepared by the sodium chloride method [7] and was distilled (105 °C/14 mm).

$Sb(OPr^i)_3$ Calcd. Sb 40.75% Found Sb 40.39%.

Preparation of Schiff bases

Schiff bases of benzaldehyde were prepared by taking equimolar amounts of amino-alcohol and benzaldehyde in benzene and refluxing for several hours, followed by the removal of water–benzene azeotrope. These Schiff bases were distilled before use; their analyses and physical characteristics are listed in Table I.

Table I

Physical properties and analyses of the Schiff bases

No.	Schiff base	State and m.p. (°C)	b.p. (°C)/pressure	Analysis (%)		
				C Found (Calcd.)	H Found (Calcd.)	N Found (Calcd.)
1	Benzylidene-2--hydroxyethyl-amine ($C_9H_{11}NO$)	Orange	98—100/0.1—0.2	72.36 (72.46)	7.35 (7.43)	9.25 (9.38)
2	Benzylidene-2--hydroxy-1--propylamine ($C_{10}H_{13}NO$)	Colourless solid 64—66	95—97/0.3—0.4	73.41 (73.58)	8.12 (8.03)	8.45 (8.59)
3	Benzylidene-3--hydroxy-1--propylamine ($C_{10}H_{13}NO$)*	Yellow liquid	103—104/0.3—0.4	73.39 (73.58)	8.15 (8.03)	8.51 (8.59)

* Used to distinguish between compounds of the same molecular formula.

Preparation of complexes

Reactions of antimony(III) isopropoxide with the Schiff bases in mole ratios 1:1, 1:2 and 1:3 were carried out. Antimony(III) isopropoxide was dissolved in benzene and then a calculated amount of the Schiff base was added. The mixture was then refluxed and the progress of the reaction followed by estimating the isopropanol fractionated azeotropically. The resulting derivatives in the form of liquids and semi-solids were isolated after removing the volatile fractions under reduced pressure; they are soluble in common organic solvents. Their analyses, physical properties and molecular weights are given in Table II.

Table II

Synthese and characteristics of antimony(III) Schiff base complexes

No.	Antimony isopropoxide (g)	Schiff base (g)	Mole ratio	Conditions and time (hr)	Compound, yield (g) nature	Isopropanol in azeotrope (g) Found (Calcd.)	Analysis (%) Sb Found (Calcd.)	Analysis (%) N Found (Calcd.)	Molecular weight Found (Calcd.)
1	1.92	$C_9H_{11}NO$ 0.96	1 : 1	Refluxing 1	$Sb(OPr^i)_2(C_9H_{10}NO)$ (2.44), yellow liquid	0.37 (0.38)	31.46 (31.39)	3.46 (3.61)	394 (387)
2	1.44	$C_9H_{11}NO$ 1.44	1 : 2	Refluxing 3	$Sb(OPr^i)(C_9H_{10}NO)_2$ (2.31), yellow semisolid	0.59 (0.58)	25.68 (25.54)	5.71 (5.87)	386 (476)
3	0.77	$C_9H_{11}NO$ 1.17	1 : 3	Refluxing 4	$Sb(C_9H_{10}NO)_3$ (1.48), yellow semisolid	0.45 (0.47)	21.10 (21.53)	7.26 (7.42)	528 (565)
4	1.44	$C_{10}H_{13}NO$ 0.79	1 : 1	Refluxing 5	$Sb(OPr^i)_2(C_{10}H_{12}NO)$ (1.85), yellow liquid	0.30 (0.29)	30.01 (30.31)	3.30 (3.48)	425 (401)
5	1.40	$C_{10}H_{13}NO$ 1.54	1 : 2	Refluxing 6	$Sb(OPr^i)(C_{10}H_{12}NO)_2$ (2.29), yellow semisolid	0.60 (0.56)	23.91 (24.13)	5.48 (5.55)	490 (504)
6	0.75	$C_{10}H_{13}NO$ 1.23	1 : 3	Refluxing 5	$Sb(C_{10}H_{12}NO)_3$ (1.53), yellow semisolid	0.43 (0.45)	19.65 (20.04)	6.68 (6.91)	592 (607)
7	1.66	$C_{10}H_{13}NO$* 0.91	1 : 1	Refluxing 3	$Sb(OPr^i)_2(C_{10}H_{12}NO)$* (2.20), yellow liquid	0.32 (0.33)	29.72 (30.31)	3.36 (3.48)	435 (401)
8	1.48	$C_{10}H_{13}NO$* 1.61	1 : 2	Refluxing $6\frac{1}{2}$	$Sb(OPr^i)(C_{10}H_{12}NO)_2^*$ (2.38), yellow semisolid	0.66 (0.59)	23.90 (24.13)	5.40 (5.55)	483 (504)
9	1.46	$C_{10}H_{13}NO$* 2.40	1 : 3	Refluxing $3\frac{1}{2}$	$Sb(C_{10}H_{12}NO)_3^*$ (2.98), yellow semisolid	0.85 (0.88)	19.86 (20.04)	6.73 (6.91)	583 (607)

Analyses and physical measurements

Antimony was estimated as antimonous pyrogallate [8], while nitrogen by Kjeldahl's method. Isopropanol was determined by the oxidimetric method [9] using $NK_2Cr_2O_7$ in 12.5% H_2SO_4.

Molecular weights were determined ebullioscopically in boiling benzene. I. R. spectra were recorded in the range of 4000—400 cm^{-1} with a Perkin Elmer 337 Grating Infrared Spectrophotometer.

Results and discussion

The reactions in mole ratios of 1 : 1, 1 : 2 and 1 : 3 (Sb(III): Schiff base) liberate 1, 2 and 3 mol of isopropanol, respectively, as shown by the equation

$$Sb(OPr^i)_3 + nSBH \rightarrow Sb\ (OPr^i)_{3-n}\ (SB)_n + nPr^iOH$$

(where $n = 1$, 2 or 3)

The isopropanol was collected azeotropically with benzene and then estimated. The resulting complexes were isolated in the form of yellow derivatives and found to be soluble in benzene.

The ebullioscopic determination of molecular weights has shown that the complexes are monomeric (Table II), indicating tetra-, penta- and hexaco-ordinate [10—12] environments for the central metal atom (**II**, **III**, **IV**).

On comparing the I. R. absorption bands of the Schiff bases with those of their metal complexes, it can be inferred that chelate formation probably takes place through the oxygen (alcoholic) and the nitrogen of the ν C = N group of the ligand moiety. This is evidenced by the disappearance of the OH bands in the 3350—3100 cm^{-1} region and by the appearance of bands in the 605 $\pm$ 5 cm^{-1} region for the metal complexes. However, the ν C = N absorption band remains almost unaffected and appears in the region 1635 $\pm$ 5 cm^{-1} in the ligands as well as in the metal complexes, probably owing to the stronger force existing in the ν C = N group. Similar observations has been made by other workers [13—17] as well as SHARMA and BAILAR [18].

Recently, BIRADAR and KULKARNI have also reported that the ν C = N frequency undergoes very little change in tin(IV) [19] and lead (IV) [20] complexes. Owing to the lack of facilities for recording the spectra in the lower region, the Sn ← N band could not be observed in these complexes.

*

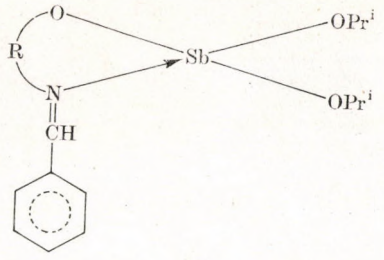

II

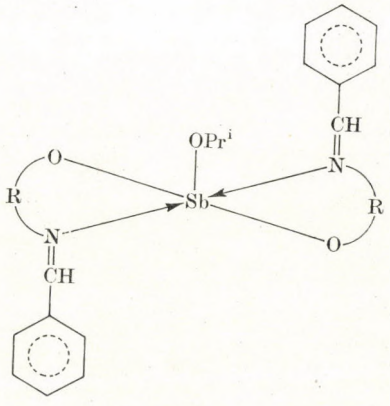

III

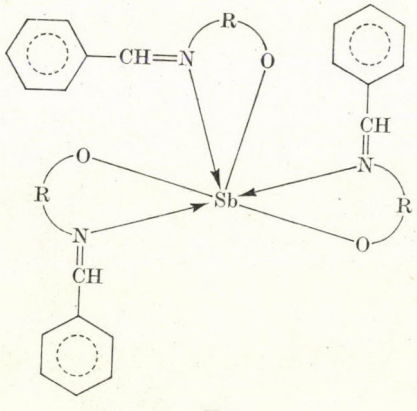

IV

*

The authors express their sincere thanks to Professor R. C. MEHROTRA and K. C. JOSHI of the Chemistry Department, University of Rajasthan, Jaipur, for providing research facilities. Thanks are also due to Dr. D. R. SINGH, Head of the Chemistry Department, R. B. S. College, Agra for his keen interest and constant encouragement.

REFERENCES

[1] MARKS, B. S., SCHOEPFLE, B. O., U. S. 1961; Chem. Abs., **56**, 323i (1962)
[2] LEWIS, F. B.: Brit. 717, 982 (1965); Chem. Abs., **62**, 11453a (1965)
[3] WETZLER, I.: French 046, 1370 (1964); Chem. Abs. **62**, 1811f (1965)
[4] LEEBRICK, J. R., REMES, N. L.: U. S., 158, 3, 530 (1971); Chem. Abs., **75**, 6106f (1971)
[5] MEHROTRA, R. C., BHATNAGAR, D. D.: J. Indian Chem. Soc., **42**, 327 (1965)
[6] MEHROTRA, R. C., RAI, A. K., BOHRA, R.: J. Indian Chem. Soc., **51**, 304 (1974)
[7] DUBROVINA, O. D., Uchenye Zapiski Kazan, Gosudarst. Univ. im. V. I. Ulyanova-Lenina, **116**, 3 (1956); Chem. Abs., **51**, 6534i (1957)
[8] FEIGL, F.: Z. angew. Chem.; **39**, 393 (1926)
[9] BRADLEY, D. C., HALIM, F. M. A., WARDLAW, W.: J. Chem. Soc. (**1950**), 3450
[10] SINGH, S. S.; Z. anorg. Chem. **384**, 81 (1971)
[11] MILICEB, S., HAZDI, D.: Inorg. Nucl. Chem. Lett. **7**, 745 (1971)
[12] KAWASAKI, Y., OKAWARA, R.: Bull. Chem. Soc. Japan, **40**, 428 (1967)
[13] DURHAM, D. A., HART, F. A.: J. Inorg. Nucl. Chem., **31**, 145 (1969)
[14] GUPTA, S. R., TANDON, J. P.: Z. Naturforsch, **25b**, 1090 (1970)
[15] MEHROTRA, R. C., DAYAL, J.: Indian J. Chem., **10**, 435 (1972)
[16] PRASAD, R. N., TANDON, J. P.: Z. Naturforsch, **28b**, 153 (1973)
[17] VIJAY, R. G., TANDON, J. P.: J. Inorg. Nucl. Chem., 1975 (In press)
[18] SHARMA, B. D., BAILAR, Jr., J. C.: J. Amer. Chem. Soc., **77**, 5476 (1955)
[19] BIRADAR, N. S., KULKARNI, V. H.: J. Inorg. Nucl. Chem., **33**, 3781 (1971)
[20] BIRADAR, N. S., KULKARNI, V. H.: Z. anorg. Chem., **381**, 312 (1971)

O. P. SINGH Chemical Laboratories, R. B. S. College, Agra
J. P. TANDON University of Rajasthan, Jaipur-302 004, India.

Acta Chimica Academiae Scientiarum Hungaricae, Tomus 89 (3), pp. 215—220 (1976)

INFLUENCE OF SINUSOIDAL A.C. ON THE BEHAVIOUR OF CADMIUM PLATING BATHS

S. S. Abd El Rehim and M. G. Helmy

(Chemistry Department, Faculty of Science, Ain Shams University, Cairo, Egypt)

Received June 20, 1975

Two plating baths, an acidic bath containing cadmium sulfate and sulfuric acid, and an alkaline bath containing cadmium sulfate, ammonium hydroxide and ammonium chloride were investigated. The influence of sinusoidal a.c. superimposed on d.c. on the anodic and cathodic polarization were traced in these baths. Results show that the effect of a.c. depends on the nature of the bath. In the acidic bath, a.c. shifts the anode potential of cadmium in the negative direction and increases the cathodic polarization, while in the alkaline bath, the shift occurs in the positive direction, which favours passivation of the electrode and depolarizes the cathode.

In addition, the effect of superimposed a.c. on the distribution of direct current and the distribution of metal on two parallel cathodes were investigated. In both plating baths examined, a.c. increases both the current and metal distribution ratios and, therefore has an unfavourable effect on the throwing power.

In previous reports [1—8] the effect on electrode potentials of a sinusoidal a.c. superimposed on d.c. was studied. The a.c. depending on its density and frequency — affects the rate of electrode processes taking place at a given potential. The observed effect of a.c. was ascribed to the asymmetric polarizabilities of the electrodes. Thus, the electrode potential changes with time and a distorted sinusoidal signal appears. Therefore, it might be expected that the a.c. would influence the distribution of d.c. between two parallel planar cathodes. This would result in changes in the metal distribution ratio and hence the throwing power of the bath.

In continuation of our previous work on the influence of superimposed a.c. on the behaviour of plating baths, we now report the results on some plating baths of cadmium.

For measuring the anodic and cathodic polarization, the circuit described earlier [9] was used, in which a cadmium anode (BDH) and a steel cathode were used. The area of each electrode was 7.5 cm^2. At the required d.c. and a.c. (50 Hz) densities ($I_{=}$ and $I_{\sim}$), the time average of the periodically changing potential of the working electrode was measured relative to a saturated calomel electrode using a potentiometer (Radelkis O. P. 201/1).

For measuring the current distribution ratio (CDR) and the metal distribution ratio (MDR), the electrode circuit described [10] was used, in which three parallel sheet electrodes, a cadmium anode and two steel cathodes, were used. The area of each electrode was 7.5 cm^2 and they had five identical

circular holes, each of which was 0.5 cm in diameter. The electrodes were arranged and fixed in a rectangular plating cell in such a manner that the distance between the anode and the nearer cathode was 2.5 cm, while that between the anode and the farther cathode was 5 cm in the same direction. Each cathode was connected in series with a copper coulometer. The a.c. passed through the cell *via* two auxiliary platinum electrodes. The required total d.c. (I_t) and a.c. ($I_\sim$) densities were conducted through the cell for 75 min. From the weights of the metal W_n and W_f deposited on the nearer and farther cathode, respectively, the MDR could be determined. The coulometers were used for calculating the individual d.c.'s, (I_n) and (I_f), passing through the nearer and farther cathode, respectively, and hence the CDR (*i. e.*, I_n/I_f).

All solutions were made from AnalaR chemicals using distilled water. The baths used were as follows:

Acidic bath: $CdSO_4 \cdot 8/3\ H_2O$, 0.8; H_2SO_4 0.05 M;

Alkaline bath: $CdSO_4 \cdot 8/3H_2O$, 0.2; NH_4OH 3.3; NH_4Cl 0.1 *M*.

Prior to each run, the electrodes were polished and cleaned using the recommended procedure, In each run, a freshly prepared solution as well as a new set of electrodes were used. All experiments were carried out at 25 $\pm$ 0.5 °C in an air thermostat.

Figure 1 presents the effect of superimposed a.c. on the anode potential of cadmium in the acidic bath. The characteristics of these curves were found to depend on both the d.c. and a.c. densities. At a given d.c. density, the anode potential suddenly shifts to a more negative value and then levels off with increasing a.c. density. This value decreases with increasing d.c. density. On the other hand, Fig. 2 shows the anode potential of cadmium in the acidic bath when the a.c. was kept constant and the d.c. density was varied. It can be seen that, at sufficiently low d.c. densities, the potential shifts sharply in the negative direction and then reaches a potential minimum. Following this, the potential of the anode shifts slowly in the positive direction with increasing d.c. density. The higher the a.c. density used, the greater the potential minimum. The results can be ascribed to the asymmetric polarizability of the electrode. Therefore, the periodical change of the electrode potential caused by superimposed a.c. has the form of a distorted sine wave. On comparing the anodic polarization curve (curve *a* in Fig. 2) and the cathodic polarization curve (curve *a* in Fig. 3) under d.c. conditions, it is clear that the cathodic polarization is greater than the anodic polarization especially at sufficiently low d.c. densities. According to the non-linear characteristics of the electrodes, the cathodic polarization during the cathodic half-cycle is greater that the anodic polarization during the anodic half-cycle of a.c. Thus the mean average potential of the anode becomes more negative than its static potential. As the ratio of d.c. to a.c. density increases, the anodic polarization becomes the predominant factor after the potential minimum.

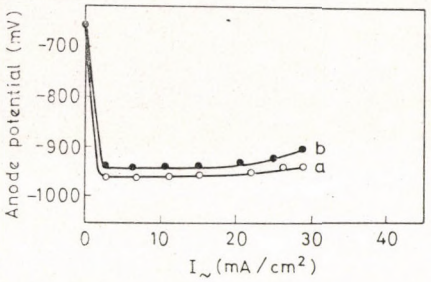

Fig. 1. Effect of a.c. on the anode potential of cadmium in the acidic bath: curve (a) $I_{=}$=20 mA/cm², (b) $I_{=}$=40 mA/cm²

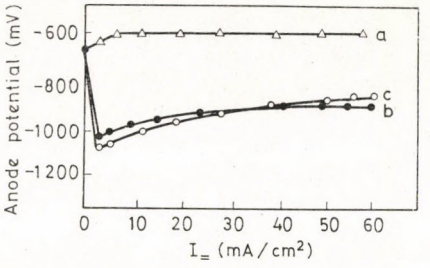

Fig. 2. Effect of a.c. on the anode potential of cadmium in the acidic bath: curve (a) $I_{\sim}$ = Ø, (b) $I_{\sim}$ = 10 mA/cm², (c) $I_{\sim}$ = = 20 mA/cm²

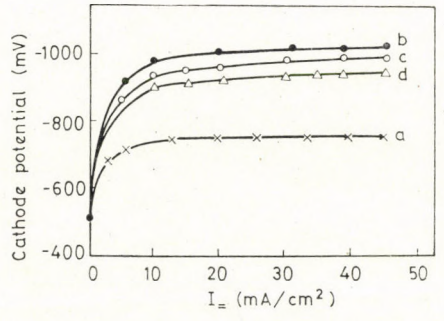

Fig. 3. Effect of a.c. on the cathode potential in the acidic bath: curve (a) $I_{\sim}$ = Ø, (b) $I_{\sim}$ = 10 mA/cm², (c) $I_{\sim}$ = 20 mA/cm², (d) $I_{\sim}$ = 40 mA/cm²

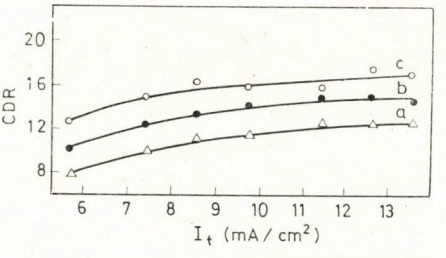

Fig. 4. Effect of a.c. on the CDR for the acidic bath: curve (a) $I_{\sim}$ = Ø, (b) $I_{\sim}$ = 50 mA/cm², (c) $I_{\sim}$ = 100 mA/cm²

Figure 3 illustrates the effect of superimposed a.c. on cathodic polarization during the deposition of cadmium from the acidic bath. As expected, a.c. shifts the cathodic polarization in the negative direction.

Figure 4 shows the variation of CDR as a function of total d.c. density I_t under the influence of a.c. in the acidic bath. The results reveal that the total d.c. is inequally distributed between the parallel cathodes with a greater portion of the current flowing through the nearer cathode. This disproportion slightly increased with increasing d.c. density. This can be explained by the fact that the cathodic polarizability of the electrode is greater at smaller d.c. densities than at higher d.c. densities. Therefore, with increasing total d.c. density, the increase in polarization of the nearer cathode becomes smaller than that of the farther cathode. Since the potentials arising at junction points should be equal to each other in every branch of the circuit according to Kirchhoff's law. Therefore, with inreasing total d.c. density, a greater portion of the current will flow through that branch of the circuit where this causes the

smaller increase in polarization. The Figure also shows that a.c. increases the CDR. The greater the a.c. density, the greater is the CDR at a given d.c. The effect of a.c. may be ascribed to its effect on the polarization of each cathode to an extent depending on its density.

Figure 5 shows that the variation of MDR as a function of I_t for the acidic bath runs parallel to that of CDR. The two ratios are interrelated by the following equation:

$$MDR = W_n/W_f = CDR \quad E_n/E_f$$

The total cathodic efficiency E_t and the individual cathodic efficiencies on each cathode, E_n and E_f are approximately the same over the whole d.c. and a.c. density range used (curve a in Fig. 10). Accordingly, the MDR is expected to be same as the CDR. It should be noted that the lower the MDR, the better is the throwing power. Figure 5 shows that superimposed a.c. has an unfavourable effect on the throwing power.

Figure 6 presents the anodic polarization curves of cadmium in the alkaline bath under the influence of different d.c. and a.c. densities. All the curves have the same general features and are characterized by the presence of a critical transition current density (I_c) (active–passive transition). In absence of a.c. the potential increases very slowly and at the I_c where passivation takes place, the potential rises steeply with increasing d.c. density. During the active region (before I_c) Cd^{2+} ions are released into the solution and finally a supersaturated solution of $Cd(OH)_2$ is formed in the vicinity of the anode surface. The subsequent adsorption and precipitation of $Cd(OH)_2$ on the anode surface results in a drop in the dissolution rate, passivation starts and the potential rises abruptly. Supersaturation is required to form nuclei in the initial stages of precipitation. As the potential rises, passivation is effected through the formation of CdO which starts to build up in the pores of the $Cd(OH)_2$ film [11—12]. Superimposed a.c. shifts the anode potential in the active region to the more positive direction. As the density of a.c. increases, anodic polarization increases. Also the Figure reveals that a.c. lowers the value of I_c and favours passivation of the cadmium electrode. The greater the a.c. density, the lower is the I_c value. The results may be due to the formation of a compact, uniform layer of $Cd(OH)_2$ under the influence of superimposed a.c., whereas with d.c. alone, the coverage is not uniform even through dissolution of the metal is greater than in the presence of a.c. [13].

Figure 7 gives the effect of superimposed a.c. on the course of cathodic polarization during the deposition of cadmium from the alkaline bath. Superimposed a.c. decreases the cathode potential. The depolarization increases with increasing a.c. density.

Figure 8 illustrates the effects of superimposed a.c. on the CDR as a function of I_t for the alkaline bath. The d.c. has no significant effect on the

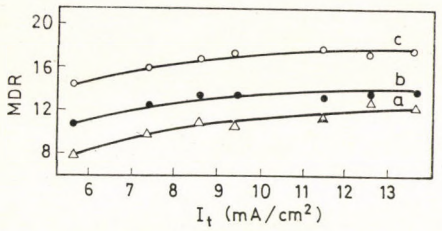

Fig. 5. Effect of a.c. on the MDR for the acidic bath: curves as in Fig. 4

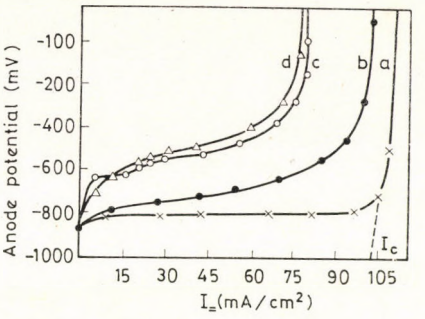

Fig. 6. Effect of a.c. on the anode potential of cadmium in the alkaline bath: curve (a) $I_\sim = Ø$, (b) $I_\sim = 5$ mA/cm², (c) $I_\sim = 10$ mA/cm², (d) $I_\sim = 20$ mA/cm²

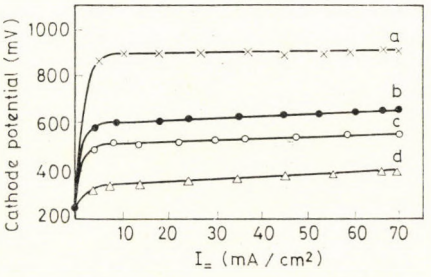

Fig. 7. Effect of a.c. on the cathode potential in the alkaline bath: curve (a) $I_\sim = Ø$, (b) $I_\sim = 10$ mA/cm², (c) $I_\sim = 15$ mA/cm², (d) $I_\sim = 20$ mA/cm²

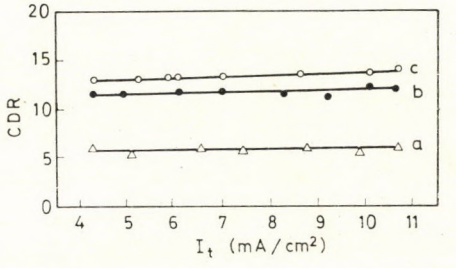

Fig. 8. Effect of a.c. on the CDR for the alkaline bath: curve (a) $I_\sim = Ø$, (b) $I_\sim = 50$ mA/cm², (c) $I_\sim = 100$ mA/cm²

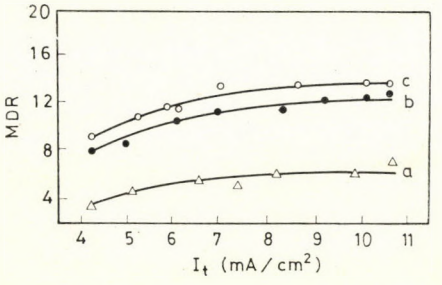

Fig. 9. Effect of a.c. on the MDR for the alkaline bath: curves as in Fig. 8

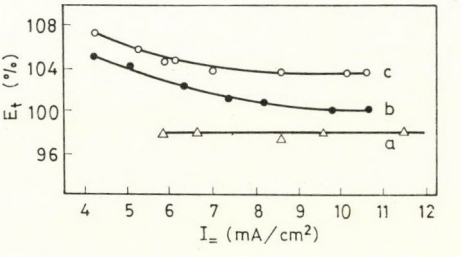

Fig. 10. E_t *vs.* I_t relation: curve (a) acidic bath, $I_\sim = Ø$, (b) alkaline bath, $I_\sim = Ø$, (c) alkaline bath, $I_\sim = 100$ mA/cm²

CDR, but a.c. increases this ratio in such a manner that as the a.c. density increases, the CDR curves shift upwards.

The data in Fig. 9 show that the MDR curves shift upwards with increasing both d.c. and a.c. densities. The lower value of the MDR at low d.c. den-

sities may be attributed to the dependence of the current efficiency on d.c. density in the alkaline solution. Curves *b* and *c* in Fig. 10 give the total cathodic efficiency E_t as a function of I_t. The efficiency decreases with d.c. density. At low d.c. densities, this decrease is large but becomes smaller with increasing d.c. density. At low d.c. densities, therefore, the MDR is lower, *i.e.* the throwing power is better than at higher d.c. densities. The favourable effect on throwing power of the decrease in current efficiency with d.c. density is reduced with increasing d.c. density. Superimposed a.c. increases the cathodic efficiency over the whole d.c. density range used. This is apparently due to the formation of a metal hydroxide during the anodic half cycle of a.c., which is subsequently incorporated in the deposit.

REFERENCES

[1] Erdey-Grúz, T. Dévay, J., Vajasdy, I., Horányi, Gy.: Acta Chim. Acad. Sci. Hung., **30**, 29 (1962)
[2] Erdey-Grúz, T., Dévay, J., Horányi, Gy. Vajasdy, I., Mészáros, L.: Acta Chim. Acad. Sci. Hung., **30**, 431 (1962)
[3] Erdey-Grúz, T., Dévay, J., Szegedi, R., Gáldi, A.: Acta Chim. Acad. Sci. Hung., **38**, 325 (1963)
[4] Dévay, J., Mészáros, L.: Acta Chim. Acad. Sci. Hung., **43**, 25 (1965)
[5] Dévay, J.: Acta Chim. Acad. Sci. Hung., **44**, 385 (1965)
[6] Dévay, J.: Veszprémi Vegyipari Egyetem Közleményei, **10**, 129 (1966)
[7] Dévay, J., Sayed Sabet Abd El Rehim; Takács, V.: Acta Chim. Acad. Sci. Hung., **52**, 201 (1967)
[8] Dévay, J., Sayed Sabet Abd El Rehim: Magyar Kém. Foly., **75**, 131 (1969)
[9] Sayed Sabet Abd El Rehim, Abd El Halim, A., M.: Acta Chim. (Budapest) **80**, 65 (1974)
[10] Sayed Sabet Abd El Rehim, Fawzy, M. H.: Acta Chim. (Budapest), **80**, 65 (1974)
[11] Lake, P. E., Casey, E. J.: J. Electrochem. Soc., **105**, 52 (1958)
[12] Abdul Azim, A. A., El Sobki, K. M.: Electrochim. Acta, **17**, 601 (1972)
[13] Rao, K. P., Rao, V. V., Udupa, H. V. K.: Electrochim. Acta, **12**, 575 (1967)

Sayed Sabet Abd El Rehim
M. G. Helmy

Chemistry Department,
Faculty of Science
Kuvait University, Kuvait

Acta Chimica Academiae Scientiarum Hungaricae, Tomus 89 (3), pp. 221—244 (1976)

MASS-SPECTROMETRIC DETERMINATION OF THERMOCHEMICAL DATA OF $CHBr_3$ and CBr_4 BY STUDY OF THEIR ELECTRON IMPACT AND HETEROGENEOUS PYROLYTIC DECOMPOSITIONS

O. KAPOSI, M. RIEDEL, K. VASS-BALTHAZÁR, G. R. SÁNCHEZ and L. LELIK

(Department of Physical Chemistry and Radiology, L. Eötvös University, Budapest)

Received July 22, 1975

With the aim of determining thermochemical data for bromo-substituted methanes, a study was made of the mechanisms of their pyrolytic decompositions as a result of electron impact and on a tungsten spiral.

A previously developed experimental method was used to determine the appearance and ionization potentials of the products formed in the decompositions of $CHBr_3$ and CBr_4. From the temperature dependence of the pyrolysis, the activation energies of the heterogeneous pyrolysis of the bromo-substituted methanes were determined, and were found to decrease in the direction $CH_3Br \rightarrow CH_2Br_2 \rightarrow CHBr_3 \rightarrow CBr_4$. It was concluded from the activation energies that on a tungsten surface the bromo-substituted methanes decompose in catalytic processes, by radical mechanisms.

The dissociation energies of the C–H and C–Br bonds were calculated for the bromo-substituted methanes; these were observed to decrease in the same direction as in the case of the activation energies. This phenomenon was interpreted qualitatively by quantum-chemical reasons.

Mass spectrometry is one of the most suitable procedures for the determination of thermochemical data (heats of formation, bond dissociation energies) of molecules. The method in essence requires study of the electron impact fragmentation, the determination of the appearance potentials of the ions formed, and the measurement of the ionization potentials of the compounds and radicals.

On this basis, therefore, radicals must be produced; this can be achieved most simply by pyrolysis of the compounds under investigation. Accordingly, study of the pyrolysis of $CHBr_3$ and CBr_4 is of fundamental importance as regards calculation of thermochemical data on these compounds. At the same time, as will be seen later, study of the heterogeneous pyrolysis of brominated methane derivatives on a tungsten filament is also of practical importance.

Following the pioneering work of ELTETON [1], ROBERTSON [2] and LE GOFF [3], many pyrolytic reactions on incandescent metal surfaces were subjected to mass-spectrometric study. The experiments have shown that under such conditions most organic molecules decompose via the formation of free radicals. Hence, study of the mechanisms of these processes requires that the analytical apparatus used, have to be suitable for the detection and identification of both stable molecules and free radicals, while the kinetic measure-

ments necessitate determination of the concentrations of the individual products too [4]. These tasks can be conveniently solved by use of the mass spectrometer even if there is a difference of several orders of magnitude between the concentrations of the components. Further, the low pressure in mass spectrometers and the possibility of extremely rapid detection of the reaction products are very favourable factors as regards study of the processes.

Our earlier mass-spectrometric experiments [5, 6] have shown that the pyrolysis of methyl bromide and methylene bromide on an incandescent tungsten surface proceeds in catalyzed processes, by radical mechanisms. As a continuation of that work, we have now carried out a similar study of the pyrolysis of bromoform and tetrabromomethane. The mass-spectrometric measurements permitted the calculation of some theoretically important thermochemical data on the brominated methane derivatives, at the same time providing important practical information on the mechanism and temperature dependence of pyrolysis in connection with halogen lamps [7, 8]. As it is well-known, in place of gaseous halogen a brominated methane derivative is added to the gas space of bromine cycle lamps [9]; during the operation of a lamp, this brominated methane derivative decomposes, partly in homogeneous [10], and partly in heterogeneous processes. For this reason, these experiments contribute to the description and understanding of the complex chemical processes taking place in halogen lamps.

Experimental

Depending on the reaction under investigation, the aim to be achieved, and the type of mass spectrometer used, many different kinds of reactors have been employed for the mass spectrometric study of heterogeneous kinetic processes [11]. In our experiments a modified Le Goff type reactor [12] was built into the ion source of an MI 13—11 mass spectrometer Fig. 1).

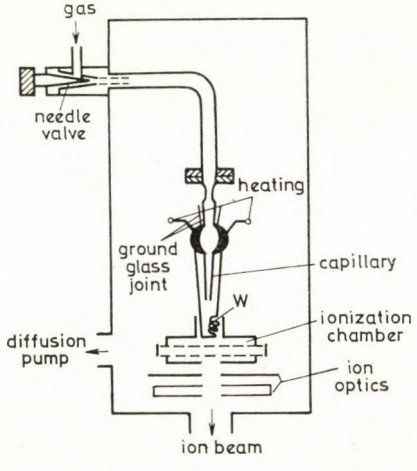

Fig. 1. Outline of the pyrolysis reactor and the ion source

A 12 V tungsten spiral (W) was incorporated into this open reactor type [6]. The temperature dependence of pyrolysis was examined under conditions ensuring molecular flow in the reactor. The reactor was situated in the immediate vicinity of the ionization chamber [6]; its time constant was very small, and it was thus suitable for the study of radicals with very short lifetimes too.

In the study of fragmentation due to electron impact, the spiral was not heated. Introduction of the $CHBr_3$ sample into the mass spectrometer, conditioning of the spiral, measurement of the temperature, and determination of the appearance and ionization potentials were carried out as reported previously [5, 6]. Since the vapour pressure of CBr_4 is substantially lower than those of the other bromo-substituted methanes, the ampoule containing CBr_4 was connected directly to the ion source by inserting a needle valve.

The $CHBr_3$ (Reanal) and the CBr_4 (BDH) were of analytical purity. Before use, the compounds were purified by repeated vacuum distillation.

Results

1. Study of the decomposition of $CHBr_3$ and CBr_4 upon electron impact

1.1. *Low-resolution mass spectra of $CHBr_3$ and CBr_4*

The low-resolution mass spectra of $CHBr_3$ and CBr_4, recorded at an electron energy of 70 eV, are given in Table 1.

The data show that the intensity of the molecular ion is very low for $CHBr_3$, and even more so for CBr_4. In the former case the base peak is that of CBr_2^+, and in the latter case that of CBr_3^+. If the data are compared with the mass spectra of CH_3Br [6] and CH_2Br_2 [5], it can be seen that the relative intensity of the molecular ions of the bromo-substituted methanes decreases with increasing number of Br atoms.

The list (Table II) of the probabilities of decomposition of the molecular ions [13, 14] serves for a numerical comparison of the differences under fragmentation conditions.

It can be seen from Table II that, at a given electron energy, the probability of decomposition of the molecular ions of the bromo-substituted methanes increases rapidly in the direction $CH_3Br \rightarrow CBr_4$. In the case of CBr_4 its value is almost 1 even at an electron energy of 15 eV. As will be seen later, this fact is in close correlation with the strengths of the bonds in the individual brominated methane derivatives.

1.2. *Fragmentation processes of $CHBr_3$ and CBr_4 resulting from electron impact*

Table I shows that, as a result of electron impact, both $CHBr_3$ and CBr_4 decompose to a very large number of ions. The unimolecular decomposition paths may be determined as described earlier [5, 6].

The principle of the procedure is the determination of the appearance potentials of all the fragments, and the ionization potentials of the radicals formed during the pyrolysis. The literature data on normal heats of formation,

Table I

Low-resolution mass spectra of $CHBr_3$ and CBr_4 at an electron energy of 70 eV

Mass number	Ion	$CHBr_3$		CBr_4	
		Peak intensity as per cent of			
		total ion current	base peak	total ion current	base peak
12	C^+	0.32	1.17	0.71	2.92
13	CH^+	0.68	2.48	—	—
79	$^{79}Br^+$	5.22	19.10	5.71	23.50
80	$H^{79}Br^+$	2.63	9.63	—	—
81	$^{81}Br^+$	5.22	19.10	5.60	23.05
82	$H^{81}Br^+$	2.59	9.49	—	—
91	$C^{79}Br^+$	5.35	19.60	4.20	17.28
92	$CH^{79}Br^+$	3.11	11.40	—	—
93	$C^{81}Br^+$	5.27	19.30	4.12	16.95
94	$CH^{81}Br^+$	3.11	11.40	—	—
158	$^{79}Br_2^+$	0.72	2.63	1.06	4.36
160	$^{79,81}Br_2^+$	1.38	5.05	2.07	8.52
162	$^{81}Br_2^+$	0.71	2.58	1.02	4.20
170	$C^{79}Br_2^+$	13.38	49.10	2.87	11.81
172	$C^{79,81}Br_2^+$	27.20	100.00	5.67	23.33
174	$C^{81}Br_2^+$	13.20	48.40	2.76	11.36
249	$C^{79}Br_3^+$	—	—	8.35	34.36
250	$CH^{79}Br_3^+$	1.25	4.58	—	—
251	$C^{79,79,81}Br_3^+$	—	—	24.30	100.00
252	$CH^{79,79,81}Br_3^+$	3.68	13.50	—	—
253	$C^{79,81,81}Br_3^+$	—	—	23.68	97.45
254	$CH^{79,81,81}Br_3^+$	3.60	13.20	—	—
255	$C^{81}Br_3^+$	—	—	7.75	31.81
256	$CH^{81}Br_3^+$	1.17	4.29	—	—
328	$C^{79}Br_4^+$	—	—	0.01	0.04
330	$C^{79,79,79,81}Br_4^+$	—	—	0.04	0.17
332	$C^{79,79,81,81}Br_4^+$	—	—	0.06	0.25
334	$C^{79,81,81,81}Br_4^+$	—	—	0.04	0.17
336	$C^{81}Br_4^+$	—	—	0.01	0.04

$\Delta H°(R^+)$, are used to calculate the possible appearance potentials. Those of the possible processes is accepted as most probable, the appearance potential of which lies closest to the measured value.

Table II

Probability of decomposition of the bromo-substituted methanes (W_z) as a function of the electron energy

Electron energy (eV)	W_z			
	CH_3Br	CH_2B_2	$CHBr_3$	CBr_4
15	0.085	0.401	0.843	0.998
17	0.165	0.420	0.867	0.997
20	0.310	0.524	0.910	0.998
25	0.409	0.599	0.905	0.999
30	0.466	0.627	0.911	0.999
70	0.555	0.663	0.920	0.999

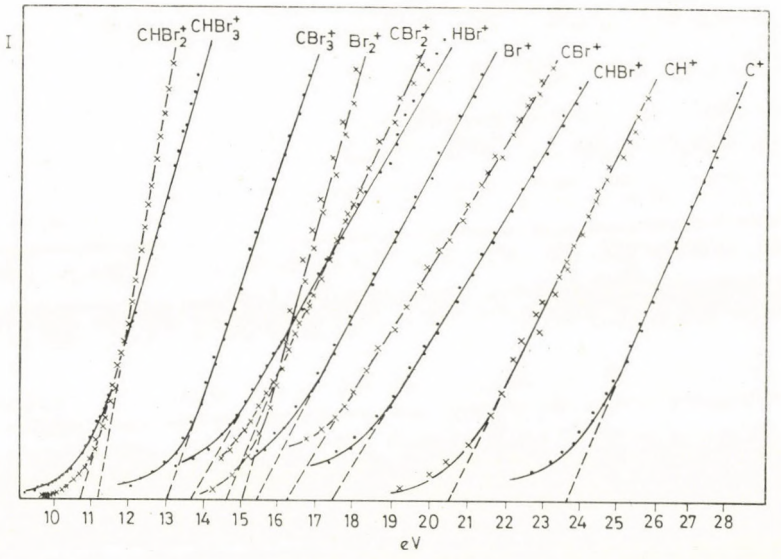

Fig. 2. Variation of the intensities of the ions formed from $CHBr_3$ as a function of the corrected electron energy

Ionization efficiency curves were recorded and evaluated as previously [5, 6]. The ionization efficiency curves for the ions produced from $CHBr_3$ and CBr_4 are shows in Figs 2 and 3, respectively. The appearance potentials were determined from the efficiency curves by the method of linear extrapolation [15]. The electron energy scale was calibrated with argon (ionization potential = 15.75 eV) and helium (ionization potential = 24.48 eV).

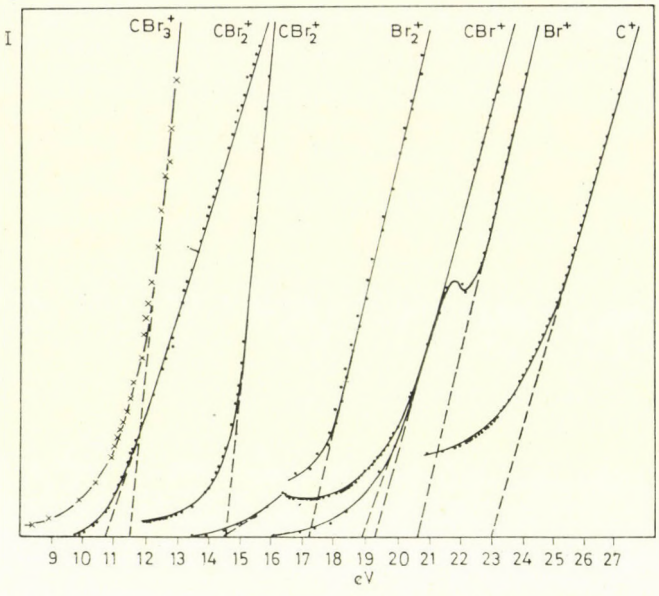

Fig. 3. Variation of the intensities of the ions formed from CBr_4 as a function of the corrected electron energy

The ionization efficiency curves for the radicals formed during pyrolysis of the bromo-substituted methanes are to be seen in Figs 4 and 5. When recording the efficiency curves, the spiral was heated to 1800—2000 K, and the ion currents were measured as a function of the electron energy under the appearance potential.

Figure 3 reveals three break-points in the ionization efficiency curve of Br. Extrapolation of the linear sections leads to appearance potentials of 14.5, 18.9 and 20.6 eV, as an indication of the fact that Br is formed via at least three different processes in the decomposition of CBr_4. The appearance potentials for the three decomposition processes, calculated from the heats of formation reported in the literature, agree well with the measured data (Table III).

Table III lists the measured appearance potentials of the fragments formed from bromomethanes the ionization potentials of the molecules and of the radicals produced in the pyrolyses, and the heats of formation calculated from our own and literature data [5,6,].

To facilitate the survey of the possible decomposition processes of $CHBr_3$ and CBr_4, it is convenient to employ the fragmentation mechanism matrix described earlier [5, 6]. The stoichiometric matrices are given in Tables IV and V. The elements of the matrices are the stoichiometric coefficients of all of the components of all of the possible decomposition reactions. The positions of the zero elements are denoted by points.

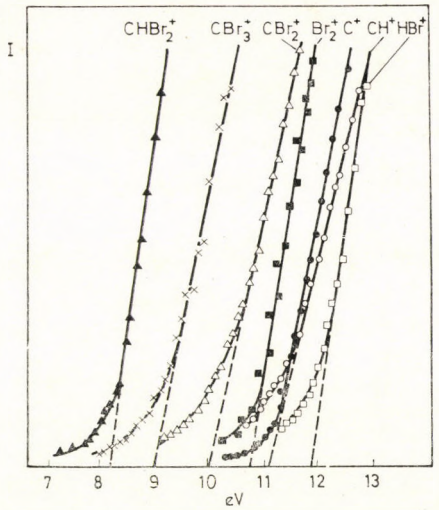

Fig. 4. Ionization efficiency curve of the radicals formed in the pyrolysis of the bromo-substituted methanes (I). Ion current intensity in arbitrary units; electron energies are corrected values

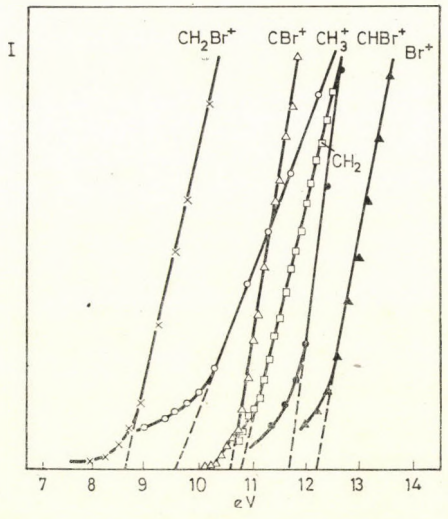

Fig. 5. Ionization efficiency curve of the radicals formed from the bromo-substituted methanes (II)

Table III

$\Delta H°$, IP and AP values of fragments formed in

Radical	$\Delta H°$ kcal/mol	IP (eV)			
		CH_3Br	CH_2Br_2	$CHBr_3$	CBr_4
C(g)	175	—	—	11.1 ± 0.2	11.1 ± 0.2
CH	143	—	—	11.1 ± 0.3	—
CH_2	84	—	10.8 ± 0.4	—	—
CH_3	38	9.6 ± 0.3	—	—	—
Br(g)	19	—	12.2 ± 0.3	—	—
Br_2(g)	3	—	—	—	10.7 ± 0.3
HBr	−15	—	11.9 ± 0.3	11.9 ± 0.4	—
CBr	144	—	12.2 ± 0.5	—	10.6 ± 0.3
CHBr	96	—	11.7 ± 0.5	11.7 ± 0.4	—
CH_2Br	51	8.3 ± 0.1	8.7 ± 0.3	—	—
CH_3Br	−8	10.5 ± 0.2	—	—	—
CBr_2	98	—	—	—	10.0 ± 0.2
$CHBr_2$	44	—	8.4 ± 0.1	—	—
CH_2Br_2	0	—	10.5 ± 0.1	—	—
CBr_3	44	—	—	—	9.1 ± 0.2
$CHBr_3$	0	—	—	10.7 ± 0.3	—
CBr_4	24	—	—	—	10.8 ± 0.3

By comparison of the calculated appearance potentials for the individual decomposition routes with those found experimentally, we may select the most probable decomposition processes. The appearance potentials measured for $CHBr_3$ and CBr_4, and the calculated values approaching most closely to the measured values, are listed in Table VI. On the basis of the good agreement of the values, the most probable decomposition routes may be chosen unambiguously.

The ion-forming fragmentation processes determined in this way are shown in Tables VII and VIII for $CHBr_3$ and CBr_4, respectively.

decomposition of bromomethanes

Ion	$\Delta H°$ kcal/mol	AP (eV)			
		CH_3Br	CH_2Br_2	$CHBr_3$	CBr_4
C^+	427	22.9 ± 0.5	22.7 ± 0.5	23.6 ± 0.5	23.0 ± 0.5
CH^+	398	21.7 ± 0.3	22.0 ± 0.5	20.5 ± 0.5	—
CH_2^+	340	14.7 ± 0.5 18.2 ± 0.5	17.1 ± 0.3	—	—
CH_3^+	255	12.8 ± 0.3	—	—	—
Br^+	308	15.8 ± 0.5	—	15.4 ± 0.4	14.5 ± 0.5 18.9 ± 0.5 20.6 ± 0.5
Br_2^+	240	—	20.7 ± 0.5	15.1 ± 0.3	17.2 ± 0.3
HBr^+	266	15.9 ± 0.3	18.2 ± 0.2	14.7 ± 0.3	—
CBr^+	390	18.8 ± 0.3	19.6 ± 0.3	16.2 ± 0.4	19.3 ± 0.4
$CHBr^+$	364	16.3 ± 0.5	16.0 ± 0.5	17.4 ± 0.4	—
CH_2Br^+	238	13.4 ± 0.3	11.1 ± 0.2	—	—
CH_3Br^+	234	10.5 ± 0.2	—	—	—
CBr_2^+	337	—	15.6 ± 0.5	13.7 ± 0.2	14.5 ± 0.3
$CHBr_2^+$	239	13.2 ± 0.5	—	—	—
$CH_2Br_2^+$	243	—	10.5 ± 0.1	—	—
CBr_3^+	254	—	—	13.0 ± 0.3	11.4 ± 0.3
$CHBr_3^+$	251	—	—	10.7 ± 0.3	—
CBr_4^+	268	—	—	—	10.8 ± 0.3

1.3. *Activation energies of the decomposition of molecular ions of bromo-substituted methanes*

In certain cases decomposition of the molecular ion requires activation (excess) energy [15], which is transferred to the neutral molecules by the ionizing electrons in the course of impact. In such cases the energy corresponding to the appearance potential must cover not only the ionization energy and the dissociation energy, but also the activation energy. After the ionization and decomposition processes, this excess energy will be present in the form of the kinetic and excitation energies of the particles formed.

Table IV

Stoichiometric matrix of electron-impact fragmentation of $CHBr_3$

	C^+				CH^+		Br^+									
H	1	1	.	.	.	.	1	1	.	.	1	.	.	.	1	.
C	.	.	.	.	.	.	1	1	.	.	.	1	.	.	.	.
CH	.	.	.	.	.	.	.	.	1	1	.	.	.	.	.	.
Br	3	1	2	.	3	1	2	.	2	.	1	1	.	1	.	.
Br_2	.	1	.	1	.	1	.	1	.	1	.	.	.	.	.	.
HBr	.	.	1	1	.	.	.	.	.	.	.	1	1	.	.	.
CBr	.	.	.	.	.	.	.	.	.	.	1	.	1	.	.	.
CHBr	.	.	.	.	.	.	.	.	.	.	.	.	.	1	.	.
CBr_2	.	.	.	.	.	.	.	.	.	.	.	.	.	.	1	.
$CHBr_2$	.	.	.	.	.	.	.	.	.	.	.	.	.	.	.	1
$CHBr_3$	−1	−1	−1	−1	−1	−1	−1	−1	−1	−1	−1	−1	−1	−1	−1	−1
C^+	1	1	1	1	.	.	.	.	.	.	.	.	.	.	.	.
CH^+	.	.	.	.	1	1	.	.	.	.	.	.	.	.	.	.
Br^+	.	.	.	.	.	.	1	1	1	1	1	1	1	1	1	1
Br_2^+	.	.	.	.	.	.	.	.	.	.	.	.	.	.	.	.
HBr^+	.	.	.	.	.	.	.	.	.	.	.	.	.	.	.	.
CBr^+	.	.	.	.	.	.	.	.	.	.	.	.	.	.	.	.
$CHBr^+$	.	.	.	.	.	.	.	.	.	.	.	.	.	.	.	.
CBr_2^+	.	.	.	.	.	.	.	.	.	.	.	.	.	.	.	.
$CHBr_2^+$	.	.	.	.	.	.	.	.	.	.	.	.	.	.	.	.
CBr_3^+	.	.	.	.	.	.	.	.	.	.	.	.	.	.	.	.
(eV)	23.2	19.5	19.5	18.0	19.6	18.1	24.3	22.8	20.7	19.2	22.1	20.6	18.5	17.7	19.3	15.3
$AP_{theor.}$																

The activation energies of decomposition of molecular ions may be calculated from the ionization potential and appearance potential data [6]. The activation energies of the decompositions of the molecular ions of bromo-substituted methanes involving formation of HBr and Br, calculated from earlier and present experimental data, are given in Table IX. ΔH in the Table IX is the total energy necessary for the decomposition, ΔH_R is the reaction heat, and $\Delta H^{\ddagger}$ is the activation energy.

Table IX shows that, in accordance with expectations [15], the molecular ions decompose in endothermic processes, and the endothermicities of decomposition processes involving formation of HBr are higher than those of processes leading to Br. (In a study of the absolute values, attention must be paid

The positions of the zero elements are denoted by points

Br_2^+				HBr^+			CBr^+			$CHBr^+$		CBr_2^+		$CHBr_2^+$	CBr_3^+
1	.	.	1	.	.	.	1	1	.	.	.	1	.	.	1
1	1	.	.	1	1	.	.	.	.	.	.	.	.	.	.
.	.	.	.	.	.	.	.	.	.	.	.	.	.	.	.
1	.	.	.	.	2	.	2	.	1	.	2	1	.	1	1
.	.	.	.	1	2	.	.	1	.	1	.	.	.	.	.
.	1	.	.	.	.	.	.	.	1	.	.	.	1	.	.
.	.	.	1	.	.	.	.	.	.	.	.	.	.	.	.
.	.	1	.	.	.	.	.	.	.	.	.	.	.	.	.
.	.	.	.	.	.	1	.	.	.	.	.	.	.	.	.
.	.	.	.	.	.	.	.	.	.	.	.	.	.	.	.
−1	−1	−1	−1	−1	−1	−1	−1	−1	−1	−1	−1	−1	−1	−1	−1
.	.	.	.	.	1	.	.	.	.	.	.	.	.	.	.
.	.	.	.	.	.	.	.	.	.	.	.	.	.	.	.
.	.	.	.	.	.	.	.	.	.	.	.	.	.	.	.
1	1	1	1	.	.	.	.	.	.	.	.	.	.	.	.
.	.	.	.	1	1	1	.	.	.	.	.	.	.	.	.
.	.	.	.	.	.	.	1	1	1	.	.	.	.	.	.
.	.	.	.	.	.	.	.	.	.	1	1	.	.	.	.
.	.	.	.	.	.	.	.	.	.	.	.	1	1	.	.
.	.	.	.	.	.	.	.	.	.	.	.	.	.	1	.
.	.	.	.	.	.	.	.	.	.	.	.	.	.	.	1
21.3	16.4	14.8	19.2	18.8	20.3	14.9	23.2	19.1	16.8	15.8	17.2	17.1	13.4	11.0	13.1

to the accuracy of the experimental appearance and ionization potential data used in the calculations, which is on average $\pm$ 0.2 eV). Table IX further permits the conclusion that the activation energy of decomposition of a bromo-substituted methane molecular ion is very close to zero (the difference from zero lies within the order of the experimental error), and thus neglect of the kinetic and excitation energies could not have involved a large error.

Table V

Stoichiometric matrix of electron-impact fragmentation of CBr_4. The positions of the zero elements are denoted by points

	C^+			Br^+						Br_2^+				CBr^+		CBr_2^+		CBr_3^+
C	.	.	.	1	1	.	.	.	.	1	1	.	.	.	.	.	.	.
Br	.	2	4	3	1	.	2	1	.	2	.	1	.	3	1	2	.	1
Br_2	2	1	.	.	1	1	.	.	.	.	1	.	.	.	1	.	1	.
CBr	.	.	.	.	.	1	1	.	.	.	.	1	.	.	.	.	.	.
CBr_2	.	.	.	.	.	.	.	1	.	.	.	.	1	.	.	.	.	.
CBr_3	.	.	.	.	.	.	.	.	1	.	.	.	.	.	.	.	.	.
CBr_4	−1	−1	−1	−1	−1	−1	−1	−1	−1	−1	−1	−1	−1	−1	−1	−1	−1	−1
C^+	1	1	1	.	.	.	.	.	.	.	.	.	.	.	.	.	.	.
Br^+	.	.	.	1	1	1	1	1	1	.	.	.	.	.	.	.	.	.
Br_2^+	.	.	.	.	.	.	.	.	.	1	1	1	1	.	.	.	.	.
CBr^+	.	.	.	.	.	.	.	.	.	.	.	.	.	1	1	.	.	.
CBr_2^+	.	.	.	.	.	.	.	.	.	.	.	.	.	.	.	1	1	.
CBr_3^+	.	.	.	.	.	.	.	.	.	.	.	.	.	.	.	.	.	1
$AP_{theor.}$ (eV)	17.1	19.1	22.1	22.2	20.7	18.5	15.0	17.2	14.1	19.2	17.2	17.1	14.1	19.8	16.5	14.9	14.1	11.4

Table VI

Measured appearance potentials for $CHBr_3$ and CBr_4, and calculated values most closely approaching the measured values

Ion	$CHBr_3$		CBr_4	
	Measured	calcd.	Measured	calcd.
	(eV)		(eV)	
C^+	23.6	23.2	23.0	22.1
CH^+	20.5	19.6	—	—
			18.9	18.5
Br^+	15.4	15.3	14.5	14.1
			20.6	20.7
HBr^+	14.7	14.9	—	—
CBr^+	16.2	16.8	19.3	19.8
$CHBr^+$	17.4	17.2	—	—
Br_2^+	15.1	14.8	17.2	17.1 17.2
CBr_2^+	13.7	13.4	14.5	14.1 14.9
$CHBr_2^+$	11.1	11.0	—	—
CBr_3^+	13.0	13.1	11.4	11.4

Table VII

Probable ion formation processes for $CHBr_3$ in the case of electron-impact ionization

Ion	Decomposition reaction
C^+	$CHBr_3 \rightarrow C^+ + H + 3\,Br$
CH^+	$CHBr_3 \rightarrow CH^+ + 3\,Br$
Br^+	$CHBr_3 \rightarrow Br^+ + CHBr_2$
HBr^+	$CHBr_3 \rightarrow HBr^+ + CBr_2$
CBr^+	$CHBr_3 \rightarrow CBr^+ + HBr + Br$
$CHBr^+$	$CHBr_3 \rightarrow CHBr^+ + 2\,Br$
Br_2^+	$CHBr_3 \rightarrow Br_2^+ + CHBr$
CBr_2^+	$CHBr_3 \rightarrow CBr_2^+ + HBr$
$CHBr_2^+$	$CHBr_3 \rightarrow CHBr_2^+ + Br$
CBr_3^+	$CHBr_3 \rightarrow CBr_3^+ + H$

Table VIII

Probable ion formation processes in unimolecular decomposition of CBr_4 in the case of electron-impact ionization

Ion	Decomposition reaction
C^+	$CBr_4 \rightarrow C^+ + 4\,Br$
Br^+	$CBr_4 \rightarrow \begin{cases} Br^+ + CBr + Br_2 \\ Br^+ + CBr_3 \\ 2\,Br^+ + Br_2 + C \end{cases}$
CBr^+	$CBr_4 \rightarrow CBr^+ + 3\,Br$
Br_2^+	$CBr_4 \rightarrow \begin{cases} Br_2^+ + CBr + Br \\ Br_2^+ + Br_2 + C \end{cases}$
CBr_2^+	$CBr_4 \rightarrow \begin{cases} CBr_2^+ + 2\,Br \\ CBr_2^+ + Br_2 \end{cases}$
CBr_3^+	$CBr_4 \rightarrow CBr_3^+ + Br$

Table IX

Activation energies of decomposition of molecular ions of bromo-substituted methanes (kcal/mol)

Process	ΔH	ΔH_R	$\Delta H^{\ddagger}$
$CH_3Br^+ \rightarrow Br + CH_3^+$	53	54	−1
$CH_2Br_2^+ \rightarrow Br + CH_2Br^+$	14	24	−10
$CHBr_3^+ \rightarrow Br + CH_2Br_2^+$	7	19	−12
$CBr_4^+ \rightarrow Br + CBr_3^+$	18	34	−16
$CH_3Br^+ \rightarrow HBr + CH_2^+$	99	91	8
$CH_2Br_2^+ \rightarrow HBr + CHBr^+$	126	115	11
$CHBr_3^+ \rightarrow HBr + CBr_2^+$	85	67	18

2. Study of the heterogeneous pyrolysis of $CHBr_3$ and CBr_4

2.1. *Temperature dependence of the pyrolysis of $CHBr_3$ on a tungsten spiral*

In the study of the temperature dependence of the pyrolysis, the temperature of the spiral of the reactor was varied while the electron energy was maintained constant.

Choice of the magnitude of the ionizing electron energy was guided by the following principles: (1) The pyrolysis may be investigated with the application of high electron energy. In this method fragmentation arises jointly on the

surface of the incandescing spiral and as a result of the ionizing electrons. In this case the change occurring in the relative intensity is primarily a consequence of the pyrolysis. (2) The other possibility is to work with a low ionizing electron energy (below the appearance potential), when there is little disturbance from electron fragmentation. At low electron energies, however, the ionization cross-section decreases strongly, and very small ion currents must be measured (particularly in the case of radicals) [16].

In our earlier measurements [5, 6], the temperature dependence of the pyrolysis was studied at an electron energy of 70 eV. However, as can be seen from Tables I and II, at higher electron energies the intensities of the molecular ions of $CHBr_3$ and CBr_4 are very low, and thus the decomposition of these compounds resulting from pyrolysis cannot be studied at high electron energy, since the electron fragmentation overlaps the effect of pyrolysis. Accordingly, in the present pyrolysis experiments the spectra were recorded at 15 eV.

In pyrolysis, the mass spectrum also changes slightly in its temperature dependence because of some other effects. One of the causes is chemical in nature; this is manifested in the fact that the surface composition of the spiral changes in the course of pyrolysis, as a result of tungsten carbide formation. This effect may be reduced by conditioning the spiral [3, 17, 18]. In addition, also physical interactions affect the intensity of the molecular beam, and hence the heights of the spectral peaks [19]. Examples of such interactions are the temperature-dependent diffuse vaporization and mirror reflection of the gas molecules from the incandescent surface [20, 21], and the change in internal energy of the gas. These effects are augmented by the fact that the gas pressure in the reactor increases during pyrolysis as a result of a rise in the number of molecules. Further, at high temperatures the molecular beam passes through the ionization chamber more rapidly, and thus the probability of ionization falls. This latter effect is not too large, since the temperature of the ionization chamber is not influenced to a great extent by the temperature of the reactor, while at a constant molecular flux the peak height is merely a square root function of the translational temperature of the molecules [22]. As a consequence of all these effects, the heights of the individual peaks of the spectrum vary in almost the same proportions, and thus, if the relative intensities are expressed as a percentage of the total ion current measured at the individual temperatures, even in spite of the above physical interactions a realistic picture may be obtained of the temperature dependence of the mass spectrum and the pyrolysis.

Figure 6 shows the temperature dependence of the quantities of those ions appearing with higher relative intensities in the mass spectrum of $CHBr_3$, while Fig. 7 gives the corresponding dependence for ions detected in lower relative intensities. The temperature dependence of the ion intensity, or of the pyrolysis, is even more striking in a plot of $\Delta I/\Delta T$ *vs.* T (Figs 8 and 9).

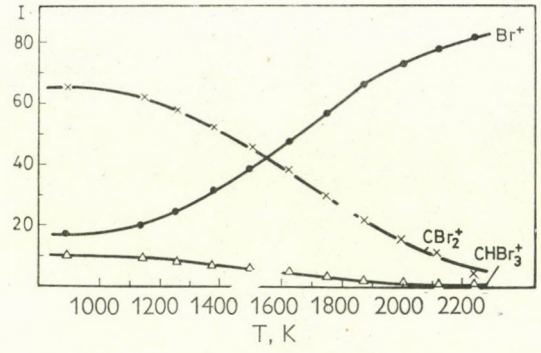

Fig. 6. Temperature dependence of the ion current of radicals formed in the pyrolysis of $CHBr_3$. Electron energy 15 eV

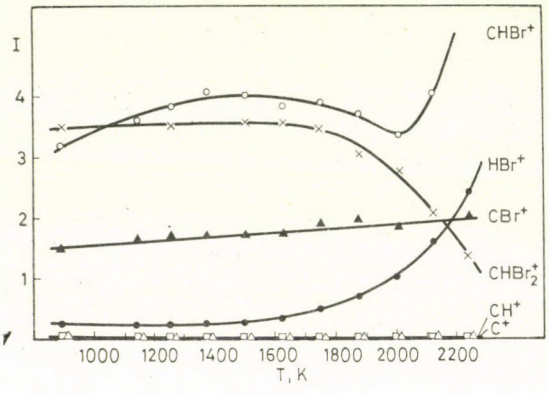

Fig. 7. Temperature dependence of the ion current of decomposition products formed in lower relative intensities in the pyrolysis of $CHBr_3$. Electron energy 15 eV

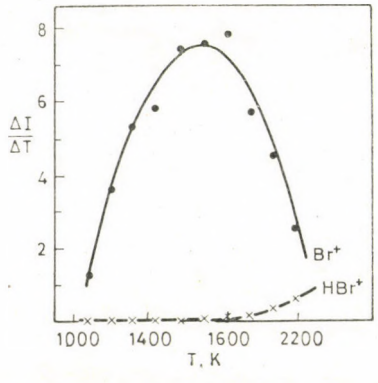

Fig. 8. Temperature dependence of the quotient of differences of the ion current of the products formed in the pyrolysis of $CHBr_3$

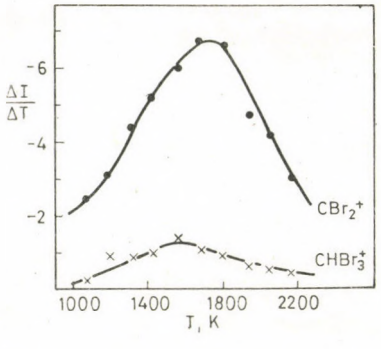

Fig. 9. Temperature dependence of the quotient of differences of the ion current of the decomposition products formed in the pyrolysis of $CHBr_3$

The Figures reveal that, with this reactor type, the pyrolysis of $CHBr_3$ begins to a detectable extent at about 800 K, while Figs 8 and 9 show that the degree of pyrolysis varies most intensively in the temperature interval 1600—1800 K. The main decomposition products of $CHBr_3$ are Br, CBr_2 and probably H, though the latter could not be detected with our apparatus. The amount of HBr formed was much less than in the pyrolysis of CH_3Br and CH_2Br_2 [5, 6]. As a consequence of futher decomposition, the relative amount of some of the radicals occurring with lower intensities (HBr, CHBr and CBr) increase, while that of $CHBr_2$ decreases as the temperature rises. The amount of C detected in very low intensities in the pyrolysis is almost constant, since the rise of temperature leads to an increase in the rate of tungsten carbide formation similar to that in the deposition of C.

2.2. *Temperature dependence of the pyrolysis of* CBr_4

Figures 10 and 11 present the temperature dependence of the spectral peaks detected in higher, and in lower relative intensities, respectively, on pyrolysis. Figures 12 and 13 show the extents of the temperature dependent changes as a function of temperature.

It can be seen from Figs 10—13 that the temperature dependence of the pyrolysis of CBr_4 is similar to that observed for $CHBr_3$. The main products of pyrolysis are the Br, CBr_3, and CBr_2 radicals. Ions indicative of the formation of CBr and Br_2 were detected in much lower relative intensities. The curve for Br_2 has a maximum at about 1500 K, for at temperatures higher than this Br_2 begins to dissociate to atoms.

2.3. *Activation energies of the heterogeneous pyrolysis of bromo-substituted methanes*

We have seen that the fragmentation resulting from the ionizing electrons can be eliminated if the ionizing electron energy is lower than the appearance potential of the decomposition products under study, but higher than the ionization potential of the radical. Thus, the values of the ion current are naturally very small, and the accompanying experimental difficulties reduce the accuracy of the measurements. If the pyrolysis unavoidably taking place on the cathode is taken into account, together with the small extent of electron fragmentation occurring because of the inhomogeneity of the electron energy [15], *i.e.* the ion current observed at the cold reactor spiral is subtracted from the measured ion currents, then we obtain the ion current originating only from the ionization of the radicals formed during pyrolysis. Hence, Fig. 14 shows the temperature dependence of the per cent increase in the ion current due to the reac-

tions of the Br atoms formed in the pyrolysis of $CHBr_3$ and CBr_4, while Fig. 15 shows the corresponding dependence in the case of HBr formed in the pyrolysis of $CHBr_3$. The amounts of Br and HBr formed on pyrolysis increase rapidly with the rise of temperature.

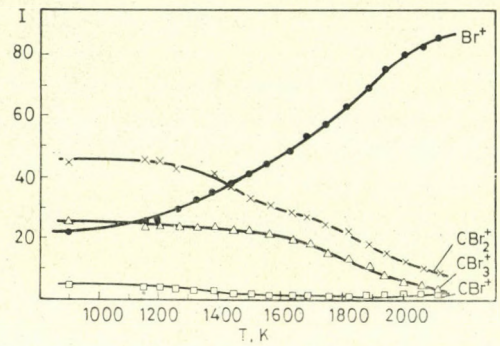

Fig. 10. Temperature dependence of the ion current of radicals formed in the pyrolysis of CBr_4. Electron energy 15 eV

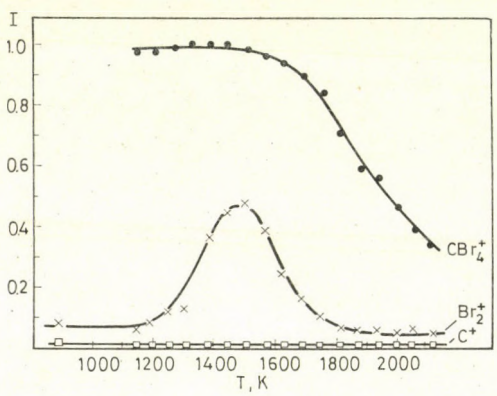

Fig. 11. Temperature dependence of the ion current of decomposition products formed in lower relative amounts in the pyrolysis of CBr_4. Electron energy 15 eV

If the ion current of the radicals formed in the pyrolysis are expressed in arbitrary units, logarithms are taken, and these are plotted as a function of 1/T, the activation energy of the decomposition process resulting in the product in question may be calculated from the linear Arrhenius plot obtained. In combination with the results of earlier measurements [5, 6], Fig. 16 gives the Arrhenius plots for the decomposition reactions of the bromo-substituted methanes leading to formation of Br, and Fig. 17 those of the heterogeneous decomposition processes accompanied by formation of HBr.

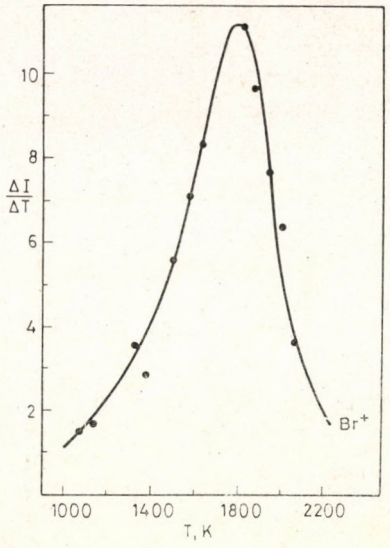

Fig. 12. Temperature dependence of the quotient of differences of the ion current of the products formed in the pyrolysis of CBr_4

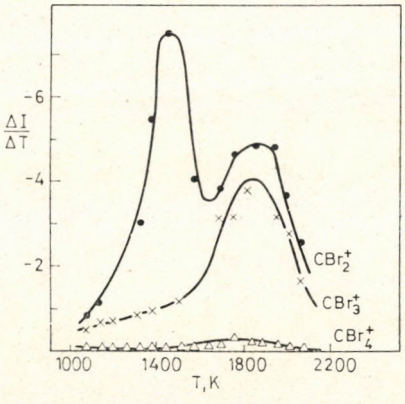

Fig. 13. Temperature dependence of the quotient of differences of the ion current of the products formed in the pyrolysis of CBr_4

The activation energies calculated for the heterogeneous pyrolysis from the straight lines are listed in Table X. The cause of the limited accuracy of the measurements is that the surface state of the tungsten spiral has a decisive effect on these pyrolytic processes. As has already been pointed out, the surface composition changes during pyrolysis. In order to reduce this effect to a minimum, the pyrolysis of the bromo-substituted methanes were measured one after another on the same, well-conditioned spiral (covered with tungsten carbide).

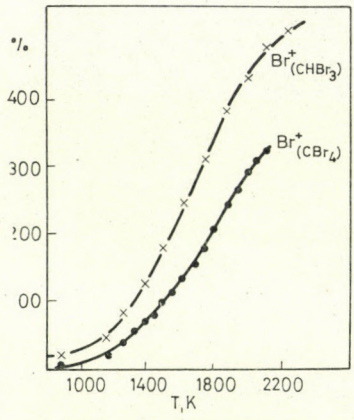

Fig. 14. Temperature dependence of the percent increase of the ion current originating from ionization of the Br atoms formed in the pyrolysis of $CHBr_3$ and CBr_4. Electron energy 13 eV

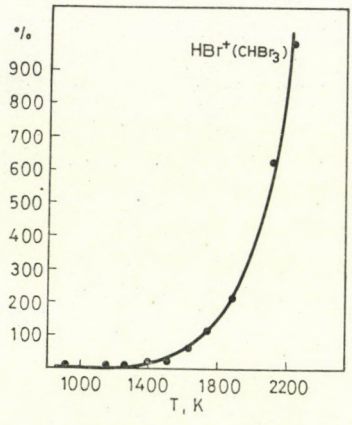

Fig. 15. Temperature dependence of the per cent increase of the ion current originating from ionization of the HBr formed in the pyrolysis of $CHBr_3$

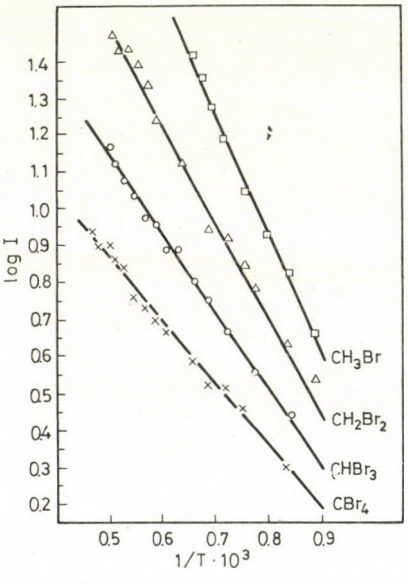

Fig. 16. Arrhenius plots of the ion current of the Br formed from the decomposition of bromo-substituted methanes

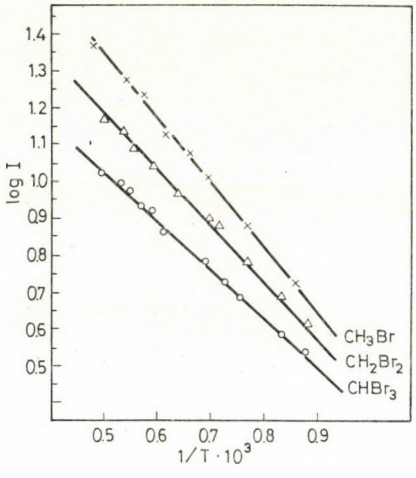

Fig. 17. Arrhenius plots of the ion current of the HBr formed from the decomposition of bromo-substituted methanes

Table X shows that the activation energies of the heterogeneous decompositions of bromo-substituted methanes leading to formation of Br and HBr are the smaller, the more H atoms in the molecule are replaced by Br. There is a systematic decrease in the activation energy values in the direction

Table X

Activation energies of pyrolytic decompositions of bromo-substituted methanes on a tungsten surface, with the formation of Br and HBr (kcal/mol)

Decomposition process	$\Delta H^{\ddagger}$
$CH_3Br \rightarrow Br + CH_3$	15.0 ± 3.0
$CH_2Br_2 \rightarrow Br + CH_2Br$	13.0 ± 3.0
$CHBr_3 \rightarrow Br + CHBr_2$	10.5 ± 2.5
$CBr_4 \rightarrow Br + CBr_3$	8.0 ± 2.0
$CH_3Br \rightarrow HBr + CH_2$	8.6 ± 2.0
$CH_2Br_2 \rightarrow HBr + CHBr$	7.4 ± 1.5
$CHBr_3 \rightarrow HBr + CBr_2$	6.3 ± 1.5

$CH_3Br \longrightarrow CBr_4$. It can also be seen that decomposition processes accompanied by HBr formation require less excess energy than the decompositions of the same molecules to Br.

If the above activation energies are compared with those to be found in the literature [23, 24] for homogeneous pyrolytic decompositions, it is observed that although these values vary according to similar regularities, their numerical values are substantially higher (about 5 times), and it follows from this that on tungsten the bromo-substituted methanes undergo pyrolysis in catalytic processes involving radical mechanisms.

A regularity similar to that for the activation energies also emerges from a comparison of the thermodynamic data relating to the bromo-substituted methanes. If the free energies of formation of the bromo-substituted methanes are examined [25] (Table XI), it is observed that these compounds are not too stable thermodynamically; their stabilities decrease with increasing number of Br atoms (the free energy of formation is slightly negative for CH_3Br and CH_2Br_2, and positive for $CHBr_3$ and CBr_4). At room temperature, however, they are

Table XI

Free energies of formation of bromo-substituted methanes (kcal/mol)

Compound	$\Delta F°$
CH_3Br (g)	−6.2
CH_2Br_2 (g)	−1.4
$CHBr_3$ (g)	3.8
CBr_4 (g)	8.6

nevertheless stable, for their decomposition requires activation energy. The activation energy required for decomposition is the smaller, the thermodynamically more labile the molecule.

From all this, the practical conclusion can be drawn that if it is wished to produce halogen for halogen lamps by either homogeneous or heterogeneous decomposition of bromo-substituted methanes, it is energetically more favourable to employ those containing more Br atoms ($CHBr_3$ or CBr_4). Because of the high operating temperature (ca. 2800 K) however, in the case of incandescent lamps, the energetic questions are overshadowed by technological factors. It is much more convenient to use CH_3Br, and even more so CH_2Br_2, to fill the lamps, the vapour pressure of the latter at room temperature being the desired few Torr.

3. Determination of bond dissociation energies of bromo-substituted methanes

In our earlier [5, 6] and present experiments, the energies necessary to split the C–Br and C–H bonds of the bromo-substituted methanes were calculated from the ionization potentials of the radicals formed on pyrolysis, and from the appearance potentials measured in the fragmentation resulting from electron impact [15]. Table XII contains the measured appearance and inoni-

Table XII

Measured appearance and ionization potentials of bromo-substituted methanes, the heats of radical formation (ΔH°) and bond dissociation energies ($D_{measd.}$) calculated from these, and the literature bond dissociation energies ($D_{lit.}$)

Bond	$\Delta H^\circ_{measd.}$ (kcal/mol)	AP (eV)	IP (eV)	$D_{measd.}$ (kcal/mol)	$D_{lit.}$ (kcal/mol)	Radical stabilization (kcal/mol)
CH_3-Br	38	12.8	9.6	74±5	66.5	
CH_2Br-Br	51	11.1	8.3	65±4	62.5	
$CHBr_2-Br$	44	11.1	8.4	62±4	55.5	
CBr_3-Br	44	11.4	9.1	53±3	49.0	
CH_2Br-H	51	13.4	8.3	118±6	106.8	−15
$CHBr_2-H$	44	13.2	8.4	111±6	101.1	−8
CBr_3-H	44	13.0	9.1	90±5	91.1	+19

zation potentials, the calculated heats of radical formation and bond dissociation energies. The bond dissociation energies were calculated by the following relationship

$$AP(R^+) = IP(R) + D(R—X)$$

where AP is the appearance potential, IP is the ionization potential, and D is the bond dissociation energy (where X = Br or H).

The Table also gives the experimental data of SEHON and SZWARC [23, 26], who studied the homogeneous pyrolysis of bromo-substituted methanes by a toluene radical-trapping technique, and from the results calculated the C–Br bond energies. We calculated the literature C—H bond energies from data on the heats of formation [15], using the relationship

$$D(R\text{–}H) = \Delta H_f(R^{\cdot}) + \Delta H_f(H) - \Delta H_f(R\text{–}Hr)$$

where ΔH_f is the appropriate heat of formation.

It can be seen from the Table that, even though the agreement between the measured and the literature data is not too good in certain cases (owing to the limited accuracy of the appearance and ionization potentials), nevertheless it can be established quite clearly in both cases that the strengths of both the C–Br and the C–H bonds decrease with increasing number of Br atoms in the molecule. This tendency may also be observed from a comparison of the mass spectra of CH_3Br and CH_2Br_2 [5, 6] and those of $CHBr_3$ and CBr_4 reported here (Table I). The spectra reveal that at a given electron energy the relative intensity of the molecular ion decreases in the direction $CH_3Br \longrightarrow CH_2Br_2 \longrightarrow CHBr_3 \longrightarrow CBr_4$. This is understandable if it is considered that the H atoms are progressively replaced by much larger Br atoms [27]. This has the result, that with increasing number of Br atoms, the repulsion between the Br atoms also increases, and thus the C–Br and C–H bond strengths decrease.

Decreases in the same direction are also exhibited by the thermodynamic stabilities of the bromo-substituted methanes (Table XI), and by the activation energies of the pyrolytic decompositions directly connected with the bond strenghts (Table X).

Besides the repulsion between the Br atoms, the effect of the resonance stabilization of the radicals formed on the dissociation energy of the C–Br bond must also be taken into account [23]. This means that the p electron of the C atom of the free radical formed from the bromo-substituted methane is uncompensated, and an interaction arises with the p electrons of the Br atoms, thereby resulting in stabilization of the radical. The stabilization increases with the number of Br atoms, and is greatest in the case of the CBr_3 radical. Stabilization of the radical is also caused by the decrease of the repulsion energy during formation of the radical. This occurs when the group (CBr_3) formed from the originally close-packed, tetrahedral molecule is converted to a planar structure during the formation of the CBr_3 radical.

The measure of complete stabilization of the radicals is defined numerically by the difference $D(CH_3\text{–}H) - D(R\text{–}H)$ [28, 29], where R is the radical formed from the bromo-substituted methane. The larger this difference, the

higher the stability of the radical formed. The value of $D(CH_3–H)$ is 103 kcal/mol [26]. Hence:

$$D(CH_3–H) - D(CH_2Br–H) = -15 \text{ kcal/mol}$$
$$D(CH_3–H) - D(CHBr_2–H) = -8 \text{ kcal/mol}$$
$$D(CH_3–H) - D(CBr_3–H) = +13 \text{ kcal/mol}$$

REFERENCES

[1] ELTETON, G. C.: J. Chem. Phys., **15**, 455 (1947)
[2] ROBERTSON, A. J. B.: Proc. Roy. Soc. (London), A **199**, 349 (1949)
[3] LE GOFF, P.: J. Chim. Phys. **50**, 423 (1953)
[4] LOSSING, F. P.: Mass Spectrometry of Free Radicals; in C. A. MCDOWELL: Mass Spectrometry. McGraw-Hill, New York 1963
[5] KAPOSI, O., RIEDEL, M., DEUTSCH, T.: Magy. Kém. Folyóirat, **79**, 505 (1973); Acta Chim. (Budapest), **81**, 43 (1974)
[6] KAPOSI, O., RIEDEL, M., SANCHEZ, G. R.: Magy. Kém. Folyóirat, **80**, 914 (1974); Acta Chim. (Budapest), **85**, 361 (1975)
[7] MOSBY, F. A., SCHUPP, L. J., STEINER, G. G., ZUBLER, E. G.: Illum. Eng. **62**, 198 (1967)
[8] HANGOS, I., DEUTSCH, T.: Kémiai Közl. **37**, 459 (1972)
[9] JAMPENS, T.: Philips Techn. Rundsch., **27**, 165 (1966)
[10] DEUTSCH, T.: Dissertation. L. Eötvös University, Budapest 1973
[11] PENTENERO, A., LE GOFF, P.: Mass Spectrometric Studies of Heterogeneous Chemical Kinetics; in R. J. REED: Mass Spectrometry. Academic Press, London 1965
[12] LE GOFF, P.: J. Chim. Phys. **53**, 269 (1956)
[13] PAHL, M.: Z. Naturforsch. **9b**, 188 (1954)
[14] PAHL, M.: Z. Naturforsch., **9b**, 418 (1954)
[15] FIELD, F. H., FRANKLIN, J. L.: Electron Impact Phenomena. Academic Press, New York 1970
[16] ROBERTSON, A. J. B.: Mass Spectrometry, Methuen et Co., Ltd., London, 1954
[17] LE GOFF, P., LETORT, M.: J. Chim. Phys., **53**, 480 (1956)
[18] LE GOFF, P., LETORT, M.: J. Chim. Phys., **54**, 3 (1957)
[19] NUTT, C. W., CARTER, A. J.: Trans. Faraday Soc., **64**, 771 (1968)
[20] DATZ, S., MOORE, G. E., TAYLOR, E. H.: J. Catal. **5**, 218 (1966)
[21] HURLBUT, F. C.: Proc. Int. Symp. Rarefied Gas Dyn., **1**, 1 (1967)
[22] CASSUTO, A.: Temperature Factors in Mass Spectrometry; pp. 283—303; in REED, R. J.: Mass Spectrometry. Academic Press, London 1965
[23] SEHON, A. H., SZWARC, M.: Proc. Roy. Soc. London, Ser. A. **209**, 110 (1951)
[24] KERR, J. A.: Chem. Rev. **66**, 465 (1966)
[25] WEST, C.: Handbook of Chemistry and Physics. 51st edn. The Chemical Rubber Co., Cleveland 1970—1971
[26] SZWARC, M.: Proc. Roy. Soc. London, Ser. A. **207**, 5 (1951)
[27] PAULING, L.: The Nature of the Chemical Bond. Cornell University Press, Ithaca, New York 1940
[28] BAUGHAN, E. C., EVANS, M. G., POLÁNYI, M.: Trans. Faraday Soc., **37**, 377 (1941)
[29] SZWARC, M.: J. Chem. Phys., **18**, 1660 (1950)

Olivér KAPOSI
Miklós RIEDEL
Katalin VASS-BALTHAZÁR
H-1088 Budapest Puskin u. 11—13.

G. Roberto SANCHEZ; C. N. J. C. Calle 25 No 258 Rpto Cubanacan, Habana, Cuba

László LELIK, Egyesült Izzólámpa és Villamossági R. T. H—1169 Budapest Váci út 77.

Acta Chimica Academiae Scientiarum Hungaricae, Tomus 89 (3), pp. 245—256 (1976)

PROPERTIES OF ALCOHOL–AMINE MIXTURES, VIII

EFFECT OF SOLVENT ASSOCIATION ON THE CONCENTRATION DEPENDENCE OF THE ELECTRIC CONDUCTANCE OF AMINE–ALCOHOL AND AMINE–WATER MIXTURES

F. RATKOVICS, M. LÁSZLÓ and T. SALAMON

(Research Group for Electrochemistry Hungarian Academy of Sciences and Department of Physical Chemistry, University of Chemical Industry, Veszprém)

Received June 26, 1975

A study was made of mixtures of *n*-butylamine and *n*-propylamine with alcohols and with water, with regard to the correlation of the electric conductance and the concentration. It was found that the variation of the specific molar conductance as a function of the concentration can be interpreted by a simple association model. In this model, ion formation is conceived as the dissociation of complexes of the type A_nB, containing a single amine molecule and several solvent molecules. The experimental data permit conclusions as to the average degree of association. The values of this for both alcohols and water fit well into the series obtained for the degree of association by other methods.

We have been studying the association conditions of alcohol–amine mixtures in the liquid phase for an appreciable time. These investigations have revealed that numerous physico-chemical characteristics of the mixtures and of the pure components are so closely correlated with the association phenomena that their study can be utilized to refine and supplement the physical picture of association. We are attempting to obtain information on the association conditions with as many methods of examination as possible, for these independent methods permit us to check the assumptions made during the interpretation of the experimental results. In our earlier publications on this topic we have dealt with the study of the vapour–liquid equilibrium of alcohol–amine mixtures, their heats of mixing, dielectric properties, viscosities, and the activation energy of viscous flow, and with the interpretation of the results [1—6]. Finally, in the most recent publication in this series [7], a study was made of the specific electric conductance and its dependence on the concentration and temperature, in mixtures of *n*-butylamine with methanol, ethanol, 1-propanol and 1-butanol. The qualitative evaluation of the results has shown that in that concentration range where we can speak of amine dis- solved in alcohol, *i.e.* when the mixture contains much alcohol compared to the amine, the association and electrolytic dissociation can probably be described by the following equilibria:

$$(\mathrm{ROH})_n + \mathrm{R'NH_2} \rightleftharpoons (\mathrm{ROH})_{n-1}\mathrm{ROH_3NR'} \rightleftharpoons \mathrm{R'NH_3^+} + (\mathrm{ROH})_{n-1}\mathrm{RO^-}$$

It was assumed that primarily the mixed associated species (consisting of both alcohol and amine molecules) containing the more alcohol molecules are

capable of electrolytic dissociation. In the present paper an account is given of further experimental results, and an attempt is made to draw quantitative conclusions from the electric conductance data as to the average composition of the associations (or ion pairs) capable of electrolytic dissociation.

Experimental

The available experimental results were supplemented with new measurements, made as described previously [7]. A study was made of the electric conductance in *n*-propylamine–methanol, *n*-butylamine–water and *n*-propylamine–water mixtures. The results are given in Tables I—IV.

Table I

Specific and molar specific conductance of n-propylamine–methanol mixtures at 20°C

Concentration (mol l^{-1})	$\varkappa$ (μS cm^{-1})	Λ_{am} (Ω^{-1} cm^2)
0.576	178.0	3.09×10^{-1}
1.100	199.0	1.81×10^{-1}
2.020	186.0	9.20×10^{-2}
2.790	156.5	5.60×10^{-2}
3.460	136.5	3.94×10^{-2}
5.040	76.8	1.52×10^{-2}
6.590	48.8	7.40×10^{-3}
8.800	20.6	2.34×10^{-3}
12.100	0.279	2.30×10^{-5}

Table II

Specific and molar specific conductance of n-propylamine–water mixtures at 20°C

Concentration (mol l^{-1}	$\varkappa$ (μS cm^{-1})	Λ_{am} (Ω^{-1} cm^2)
0.576	2930.0	5.10
1.100	3070.0	2.79
2.020	2420.0	1.20
2.790	1835.0	6.58×10^{-1}
3.460	1410.0	4.07×10^{-1}
5.040	571.0	1.13×10^{-1}
6.590	180.0	2.73×10^{-2}
8.800	53.5	6.08×10^{-3}
12.100	0.279	2.30×10^{-5}

Table III

Specific and molar specific conductance of n-butylamine–water mixtures at 20°C

Concentration (mol l^{-1})	$\varkappa$ ($\mu S\ cm^{-1}$)	Λ_{am} ($\Omega^{-1}\ cm^2$)
0.481	2745	5.70
0.631	2910	4.61
0.918	2790	3.04
1.680	2420	1.44
2.330	1720	7.35×10^{-1}
2.880	1535	5.31×10^{-1}
3.880	838	2.16×10^{-1}
5.050	212	4.20×10^{-2}
6.220	111	1.78×10^{-2}
8.420	17.9	2.12×10^{-3}
10.10	0.18	1.78×10^{-5}

Table IV

Specific and molar specific conductance of n-butylamine–water mixtures at 0°C

Concentration (mol l^{-1})	$\varkappa$ ($\mu S\ cm^{-1}$)	Λ_m ($\Omega^{-1}\ cm^2$)
0.631	1780	2.82
0.918	1910	2.08
1.200	2120	1.77
1.680	1445	8.60×10^{-1}
2.330	1115	4.78×10^{-1}
2.880	865	3.00×10^{-1}
3.880	534	1.38×10^{-1}
5.050	200	3.96×10^{-2}
5.050	200	3.96×10^{-2}
6.220	58.6	9.40×10^{-3}
8.420	11.15	1.32×10^{-3}
10.10	0.40	3.96×10^{-5}

In the Tables c is the concentration of the amine, while $\varkappa$ is the specific, and Λ_{am} the specific molar conductance. In these latter calculations the amine was regarded as the solute.

Discussion

The experimental results show that there is barely any difference between the concentration dependences of the specific conductance of aqueous or methanolic solutions containing *n*-propylamine and *n*-butylamine. It appears, therefore, that in this respect the decisive role is played not by the dissolved amine, but by the properties of the solvent. The results obtained with the aqueous solutions fit in with the series of measurements made in mixtures of various alcohols with *n*-butylamine [7], since the nature of the curves describing the conductance as a function of concentration is the same in every system examined. Similarly as in alcoholic solutions, the maximum in the specific conductance is to be found at an amine concentration of about 1 *M* in aqueous solutions. Thus, in the evaluation, water was regarded as the first member of a solvent series consisting of alcohol homologues. (In this conception, the alcohols are regarded as derivatives of water, in which one of the hydrogens of the water has been replaced by an alkyl group.)

Evaluation is facilitated by considering the correlation between the specific molar conductance and the amine concentration. This was not dealt with in the preceding paper [7]. The earlier data supplement the more recent results given in Tables I—IV, and thus the evaluation can be extended to every amine–alcohol mixture investigated to date.

The first question to which an answer was sought was whether the electric conductance of the amine–water and amine–alcohol mixtures can be interpreted in the classical way, *i.e.* by the assumption of a formal dissociation equilibrium such as can be written e.g. in the case of ammonium hydroxide. In the present case, the equilibrium in question would be:

$$ROH_3NR' \rightleftharpoons RO^- + R'NH_3^+$$

where R and R' are any alkyl groups or hydrogen. For the equilibrium constant of the dissociation we may write:

$$K_d = \frac{\alpha^2 c}{1 - \alpha} \tag{1}$$

where K_d is the dissociation constant, and α is the degree of dissociation, which can be expressed by the specific molar conductance. The amines involved are not strongly basic, and therefore the dissociation is presumably only slight, so that:

$$\alpha = \frac{\Lambda_{am}}{\Lambda_{am,\,\infty}} \ll 1 \tag{2}$$

Thus:

$$K_d \approx \alpha^2 c \tag{3}$$

It follows from Eqs (2) and (3) that:

$$K_d \Lambda_{\mathrm{am},\infty}^2 = \Lambda_{\mathrm{am}}^2 c \tag{4}$$

This indicates that, at a given temperature, the product of the concentration and the square of the specific molar conductance is constant. In practice, it was found that for the solutions examined this correlation does not hold, for the above product varies considerably as a function of concentration. As examples, data on the *n*-butylamine–water and *n*-butylamine–methanol systems are presented in Table V.

Table V

Value of the product $\Lambda_{\mathrm{am}}^2 c$ in aqueous and methanolic solutions of n-butylamine, as a function of the concentration (c) at 20 °C

Water		Methanol	
c (mole l^{-1})	$\Lambda_{\mathrm{am}}^2 c$	c (mol l^{-1})	$\Lambda_{\mathrm{am}}^2 c$
0.481	15.70	0.481	6.97×10^{-2}
0.631	13.45	1.082	4.74×10^{-2}
0.918	8.49	1.683	2.11×10^{-2}
1.680	3.50	2.754	5.51×10^{-3}
2.330	1.26	5.050	4.04×10^{-4}
2.880	8.18×10^{-1}	6.730	6.73×10^{-5}
3.880	1.81×10^{-1}	7.855	3.99×10^{-6}
5.050	8.90×10^{-3}	8.978	4.85×10^{-8}
6.200	1.97×10^{-3}		
8.420	3.79×10^{-5}		

It can be seen that the value of the product $\Lambda_{\mathrm{am}}^2 c$ decreases rapidly with increasing amine concentration, and thus the value of the dissociation constant defined in the above manner is strongly concentration-dependent. This finding can be explained in several ways, but it does not contradict our earlier conceptions, for those investigations carried out earlier by other methods [2—4] led to the conclusion that the associated amine–alcohol species, whose dissociation is used to interpret the conductance, do not generally consist only of one alcohol and one amine molecule, but contain several alcohol molecules. Thus, the association process we assumed was the following:

$$(\mathrm{ROH})_n + \mathrm{H_2NR'} \rightleftharpoons (\mathrm{ROH})_{n-1}\,\mathrm{ROH_3NR'}$$

where the value of n giving the degree of alcohol association may be 1, 2, 3, . . . etc. We assume that the mixed associated species (or the ion pair formed from

it as described in the literature) may dissociate in the following manner:

$$(ROH)_{n-1}ROH_3NR' \rightleftharpoons [(ROH)_{n-1}RO^-]\,[^+H_3NR'] \rightleftharpoons (ROH)_1RO_{n-1} + \\ + R'NH_3^+$$

If it is taken into consideration that the mixed species is held together by three hydrogen bonds when $n = 1$ [8], whereas if $n > 1$ then the number of hydrogen bonds linking the nitrogen and oxygen atoms is at most two, it must be concluded that mixed species containing more alcohol molecules are more likely to dissociate. It must be noted here that essentially the same assumption is accepted for water, when the high ionic mobilities of H^+ and OH^- are explained by the prototropic conductance mechanism, and these ions are conceived of as a cluster of water molecules with a proton excess or deficiency. This conception is not contradicted by the assumption of the solvation of the RO^- ions, for if the solvation is accompanied by the formation of hydrogen bonds, then the final product is the assumed anion $(ROH)_{n-1}RO^-$. Solvation of the cations $R'NH_3^+$ may also be considered, but the formation of such a solvated $R'NH_3^+$ ion would imply dissociation of the alcohol–amine mixed species in such a way that the alcohol molecules would separate into two groups: either bound to the cation, or forming an independent anion. The possibility of this cannot be excluded, but we do not regard it as probable, since the assumption of such a separation of the alcohol molecules is in contradiction with the finding that the pure alcohols are very poor conductors, for the very reason that the alcohol associations do not separate into groups with either proton excess or proton deficiency, *i.e.* into ions. (The specific electric conductances of the pure alcohols are at least one order of magnitude smaller than those of the solutions examined.) From all these considerations, therefore, the above dissociation equilibrium is regarded as the most probable.

An attempt was made to use the physical picture outlined above to form a model for the interpretation of the phenomena studied: a model which also allows conclusions to be drawn as to the average compositions of the alcohols and the associated alcohol–amine species.

The fact that the association conditions of alcohols can by no means be regarded as clarified, compels us a priori to make assumptions with respect to alcohol association. However, this does not exclude the possibility of applying a model, as numerous examples can be found in the literature where a given phenomenon can be equally well interpreted by different association models. (For example, the vapour–liquid equilibrium data for *n*-propylamine-*n*-hexane mixtures can be calculated with practically the same accuracy with the MECKE—KEMPTER model, which assumes an infinite chain association for the amine, or with the model based on the assumption of cyclic tetramers [9].)

In these models it is customarily assumed that the associated species and the monomers form ideal mixtures with each other [10].

On the above basis, the mixed clusters of the alcohol–amine mixture should be replaced in the model by an association complex of composition A_nB, consisting of n molecules of alcohol and one molecule of amine (A and B, respectively). Thus, the electric conductance of the mixture may be attributed to the ions formed upon dissociation:

$$A_nB \rightleftharpoons A_n^- + B^+$$

(It must be noted that the number, n, of alcohol molecules forming the assumed anion is definitely closely connected with the average degree of association of the mixed species formed in the actual system, although it is not necessarily identical with this, for it is conceivable that the species AB dissociate to a lesser extent than the species A_nB ($n > 1$) and thus the average number of alcohol molecules in the mixed clusters differs from the average number of alcohol molecules comprising the anions. In the case assumed here the latter quantity is larger than the former.)

The dissociation constant of the complex described in the model is:

$$K_d = \frac{[A_n^-]\,[B^+]}{[A_nB]} = \frac{\alpha^2 c}{1-\alpha} \approx \alpha^2 c \tag{5}$$

where α is the degree of dissociation, presumably much less than unity, and c is the concentration of the mixed complex A_nB. If the degree of dissociation is expressed in terms of the specific molar conductance:

$$\alpha = \frac{\Lambda}{\Lambda_\infty} = \frac{\varkappa}{\Lambda_\infty c} \tag{6}$$

and thus:

$$K_d \Lambda_\infty^2 \approx \frac{\varkappa^2}{c} \tag{7}$$

where Λ is the molar specific conductance of the mixed complex, and Λ_∞ is the same quantity at infinite dilution.

Let us regard the alcohol as an ideally associated mixture as proposed by PRIGOGINE [10], *i.e.* let us assume that the associated complex and the monomer in the pure alcohols form an ideal mixture with each other. We may then write the equilibrium constant, K_n, for the association reaction of the alcohol in terms of the concentrations of the complex, A_n, and the monomer, A_1:

$$K_n = \frac{[A_n]}{[A_1]^n} \tag{8}$$

The equilibrium constant of mixed association can be written in a similar manner, assuming that the previous model for the alcohol is valid in the presence of the amine too:

$$K_a = \frac{[A_nB]}{[A_n][B_1]} = \frac{[A_nB]}{K_n[A_1]^n[B_1]} \tag{9}$$

where $[B_1]$ is the concentration of the monomeric amine molecules. As regards the concentrations of monomeric alcohol and amine, these are proportional to the nominal concentrations of the components, c_{alc} and c_{am}, since our viscosity measurements [4] show that in an amine–alcohol mixture the average degree of association of the mixture decreases monotonously and almost linearly, on proceeding from the pure alcohol towards the pure amine. Accordingly, the equilibrium constant of association can be given in terms of the nominal concentrations too.

To a first approximation, let:

$$[A_1] = k_a c_{alc} \tag{10}$$

$$[B_1] = k_b c_{am} \tag{11}$$

and thus, from Eq. (9):

$$K_a = \frac{[A_nB]}{K_n k_a^n c_{alc}^n k_b c_{am}} \tag{12}$$

If the constants are combined: $K_a K_n k_a^n k_b = \beta$, and if the substitution $[A_nB] = \beta c_{alc}^n c_{am} \approx c$ is performed, taking into account Eqs (12) and (5), since in the sense of (6) $\alpha = \varkappa / c\Lambda_\infty$, for the degree of dissociation of the mixed association we obtain that:

$$\alpha = \frac{\varkappa}{\Lambda_\infty \beta_{alc}^n c_{am}} \tag{13}$$

Hence, on the basis of Eq. (5):

$$\Lambda_\infty^2 K_d = \frac{\varkappa^2}{\beta c_{alc}^n c_{am}} = \frac{\varkappa^2}{c_{am}^2} \cdot \frac{c_{am}}{\beta c_{alc}^n} \tag{14}$$

The first factor on the right-hand side of this relation is the square of the specific molar conductance calculated with the nominal concentration, *i.e.* the square of Λ_{am} given in the Tables, and thus:

$$c_{alc}^n \beta K_d \Lambda_\infty^2 = \Lambda_{am}^2 c_{am} \tag{15}$$

Taking logarithms in Eq. (5):

$$n \log c_{alc} + \log(\beta K_d \Lambda_\infty^2) = \log(\Lambda_{am}^2 c_{am}) \tag{16}$$

It follows from Eq. (16) that if the model is suitable for describing the phenomenon, then the expression log $(\Lambda_{am}^2 c_{am})$ will give a straight line as a function of the logarithm of the alcohol concentration, and the slope of this straight line will yield the number of alcohol molecules in the mixed complex assumed in the model, *i.e.* the value of n.

For purposes of clarity, the simplifying assumptions made in the course of the derivation of (16) are listed below:

1. It was assumed that the electric conductance of the amine–alcohol mixtures is due to ions formed from the mixed complex of type A_iB.

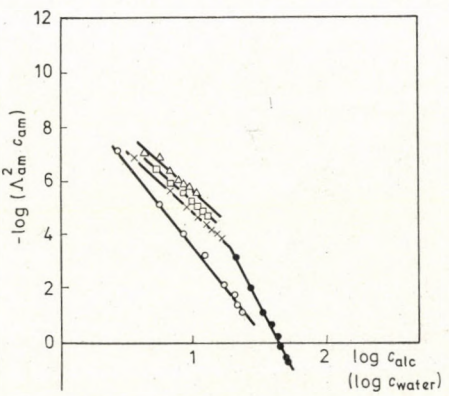

Fig. 1. μlog(Λ_{am} c_{am}) *vs.* log $c_{solvent}$ plots for n-butylamine alcohol and *n*-butylamine–water mixtures. Data measured at 0 °C (○ methanol, × ethanol, □ 1-propanol, △ 1-butanol, ● water)

2. In the model employed to interpret the conductance the various complexes A_iB were replaced by an association complex of composition A_nB.

3. It was assumed that the ideally associated mixture model proposed by PRIGOGINE [10] is valid in the amine–alcohol mixture and in pure alcohol too.

4. It was assumed for the degree of dissociation of the mixed complex than $\alpha \ll 1$.

5. It was assumed that to a first approximation the concentrations of the monomeric alcohol and amine molecules in the alcohol mixture are proportional to the nominal concentrations of the alcohol and amine.

The $-\log(\Lambda_{am}^2 c_{am})$ *vs.* log c_{alc} plots of the experimental results are shown in Figs 1—3.

The diagrams reveal that, in accordance with expectations, these plots are linear for the various alcohols and for water too. The deviations from linearity can be attributed partly to errors in the measurements, and partly to the simplifying assumption that the concentrations of the monomers of the solvent and solute in the mixtures in question vary linearly as a function of the nominal concentrations. In the alcoholic solutions there is a larger deviation

only for $\log c_{alc} < 0.4$, *i.e.* when the mixture consists predominantly of amine and not of alcohol. In this range it can no longer be expected that a significant amount of mixed complex A_nB be formed. This is also indicated by the fact that mixtures containing little alcohol have very low electric conductances.

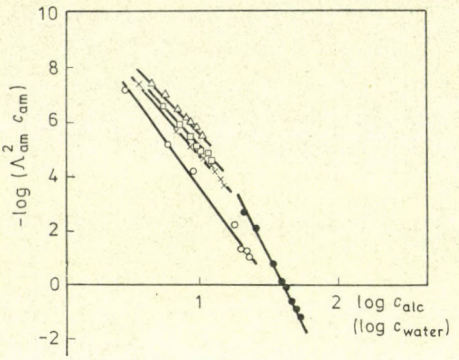

Fig. 2. $\mu\log (\Lambda_{am}^2 c_{am})$ *vs.* $\log c_{solvent}$ plots for *n*-butylamine–alcohol and *n*-butylamine–water mixtures. Data measured at 20 °C (○ methanol, × ethanol, □ 1-propanol, △ 1-butanol, ● water)

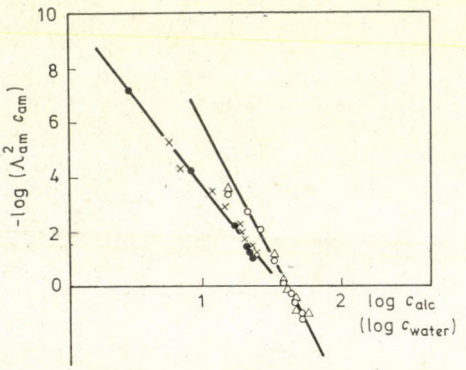

Fig. 3. $\mu\log (\Lambda_{am}^2 c_{am})$ *vs.* $\log c_{solvent}$ plots for aqueous and methanolic solutions of *n*-butylamine and *n*-propylamine. Data measured at 20 °C (× *n*-butylamine in methanol, △ *n*-butylamine in water, ● propylamine in methanol, ○ *n*-propylamine in water)

The results obtained in methanolic solution show that in solutions containing little amine ($\log c_{alc} > 1.2$) the value of n is larger, and becomes similar to the value observed in the other alcohols only in systems containing more amine. This was not taken into consideration in the evaluation, but the average value of n was determined.

By the exchange of roles of the solvent and solute we can probably also explain the fact that the temperature coefficient of the specific conductance changes its sign in roughly this concentration interval [7].

The data measured in aqueous solution give a straight line only for log $c_{water} < 1.3$, *i.e.* up to a concentration of 20 *M*. This can probably be explained by the significantly different association properties of water and the alcohols. The negative slopes of the straight lines in the Figure give the number of solvent molecules participating in the assumed association reaction. These are listed in Table VI.

Table VI

Negative slopes (n) of the $-\log(\Lambda^2_{am}\, c_{am})$ *vs.* $\log c_{solvent}$ *plots*

Mixture	$-\tan\theta = n$	
	20 °C	0 °C
n-butylamine–1-butanol	5.10	4.43
n-butylamine–1-propanol	5.34	4.54
n-butylamine–ethanol	5.60	4.62
n-butylamine–methanol*	6.55	6.25
n-butylamine–water	10.30	10.20
n-propylamine–methanol	6.55	—
n-propylamine–water	10.30	—

* Average value over the range studied

Figure 3 depicts the results obtained for methanolic and aqueous solutions of *n*-butylamine and *n*-propylamine. It appears that the results for the two amines do not differ with regard to the solvent: the data for aqueous and methanolic solutions lie on one straight line for a given amine. Accordingly, in agreement with our conceptions, the phenomenon under examination depends primarily on the association properties of the solvent.

If the data of Table VI are inspected, two tendencies can be established. It is clear that the number of solvent molecules involved in the assumed mixed association increases with the decrease of the molar mass of the solvent; it also decreases to a slight extent with the decrease of temperature. The values of *n* from 4.43 to 6.55 agree with the results of our earlier investigations by a different method. Viscosity measurements gave a value increasing from 3.24 to 3.70 upon going from 1-butanol to methanol for the average degree of association of the alcohol. The activation energy of viscous flow yielded results increasing from 3.66 to 4.43 for this same quantity. If we set out from the consideration mentioned earlier, that, as regards the mixed complexes, those containing several alcohol molecules will have lower dissociation energies than AB, it appears understandable that we obtain results somewhat higher than the average degree of association of the alcohol for the value of *n* on the basis of the electric conductance data.

With regard to the aqueous solutions, data suitable for such a comparison were not found, but various authors [11—14] maintain that in this temperature range the number of hydrogen bonds broken at a given instant can be estimated as about 10—15% of the total number of possible hydrogen bonds. This physical picture can be compared with the value of $n = 10.3$ which we determined.

The similar nature of the properties of alcoholic and aqueous solutions permits the conclusion that in the amine-containing solutions in question the relatively high electric conductance in both aqueous and alcoholic solutions can be explained by the high mobilities of the anions. It follows from this, however, that the prototropic conductance mechanism may play an important role in alcoholic solutions too. It seems very probable that a significant proportion of the electric conductance of the amine alcohol mixtures stems from the phenomenon that an alcohol complex deficient in one proton, and acting as anion, acquires a proton from a neighbouring neutral molecular cluster, thereby becoming neutral, while the previously neutral species takes over the role of anion as a result of its proton deficiency. This physical picture is in agreement with the finding that at lower temperature, where the average degree of association of the dissociating mixed complexes is smaller (see Table VI), in the concentration range considered the specific conductance decreases with the decrease of temperature [7]. With regard to why the mixed complexes containing fewer alcohol molecules dissociate to a larger extent at lower than at higher temperature, we cannot as yet give a definite explanation, but we consider it possible that the phenomenon is connected with a change in the association conditions of the alcohols, with enhanced ring-formation, and hence with the decrease average number of monomers in the alcohol clusters.

REFERENCES

[1] RATKOVICS, F., LISZI, J., LÁSZLÓ, A.: Magy. Kém. Foly. **79,** 273 (1973)
[2] RATKOVICS, F., LÁSZLÓ, A.: Magy. Kém. Foly. **79,** 276 (1973)
[3] LISZI, J., SALAMON, R., RATKOVICS, F.: Magy. Kém. Foly. **79,** 468 (1973)
[4] RATKOVICS, F., SALAMON, T., DOMONKOS, L.: Magy. Kém. Foly. **80,** 155 (1974)
[5] RATKOVICS, F., GUTI, Zs].: Magy. Kém. Foly. **80,** 159 (1974)
[6] RATKOVICS, F., SALAMON, T., DOMONKOS, L.: Magy. Kém. Foly. **80,** 264 (1974)
[7] RATKOVICS, F., LÁSZLÓ, A.: Magy. Kém. Foly. **80,** 310 (1974)
[8] HUYSKENS, P., HUYSKENS, T. Z.: Bull. Soc. Chim. Belg., **69,** 267 (1960)
[9] KEHIAIAN, H.: Bull. Acad. Polon. Sci. Chim., **14,** 703 (1966)
[10] PRIGOGINE, I., DEFAY, R.: Chemische Thermodynamik. VEB Deutscher Verlag, Leipzig 1962.
[11] HORNE, R. A.: Water and Aqueous Solutions. Wiley, London 1971
[12] LUCK, W.: Disc. Faraday Soc., **43,** 115 (1967)
[13] HINDMAN, J.: J. Chem. Phys., **44,** 4582 (1966)
[14] MULLER, N.: J. Chem. Phys., **43,** 2555 (1965)

Ferenc RATKOVICS
Mária LÁSZLÓ
Tamás SALAMON
H—8201 Veszprém Pf. 28.

Acta Chimica Academiae Scientiarum Hungaricae, Tomus 89 (3), pp. 257—263 (1976)

SOLUTE–SOLVENT INTERACTION IN AQUEOUS SOLUTIONS OF NON-ELECTROLYTES: VISCOSITY EFFECTS

AMINA M. HAFEZ and H. SADEK

(Chemistry Department, Faculty of Science, Alexandria University, Alexandria, A. R. E.)

Received September 5, 1975

Solute–solvent interactions were studied by viscosity measurements in the aqueous solutions of methanol, ethanol, *t*-butanol–glycerol, dioxan, methylcellosolve, acetone, acetonitrile and dimethylsulfoxide. Molecular complexes can be detected in all systems. The data were discussed in the light of HARMS' theory.

Introduction

In recent years several publications appeared concerning the nature of the intermolecular structure of water. The main assumption involved was that liquid water exists in the form of aggregates, in which water molecules are connected into a network-like structure through hydrogen bonds. The aggregates which may take different shapes can be dimers with a structure similar to that of diborane, or rings of 3, 4, 5 or 6 molecules as suggested by AGENO [1], who developed structural models based on the assumption that each oxygen atom has four tetrahedral orbitals. Each collective bond involves one lone and one occupied orbital. Thus, each molecule of water can participate in no more than two hydrogen (collective) bonds. On the other hand aggregates may assume the "iceberg" form suggested by FRANKS and EVANS [2] or the "cluster" form as proposed by NÉMETHY and SCHERAGA [3]. These authors based their suggestions on the "flickering-cluster" model of FRANKS and WEN [4].

On mixing alcohol with water, contraction in volume is observed in many systems [5—11]. This contraction can be attributed to the occupation of free volume or cavities in the open solvent structure by the other component, and can be expressed by the relationship:

$$\Delta V = \frac{x_1 M_1 + x_2 M_2}{d_{12}} - \left[x_1 \frac{M_1}{d_1^\circ} + x_2 \frac{M_2}{d_2^\circ} \right]. \qquad (1)$$

Thus, a plot of ΔV *vs.* x_1 (the mole fraction of the solute) shows a minimum at which the organic solvent–water "complex" is assumed to be present.

In this paper these studies will be extended to viscosity measurements in various organic solvent–water systems. Use is made of the data in the literature as well as those obtained in this laboratory. This study includes the following systems:

(1) MeOH—H_2O [12], (2) EtOH—H_2O [13], (3) *t*-BuOH—H_2O [14], (4) glycerol (GOH)—H_2O [7], (5) dioxane (D)—H_2O [8], (6) methylcellosolve (MCS)—H_2O [11], (7) Me_2CO—H_2O [13], (8) MeCN—H_2O [15], and (9) Me_2SO—H_2O [16].

The suggested "complex" formation will be discussed in the light of HARMS' [17] theory.

Results and discussion

I. Absolute viscosity vs. mole fraction curves

Figure 1 shows the variation of the absolute viscosity of the mixture with the mole fraction (x_1) of the organic component for the 6 systems. As can be readily seen, maxima are observed with the exception of system (4). These maxima can be attributed to the variation of water structure upon the addition of alcohol, since the structure collapses owing tothe breaking of H-bonds in the water aggregates. The maxima represent a 1 : 2 organic solvent–water "complex".

AGENO [18] explains the presence of a maximum in the MeOH—H_2O system assuming that, at this concentration, all hydrogen bonds available in water at the given temperature are saturated by alcohol molecules. If the alcohol concentration is further increased, the viscosity of the mixture should decrease toward that of pure methanol.

KAY *et al.* [19] studied systems (2) and (5) and suggested that the structural effect is a maximum at low ethanol concentration, and the composition corresponding to the viscosity maximum is the result of two conflicting effects much like the maximum on the density curve of pure water.

FRANKS [10] have found that in the case of system (2), $d\eta/dc$ increases with increasing concentration, indicating an increased structural effect, which reaches a maximum, whereas according to KAY and BROADWATER [20], $d\eta/dc$ decreases with increasing dioxan concentration for system (5). FRANKS [10] put forward an explanation for these two types of behaviour. Small additions of non-electrolytes to water cause an increase in long-range order or an increase in the half-life of the structured entities existing in water. Through hydrogen bonding, the structural integrity of liquid water is probably enhanced. The maximum occurring in systems (2) and (5) was attributed to structure promotion.

However, in glycerol–water the "complex" cannot be detected from the η *vs.* x_1 plot. On the basis of the ΔV *vs.* x_1 plot it should have the composition [GOH·3(H_2O)] [7]. On the other hand, DARBARI *et al.* [21] studied the sound adsorption in this system and deduced the formula [GOH·6(H_2O)].

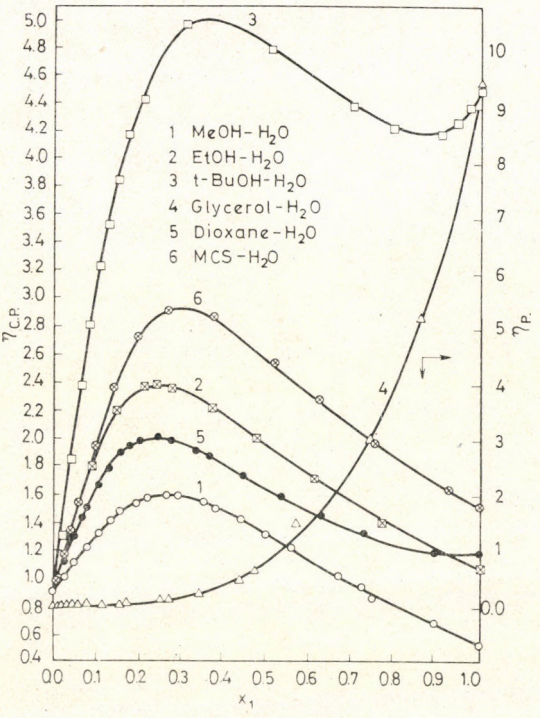

Fig. 1. Variation of absolute viscosity with composition

Apparently, systems (5) and (6) show viscosity variations similar to those observed for alcohol–water systems. This behaviour is expected since hydrogen bond formation would be strong with structures containing more than one oxygen atom.

Figure 2 comprises a second group of systems (7—9), in which the organic liquid possesses unsaturation at a carbon atom $\left(\begin{matrix}Me\\Me\end{matrix}\!\!>\!C=O\right)$, a nitrogen atom (Me—C=N), or at a sulfur atom $\left(\begin{matrix}Me\\Me\end{matrix}\!\!>\!S=O\right)$.

The "complex" [1 organic solvent·6(H_2O)] can be easily detected from Figure 2 in systems (7) and (8). At the same time the data of COWIE and TOPOROWSKI [16] show that probably a $Me_2SO \cdot 2(H_2O)$ "complex" is formed. These authors have found that the maximum on the viscosity isotherm de-

creases with increasing temperature. This led them to suggest that "the system Me_2SO–H_2O" belongs to the class of solutions possessing numerous solute water bonds which are stronger than the hydrogen bonds between water molecules. The "complex" formed is thermally labile and would only be expected to exist in a completely undissociated state at low temperatures.

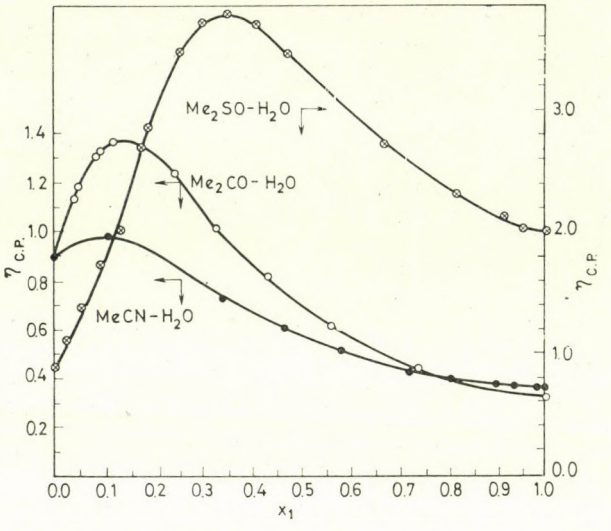

Fig. 2. Variation of absolute viscosity with composition

II. Deviations in the viscosity of binary mixtures

Many authors [22—31] have suggested equations which correlate the viscosity of binary mixtures with those of the components. The conclusion drawn was that viscosity is a non-additive property and there is always deviation from linear additivity.

HARMS' *et al.* [17] suggested the following relationship for the viscosity of a binary liquid mixture:

$$\eta_{M_{12}} = x_1 \eta_{M_1} + x_2 \eta_{M_2}, \tag{2}$$

where η_M is the molar viscosity representing the force which acts via the linear velocity gradient on a stationary plane of area $V_M^{2/3}$ at a distance $V_M^{1/3}$ (V_M is the molar volume). It is independent of the state of matter and the type of the molecules and is given by

$$\eta_M = \eta \, V_M^{1/3} . \tag{3}$$

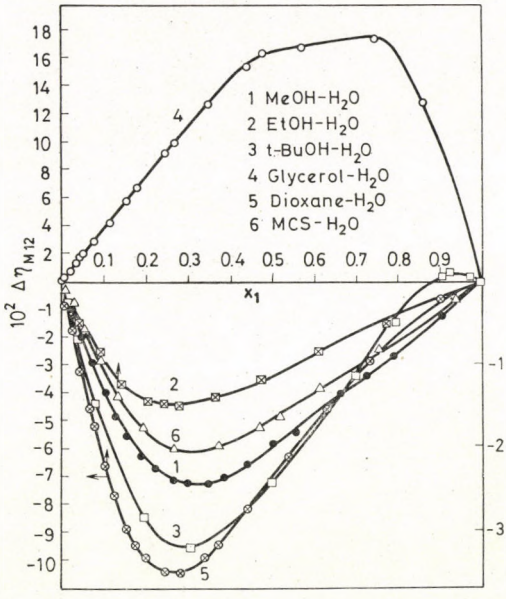

Fig. 3. Variation of $\Delta\eta_{M_{12}}$ with composition

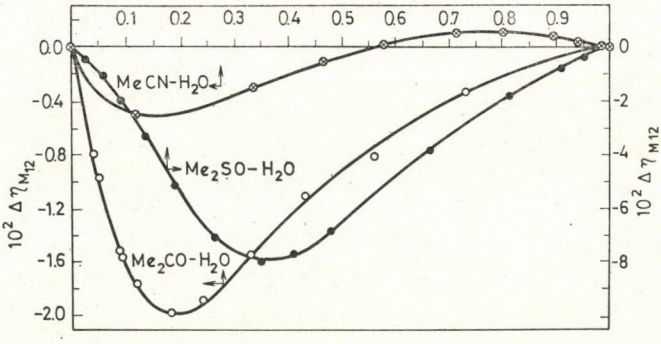

Fig. 4. Variation of $\Delta\eta_{M_{12}}$ with composition

The divergence from linearity ($\Delta\eta_{M_{12}}$) can be obtained from the relationship

$$\Delta\eta_{M_{12}} = \eta^{\text{calcd.}} - \eta^{\text{exptl.}}$$
$$= x_1\eta_1 V_{M_1}^{1/3} + x_2\eta_2 V_{M_2}^{1/3} - \eta_{12} V_{M_{12}}^{1/3} \qquad (4)$$

Figures 3 and 4 show variation of the deviation $\Delta\eta_{M_{12}}$ with x_1. As can be readily seen, a maximum is only observed in the case of system (4). The minima in the other systems occur at mole fractions approximately equal to those corresponding to the maxima in the η *vs.* x_1 plot. Also, it is obvious

that the depth of the minimum can be regarded as a measure of the interaction, which decreases in the following order

$$D\text{–}H_2O > t\text{-BuOH–}H_2O > MeOH\text{–}H_2O > MCS\text{–}H_2O > EtOH\text{–}H_2O .$$

For the unsaturated organic solvent–water systems the following order is obtained

$$Me_2CO\text{–}H_2O > Me_2SO\text{–}H_2O > MeCN\text{–}H_2O .$$

HARMS' *et al.* [17] obtained positive $\Delta\eta_{M_{12}}$ values for the systems CCl_4 with hexane, CS_2, C_6H_6, EtOH, PrOH and BuOH, benzene with MeOH, EtOH, BuOH or Me_2CO, EtOH with CS_2 or dioxan, and acetone with hexane, where maxima were always observed. No negative values of $\Delta\eta_{M_{12}}$ were reported by these authors. Positive and negative $\Delta\eta_{M_{12}}$ values were explained by HARMS' *et al.* [17] in the light of the molecular theory of internal friction (or lubrication) due to mixing. They considered the mixing of two liquids, one consisting of molecules with free polar groups which form large molecules (*e. g.* alcohols), and the other consisting of non-polar molecules which do not tend to associate. On dilution of the polar with the nonpolar component, association and/or dissociation of the aggregates occur. With further dilution, the equilibrium between these two processes will be shifted towards the formation of simple molecules. Therefore, they were able to explain the viscosity data in terms of two possibilities:

1. Single, large polar molecules which interact but weakly with the molecules of the nonpolar component. Through breakdown of the large aggregates, the number of loose positions increases thus the internal friction will be small. The mixing process is generally associated in this case with enhanced internal lubrication.

2. Single, large polar molecules interact strongly with the molecules of the nonpolar component. Through breakdown of the large units of the polar component, a number of new loose positions appears. On the other hand, a great number of the loose points already present are fixed through interaction between the large polar molecules and the molecules of the nonpolar component (solvation).

According to this concept, it is clear that internal lubrication occurs in the GOH–H_2O system and, at low water concentrations, also in the *t*-BuOH–H_2O and MeCN–H_2O systems, while negative $\Delta\eta_{M_{12}}$ values enhance internal friction in the other systems. It is very difficult to predict whether molecules in a given pair of liquids will facilitate or hinder each other's hydrodynamic motion.

It can be suggested that HARMS' theory is applicable to systems in which both components are polar liquids.

REFERENCES

[1] AGENO, M.: Proc. Natl. Acad. Sci., **57**, 567 (1967)
[2] FRANK, H. S., EVANS, M. V.: J. Chem. Phys., **13**, 507 (1945)
[3] NÉMETHY, G., SCHERAGA, H. A.: J. Chem. Phys., **36**, 3382, 3401 (1962)
[4] FRANK, F. S., WEN, Y. M.: Disc. Faraday Soc., **24**, 133 (1957)
[5] FRANKS, F., IVES, D. J. G.: Quart. Rev. **20**, 1 (1966)
[6] NAKANISHI, K., KATO, N., MARUYAMA, M.: J. Phys. Chem., **71**, 814 (1967)
[7] SADEK, H., HAFEZ, A. M., KHALIL, F. Y.: Electrochim. Acta, **14**, 1089 (1969)
[8] SADEK, H., HAFEZ, A. M.: to be published
[9] GRIFFITHS, V. S.: J. Chem. Soc. (**1952**), 1326
[10] FRANKS, F.: In "Physico-chemical Processes in Mixed Aqueous Solvents" ed. F. Franks, p. 50 Heinemann, London 1967
[11] SADEK, H., EL-HARAKANY, A.: Electrochim. Acta, **16**, 339 (1971)
[12] Unpublished results
[13] International Critical Tables, McGraw-Hill, New York, **5**, 22 (1929)
[14] BROADWATER, T. L., KAY, R. L.: J. Phys. Chem., **74**, 3802 (1970)
[15a] D'APRANO, A., FUOSS, R. M.: J. Phys. Chem., **73**, 400 (1969)
[15b] COPLAN, M. A., FUOSS, R. M.: J. Chem. Phys., **68**, 1181 (1964)
[16] COWIE, J. M. G., TOPOROWSKI, P. M.: Can. J. Chem., **39**, 2240 (1961)
[17] HARMS, H., RÖSSLER, H., WOLF, K. L.: Z. phys. Chem. B **41**, 321 (1938)
[18] AGENO, M.: Proc. Natl. Acad. Sci., **57**, 856 (1967)
[19] KAY, R. L., cited in Ref. [10] p. 70
[20] KAY, R. L., BROADWATER, T. L.: Electrochim. Acta, **16**, 667 (1971)
[21] DARBARI, G. S., SINGH, R. P., VERMA, G. S., RAJAGOPLAN, S.: Nuovo Cimento, B **52** 1 (1967)
[22] KENDALL, J., VENTESKAPSAKED, M. K.: Nobelinst., **2**, (1913)
[23] LEES, C. H.: Phil. Mag., **6**, 128 (1901)
[24] BINGHAM, E. C.: Am. Chem. J., **34**, 481 (1905): Phys. Rev., **35**, 407 (1912)
[25] DRUCKER, K., KASSEL, R.: Z. phys. Chem., **76**, 367 (1911)
[26] LANTIÉ, R.: Bull. Soc. Chim., 168 (1946)
[27] ARRHENIUS, S.: Z. phys. Chem., **1**, 285 (1887)
[28] NOYES, A. A., FALK, K. G.: J. Amer. Chem. Soc., **34**, 454 (1912)
[29] KENDALL, J., WRIGHT, A. H.: J. Amer. Chem. Soc. **42**, 1776 (1920)
[30] KENDALL, J., MONROE, K. P.: J. Amer. Chem. Soc., **39**, 1802 (1917)
[31] KENDALL, J., MONROE, K. P.: J. Amer. Chem. Soc., **43**, 115 (1921)

AMINA M. HAFEZ
H. SADEK
Chemistry Department, Faculty of Science,
Alexandria University, Alexandria, A.R.E.

Acta Chimica Academiae Scientiarum Hungaricae, Tomus 89 (3), pp. 265—273 (1976)

HETEROCYCLISCHE β-ENAMINOESTER, 16[1]

ZUR REAKTION HETEROAROMATISCHER β-ENAMINOESTER MIT MALEINSÄUREANHYDRIDEN DIE PHOTO-DIMROTH-UMLAGERUNG VON 5-AMINO-4-ÄTHOXYCARBONYL-1-PHENYL-1,2,3-TRIAZOL

G. SZILÁGYI* und H. WAMHOFF

(Organisch-Chemisches Institut der Universität Bonn D 5300–Bonn, Max-Planck-Str. 1)

Eingegangen am 10. Januar 1975

2-Amino-3-äthoxycarbonyl-4,5,6,7-tetrahydro-benzothiophen **1** und 5-Amino-4-äthoxycarbonyl-pyrazol **4** reagieren mit Maleinsäureanhydriden unter Bildung substituierter Maleamidsäure-Derivate (**3**, **5**). Die Reaktivität von **3** und **5** sowie die Bereitschaft zu Ringschlußreaktionen werden untersucht. 5-Amino-4-äthoxycarbonyl-1-phenyl-1,2,3-triazol **12** lagert sich photosensibilisiert in das 5-Anilino-4-äthoxycarbonyl-1,2,3-triazol **14** um.

Die cyclophile Doppelbindung des Maleinsäureanhydrids und seiner Derivate reagiert bei UV-Bestrahlung mit zahlreichen Doppel- und Dreifachbindungen unter $2 + 2 \rightarrow 4$ Cycloaddition [2]. Es lag daher nahe, die photochemische Reaktivität der Doppelbindung eines heterocyclischen β-Enaminocarbonyl-System gegenüber diesem Cyclophilen zu untersuchen [3]: Wie wir früher berichten konnten [4], reagiert β-Amino-crotonsäureäthylester mit Maleinsäureanhydrid anstatt einer Cycloaddition unter Bildung von 3-Äthoxycarbonyl-4-carbomethoxy-2-methyl-2-pyrrolin-5-on.

Bei der UV-Bestrahlung der heterocyclischen β-Enaminoester (wie z. B. 1,2,3-Triazolyl-, 1,2-Oxazolyl-, 4,5-Dihydro-furyl- und Thienyl-, 1-Methyl (oder Phenyl)-pyrazolyl- und 4,5,6,7-Tetrahydro-benzthienyl-) in Gegenwart von Maleinsäureanhydriden **2a—c** konnten wir jedoch keine Photo-Reaktion feststellen. Diese geringe cyclophile Aktivität der heterocyclischen β-Enaminoester gegenüber dem Maleinsäureanhydrid erklären wir mit der β-Enaminocarbonyl-Struktur: die nukleophile Kraft der Aminogruppe ist zu schwach ausgebildet (nukleophiles Zentrum: C–3 Atom [5]). Die Reaktivität der olefinischen Doppelbindung ist zudem wegen der "push-pull"-artigen-Resonanzstabilisierung nur mäßig ausgebildet.

Bei der thermischen Umsetzung äquimolarer Mengen von 2-Amino-3-äthoxycarbonyl-4,5,6,7-tetrahydro-benzothiophen **1** [6] mit Maleinsäureanhydrid **2a** (in Tetrahydrofuran) bildet sich — nach nukleophilem Angriff der Aminogruppe an ein Anhydrid –C=O– N-(3-Äthoxycarbonyl-4,5,6,7-tetrahydro-2-benzthienyl)-maleamidsäure **3a**. Mit Dibrom-maleinsäureanhydrid

*Stipendiat der Alexander von Humboldt-Stiftung von Febr. 1972 bis Mai 1973.

2b und Phatalsäureanhydrid **2c** reagiert **1** ferner zu den entsprechenden Derivaten von **3**:

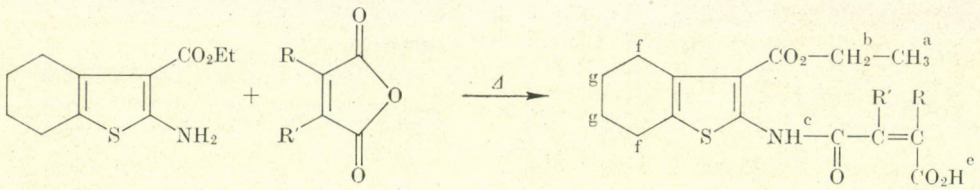

1 **2a–c** **3a–c**

a R = R′ = H
b R = R′ = Br
c R = R′ = —(CH=CH—CH=CH)—

Auf analoge Weise reagiert 5-Amino-4-äthoxycarbonyl-pyrazol [7] **4** mit **2a** und **2c** zum Derivat **5**:

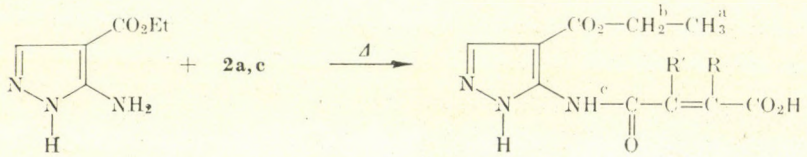

5a,b

a R = R′ = H
b R = R′ = —(CH=CH—CH=CH)—

Nach Hydrierung (**6**) (Pd/C) erhält man unter nachfolgender Decarboxylierung die Propionamido-Derivate **7**.

Mit Methanol/Borfluorid-äthylätherat [8] gelingt eine Überführung von **3a**, **b**, **6** in die Methylester **8a–c**. **3a** reagiert mit Thionylchlorid und anschließend mit Allylamin zu dem Allylamido-Derivate **9** (s. Tab. I).

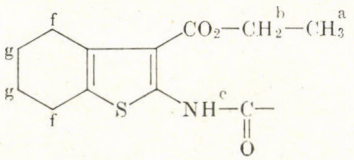

6 $CH_2^dCH_2^{d'}CO_2H$
7 $CH_2^dCH_3^{d'}$
8a $CH^d{=}CH^{d'}CO_2CH_3^e$
b $CBr{=}CBrCO_2CH_3^e$
c $CH_2^dCH_2^{d'}CO_2CH_3^e$
9 $CH^d{=}CH^{d'}CONH\text{-}allyl^{e_{1-3}}$

Tabelle I

Ausbeuten, Schmelzpunkte und analyt. Daten von **3a—c, 5a—b, 6, 7, 8a—c,** *und* **9**

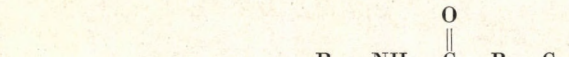

Verb.	R	B	C	Ausb. %	Schmp.	Summenformel (Mol.-Gew.)		Analyse C	Analyse H	Analyse N
3a	R^1	CH=CH	CO_2H	79,0	181—183°	$C_{15}H_{17}NO_5S$ (323,36)	Ber.	55,71	5,30	4.33
							Gef.	55,45	5,18	4,32
3b	R^1	CBr=CBr	CO_2H	62,3	178—180°	$C_{15}H_{15}Br_2NO_5S$ (481,18)	Ber.	37,44	3,14	2,91
							Gef.	37,38	3,20	2,84
3c	R^1	o · C_6H_4	CO_2H	32,2	172—174°	$C_{19}H_{19}NO_5S$ (373,42)	Ber.			3,75
							Gef.			3,75
5a	R^2	CH=CH	CO_2H	54,0	182—184°	$C_{10}H_{11}N_3O_5$ (253,21)	Ber.	47,43	4,38	16,60
							Gef.	47,49	4,41	16,82
5b	R^2	o · C_6H_4	CO_2H	46,2	161—163°	$C_{14}H_{13}N_3O_5$ (303,27)	Ber.			13,86
							Gef.			13,88
6	R^1	CH_2—CH_2	CO_2H	38,5	165—168°	$C_{15}H_{19}NO_5S$ (325,38)	Ber.			4,30
							Gef.			4,28
7	R^1	CH_2—CH_2	H	40,5	210—212°	$C_{14}H_{19}NO_3S$ (281,37)	Ber.			4,98
							Gef.			4,79
8a	R^1	CH=CH	CO_2CH_3	86,0	119—120°	$C_{16}H_{19}NO_5S$ (337,39)	Ber.			4,15
							Gef.			4,15
8b	R^1	CBr=CBr	CO_2CH_3	52,0	146—148°	$C_{16}H_{17}Br_2NO_5S$ (495,20)	Ber.			2,82
							Gef.			2,82
8c	R^1	CH_2CH_2	CO_2CH_3	64,5	93— 96°	$C_{16}H_{21}NO_5S$ (339,41)	Ber.			4,13
							Gef.			3,99
9	R^1	CH=CH	CONH-allyl	21,0	192—193°	$C_{18}H_{22}N_2O_4S$ (362,44)	Ber.			7,73
							Gef.			7,30

Tabelle II

Spektroskopische Daten

Verb.	UV (in Methanol)[a] λ_{max} (nm)	IR (cm^{-1}) in KBr[b]				
		ν_{N-H}[d]	$\nu_{C=O}$ (Ester)	$\nu_{C=O}$ (Amid)	$\nu_{CO(OH)}$	$\nu_{asCOO^{(-)}}$
3a	339, 263, 214	3400—2300[b,d] (3160)	1725	1670	1715	—
b	343, 262, 216	3500—2300[d] (3140)	1710	1655	1670	—
c	331, 263, 256, 227, 208	3500—2300[d] (3280)	1740	1650	1700	—
5a	272, 212	3300, 3220[d]	1725	1670	—	1600—1640
b	263, 223, 207	3600—1750[d] (3310, 2500)[e] 1900	1705	1675	—	~1600
6	315, 261, 253, 226	3400—3000[d] (3280, 3190)	1680	1650	1735	—
7	319, 261, 255, 226	~3240	1685	1660	—	—
8a	340, 263, 213	~3220	1725, 1675	1650	—	—
b	355, 239, 215	~3150	1740, 1660	1655	—	—
c	319, 263, 255, 227, 207	~3260	1735, 1680	1660	—	--
9	357, 263, 218	~3390 und ~3450	1715	1635, 1620	—	—

a in 96% Äthanol
b in $CHCl_3$
c in d^6—DMSO
d überlappt von $\nu_{OH}(-CO_2H)$, breit
e $=NH^+$ (Zwitterion) ——

Cyclisierung von **3a** mit Essigsäureanhydrid führt zu 3-Äthoxycarbonyl-2-(1-maleinimido)-4,5,6,7-tetrahydro-benzothiophen **10**:

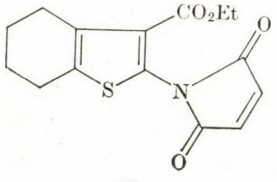

10

von **3a—c, 5a,b, 6, 7, 8a—c, und 9**

N M R (TMS: $\tau = 10$) (J in Hz) in $CDCl_3$[c]

H^a	H^b	H^c	H^d	$H^{d'}$	H^e	H^f	H^g
8,60 t [7]	5,60q [7]	—2,4		3,50s		~7,3m	~8,2m
8,65t[c] [7]	5,65q [7]	—1,9	—	—		~7,3m	~8,25m
8,70t [7]	5,75q [7]	0,25[f] —1,60		2,4m		~7,3m	~8,25m
8,75t[c] [7]	5,75q [7]	—0,6	3,34	3,61d [12]		1,90s	
8,75 [c] [7]	5,75q [7]	~—0,1		2,3m		1,95s	
8,60t [7]	5,65q [7]	~0,5[f] ~—1,4		7,20s		~7,35m	~8,2m
8,65t[c] [7]	5,65q [7]	~—1,1	~7,4d[i]	~8,65t[j]		~7,4m	~8,25m
8,60t [7]	5,65q [7]	~—1,6	3,50[h]	3,70[h] [12]	6,20s	~7,25m	~8,2m
8,65t [7]	5,65q [7]	~—2,2	—	—	6,10s	~7,25m	~8,2m
8,65t [7]	5,65q [7]	~—1,4		7,20s	6,30s	~7,35m	~8,2m
8,70t[c] [7]	5,70q [7]	~—1,3 +1,2[g]		2,95s	e_1 6,15m e_2 4,2 m e_3 4,8 m	~7,35m	~8,3m

f NH und OH
g NH (Seitenkette)
h AB-Spektrum
i überlappt von H^f
j überlappt von H^a

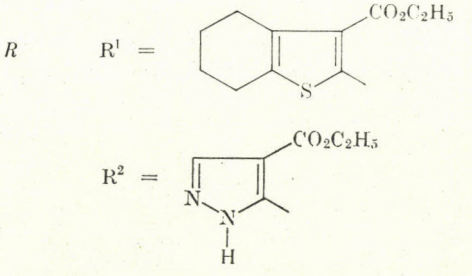

Im Falle von **5a** ist es auch unter Verwendung zahlreicher Kondensationsmittel (z. B. DCC, $POCl_3$, PPA) nicht gelungen, einen weiteren Ring anzukondensieren. Mit Essigsäureanhydrid gewinnt man **11**, dessen Entstehung durch Abspaltung der Seitenkette und nachfolgende Acetylierung zu deuten ist. In Schmelzpunkt und IR-Daten stimmt **11** mit einer von HARTKE [9] durch Acetylierung von **4** erhaltene Verbindung überein:

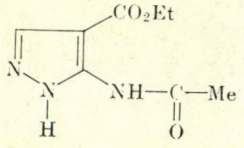

11

Photo-Dimroth-Umlagerung von 5-Amino-4-äthoxycarbonyl-1-phenyl-1,2,3-triazol 12 [10]

Wie in der Literatur bekannt ist, reagieren einige 1,2,3-Triazole bei UV-Bestrahlung unter N_2-Abspaltung zu Ketene-iminen [11] oder zu Aziridinen [12—14]. **12** *alleine* bestrahlt wurde, in sämtlichen Lösungsmitteln, ohne daß wir eine N_2-Entwicklung beobachten konnten.

12 reagiert mit **2a** weder unter thermischen noch photochemischen Bedingungen. Bei UV-Bestrahlung (Quarzapparatur/Dioxan) in Gegenwart von Triphenylen als Sensibilisator lagert sich **12** in 5-Anilino-4-äthoxycarbonyl-1,2,3-triazol **14** [15] um. Diese Reaktion stellt das erste Beispiel einer photoinduzierten Dimroth-Umlagerung dar. Diese Reaktion wurde bisher stets thermisch unter in wäßrigem oder basischem Milieu durchgeführt [15, 16]. Parallel-Versuch (=Rühren ohne Licht) ruft keine Umlagerung hervor, womit sichergestellt wird, daß es sich hier tatsächlich um Photo- und nicht Thermo-Reaktion handelt.

Die Reaktion führt zu einem Gleichgewicht [17] zwischen **12** und **14.** Als ersten Schritt diskutieren wir eine Homolyse zwischen N–1 und N–2 (**12** → **13**) gefolgt von einer Umlagerung + Rekombination zum isomeren Dimroth-Produkt **14**.

Die Strukturen der erhaltenen Verbindungen befinden sich im Einklang mit den spektroskopischen Daten (s. Tab. II).

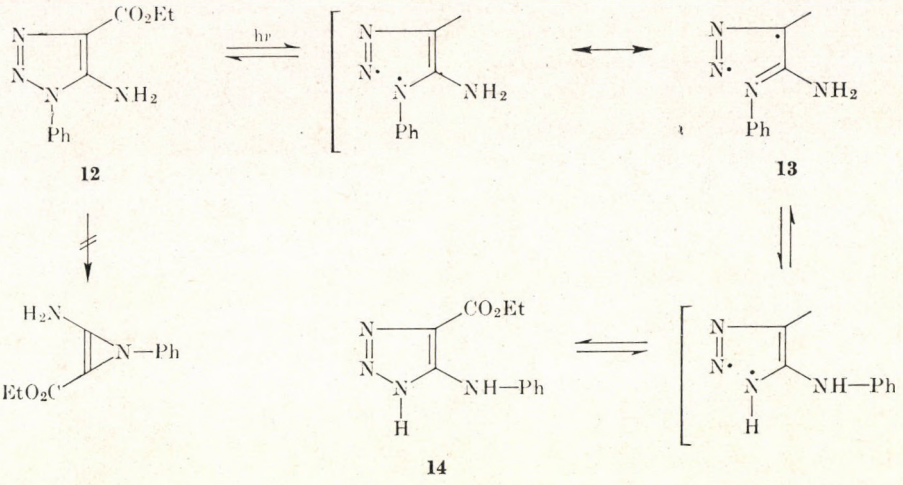

12 13 14

Experimenteller Teil

Für die spektroskopischen Untersuchungen dienten folgende Geräte: UV: Cary 15 und Unicam SP 700, IR: Perkin–Elmer 237 und 457, NMR: Varian A 60 und A 60 D.

Allgemeine Vorschrift zur Darstellung der Maleamidsäuren 3a–c und 5a, b: 20 mmol **1** (oder **4**) und 20 mmol **2a–c** werden in 50 ml Tetrahydrofuran bei Raumtemperatur gerührt und eine Nacht belassen. Das Produkt wird abfiltriert und aus Äthanol umkristallisiert (Daten s. Tab. I.).

N-(3-Äthoxycarbonyl-4,5,6,7-tetrahydro-2-benzthienyl)-bernsteinamidsäure 6: 10 mmol **3a** wird in 50 ml Äthanol in Gegenwart von 10% Pd/C bei Raumptemp. hydriert. Nach der Aufnahme eines Moles H_2 wird der Katalysator abfiltriert, das Lösungsmittel abgezogen und der Rückstand aus Äthanol umkristallisiert (Daten s. Tab. I).

3-Äthoxycarbonyl-2-propionamino-4,5,6,7-tetrahydro-benzothiophen 7: 20 mmol **6** werden auf 250—270 °C erhitzt, nach der Beendigung der CO_2-Abspaltung wird der Rückstand abgekühlt und aus Isopropanol umkristallisiert (Daten s. Tab. I).

Allgemeine Vorschrift zur Veresterung von 3a, b und 6: 10 mmol **3a, b** oder **6** werden in 50 ml Methanol in Gegenwart von 2 ml Borfluorid/Äthylätherat 3 h zum Sieden erwärmt. Das Lösungsmittel wird in Vakuum entfernt und der Rückstand aus Äthanol umkristallisiert (Daten s. Tab. I).

N-Allyl-N'-(3-äthoxycarbonyl-4,5,6,7-tetrahydro-2-benzthienyl)-maleinsäurediamid (9): 4,1 g (12 mmol) **3a** und 4,1 ml $SOCl_2$ werden in 30 ml Benzol gelöst und 1 h zum Sieden erhitzt. Das Reaktionsgemisch wird in Vakuum eingeengt, in 30 ml Dioxan gelöst und innerhalb 0,5 h zu einer Lösung von 1,71 g (30 mmol) Allylamin in 30 ml Dioxan zugetropft. Das Gemisch wird 6 h bei Raumtemp. gerührt, in Wasser gegossen, mit 3×50 ml Benzol extrahiert und über $MgSO_4$ getrocknet. Der Rückstand (nach dem Abdampfen des Lösungsmittels) wird aus Äthanol umkristallisiert (Daten s. Tab. I).

3-Äthoxycarbonyl-2-(1-maleinimido)-4,5,6,7-tetrahydrobenzothiophen 10: 3,23 g (10 mmol) **3a** werden in 16 ml Essigsäureanhydrid 4 h zum Sieden erwärmt. Nach Abkühlen wird das Reaktionsgemisch in Wasser gegossen, mit Ammoniak neutralisiert, mit Chloroform

extrahiert und über $MgSO_4$ getrocknet. Nach Verdampfen des Lösungsmittels wird der Rückstand aus Äthanol umkristallisiert. Ausb. 1,0 g (33%) vom Schmp. 134—136 °C.

UV (96% C_2H_5OH): λ_{max} 409, 347, 256, 217 nm.
IR(KBr): ν C=O_{Imid} 1800, 1780 und 1705, ν C=O_{Ester} 1710, ν C=C 1655, 1635, 1560 und 1530 cm^{-1}.
NMR($CDCl_3$): Ester τ 8,65 t u. τ 5,68 q (7,0 Hz), C–H_{Vinyl} τ 3,33 d u. τ 2,64 d (5,0 Hz), CH_2(5,6) τ 8,2 m (4,0 Hz) u. CH_2 (4,7) τ 7,3 m (4,0 Hz).
$C_{15}H_{15}NO_4S$ (305,34) ber. N 4,59, S 10,50, gef. N 4,69, S 10,29.

5-Acetamido-4-äthoxycarbonyl-pyrazol 11: Aus **5a** ausgehend, nach der Vorschrift **10**, erhält man **11**. Ausb. 0,57 g (29%) vom Schmp. 201—202 °C (Lit [9] 200 °C).

IR(KBr): ν NH 3340 und 3250, ν C=O 1695 und 1680 cm^{-1} (Lit [9] Nujol) 3340, 3250, 1700 und 1680 cm^{-1}).
NMR(d^6–DMSO): Ester τ 8,72 t und τ 5,71 q (7,0 Hz), $CH_{3Acetyl}$ τ 7,87 s, C–H τ 2,0 s, τ N–H 0,3.
$C_8H_{11}N_3O_3$ (197,19) ber. C 48,72, H 5,62, N 21,31, gef. C 48,61, H 5,67, N 21,24.

Photo-Dimroth-Umlagerung von 5-Amino-4-äthoxycarbonyl-1-phenyl-1,2,3-triazol 12: 4,64 g (20 mmol) **12** werden in ca. 220 ml Dioxan gelöst, 10 mg Triphenylen als Sensibilisator zugefügt und in einer Bestrahlungsapparatur (mit Wasser gekühlter Quarzfinger) unter magnetischem Rühren mit einem Hg-Hochdruckbrenner (Philips HPK 125 W) bestrahlt. Der Reaktionsablauf wird mit DC verfolgt (System Benzol/Aceton 80:20). Nach 36—48 h Bestrahlungsdauer wird kein weiteres Photoprodukt mehr gebildet. Nach dem Verdampfen des Lösungsmittels wird der Rückstand an Kieselgel in Systemen steigender Polarität chromatographiert (1. Benzol, 2. Benzol/Essigester 9:1). **14** fällt als Feststoff an, der aus Äthanol umkristallisiert wird.

Ausb. 1,77 g (38,0%) vom Schmp. 136—138 °C (Lit. [15] 129—130 °C).

IR(KBr): ν NH 3380 (Ph–NH) und 3500—2600 (3150, 2940) (Azol-NH), ν C=O 1700, aromatische und heteroaromatische CH-Schwingungen +β NH-Banden 1620, 1590, 1545, 1490, 1475 und 1440 cm^{-1} (Lit. [18] 3455, 3280, 1712, 1620 und 1560 cm^{-1} für **12**).

NMR($CDCl_3$): Ester τ 8,52 t und τ 5,43 q (7 Hz), Ph–NH τ 4,6, Azol–NH τ 2,1.

$C_{11}H_{12}N_4O_2$ (232,24) ber. N 24,25, gef. N 24,17.

*

G. Sz. dankt der Alexander von Humboldt-Stiftung für ein Forschungsstipendium. Herrn P. Sohár danken wir für wertvolle Diskussionen, der Deutschen Forschungsgemeinschaft für Sachbeihilfen.

LITERATUR

[1] 15. Mitteil.: Wamhoff, H., Hartlapp, J.: Chem. Ber., **109**, 1269 (1976)
[2] Chapman, O. L.: Organic Photochemistry, Bd. 1. S. 307, Marcel Dekker, New York 1967
[3] Szilágyi, G., Wamhoff, H., Sohár, P.: Chem. Ber., **108**, 464 (1975)
[4] Szilágyi, G., Wamhoff, H.: Acta Chim. (Budapest), **82**, 375 (1974)
[5] Wamhoff, H.: Tetrahedron, **26**, 3849 (1970)
[6] Gewald, K.: Chem. Ber., **99**, 1002 (1966)
[7] Schmidt, P., Druey, J.: Helv. Chim. Acta, **39**, 986 (1956)
[8] Marshall, J. L., Erickson, K. C., Folsom, T. K.: Tetrahedron Letters, **1970**, 4011
[9] Hartke, K., Alarcon, R., Ramirez, D., Bartulin, J.: Arch. Pharm. (Weinheim), **299**, 214 (1966)
[10] Dimroth, O.: Ber. Deut. Chem. Ges., **35**, 4059 (1902) und Liebigs Ann. Chem., **364**, 203 (1908)

[11] BURGESS, E. M., CARITHERS, R., MCCULLAGH, L.: J. Amer. Chem. Soc., **90**, 1923 (1968)
[12] SCHEINER, P.: Tetrahedron, **24**, 2757 (1968) und J. Amer. Chem. Soc., **90**, 988 (1968)
[13] MAERKY, M., DOPPLER, Th., HANSEN, H. J., SCHMID, H.: Chimia **23**, 230 (1969)
[14] TSUJIMOTO, K., OHASHI, M., YONEZAWA, T.: Bull. Chem. Soc. Japan, **46**, 3605 (1973)
[15] DIMROTH, O.: Liebigs Ann. Chem. **364**, 183 (1908)
[16] BROWN, D. J. in Thygarajan, B. S. edit., Mechanisms of Molecular Migrations, Vol. I., S. 209, Interscience, New York 1968
[17] LIEBER, E., TAI SIANG CHAO, RAMANCHANDRA RAO, C. N.: J. Org. Chem., **22**, 654 (1957)
[18] WAMHOFF, H., DÜRBECK, H., SOHÁR, P.: Tetrahedron, **27**, 5873 (1971)

Géza SZILÁGYI; Institut für Arzneimittelforschung, H–1325, Budapest, Pf. 82.
H. WAMHOFF; Organisch-Chemisches Institut der Universität Bonn,
D 5300–Bonn, Max–Planck–Str. 1. BRD.

Acta Chimica Academiae Scisntiarum Hungaricae, Tomus 89 (3), pp. 275—277 (1976)

CONVERSIONS OF TOSYL AND MESYL DERIVATIVES IN THE MORPHINE GROUP, XVI*

NEW DATA TO THE MECHANISM OF ALLYLIC REARRANGEMENT

S. MAKLEIT, T. MILE and R. BOGNÁR

(Department of Organic Chemistry, L. Kossuth University, Debrecen)

Received May 28, 1975

Additional evidence is presented for the complex ($S_N2 + S_Ni'$) mechanism of the transformation of the allylic system occurring in morphine alkaloids. Starting with codeine tosylate, alteration of the reaction conditions made possible the preparation of both chloro derivatives, α- and β-chlorocodide; the isolated α-derivative was isomerized into the β-derivative under similar conditions as for the preparation of the later.

Theoretical considerations and experimental observations during our previous work [1, 2] led to the conclusion that those nucleophilic substitution reactions of the *pseudo-equatorial* tosyloxy group in codeine-, 3-0-acetylmorphine- and 14-hydroxycodeine tosylates which yield "pseudo" compounds (C–8 substituted derivatives), can be described by a combined S_N2+S_Ni' mechanism.

In the present paper further experimental evidence is presented in connection with this problem.

It has been described in the literature that codeine tosylate (3-methoxy-4,5α-epoxy-6α-tosyloxy-7,8-didehydro-17-methylmorphinan) (**I**) reacts with lithium chloride in acetone solution to yield α-chlorocodide (3-methoxy-4,5-α-epoxy-6β-chloro-7,8-didehydro-17-methylmorphinan) (**II**); the reaction has S_N2 mechanism [3].

On the basis of earlier observations [1, 2], this reaction was examined in detail and it has been found that relatively slight changes in the experimental conditions are sufficient also in this case to allow the preparation of both the α- (C–6) (**II**) and the β- (C–8) (**III**) isomers, and to convert the isolated C–6 isomer, which is a kinetic product, into the C–8 thermodynamic isomer, by applying similar conditions as for the synthesis of the β-isomer (3-methoxy-4,5α-epoxy-6,7-didehydro-8β-chloro-17-methylmorphinan) (**III**).

The transformations are shown in Fig. 1.

Recently, the 6-deoxy-6-thiocyanato derivative [1] (called product *a* in the reference cited), whose formation had been assumed in the course of the

* Part XV: S. MAKLEIT, G. SOMOGYI, R. BOGNÁR: Acta Chim. (Budapest) (in press and Magyar Kém. Foly. **81**, 517 (1975).

conversion of codeine tosylate into the 8-deoxy-8-isothiocyanate derivative, could also be isolated under special conditions and its isomerization (C–6 → C–8 transition) has been achieved [4].

The isomerization of 6-deoxy-6-azido-14-hydroxyisocodeine to 8-deoxy-8-azidopseudocodeine has also been reported by us [2].

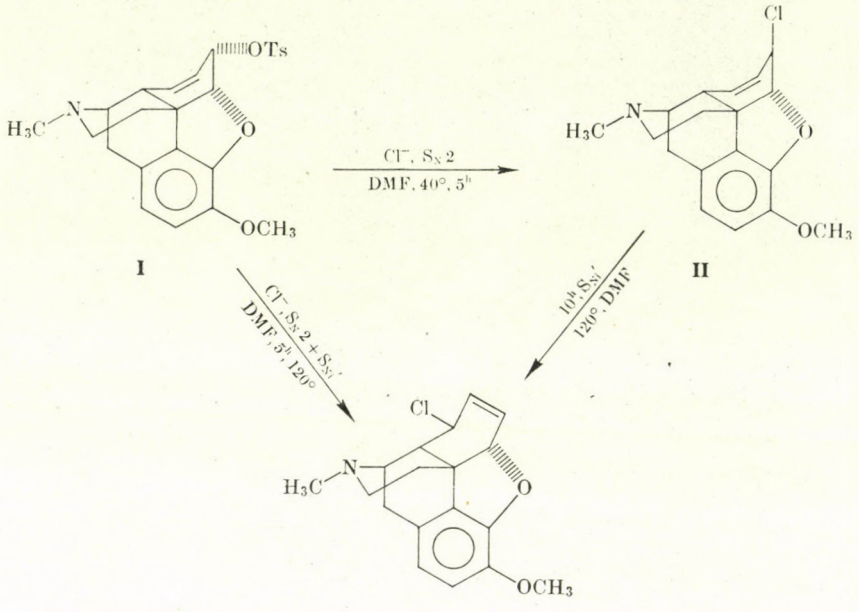

Fig. 1

The SNi" part-processes in the two latter reaction have been explained by a [3,3] -suprafacial sigmatropic rearrangement proceeding through the formation of a quasi-cyclic intermediate [4].

The reaction of codeine tosylate with potassium thiolacetate in DMF [5] yielded the 8-deoxy-8-acetylthio derivative. The corresponding 6-deoxy-6-acetylthio derivative has not been isolated, but the S_N2 mechanism of its formation was assumed, and its transformations by S_Ni' reaction was suggested to take place probably through a tight ion pair [4].

The S_Ni' partial mechanism in the transition **II** → **III** can also be explained similarly by the formation of an ion pair, since the chlore derivative was obtained exclusively, even on the addition of foreign anions (Br^-, N_3^-) [6].

Experimental

α-Chlorocodide (II)

6-O-Tosylcodeine (4.0 g; 8.8 m.moles) and lithium chloride (1.36 g; 32 m.moles) were dissolved in dry DMF (120 ml) and kept at 40 ± 2 °C for 5 hrs. The reaction mixture was poured into ice-water (600 ml) and extracted with benzene (3 × 100 ml). The benzene solution was washed with water saturated with sodium chloride (2 × 50 ml), dried over magnesium sulfate and evaporated to dryness. The residue was crystallized from ethanol to obtain 2.13 (76%) of the product, m.p. 152 °C (lit. m.p. 151—154 °C [3]; mixed m.p. 151—152 °C.

β-Chlorocodide (III)

6-O-Tosylcodeine (3.0 g; 6.6 m.moles) and lithium chloride (1.02 g; 24 m.moles) were dissolved in dry DMF (90 ml) and kept at 120 ± 4° C for 5 hrs. The reaction mixture was processed as described above, to obtain 0.7 g (33.3%) of the product, m.p. 155—157 °C (from ethanol) (lit. m.p. 153—154 °C) [3].

Conversion of (II) into (III)

Compound **(II)** (1.5 g) was heated in DMF (30 ml) at 120 °C for 10 hrs; the progress of the reaction was followed by TLC. After the disappearance of the spot due to **II**, the reaction mixture was processed as above, to yeield 0.62 g (41.2%) of the product, m.p. 155—156 °C (mixed m.p. 155° C).

*

The authors' thanks due are to the Natural Science Department I of the Hungarian Academy of Sciences and to the Alkaloida Chemical Works, Tiszavasvári, for supporting this work.

REFERENCES

[1] Bognár, R., Makleit, S., Mile, T., Radics, L.: Mh. Chem. **103,** 143 (1972); Magyar Kém. Foly. **78,** 163 (1972)
[2] Makleit, S., Radics, L., Bognár, R., Mile, T., Oláh, É.: Acta Chim. (Budapest) **74(1),** 99 (1972); Magyar Kém. Foly. **78,** 223 (1972)
[3] Stork, G., Clarke, F. H.: J. Am. Chem. Soc. **78,** 4619 (1956)
[4] Makleit, S.: Theses of doctorate at the Academy (1972), Debrecen
[5] Bognár, R., Makleit, S., Mile, T., Radics, L.: Acta Chim. (Budapest) **64,** 273 (1970); Magyar Kém. Foly. **76,** 102 (1970)
[6] Bordwell, F. G., Schexnayder, D. A.: J. Org. Chem. **33,** 3233, 3236, 3240 (1968)

Sándor Makleit
Teréz Mile
Rezső Bognár

Institute of Organic Chemistry, University of Debrecen
H–4010. Debrecen.

Acta Chimica Academiae Scientiarum Hungaricae, Tomus 89 (3), pp. 279—284 (1976)

SYNTHESIS OF SOME COUMARIN-AMINO ACID METHYL ESTER DERIVATIVES

A. M. EL-NAGGAR, M. H. A. EL-GAMAL, B. A. H. EL-TAWIL and F. S. M. AHMED

(Chemistry Department, Faculty of Science, Al-Azhar University, Nasr-City, Cairo and Nat. Res. Centre, Dokki, Cairo, Egypt A.R.E.)

Received June 13, 1975;

in revised form October 18, 1975

Coumarin-3-CO-Gly-OMe (**II**) and the corresponding L-Ala, L-Leu, L-Ser, D-Val, L-Tyr, D-Phe, L-Pro, L-Trp, L-Thr and β-Ala methyl ester derivatives (**III**—**XIV**) have been synthesized by the action of coumarin-3-acid chloride (**I**) on amino acid methyl ester hydrochlorides in dioxan containing Et_3N. Hydrazinolysis of coumarin-3-CO--L-Leu-OMe (**IV**) in dioxan gave the corresponding hydrazide in 85% yield. 3-[5-(6,7--dimethoxybenzofuryl)] propenoyl-Gly-OMe (**XVII**) and the corresponding L-Ala, D-Phe, L-Tyr, L-Thr, L-Trp and L-Ser-methyl ester derivatives (**XVIII**—**XXII**) have been prepared by the reaction of 3-[5-(6,7-dimethoxybenzofuryl)] propenoic acid chloride (**XVI**) with the appropriate amino acid methyl ester in dioxan containing Et_3N.

Introduction

The coumarin group of natural products has aroused in the past twenty years considerable interest on account of various aspects of biological activity [1, 2]. It seems therefore desirable to synthesize some coumarin-amino acid derivatives which may be of verified or intensified pharmaceutical effects. In continuation of our previous work [3, 4], the synthesis of coumarin-3-CO-amino acid esters (**II**—**XIV**) and 3-[5-(6,7-dimethoxybenzofuryl)] propenoyl-amino acid esters (**XVII**—**XXIII**) is described in this paper.

Results and discussion

For the preparation of the title compounds, **I** [5] was treated with the appropriate amino acid methyl ester hydrochloride (1:1.2 mole) in dioxan–Et_3N medium to afford coumarin-3-CO-amino acid methyl esters (**II**—**XIV**). Coumarin-3-CO-Gly-OMe (**II**) was successively synthesized and the product easily isolated, purified and recrystallized.

The reaction of **I** with Ala- or β-Ala, Val, Leu, Phe, Glu and Pro was carried out under the same conditions as used for the preparation of the glycine derivative, and the time required for completion of the reaction (5 min, — 2 hrs) was monitored by TLC.

In the preparation of the Ser, Tyr, Thr and Trp derivatives (**V**, **IX**, **XII** and **XIII**), the coupling reactions did not require the prior protection of the side chain group of the amino acid, and no side reactions were observed.

Most of the products were obtained in crystalline form in 50—85% yield. The compounds (**II**—**XIV**) were chromatographically homogeneous and gave negative ninhydrin reaction.

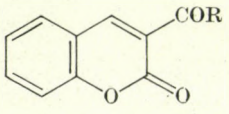

(Structure **II**—**XV**)

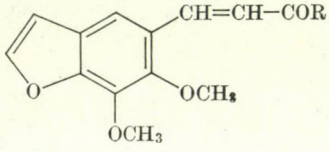

(Structure **XVII**—**XXII**)

The electrophoretic mobility (E) was found to be zero for all derivatives indicating the high purity of the products from any unreacted amino acid esters.

The IR spectrum of coumarin-3-CO-Gly-OMe (**II**) in KBr showed the characteristic bands at 3460, 3340 and 3040 (NH and CONH); 1740, 1650 and 1560 (α-pyrone); 1655, 1520 and 1280 (amide I, II, III); 1445, 1360 ($-COOCH_3$) and 1690 (ν C=O) cm^{-1}, thereby supporting the structure of **II**.

The IR spectra of the other compounds (**III**—**XIV**) had analogous peaks, confirming the structures of these compounds.

The UV spectra of **II**—**XIV** in ethanol showed λ_{max} (log ε) at 210 nm (4.55) and 295 nm (4.43), characteristic of the coumarin residue.

The attempted coupling reaction of coumarin-3-carboxylic acid with amino acid esters in DMF, benzene or THF using the dicyclohexylcarbodiimide method was fruitless. The azide method also failed owing to the unstability of the coumarin ring towards hydrazinolysis reaction in ethanol.

Treatment of coumarin-3-CO-L-Leu-OMe (**IV**, 1M) with a 0.5M (or 1M) solution of hydrazine hydrate in ethanol at 20° C (or even at 5 °C) for 2 hrs lead to the destruction of the α-pyrone ring as indicated by the UV data. However, when **IV** was refluxed (90 °C) with 0.5M hydrazine hydrate in dioxan–ethanol mixture for 6 hrs, the desired hydrazide (**XV**) was obtained and no side reactions were observed. The stability of the α-pyrone ring was established by the UV spectrum, elemental analysis, chromatographic studies and the IR

spectrum. Similarly, some authors [6, 7] found that the α-pyrone ring in other coumarins was cleaved by treatment with hydrazine hydrate, when toluene, benzene, xylene, acetic acid and alcohols were used as the solvent. However, when phenetole or tetraline were applied instead of the mentioned solvents, no detectable destruction of the coumarin molecule was observed.

Several 3-[5-(6,7-dimethoxy-benzofuryl)] propenoyl-amino acid esters were prepared by the reaction of **XVI** with the amino acid methyl ester, using the procedure described for the preparation of **II—XIV**. The time required for completion of the reaction (35 min — 2 hrs) was found out by TLC. However, coupling reactions with L-Ala, L-Tyr and L-Trp yielded products which contained small traces of undesired by-products. Compounds **XVIII**, **XX** and **XXII** were isolated and purified by preparative TLC and repeated recrystallizations. In general, the desired 3-[5-(6,7-dimethoxybenzofuryl)] propenoyl-amino acid esters were obtained in crystalline form in 30—80% yield.

The IR spectrum of **XVII** in KBr had the characteristic bands at 3260, 3040 (NH and CONH); 3165, 1560, 1030 (benzofuran system); 1670, 1550, 1280 (amide I, II and III); 2920, 2820, 1450, 1340 (Ar–OCH_3); 1120, 1240, 1735 ($COOCH_3$); 1620, 1450, 1220 cm^{-1} (C=C) thereby confirming the structure of **XVII**. The UV spectra of **XVII—XXII** (in EtOH) showed λ_{max} (log ε) at 248 nm (4.46) and 285 nm (4.48) characteristic of the benzofuran structure.

Compounds **II—XV** and **XVII—XXII** were prepared and characterized for the first time. The biological and pharmacological properties of the synthesized compounds are still under screening.

Experimental

Optical rotations $[\alpha]_D^{20}$ were measured in DMF (unless otherwise stated). The R_f values (TLC) were determined on silica gel, developed with benzene-ethyl acetate (1:1) and detected with iodine in KI solution (20%) as the spraying agent. Benzidine, ninhydrin, silver nitrate and hydroxamate reactions were used for detection of the amino acid derivatives on paper chromatograms (spot reactions) [8]. The electrophoretic mobilities, E, were measured with 1000 V, 2 hrs in pyridine–acetate buffer [8]. UV spectra were taken in ethanol and the IR spectra in KBr pellets.

Coumarin-3-acid chloride (I)

This compound was synthesized from coumarin-3-carboxylic acid using the procedure described in [5].

General procedure for the synthesis of coumarin-3-CO-amino acid methyl esters (II—XIV)

Coumarin-3-acid chloride (**I**) (0.63 g; 0.003 mole) was dissolved in dioxan (20 ml) and added to a solution of the amino acid methyl ester hydrochloride (0.0036 mole) in dioxan (20 ml) containing triethylamine (1 ml). The reaction mixture was stirred at room temperature followed by refluxing until completion of the reaction as checked by TLC. After cooling

Table I

Coumarin-3-CO-amino acid methyl esters (**II—XV**)

Comp. No.	R = Amino acid residue	Yield, %	M.p., °C	R_f	$[\alpha]_D^{20}$	Mol. formula	Elementary analysis, %					
							Found			Calculated		
							C	H	N	C	H	N
II	Gly-OMe	65	193—195	0.63	—	$C_{13}H_{11}NO_5$	60.27	4.37	5.19	59.77	4.2	5.3
III	L-Ala-OMe	60	108—110	0.70	+49.7(c, 0.64)	$C_{14}H_{13}NO_5$	61.24	4.94	4.92	61.09	4.7	5.0
IV	L-Leu-OMe	70	120—122	0.81	+51.4 (c, 0.5)	$C_{17}H_{19}NO_5$	64.62	6.06	4.56	64.34	6.04	4.41
V	L-Ser-OMe	50	98—100	0.71	+105.4 (c, 0.4)	$C_{14}H_{13}NO_6$	58.21	4.9	4.57	57.73	4.5	4.82
VI	D-Val-OMe	70	91— 92	0.68	+47.8 (c, 0.7) +15.2 (c, 0.5 acetone)	$C_{16}H_{17}NO_5$	63.36	5.74	4.7	63.36	5.61	4.62
VII	L-Val-OMe	85	85— 87	0.68	+60.8 (c, 0.5); −17.2 (c, 0.5 acetone)	$C_{16}H_{17}NO_5$	63.87	5.64	4.34	63.36	5.61	4.62
VIII	L-Glu-OMe	70	103—105	0.51	+17.3 (c, 0.5)	$C_{17}H_{17}NO_7$	58.95	5.03	6.06	58.78	4.8	4.03
IX	L-Tyr-OMe	65	95— 98	0.59	+72.1 (c, 0.5)	$C_{20}H_{17}NO_6$	65.41	4.7	3.84	65.3	4.6	3.8
X	D-Phe-OMe	30	105—107	0.68	+17.7 (c, 0.6)	$C_{20}H_{17}NO_5$	68.48	4.93	3.59	68.37	4.8	3.9
XI	L-Pro-OMe	82	145—147	0.82	−33.3 (c, 0.6)	$C_{16}H_{15}NO_5$	63.56	4.88	4.81	63.78	4.98	4.6
XII	L-Trp-OMe	55	107—109	0.70	+74.8 (c, 0.5)	$C_{22}H_{18}N_2O_5$	67.68	4.88	7.66	67.69	4.6	7.2
XIII	L-Thr-OMe	30	160—162	0.47	+58.5 (c, 0.7)	$C_{15}H_{15}NO_6$	59.23	5.08	4.76	59.01	4.91	4.5
XIV	β-Ala-OMe	75	150—152	0.48	—	$C_{14}H_{13}NO_5$	61.38	5.05	4.99	61.09	4.7	5.09
XV	L-Leu-N_2H_3	85	225—226	0.90	+7.2 (c, 0.5 acetone)	$H_{16}H_{19}N_3O_4$	60.77	7.12	13.5	60.5	6.9	13.2

Table II

3-[5-(6,7-Dimethoxybenzofuryl)]propenoyl amino acid methyl esters (**XVII—XXII**)

Comp. No.	R = Amino acid residue	Yield, %	M.p., °C	R_f	$[\alpha]_D^{20}$	Mol. formula	Elementary analysis, %					
							Found			Calculated		
							C	H	N	C	H	N
XIII	Gly-OMe	40	152—153	0.43	—	$C_{16}H_{17}NO_6$	60.31	5.75	4.53	60.18	5.32	4.39
XVIII	L-Ala-OMe	66	105—107	0.56	+75.0 (c, 0.53)	$C_{16}H_{19}NO_6$	59.95	5.96	4.49	59.81	5.91	4.36
XIX	D-Phe-OMe	64	147—150	0.73	+103.3 (c, 0.7)	$C_{23}H_{23}NO_6$	67.98	5.91	3.48	67.48	5.62	3.42
XX	L-Tyr-OMe	30	135—137	0.58	+18.0 (c, 1.4)	$C_{23}H_{23}NO_7$	64.95	5.93	3.39	64.9	5.41	3.29
XXI	L-Thr-OMe	82	183—185	0.26	+46.0 (c, 1.7)	$C_{18}H_{21}NO_7$	59.85	5.94	3.93	59.5	5.78	3.85
XXII	L-Trp-OMe	35	95— 97	0.65	+23.0 (0.78)	$C_{25}H_{24}N_2O_6$	66.96	5.95	6.55	66.96	5.35	6.25

of the reaction mixture, $Et_3N \cdot HCl$ was filtered off and a benzene–ether mixture (250 ml) (1:1) was added. The reaction mixture was washed with H_2O, 10% $NaHCO_3$, H_2O and dried over Na_2SO_4. Evaporation of the solvent in vacuum gave a solid product which was recrystallized from ethanol, methanol, hexane or their mixtures. Compounds (**II**—**XIV**) were chromatographically homogeneous when detected with benzidine, iodine solution, hydroxamate reactions, and all gave negative ninhydrin test. E = zero (for compounds **II**—**XIV**) (*c.f.* Table I, Compounds **II**—**XIV**).

Synthesis of coumarin-3-CO-L-Leu-N_2H_3 (XV)

Coumarin-3-CO-L-Leu-OMe (**IV**) (1 g) was dissolved in dioxan (25 ml) and hydrazine hydrate (0.88 ml) (0.5 *M*) dissolved in a mixture of 15 ml ethanol and 20 ml dioxane was added. The solution was refluxed for 6 hrs at 90 °C. The time required for the formation of the hydrazide was established by TLC. Evaporation of the solvent in vacuum gave a solid material which was recrystallized from abs. ethanol. The material was chromatographically homogeneous and gave positive reaction with silver nitrate (*c.f.* Table I, Compound **XV**).

General procedure for the synthesis of 3-[5-(6,7-dimethoxybenzofuryl)]propenoyl-amino acid methyl esters (XVII—XXII)

(*a*) 3-[5-(6,7-Dimethoxybenzofuryl)]propenoic acid chloride (**XVI**): 3-[5-Dimethoxybenzofuryl)] propenoic acid (0.55 g) was dissolved in chloroform (20 ml), PCl_5 (1.5 g) was added, and the mixture refluxed for 1 hr; the excess PCl_5 was then filtered off. Evaporation of the solvent in vacuum gave the acid chloride (**XVI**) as a hygroscopic crystalline material (0.533 g; 90%).

(*b*) Synthesis of **XVII**—**XXII**:

Compound **XVI** (0.533 g; 0.002 mole) was dissolved in dioxan (20 ml) and added to a solution of the amino acid methyl ester hydrochloride (0.0024 mole) in dioxan (20 ml) containing triethylamine (2 ml). The reaction mixture was refluxed for a period of 30 min to 2 hrs; the time required for completion of the reaction was determined by TLC. The same procedure was then followed as described for **II**—**XIV**. The compounds (**XVII**—**XXII**) were recrystallized from petroleum ether, ethanol or methanol, to obtain well-crystallized substances. All products were chromatographically homogeneous after their isolation and purification (*c.f.* Table II, Compounds **XVII**—**XXII**).

*

The authors are greatly indebted to the NRC, Cairo, Egypt, for laboratory facilities.

REFERENCES

[1] SOINE, T. O.: J. Pharm. Sci. **53**, 231 (1964)
[2] NIELSEN, B. E.: "Coumarins of Umbelliferon Plants", Ph. D. Thesis, Royal Danish School of Pharmacy, Copenhagen, 1970
[3] EL-NAGGAR, A. M., EL-GAMAL, M. H. A., EL-TAWIL, B. A. H., ABD-EL-SALAM, A. M.: Ind. J. Chem. **13** (3), 305 (1975)
[4] EL-NAGGAR, A. M., EL-GAMAL, M. H. A., EL-TAWIL, B. A. H., AHMED, F. S. M.: Ind. J. Chem. **13** (4), 424 (1975)
[5] WOODS, L. L., SAPP, J.: J. Org. Chem. **30**, 312 (1965)
[6] ALY, M. I., SAMI, S. M.: Egypt J. Chem. **16**, 169 (1973)
[7] MORIMATO, Y.: Yakugaki Zasshi **82** (2), 3422f (1963), 389—394 (1962); C. A. **58** (2), 3422 (1963)
[8] EL-NAGGAR, A. M.: Ind. J. Chem. **9** (12), 1326 (1971)

Ahmed M. EL-NAGGAR
M. H. A. EL-GAMAL
B. A. H. EL-TAWIL
F. S. M. AHMED

Chemistry Department, Faculty of Science, Al-Azhar University, Nasr-City, Cairo, Egypt, A.R.E.

RECENSIONES

Gy. SZEKÉR: *Significance of Aluminium in Technical Development*

(Advances in Chemistry, Vol. 25)

Akadémiai Kiadó, Budapest 1975, 194 pages

The series "Advances in Chemistry" gives information not only about basic research and not only summarizes the technological and operational results but discloses the full and easily intelligible notion of an economic matter — as it is done in this present work, too.

The review starts with the presentation of the importance of aluminium which is best reflected by the slogan: "Aluminium is the XXth century's metal". Here is about the career aluminium has made and makes in several fields of its application.

The description of bauxite, the main mineral of aluminium, and the aluminium production from it not only gives a possibility for specialists to survey the problem but is readable for the public as well.

The aluminium is a world economical factor. We gain a picture of the part played by the capitalist companies in such a deepness like dual pricing system, which gives an idea about the industry-politics of world concerns.

The chapter about the situation of the Hungarian bauxite-aluminium industry is especially of historical interest. In it the author presents the development and results contributed by domestic research. During the last decade this developing tendency has speeded up as a result of the close socialist co-operation. Concerning the entire industry we have reached the world standard and Hungarian scientists definitely take a prominent part in solving futher problems, too.

The intellectual export transacted by ALUTERV is a striking eloquent proof of this. The comment upon the future tendency of development, the objective criticism of some almost phantasmagorial ideas concludes the book.

There is a little flaw: in the names of American companies Aluminium is used instead of Aluminum.

Z. G. SZABÓ

Structure and Bonding, Vol. 21

Springer-Verlag, Berlin, Heidelberg, New York, 1975. 144 pages

The continuous increase of the number and size of chemical periodicals is slowly becoming hard to grasp even by the aid of reference journals. Doubtless, this is in connection with the fact that the periodicals themselves, but even more so the referring abstracts — aspiring after entirety — accomplished their work with less criticism than needed. This is the reason why already decades ago the publication of annual reviews and reports was started, which informed on the most significant results of each field. Structure and Bonding is one of these, and in fact is one of the most successive and most useful summaries. This enterprise is *problem-oriented* and from time to time summarizes the theoretical and experimental results of different topics. The fact that it is dealing with the correlations between macroscopic, *i.e.* classical chemical, and microscopic, i.e. atomic phenomena makes this review exceptional. The opinion becomes more and more general that we have made considerable progress toward being able to deduce the properties of bulk substances from atomic and structural parameters.

The first review of volume XXI, "The Study of Covalency by Magnetic Neutron Scattering" by B. C. TOFIELD (Bell Laboratories), summarizes those results published on the application of magnetic neutron scattering since 1965 when HUBBARD's and MARSHALL's paper was printed. The study of neutron scattering has provided numerous and interesting results that could not have been obtained in any other way. This new technique makes possible to study the covalency in metals, alloys, semi-metals as well as in insulators. As the author himself expresses, his main purpose is to draw attention and interest to this new technique.

The second review of the book is on the superheavy elements. B. FRICKE very practically describes those efforts which aim at the prediction of chemical and physical properties of elements following the second rare-earth group. Actually this is not only a new adaption of the more than 100 years old Mendeleev idea but an up-to-date and complete formulation of it.

Numerous efforts have quite unanimously lead to the statement that the 6d transition metal group and even further elements up to atomic number 172 have not at all monotonous by decreasing stability but certain nuclei with large atomic numbers — around 112–114 — and with neutron numbers of 178–184 have additional stability and therefore their production by bombarding two heavy nuclei with each other is an effect that bids fair prospects. The fact that the relativistic effect, too, was taken into consideration in the ab initio calculations contributes to a better estimation of the atomic stability.

A surprising result is that with the increase of the atomic number and of the shells, the size of the atom does not monotonously increase, moreover, it actually shows a decreasing tendency already from cesium. In other words cesium seems to be the largest atom in the entire periodic system. JØRGENSEN's work made in this field on the legitimacy of extrapolations should be especially emphasized. In these the double series of magic numbers has given a great assistance.

The predictions may, or rather must be taken sceptically if they are not made on such a sound scientifical basis.

Z. G. SZABÓ

Inorganic Chemistry, Series Two, Volume 10, *Solid State Chemistry*

Butterworths, London, University Park Press, Baltimore, 1975. 264 pages

Since the revival of inorganic chemistry, the far reaching development has at the same time started a great number of new pediodicals and summarizing series, too. One of the most excellent representatives of these is, within the framework of the "International Review of Science", the "Inorganic Chemistry Series" which now in its second serial volume 10 gives a review about the chemistry of solid phase.

These series compile the new results of topics in inorganic chemistry in *field-oriented* chapters. The fact that H. J. EMELÉUS is the Consultant Editor of the publication automatically garantees the high level of the compilation.

The present volume consists of 7 reviews by the following authors:

High-pressure studies of electronic structure in solids
H. G. DRICKAMER, University of Illinois
Oxide glasses
T. I. BARRY, National Physical Laboratory, Middlesex
Crystallographic shear structures
R. J. D. TILLEY, University of Bradford
III—V Compounds and alloys
G. B. STRINGFELLOW, Hewlett-Packard Laboratories, California
Decomposition reaction of solids
A. K. GALWEY, Queen's University, Belfast
Mass transport in ionic solids
B. C. H. STEELE and G. J. DUDLEY, Imperial College of Science and Technology, University of London
Oxide bronzes and related phases
P. G. DICKENS and P. J. WISEMAN, University of Oxford

Though the titles are speaking for themselves, those extremely interesting results must be emphasized according to which the application of high-pressures (over 100.000 atm) may result in radical changes of the physical and chemical properties of solid phases. A pressure of such an order of magnitude already influences the structure of atoms, the electron zones melt together and there is a significant shift in the energies.

Glass can show numerous excellent characteristics of single crystals such as homogeneity, transparency and high mechanical strength without the difficulties of single crystal production. It has not only theoretical but continuously increasing practical importance, too. The short-range order can be easily influenced and therefore the production of glasses appropriate for particular applications has become possible. The production of crystals or glass from melt depends on the rate of nucleation and growth and these are exactly the parameters that can be easily influenced. Apart from the previously used glasses of simple composition based mainly on silicic acid today practically all the semi-metals play a part in the formation of glass, moreover further elements such as Ga, In have joined them, too.

GALWAY's extremely useful summary on decompositions in solid phases clearly emphasizes those mechanistic possibilities that we have to regard as first elementary steps in these transformations.

To this are added the chapters on crystallographic shear structures and mass transport in ionic solid phase. These together provide a clearer picture for the better understanding of these processes than ever before.

Z. G. SZABÓ

J. C. JOHNSON: *Antioxidants. Syntheses and Applications*

Park Ridge, New Jersey, London, England, Noyes Data Corporation 1975. 320 pages

The Chemical Technology Review series of Noyes Data Corporation is an undertaking extremely useful to practical experts. This Volume is member 44 of the series. As mentioned by the editor in the preface of the volume, the basic source of the work of practical experts is patent literature. This idea may have guided the publishers in their decision to review the US patents on a given topic at intervals of 4—5 years. The present volume is a review of US patents published between 1966 and 1974. It discusses a total of 247 patents, classified according to two principles. The first principle of classification is the chemical structure of antioxidants, the following groups being discussed:

Phenol antioxidants,
Sulfur-containing phenol antioxidants,
Nitrogen-containing phenol antioxidants,
Amine and imine antioxidants,
Triazine and cyanurate antioxidants,
Phosphorus-containing antioxidants, and
Miscellaneous antioxidants.

The second principle is the application of antioxidants. Accordingly, the head titles are:

Stabilization of petroleum products,
Antioxidants of lubricants,
Antioxidants of elastomers (antiozonants),
Antioxidants of polyolefins,
Antioxidants of other polymers,
Antioxidants in food industry.

The practical applicability of the volume is very wide. It is useful for experts dealing with the preparation of antioxidants as well as for those utilizing antioxidants. It is the merit of the editors that the legal formalities that make patent specifications only harder to understand have been peeled off, and the text contains only the detailed description of preparation and application methods. For those who wish to study the literature of this field it takes only some hours to gather the information from this volume that would require the hard wor of days, or sometimes weeks, if it were to be collected from reference periodicals.

B. LOSONCZI

INDEX

Printed in Hungary

A kiadásért felel az Akadémiai Kiadó igazgatója. Műszaki szerkesztő: Zacsik Annamária

A kézirat nyomdába érkezett: 1976. II. 27. — Terjedelem: 9,10 (A/5) ív 50 ábra

76.2849 Akadémiai Nyomda, Budapest — Felelős vezető: Bernát György

ACTA CHIMICA

ТОМ 89 – ВЫП. 3

РЕЗЮМЕ

Кинетика реакции, протекающей между двухлористым галлием и йодистым этилом, I

А. МЕСТИЦКИ, Д. КНАУС. Б. ЧАКВАРИ и Я. ЭММЕР

Была исследована реакция восстановления, протекающая между двухлористым галлием и йодистым этилом, используя в качестве растворителя избыток одного из реакционных партнеров, а именно йодистый этил. Следза реакцией осуществился с помощью измерения объема образующегося этана. На основе наших измерений были получены следующие результаты: энергия активации равна $-6{,}5 \pm 1$ ккал/моль, энтальпия активации равна $-6{,}8 \pm 1$ ккал/моль и энтропия активации равна -101 ± 4 кал/°К. На основе этих данных были сделаны заключения относительно механизма реакции.

Комплексы сурьмы(III) с основаниями Шиффа, полученными из бензальдегида и аминоспиртов

О. П. СИНГ и ДЖ. П. ТАНДОН

Сообщается синтез комплексов сурьмы(III) с шиффовыми основаниями с различным координационным числом. Они были синтезированы взаимодействием изопропоксида сурьмы(III) с монофункциональными основаниями Шиффа с двумя координирующими местами, имеющие основную формулу $C_6H_5CH : NROH$ (где $R = -(CH_2)_2-$, $-CH_2CH(CH_3)-$ и $(CH_2)_3-$) с ралучной стехиометрией. Проведение реакции с молярными отношениями компонентов 1 : 1, 1 : 2 и 1 : 3 приводит к образованию следующих производных $Sb(OPr^i)_2$ (SB), $Sb(OPr^i)$ $(SB)_2$ и $Sb(SB)_3$ (где SBH — молекула монофункцинального основания Шиффа с двумя координирующими местами), соответственно. В образующихся производных центральный атом металла оказывается в тетра-, пента- и гекса-координированном окружении, соответственно, что следует из их мономерной природы в кипящем бензоле. Были сняты ИК спектры этих производных и сделаны возможные ассигнации.

Влияние синусоидального переменного тока на поведение гальванических ванн для кадмиевых покрытий

С. С. АБД ЭЛЬ РЕХИМ и М. Г. ХЕЛМИ

Были исследованы два типа гальванических ванн: кислая ванна, содержащая сульфат кадмия и серную кислоту, и щелочная ванна, содержащая сульфат кадмия, гидроокись аммония и хлористый аммоний. Было изучено влияние синусоидального переменного тока, наложенного на постоянный ток, на анодную и катодную поляризацию. Результаты указывают на то, что эффект переменного тока зависит от природы ванны. В кислой ванне переменный ток сдвигает анодный потенциал кадмия в направлении менее благородных металлов и увеличивает катодную поляризацию, в то время как в щелочной ванне переменный ток сдвигает анодный потенциал кадмия в направлении более благородных металлов и благоприятствует пассивации электрода, а также деполяризует катодный потенциал.

Помимо этого был изучен эффект наложенного переменного тока на распределение постоянного тока, а также на распределение металла между двумя параллельными катодами. В обоих изученных гальванических ваннах переменный ток увеличивает доли распределения как тока, так и металла, и тем самым, неблагоприятно сказывается на равномерности покрытия.

Определение термохимических данных молекул $CHBr_3$ и CBr_4 с помощью масс-спектрометрии на основе исследования разложения за счет электронных столкновений и гетерогенного пиролиза

О. КАПОШИ, М. РИДЕЛЬ, К. ВАШ-БАЛЬТАЗАР, Р. САНЧЕЗ и Л. ЛЕЛИК

С целью определения термохимических данных бромметанов был исследован механизм разложения за счет электронных столкновений и пиролиза на вольфрамовой спирали.

С помощью метода, разработанного авторами ранее, были определены потенциалы появления и ионизации продуктов, образующихся при разложении $CHBr_3$ и CBr_4. Исходя из температурной зависимости пиролиза, были определены энергии активации гетерогенного пиролиза бромметанов и было найдено, что они уменьшаются в направлении: $CH_3Br \rightarrow CH_2Br_2 \rightarrow CHBr_3 \rightarrow CBr_4$. На основе величин энергий активации можно заключить, что бромметаны каталитически разлагаются на поверхности вольфрама согласно радикальному механизму.

Были рассчитаны энергии диссоциации связей C—H и C—Br в бромметанах и для них наблюдалась та же самая понижающая тенденция, как и в случае энергий активации. Количественно это явление интерпретируется на квантовохимических основах.

Свойства смесей спирт-амин, VIII

Влияние ассоиации ралтворителя на зависимость электропроводности от концентрации для систем амин — спирт и амин — вода

Ф. РАТКОВИЧ, М. ЛАСЛО и Т. ШАЛАМОН

Были исследованы смеси н-бутил и н-пропиламинов со спиртами и водой. Была измерена их электропроводность в зависимости от концентрации. Было установлено, что изменение удельной молярной электропроводности в зависимости от концентрации может быть объяснено на основе простой ассоциационной модели. Образование ионов типа A_nB является результатом диссоциации ассоциатов, содержащих единственную молекулу амина и более молекул растворителя. На основе данных измерений можно было сделать заключения относительно средней степени ассоциации. Эта величина для спиртов и воды хорошо укладывается в тот ряд данных, который был получен для степеней ассоциации с помощью других методов.

Взаимодействия растворенного вещества с растворителем в водных растворах неэлектролитов

Эффекты вязкости

А. М. ХАФЕЗ и Х. САДЕК

Взаимодействия между растворенным веществом и растворителем были исследованы на основе измерения вязкости водных растворов метанола, этанола, *трет*-бутанола, глицерина, диоксана, метилцеллозольва, ацетона, ацетонитрила и диметилсульфоксида. Во всех системах были детектированы молекулярные комплексы. Данные обсуждаются в свете теории Хармса.

Взаимодействие гетероароматических β-энаминоэфиров с малеиновым ангидридом

Фото—Димрот превращения 5-амино-4-этоксикарбонил-1,2,3-триазоля

Г. СИЛАДИ и Х. ВАМХОФФ

2-Амино-3-этоксикарбонил-4,5,6,7-тетрагидробензотиофен (**1**) и 5-амино-4-этоксикарбонилпиразоль (**4**) реагируют с малеиновым ангидридом, давая при этом производные замещенной малеамидной кислоты (**3** и **5**, соответственно). Были исследованы реакционная способность соединений **3** и **5**, а также их склонность к циклизации. 5-Амино-4-этоксикарбонил-1-фенил-1,2,3-триазоль (**12**), подверженный фотосенсибилизации, превращается в 5-анилино-4-этоксикарбонил-1,2,3-триазоль (**14**).

Превращения тозиловых и мезиловых производных в ряду морфина, XVI

Новые данные в связи с механизмом аллильной перегруппировки

Ш. МАКЛЕЙТ, Т. МИЛЕ и Р. БОГНАР

Приводятся новые данные, доказывающие сложный механизм ($S_S2 + S_{Si}'$) аллильной перегруппировки в случае морфиновых алкалоидов. Исходя из тозилата кодеина и с некоторыми модификациями условий реакции, были приготовлены оба изомера хлорных производных, т. наз., α-и β-хлорокодиды. Изолированное α-производное было изомеризовано в β-производное, используя условия синтеза β-производного.

Синтез некоторых производных метиловых эфиров кумаринаминокислоты

А. М. ЭЛЬ-НАГАР, М. Х. А. ЭЛЬГАМАЛЬ, Б. А. Н. ЭЛЬ-ТАВИЛ и Ф. С. М. АХМЕД

Кумарин-3-CO-Gly-OMe (II) и соответствующие метиловые эфиры (III—XIV) L—Ala, L—Leu, L—Ser, D—Val, L—Tyr, D—Phe, L—Pro, L—Trp, L—Thr и β-Ala были синтезированы действием хлорида кумарин-3-кислоты (I) на гидрохлориды метилового эфира аминокислоты в диоксане, содержащем Et_3N. Кумарин-3-CO-L-Leu-OMe (IV) в диоксане был превращен с выходом 85% в соответствующий гидразид: 3 [5-(6,7-Диметоксибензофурил)] пропеноил-Gly-OMe (XVII) и соответствующие метиловые эфиры (XVIII—XXII) L-Ala, D-Phe,L-Tyr, L-Thr, L-Trp и L-Ser были приготовлены с помощью взаимодействия хлорида 3[5-(6,7-диметоксибензофурил)] акриловой кислоты (XVI) с метиловым эфиром соответствующей аминокислоты в диоксане, содержащем Et_3N.

The Acta Chimica publish papers on chemistry, in English, German, French and Russian.

The Acta Chimica appear in volumes consisting of four parts of varying size, 4 volumes being published a year.

Manuscripts should be addressed to

Acta Chimica
H-1521 Budapest, Hungary

Correspondence with the editors should be sent to the same address.

The rate of subscription in $ 32.00 a volume.

Orders may be placed with »*Kultúra*« Foreign Trade Company for Books and Newspapers (H-1389 Budapest 62, P. O. B. 149. Account No. 218 10990) or with representatives abroad.

Les Acta Chimica paraissent en français, allemand, anglais et russe et publient des mémoires du domaine des sciences chimiques.

Les Acta Chimica sont publiés sous forme de fascicules. Quatre fascicules seront réunis en un volume (4 volumes par an).

On est prié d'envoyer les manuscrits destinés à la rédaction à l'adresse suivante:

Acta Chimica
H-1521 Budapest, Hongrie

Toute correspondance doit être envoyée à cette même adresse.

Le prix de l'abonnement est de $ 32,00 par volume.

On peut s'abonner à l'Entreprise pour le Commerce Extérieur de Livres et Journaux «*Kultúra*» (1389 H-Budapest 62, P. O. B. 149 Compte-courant No. 218 10990) ou à l'étranger chez tous les représentants ou dépositaires.

«*Acta Chimica*» издают трактаты из области химической науки на русском, французском, английском и немецком языках.

«*Acta Chimica*» выходят отдельными выпусками разного объема. 4 выпуска составляют один том, 4 тома публикуются в год.

Предназначенные для публикации рукописи следует направлять по адресу:

Acta Chimica
H-1521 Budapest, ВНР

По этому же адресу направлять всякую корреспонденцию для редакции.

Подписная цена — $ 32,00 за том.

Заказы принимает предприятие по внешней торговле книг и газет «*Kultúra*» (1389 H-Budapest 62, P. O. B. 149. Текущий счет № 218 10990) или его заграничные представительства и уполномоченные.

Reviews of the Hungarian Academy of Sciences are obtainable at the following addresses:

AUSTRALIA

C. B. D. Library and Subscription Service
Box 4886, G. P. O.
Sydney N. S. W. 2001

Cosmos Bookshop
145 Acland St.
St. *Kilda 3182*

AUSTRIA

Globus
Höchstädtplatz 3
A—1200 Wien XX

BELGIUM

Office International de Librairie
30 Avenue Marnix
1050-Bruxelles

Du Monde Entier
162 Rue du Midi
1000—Bruxelles

BULGARIA

Hemus
Bulvar Ruszki 6
Sofia

CANADA

Pannonia Books
P. O. Box 1017
Postal Station "B"
Toronto, Ont. M5T 2T8

CHINA

C N P I C O R
Periodical Department
P. O. Box 50
Peking

CZECHOSLOVAKIA

Mad'arská Kultura
Národní třida 22
115 66 Praha

PNS Dovoz tisku
Vinohradská 46
Praha 2

PNS Dovoz tlače
Bratislava 2

DENMARK

Ejnar Munksgaard
Nörregade 6
DK—1165 Copenhagen K

FINLAND

Akateeminen Kirjakauppa
P. O. Box 128
SF-00101 Helsinki 10

FRANCE

Office International de Documentation et Librairie
48, Rue Gay-Lussac
Paris 5

Librairie Lavoisier
11 Rue Lavoisier
Paris 8

Europeriodiques S. A.
31 Avenue de Versailles
78170 La Celle St-Cloud

GERMAN DEMOCRATIC REPUBLIC

Haus der Ungarischen Kultur
Karl-Liebknecht-Strasse 9
DDR—102 Berlin

Deutsche Post
Zeitungsvertriebsamt
Strasse der Pariser Kommüne 3—4
DDR-104 Berlin

GERMAN FEDERAL REPUBLIC

Kunst und Wissen
Erich Bieber
Postfach 46
7 Stuttgart 5

GREAT BRITAIN

Blackwell's Periodicals
P. O. Box 40
Hythe Bridge Street
Oxford OX1 2EU

Collet's Holdings Ltd.
Denington Estate
London Road
Wellingborough Northants NN8 2QT

Bumpus Haldane and Maxwell Ltd.
5 Fitzroy Square
London W1P 5AH

Dawson and Sons Ltd.
Cannon House
Park Farm Road
Folkestone, Kent

HOLLAND

Swets and Zeitlinger
Heereweg 347b
Lisse

Martinus Nijhoff
Lange Voorhout 9
The Hague

INDIA

Hind Book House
66 Babar Road
New Delhi 1

India Book House
Subscription Agency
249 Dr. D. N. Road
Bombay 1

ITALY

Santo Vanasia
Via M. Macchi 71
20124 Milano

Libreria Commissionaria Sansoni
Via Lamarmora 45
50121 Firenze

JAPAN

Kinokuniya Book-Store Co. Ltd.
826 Tsunohazu 1-chome
Shinjuku-ku
Tokyo 160—91

Maruzen and Co. Ltd.
P. O. Box 5050
Tokyo International 100—31

Nauka Ltd.-Export Department
2—2 Kanda
Jinbocho
Chiyoda-ku
Tokyo 101

KOREA

Chulpanmul
Phenjan

NORWAY

Tanum-Cammermayer
Karl Johansgatan 41—43
Oslo 1

POLAND

Węgierski Instytut Kultury
Marszalkowska 80
Warszawa

BKWZ Ruch
ul. Wronia 23
00—840 Warszawa

ROUMANIA

D. E. P.
Bucureşti

Romlibri
Str. Biserica Amzei 7
Bucureşti

SOVIET UNION

Sojuzpechatj — Import
Moscow

and the post offices in each town

Mezhdunarodnaya Kniga
Moscow G—200

SWEDEN

Almqvist and Wiksell
Gamla Brogatan 26
S—101 20 Stockholm

A. B. Nordiska Bokhandeln
Kunstgatan 4
101 10 Stockholm 1 Fack

SWITZERLAND

Karger Libri AG.
Arnold-Böcklin-Str. 25
4000 Basel 11

USA

F. W. Faxon Co. Inc.
15 Southwest Park
Westwood, Mass. 02090

Stechert-Hafner Inc.
Serials Fulfillment
P. O. Box 900
Riverside N. J. 08075

Fam Book Service
69 Fifth Avenue
New York N. Y. 1003

Maxwell Scientific International Inc.
Fairview Park
Elmsford N. Y. 10523

Read More Publications Inc.
140 Cedar Street
New York N. Y. 10006

VIETNAM

Xunhasaba
32, Hai Ba Trung
Hanoi

YUGOSLAVIA

Jugoslavenska Knjiga
Terazije 27
Beograd

Forum
Vojvode Mičića 1
21000 Novi Sad

ACTA CHIMICA

ACADEMIAE SCIENTIARUM HUNGARICAE

TOMUS 89 FASCICULUS 4

AKADÉMIAI KIADÓ, BUDAPEST

1976

ACTA CHIM. (BUDAPEST) ACASA 2 89 (4) 289–416 (1976)

ACTA CHIMICA

A MAGYAR TUDOMÁNYOS AKADÉMIA KÉMIAI TUDOMÁNYOK OSZTÁLYÁNAK IDEGEN NYELVŰ KÖZLEMÉNYEI

SZERKESZTI

LENGYEL BÉLA

TECHNIKAI SZERKESZTŐK

DEÁK GYULA és HARASZTHY-PAPP MELINDA

Az Acta Chimica német, angol, francia és orosz nyelven közöl értekezéseket a kémiai tudományok köréből.

Az Acta Chimica változó terjedelmű füzetekben jelenik meg, egy-egy kötet négy füzetből áll. Évente átlag négy kötet jelenik meg.

A közlésre szánt kéziratok a szerkesztőség címére ((1521 Bp., Műegyetem) küldendők. Ugyanerre a címre küldendő minden szerkesztőségi levelezés. A szerkesztőség kéziratokat nem ad vissza.

Megrendelhető a belföld számára az „Akadémiai Kiadó"-nál (1363 Budapest, Pf 24. Bankszámla 215 11488), a külföld számára pedig a „Kultúra" Könyv- és Hírlap Külkereskedelmi Vállalatnál (1389 Budapest 62, P.O.B. 149. Bankszámla: 218 10990) vagy annak külföldi képviseleteinél és bizományosainál.

Die Acta Chimica veröffentlichen Abhandlungen aus dem Bereiche der chemischen Wissenschaften in deutscher, englischer, französischer und russischer Sprache.

Die Acta Chimica erscheinen in Heften wechselnden Umfanges. Vier Hefte bilden einen Band. Jährlich erscheinen 4 Bände.

Die zur Veröffentlichung bestimmten Manuskripte sind an folgende Adresse zu senden:

Acta Chimica
H-1521 Budapest

An die gleiche Anschrift ist auch jede für die Redaktion bestimmte Korrespondenz zu richten. Abonnementspreis pro Band: $ 32,00.

Bestellbar bei dem Buch- und Zeitungs-Außenhandels-Unternehmen »*Kultúra*« (1389 Budapest 62, P.O.B. 149 Bankkonto Nr. 218 10990) oder bei seinen Auslandsvertretungen und Kommissionären.

Acta Chimica Academiae Scientiarum Hungaricae, Tomus 89 (4), pp. 289–295 (1976)

ANWENDUNG DES HYDROPYROLYSE-VERFAHRENS ZUR BESTIMMUNG DES HALOGENGEHALTS ORGANISCHER VERBINDUNGEN

L. MÁZOR

(Lehrstuhl für allgemeine und analytische Chemie, Technische Universität, Budapest)

Eingegangen am 18. Juni 1975

Werden Dämpfe oder Pyrolyseprodukte von organischen Halogenverbindungen mit Hilfe eines mit Wasserdampf gesättigten inerten Gasstroms durch eine Platinkatalysatorschicht der Temperatur 800—1100 °C geleitet, so zersetzen sie sich völlig unter Bildung von Halogenwasserstoff und Kohlenoxiden. Das im Kühler kondensierte und aufgefangene Destillat hat ein verhältnismäßig geringes Volumen und ist von störenden Ionen frei; die Halogenwasserstoffsäuren oder die Halogenidionen können darin mittels geeigneter volumetrischer oder sonstiger analytischer Verfahren genau bestimmt werden.

Einleitung

Das Hydropyrolyse-Verfahren wird bereits seit mehr als 30 Jahren verwendet, besonders zur Bestimmung des Fluor- und Chlorgehalts von Schwermetallsalzen (z. B. Uranfluorid) und Silikaten [1].

Unter der Einwirkung von Wasserdampf (und Sauerstoff) wird der Halogengehalt (X) dieser Verbindungen bei Temperaturen über 1000 °C nach dem folgenden Reaktionsschema frei:

$$MeX_{2_n} + nH_2O \rightleftharpoons MeO_2 + 2nHX\,.$$

Der mit dem Wasserdampf abdestillierende Halogenwasserstoff kann im Destillat acidimetrisch oder nach einem für die Bestimmung von Halogenidionen geeigneten Verfahren erfaßt werden.

Entgegen dem zur Trennung und Anreicherung geringer Fluoridmengen in anorganischen Stoffen früher üblichen Verfahren von WILLARD und WINTER [2] besteht der Vorteil der Hydropyrolyse-Destillation darin, daß die Anreicherung viel stärker ist und die Halogenidionen im Destillat in Abwesenheit störender Ionen bestimmt werden können.

Literaturüberblick

C. A. HORTON [3] machte den Versuch, das Hydropyrolyse-Verfahren zum Bestimmen von Fluor in organischen Verbindungen zu verwenden; der Erfolg blieb jedoch aus, die Dämpfe bzw. Pyrolyseprodukte der organischen

Stoffe durchliefen das leere Hochtemperaturrohr, ohne vollkommen zersetzt zu werden. Unsere Versuche zeigten, daß durch das Einsetzen einer Platinkatalysatorschicht in den geheizten Rohrteil die Dämpfe bzw. Pyrolyseprodukte der Fluor- oder sonstigen halogenhaltigen organischen Verbindungen selbst bei Temperaturen unterhalb von 1000 °C völlig zersetzt werden. Auch Methan und Benzoldämpfe wurden während des Durchgangs durch die ca. 100 mm lange Platinkatalysator-Schicht (Durchmesser ca. 8 mm) bei einer Temperatur von 1000 °C vollkommen verbrannt, die Dämpfe wurden in einem mit Wasserdampf gesättigten inerten Trägergasstrom (Stickstoff, Argon) mit einer Geschwindigkeit von 3—4 cm^3 min durch das Rohr geleitet. Die Katalysatorschicht bestand aus einem locker zusammengedrehten Netz, gewoben aus dünnem Platindraht. Bei der gleichen Versuchsanordnung wurden Fluorverbindungen bei 900—1100 °C, Chlorverbindungen bei 800—900 °C, Bromverbindungen bei 700—800 °C völlig zersetzt. Die Zersetzung von Jodverbindungen erfolgte bei noch niedrigeren Temperaturen. Die Gegenwart von Wasserdampf verhinderte den Zerfall des Jodwasserstoffs, es wurde kein elementares Jod gebildet.

Theoretische Grundlagen des Vorganges

Die Hydropyrolyse ist ein komplexer Vorgang, in dem — in Abhängigkeit von den Eigenschaften der sich zersetzenden Verbindung — gleichzeitig und nacheinander zahlreiche Elementarvorgänge verlaufen, bis endlich die Moleküle der Verbindungen in ihre elementaren Bestandteile bzw. einfache anorganische Zerfallsprodukte zersetzt werden.

Zahlreiche Halogenverbindungen reagieren mit den polaren Wasserdampfmolekülen in einer nukleophilen Substitutionsreaktion unter Bildung von Halogenwasserstoff bereits bei Temperaturen von 200—400 °C, z. B.

$$CH_3CH_2X + {}^-OH...H^+ \rightarrow CH_3CH_2OH + HX\,,$$

$$C_6H_5X + {}^-OH...H^+ \rightarrow C_6H_5OH + HX\,.$$

Solche nukleophile Substitutionsreaktionen gehen besonders leicht vor sich bei Verbindungen, deren Halogenatom durch die Wirkung eines elektrophilen Substituenten gelockert ist. Jedoch reagiert z. B. Chlorbenzol mit Wasserdampf nur bei Temperaturen um 450 °C, unter Bildung von Phenol und Salzsäure (*Raschig*sches Verfahren zur Herstellung von Phenol).

Jedoch zersetzen sich im allgemeinen auch solche Verbindungen unterhalb von 500 °C, die nicht zu nukleophilen Substitutionsreaktionen neigen. Diese Vorgänge verlaufen auf sehr komplexe Art, es sind nur allgemeine Prinzipien ihres Ablaufs bekannt. Bei Halogenverbindungen können Eliminationsreaktionen auftreten, bei denen auch Halogenwasserstoff als Zersetzungs-

produkt erscheint. Der Energiebedarf von thermischen Zersetzungsvorgängen ist von der Energie der Kohlenstoff–Halogen-Bindung sowie von der Größe und Struktur des Moleküls abhängig. Bei zunehmender Temperatur entstehen stets kleinere und wärmebeständigere Zersetzungsprodukte; diese Regel ist für sämtliche Halogenverbindungen gültig. Aus Jod- und Bromverbindungen entstehen — infolge der verhältnismäßig geringen Energie der Kohlenstoff–Jod- bzw. Kohlenstoff–Brom-Bindung — nur selten stabile thermische Zersetzungsprodukte. Der aus Chlorverbindungen und besonders der aus Fluorverbindungen entstehende Tetrachlorkohlenstoff bzw. Tetrafluorkohlenstoff gehört infolge seiner symmetrischen Struktur zu den wärmebeständigsten Verbindungen. Aus den niedermolekularen wärmebeständigen halogenhaltigen Zersetzungsprodukten kann das elementare Halogen oder der Halogenwasserstoff nur mittels einer Oxidationsreaktion freigesetzt werden. Eine solche Reaktion verläuft auf der Oberfläche des Platinkatalysators bei entsprechend hoher Temperatur unter Teilnahme des Sauerstoffs des Wasserdampfes, wobei anstelle der Kohlenstoff–Halogen-Bindung die energiereichere Kohlenstoff–Sauerstoff-Bindung gebildet wird. In dem allgemein bekannten Vorgang der Wassergasherstellung tritt die Reaktion bereits bei 450 °C unter Bildung von Kohlenmonoxid und Wasserstoff ein, und die Gleichgewichtskonstante der Reaktion erreicht bei 830 °C den Wert 1. Als Ergebnis dieser Reaktion entsteht aus den Halogen–Kohlenstoff Verbindungen Kohlenmonoxid, Kohlendioxid und Halogenwasserstoff. Bei Temperaturen unterhalb von 900 °C erscheint bereits das Methan, und bei der Pyrolyse von cyclischen Verbindungen auch das Benzol in dem (hinsichtlich der Reaktion inerten aus dem Rohr austretenden) Trägergas.

Apparatur

In unseren Hydropyrolyse-Versuchen verwendeten wir die in Abb. 1 gezeigte Apparatur. Diese ist zweckmäßig so aufzustellen, daß das Rohrsystem in Richtung des Kühlers etwa 5° abfällt. Dadurch wird erreicht, daß das in den kalten Teilen des Rohrsystems kondensierte Wasser zu den Öfen abfließt und dort verdampft.

Der wesentliche Teil der Apparatur ist das etwa 400 mm lange Quarzrohr mit einem inneren Durchmesser von 8—10 mm, an dessen rechtes Ende sich das Zwischenstück *5*, *6*, an das linke Ende der Liebigkühler *10* mit Schliffen anschließt. Das vierfach verzweigte Zwischenstück kann aus Glas verfertigt sein; der zweig *6* dient zum Einführen des Trägergases, welches das Rohr nach außen hin spült. Im horizontalen Zweig *5* befindet sich der mittels eines Magneten von außen her verschiebbare Stab, dessen Kopf aus Eisen ist. Das in das Brennrohr eindringende Ende des Stabes ist schaufelförmig ausgebildet; auf dieses Ende wird das Schiffchen mit der Einwaage der zu untersuchenden Substanz aufgesetzt. Wird eine flüchtige Flüssigkeit untersucht, so wird sie auf die übliche Weise in eine Kapillare gewogen und diese mit ihrer Öffnung in Richtung zum beweglichen Ofen in das Schiffchen eingesetzt. Mit der Apparatur können auch gasförmige Substanzen untersucht werden. Die Gase werden mit Hilfe einer durch den PTFE-Stopfen im Stutzen *5* durchgestochenen Injektionsnadel in das Rohr eingeführt. Eine andere Möglichkeit besteht darin, das Gas im Glasbehälter gemäß Abb. 2 zu wägen und mit dem Trägergas in die Apparatur zu spülen. Ein ähnlicher Behälter, der leichter ist als 20 g, kann auch auf einer Mikrowaage gewogen werden.

Der dritte Zweig des Mittelstückes schließt sich an die Wasserdampfquelle an; in dieser taucht eine aus Widerstanddraht hergestellte Spirale passender Abmessung in destilliertes

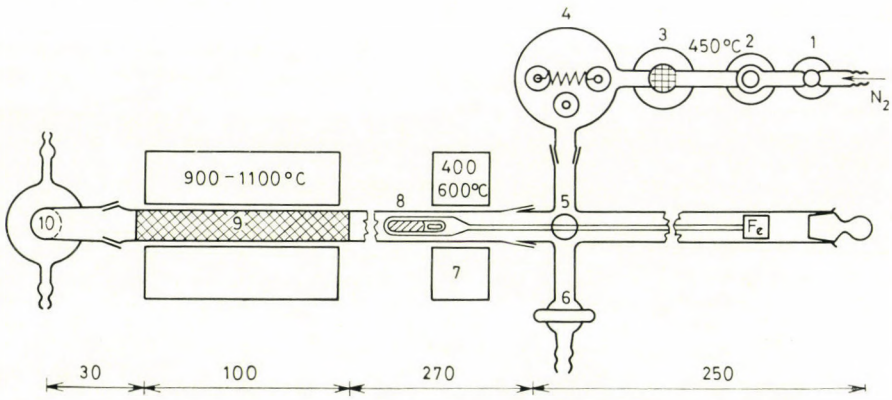

Abb. 1. Schema der Hydropyrolyse-Apparatur; Aufsicht: *1* Druckausgleichgefäß, *2* Rotameter, *3* Rohrofen für die Gasreinigung, *4* Wasserdampfentwickler, *5* vertikaler Rohrstutzen mit PTFE-Stopfen, *6* Einweghahn zum Einleiten des Spülgases, *7* beweglicher elektrischer Rohrofen, *8* Schiffchen aus Platin, *9* Katalysatorschicht (zusammengerolltes Platinnetz), *10* Liebig-Kühler. Maßbezeichnungen in mm

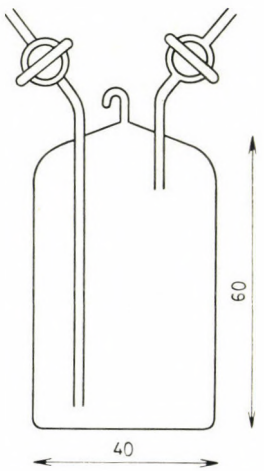

Abb. 2. Gefäß zum Einwägen gasförmiger Substanzen. Maßbezeichnungen in mm

Wasser. Der Heizstrom der Spirale wird mit einem Toroidtransformator geregelt, so daß — durch stärkeres oder schwächeres Sieden des Wassers — die nötige Wasserdampfmenge hergestellt wird. Der Wasserdampf wird durch das Trägergas in die Apparatur transportiert; dieses wird aus einer Stahlflasche oder einem Gasometer zuerst in den gegen Überdruck sichernden Behälter *1*, und anschließend in das Rotameter *2* (5—25 cm^3 Gas/min) geführt. Das Gas gelangt dann in den Rohrofen *3*. Das Rohr des Ofens ist mit Stückchen aus metallischem Kupfer gefüllt und entfernt bei einer Temperatur von ungefähr 450 °C die Sauerstoffverunreinigung des Trägergases.

Es wird so viel der zu prüfenden Substanz in das Schiffchen eingewogen, daß ihr Halogengehalt 2—5 mg betragen soll.

Durchführung der Prüfung

Die Apparatur wird zuerst mit einem schnellen (10—15 cm^3/min) Trägergasstrom 10—20 Minuten lang gespült, wobei das Wasser des Wasserdampfentwicklers in lebhaftem Sieden gehalten wird. Zugleich wird der große Ofen auf die nötige Temperatur aufgeheizt. Temperaturen über 1100 °C erwiesen sich selbst bei der sehr schwer zersetzbaren Trifluoressigsäure als unnötig. Der bewegliche Ofen wird mit einer Temperatur von etwa 500 °C in Betrieb gesetzt und mit seiner Hilfe das im Rohr kondensierende Wasser verdampft. Danach wird der bewegliche Ofen vom Rohr abgenommen (dieser Ofen kann auseinandergeklappt werden). Nach dem Abkühlen des Rohres wird der Stopfen des Zwischenstücks entfernt und das Schiffchen mit der Einwaage in das Rohr geschoben. Inzwischen wird der Hahn *6* des Zwischenstücks geöffnet und die Luft im Rohr mit dem Trägergasstrom verdrängt. Dann wird das Rohr mit dem Stopfen verschlossen und das Schiffchen mit Hilfe eines Magneten so weit im Rohr vorgeschoben, bis es sich etwa 30 mm vor dem großen Ofen befindet. Inzwischen wird die Trägergasgeschwindigkeit auf 5—7 cm^3/min herabgesetzt und das Wasser im Wasserdampfentwickler in nur schwachem Sieden gehalten. Unter das Ausflußrohr des Kühlers wird ein kleiner Titrierkolben gestellt. Dann wird der bewegliche Ofen auf das rechte Ende des Brennrohres aufgesetzt und mit einer Geschwindigkeit von 0,5—1 cm/min in Gang gesetzt. Sobald der Ofen einen Abstand von 1—2 cm vom Schiffchen erreicht hat, wird seine Geschwindigkeit verringert, oder er wird von Hand mit einer Geschwindigkeit von einigen mm pro Minute vorgeschoben. Die Art des Pyrolysierens hängt übrigens — wie bei allen ähnlichen Brennverfahren — von den Eigenschaften der untersuchten Substanz ab. Es ist wichtig, daß die Dämpfe bzw. Pyrolyseprodukte der untersuchten Substanz langsam und gleichmäßig in die Katalysatorschicht gelangen. Sobald der bewegliche Ofen die Front des großen Ofens erreicht hat, wird etwa 10 Minuten lang gewartet, bis die Pyrolyseprodukte mit dem mit Wasserdampf gesättiampfentgergas die Katalysatorschicht durchlaufen. Danach wird das Wasser im Wasserdgten Träwickler in lebhaftes Sieden gebracht und im Laufe von etwa 15 Minuten wird so viel Wasserdampf durch die Apparatur getrieben, daß ungefähr 10 cm^3 Wasser im Titrierkolben gesammelt werden. Diese Wasserdampf- bzw. Wassermenge ist ausreichend, um den Halogenwasserstoff aus der Katalysatorschicht und dem Kühler zu spülen. Werden Fluorverbindungen untersucht, so ist das Kühlerrohr aus Quarz angefertigt und mit Quarzstückchen gefüllt, während das Sammelgefäß aus Quarz oder Kunststoff (z. B. Polyäthylen) bestehen kann.

Die Gesamtdauer der Bestimmung hängt davon ab, wie schnell die Pyrolyseprodukte der untersuchten Substanz durch die Katalysatorschicht getrieben werden können. Der höchste Zeitbedarf tritt bei der Analyse von Fluorverbindungen auf, besonders bei Verbindungen, aus denen im Laufe der Pyrolyse Trifluormethyl-Gruppen enthaltende Zersetzungsprodukte entstehen. Zur völligen Zersetzung von Verbindungen mit solchen Gruppen (z. B. Trifluoressigsäure) sind selbst bei Temperaturen von 1000—1100 °C Verweilzeiten von 10—15 Minuten in der Platinkatalysatorschicht notwendig. Demgemäß kann die Dauer der Bestimmung 35—45 Minuten betragen, während Chlor-, Brom- und Jodverbindungen im allgemeinen im Laufe von 25—35 Minuten bestimmbar sind. Bei der Analyse von organischen Verbindungen mit hohem Jodgehalt (z. B. Jodoform) ist es empfehlenswert, 50—70 mg eines wasserstoffreichen Zusatzstoffes (Dodecylalkohol, Paraffinöl) in das Schiffchen zu geben, damit aus dem freiwerdenden elementaren Jod sofort Jodwasserstoff gebildet wird.

Im Destillat wird der größte Teil des Fluors in Form von Wasserstoffsilikofluorid vorliegen. Diese Verbindung kann z. B. mit einer 0,02 *n* NaOH-Meßlösung unter Anwendung eines säureempfindlichen Indikators (z. B. ein Mischindikator aus Methylrot und Methylenblau) titriert werden. Genauere Ergebnisse werden jedoch mit für Fluorid-Ionen spezifischen Meßmethoden erhalten. So kann man z. B. mit 0,02 *n* Thoriumnitrat-Meßlösung, unter Anwendung von alizarinsulfosaurem Natrium oder Methylthymolblau als Indikator titrieren, oder es kann der Titrationsendpunkt mit Thoriumnitrat potentiometrisch, mit Hilfe einer für Fluoridionen spezifischen Elektrode, angezeigt werden [4]. Die aus Chlorverbindungen entstehende Salzsäure kann acidimetrisch titriert werden, oder es kann das Chlorid-Ion mit Silbernitrat-Meßlösung, mit potentiometrischer Endpunktsanzeige, unter Anwendung eines für Chlorid-Ionen spezifischen Membranelektrodensystems titriert werden. Ähnlich werden Bromidionen bzw. Bromwasserstoff titriert. Die potentiometrische Titration von Jodidionen mit spezifischen Membranelektroden ist infolge des hohen Potentialsprungs recht empfindlich, es kann selbst mit einer 0,005 *n* Silbernitrat Meßlösung auf einen Tropfen genau titriert werden. Jedoch ist — wenn keine Elektrode zur Verfügung steht — auch die jodometrische Methode ähnlich empfindlich. Dabei wird in das Sammelgefäß eine natriumacetathaltige Bromlösung in Eisessig gegeben, welche die mit dem Destillat zutropfenden Jodidionen sofort zu Jodationen oxidiert. Nach dem Entfernen des Bromüberschusses wird aus der mit Schwefelsäure angesäuerten Lösung mit Jodidionen Jod freigesetzt, das mit 0,02 *n* Natriumthiosulfat-Meßlösung titriert wird.

Ergebnisse

Mit dem beschriebenen Verfahren untersuchten wir zahlreiche Fluor-, Chlor-, Brom- und Jodverbindungen. Die Einwaage lag zwischen 2 und 15 mg. Die Ergebnisse sind in den Tabellen I—IV angeführt.

Tabelle I

Fluorverbindungen

Verbindung	Theoretischer F-Gehalt, %	Mittelwert der Ergebnisse von 10 Bestimmungen %	Streuung %
Triamcinolonacetonid $C_{22}H_{27}O_6F$	4,67	4,67	0,35 (0,075)
Haloperidol $C_{21}H_{23}O_2NFCl$	5,05	5,12	0,16 (0,031)
3-Chlor-4-bromfluorbenzol C_6H_3ClBrF	9,07	9,03	0,44 (0,049)
p-Fluoranilin $H_2N.C_6H_4.F$	12,87	12,83	0,36 (0,028)
Freon 12 CF_2Cl_2	31,40	31,23	1,41 (0,045)
Polytetrafluoräthylen $(CF_2—CF_2)_n$	75,88	75,99	2,32 (0,030)

Tabelle II

Chlorverbindungen

Verbindung	Theoretischer Cl-Gehalt, %	Mittelwert der Ergebnisse von 10 Bestimmungen %	Streuung %
2,4-Dinitrochlorbenzol $(O_2N)_2C_6H_3Cl$	17,42	17,55	0,35 (0,020)
3-Fluor-4-chloranilin $H_2N.C_6H_3FCl$	24,22	24,19	0,24 (0,01)
p-Chlorphenol $HO.C_6H_4Cl$	27,57	27,46	0,38 (0,014)
Monochloressigsäure $CH_2ClCOOH$	37,53	37,41	0,64 (0,017)
Hexachlorcyclohexan $C_6H_6Cl_6$	75,60	75,13	0,80 (0,010)
Chloroform $CHCl_3$	89,08	88,70*	0,86 (0,010)
Tetrachlorkohlenstoff CCl_4	92,18	91,33*	1,12 (0,013)

* Mittelwert aus 5 Bestimmungen.

Der in Klammern angeführte Wert in der Spalte Streuung ist die sog. relative Streuung, d. h. die Streuung dividiert durch den Wirkstoffgehalt, in Prozenten. Die relative Streuung charakterisiert die Genauigkeit des Verfahrens besser als die Streuung selbst.

Tabelle III

Bromverbindungen

Verbindung	Theoretischer Br-Gehalt, %	Mittelwert der Ergebnisse von 10 Bestimmungen, %	Streuung %
α-Brom-iso-valerylkarbamid $(CH_3)_2CHCHBrCONHCONH$	35,83	35,85	0,30 (0,011)
N-Bromsuccinimid $(H_2C-CO)_2=NBr$	44,89	44,83	0,35 (0,008)
p-Bromphenol $HO.C_6H_4Br$	46,23	46,17	0,38 (0,008)
p-Bromanilin $H_2N.C_6H_4Br$	46,46	46,49	0,22 (0,005)
Brombenzol C_6H_5Br	51,10	51,16*	0,38 (0,007)
Bromoform $CHBr_3$	94,85	94,72	0,33 (0,008)

* Mittelwert aus 5 Bestimmungen.

Tabelle IV

Jodverbindungen

Verbindung	Theoretischer J-Gehalt, %	Mittelwert der Ergebnisse von 10 Bestimmungen %	Streuung %
7-Jod-5-chlor-8-hydroxychinolin JC_9NH_4ClOH	41,55	41,49	0,42 (0,010)
Jodvanillin $JC_6H_2OH.CHO.OCH_3$	45,65	45,54*	0,39 (0,009)
p-Nitrojodbenzol $O_2N.C_6H_4J$	50,96	50,77	0,29 (0,006)
p-Jodanilin $H_2N.C_6H_4J$	57,95	57,98	0,28 (0,005)
Monojodessigsäure CH_2JCOOH	68,15	67,82*	0,73 (0,011)
Jodoform CHJ_3	97,05	96,23	0,70 (0,007)

* Mittelwert aus 5 Bestimmungen.

LITERATUR

[1] Domange, L.: Anal. Chem., **7,** 225 (1937); Warf, J. C., Cline, W. D., Tevebough, R. F.: Anal. Chem., **26,** 342 (1954); Lee, J. E. jr., Edegerton, J. H., Kelley, M. T.: Anal. Chem., **28,** 1441 (1956); Hibbits, J. O.: Anal. Chem., **29,** 1760 (1957)
[2] Willard, H., Winter, O. B.: Ind. Eng. Chem. Anal. Ed., **5,** 7 (1933)
[3] Kolthoff, I. M., Elving, P. J., Sandell, E. B.: Treatise on Anal. Chem. of the Elements, Vol. 7, Sect. A; Horton, A. H.: Fluorine, S. 237, B: Decomposition of Organic Fluorine Compounds, 2. Hydrolytic Methods
[4] Mázor, L.: Analytical Chemistry of Organic Halogen Compounds, S. 159—163. Akadémiai Kiadó—Pergamon Press, Budapest—Oxford, 1975

László Mázor; H-1111 Budapest, Gellért tér 4.

Acta Chimica Academiae Scientiarum Hungaricae, Tomus 89 (4), pp. 297—305 (1976)

EXTRACTION OF PRASEODYMIUM WITH TRIBUTYL PHOSPHATE FROM AN AQUEOUS PHASE CONTAINING MINERAL SALT MIXTURES

L. GENOV and I. DUKOV

(Department of Inorganic Chemistry, Institute of Chemical Technology, Sofia, 56, Bulgaria)

Received February 8, 1975

The extraction of Pr with TBP solutions in CCl_4 from an aqueous phase containing mixtures of $NaClO_4$ and $NaNO_3$, $NaClO_4$ and NaSCN, or $NaNO_3$ and NaSCN has been investigated. In the presence of salt mixtures the extraction of Pr was found to increase. The highest increase was observed on the addition of small quantities of NaSCN to $NaClO_4$ and $NaNO_3$.

The investigations show that the increased extraction is associated with increased activity coefficients in the presence of mixtures of $NaClO_4$ and $NaNO_3$ and also with the formation of mixed complexes in the presence of NaSCN and $NaClO_4$ or NaSCN and $NaNO_3$.

Introduction

In recent years there appeared a number of publications [1—14] on the extraction of various metals from an aqueous phase containing mixtures of mineral acids or salts. The investigations have shown that in most cases the extraction of the metals studied is increased, as compared with their extraction from an aqueous phase containing a single inorganic anion. In some of the papers cited above, it has been pointed out that the increase of extraction is due to an increase in the activity coefficients [7—13], while others [4—6, 14] state that this increase is due to the formation of mixed complexes containing both anions from the aqueous phase. The third concept [1—3] is that the increase of extraction is caused both by the increase of the activity coefficients and the formation of mixed complexes.

The present work was carried out for investigating the extraction of Pr with tributyl phosphate (TBP) solutions in CCl_4 from an aqueous phase containing mineral salt mixtures, and to determine their influence the extraction of Pr.

Experimental

Reagents

All chemicals employed were of analytical grade (p. a.); TBP ("Fluka") was purified before use [15]. In all experiments the concentration of Pr was 3.55×10^{-4} *M*. To avoid hydrolysis, the pH was maintained at 2.

Procedure

10 ml each, of the aqueous and the organic phases, were shaken for 30 min. As established beforehand, this time is sufficient for equilibrium to be reached. After standing for 1 hr, the phases were separated. The concentration of Pr was determined photometrically with Arsenazo III [20]. To determine Pr in the organic phase, a back extraction was first carried out.

In the photometric determination of Pr, its concentration was maintained within the limits of the optimum [20], so that maximum accuracy (offered by the method) could be attained.

Results and discussion

The distribution coefficients, D, obtained for the extraction of Pr from an aqueous phase containing either the individual salts $NaNO_3$, $NaClO_4$ and NaSCN or their mixtures are given in Figs 1—3 and Tables I—III. Figures

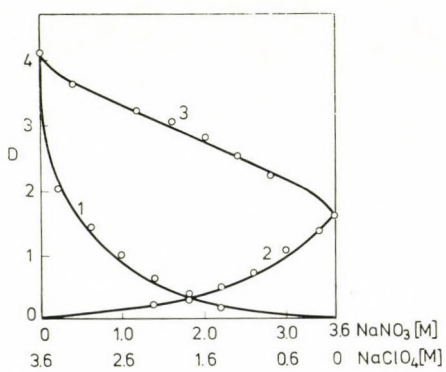

Fig. 1. Values of D for the extraction of Pr with a 2 *M* solution of TBP in CCl_4 from an aqueous phase containing $NaClO_4$ (1), $NaNO_3$ (2), and their mixture (3); $NaClO_4 + NaNO_3 = 3.6$ *M*

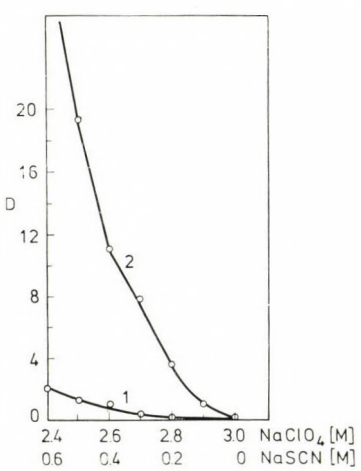

Fig. 2. Values of D for the extraction of Pr with a 1.5 *M* solution of TBP in CCl_4 from an aqueous phase containing NaSCN (1) and a mixture of NaSCN and $NaClO_4$ (2); $NaSCN + NaClO_4 = 3.0$ *M*

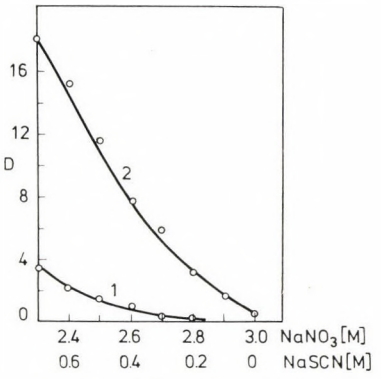

Fig. 3. Values of D for the extraction of Pr with a 1.5 *M* solution of TBP in CCl_4 from a n aqueous phase containing NaSCN (1) and a mixture of NaSCN and $NaNO_3$ (2); NaSCN + + $NaNO_3$ = 3.0 *M*

Table I

Distribution coefficients for the extraction of Pr with a 2 M solution of TBP in CCl_4 from an aqueous phase containing $NaClO_4$ (D_1), $NaNO_3$ (D_2) and their mixture (D_{12})

No.	$NaClO_4$ [*M*]	D_1	$NaNO_3$ [*M*]	D_2	$NaClO_4 + NaNO_3$		D_{12}
					$NaClO_4$ [*M*]	$NaNO_3$ [*M*]	
1	3.6	4.10	—		—	—	—
2	3.2	1.70	0.4	0.05	3.2	0.4	3.62
3	2.4	0.70	1.2	0.18	2.4	1.2	3.20
4	2.0	0.44	1.6	0.25	2.0	1.6	3.00
5	1.6	0.27	2.0	0.38	1.6	2.0	2.78
6	1.2	0.16	2.4	0.55	1.2	2.4	2.50
7	0.8	0.10	2.8	0.78	0.8	2.8	2.20
8	—	—	3.6	1.57	—	—	—

Table II

Distribution coefficients for the extraction of Pr with a 1.5 M solution of TBP in CCl_4 from an aqueous phase containing $NaNO_3$ (D_1), NaSCN (D_2) and their mixture (D_{12})

No.	$NaNO_3$ [*M*]	D_1	NaSCN [*M*]	D_2	$NaNO_3$ + NaSCN		D_{12}
					$NaNO_3$ [*M*]	NaSCN [*M*]	
1	3.0	0.40	—	—	—	—	—
2	2.9	0.37	0.1	0.01	2.9	0.1	1.6
3	2.8	0.33	0.2	0.12	2.8	0.2	3.1
4	2.7	0.30	0.3	0.42	2.7	0.3	5.8
5	2.6	0.27	0.4	0.94	2.6	0.4	7.6
6	2.5	0.24	0.5	1.44	2.5	0.5	11.5
7	2.4	0.21	0.6	2.08	2.4	0.6	15.1
8	2.3	0.19	0.7	3.35	2.3	0.7	18.0

Table III

Distribution coefficients for the extraction of Pr with a 1.5 M solution of TBP in CCl_4 from an aqueous phase containing $NaClO_4$ (D_1), NaSCN (D_2) and their mixture (D_{12})

No.	$NaClO_4$ [M]	D_1	NaSCN [M]	D_2	$NaClO_4$ + NaSCN		D_{12}
					$NaClO_4$ [M]	NaSCN [M]	
1	3.0	0.25	—	—	—	—	—
2	2.9	0.23	0.1	0.01	2.9	0.1	1.1
3	2.8	0.20	0.2	0.12	2.8	0.2	3.7
4	2.7	0.18	0.3	0.42	2.7	0.3	7.9
5	2.6	0.15	0.4	0.94	2.6	0.4	11.1
6	2.5	0.12	0.5	1.44	2.5	0.5	19.6
7	2.4	0.10	0.6	2.08	2.4	0.6	29.3

2 and 3 do not show the extraction from an aqueous phase containing only $NaClO_4$ or $NaNO_3$ because, under the experimental conditions, it is negligibly small. From the data indicated in Figs 1—3 and Tables I—III, it is evident that on using salt mixtures the extraction of Pr is in all cases under consideration greater than the sum of effects, due to the same salts employed separately. This is a peculiar kind of synergic effect, caused not by the presence of mixtures of the extracting agent in the organic phase, but rather by the presence of salt mixtures in the aqueous phase.

The investigations made so far offer no possibility to explain the increased extraction. This requires some additional studies.

I. Extraction from an aqueous phase containing mixtures of $NaClO_4$ and $NaNO_3$

One of the problems in the present work was to establish whether mixed complexes are extracted with $NaClO_4$ and $NaNO_3$ present in the aqueous phase. In principle, the increased distribution coefficient of Pr for extraction from an aqueous phase containing mixtures of the two salts (Fig. 1 and Table I) may be explained either by the increase of the activity coefficients or by the formation of mixed complexes containing anions of both salts. Let us assume that the better extraction is due to the increase of the activity coefficients, *i.e.* no mixed complexes are formed and the complexes extracted contain only one of the anions present in the aqueous phase. It has been found [16, 17] that these complexes are of the composition $Pr(NO_3)_3.3TBP$ and $Pr(ClO_4)_3.6TBP$. In this case

$$D = K_{30}[TBP]^3 [NO_3^-]_3 \gamma_{1\pm 3}^4 + K_{03}[TBP]^6 [ClO_4^-]^3 \gamma_{2\pm}^4 \qquad (1)$$

In the above expression K_{30} and K_{03} are the extraction constants for the complexes $Pr(NO_3)_3.3TBP$ and $Pr(ClO_4)_3.6TBP$, respectively, while $\gamma_{1\pm}$ and $\gamma_{2\pm}$ stand for the mean activity coefficients.

In order determine the validity of the above assumption it is necessary to measure the activity coefficients of $Pr(NO_3)_3$ and $Pr(ClO_4)_3$ in a solution of $NaNO_3$ and $NaClO_4$. The isopiestic method [21] was employed for the purpose. It was established that with a total concentration of 3.6*M* the activity coefficient of $Pr(NO_3)_3$ changes from 0.165 (in a solution of $NaNO_3$) to 0.631 (in a solution of $NaClO_4$), while the activity coefficient of $Pr(ClO_4)_3$ is changed from 0.821 (in a solution of $NaClO_4$) to 0.231 (in a solution of $NaNO_3$).* Substitution of the above values into expression (1) leads to a satisfactory agreement with the data on the extraction of Pr from an aqueous phase containing mixtures of $NaNO_3$ and $NaClO_4$. Therefore, one may conclude that the enhanced extraction is due to the change in the activity coefficients. However, the possibility of formation and extraction of mixed complexes cannot be excluded as this has been found in Refs [1, 2] for the extraction of Zr and Hf with TBP. Nevertheless, in our case the influence of mixed complexes on the increase of Pr extraction must be insignificant.

II. Extraction from mixtures of $NaSCN—NaClO_4$ and $NaSCN—NaNO_3$

A strong influence of NaSCN on the extraction of Pr is observed in both cases under consideration. Figures 2 and 3 and Tables II and III make evident that the addition of small amounts of this salt leads to strongly increased extraction. In our opinion this increase is due primarily to the extraction of mixed complexes as the concentration of added NaSCN is too small to cause (at a constant ionic strength) a significant increase in the activity coefficients. However, before considering the influence of these mixtures, it is necessary to investigate the extraction of Pr from an aqueous phase that contains only NaSCN and to determine the solvation number of the extracted complex, because the data available in the literature are quite diverse [8, 18, 19]. The authors of Ref. [18] have found that La, Eu, and Lu form complexes which have solvation numbers of 5, 4 and 3, respectively. Our investigations (Fig. 4) have shown that the extracted complexes have a solvation number of 5, *i.e.* their composition is $Pr(SCN)_3.5TBP$. An extraction constant of $K_{30} = 1.2$ was established.

To determine the solvation number of the assumed mixed complexes for their extraction from an aqueous phase containing $NaClO_4$ and NaSCN,

* The complete data on the investigation of the activity coefficients will be the subject of a separate communication.

the dependence of lg D on log [TBP] was studied at NaSCN concentrations of 1.8 *M* and 0.9 *M* and at 0.9 and 1.8 *M* $NaClO_4$, respectively (Fig. 5). In both cases linear relationship with a slope of 5, were obtained which indicates

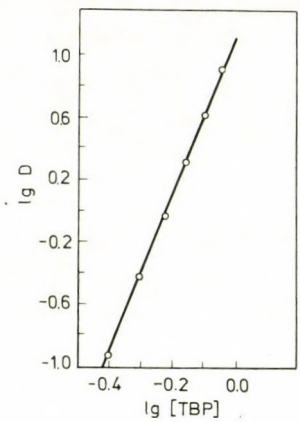

Fig. 4. Dependence of lg D on lg [TBP] for the extraction of Pr from an aqueous phase containing 2.1 *M* NaSCN

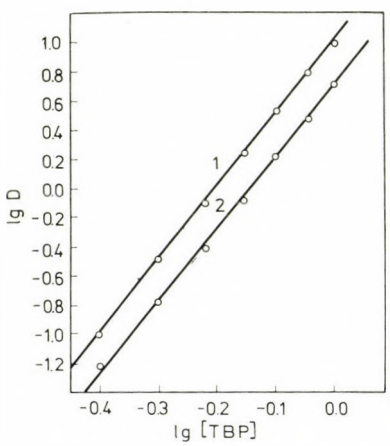

Fig. 5. Dependence of lg D on lg [TBP] for the extraction of Pr from an aqueous phase containing NaSCN and $NaClO_4$: 1. NaSCN = 1.8 *M*, $NaClO_4$ = 0.9 *M*; 2. NaSCN = 0.9 *M*, $NaClO_4$ = = 1.8 *M*

that only penta-solvates are extracted. Presumably, it would impossible to detect the complex $Pr(ClO_4)_3$. 6TBP, it being extracted to a lesser extent. The availability of only the penta-solvates reduces the number of probable complexes to three, namely, $Pr(SCN)_3$.5TBP with an extraction constant of K_{30}; $Pr(SCN)_2(ClO_4)$.5TBP with an extraction constant of K_{21}; and Pr(SCN)

$(ClO_4)_2.5TBP$ with an extraction constant of K_{12}. If the activity coefficients remain constant, the distribution coefficient will be determined by

$$D = K_{30}[SCN^-]^3[TBP]^5 + K_{21}[SCN^-]^2[ClO_4^-][TBP]^5 + \\ + K_{12}[SCN^-][ClO_4^-]^2 \cdot [TBP]^5 \quad (2)$$

On dividing both sides of Eq. (2) by $[TBP]^4$, one

$$D/[TBP]^4 = [TBP]\{K_{30}[SCN^-]^3 + K_{21}[SCN^-]^2[ClO_4^-] + K_{12}[SCN^-][ClO_4^-]^2\} \quad (3)$$

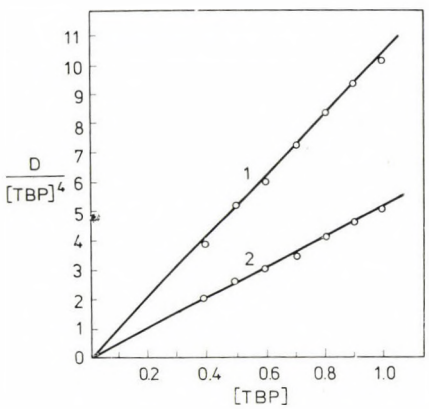

Fig. 6. Dependence of $D/[TBP]^4$ on [TBP] for the extraction of Pr from an aqueous phase containing NaSCN and $NaClO_4$: 1. NaSCN = 1.8 *M*, $NaClO_4$ = 0.9 *M*; 2. NaSCN = 0.9 *M*, $NaClO_4$ = 1.8 *M*

As $[SCN^-]$ = const and $[ClO_4^-]$ = const, Eq. (3) corresponds eq. to a straight line passing through the origin of the co-ordinate system. If the assumption made about the complexes existing in the organic phase is correct, then — at a definite and constant ratio of the two salts — the experimental data should confirm the above considerations. It is evident from Fig. 6 that the dependences of $D/[TBP]^4$ on [TBP], obtained with two ratios of NaSCN and $NaClO_4$ give straight lines passing through the origin. This is additional evidence for the extraction of penta-solvates and at the same time it proves the absence of tetra-solvates. If the latter had been available, the straight lines would have been characterized by an intercept on the ordinate axis. This is observed in Fig. 7, which illustrates the dependence of $D/[TBP]^4$ on [TBP] for the extraction of Pr from an aqueous phase containing NaSCN and $NaNO_3$. The experimental results indicate that with 1.8 *M* NaSCN and 0.9 *M* $NaNO_3$ only penta-solvates are extracted, while at concentrations of 0.9 *M* NaSCN and 1.8 *M* $NaNO_3$ tetra-solvates are extracted together with the penta-solvates.

The data illustrated by Figs. 6 and 7 permit some further conclusions. The slope of curves 1 in both figures is approximately the same. These curves correspond to 1.8 *M* NaSCN and the to 0.9 *M* $NaClO_4$ or $NaNO_3$. Hence, the exchange of $NaClO_4$ for $NaNO_3$ affects the extraction but very little. This fact indicates that at high NaSCN concentrations, it is the complexes $Pr(SCN)_3.5TBP$ that are predominantly extracted. In this case, constants K_{21} and K_{12} in the right-hand side of Eq. (3) will have a small value, as compared with K_{30} but the relationship will remain a straight line. At the same time,

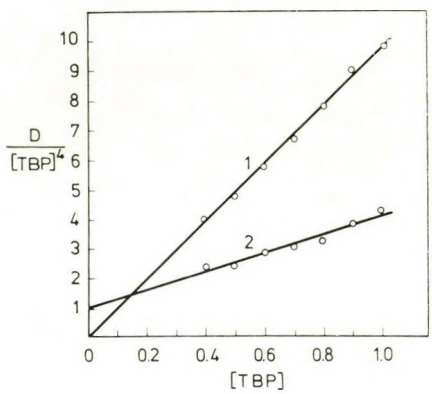

Fig. 7. Dependence of $D/[TBP]^4$ on [TBP] for the extraction of Pr from an aqueous phase containing NaSCN and $NaNO_3$: 1. NaSCN = 1.8 *M*, $NaNO_3$ = 0.9 *M*; 2. NaSCN = 0.9 *M*, $NaNO_3$ = 1.8 *M*

the data for curves 2 in Figs. 6 and 7, obtained for 0.9 *M* NaSCN and 1.8 *M* $NaClO_4$ or $NaNO_3$ differ appreciably. The different slopes of the straight lines, as well as the differences in the distribution coefficients permit to assume the extraction of mixed complexes with solvation number 5 when NaSCN and $NaClO_4$ are available in the aqueous phase, and of mixed complexes with solvation number 4 in the presence of NaSCN and $NaNO_3$.

REFERENCES

[1] Rozen, A. M.: Radiokhimiya, **10,** 273 (1968)
[2] Reznik, A. M., Rozen, A. M., Korovin, S. S., Apraksin, I. A.: Radiokhimiya, **5,** 49 (1963)
[3] Apraksin,I. A., Korovin, S. S., Reznik, A. M., Rozen, A. M.: Radiokhimiya, **12,** 17 (1970)
[4] Korovin, S. S., Berezkho, P. G., Reznik, A. M.: Khimiya protsessov ekstraksii, p. 172. Nauka Moskow 1972
[5] Sekine, T., Hamada, T., Sakairi, M.: Bull. Chem. Soc. Japan, **39,** 244 (1966)
[6] Hasegawa, Y.: Bull. Chem. Soc. Japan, **43,** 2665 (1970)
[7] Hasegawa, Y., Sekine, T.: J. Inorg. Nucl. Chem., **36,** 421 (1974)
[8] Sekine, T.: Bull. Chem. Soc. Japan, **38,** 1972 (1965)

[9] SEKINE, T.: Acta Chim. Scand., **19,** 1435 (1965)
[10] MORIYA, H., SEKINE, T.: Bull. Chem. Soc. Japan, **44,** 3347 (1971)
[11] SEKINE, T., KOMATSU, YU., SAKAIRI, M.: Bull. Chem. Soc. Japan, **44,** 1480 (1971)
[12] TEBELEV, L. G., MELKAYA, R. F.: J. Neorg. Khim. **18,** 2814 (1973)
[13] SAMODELOV, A. P.: Radiokhimiya, **6,** 568 (1964)
[14] GENOV, L., SACHARIEVA, M.: Monatsh. Chem., **104,** 470 (1973)
[15] DE, A. K., KHOPKAR, S. M., CHALMERS, R. A.: Solvent Extraction of Metals, p. 172. Van Nostrand, London
[16] YOSHIDA, H.: J. Inorg. Nucl. Chem., **26,** 619 (1964)
[17] KERTES, A.: Poslednie dostizheniya v oblasti zhidkostnoi ekstraktsii, p. 49, Khimiya, Moskow
[18] KHOPKAR, P. K., NARAYANKUTTY, P.: J. Inorg. Nucl. Chem., **34,** 2617 (1972)
[19] YOSHIDA, H.: J. Inorg. Nucl. Chem., **24,** 1257 (1962)
[20] SAVVIN, S. V.: Arsenazo III, p. 177 Moskow, Atomizdat, 1966
[21] MIKULIN: Voprosy fizicheskoi khimii rastvorov elektrolitov p. 222. Khimiya, Moskow 1968

L. GENOV, I. DUKOV
Department of Inorganic Chemistry,
Institute of Chemical Technology, Sofia 56, Bulgaria.

Acta Chimica Academiae Scientiarum Hungaricae, Tomus 89 (4), pp. 307—317 (1976)

CALORIMETRIC INVESTIGATIONS ON THE POLYMERIZATION OF *CIS*-2,4-DIMETHYL-2,4,8,10,10--HEXAPHENYL-SPIRO(5,5)-PENTASILOXANE

T. Székely, M. Lengyel

(Research Laboratory for Inorganic Chemistry of the Hungarian Academy of Sciences, Budapest)

and

V. S. Papkov, A. E. Zachernyuk, A. A. Zhdanov, K. A. Andrianov

(Institute of Elementorganic Compounds, Academy of Sciences, Moscow, USSR)

Received April 26, 1975

The caloric changes of *cis*-2,4-dimethyl-2,4,8,8,10,10-hexaphenyl-spiro(5,5) pentasiloxane were investigated by the DSC technique. It has been found that the melting of this compound is accompanied by a recrystallization process, in which the original compound transforms into a modification with a higher melting point. The polymerization of the above compound in the presence of various amounts of KOH as catalyst has also been studied. The process was found to be a complex, multi-step reaction. The characteristic temperatures, and the heats of polymerization and melting were determined from the calorimetric curves. The activation energy of polymerization, calculated by approximate methods, is 30 kcal/mol.

Owing to the easy deformability of the O—Si—O valence angles, the structures of organosilicon polymers and oligomers depend very strongly on the nature of the substituents. The medium also plays an important role, and these factors may exert a major influence on the thermal changes, such as phase transitions or polymerization.

The accurate measurement of these thermal changes permits to study the polymerization process and the resulting isomers, stereoisomers and conformers.

In this respect *cis*-2,4-dimethyl-2,4,8,8,10,10-hexaphenyl-spiro(5,5)-pentasiloxane (**I**) is a very interesting compound since it contains di- and tetrafunctional units and has a spirocyclic structure. This compound is solid and crystalline at room temperature, but is also capable of phase transition and polymerization, and thus it can be used to adventage. The substance was prepared [1] *via* the reaction given in Fig. 1. The reaction conducted in solution phase at room temperature yields the pure *cis* isomer shown in the Figure.

This spirosiloxane compound can be regarded as a condensation product of two trisiloxane (D_3) rings. Its infrared spectrum is, like that of D_3, considerably different from those of simple, linear polysiloxanes.

The thermal effects were measured with a Perkin—Elmer DSC-1B instrument, the maximum sensitivity of which is 1 mcal/sec. First the process of

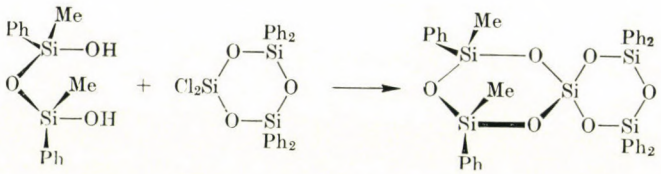

Fig. 1. Synthesis of compound **I**

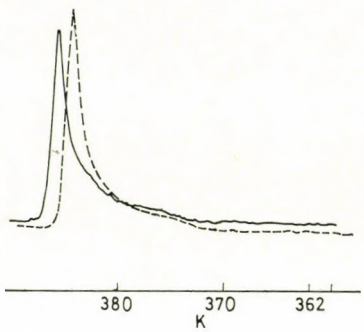

Fig. 2. Melting curve of **I** in various specimen holders. — — — Pt holder, sample weight 3.340 mg; ——— Al holder, sample weight: 3.199 mg; $\Delta H_1 = \Delta H_2 = 11.35$ cal/g; heating rate (β) = 8 °C/min

melting was studied, mainly in order to determine the stability of the compound at its melting point and in molten state. As the compound produces a fairly sharp peak, it is sufficiently pure, and does not decompose during melting. Figure 2 shows two melting curves, corresponding to aluminium and platinum specimen holders, respectively. Both the shapes of the curves and the heats of melting obtained, which agree to within two decimals, indicate an excellent reproducibility. The shift in the location of maximum is due to the fact that the two curves were measured on two subsequent days, and the instrument was not re-calibrated, *i.e.* the curves were plotted against the same temperature scale.

If a sample once melted (a) is cooled and remelted, the curve shown in Fig. 3 can be obtained.

As can be seen, in the second melting process (b) an extra peak appears at higher temperatures, which becomes the only peak in the third melting (c). It may be assumed as an explanation that in the melt — owing to the remarkable temperature dependence of the substituent effect known in silicon chemistry — the original *cis* form is converted into the *trans* derivative with a higher melting point. It cannot be excluded, however, that the two melting peaks correspond to the same molecular form, but to two crystal modifications.

Upon the effect of a catalyst (0.02% KOH), the spirosiloxane undergoes polymerization [1], which can be monitored through the increase in molecular weight or the extensive changes in the infrared spectrum. This catalytic poly-

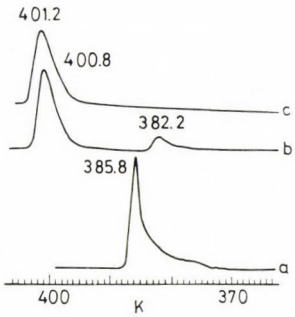

Fig. 3. Melting curve of **I** in repeated melting. Sample weight: 3.199 mg, $\beta = 8$ °C/min

merization, with an essentially ionic mechanism, is widely known for siloxanes. It is also well known that these reactions, unlike several organic polymerization processes which are controlled kinetically, tend towards thermodynamic equilibria, *i.e.* after a relatively short time they reach an equilibrium molecular weight distribution corresponding to the given temperature.

The polymerization performed at various temperatures (120, 130 and 150 °C [1]) was found to occur quite rapidly, which is easy to understand if it is taken into account that the spirocyclic compound is also a strained system of D_3 type. However, to follow the process of polymerization, the gel content of the resulting product was also measured besides the above measurements. This proved to be necessary, because these molecules, unlike the simple starting compounds of types D_3, D_4, etc., which contain only bifunctional units, also include one tetrafunctional segment (Q) per molecule, which makes the monomer itself tetrafunctional if both rings are opened. The extent of cross-linking increases monotonously at 120 and 130 °C, as shown by the gel content data, passes a maximum at 150 °C, and then decreases to a very small value. The latter phenomenon can be attributed to the substituent effect, by assuming that, instead of the disordered cross-linked structure, spirocyclic chain polymers are formed, which are soluble again in the organic solvent employed.

These processes can be illustrated by the following scheme:

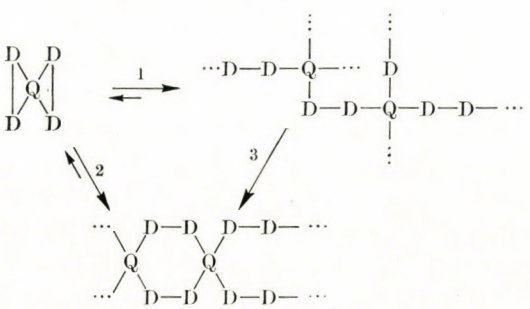

It is of particular interest whether these delicate transformations in molecular structure, which do not exceed the low energies associated with phase transitions, can be detected. The DSC technique appeared to be promising for this purpose. The polymerization was therefore performed in the DSC apparatus using various catalyst concentrations and heating rates. The measurements were similar to the melting experiments on the crystalline monomer, first with a catalyst concentration of 0.02% (as employed in Ref. [1]), and then with potassium hydroxide concentrations of 0.03, 0.05 and 0.2%.

The results can be summarized as follows. At low concentrations (0.02, 0.03 and 0.05%) and high heating rates two or three small but unambiguously observable exothermic peaks could be measured after the melting peak (*cf.* Figs 9 and 10).

With regard to the relative complexity of the system and to the unexpectedly varying nature of the DSC signal, it had to be proved that this DSC curve is really characteristic of the process. All measurements performed by the non-isothermal technique are open to justified doubts, since it is known that "apparent" peaks may often occur due to certain steady states caused by accidental phenomena. The interpretation of DSC measurements deserves particular care, since in this case the above difficulties are multiplied by the perturbation effects of the small amount of sample, the transition thermal resistance and other experimental parameters. As indicated by Fig. 4, the reproducibility on two different samples is quite perfect, proving that accidental effects do not play a role.

Figure 5 illustrates the result of an experiment in which the instrument was set at isothermal mode after the melting. The exothermic signals are still clearly observable, although they are, of course, less expressed than in the non-isothermal mode. Accordingly, as also proved by the isothermal measurement, the exothermic peaks are real, and can be attributed to the polymerization process.

In further measurements low catalyst concentrations were employed again, and we studied the effect of heating rate on the nature of the DSC curve. Figure 6 shows the result of a measurement in which the sample contained 0.02% of catalyst and the heating rate was 2 °C/min. The shape of the curve is remarkably different from that recorded at a heating rate of 32 °C/min (Fig. 4), insofar as two endothermic melting peaks appear, similarly to the melting curves obtained in the absence of catalyst. However, the extra peak appears already in the first experiment, whereas with the systems containing no catalyst the substance of higher melting point is produced only after the second or subsequent heating runs. Unlike with the simple melting curves, there is a sharp exothermic peak here between the two endothermic peaks, with an area approximately equal to that of the second melting peak. Consequently, upon the effect of catalyst a phase transition takes place, which cor-

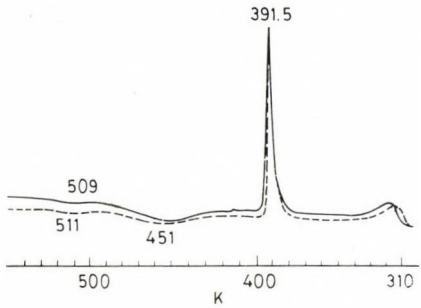

Fig. 4. Polymerization of **I** in the presence of 0.05% KOH; — — — sample weight: 3.328 mg, ——— sample weight: 3.665 mg, $\beta = 32$ °C/min

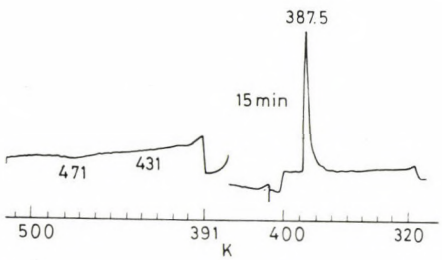

Fig. 5. Polymerization of **I** in the presence of 0.02% KOH as catalyst. Sample weight: 9.326 mg; $\beta = 8$ and 0 °C/min

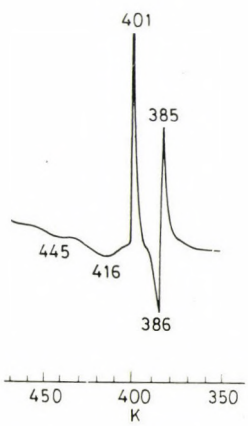

Fig. 6. Polymerization of **I** in the presence of 0.02% KOH. Weight: 8.260 mg, $\beta = 2$ °C/min

responds presumably to the crystal modification of the *trans* form, and the rate of this transition, relative to the melting process, is increased by the catalyst to such an extent that its thermal effect, the heat of transition, becomes readily measurable.

To decide whether the peaks at 385 and 401 K correspond to the spirocyclic monomer, the samples were cooled abruptly after the second melting peak, and their infrared spectra were recorded. The spectra show the invariable presence of the monomer, indicating that the two endothermic peaks and the exothermic peak correspond, even in the presence of catalyst, to the phase transition preceding the polymerization. It is worth noting that, similarly to the endothermic peaks, the exothermic peak located between them at 386 K is also reproducible in position.

As to the further shape of the curve, the third, smallest polymerization peak is absent, like on all the curves recorded at low heating rates, and after the second melting peak there are only two well-defined exothermic peaks. These signals are different in shape from a sharp melting curve, and their flatness is characteristic of chemical reactions or processes involving mass transfer.

As indicated by Figs 7 to 10, at a potassium hydroxide concentration of 0.02%, and higher heating rates, the relative proportions of the two melting peaks vary in favour of the first one, and the height of the exothermic peak between them also decreases significantly.

These facts are apparently easy to interpret if it is assumed that the catalyst plays a role not only in the polymerization but also in the isomerization process.

The specimen was cooled abruptly after the first and second polymerization peaks, respectively, and the infrared spectra of these samples were found to be identical. It is possible that the third exothermic peak is connected, in fact, to the formation of the cyclolinear polymer, which is soluble in organic solvents. Its thermal effect is, however, so small that it could not be investigated so far in detail. The observability of the third peak depends, owing to its low intensity, on the heating rate. Namely, when the effects become more prolonged at low heating rates, the third step may easily merge with the base line, as a result of the limited sensitivity of the equipment.

It is interesting to investigate whether our hypotheses concerning the shape of the curve are supported our measurements at higher catalyst concentrations.

It is apparent from Figure 11 that under such conditions the second melting peak is absent, but the second exothermic polymerization peak is also suppressed, indicating that there is a close correlation between them. Thus, at sufficient rates of polymerization there is no time for competitive isomerization and phase transition and the sample becomes cross-linked in a single step.

The following experiments were aimed as checking the results and the relationship between the catalytic effect and the DSC curve. The potassium hydroxide content was again 0.02%, but the sample was exposed to air for

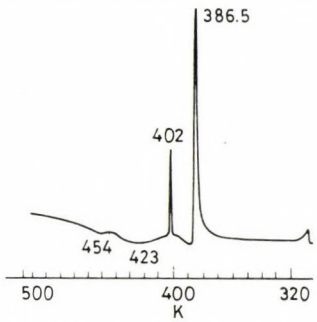

Fig. 7. Polymerization of **I** in the presence of 0.02% KOH. Weight: 4.840 mg, $\beta = 4$ °C/min

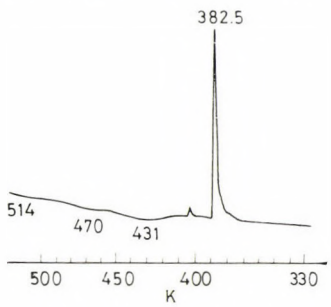

Fig. 8. Polymerization of **I** in the presence of 0.02% KOH. Weight: 4.629 mg, $\beta = 8$ °C/min

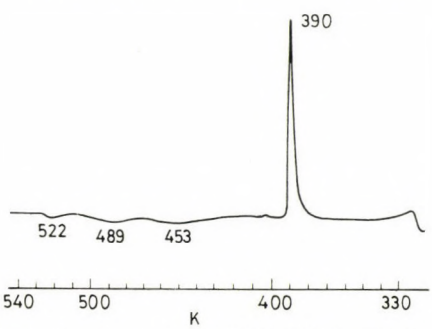

Fig. 9. Polymerization of **I** in the presence of 0.02% KOH. Weight: 5.461 mg, $\beta = 16$ °C/min

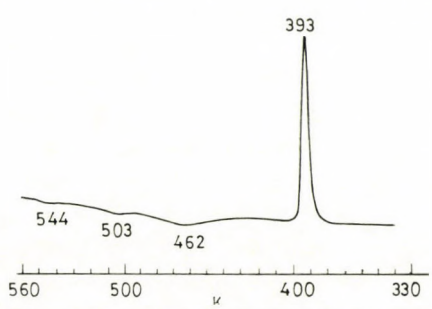

Fig. 10. Polymerization of **I** in the presence of 0.02% KOH. Weight: 3.726 mg, $\beta = 32$ °C/min

a longer period, during which the potassium hydroxide catalyst could certainly carbonize upon the effect of atmospheric carbon dioxide, and there was a possibility for incidental room-temperature reactions. The measurements on these samples gave results identical, to the finest details, with of those the measurements on catalyst-free samples, proving that the mixing involves no changes in the heat capacity or specific heat function, and no chemical change occurs, either, at this temperature. At a catalyst concentration of 0.01% no catalytic effect can be observed at all.

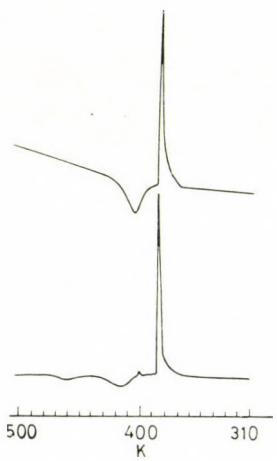

Fig. 11. DSC curves of the polymerization processes in the presence of low and extremely high amounts of catalyst. $\beta = 4$ °C/min. Upper diagram: 0.2% KOH, lower diagram: 0.05% KOH

In the next experiments attempts were made to determine the characteristic temperature and characteristic heat by varying a sufficient number of parameters, relying on the fact of good reproducibility. Some informative kinetic calculations were also performed on the data obtained. It must be emphasized that these calculations are only approximate, semi-quantitative in nature, because the processes are complex and partly overlap each other.

Kinetic calculations can be based only on the characteristic temperature which belongs to the maximum of reaction rate (peak temperature). In this respect the DSC technique is very convenient, because the reaction rate (more particularly the proportional amount of heat evolved), and not the conversion is measured directly. Under the conditions of the given transformations, therefore, we must be satisfied with varying the heating rate systematically at fixed other parameters, and determining the shift in the maximum temperature.

The data obtained are shown in Table I.

Table I

Sample weight (mg)	KOH (%)	Heating rate (°C/min)	$T_{1\,\mathrm{m.p.}}$ (K)	$T_{2\,\mathrm{m.p.}}$ (K)	$T_{1\,\mathrm{pol}}$ (K)	$T_{2\,\mathrm{pol}}$ (K)	ΔH_{melt} (cal/g)	$\Sigma\Delta H_{\mathrm{pol}}$ (cal/g)
8.622	0.02	2	388.1	402.7	416.7	443.8	10.0	9.1
4.649	0.02	4	388.6	402.8	422.0	457.0	10.3	9.8
5.086	0.02	8	391.1	—	432.0	467.0	11.0	9.7
4.629	0.02	8	389.1	402.0	430.0	467.0	10.7	9.3
4.285	0.02	16	389.5	—	439.0	481.0	11.2	9.0
4.123	0.02	16	390.4	—	440.0	481.0	11.2	9.5
3.472	0.02	32	389.6	—	449.0	493.0	11.8	9.8
3.726	0.02	32	390.3	—	456.0	496.0	11.5	8.6
8.005	0.03	2	388.2	402.8	415.0	440.0	11.6	6.8
4.379	0.03	4	388.6	402.3	420.0	452.0	10.6	8.8
4.479	0.03	8	388.6	402.0	431.0	467.0	11.7	9.3
4.906	0.03	16	388.1	—	441.5	482.0	11.7	9.2
3.462	0.03	32	389.1	—	448.0	487.0	11.6	9.5
8.020	0.05	2	388.0	402.7	410.3	446.0	11.4	8.8
4.666	0.05	4	388.3	402.3	415.0	457.0	11.5	9.9
4.613	0.05	8	388.7	—	421.0	476.0	11.4	9.4
6.123	0.05	16	389.5	—	434.0	491.0	11.2	9.8
3.825	0.05	32	389.6	—	399.0	—	11.8	8.8
8.095	0.05	32	391.2	—	454.0	504.0	11.6	9.6
8.002	0.05	32	391.2	—	454.0	504.0	11.7	9.2
8.143	0.05	32	391.2	—	454.9	504.0	11.6	9.8
6.314	0.02	2	386.5	—	399.6	—	9.9	7.4
6.354	0.20	4	387.8	—	406.0	—	10.6	8.2
6.199	0.20	4	387.3	—	405.0	—	11.2	8.1
6.319	0.20	4	388.6	—	407.0	—	10.5	7.9

Since the maximum temperatures in the curves were reproducible within the accuracy of the measurements, the reference method [2] could be applied.

The basic equation of this method is as follows:

$$E = \frac{nRT_{\max}}{x_{\max}} - \left(\frac{\mathrm{d}x}{\mathrm{d}t}\right) \tag{1}$$

where x is the reaction coordinate, the other symbols have the conventional meaning, and subscript "max" refers to the maximum reaction rate.

Eq. (1) can be rewritten, after well known simplifications, as

$$\frac{\mathrm{d}\lg|10^{\beta}|}{\mathrm{d}\left(\frac{1}{T}\right)} = -0.457\frac{E}{R} \tag{2}$$

where E, T and R have the conventional meaning and β is the heating rate.

Figure 12 illustrates that the correlation given by Eq. (2) really holds. For both polymerization processes $E = 30$ kcal/mol can be obtained from Eq. (2), which can be considered as reasonable.

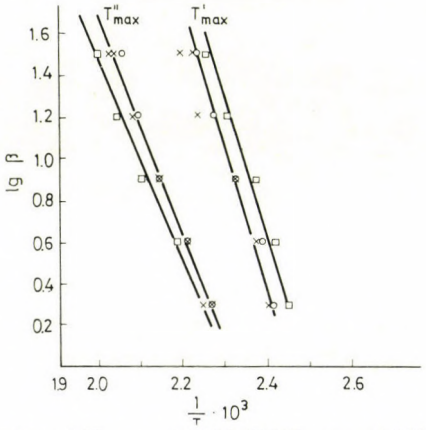

Fig. 12. Plot of lg 10β against $1/T$. × — 0.02% KOH, ○ — 0.03% KOH, □ — 0.05% KOH

It can be stated as a conclusion that the DSC technique, as indicated by the reaction investigated, can be applied to advantage in quantitative studies on ionic polymerization processes in organoelement chemistry.

The results support our statement that the process is very complex and proceeds in several steps. It has also been clarified that there is a very close relationship between the phase transitions observed during the melting of the monomer and the polymerization processes.

REFERENCES

[1] ANDRIANOV, K. A., ZACHERNYUK, A. E.: Vysokomol. Soedin., **16b**, 307 (1974)
[2] PAPKOV, V. S., SHLONIMSKII, G. L.: Vysokomol. Soedin., **10a**, 1204 (1968); OZAWA, T.: Bull. Chem. Soc. Japan, **38**, 1881 (1965)

Tamás SZÉKELY, Mária LENGYEL — Research Laboratory for Inorganic Chemistry of the Hungarian Academy of Sciences, 1502 Budapest, Pf. 132 Hungary

V. S. PAPKOV, A. E. ZACHERNYUK, A. A. ZHDANOV, K. A. ANDRIANOV — Institute of Elementorganic Compounds of the Academy of Sciences of the USSR, Moscow.

Acta Chimica Academiae Scientiarum Hungaricae, Tomus 89 (4), pp. 317—323 (1976)

REACTIONS OF OSMIUM(VIII) COMPOUNDS WITH AMMONIA

J. NYILASI and P. ORSÓS

(Department of General and Inorganic Chemistry, L. Eötvös University, Budapest)

Received July 2, 1975

The reaction of osmium tetroxide and ammonia in a medium containing potassium hydroxide leads to potassium nitridoosmate(VIII), whose nitrogen content cannot be measured by the Kjeldahl method directly, only after reduction with Devarda's alloy. The nitridoosmate(VIII) ions exert a catalytic action in the course of the digestion by concentrated sulphuric acid applied in the nitrogen determination according to Kjeldahl, provided the mixture contains also potassium sulphate, an additive raising the boiling point. Under these conditions ammonia is oxidized to nitrogen. As long as ammonia is present in the system, nitridoosmate(VIII), or more likely the compound formed from it, containing osmium of a lower oxidation state is present. However, after the ammonia has been completely oxidized to elementary nitrogen, the catalytic osmium compound is removed from the sulphuric acid medium, presumably as OsO_4. The extent of oxidation depends on the HSO_4^- to H_2SO_4 mole ratio and attains its maximum when this ratio becomes equal to unity. Osmium tetroxide does not show a catalytic effect of this type. When, however, prior to digestion with sulphuric acid, nitridoosmate(VIII) has been formed, it may interfere with, or even completely inhibit the nitrogen determination according to Kjeldahl.

Introduction

Of the compounds of osmium(VIII), mainly osmium tetroxide has been studied from the aspect of reactions with ammonia. These investigations were concerned with the formation of nitridoosmate(VIII) in an alkaline medium [1]:

$$OsO_4 + NH_3 + OH^- \rightarrow OsO_3N^- + 2H_2O$$

and with the elucidation of its structure [2]. The reactions of solid OsO_4 with gaseous and liquid ammonia have also been studied [3]. Under these conditions, the product is first yellow then becomes brown and finally black. Based on the composition of this product, WATT and POTRAFKE [4] described the reaction by the following equation:

$$3OsO_4 + 9NH_3 \rightarrow Os_3N_7O_9H_{21} + N_2 + 3H_2O$$

The reaction of potassium nitridoosmate(VIII) with ammonia has been studied by WATT and MCMORDIE [5]. Solid $KOsO_3N$ and ammonium iodide were dissolved in liquefied ammonia at —70 °C. On heating the yellow solution

to room temperature, a dark brown precipitate, later turning black, was obtained and nitrogen gas evolved. The composition of the product, insoluble in water and various organic solvents, was identical with that of the trinuclear osmium complex in the above equation:

$$3NH_4OsO_3N + 3NH_3 \rightarrow Os_3N_7O_9H_{21} + N_2$$

The formation of the osmium(VI) complex involves the oxidation of a part of the ammonia to nitrogen. In a strongly alkaline media, only part of the nitrogen content is deaminated from the trinuclear osmium complex, *i.e.* the Os—N bonds are not all identical.

Our present experiments aimed at elucidating whether a chemical reaction occurs between OsO_4 or $KOsO_3N$ and ammonia under the conditions of the Kjeldahl nitrogen determination and whether this reaction affects the determination of ammonia. Concerning potassium nitridoosmate(VIII) we have previously found [6] that it nitrogen content is not deaminated in alkaline media even at higher temperatures and its nitrogen content cannot be measured even after digestion with concentrated sulphuric acid as performed in the Kjeldahl method. However, it can be determined quantitatively as ammonia, on reduction in alkaline media with Devarda's alloy. In possession of the above informations, the experiments were carried out as follows.

Experimental

OsO_4 was a Merck product of analytical purity; $KOsO_3$ was prepared in this laboratory by reacting osmium tetroxide with ammonia in an alkaline medium [7] followed by repeated recrystallization. All the other chemicals were Reanal products of analytical purity.

Mixtures of a volume of 7.5 cm^3 were prepared for the experiments. The mixtures contained 2×10^{-2} mol/dm^3 ammonia, 2×10^{-3} mol/dm^3 OsO_4 or $KOsO_3N$ and 0.05—4.0 mol/dm^3 potassium hydroxide. First the osmium compound and subsequently the required amount of potassium hydroxide was added. The closed flasks were kept in thermostat at 20 °C. Some of the samples withdrawn periodically were treated with 2 cm^3 concentrated sulphuric acid and then boiled until they became colourless (for about 4 hrs). The sulphuric acid solutions were made alkaline and ammonia was determined in a Parnas type distillation apparatus. Titrations were performed with 1/70 *N* sulphuric acid and a mixture of Methyl Red and Methylene Blue indicator.

The other samples were directly transferred from the thermostat into the distillation apparatus and the amount of ammonia determined as specified above.

Results and discussion

In the case of mixtures of various alkalinity, containing osmium tetroxide and ammonia, a deficiency of ammonia was observed in both series of experiments. When *boiling with sulfuric acid was not applied*, the ammonia deficiency was 2×10^{-3} mol independently of the concentration of alkali, *i.e.* identical with the amount of OsO_4. Under such conditions nitridoosmate(VIII) is formed.

This is proved among others also by the observation that, on adding Devarda's alloy to the alkaline mixtures obtained after the removal of ammonia, the amount of ammonia appearing previously as a deficiency can be quantitatively removed by repeated steam distillation.

In the mixtures which contained 2×10^{-3} mol of OsO_4 but *were boiled with concentrated sulphuric acid* (after being kept at 20 °C in a medium of 0.05—1.0 molar potassium hydroxide) an ammonia deficiency of 3×10^{-3} mol was observed as a limit. This amount of nitrogen could not be found even after reduction with Devarda's alloy (after the boiling with sulphuric acid). The time

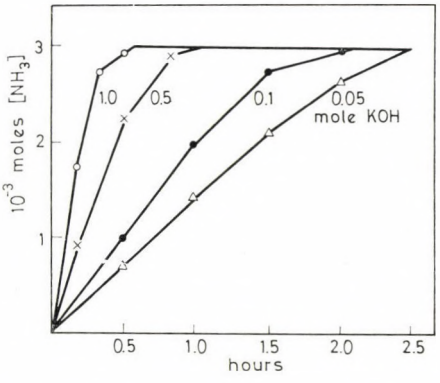

Fig. 1. Amount of ammonia appearing as deficiency, against the time and the concentration of potassium hydroxide

required for the nitrogen deficiency to develop depends strongly on the concentration of potassium hydroxide but the limiting value is independent of this concentration (Fig. 1).

The amount of ammonia added can be quantitatively removed from the mixtures containing potassium nitridoosmate(VIII) and ammonia by steam distillation applied after keeping the samples at 20 °C. When, however, boiling with concentrated sulphuric acid is also applied, 1×10^{-3} mol of the excess ammonia cannot be determined because of the 2×10^{-3} mol $KOsO_3N$, present provided the concentration of the initially applied potassium hydroxide does not exceed 1 mol/dm^3. The amount of ammonia deficiency is, up to this value, quite independent of the alkali concentration and, according to our findings is, just the same also in a medium free of potassium hydroxide. Even the reaction time is independent of the alkali concentration, within the periods tested in the experiments. Namely, when the solution of $KOsO_3N$ is added to the ammonia solution and immediately also concentrated sulphuric acid is added, the ammonia deficiency mentioned is detectable even in such cases.

In our experiments carried out thus far, at KOH concentrations between 0.05 and 1.0 mol/dm^3, ammonia deficiences corresponding to the ratio

$2OsO_4 : 3NH_3$ and $2OsO_3N^- : 1\ NH_3$ were observed. On increasing the concentration of potassium hydroxide in the mixtures, the ammonia deficiency increases after boiling the mixtures with 2 cm^3 of concentrated sulphuric acid (Fig. 2).

If the mixtures containing OsO_4 and ammonia, or $KOsO_3N$ and ammonia, were 4.0 molar with respect to potassium hydroxide, the ammonia could not be determined after boiling with 2 cm^3 concentrated sulphuric acid even if the ammonia concentration was a hundred times higher than that of the osmium compound.

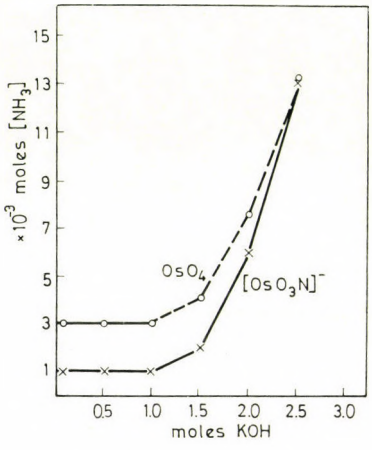

Fig. 2. Limiting value of the ammonia deficiency against the concentration of potassium hydroxide

In the mixtures containing osmium tetroxide and ammonia, a deficiency of ammonia was observed only in the case when OsO_4 had been previously contacted with ammonia in an alkaline medium, *i.e.* the formation of nitridoosmate(VIII) ions had been possible. If ammonia is treated first with concentrated sulphuric acid, then with osmium tetroxide and finally with the required amount of potassium hydroxide, the quantity of ammonia added can be measured quantitatively after boiling the system.

According to our investigations, the reaction leading to ammonia deficiency occurs during the boiling with sulphuric acid provided that OsO_3N^- ions are present. As in mixtures containing potassium hydroxide, HSO_4^--ions are formed on the addition of excess sulphuric acid, the ammonia deficiency depends obviously on the mole ratio $HSO_4^- : H_2SO_4$. If this mole ratio is low, an ammonia deficiency corresponding to the ratio $2OsO_3N^- : 1NH_3$ appears. (It may be presumed that under these conditions a dinuclear osmium complex is formed in which N plays the role of a bridging ligand and, under the conditions mentioned this nitrogen cannot be measured similarly to the nitrogen content of

Table I

Changes in the amount of measurable ammonia as a function of the HSO_4^-/H_2SO_4 mole ratio

Composition of the mixtures: 0.03 mmol $KOsO_3N$; 5.8—23 mmol K_2SO_4; 36—72 mmol H_2SO_4

Mole ratio HSO_4^-/H_2SO_4	Amount of ammonia added (mmol)				
	0.052	0.104	0.210	0.432	0.864
0.24	0.044	0.088	0.196	0.416	0.850
0.36	0.039	0.087	0.182	0.370	0.793
0.48	0.032	0.083	0.160	0.308	0.719
0.60	0.027	0.081	0.144	0.275	0.640
0.75	0.026	0.059	0.130	0.170	0.414
1.00	—	0.007	0.010	0.015	—
1.10	—	—	—	—	—

the nitridoosmate(VIII) ion.) When the HSO_4^- : H_2SO_4 mole ratio is sufficiently high, the catalytic effect of OsO_3N^- ions will prevail.

Mixtures containing $KOsO_3N$ and great amounts of ammonia were boiled, to which potassium sulphate and concentrated sulphuric acid were added in various mole ratios. At the same time also mixtures containing no nitridoosmate(VIII) ions were also investigated for the sake of comparison (Table I).

The amount of ammonia which can be determined decreases with increasing HSO_4^- : H_2SO_4 mole ratio. If this ratio is equal to unity, no ammonia can be measured at all after digestion with sulphuric acid.

As regards the catalytic effect of OsO_3N^- ions it is irrelevant whether the mixtures have been boiled in an oxygen or nitrogen atmosphere.

Concerning the fate of ammonia during the catalytic reaction, the experiments with Devarda's alloy indicated that nitrite or nitrate is not formed, and no nitrogen oxides could be detected either. Subsequently, oxidation to elementary nitrogen appeared to be likely. In order to obtain information on this point, the reaction was carried out in a closed system and changes in the gas volume were measured.

The mixtures examined were transferred into 50 cm^3 Kjeldahl flasks connected with traps containing a potassium hydroxide solution. To the trap placed at the greatest distance from the boiling flask, a gas burette was attached in order to determine the gas volume. For the sake of comparison also mixtures without potassium nitridoosmate(VIII) were investigated (Table II).

Thus, according to our investigations, at a HSO_4^- to H_2SO_4 mole ratio of 1 ammonia is oxidized to elementary nitrogen at the boiling temperature of the mixture, under the catalytic effect of OsO_3N^-.

Subsequent to the reaction, in the mixtures digested in open flasks until they became colourless, no osmium content could be detected by polarography

Table II

Amounts of N_2 measured during digestion carried out in a closed system

Composition of mixtures: 0.03 mmol $KOsO_3N$; 2.58 mmol of NH_3; 11.5 mmol K_2SO_4; 36 mmol H_2SO_4

Calculated amount of N_2 (cm^3) (20 °C, 1 atm)	Measured amount of N_2 (cm^3) (20 °C, 1 atm)
16.8	15.7
	14.6
	15.1
31.0	28.5
	30.5
	28.8

[8] or by the spectrophotometric method developed by us earlier [9]. When however, digestion was interrupted prior to the complete decolouration of the system, a part of the ammonia and also certain part of the osmium could be determined. For example, in samples which still contained 20—30% of the initial amount of ammonia, about 60—70% of the initial osmium could be determined.

Thus, while ammonia is present in the system, also the nitridoosmate(VIII) or more likely the compound formed from it, containing osmium of lower oxidation state, will be present. However, after the ammonia has been oxidized completely to elementary nitrogen, the catalytic osmium compound will be oxidized in concentrated sulphuric acid to osmium tetroxide or to another volatile compound, and will leave the open system. In investigations carried out in a closed system, the vapours of the volatile osmium compound can be condensed and the osmium can be detected.

These observations direct attention to the fact that the presence of even relatively small amounts of certain osmium compounds may interfere with, or inhibit nitrogen determinations according to Kjeldahl.

REFERENCES

[1] Fritzsche, J., Struve, R.: J. prakt. Chem. **41,** 97 (1847); Bull. Acad. Sci. St. Petersburg, **6,** 81 (1848)
Gerhardt, G.: J. Pharmac. **12,** 304 (1847)
Joly, A.: C. R. hebd. Seances Acad. Sci., **112,** 1442 (1891)
Dufet, H.: Bull. Soc. France. Mineral, **14,** 214 (1891)
Brizard, L.: C. R. Hebd. Seances Acad. Sci., **123,** 182 (1896), Bull. Soc. chim., France, **21,** 170 (1899); Ann. Chim. Physique, **7,** 21, 372 (1900)
[2] Werner, A.: Ber. chem. Ges., **34,** 2689 (1901)
Werner, A., Dinklage, K.: Ber. chem. Ges., **34,** 2689 (1901)

FRITZMANN, E.: Z. anorg. Allg. Chem., **172,** 213 (1928)
JAEGER, F. M., ZANSTRA, J. E.: Proc. Roy. Acad. (Amsterdam), **35,** 611, 778, 787 (1932)
BELOV, N. V.: Ann. sect. Plat. URSS, **18,** 112 (1945)
WOODVARD, L. A., ROBERTS, H. L.: Trans. Faraday Soc., **52,** 615 (1956)
WOODVARD, L. A., CREIGHTON, J. A., TAYLOR, K. A.: Trans. Faraday Soc., **56,** 1267 (1960)
GRIFFITH, W. P.: J. Chem. Soc., **3694** (1965)
UEKI, T., ZALKIN, A., TEMPLETON, D. H.: Acta Crystallogr. **19,** 157 (1965)
SEIP, H. M., STOLEVIK, R.: Acta Chem. Scand., **20,** 385 (1966)
MÜLLER, A., KREBS, B., CYVIN, S. J.: Acta Chem. Scand., **21,** 2399 (1967)
BARAN, E. J., AYMONINE, P. J.: An. Asoc. Quim. Argent., **56,** 11 (1968)
MÜLLER, A., BOLLMANN, F., BARAN, E. J.: Z. anorg. allg. Chem. **370** (1969)
BARAN, E. J., AYMONINO, P. J., MÜLLER, A.: Z. Naturforsch., **24,** 271 (1969)
MÜLLER, A., BOLLMANN, F., KREBS, B.: Z. anorg. allg. Chem., **368,** 155 (1969)
[3] VASKA, L.: Thesis, University Texas 1956
DODD, R. E.: Trans. Faraday Soc., **55,** 1480 (1956)
LEWIS, J., WILKINSON, G.: J. Inorg. Nucl. Chem., **6,** 12 (1958)
BERTIN, E. P., NAKAGAWA, I., MIZUSHIMA, S., LANE, T. J., QUAGLIANE, J. V.: J. Amer. Chem. Soc., **80,** 525 (1958)
BARRACLOUGH, C. G., LEWIS, J., NYHOLM, R. S.: J. Chem. Soc., **3552** (1959)
HAIR, M. L., ROBINSON, P. L.: J. Chem. Soc., **2775** (1960)
GRIFFITH, W. P.: J. Chem. Soc., **3248** (1962); **245** (1964); **899** (1966)
CLEARE, M. J., GRIFFITH, W. P.: J. Chem. Soc., **7,** 1117 (1970)
[4] WATT, G. W., POTRAFKE, E. M.: J. Inorg. Nucl. Chem., **17,** 248 (1961)
[5] WATT, G. W., MCMORDIE, W C.: J. Inorg. Nucl. Chem., **27,** 1130, 2013 (1965)
[6] NYILASI, J., ORSÓS, P.: Acta Chim. (Budapest) **75,** 405 (1973); Magy. Kém. Foly., **78,** 407 (1972)
[7] Gmelins Handbuch der Anorganischen Chemie, 66, 69 (1939); Inorg. Synt., **6,** 204 (1960)
[8] ORSÓS, P.: Acta Chim. (Budapest) **77,** 369 (1973); Magy. Kém. Foly., **79,** 94 (1973)
[9] ORSÓS, P., NYILASI, J.: Acta Chim. (Budapest) **74,** 267 (1972); Magy. Kém. Foly., **78,** 256 (1972)

János NYILASI
Piroska ORSÓS
H-1088 Budapest, Múzeum krt 6—8.

Acta Chimica Academiae Scientiarum Hungaricae, Tomus 89 (4), pp. 325—330 (1976)

PROPERTIES OF ALCOHOL–AMINE MIXTURES, IX

F. RATKOVICS and L. DOMONKOS

(Department of Physical Chemistry, University of Chemical Industry, Veszprém; Research Group for Electrochemistry of the Hungarian Academy of Sciences)

Received July 7, 1975

The dipole moments of secondary amines such as diethyl-, di-*n*-propyl- and di-*n*-butylamine, decrease with increasing temperature. This phenomenon can be interpreted by the self-association of secondary amines and the parallel alignment of the associated molecules. The heat of formation of N—H...N bonds is ca. 2 kcal/mole according to calculations based on the Mecke—Kempter model. The dipole moments of tertiary amines increase with increasing temperature. This behaviour indicates a strong interaction between the molecules in the liquid phase, and suggests that this interaction causes an antiparallel alignment of the molecules.

The data published so far on secondary and tertiary amines and their mixtures do not permit to determine unambigously whether the hydrogen-bonded association of secondary amines yields cyclic or linear polymers. The data are also insufficient to determine whether the molecules of tertiary amines are oriented to an observable extent by polar interactions. Since the knowledge of the association conditions of the pure components is a prerequisite for a study of alcohol–amine mixtures, we have investigated the relative permittivities of some secondary and tertiary amines in the liquid phase as a function of temperature. The question to be answered is whether the species formed in the self-association of diamines are predominantly cyclic or linear, and whether they are of antiparallel or parallel alignment. The investigation of tertiary amines is also concerned with the parallel or antiparallel character of the orientation caused by the interaction.

The relative permittivity was measured with a precision dielectrometer of type OH-302 in a static frequency range (3—4 MHz), between +50 and —40 °C. The sample cell was provided with a thermostating jacket, and the thermostating liquid was water above 20 °C, and methanol below is temperature.

The density measurements were performed with a digital densitometer DMA O2C, in the above temperature range. As reference, methanol was used; its density data are known from the literature [1].

The refractive index was measured with an Abbe-type refractometer. The measured data are shown in Tables I—III.

Table I

Static relative permittivity and density of triamines as a function of temperature

t (°C)	Diethylamine		Di-*n*-propylamine		Di-*n*-butylamine	
	relative permittivity (ε)	density ϱ (g/cm³)	relative permittivity (ε)	density ϱ (g/cm³)	relative permittivity (ε)	density ϱ (g/cm³)
50	3.289	0.67241	2.785	0.70958	2.603	0.73515
40	3.374	0.68472	2.824	0.72031	2.650	0.74423
30	3.520	0.69618	2.881	0.73019	2.697	0.75248
20	3.680	0.70340	2.923	0.73751	2.765	0.75814
10	3.906	0.72494	3.040	0.74881	2.841	0.77434
0	4.110	0.73446	3.130	0.76002	2.910	0.78439
− 5	4.185	0.73803	3.210	0.76427	2.935	0.78975
−10	4.380	0.75392	3.252	0.76892	2.970	0.79273
−15	4.530	0.75955	3.274	0.77523	3.020	0.79954
−20	4.670	0.76562	3.380	0.78029	3.065	0.80330
−25	4.890	0.77224	3.443	0.78540	3.075	0.80758
−30	5.120	0.77893	3.508	0.79322	3.085	0.81310

Table II

Static relative permittivity and density of triamines as a function of temperature

t (°C)	Triethylamine		Tri-*n*-propylamine		Tri-*n*-butylamine	
	ε	ϱ (g/cm³)	ε	ϱ (g/cm³)	ε	ϱ (g/cm³)
20	2.418	0.72908	2.380	0.75611	2.340	0.77809
15	2.412	0.73379	2.378	0.76065	2.342	0.78164
10	2.413	0.74022	2.355	0.76686	2.343	0.78633
5	2.417	0.74573	2.354	0.77102	2.344	0.79078
0	2.424	0.75104	2.350	0.77571	2.346	0.78996
− 5	—	—	2.342	0.77984	2.345	0.79162
−10	2.450	0.76039	2.340	0.78364	2.345	0.78954
−15	2.453	0.76670	2.326	0.78959	2.346	0.79317
−20	2.468	0.77138	2.323	0.79404	2.349	0.79496
−25	2.477	0.77716	2.323	0.79804	2.348	0.79458
−30	2.497	0.78284	2.325	0.80444	2.346	0.79690
−35	2.521	0.78852	—	—	2.346	0.79787
−40	2.540	0.79282	—	—	2.344	0.79932

Table III

Refractive indexes (n_D) measured at 20 °C

Compound	n_D^{20}
Diethylamine	1.3851
Di-*n*-propylamine	1.4046
Di-*n*-butylamine	1.4183
Triethylamine	1.4008
Tri-*n*-propylamine	1.4171
Tri-*n*-butylamine	1.4297
n-hexane	1.3750

The results were interpreted on the basis of Eq. (1), corresponding the KIRKWOOD—FRÖHLICH theory [2]:

$$g\mu_g^2 = \frac{(\varepsilon_0 - \varepsilon_\infty)(2\varepsilon_0 - \varepsilon_\infty)}{3\varepsilon_0}\left(\frac{3}{\varepsilon_\infty + 2}\right)^2 \frac{3VkT\varepsilon^0}{N} = \mu_f^2 \qquad (1)$$

where μ_g is the vapour phase dipole moment of the molecule, N is the number of molecules in volume V, k is Boltzmann's constant, ε_0 is the static relative permittivity, ε^0 is the absolute permittivity of vacuum 8.85415×10^{-12} Fm^{-1}), ε_∞ is the square of the intrinsic refractive index ($\varepsilon_\infty \to n_\infty^2$), and μ_f is the effective dipole moment of the liquid. Factor g in Eq. (1) is used to take into account the rotational barrier formed by the intermolecular interactions that may also lead to association. The dipole moment generally increases if the orientation of the molecular dipoles is parallel. In these cases g is greater than unity. For antiparallel orientation g is less than 1.

The determination of g involves, in practice, two difficulties. The first one is the determination of n_∞, *i.e.* the intrinsic refractive index. If n_∞ cannot be determined experimentally or theoretically, it is most convenient to measure the refractive index with respect to the Na D line (n_D), and to use it in place of n_∞ [2, 3].

The second problem is posed by the determination of μ_g occurring in Eq. (1). The most widespread method is to determine the orientation polarization as a function of concentration in a dilute solution of some non-polar solvent, and to extrapolate to infinite dilution. According to ONSAGER, the resulting dipole moment and the dipole moment in the vapour phase are related by the equation [3]

$$\mu_s = \frac{(\varepsilon_\infty + 2)(2\varepsilon_0 + 1)}{3(2\varepsilon_0 + \varepsilon_\infty)}\,\mu_g \qquad (2)$$

where ε_0 and ε_∞ refer to the non-polar solvent.

The effective dipole moments were determined from Eq. (1) as a function of temperature, n_∞ being replaced by the corresponding n_D values given in Table III. The results are shown in Table IV. The variation of the dipole moment with the temperature is illustrated in Fig. 1. It can be seen from the diagram that the dipole moments of diamines and triamines change with the temperature in opposite directions.

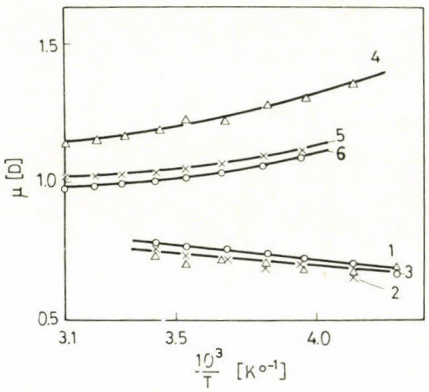

Fig. 1. Effective dipole moment of tertiary and secondary amines against the reciprocal absolute temperature. (1) triethylamine, (2) tri-*n*-propylamine, (3) tri-*n*-butylamine, (4) diethylamine, (5) di-*n*-propylamine, (6) di-*n*-butylamine

Table IV

Dipole moment of di- and triamines as a function of temperature

t (°C)	Diethylamine	Di-*n*-propylamine	Di-*n*-butylamine	Triethylamine	Tri-*n*-propylamine	Tri-*n*-butylamine
50	1.155	1.026	0.978			
40	1.158	1.025	0.991			
30	1.179	1.032	1.002			
20	1.204	1.031	1.026	0.738	0.774	0.772
10	1.255	1.060	1.043	0.716	0.731	0.758
0	1.229	1.073	1.055	0.707	0.709	0.747
−10	1.281	1.097	1.063	0.707	0.689	0.732
−20	1.310	1.114	1.080	0.701	0.649	0.720
−30	1.363	1.126		0.699	0.634	0.702
−40				0.706		0.684

The decrease in the dipole moment of diamines with increasing temperature is due probably to the presence of association polymers in parallel alignment. The result of two opposite effects can be observed: the energy of thermal motion, which tends to break this parallel alignment, acts against the parallel orientation produced by the association. For this reason the parallel

alignment becomes less preferred at higher temperatures, and thus the dipole moment decreases with increasing temperature. It is obvious for similar reasons that the result of the interactions of triamines is a slight antiparallel alignment, and thus their dipole moments increase with increasing temperature, *i.e.* with a decrease in the orientation effect.

We have determined the variation of KIRKWOOD's g factor as a function of temperature. The vapour phase dipole moment of diethylamine and the dipole moments of di-*n*-propyl and di-*n*-butylamine in infinitely dilute solution were taken from the literature [4]:

μ_S (in *n*-hexane)

for di-*n*-propylamine	0.99 D
for di-*n*-butylamine	1.00 D

The data were converted to vapour phase values by means of Eq. (2); the following values of μ_g were used:

$$\mu_g\,(\text{DEA}) \rightarrow 0.920\ \text{D}$$
$$\mu_g\,(\text{DPA}) \rightarrow 0.915\ \text{D}$$
$$\mu_g\,(\text{DBA}) = 0.905\ \text{D}$$

Provided that the association model of MECKE and KEMPTER [5] holds, the following relationship connects the equilibrium constant of association (K) with the g factor [6]:

$$KC_0 = \frac{g^2 - 1}{4} \tag{3}$$

where C_0 is the nominal concentration. Eq. (3) can be used to determine graphically, by means of a $\log (g^2 - 1)$ *vs.* $1/T$ diagram, the heat of association (Fig. 2). The calculated data are given in Table V.

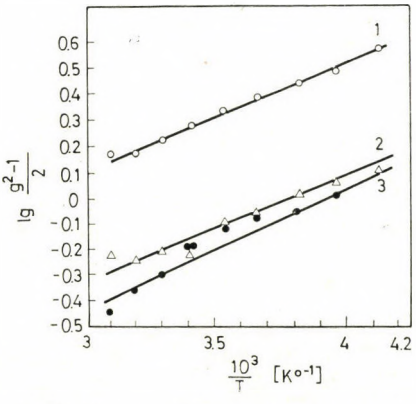

Fig. 2. The $\log \frac{g^2 - 1}{2}$ *vs.* $10^3/T$ diagrams of secondary amines. (1) diethylamine, (2) di-*n*-propylamine, (3) di-*n*-butylamine

Table V

The Kirkwood g-factors of diamines

t (°C)	$10^3/T$ (K^{-1})	Diethylamine		Di-*n*-propylamine		Di-*n*-butylamine	
		g	$\log(g^2-1)$	g	$\log(g^2-1)$	g	$\log(g^2-1)$
50	3.096	1.576	0.1714	1.258	−0.2343	1.167	−0.4410
40	3.195	1.583	0.1778	1.253	−0.2441	1.200	−0.3556
30	3.300	1.643	0.2276	1.271	−0.2111	1.227	−0.2959
20	3.413	1.713	0.2865	1.269	−0.2197	1.286	−0.1851
10	3.534	1.790	0.3432	1.342	−0.0969	1.328	−0.1163
0	3.663	1.860	0.3909	1.374	−0.0516	1.360	−0.0706
−10	3.802	1.939	0.4409	1.432	0.0216	1.376	−0.0492
−20	3.953	2.029	0.4937	1.481	0.0766	1.423	0.0116
−30	4.115	2.195	0.5818	1.514	0.1113		

The changes in the enthalpy of association were calculated on the basis of Fig. 2. The values obtained are −2.01 kcal/mole for diethylamine, −2.00 kcal/mole for di-*n*-propylamine and −2.15 kcal/mole for di-*n*-butylamine, in good agreement with the enthalpies of formation of the N—H...N bond obtained by other authors using other methods, varying between −2.0 and −2.3 kcal/mole [7].

REFERENCES

[1] TIMMERMANS, J.: Sci. Proc. Dublin Soc., **13,** 310 (1912)
[2] KIRKWOOD, J. G.: J. Chem. Phys., **7,** 911 (1939)
[3] SACHPARANOV, M. J.: Wissenschaftl. Z., **9,** 137 (1967)
[4] PARTINGTON, J. R.: An Advanced Treatise on Physical Chemistry, Vol. V, p. 518. Longmans 1954
[5] KEMPTER, H., MECKE, R.: Z. Phys. Chem., B**46,** 229 (1940)
[6] HILL, N. E., VAUGHAN, W. E., PRICE, A. H., DAVIES, M.: Dielectric Properties and Molecular Behaviour. Van Nostrand—Reinhold, London 1969
[7] KEHIAIAN, H.: Bull. Acad. Pol. Sci., **14,** 703 (1966)

Ferenc RATKOVICS
László DOMONKOS
H-8201 Veszprém, Pf. 28.

Acta Chimica Academiae Scientiarum Hungaricae, Tomus 89 (4), pp. 331—335 (1976)

PROPERTIES OF ALCOHOL–AMINE MIXTURES, X

VISCOSITY OF SECONDARY AMINES

F. RATKOVICS and T. SALAMON*

*(Department Physical Chemistry, University of Chemical Industry, Veszprém and *Research Group for Electrochemistry of the Hungarian Academy of Sciences, Veszprém)*

Received July 23, 1975

The variation of average degree of association as a function of the temperature has been investigated by measuring the viscosity of di-*n*-propyl and di-*n*-butylamine in the temperature range from —20 to +80 °C. It has been found that the activation enthalpy of viscous flow and the average degree of association increase rapidly with decreasing temperature. This phenomenon can be interpreted in terms of the-Mecke–Kempter model, assuming infinite chain association. The enthalpy of formation of the hydrogen bond, calculated from viscosity data, is —2.4 kcal/mol, in good agreement with the values calculated from the dielectric data.

In the liquid phase secondary amines form associates in which, according to dielectric investigations [1], the molecules are mostly in parallel position. The most obvious reason for such dipole orientation might be the formation of chain-type association polymers. The present communication reports on further studies aimed at the elucidation of the cyclic or chain-like structure of the associates. Viscosity and the activation enthalpy of viscous flow are related to the degree of association of the polymers formed by liquids [2, 3]. Viscosity measurements as a function of the temperature make thus possible to follow changes in the average degree of association, and thereby to determine indirectly also the enthalpy of the association reaction and to draw conclusion on the cyclic or chain-like structure of the associates. In addition, by measuring the viscosity of secondary amines we also intended to check whether the conclusions from dielectric and viscosity measurements are consistent.

The viscosities of di-*n*-propylamine and di-*n*-butylamine have been determined.

The dynamic viscosity of the components investigated has been measured at atmospheric pressure, with a Höpplet type rheoviscosimeter in the temperature range between —20 and +80 °C. Our results are summarized in Table I.

It can be seen from Fig. 1 that a plot of the logarithm of the dynamic viscosity against the reciprocal absolute temperature does not give straight lines for the two diamines, as opposed to the alcohols investigated earlier [2]. With decreasing temperature, a steadily increasing deviation from the Arrhenius-Andrade linear ralationship can be observed. This means that the activation enthalpy of viscous flow is not constant, decreasing with increasing temperature.

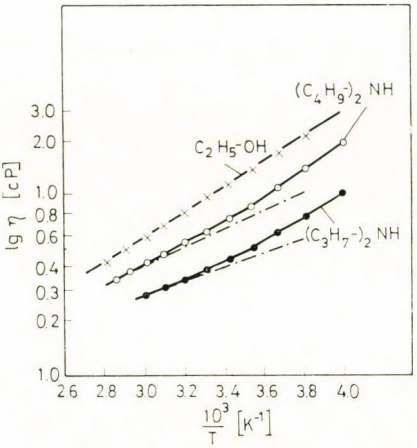

Fig. 1.

It has been shown in our investigation of alcohols [3] that the activation enthalpy of viscous flow is proportional to the average degree of association, at least in the case of low molecular weight alcohols. The slope of the log η *vs.* $\frac{1}{T}$ curves changes with the temperature in the case of diamines, thus these components probably form associates in which the number of the components varies within wide limits. This qualitative finding is indicative of chain association, and is thus in accord with conclusions drawn form dielectric prop-

Table I

Dynamic viscosity as a function of temperature

Temperature (K)	Dynamic viscosity (cP)	
	di-*n*-propylamine	di-*n*-butylamine
253	1.12	2.37
263	0.91	1.65
273	0.73	1.26
283	0.60	1.02
293	0.50	0.85
303	0.44	0.73
313	0.39	0.64
323	0.36	0.55
333	0.32	0.49
343	—	0.43
353	—	0.39

erties [1]. In the case of formation of cyclic association polymers, the maximum possible degree of association is determined by the number of monomers participating in the ring. Since this number can be estimated to be not larger than four, for such cyclic structures, the average degree of association may vary only between 1 and 4.

It is known that in the case of chain association, the model introduced by KEMPTER and MECKE [4], assuming ideal, infinite chain association, describes the experimental results rather well, and is based on a physical concept closely approaching the real situation. We have attempted therefore to interpret the results in terms of this model and on the basis of the linear relationship found between the activation enthalpy of viscous flow and the average degree of association.

According to the model, the standard enthalpies and entropies of consecutive association reactions are identical

$$\Delta H_i^\circ = \Delta H^\circ \text{ (independent of } i\text{)}, \tag{1}$$

$$\Delta S_i^\circ = \Delta S^\circ \text{ (independent of } i\text{)}, \tag{2}$$

i. e. the changes in enthalpy and entropy accompanying the formation and rupture of hydrogen bonds, do not depend on the number of monomers constituting the association multimers. It follows from relationships (1) and (2) that the equilibrium constants of consecutive association reactions are also the same, so that association equilibrium can be unequivocally described by a single equilibrium constant, independent of the value of i.

$$K = K_i = \frac{X_{i+1}}{X_i X_1} \qquad (i = 1,2,\ldots) \tag{3}$$

where X is a real mole fraction and i the number of monomer units forming the associate.

Using van't Hoff's equation, the temperature dependence of the equilibrium constant can be expressed as

$$\frac{\mathrm{d} \ln K}{\mathrm{d}T} = \frac{\Delta H}{RT^2} \tag{4}$$

Integration under the assumption that ΔH is constant yields

$$\ln K = -\frac{\Delta H}{RT} + C \tag{5}$$

Where K is the association equilibrium constant defined by relationship (3), T the absolute temperature, R the universal gas constant, ΔH the enthalpy

of formation of the hydrogen bond, and C is a constant. The equilibrium constant decreases with increasing temperature because the hydrogen bonds are ruptured and the degree of association diminishes.

In addition to this, the correlation found between the average molecular weight of the associates and the activation enthalpy of viscous flow, discussed in our earlier communications [2, 3], has been used for the interpretation of the experimental results. Accordingly

$$\alpha = \frac{\overline{M}}{M_1} = A_1 \Delta \mathrm{H}_v + B_1 \tag{6}$$

where α is the average degree of association, $\overline{M}$ the average molecular weight of the associates ($\overline{M} = X_i M_i$), M_1 the molecular weight of the monomer, while A_1 and B_1 are constants.

In one of our earlier communications [3], the following relationship has been found between the average molecular weight of the pure substance and the equilibrium constant of the Mecke—Kempter model

$$\alpha = \frac{\overline{M}}{M_1} = K + 1. \tag{7}$$

Thus, using Eqs (6) and (7), the relationship between the activation enthalpy of viscous flow ($\Delta \mathrm{H}_v$) and the equilibrium constant (K) is,

$$\Delta \mathrm{H}_v = A_2 + B_2 K \tag{8}$$

where the new constants are denoted by A_2 and B_2. From the definition of the activation enthalpy of viscous flow, we have

$$\frac{\mathrm{d}\, ln\, \eta}{\mathrm{d}T} = \frac{\mathrm{H}_v}{RT^2}$$

and from Eqs (5) and (8), the following relationship is obtained

$$\ln \eta = a + \frac{b}{T} + ce^{-\frac{\Delta \mathrm{H}}{\mathrm{RT}}} \tag{9}$$

where η is the dynamic viscosity (cP)
T the temperature (K)
Δ H the enthalpy of the hydrogen bond (cal/mol)
R the universal gas constant (A 1.98 cal/mol K)
a, b and c are constants.

To check the validity of the relationship deduced from the model, the bonding energy of the hydrogen bond has been calculated from the dynamic viscosity in temperature data in Table I, using relationship (9). Calculations were performed on an ODRA computer. For the energy of the hydrogen bond, a value of —2.4 kcal/mol has been obtained in the case of both di-*n*-propylamine and di-*n*-butylamine. These results agree well with the bonding energies of —2.00 and —2.15 kcal/mol, respectively determined by dielectric measurements for the two compounds and also with the data of other authors obtained by measuring the heats of mixing [5]. The variance σ_2, determined from the differences of the measured and calculated values of ln η is 0.00092 and 0.00110, respectively.

Both model calculations and a qualitative evaluation of experimental results show that in the pure liquid state di-*n*-propylamine and di-*n*-butylamine presumably form mainly chain associates. The enthalpy of formation of the hydrogen bonds is about —2.0 to —2.5 kcal/mol. The charge with temperature of the activation energy of viscous flow is consistent with the change in the average degree of association.

On the basis of this, the probable structure of the associates is

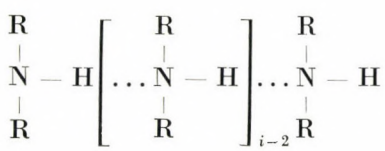

It seems that the above method for the evaluation of the results of viscosity measurements is in accord with the dielectric properties and may be suitable for the distinguishing ring and chain-type polymers association as well as for the determination of the enthalpy of the association reaction.

REFERENCES

[1] RATKOVICS, F., DOMONKOS, L.: Acta Chim. (Budapest). (In press)
[2] RATKOVICS, F., SALAMON, T., DOMONKOS, L.: Acta Chim. (Budapest), **83**, 53 (1974)
[3] RATKOVICS, F., SALAMON, T., DOMONKOS, L.: Acta Chim. (Budapest), **83**, 71 (1974)
[4] KEMPTER, M., MECKE, R.: Z. Phys. Chem. (B) **46**, 229 (1940)
[5] KEGIAIAN, H.: Bull. Acad. Pol. Sci., **14**, 703 (1966)

Ferenc RATKOVICS
Tamás SALAMON
H-8201. Veszprém, Pf. 28.

Acta Chimica Academiae Scientiarum Hungaricae, Tomus 89 (4), pp. 337–346 (1976)

π-ELECTRON SCF-MO CALCULATIONS FOR DISUBSTITUTED BENZENE DERIVATIVES CONTAINING A DONOR AND AN ACCEPTOR GROUP

Á. I. KISS and J. SZŐKE

(Department of Physical Chemistry, Technical University and Department of Optical Spectroscopy, Central Research Institute for Physics)

Received July 5, 1975

The π-electronic structure and spectra of disubstituted benzene derivatives containing an electron donor and an acceptor group have been calculated by the Pariser—Parr—Pople method. The applicability of a uniform parameter system to a wider range of benzene derivatives is discussed in detail. The calculations give good results for the spectral characteristics, ground state charge densities and bond orders. Comparison is made with other π-electron calculations reported in the literature.

Several papers have been published on π-electron SCF MO calculations for limited groups of donor-acceptor disubstituted benzenes. Primarily nitrobenzene derivatives *e.g.* amino- [1—5], hydroxy- [4, 6], and halo-nitrobenzenes [7, 8] have been investigated. Less information is available on benzaldehyde and benzoic acid derivatives. The electronic structure and spectra of methyl- [9], hydroxy- [10], and halo-benzaldehydes [11] have been studied as well as the steric hindrance in methylbenzoic acids [12], and the intramolecular hydrogen bonding in hydroxybenzaldehydes and -benzoic acids [13] were investigated.

The aim of the present work is a systematic study of the π-electronic structure and spectra for a larger number of disubstituted benzene derivatives containing an electron donor and an acceptor group. The method used has been the Pariser—Parr—Pople (PPP) approximation [14] with the same starting values worked out for the monosubstituted compounds [15] and applied for derivatives containing two donor [16], and two acceptor [17] groups. The applicability of uniform starting parameters to the description of π-electron properties of a wider range of compounds has been investigated.

Method of calculation

The details of the PPP method, as used in this work, are given in Ref. [15]. The fluoro, chloro, hydroxy and amino groups were considered as donors, and the formyl, carboxy and nitro groups as acceptors. The π-electronic structure and spectra of all possible disubstituted benzenes built up with the above substituents have been calculated. Throughout the calculations, the starting values giving best fit for the spectral data of the monosubstituted derivatives

Table I

Starting parameters of the substituents

Atomic parameters		
Atom	I_μ (eV)	A_μ (eV)
F	34.00	12.61
Cl	24.37	11.34
Ö	30.07	10.83
N̈	25.73	8.97
C	11.16	0.03
N	14.12	1.78
O	17.70	2.47
Bond parameters		
Bond	$r_{\mu\nu}$ (Å)	$-\beta_{\mu\nu}$ (eV)
C—C aromatic	1.397	2.39
C—F	1.30	2.2
C—Cl	1.69	2.2
C—O hydroxy	1.36	2.5
C—N amino	1.38	2.3
C—C exocycl.	1.50	2.39
C=O carbonyl	1.215	2.7
C=O carboxy	1.245	2.6
C—O carboxy	1.31	2.5
C—N nitro	1.38	2.1
C—O nitro	1.21	3.0

have been used. The atomic and bond parameters of the substituents are collected in Table I.

Planar molecular structures were assumed in each case. With the benzaldehyde and benzoic acid derivatives the calculation was performed for all planar conformations. In this paper, as in the calculation of the di-acceptor derivatives [17], only the O-*cis* forms are considered. The reason for giving preference to this rotamer in the study of carboxylic acids is the smaller steric demand of the carbonyl group and the greater separation of identical hydroxy groups in the O-*cis* form. For comparison the same conformer was considered with the corresponding aldehydes. The PPP calculation gives the O-*cis* form as the more stable conformer of aldehydes, and the O-*trans* form as that of carboxylic acids, because of the proximity of large π-charges. According to the experimental results, the O-*trans* form generally predominates except for derivatives containing groups giving rise to intramolecular hydrogen bonding

and for the bulky halogen substituents preferring the O-*cis* form [18, 19]. The results of calculations with different rotamers will be given in a subsequent paper [20].

Some control calculations have been carried out with variation of the parameters adopted in this work, or with some other starting values, respectively, on some derivatives, primarily on the nitroanilines, in order to check whether our parameter system really gives the most acceptable results. The sensitivity of the calculation to molecular structural data was checked by the variation of the C–N bond distances. Both the bond distance characteristics of aromatic amines (1.38 Å) and those of aromatic nitro compounds (1.46 Å) was used. The results show that the method is not very sensitive to changes in the bond distances. For instance, the calculation of the nitroanilines was performed using 1.38 and 1.46 Å for both C–N distances. The largest difference in charge density is 0.0088 (on the amino nitrogen atom of the *o*-derivative), and that in transition energy 0.025 eV (for the first band of the *m*-derivative). In the calculation of fluoro- and chloronitrobenzenes with the same C–N bond distances the difference was always smaller than the figures given above. Throughout this paper 1.38 Å was used for the C–N distances.

The method is much more sensitive to the one- and two-center integrals. The variation of the resonance integrals ($\beta_{\mu\nu}$) demonstrates that the changes in the $\beta_{\mu\nu}$ values of the bonds involving the substituent atoms influence the calculated transition energies to a smaller extent than does the variation of the ring β_{cc} parameters because of the repeated occurrence of the latter. The results for the nitrophenols, nitroanilines and fluorobenzaldehydes show that the transition energies are changed only by some hundredths of an eV as a result of the change of β_{C-O}, β_{C-N} and β_{C-F} by 0.2 eV. The reasonable $\beta_{\mu\nu}$ interval of 1.0 eV usually produces changes of 0.1—0.2 eV in the transition energies. This means that deviation from the experimental value by 0.3—0.4 eV (*e.g.* in *p*-nitroaniline) cannot be eliminated in this way. The agreement can further be improved by changing the ring β_{CC} by 0.1—0.2 eV, the separate fitting of the ring resonance integrals would, however, remove the generality of the treatment.

In order to get information on the reliability of the atomic parameters given in Table I, calculations have been performed with a different set of ionization potentials ($I\mu$) and electrons affinities ($A\mu$) for the atoms contributing two electrons to the π-system. The values taken from HINZE's tables [21] were considered, which produce much less satisfactory results: the transition energy of the first band for *o*- and *m*-nitroaniline is by about 0.05 eV higher, that of the second band by 0.5—0.6 eV lower, and the energies of the first two bands for the *p*-derivative are by 0.1—0.2 eV lower. Comparison with the experimental data shows that the agreement is better only for the first band of *p*-nitroaniline (the calculated value is 3.982 instead of 4.206 eV).

it is, however, worse for the second band of the *p*-isomer (4.241 instead of 4.348 eV), and for the first three bands of the *o*- and *m*-derivative. Similar deviations are obtained with nitrobenzene and the other derivatives investigated.

The results for benzene derivatives containing atoms contributing two electrons show that the transition energies obtained in most cases differ by several tenths of an eV from the experimental values when using I_μ and A_μ values evaluated from HINZE's tables [21]. Satisfactory results are produced by the reduced I_μ and A_μ values, suggested by BAILEY [22] and adopted in our calculations.

The parameter control outlined above seems to be convincing as to the applicability of the parameters selected.

Results and discussion

Spectral data

Table II contains the calculated and experimental spectral data (singlet transition energies, oscillator strengths and polarization directions) for the three isomers of fluoro-, chloro-, hydroxy- and aminonitrobenzenes. The results for the benzaldehyde and benzoic acid derivatives are given in [20]. The agreement for the transition energies is satisfactory, the deviation does not exceed those of the calculation for the di-donor and di-acceptor compounds. The largest deviation for the first band was found with *o*-nitrophenol (9.608%), that for the second band with *p*-nitroaniline (7.408%).

The experimental oscillator strengths were evaluated by the equation $\varepsilon = 41\,700\,f$ [27]. There is no numerical correspondence between the calculated and experimental oscillator strengths. The calculation reproduces, however, for most molecules, the intensity ratios of the different bands.

There is an overall agreement between the calculated and experimental values within the series of the three isomers and within the series of the four donor groups.

The calculated polarization directions are given as α, which measures the angle from the y axis in clockwise direction, the bond between the substituent and the ring carbon atom in position 1 lying on the positive y axis (the coordinate system and the numbering of atoms is given in Fig. 1). The calculated polarization directions correspond to those expected from the vectorial addition of the components of the transition moment.

The experimental determination of the polarization vectors was reported for *p*-nitroaniline by TANAKA [28]. In place of the longest wavelength band of the solution spectrum, two bands appear: the high-intensity charge transfer (CT) band near 320 nm polarized in the y direction and a weak band at 264 nm corresponding to the x polarized benzenoid transition. The results of our calculation on *p*-nitroaniline are in complete accordance with the experimental

Table II

Calculated and experimental spectral data

Nitrobenzene	Calculated			Experimental[a]		Ref.
	E (eV)	f	α°	E (eV)	f	
o-fluoro-	4.213	0.123	136.0	4.460	0.044	[23]
	4.931	0.265	182.7	5.123	0.174	
	5.703	0.074	32.6			
	5.991	0.142	142.0			
	6.161	0.501	217.5			
	6.900	0.625	281.0			
m-fluoro-	4.283	0.073	53.3	4.366	0.044	[23]
	4.993	0.320	181.5	4.959	0.204	
	5.705	0.138	148.8	5.904	0.192	
	5.990	0.173	90.1			
	6.111	0.433	332.2			
	6.900	0.629	243.3			
p-fluoro-	4.545	0.004	90.0	~4.428		[23]
	4.724	0.499	180.0	4.843	0.228	
	5.788	0.071	90.0			
	6.086	0.386	90.0			
	6.304	0.086	180.0			
	6.938	0.845	0.0			
o-chloro-	4.027	0.149	132.8	4.335	0.031	[24]
	4.878	0.177	181.0	5.081	0.096	
	5.582	0.149	27.7	5.904	0.384	
	5.864	0.301	191.0			
	6.104	0.405	54.5			
	6.675	0.420	265.4			
m-chloro-	4.172	0.082	232.8	4.275	0.032	[24]
	4.960	0.269	183.4	4.881	0.187	
	5.574	0.286	329.7	5.821	0.456	
	5.921	0.256	157.7			
	6.009	0.327	114.5			
	6.684	0.239	228.8			
p-chloro-	4.524	0.002	90.0	4.275	0.072	[24]
	4.559	0.562	180.0	4.678	0.288	
	5.718	0.113	90.0	5.794	0.257	
	6.089	0.366	90.0			
	6.210	0.011	180.0			
	6.772	0.870	0.0			

Table II (continued)

Nitrobenzene	Calculated			Experimental[a]		Ref.
	E (eV)	*f*	α°	*E* (eV)	*f*	
o-hydroxy-	3.916	0.172	139.1	3.573	0.089	[25]
	4.871	0.156	184.4	4.592	0.174	
	5.516	0.104	21.4	5.876	0.348	
	5.805	0.360	186.1			
	6.118	0.336	56.5			
	6.715	0.557	275.2			
m-hydroxy-	4.030	0.098	48.5	3.948	0.053	[25]
	4.937	0.208	185.1	4.805	0.148	
	5.480	0.294	156.1	~5.585		
	5.852	0.329	151.8			
	6.011	0.291	111.9			
	6.633	0.215	228.8			
p-hydroxy-	4.490	0.556	180.0	4.350	0.148	[25]
	4.493	0.000	270.0			
	5.652	0.155	90.0	5.661	0.229	
	6.111	0.371	90.0			
	6.150	0.005	180.0			
	6.815	0.980	0.0			
o-amino-	3.537	0.184	137.2	3.280	0.103	[25]
	4.738	0.041	176.7	4.592	0.101	
	5.284	0.057	357.3			
	5.442	0.611	208.0	5.438	0.456	
	6.073	0.076	69.8			
	6.289	0.495	247.4			
m-amino-	3.666	0.096	48.8	3.583	0.049	[25]
	4.821	0.056	217.1	4.592	0.098	
	5.220	0.512	160.9	5.438	0.417	
	5.457	0.406	136.0			
	6.003	0.128	107.1			
	6.052	0.099	95.0			
p-amino-	4.206	0.616	0.0	3.850	0.355	[25]
	4.348	0.009	90.0	~4.696		
	5.437	0.186	270.0	5.462	0.186	
	5.838	0.020	0.0			
	6.116	0.333	270.0			
	6.677	0.857	0.0			

a) The experimental data refer to cyclohexane solution.

assignment. The calculation of *p*-nitrophenol gives similar spectral characteristics. The calculated energy difference between the first two bands of these compounds is considerably smaller than the experimental value. Parameter variation as outlined in the preceding section, does not alter essentially this picture.

It should be mentioned that the deviation of the calculated energy from the experimental value for the first transition is larger than expected with *o*-nitrophenol, and the situation is the same, although to a smaller extent, with *o*-nitraniline and *o*-hydroxybenzaldehyde. The difference between the calculated and experimental value is larger than 3% for the above compounds, with *o*-hydroxy and *o*-aminobenzoic acid, on the other band, it is smaller

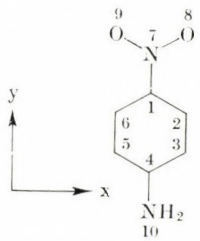

Fig. 1.

than 2%. This behaviour may be attributed to intramolecular hydrogen bonding which is stronger in the former and weaker in the latter molecules, and tends to lower the transition energy. This effect was not included in the original framework. The effect of hydrogen bonding may be considered by alteration of the ionization potentials (I_μ) of the atoms involved [13]. By inclusion of this modification better agreement was reached.

It may be concluded from the above discussion that the calculated spectral characteristics are in overall agreement with the experimental interpretation of the spectra.

It is of interest to compare our results with some other PPP calculations given in the literature. The calculation by LUTSKII and GOROKHOVA [5, 6] with similar parameterization except for the I_μ and A_μ values of atoms contributing two electrons to the π-system, produced smaller transition energies for the nitroanilines and nitrophenols than did our calculation. Their values are larger for the first band and smaller for the second and third bands than the experimental energies. They obtained better agreement for the first band of *p*-nitroaniline but in all other cases their calculated energies and intensities show larger deviations from the experimental values. The experimental data cited in Refs [5, 6] are taken partly from vapour spectra, partly from spectra in polar solvents. In the latter case, large shifts can be observed, *e.g.* the band near 5.0 eV in the spectra of *o*- and *m*-nitroaniline, and that at 5.3 eV with *o*- and *m*-nitrophenol [29] do not appear of the same energy in nonpolar sol-

vents, the bands near 5.6—5.8 and 5.45 eV, respectively, may correspond to them. Accepting the latter values, the present calculation seems to give better results.

GHIRVU and GROPEN [7] obtained nearly identical results for chloronitrobenzenes, using a different parameterization scheme. Their calculated transition energies are somewhat higher for the *o*- and *m*-isomers, and lower for the *p*-isomer than in our calculation. The energies calculated by LUTSKII and GOROKHOVA [8] are considerably lower both for fluoro- and for chloronitrobenzenes because of the use of the atomic parameters (I_μ and A_μ) of HINZE's tables for the halogen atoms just as with the hydroxy- and aminonitrobenzenes. These deviations justify the use of BAILEY's [22] parameters.

It seems that detailed calculations are not available for the benzaldehydes and benzoic acids. The present calculations on the O-*cis* conformers give satisfactory results: the deviation from the experimental transition energies is always smaller than the highest deviation given for the nitro-compounds.

The calculations [10] for the O-*cis* form of the hydroxybenzaldehydes produced somewhat smaller transition energies than the present work. The situation is the same as with the nitro derivatives. The transition energies calculated by LUTSKII *et al.* [11] for halogenobenzaldehydes are larger than the experimental values. Our results are in general smaller than the experimental values, but they seem to give better agreement except the *o*-derivatives.

Charge densities and bond orders

The charge densities of the characteristic substituent atoms and of the unsubstituted ring carbon atoms are given in Table III for the nitrobenzene derivatives. The complete molecular diagrams can be found in the Appendix [26].

The charge density increases on the donor atom, and decreases on the oxygen atoms of the acceptor carbonyl and nitro groups in the order *ortho*, *para*, *meta*. In the molecules investigated the charge density of the donor substituents is smaller, and that of the acceptor atoms larger than in the corresponding mono- and homo-disubstituted derivatives. The order of increasing $+M$ effect of the donor groups (F, Cl, OH, NH_2) corresponds to that expected. The charge density on the ring carbon atoms and the bond orders vary in accordance with the substituent effect.

The charge densities calculated for the fluoronitrobenzenes are in good agreement with the π-charge densities from CNDO/2 calculations [30]. The latter calculations produce somewhat larger interactions, *i.e.* the differences between the charge densities of the ring carbon atoms are somewhat larger. The deviation is 0.01—0.02 charge unit.

For the chloronitrobenzenes GHIRVU has recently reported CNDO/2 and PPP calculations [31]. From a comparison of the charge densities, it can be

Table III

Charge densities of nitrobenzene derivatives

	P_{55}	P_{66}	P_{88}	P_{1010}
o-fluoro-	1.0121	0.9560	1.5118	1.9083
m-	0.9857	0.9826	1.4981	1.9208
p-	1.0326	0.9553	1.5011	1.9150
o-chloro-	1.0165	0.9569	1.5149	1.8929
m-	0.9868	0.9864	1.4989	1.9109
p-	1.0357	0.9563	1.5025	1.9030
o-hydroxy-	1.0254	0.9540	1.5225	1.8414
m-	0.9840	0.9966	1.4995	1.8642
p-	1.0555	0.9532	1.5046	1.8539
o-amino	1.0337	0.9533	1.5312	1.7797
m-	0.9840	1.0057	1.5007	1.8159
p-	1.0663	0.9531	1.5075	1.7998

concluded that our PPP results give a slightly better agreement with the CNDO/2 calculations (our PPP values are by several hundredths of a charge unit lower) than GHIRVU's PPP results. A calculation of bond distances from our bond orders by the formulas given in Ref. [31] gave results in good agreement with GHIRVU's results.

π-dipole moment

The dipole moment contribution of the π-electrons (μ_π) is increasing in the order *ortho, meta, para* with all the investigated molecules. The experimental dipole moments vary in the same order for the hydroxy and amino compounds but in the reverse order for the halogene derivatives.

In series of compounds containing the same acceptor but different donors, the calculated μ_π varies in the experimental order $F < Cl \leq OH < NH_2$, except for the *o*-derivatives. In series with an identical donor group, the experimental order is $COOH \leq CHO < NO_2$ with the exception of the fluoro derivatives. The calculated order is $CHO < COOH < NO_2$, the μ_π value of the carboxy compounds being relatively too high. The same order holds both for the O-*cis* and O-*trans* conformers, only the magnitude of μ_π is larger in the latter case. The situation is the same with the monosubstituted aromatic carbonyl compounds (C_6H_5COX). The value increases in the given donor order, *i.e.* $CHO < COCl < COOH < CONH_2$, the experimental order being $COOH < < CHO < COCl < CONH_2$. The trends are the same except for the location of the carboxy derivatives.

The present calculations of the π-dipole moments of benzenedialdehydes are in good accordance with the PPP calculation by KLABUHN *et al.* [32]. The π-dipole moments of the nitrophenols and nitroanilines were calculated by LUTSKII *et al.* [33]. Their calculations gave better results for the nitroanilines and poorer ones for the nitrophenols.

It can be established that reduced I_μ and A_μ values used in our calculations give the spectral data in better agreement with the experiment than the π-dipole moments. The reason is that the starting parameters are fitted to spectral data which seem to be the better comparable experimental value.

The detailed results of the calculations are collected in Ref. [26].

REFERENCES

[1] LABHART, H., WAGNIERE, G.: Helv. Chim. Acta, **46**, 1314 (1963)
[2] LIPTAY, W., EBERLEIN, W., WEIDENBURG, H., ELFLEIN, O.: Ber. Bunsenges., **71**, 548 (1967)
[3] GROPEN, O., SKANCKE, P. N.: Acta Chem. Scand., **23**, 2685 (1969)
[4] BEVERIDGE, D. L., HINZE, J.: J. Amer. Chem. Soc., **93**, 3107 (1971)
[5] LUTSKII, A. E., GOROKHOVA, N. I.: Opt. Spektr., **27**, 917 (1969)
[6] LUTSKII, A. E., GOROKHOVA, N. I.: Teor. Eksp. Khim., **6**, 490 (1970)
[7] GHIRVU, C. I., GROPEN, O.: Acta Chem. Scand., **25**, 1011 (1971)
[8] LUTSKII, A. E., GOROKHOVA, N. I.: Teor. Eksp. Khim., **6**, 587 (1970)
[9] MISHRA, P. C., RAI, D. K.: Indian J. Pure Appl. Phys., **8**, 691 (1970)
[10] LYUBARSKAYA, A. E., MINKIN, V. I., KNYAZHANSKII, M. I.: Teor. Eksp. Khim., **8**, 71 (1972)
[11] LUTSKII, A. E., NAIDENOVA, I. I., GOROKHOVA, N. I., ROMODANOV, I. S.: Teor. Eksp. Khim., **9**, 592 (1973)
[12] SMEYERS, Y. G., SIEIRO, C.: Theor. Chim. Acta, **28**, 355 (1972)
[13] RAZAFINDRAKOTO, E., BESNAINOU, S.: Theor. Chim. Acta, **7**, 321 (1967)
[14] PARR, R. G.: Quantum Theory of Molecular Electronic Structure. Benjamin, New York 1964
[15] KISS, A. I., SZŐKE, J.: Chem. Phys. Lett., **11**, 52 (1972); Acta Chim. Acad. Sci. Hung., **74**, 59 (1972)
[16] KISS, A. I., SZŐKE, J.: Chem. Phys. Lett., **18**, 195 (1973)
[17] KISS, A. I., SZŐKE, J.: J. Mol. Struct., **18**, 457 (1973)
[18] SMITH, W. B., DAEVENPORT, D. L., IHRIG, A. M.: J. Amer. Chem. Soc., **94**, 1959 (1972)
[19] EGLINTON, G., FERGUSON, G., ISLAM, K. M. S., GLASBY, J. S.: J. Chem. Soc. (B) 1141 (1967)
[20] KISS, A. I., SZŐKE, J.: Acta Chim. (Budapest), to be published
[21] HINZE, J., JAFFÉ, H. H.: J. Amer. Chem. Soc., **84**, 540 (1962)
[22] BAILEY, M. L.: Theor. Chim. Acta, **13**, 56 (1969)
[23] FORBES, W. F.: Can. J. Chem., **37**, 1977 (1959)
[24] FORBES, W. F.: Can. J. Chem., **38**, 1104 (1960)
[25] KISS, A. I., HORVÁTH, G.: Acta Chim. Acad. Sci. Hung. **42**, 15 (1964)
[26] KISS, A. I., SZŐKE, J.: KFKI Report 75—13
[27] ALLINGER, N. L., STUART, T. W., TAI, J. C.: J. Am. Chem. Soc. **90**, 2819 (1968)
[28] TANAKA, J.: Bull. Chem. Soc. Japan **36**, 833 (1963)
[29] DOUB, L., VANDENBELT, J. M.: J. Am. Chem. Soc. **69**, 2714 (1947); **71**, 2414 (1949)
[30] JONES, R. G., PARTINGTON, P.: J. Chem. Soc. Faraday Trans. **2**, 68, 2087 (1972)
[31] GHIRVU, C. I. Rev. Roum. Chim. **17**, 1951 (1972)
[32] KLABUHN, B., CLAUSEN, E., GOETZ, H.: Tetrahedron **29**, 1153 (1973)
[33] LUTSKII, A. E., MINKIN, V. I., GOROKHOVA, N. I.: Zh. Struct. Khim. **12**, 1126 (1971)

Árpád KISS; H-1511 Budapest, Budafoki út 8.
József SZŐKE; H-1525 Budapest, Pf. 49.

Acta Chimica Academiae Scientiarum Hungaricae, Tomus 89 (4), pp. 347—363 (1976)

ÄQUIDENSITOMETRIE — EINE METHODE ZUR BEURTEILUNG DER STRUKTUR VON PLASMEN, III*

BEURTEILUNG DES GALLIUMARSENID- UND GERMANIUMDIOXID-GLEICHSTROMBOGENPLASMAS DURCH ÄQUIDENSITOMETRIE VON MONOCHROMATISCHEN BOGENPHOTOGRAPHIEN

K. Dittrich, H. Rößler und K. Niebergall

(Sektion Chemie der Karl-Marx-Universität Leipzig, Leipzig, DDR

Eingegangen am 20. November 1975

Die Charakterisierung des Gleichstrombogenplasmas, welches durch Verdampfen von Galliumarsenid oder Germaniumdioxid entsteht, erfolgt auf experimentellem Weg durch spektrale Photographie und photographisch-äquidensitometrische Auswertung der erhaltenen Photogramme. Es ist möglich, qualitative Aussagen über die Axialverteilung der Elemente zu gewinnen.

Es konnte gezeigt werden, daß sich die Verteilung sowohl der Matrixelemente als auch der Spuren nach dem jeweiligen Ionisationspotential richtet. Elemente mit niedrigem Ionisationspotential reichern sich an der Kathode, Elemente mit hohem Ionisationspotential an der Anode an. Sowohl die Temperatur des Plasmas als auch die Matrix sind von Einfluß auf die Verteilung der Teilchen im Plasma. Die Ergebnisse werden ausführlich diskutiert.

1. Einführung

Das Galliumarsenid- bzw. Germaniumdioxid-Gleichstrombogenplasma, welches bei Verdampfung eines Galliumarsenid- bzw. Germaniumdioxid—Graphitpulver-Gemisches aus einer Graphit-Kraterelektrode in einem Gleichstrombogen erhalten wird, hat eine komplizierte Zusammensetzung und Struktur.

Die Heterogenität der Zusammensetzung nimmt noch zu, wenn sich im Galliumarsenid bzw. Germaniumdioxid Nebenbestandteile oder Spuren anderer Metalle befinden. Die Heterogenität des Plasmas ist auf die unterschiedliche Verdampfung der Teilchen, ihre Konvektion und Wanderung im elektrischen Feld des Gleichstrombogens und auf chemische Reaktionen zurückzuführen.

Die rechnerische Ermittlung der Zusammensetzung eines solchen Vielkomponentenplasmas ist wegen der großen Zahl von Einflußgrößen praktisch nicht möglich. Sie ist aber für die analytische Spektrochemie — besonders für die Spurenanalyse — von Bedeutung. Wir wandten auf die Behandlung dieses Problems die von uns entwickelte und beschriebene Methode [1, 2] der Kombination der Photographie im monochromatischen Licht mit der photographischen Äquidensitometrie an. Diese Methode gestattet es, qualitative Aussagen über die Verteilung sowohl der Matrixelemente als auch der Spurenbestandteile im Plasma zu machen.

* Teil II. Spectrochimica Acta, im Druck

2. Experimentelles

2.1 Herstellung von spektral aufgelösten Photogrammen des Galliumarsenid- und Germaniumdioxid-Gleichstrombogenplasmas

Die Photogramme wurden, wie in unserer II. Mitteilung beschrieben, unter Verwendung des Plangitterspektrographen PGS 2 (VEB Carl Zeiss Jena) hergestellt.

Am Plangitterspektrograph wurde der Spalt und der Spaltkopf entfernt und durch einen Zentralverschluß mit 5 mm Durchmesser ersetzt. Die abzubildenden Lichtbögen wurden mit einem Achromaten (f = 75,8 mm) im Verhältnis 5 : 1 verkleinert und scharf in der ehemaligen Spaltebene des Spektrographen abgebildet.

Die Anregungs- und Aufnahmebedingungen sind in Tabelle 1 zusammengefaßt. Die Vorbrennzeit von 20 sec wurde nach Auswertung der Fahrspektren gewählt. Diese zeigten

Tabelle I

Anregungs- und Aufnahmebedingungen

Spektrograph	Plangitterspektrograph PGS 2
Gitter	651 Strich/mm, Blaze 1020 nm
Dispersion (Plattenmitte)	0,235 nm/mm 3. Ordnung (315 nm) 0,176 nm/mm 4. Ordnung (236,3 nm)
Ordnungsfilter	UG 5
Anregung	Universalbogenimpulsgenerator UBI 1
Stromstärke	6 und 12 A Gleichstrom
Elektroden	siehe Abb. 1
Elektrodenabstand	3 mm, von Hand nachgeregelt
Probematerial	GaAs (Matrix), je 500 ppm Al, Sn, Ge, Mg GeO_2 (Matrix), je 500 ppm Al, Sn
Probemenge	20 mg Matrix-Kohlepulver-Mischung (1 : 3)
Atmosphäre	Luft oder Argon-Sauerstoff (3 : 2) (120 l/h : 80 l/h)
Vorbrennzeit	20 sec
Belichtungszeit	0,5 sec
Außenoptik	Achromat (f = 75,8 mm), Direktabbildung, Maßstab 5 : 1
Spektralplatten	ORWO WU 3 spektralblau, extrahart
Entwicklung	4 min, ORWO MH 28 (1 : 4), 19 °C
Unterbrechung	10 sec 5%ige Essigsäure, 19 °C
Fixierung	6 min ORWO A 304, 200 g/l, 19 °C
Wässern	10 min
Trocknen	25 min, 27 °C

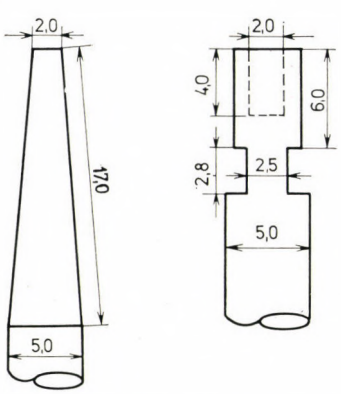

Abb. 1. Elektrodenkombination (Maßangaben in mm)

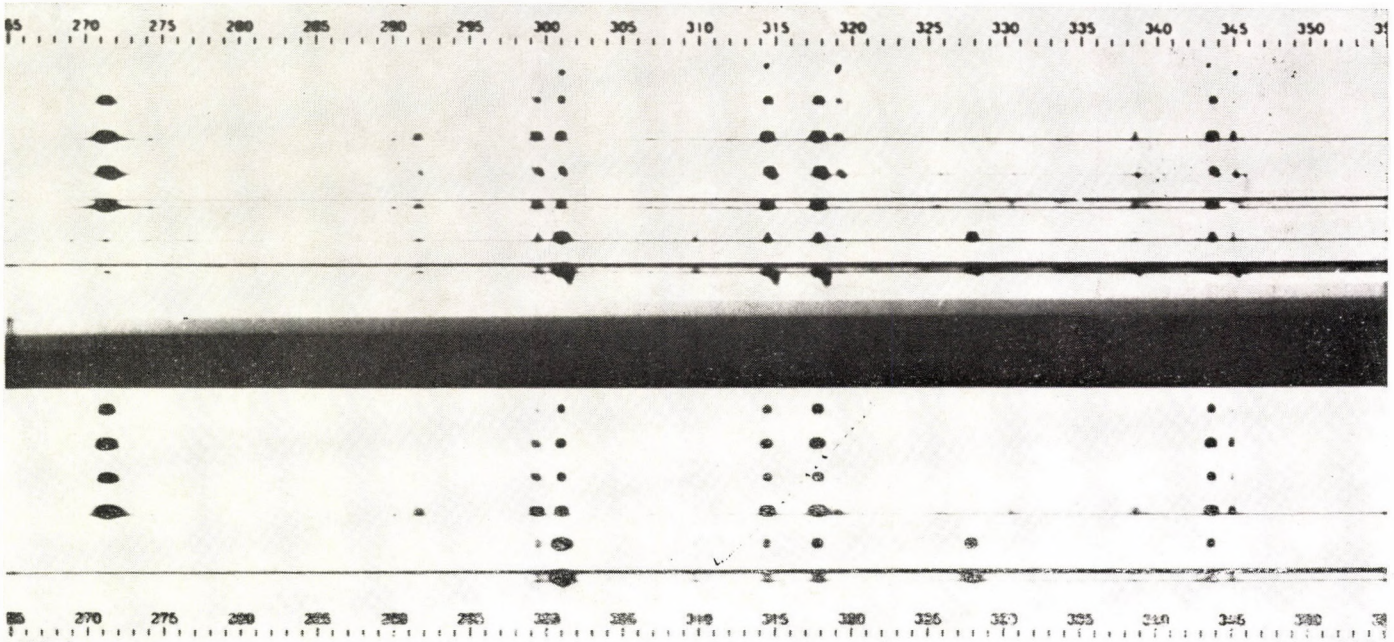

Abb. 2. Originalnegativ von Lichtbogenphotogrammen

sowohl für die Matrix als auch für die Spuren ein Verdampfungsmaximum nach 20 sec Brenndauer und danach einen in Abhängigkeit von der Stromstärke mehr oder weniger steilen Intensitätsabfall an.

Die Abbildung 2 zeigt eine typische Aufnahme. Es ist zu erkennen, daß bei Verwendung der 3. oder 4. Ordnung des Gitters fast keine Überlappungen auftreten und eine genügende Anzahl freiliegender Bogenabbildungen vorhanden ist.

2.2 Herstellung der Äquidensiten

Die Herstellung der Einzeläquidensiten erfolgte auf ORWO-Planfilm FU 5 gleichzeitig für die gesamte Photoplatte auf halbautomatischem Weg [3].

Die exakte Zuordnung einer Schwärzung des Originalphotogramms gelingt durch Mitäquidensitometrieren eines graduierten Graukeils. Die Montage der Einzeläquidensiten zu einem Gesamtäquidensitenbild erfolgte in der bereits beschriebenen Weise [2].

3. Ergebnisse und Diskussion

3.1 Ergebnisse

Die Abbildungen 3, 4, 5, 6, 7, 8 und 9 zeigen die Äquidensitogramme für die Übergänge verschiedener Atome und Ionen in Luft- bzw. Argon-Sauerstoff-Atmosphäre.

Tabelle II

Wellenlängen, Intensitäten und Anregungspotentiale der mit Hilfe von Äquidensitogrammen untersuchte Übergänge

Element	Übergang in nm	Relative Intensität im Bogen	Anregungs-potential in eV	Ionisations-potential in eV
Al I	308,215	800	4,02	5,98
Sn I	317,502	500	4,33	7,33
Ge I*	303,906	1000	4,96	8,13
As I**	289,871	25	—	9,81
Ga I**	287,424	10	4,29	5,99
C I***	247,857	400	7,69	11,26
Mg I	309,689	150	6,72	7,64
Mg II	280,269	150	4,42	15,03

* Sowohl Matrix als auch Nebenbestandteil im GaAs.
** Matrixelemente.
*** Elektrodenmaterial.

Die verwendeten Übergänge sind in der Tabelle III näher charakterisiert. Die Äquidensite höchster Schwärzung in jedem Bild ist mit einer Zahl gekennzeichnet, die eine Zuordnung zur Originalschwärzung ermöglicht (siehe Tabelle III). Die äußerste Äquidensite eines jeden Bildes trägt die Zahl 1. Die Äquidensiten 2, 6 und 11 wurden wegen der geringen Schwärzungsunterschiede zu den jeweils vorher liegenden Äquidensiten nicht mit eingezeichnet.

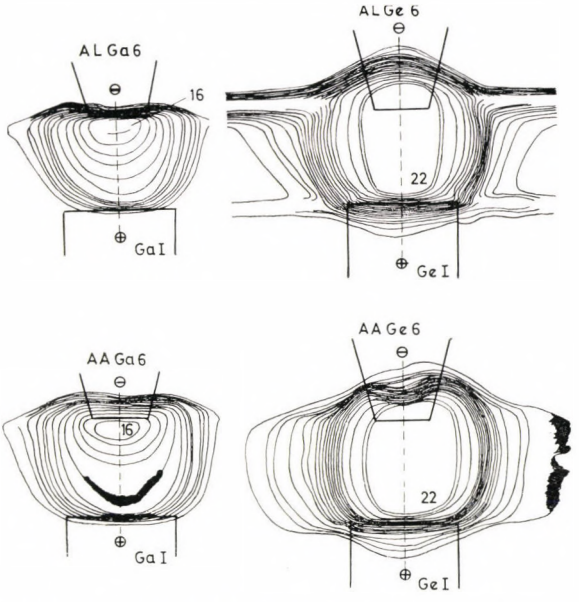

Abb. 3. Monochromatische Äquidensitogramme für die Matrixelemente Gallium (in GaAs) und Germanium (in GeO_2)
AL Ga6: anod. Verdampfung in Luft bei 6A für Ga I 287,424 nm
AA Ga6: anod. Verdampfung in Ar/O_2 bei 6A für Ga I 287,424 nm
AL Ge6: anod. Verdampfung in Luft bei 6A für Ge I 303,906 nm
AA Ge6: anod. Verdampfung in Ar/O_2 bei 6A für Ge I 303,906 nm

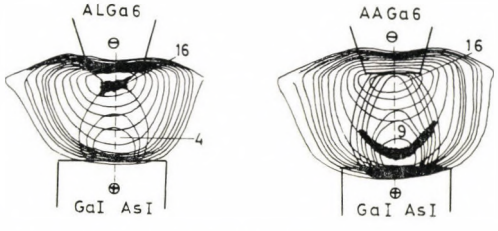

Abb. 4. Monochromatische Äquidensitogramme für die Elemente Gallium und Arsen (in GaAs) (Photomontage von Gesamtäquidensiten des Ga und As) AL Ga6, AA Ga6: siehe Erläuterung Abbildung 3
Ga I: 287,424 nm, As I 289,871 nm

Mit Hilfe der Tabelle III ist es außerdem möglich, den einzelnen Äquidensiten relative Intensitäten zuzuordnen. Dazu war es erforderlich, die Plattengradation in Abhängigkeit von der Wellenlänge mit Hilfe der kontinuierlichen Spektren näherungsweise zu ermitteln (siehe Abb. 2). Es kann eingeschätzt werden, daß die Schwärzungswerte der Tabelle III mit einem absoluten Fehler von etwa $\pm 0{,}02$ behaftet sind. Die Elektroden wurden in die Äquidensitogramme nachträglich eingezeichnet.

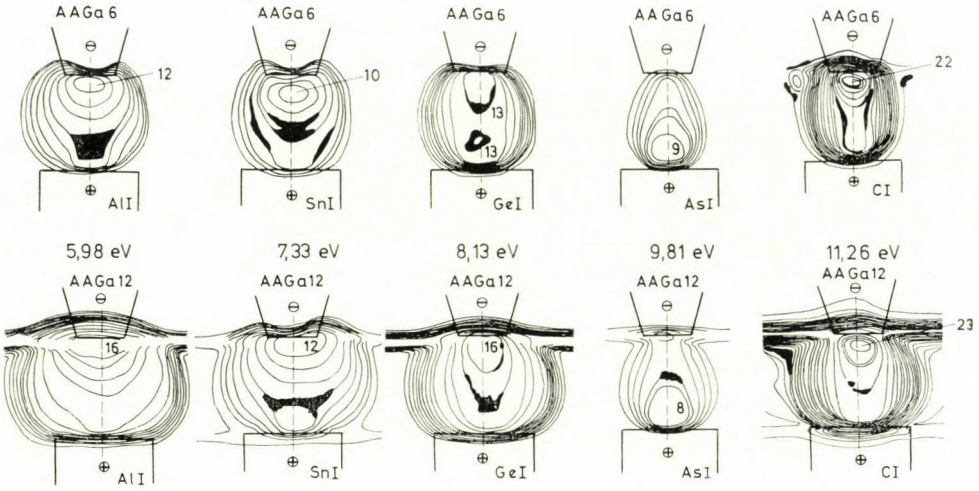

Abb. 5. Monochromatische Äquidensitogramme für die Nebenbestandteile Aluminium, Zinn, Germanium, für Arsen und Kohlenstoff (Matrix GaAs) in Luft
AL Ga6: anod. Verdampfung in Luft bei 6A für GaAs
AL Ga12: anod. Verdampfung in Luft bei 12A für GaAs
Liniencharakteristik siehe Tabelle II

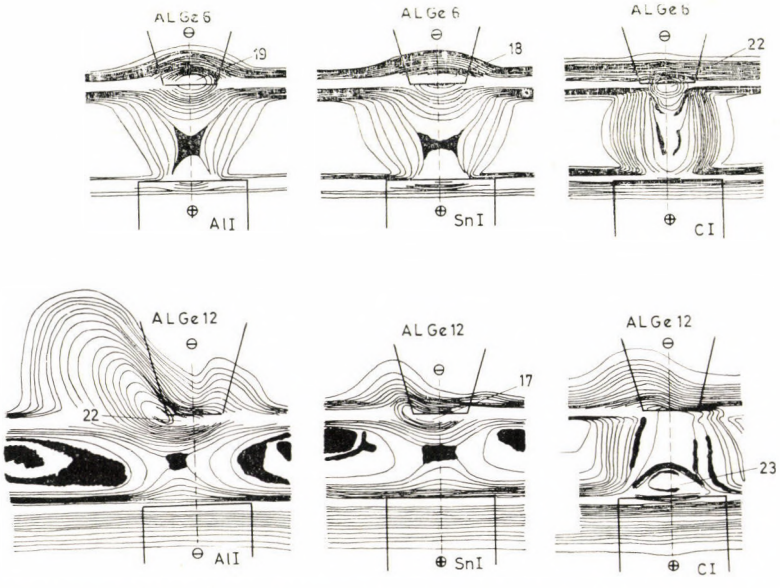

Abb. 6. Monochromatische Äquidensitogramme für die Nebenbestandteile Aluminium und Zinn und für Kohlenstoff (Matrix GeO_2) in Luft
AL Ge6: anod. Verdampfung in Luft bei 6A für GeO_2
AL Ge12: anod. Verdampfung in Luft bei 12A für GeO_2
Liniencharakteristik siehe Tabelle II

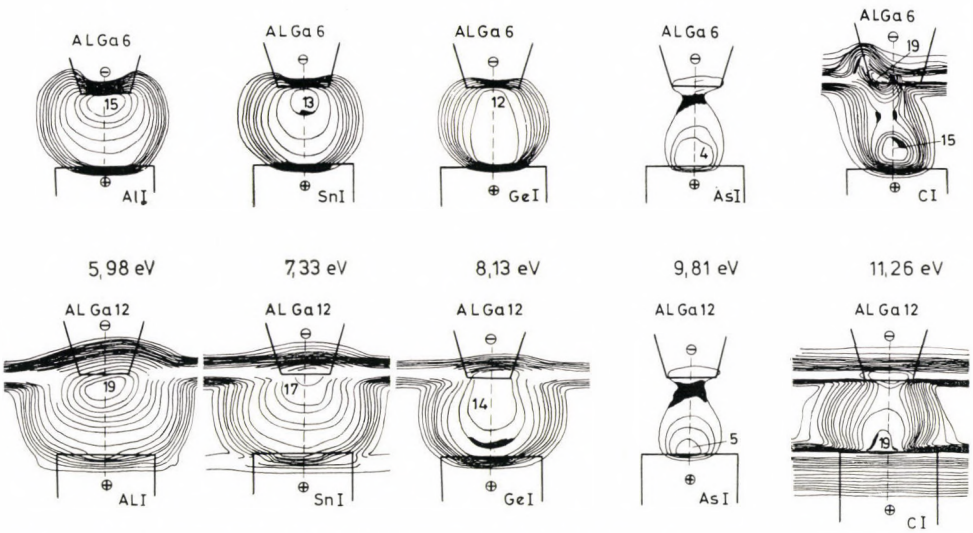

Abb. 7. Monochromatische Äquidensitogramme für die Nebenbestandteile Aluminium, Zinn, Germanium, für Arsen und Kohlenstoff (Matrix GaAs) in Argon Sauerstoff-Atmosphäre (3 : 2)
AA Ga6: anod. Verdampfung in Ar/O_2 bei 6A für GaAs
AA Ga12: anod. Verdampfung in Ar/O_2 bei 12A für GaAs
Liniencharakteristik siehe Tabelle II

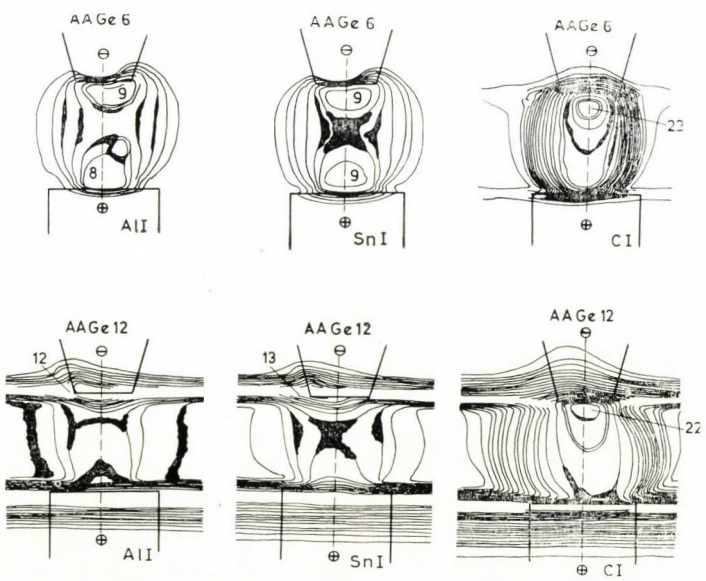

Abb. 8. Monochromatische Äquidensitogramme für die Nebenbestandteile Aluminium und Zinn und für Kohlenstoff (Matrix GeO_2) in Argon-Sauerstoff-Atmosphäre (3 : 2)
AA Ge6: anod. Verdampfung in Ar/O_2 bei 6A für GeO_2
AA Ge12: anod. Verdampfung in Ar/O_2 bei 12A für GeO_2
Liniencharakteristik siehe Tabelle II

Tabelle III

Äquidensiten-Nummern, Schwärzungen S und spektrale relative Intensitäten I

Äquidensiten-Nummer	S	$I_{280\,nm}$	$I_{310\,nm}$
1	0,20	1,937	2,104
(2)	0,23		
3	0,28	2,193	2,382
4	0,33	2,371	2,571
5	0,42	2,729	2,952
(6)	0,43		
7	0,46	2,904	3,140
8	0,52	3,192	3,444
9	0,62	3,721	4,018
10	0,72	4,355	4,677
(11)	0,73		
12	0,81	5,012	5,370
13	0,93	6,039	6,457
14	1,00	6,730	7,195
15	1,11	7,998	8,531
16	1,20	9,205	9,795
17	1,32	11,09	11,88
18	1,40	12,56	13,30
19	1,52	15,17	16,00
20	1,68	19,45	20,46
21	1,83	24,55	25,76
22	1,91	27,86	29,17
23	2,13	39,26	40,83
24	2,33	53,58	55,99

Alle Abbildungen zeigen deutlich eine Struktur des Plasmas, wobei allerdings zu berücksichtigen ist, daß es sich um Flächenprojektionen eines räumlichen Strahlers handelt.

Eine nähere Beurteilung der Radialverteilung der Teilchen ist wegen des radialen Temperaturgradienten nicht möglich. Die qualitative Beurteilung der Axialverteilung — besonders durch Vergleichsbetrachtungen — ist möglich.

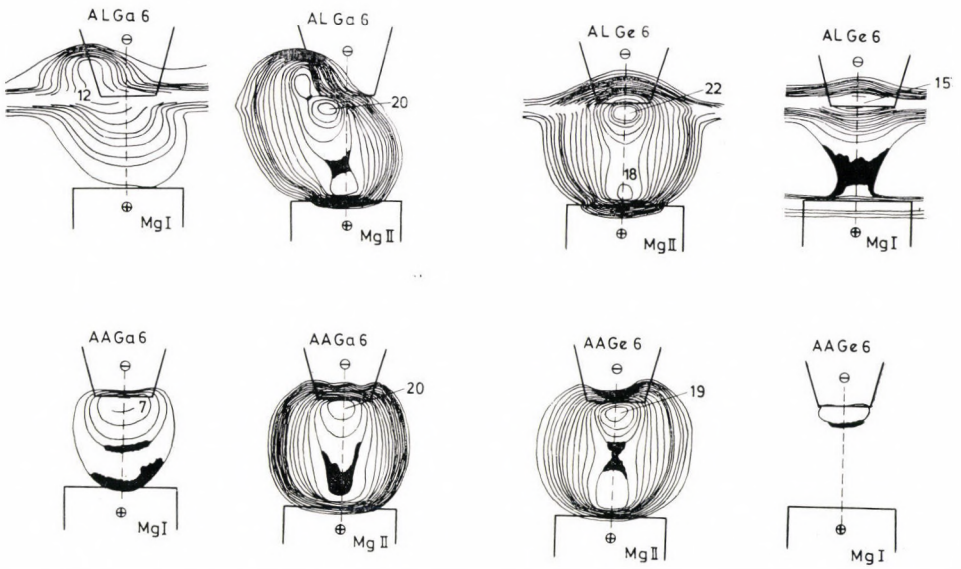

Abb. 9. Monochromatische Äquidensitogramme für die Magnesiumatome und -ionen in Luft und Ar/O_2 (Matrix GaAs und GeO_2)
AL Ga6, AL Ge6, AA Ga6, AA Ge6: siehe Abb. 3
Liniencharakteristik siehe Tabelle II

3.2 Äquidensitogramme von Übergängen der Matrixelemente Gallium, Arsen und Germanium

Die Abbildung 3 zeigt Äquidensitogramme für Übergänge des Galliums und Germaniums. Es sind deutlich Unterschiede zu erkennen. Das Gallium reichert sich an der Kathode an, das Germanium ist über die gesamte Bogensäule homogen verteilt. Die Abbildung 4 zeigt 2 Äquidensitogramme des Galliums und Arsens (aufgenommen als Galliumarsenid). Hier ist ebenfalls zu erkennen, daß das Gallium aus Kathodennähe, das Arsen jedoch aus Anodennähe strahlt. Ein Einfluß der Atmosphäre (Luft oder Argon : Sauerstoff 3 : 2) ist kaum feststellbar. Lediglich im Falle des Arsens macht sich die höhere Temperatur des Argon–Sauerstoff-Plasmas in einer Zunahme der Strahlungsintensität bemerkbar. In den anderen Fällen ist nur eine geringfügige Bogenaufweitung zu erkennen.

Die Ursache für dieses unterschiedliche Verhalten der Elemente ist in ihren Ionisierungspotentialen zu suchen (s. a. Tab. II). Damit läßt sich zeigen, daß ein dem bereits 1931 von MANNKOPF und PETERS [4] gefundenen Kathodenschichteffekt ähnlicher Effekt auch bei Matrixsubstanzen auftritt. Die Verdampfungsraten betrugen in unserem Fall etwa 3 mg/min. Eine weitere Erhöhung der Verdampfungsgeschwindigkeit wurde nicht vorgenommen.

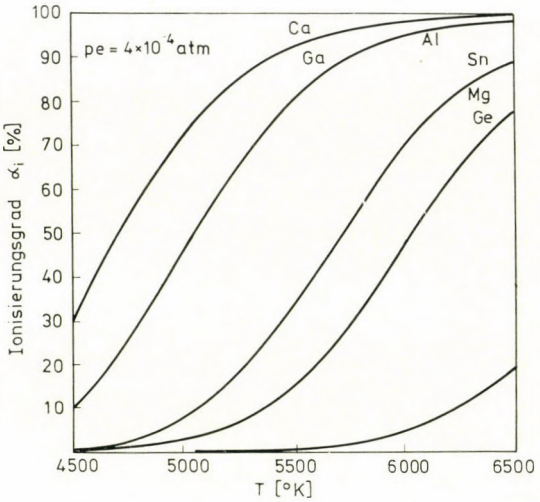

Abb. 10. Ionisierungsgrad in Abhängigkeit von der Temperatur bei einem vorgegebenen Elektronendruck von 4×10^{-4} at für verschiedene Elemente

Es ist weiterhin zu schlußfolgern, daß auch in Bögen mit hohen Metalldampfkonzentrationen der Ionisationsgrad wesentlich zur Verteilung der Elemente im Plasma beiträgt. Berechnet man den Ionisationsgrad des Galliums, Arsens und Germaniums und für einige andere Elemente für verschiedene Temperaturen bei einem vorgegebenen (nicht ermittelten) Elektronendruck, so ergeben sich die in Abbildung 11 gezeigten Kurven. Die für die Berechnung benötigten Werte wurden der Literatur entnommen [5].

Die Temperaturen der Bogenachse wurden durch Messung der Intensitätsverhältnisse von Linien der 420 nm Bande des Cyanradikals bestimmt [6, 7]. Für die Temperaturbestimmung wurden Linien-Querspektrogramme aufgenommen. Die aus den Schwärzungen errechneten relativen Intensitäten wurden mit Hilfe der Abelschen Integralgleichung in relative Radialintensitäten umgerechnet. Die für das Zentrum der Bogenachse erhaltenen Werte wurden zur Temperaturberechnung benutzt. Der Argon–Sauerstoff-Atmosphäre wurde für die Temperaturbestimmung eine geringe Menge Stickstoff zugefügt (105 l/h Ar, 75 l/h O_2, 20 l/h N_2). Diese Menge genügte einerseits für die Bildung des Cyanradikals in der erforderlichen Konzentration, andererseits werden die Verhältnisse eines reinen Argon–Sauerstoff-Bogens nicht wesentlich verändert. Die gemessenen Werte sind in der Tabelle IV zusammengefaßt.

Der Tabelle IV ist zu entnehmen, daß die Temperatur des Germaniumdioxid-Bogens um etwa 500 °C höher liegt als die des Galliumarsenid-Bogens und daß zwischen den Luft- und den Argon–Sauerstoff-Bögen ebenfalls eine Differenz von etwa 500° liegt.

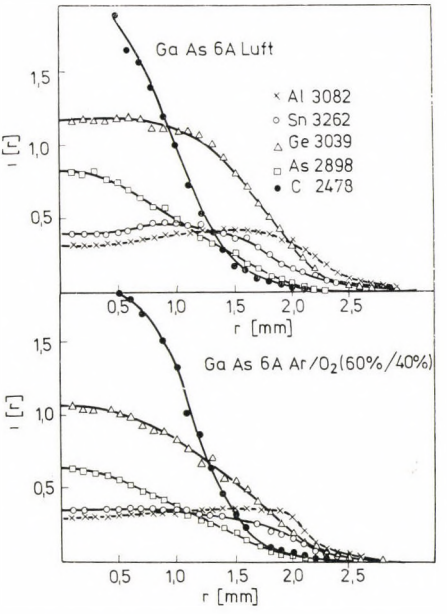

Abb. 11. Radialverteilung der Leuchtdichte (relative Volumenstrahlintensitäten) im GaAs-Gleichstrombogen für verschiedene Elemente

Tabelle IV

Plasmatemperaturen der Bogensäule

Matrix	Atmosphäre	Stromstärke A	Temperatur °K
GaAs	Luft	6	5450
GaAs	Luft	12	5800
GaAs	Ar/O_2	6	5850
GaAs	Ar/O_2	12	6350
GeO_2	Luft	6	5950
GeO_2	Luft	12	6400

Entnimmt man der Abbildung 11 bei den gemessenen Temperaturen die Ionisationsgrade, so erhält man für Gallium etwa 80% (Luft) und 90% (Argon-Sauerstoff), für Germanium etwa 40% (Luft) und 65% (Argon-Sauerstoff) und für Arsen etwa 2% bzw. 4%.

Damit ist u. E. erwiesen, daß die axiale Verteilung der Matrixelemente unter unseren Bedingungen wesentlich von der Transportgeschwindigkeit und damit vom Ionisationsgrad beeinflußt wird. Außerdem spielen natürlich die Ionenbeweglichkeit und die Feldstärke eine Rolle [6].

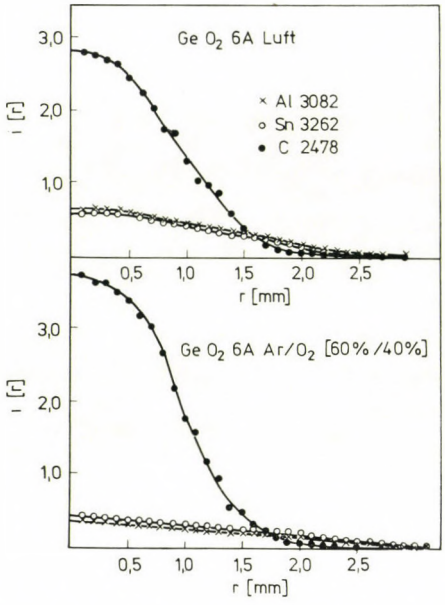

Abb. 12. Radialverteilung der Leuchtdichte (relative Volumenstrahlintensitäten) im GeO_2-Gleichstrombogenplasma für verschiedene Elemente

3.3 Äquidensitogramme von Übergängen der Nebenbestandteile in Galliumarsenid und Germaniumdioxid in Luftatmosphäre

Nach den für die Matrixelemente gefundenen Ergebnissen war anzunehmen, daß auch das Ionisationspotential der Nebenbestandteile einen Einfluß auf die Verteilung der Spezies im Plasma hat (s. a. [2]), denn besonders für Spuren hatten MANNKOPF [7] und auch VUKANOVIĆ [8] eine Verstärkung der Atomspektren in Kathodennähe festgestellt.

Die Abbildungen 6 und 7 stellen entsprechende Äquidensitogramme für Nebenbestandteile im Galliumarsenid bzw. Germaniumdioxid bei zwei Stromstärken dar.

Arsen wurde hier ebenfalls abgebildet, da es entsprechend seiner hohen Verdampfungsgeschwindigkeit und des bei 1000 °C nahezu vollständigen thermischen Zerfalls des Galliumarsenids zum Zeitpunkt der Aufnahme nur als Nebenbestandteil vorhanden war. Die Emission der Kohlenstofflinie wird durch sublimierten Kohlenstoff der Elektroden verursacht.

Die Abbildungen zeigen deutlich, daß sich die Verteilung der Leuchtdichte nach dem Ionisationspotential der Elemente richtet. Der eigentliche Faktor dürfte dabei wieder der Ionisationsgrad des jeweiligen Elementes und die sich daraus ergebende Transportgeschwindigkeit im elektrischen Feld sein. Es ist sicher auch der in Kathodennähe höhere Elektronendruck (s. a. 3.6), der zur verstärkten Bildung freier Atome führt, zu berücksichtigen.

Zur quantitativen Charakterisierung der Leuchtdichteverteilung im Bogen wurde das Verhältnis der relativen Intensitäten des Kathoden- bzw. Anodenbereiches zur relativen Intensität der Bogenmitte (jeweils auf der Bogenachse) gebildet.

$$\frac{I_{\text{rel. Kath.}}}{I_{\text{rel. Mitte}}} = \text{VF}_{\text{Kath.}} \qquad \frac{I_{\text{rel. Anode}}}{I_{\text{rel. Mitte}}} = \text{VF}_{\text{Anode}}$$

VF = Verstärkungsfaktor.

Diese Verstärkungsfaktoren sind ein Maß für die Leuchtdichteverstärkung oder -abschwächung in den entsprechenden Bogenzonen. Sie sind unabhängig von den Unterschieden der Intensitäten der einzelnen Linien und lassen somit einen besseren Vergleich zu.

Tabelle V

Verstärkungsfaktoren der relativen Intensitäten in Luft

Stromstärke	Element	$VF_{Kathode}$		VF_{Anode}	
		in GaAs	in GeO_2	in GaAs	in GeO_2
6	Al I	1,52	3,08	0,68	1,16
6	Sn I	1,20	1,98	0,74	1,16
6	Ge I	1,00	—	1,00	—
6	As I	0,88	—	1,08	—
6	C I	3,03	2,20	1,59	0,92
12	Al I	1,74	3,56	0,43	1,48
12	Sn I	1,30	2,50	0,52	1,40
12	Ge I	1,01	—	0,75	—
12	As I	0,73	—	1,24	—
12	C I	1,21	1,00	1,21	1,99

In der Tabelle V sind die ermittelten Verstärkungsfaktoren zusammengefaßt. Trägt man die Verstärkungsfaktoren der Elemente gegen die Ionisationspotentiale in einem linearen Maßstab auf, so können die Punkte durch eine Gerade verbunden werden. Die Verstärkungsfaktoren des Kohlenstoffs sind mit den anderen nicht vergleichbar, da sowohl die Kathode als auch die Anode aus Kohlenstoff besteht.

Vergleicht man die Verteilung der Elemente Aluminium und Zinn im Galliumarsenid- und Germaniumdioxid. Bogenplasma miteinander (Abb. 5 und 7 und Tabelle V), so stellt man im Germaniumdioxid-Plasma eine stärkere Anreicherung an der Kathode und einen größeren Verstärkungsfaktor fest. Dieses Ergebnis erklären wir damit, daß der Elektronendruck im Germaniumdioxid-Bogen trotz der höheren Temperatur infolge des niedrigen Ioni-

sationsgrades niedriger als im Galliumarsenid-Bogen ist. Dies führt zu einer stärkeren Ionisation des Aluminiums und Zinns und damit zu einem stärkeren Transport.

Bemerkenswert bei der Abbildung 6 ist noch die starke Asymmetrie des Bogens. Zum Zeitpunkt der Aufnahme des Photogramms erfolgte bei Verlagerung des Kathodenbrennfleckes an die Kante offensichtlich eine Eruption des Plasmas. Die Temperatur dieser Plasmawolke reichte besonders zur weiteren Anregung der leicht anregbaren Teilchen aus. Die Andeutung eines zweiten Leuchtdichtemaximums in Anodennähe ist offensichtlich auf die bei der Stromstärke von 12 A stark zunehmende Verdampfung zurückzuführen.

Auch die Kontinuumstrahlung der Elektroden nimmt, wie an den oben und unten gelegenen parallelen Äquidensiten zu erkennen ist, mit Temperaturzunahme stark zu.

3.4 Äquidensitogramme von Übergängen der Nebenbestandteile in Galliumarsenid und Germaniumdioxid in Argon-Sauerstoff-Atmosphäre

Argon- und Argon–Sauerstoff-Atmosphären werden in der analytischen Spektrochemie oft zur Vermeidung der störenden Cyanbanden und auch zur Erhöhung der Plasmatemperatur angewendet. Aus diesem Grund untersuchten wir den Einfluß der Argon–Sauerstoff-Atmosphäre auf das Galliumarsenid- und Germaniumdioxid-Gleichstrombogenplasma.

Die Abbildungen 7 und 8 stellen die Äquidensitogramme verschiedener Nebenbestandteile in Galliumarsenid bzw. Germaniumdioxid dar.

Ähnlich wie in Luftatmosphäre ergibt sich auch in Argon–Sauerstoff-Atmosphäre eine Leuchtdichteverteilung in Abhängigkeit vom Ionisationspotential des jeweiligen Elementes. Dies ist besonders deutlich beim Galliumarsenid-Plasma sichtbar.

Infolge der höheren Temperatur dieses Plasmas (s. Tabelle IV) im Vergleich zum Luftbogen ist eine Verschiebung des Leuchtdichtemaximums des Germaniums im Galliumarsenid zur Kathode zu erkennen. Die höhere Temperatur bewirkt eine stärkere Ionisation und somit eine solche Verteilung.

Die Verhältnisse im Germaniumdioxid-Bogen liegen offensichtlich etwas anders als im entsprechenden Luftbogen. Es ist gegenüber dem Luftbogen eine deutliche Schwächung der Maximalintensitäten und eine Homogenisierung des Bogenplasmas eingetreten.

Es ist weiterhin zu erkennen, daß der Kohlenstoff kein Anodenmaximum mehr aufweist, obwohl entsprechend dem Ionisationspotential des Kohlenstoffs im Anodenbereich sehr intensive Strahlung auftreten sollte. Wir führen diesen Effekt auf den erhöhten Partialdruck des Sauerstoffs in dem verwendeten Gasgemisch zurück. Da wir außerdem feststellten, daß der Abbrand der Elektroden im Argon–Sauerstoff-Gemisch schneller erfolgt, müßte eigentlich

eine stärkere Konzentration von Kohlenstoffatomen im Plasma sein und ein starkes Anodenmaximum auftreten. Da dies nicht der Fall ist, nehmen wir an, daß durch den hohen Partialdruck des Sauerstoffs der Abbau der Anode hauptsächlich durch Oxydation und nicht durch Sublimation erfolgt. Das gebildete CO trägt jedoch nicht zur Kohlenstoffatomemission bei.

Tabelle VI

Verstärkungsfaktoren der relativen Strahlungsintensitäten in Ar/O_2

Stromstärke	Element	$VF_{Kathode}$		VF_{Anode}	
		in GaAs	in GeO_2	in GaAs	in GeO_2
6	Al I	1,43	1,24	0,83	1,06
6	Sn I	1,36	1,17	0,85	1,17
6	Ge I	1,02	—	1,00	—
6	As I	0,74	—	1,17	—
6	C I	2,14	1,84	0,68	0,83
12	Al I	1,48	2,28	0,81	2,28
12	Sn I	1,26	2,21	0,86	2,21
12	Ge I	1,10	—	0,86	—
12	As I	1,00	—	1,14	—
12	C I	1,98	1,43	0,63	0,57

Errechnet man die Verstärkungsfaktoren (siehe Tabelle VI), so sind die genannten Tendenzen eindeutig ablesbar. Die Darstellung der Verstärkungsfaktoren gegenüber dem Ionisationspotential der einzelnen Elemente liefert im Falle des Galliumarsenid-Bogens wiederum Geraden.

3.5 Radialverteilung der Leuchtdichte der Nebenbestandteile des Galliumarsenid- und Germaniumdioxid-Bogens

Die Radialverteilung ist aus den Äquidensitogrammen nicht ohne weiteres ablesbar. Eine Möglichkeit, qualitative Angaben zu erhalten, besteht darin, mit Hilfe der Abelschen Integralgleichung die aus den Schwärzungswerten der Äquidensiten erhaltenen relativen Flächenintensitäten in relative Volumenstrahlintensitäten umzurechnen.

Die erhaltenen Ergebnisse sind in den Abbildungen 11 und 12 dargestellt. Für die Ermittlung der Volumenstrahlintensitäten wurde jeweils die Bogenmitte gewählt. Es zeigt sich, daß die Leuchtdichte des Aluminiums und Zinns über einen großen Querschnitt homogen verteilt ist. In einigen Fällen nimmt die Strahlungsintenstität zum Bogenzentrum sogar ab. Im Falle des Germaniums, Arsens und Kohlenstoffs ist eine stärkere Abhängigkeit der Volumenstrahlintensität vom Bogenradius erkennbar.

Vergleicht man diese Kurven mit den dazugehörigen Äquidensitogrammen, so sieht man, daß die Äquidensitendichte im Zentrum der Bogensäule zur qualitativen Beurteilung der relativen Volumenstrahlintensität herangezogen werden kann. Hohe Dichte bedeutet ein starkes Maximum, geringe Dichte im Zentrum und hohe Dichte in den Außenbezirken bedeutet homogene Verteilung der Volumenstrahlintensität in einer relativ breiten Bogensäule.

Eine Aussage über die Verteilung der Teilchen ist aus diesen Angaben wegen des steilen Temperaturgradienten nicht möglich.

3.6 Vergleich der Äquidensitogramme von Übergängen der Magnesiumatome und -ionen im Galliumarsenid- und Germaniumdioxid-Gleichstrombogenplasma

Der Vergleich der Leuchtdichteverteilung von Strahlungen von Atomen und Ionen wurde am Beispiel des Magnesiums (s. Tab. 2) sowohl im Luftbogen als auch im Argon–Sauerstoffbogen durchgeführt. Die entsprechenden Äquidensitogramme sind in Abbildung 9 dargestellt.

Sowohl für die Leuchtdichte der Atom- als auch der Ionenlinie hat sich ein Maximum vor der Kathode ausgebildet. Größere Unterschiede sind vor allem bei der Ionenlinie in Abhängigkeit von der Matrix und der Atmosphäre nicht zu erkennen.

Die Reduzierung der Leuchtdichte der Atomlinien des Magnesiums beim Übergang von der Galliumarsenid- zur Germaniumdioxid-Matrix und beim Übergang von Luft- zu Argon-Sauerstoff-Atmosphäre ist auf die damit verbundene Temperaturerhöhung zurückzuführen, die der Rekombination der Ionen zu Atomen entgegenwirkt. Infolge des niedrigeren Elektronendruckes im Germaniumdioxid-Plasma ist die Rekombination nur noch in unmittelbarer Nähe der Kathode zu beobachten.

4. Allgemeine Schlußfolgerungen

Das Verfahren der Kombination der spektralen Photographie und der photographischen Äquidensitometrie erwies sich als nützliches Hilfsmittel für die Charakterisierung des Galliumarsenid- und Germaniumdioxid-Plasmas.

Es konnte gezeigt werden, daß sowohl für die Matrixelemente als auch für die Nebenbestandteile eine axiale Verteilung der Atome im Plasma in Abhängigkeit vom Ionisationspotential erfolgte.

Bei niedrigem Ionisationspotential existiert sowohl für Atome als auch Ionen ein Leuchtdichtemaximum an der Kathode, bei hohem Ionisationspotential ist ein solches an der Anode vorhanden, bei mittleren Ionisationspotentialen bildet sich eine homogene Bogensäule aus.

Der Elektronendruck, der durch die Matrix hervorgerufen wird und die durch ihn und die Atmosphäre und Stromstärke hervorgerufenen Temperaturänderungen beeinflussen diesen Effekt.

Im Falle höherer Temperatur wird der Verstärkungsfaktor an der Kathode im allgemeinen größer, weil in den übrigen Teilen des Bogens die Leuchtdichte stark reduziert ist. Einen Einfluß hat dabei auch der Elektronendruck, der im wesentlichen durch die Matrix bestimmt wird. Diese Ergebnisse stimmen damit überein, daß der Kathodenschichteffekt vor allem für Spuren im Kohlelichtbogen von Bedeutung ist.

Die im matrixbeeinflußten Bogen erreichten Verstärkungsfaktoren von etwa 2 bieten trotzdem die Möglichkeit zur Verbesserung des Linie-Untergrund-Verhältnisses bei der spektrographischen Spurenanalyse.

*

Herrn W. Högner vom Zentralinstitut für Astrophysik der AdW der DDR Karl-Schwarzschild-Observatorium Tautenburg danken wir hiermit für die Anfertigung der Äquidensiten.

LITERATUR

[1] Dittrich, K., Niebergall, K., Rößler, H.: Z. Chem. **13,** 231 (1973)
[2] Dittrich, K., Niebergall, K., Rößler, H.: Spectrochim. Acta (im Druck)
[3] Högner, W.: Privatmitteilung
[4] Mannkopf, R., Peters, C.: Z. Phys. **70,** 444 (1931)
[5] Boumans, P. W. J. M.: Theory of spectrochemical excitation. Hilger & Watts, London, 1966
[6] Boumans, P. W. J. M.: Proc. Coll. Spectr. Intern. XIV., Debrecen 1967, S. 23—63
[7] Mannkopf, R.: Z. Phys. **76,** 396 (1932)
[8] Vukanović, D.: Proc. 7. Intern. Conf. on Phenomena in Ionized Gases, Beograd, 1965, Bd. I, 762

Klaus Dittrich
Helmut Rößler
Knut Niebergall

Sektion Chemie der Karl-Marx-Universität Leipzig, 701 Leipzig, Liebigstr. 18. DDR.

Acta Chimica Academiae Scientiarum Hungaricae, Tomus 89 (4), pp. 365—380 (1976)

ÄQUIDENSITOMETRIE — EINE METHODE ZUR BEURTEILUNG DER STRUKTUR VON PLASMEN, IV

UNTERSUCHUNG DER LEUCHTDICHTEVERTEILUNG IM GLEICHSTROMBOGENPLASMA BEI KATHODISCHER VERDAMPFUNG DER ANALYSENSUBSTANZ IN GEGENWART UND ABWESENHEIT EINES MAGNETFELDES

K. Dittrich, K. Niebergall und H. Rößler

(Sektion Chemie der Karl-Marx-Universität Leipzig, Leipzig, DDR)

Eingegangen am 20. November 1975

Die Charakterisierung von Gleichstrombogenplasmen, die durch kathodische Verdampfung von Lanthansesquioxid, Galliumarsenid und Germaniumdioxid in Gegenwart und Abwesenheit von homogenen Magnetfeldern entstehen, erfolgt auf experimentellen Wege durch spektrale Photographie und photographisch-äquidensitometrische Auswertung der erhaltenen Photogramme. Es ist möglich, qualitative Aussagen über die Axialverteilung der Elemente zu gewinnen. Es konnte gezeigt werden, daß sowohl in Gegenwart als auch in Abwesenheit des Magnetfeldes ein Leuchtdichtemaximum vor der Kathode vorhanden ist. Die Größe der kathodischen Anreicherung richtet sich nach dem Ionisationspotential des Neben- und Hauptbestandteiles.

Der Einfluß des Magnetfeldes macht sich besonders bei schwerer ionisierbarer Matrix in einer Bogenaufweitung bemerkbar.

1. Einführung

In der Literatur ist beschrieben [1, 2], daß bei kathodischer Verdampfung gegenüber der anodischen Verdampfung bei stark reduzierter Probemasse gleiche, zum Teil auch verbesserte Nachweisgrenzen für die Bestimmung von Spurenbestandteilen erzielt werden können.

Bei unseren Untersuchungen über die Anwendung des homogenen Magnetfeldes auf ein Gleichstrombogenplasma, das eine große Menge leicht ionisierbarer Teilchen enthält, die anodisch verdampft werden, stellten wir fest, daß kein stabiles Bogenplasma erhalten werden kann. Bei Anwendung der kathodischen Verdampfung für einen magnetfeldbeeinflußten Gleichstrombogen war das Plasma stabil und es wurde ein gleichmäßiger Abbrand erzielt.

Aufgrund dieser Ergebnisse stellten wir uns die Aufgabe, die Verteilung der Leuchtdichte der einzelnen Plasmabestandteile in diesen Bogenplasmen mit Hilfe der von uns entwickelten Methode der Kombination der spektralen Photographie mit der photographischen Äquidensitometrie zu untersuchen [3, 4, 5]. Diese Methode gestattet es, qualitative Aussagen über die Axialverteilung der Elemente in einem Bogenplasma und über die Bogengeometrie zu machen. Die Untersuchungen wurden an Bogenplasmen durchgeführt, die weitgehend durch die kationischen Bestandteile der Matrixsubstanzen

Lanthan (La_2O_3), Gallium (GaAs) und Germanium (GeO_2) bestimmt wurden. Es wurde in der Hauptsache die Leuchtdichteverteilung der in diesen Matrixsubstanzen vorhandenen Spurenbestandteile untersucht.

2. Experimentelles

2.1 Herstellung von spektral aufgelösten Photogrammen

Die Photogramme wurden, wie in unserer II. Mitteilung [4] näher beschrieben, unter Verwendung des Plangitterspektrographen PGS 2 (VEB C. Zeiss, Jena) hergestellt. Die Anregungs- und Aufnahmebedingungen sind in Tabelle 1 zusammengefaßt. Die Vorbrennzeiten wurden so gewählt, daß jeweils in einem Verdampfungsmaximum aufgenommen werden konnte.

Die in Abbildung 1 dargestellten unterschiedlichen Elektrodenkombinationen und -formen sind für die Erzeugung eines stabilen Bogens und eines gleichmäßigen Abbrandes erforderlich. Eine breite Gegenelektrode ist in Gegenwart des Magnetfeldes notwendig, weil durch die infolge der Rotationsbewegung des Bogens veränderten Außenströmungen nur bei dieser breiten Auflage ein stabiler Bogen erhalten wird. Ohne Magnetfeld führt jedoch diese

Tabelle I

Anregungs- und Aufnahmebedingungen

Spektrograph	Plangitterspektrograph PGS 2
Gitter	651 Strich/mm, Blaze 1020 nm
Dispersion (Plattenmitte)	2. Ordnung 0,370 nm/mm (410 nm) für Ca und (650 nm) für La 3. Ordnung 0,234 nm/mm (315 nm) und 4. Ordnung 0,176 nm/mm (236,4 nm) für Ga und Ge
Ordnungsfilter	WG1 für 2. Ordnung, UG 5 für 3. u. 4. Ordn.
Außenoptik	Achromat (f = 75,8 mm), Direktabbildung Maßstab 5 : 1
Anregung	Universalbogenimpulsgenerator UBI 1
Stromstärke	10 A für La, 6 A und 12 A für Ge und Ga
Magnetfeld	0—350 G, homogen, axial
Elektroden	siehe Abbildung 1
Elektrodenabstand	3 mm, von Hand nachgeregelt
Probematerial	La_2O_3 (Matrix), 1000 ppm CaO, GaAs (Matrix), je 500 ppm Al, Sn, Ge, Mg GeO_2 (Matrix), je 500 ppm Al, Sn
Probemenge	40 mg La_2O_3 : C (1 : 1) 20 mg GaAs : C (1 : 3) 20 mg GeO_2 : C (1 : 3)
Atmosphäre	Luft
Vorbrennzeit	10 A La, 150 sec 10 A Ca, 90 sec 6 A und 12 A Ga und Ge, 20 sec
Belichtungszeit	10 A La 0,1 sec 10 A Ca 0,2 sec 6 A und 12 A Ga und Ge-Matrix 0,5 sec
Spektralplatten	ORWO WP 3 rot extrahart für La Ca ORWO WU 3 blau extrahart für Ga und Ge
Entwicklung	4 min ORWO MH 28 (1 : 4), 19°
Unterbrechung	10 sec, 5%ige Essigsäure, 19°
Fixierung	6 min, ORWO A 304, 200 g/l, 19°
Wässern	10 min
Trocknung	25 min, 27°

breite Gegenelektrode zu einem »wandernden« Bogen. Die als Kathode eingesetzten Becherelektroden hatten sich bei analytischen Bestimmungen in La_2O_3-Matrix bzw. GaAs- und GeO_2-Matrix bewährt. Die größere Wandstärke des Bechers für die La_2O_3-Matrix erwies sich wegen des geringen Kohlenstoffanteils in der La_2O_3-Kohle-Pulvermischung für einen gleichmäßigen Abbrand als vorteilhaft.

Zur Ermittlung der Plattengradation wurde ein Kontinuum mit der Xenonbogenlampe XBO 500 und einem 6 Stufenfilter aufgenommen.

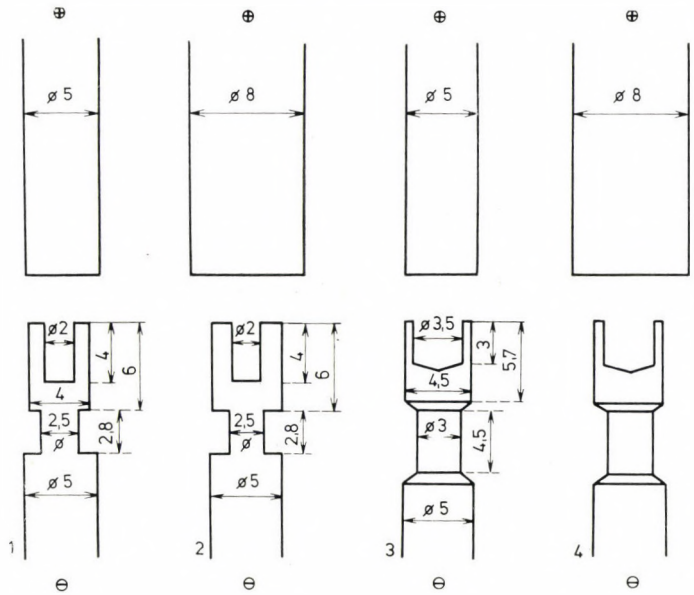

Abb. 1. Elektrodenkombinationen: 1 für La_2O_3, 2 für La_2O_3 im Magnetfeld, 3 für GaAs und GeO_2, 4 für GaAs und GeO_2 im Magnetfeld

2.2 Herstellung der Äquidensiten

Die Herstellung der Einzeläquidensiten erfolgte auf ORWO-Planfilm FU 5 gleichzeitig für die gesamte Photoplatte auf halbautomatischem Weg (6) wie in der III. Mitteilung beschrieben.

3. Ergebnisse und Diskussion

3.1 Ergebnisse

Die Abbildungen 2, 3 und 5—10 zeigen die Äquidensitogramme für Übergänge verschiedener Atome und Ionen in Luftatmosphäre in Gegenwart und Abwesenheit eines homogenen Magnetfeldes bei kathodischer Verdampfung. Die verwendeten Übergänge sind in der Tabelle II näher charakterisiert. Die Äquidensite höchster Schwärzung in jedem Bild ist mit einer Zahl gekennzeichnet, die eine Zuordnung zur Originalschwärzung (s. Tabelle III) ermöglicht. Die äußerste Äquidensite trägt die Nummer 1. Zwischen diesen Werten

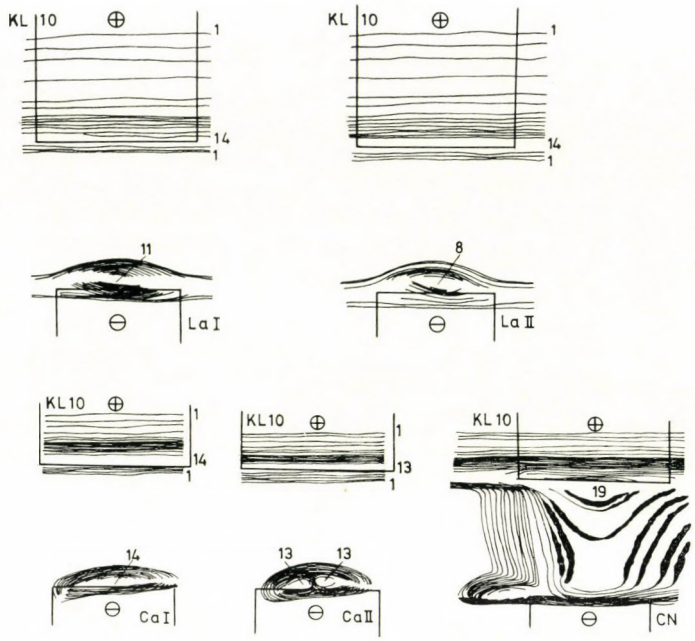

Abb. 2. Monochromatische Äquidensitogramme für das Matrixelement Lanthan, den Nebenbestandteil Calcium und das Cyanradikal bei kathodischer Verdampfung in Luft
KL 10 La I: kathod. Verdampfung in Luft bei 10A für La 654,315 nm
KL 10 La II: kathod. Verdampfung in Luft bei 10A für La 652,699 nm
KL 10 Ca I: kathod. Verdampfung in Luft bei 10A für Ca 422,673 nm
KL 10 Ca II: kathod. Verdampfung in Luft bei 10A für Ca 396,847 nm
KL 10 CN: kathod. Verdampfung in Luft bei 10A für CN 421,6 nm

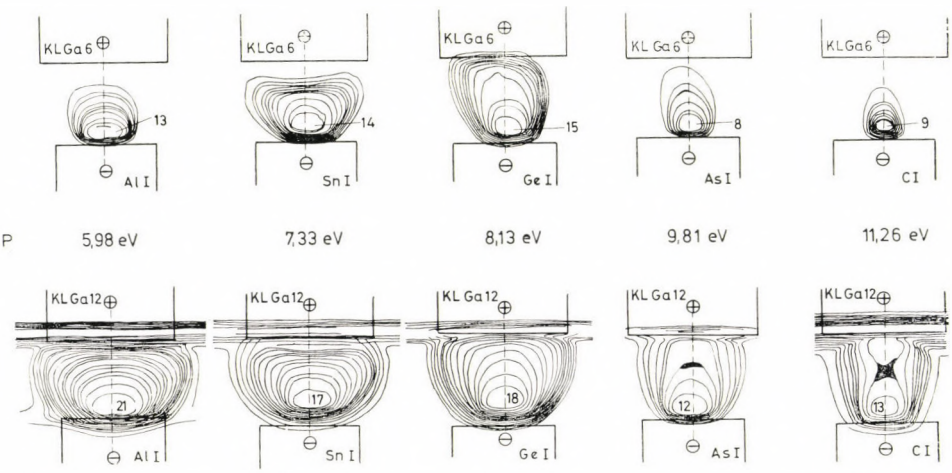

Abb. 3. Monochromatische Äquidensitogramme für die Nebenbestandteile Aluminium, Zinn und Germanium und für Arsen und Kohlenstoff (Matrix GaAs):
KL Ga6: kathod. Verdampfung in Luft bei 6A in GaAs Matrix
KL Ga12: kathod. Verdampfung in Luft bei 12A in GaAs Matrix
Liniencharakteristik siehe Tabelle II

Tabelle II

Wellenlängen, Intensitäten und Anregungspotentiale der mit Hilfe von Äquidensitogrammen untersuchten Übergänge

Element	Übergang in nm	Relative Intensität in Bogen	Anregungs-potential in eV	Ionisations-potential in eV
La I	654,315	125	2,23	5,61
La II	652,699	125	2,13	11,43
Ca I	422,673	500 R	2,93	6,11
Ca II	396,847	500 R	3,12	11,87
Al I	308,215	800	4,02	5,98
Sn I	317,502	500	4,33	7,33
Ge I	303,906	1000	4,96	8,13
As I	289,871	25	—	9,81
C I	247,857	400	7,69	8,13
Mg I	309,689	150	6,72	7,64
Mg II	280,269	150	4,42	15,03

ist entsp rechend der Tabelle III zu numerieren. Außerdem ist es mit Hilfe der Tabelle III möglich, den einzelnen Äquidensiten relative Intensitäten zuzuordnen. Dazu war es erforderlich, die Plattengradation in Abhängigkeit von der Wellenlänge mit Hilfe der kontinuierlichen Spektren zu ermitteln. Die Elektroden wurden nachträglich im entsprechenden Maßstab eingezeichnet. Es wurde keine kegelförmige Gegenelektrode (Anode) verwendet, da der Abbrand infolge der hohen Temperatur zu groß war und ein gleichbleibender Elektrodenabstand deshalb nicht eingehalten werden konnte.

3.2 Äquidensitogramme von Übergängen des La I, La II (Matrix), Ca I, Ca II und CN bei kathodischer Verdampfung

Die Abbildung 2 stellt Äquidensitogramme für Lanthan- und Calciumübergänge und des Cyanbandenkopfes bei kathodischer Verdampfung dar.

Im Gegensatz zu den Ergebnissen bei anodischer Verdampfung [4] ist die Strahlung der Metallatome und -ionen auf den kathodischen Raum beschränkt. Der Äquidensite für den Cyanbandenkopf ist zu entnehmen, daß zum Zeitpunkt der Aufnahme ein vollständig ausgebildeter Lichtbogen existierte. Der Lanthanübergang, der mit dem Cyanbandenkopf überlappt, zeigt die gleiche Struktur, wie sie bei den freiliegenden Übergängen zu beobachten ist. Wir sind der Auffassung, daß sich ein Gleichgewicht zwischen dem Teilchentransport durch Diffusion und Konvektion und dem Teilchentransport durch Wanderung im elektrischen Feld einstellt. Im Gegensatz zur

Tabelle III

Äquidensiten-Nummern, Schwärzungen S und spektrale relative Intensitäten I

Nr.	S_1	$I_{395\,nm}$	$I_{420\,nm}$	$I_{650\,nm}$	S_2	$I_{280\,nm}$	$I_{310\,nm}$
1	0,2	1,819	1,896	1,818	0,2	1,937	2,104
2	0,22	1,841	1,899	1,841	0,23		
3	0,27	1,911	1,974	1,874	0,28	2,193	2,382
4	0,35	2,067	1,958	1,98	0,33	2,371	2,571
5	0,41	2,196	2,023	2,091	0,41	2,729	2,952
6	0,48	2,356	2,175	2,241	0,43		
7	0,53	2,486	2,281	2,347	0,46	2,904	3,140
8	0,70	2,929	2,705	2,721	0,52	3,192	3,444
9	0,74	3,024	2,791	2,809	0,62	3,721	4,018
10	0,82	3,279	2,997	2,978	0,72	4,355	4,677
11	0,92	3,529	3,266	3,203	0,73		
12	1,01	3,777	3,515	3,401	0,81	5,012	5,370
13	1,03	3,819	3,579	3,44	0,93	6,039	6,457
14	1,12	4,093	3,831	3,631	1,00	6,73	7,195
15	1,22	4,352	4,132	3,834	1,11	7,998	8,531
16	1,3	4,57	4,369	3,973	1,20	9,205	9,795
17	1,53	5,188	5,071	4,394	1,32	11,09	11,88
18	1,67	5,609	5,523	4,656	1,40	12,56	13,30
19	1,85	6,034	6,08	4,931	1,52	15,17	16,00
20	1,97	6,369	6,467	5,112	1,68	19,45	20,46
21					1,83	24,55	25,76
22					1,91	27,86	29,17
23					2,13	39,26	40,83
24					2,33	53,58	55,99

S_1 Angaben für La-Matrix und Ca.
S_2 Angaben für Ga und Ge-Matrix und Nebenbestandteile.
Die Äquidensiten Nr. 2, 6 und 11 wurden wegen ihrer Ähnlichkeit mit Nr. 1, 5 und 10 nicht in die Äquidensitogramme eingezeichnet.

anodischen Verdampfung sind diese Transportfaktoren bei kathodischer Verdampfung entgegengesetzt gerichtet. Infolge der hohen Frequenz, mit der sich das dynamische Gleichgewicht zwischen Atomen und Ionen einstellt, wirkt sich dieser Faktor sowohl auf die Verteilung der Strahlung der neutralen Atome als auch der der Ionen aus.

3.3 Äquidensitogramme von Übergängen der Nebenbestandteile des Galliumarsenid und Germaniumdioxid bei kathodischer Verdampfung

Ähnlich wie bei der anodischen Verdampfung (5) wurde festgestellt, daß das Ionisationspotential sowohl des Matrixelementes als auch der Spurenbestandteile einen Einfluß auf die Leuchtdichteverteilung der Spurenelemente im Gleichstrombogenplasma hat. Die Abbildung 3 zeigt die Äquidensitogramme für die Nebenbestandteile Aluminium, Zinn und Germanium im Galliumarsenid und für Arsen und Kohlenstoff in Gegenwart dieser Matrix bei zwei Stromstärken. Mit zunehmendem Ionisationspotential, d. h. schwächerem Ionisationsgrad des Nebenbestandteils unter den gleichbleibenden Bedingungen der Galliumarsenidmatrix streckt sich die Strahlungsverteilung von der Kathode zur Anode. Das ist wiederum erklärbar durch die Reduzierung des feldbedingten Transportes zur Kathode für die schwerer ionisierbaren Teilchen. Die Temperaturerhöhung beim Übergang von 6 A auf 12 A vergrößert die Verdampfungsgeschwindigkeit, so daß eine Homogenisierung des Bogenplasmas erkennbar ist. Berechnet man jedoch die Verhältnisse der relativen Lichtintensitäten des kathodischen Raumes zur Bogenmitte, so ist kein wesentlicher Unterschied zwischen den Plasmen bei 12 A und 6 A zu erkennen (s. Tabelle IV). In beiden Fällen ist eine Korrelation mit dem Ionisationspotential festzustellen (s. Abb. 4). Eine Ausnahme bilden die Kohlenstoffäquidensitogramme und deren Verstärkungsfaktoren. Im Fall des 6 A Bogens ist die Temperatur im Plasma so niedrig, daß zu wenig Kohlenstoff von der Kathode und gar kein Kohlenstoff von der Anode verdampft. Im Fall des 12 A Bogens verdampfen nennenswerte Mengen Kohlenstoff von der Anode und Kathode. Das ist zu berücksichtigen, wenn man die richtige Tendenz des Verstärkungsfaktors 1,2 beurteilt.

Die Abbildung 5 zeigt die Äquidensitogramme für Aluminium und Zinn und auch für Kohlenstoff in einer Germaniumdioxid-Matrix. Im Vergleich

Tabelle IV

Verstärkungsfaktoren der relativen Strahlungsintensitäten des kathodennahen Raumes bezogen auf die Bogenmitte für die kathodische Verdampfung

Stromstärke	6 A		12 A	
Matrix	GaAs	GeO_2	GaAs	GeO_2
Element	kathodische Verstärkungsfaktoren $VF_{kath.}$			
Al I	2,20	3,20	2,60	3,85
Sn I	1,75	2,90	1,90	3,42
Ge I	1,59	—	1,65	—
As I	1,28	—	1,35	—
C I	1,57	1,00	1,20	1,00

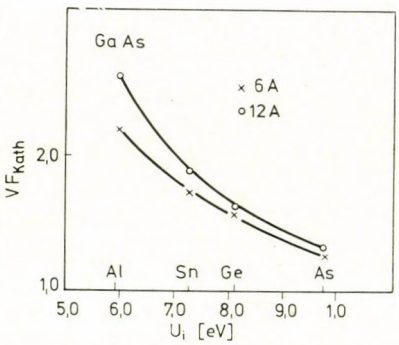

Abb. 4. Abhängigkeit der Verstärkungsfaktoren vom Ionisationspotential für Aluminium, Zinn, Germanium und Arsen (Matrix GaAs) bei kathodischer Verdampfung in Luft

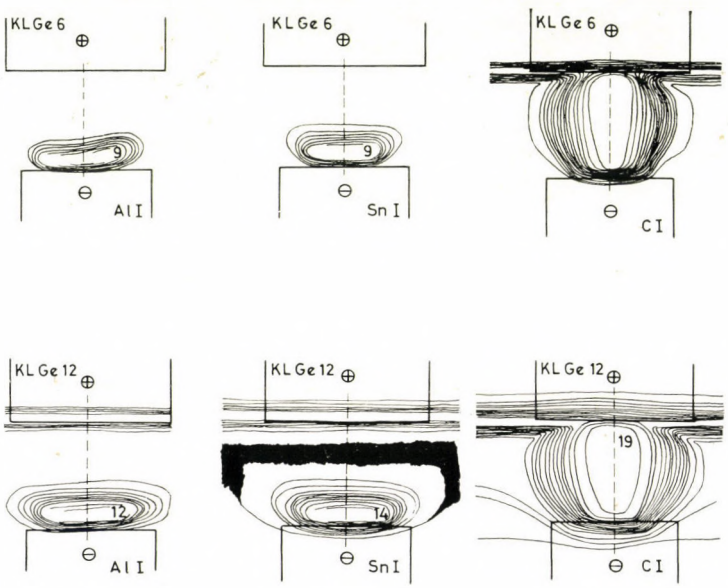

Abb. 5. Monochromatische Äquidensitogramme für die Nebenbestandteile Aluminium und Zinn und für Kohlenstoff (Matrix GeO_2)
KL Ge6: kathod. Verdampfung in Luft bei 6A Matrix GeO_2
KL Ge12: kathod. Verdampfung in Luft bei 12A Matrix GeO_2
Linien charakteristik siehe Tabelle II

zum Gallium-Bogen sind die Bestandteile noch stärker auf den kathodennahen Raum konzentriert (s. a. Tabelle IV). Dies kommt besonders bei der Stromstärke von 12 A zum Ausdruck. Auch dieses Verhalten läßt sich mit Hilfe der unterschiedlichen Ionisationspotentiale und Ionisationsgrade erklären. Der Ionisationsgrad für Aluminium und Zinn wird in der schwerer ionisierbaren Matrix Germanium höher als im Gallium sein, so daß der feldbedingte

Transport größer wird. Allerdings ist in diesem Fall auch die geringere Verdampfungsgeschwindigkeit der Matrix zu berücksichtigen, denn der Siedepunkt des elementaren Germaniums liegt mit 2700 °C um etwa 700 °C höher als der des Galliums.

Der Abbildung 5 ist auch zu entnehmen, daß es sich um eine echte Konzentrationsabnahme im Plasma handeln muß und nicht nur um veränderte Anregungsbedingungen, z. B. einen axialen Temperaturgradienten, denn für den Kohlenstoffübergang ist eine homogene Leuchtdichte-Verteilung erkennbar. Diese homogene Leuchtdichte-Verteilung widerspricht eigentlich wegen des sehr hohen Ionisationspotentials des Kohlenstoffs dem bisher Gesagten. Es ist hier jedoch zu berücksichtigen, daß auch die Anode aus Kohlenstoff besteht und auch dort eine Verdampfung möglich ist. Auch im Galliumarsenid-Bogenplasma ist die Homogenität der Leuchtdichteverteilung des Kohlenstoffs bei 12 A erkennbar. Bei einer Stromstärke von 6 A reicht offensichtlich die Temperatur der Anode für eine nennenswerte Verdampfung des Kohlenstoffs nicht aus.

3.4 Äquidensitogramme von Übergängen der Magnesiumatome und -ionen in Galliumarsenid- und Germaniumdioxid-Plasmen bei kathodischer Verdampfung

Auch in der Galliumarsenid- und Germaniumdioxid-Matrix sollte der Einfluß des Ionisationszustandes der Nebenbestandteile auf deren Leuchtdichteverteilung bei kathodischer Verdampfung untersucht werden. Als Beispiel wurde wie bei der anodischen Verdampfung (s. a. (5)) ein Atom- und ein Ionenübergang des Magnesiums ausgewählt. Die erhaltenen Äquidensitogramme sind in der Abb. 6 dargestellt. Entsprechend dem Ionisationspotential des Magnesiums lassen sich die Äquidensitogramme von Mg I zwischen Sn I und Ge I einordnen (s. a. Abb. 3). Da diese Aufnahmen bei einem zweiten Bogenabbrand erhalten wurden, wird durch dieses Ergebnis die Objektivität der Methode bestätigt. Der Vergleich der Magnesium I-Äquidensitogramme für die Galliumarsenid- und die Germaniumdioxid-Matrix zeigt ebenfalls, daß sich die Magnesiumatome in der Matrix mit höherem Ionisationspotential stärker vor der Kathode konzentrieren.

Sowohl in der Gallium- als auch in der Germanium-Matrix weisen die Magnesium II-Übergänge ein starkes Maximum in Kathodennähe auf. Die im Vergleich zum Magnesium I-Übergang höhere Intensität bestätigt den hohen Ionisationsgrad.

Der Vergleich der Äquidensitogramme des Magnesium II-Überganges in Gallium- und Germanium-Matrix bei 12 A zeigt, daß die Annahme, daß der Ionisationsgrad des Magnesiums im schlechter verdampfenden und schwerer ionisierenden Germanium höher liegt, richtig ist, denn in der Germanium-

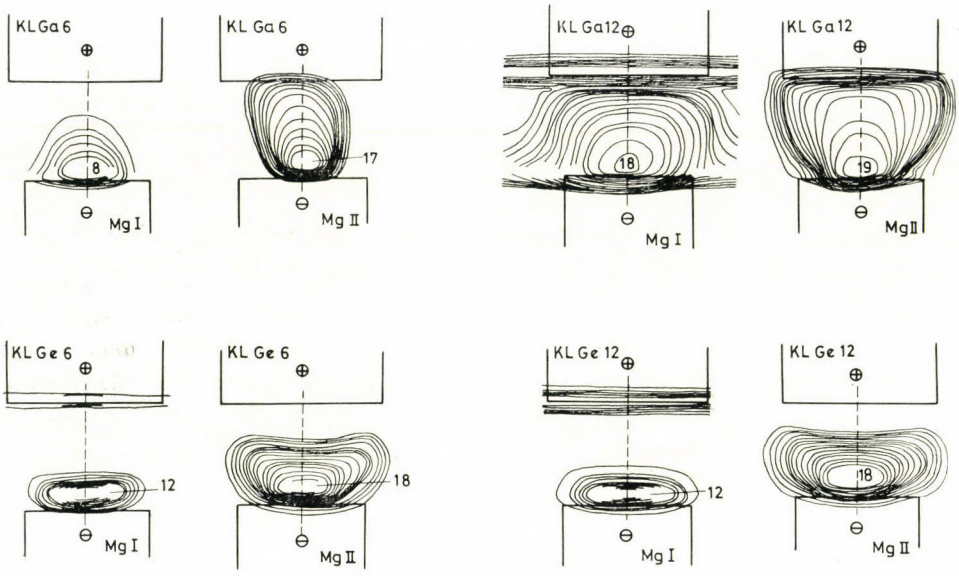

Abb. 6. Monochromatische Äquidensitogramme für Magnesiumatome und -ionen
KL Ga6: kathod. Verdampfung in Luft bei 6A Matrix GaAs
KL Ga12: kathod. Verdampfung in Luft bei 12A Matrix GaAs
KL Ge6: kathod. Verdampfung in Luft bei 6A Matrix GeO_2
KL Ge12: kathod. Verdampfung in Luft bei 12A Matrix GeO_2

Tabelle V

Verstärkungsfaktoren der relativen Strahlungsintensitäten des kathodennahen Raumes bezogen auf die Bogenmitte für die kathodische Verdampfung

Stromstärke	6 A		12 A	
Matrix	GaAs	GeO_2	GaAs	GeO_2
Element	kathodische Verstärkungsfaktoren $VF_{kath.}$			
Mg I	1,64	2,70	1,46	3,20
Mg II	1,86	4,32	1,56	4,60

Matrix ist das kathodennahe Maximum der Leuchtdichte viel ausgeprägter. Die Verstärkungsfaktoren für diese Übergänge sind in der Tabelle V zusammengefaßt. Sie bestätigen die gezogenen Schlußfolgerungen.

3.5 Äquidensitogramme von Übergängen von Atomen und Ionen in Lanthan-, Gallium- und Germanium-Matrix im magnetfeldbeeinflußten Bogen bei kathodischer Verdampfung

Es ist bekannt, daß die intensitätsverstärkende Wirkung eines homogenen Magnetfeldes durch einen Konzentrationsanstieg der Elemente vor der Kathode und durch verstärkte Anregungsprozesse infolge von Temperaturer-

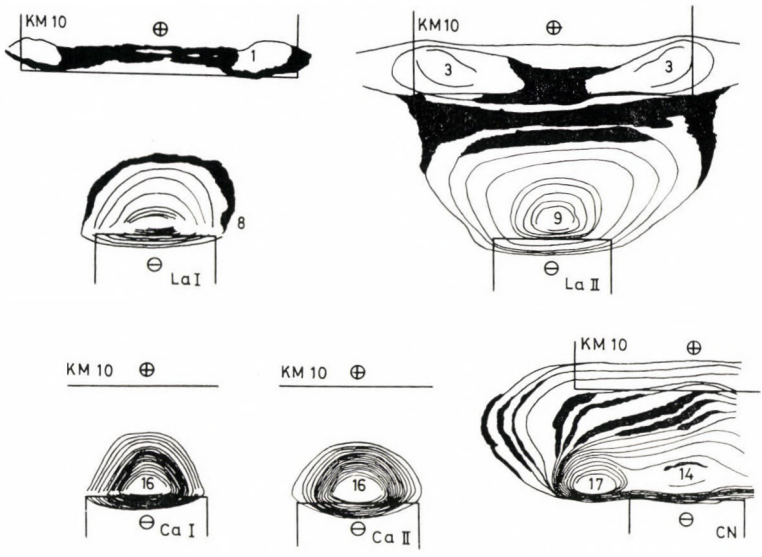

Abb. 7. Monochromatische Äquidensitogramme für das Matrixelement Lanthan, den Nebenbestandteil Calcium und das Cyanradikal im Magnetfeld
KM 10 La I, II: kathod. Verdampfung in Luft bei 10A und 200G für La
KM 10 Ca I, II: kathod. Verdampfung in Luft bei 10A und 20G für Ca
KM 10 CN: kathod. Verdampfung in Luft bei 10A und 200G für CN
(Cyanbandenkopf bei 421,6 nm)
Liniencharakteristik siehe Tabelle II

höhung verursacht wird [6]. Da bei anodischer Verdampfung einer leicht ionisierbaren Matrix bei Anwendung eines homogenen Magnetfeldes von uns keine Linienverstärkung beobachtet und kein stabiler Bogen erhalten wurde, setzten wir die kathodische Verdampfung in Verbindung mit einem Magnetfeld ein. Orientierende Versuche von LEUSHACKE [6] hatten ergeben, daß bei kathodischer Verdampfung ein noch ausgeprägteres Maximum der Intensität vor der Kathode erhalten wird.

Wir untersuchten diese Plasmen ebenfalls durch Äquidensitometrieren spektraler Photographien.

Die erhaltenen Äquidensitogramme werden in den Abbildungen 7, 8, 9 und 10 dargestellt. Wir verwendeten als Gegenelektrode Kohlestäbe mit einem Durchmesser von 8 mm (s. Abb. 1), um die durch das Magnetfeld und die Konvektion hervorgerufenen Strömungsverhältnisse günstig zu beeinflussen.

Im Falle der Lanthan-Matrix (Abb. 7) ist im Vergleich zum magnetfeldfreien Bogen eine starke Aufweitung besonders bei La II infolge der durch die Helixbildung bedingten Bogenverlängerung und infolge der veränderten Strömungsbedingungen zu beobachten. Diese Bogenaufweitung drückt sich in einer axialen Streckung des strahlenden Plasmagebietes und in der auftretenden Pinch-Konfiguration aus. Auch die von BRIL und Mitarbeitern [7]

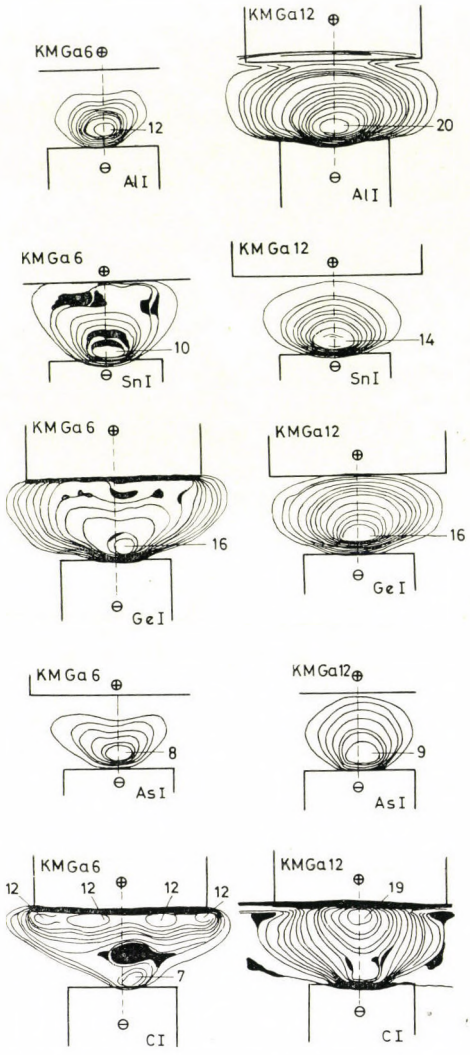

Abb. 8. Monochromatische Äquidensitogramme für die Nebenbestandteile Aluminium, Zinn und Germanium, für Arsen und Kohlenstoff (Matrix GaAs) bei kathodischer Verdampfung in Luft in Gegenwart eines Magnetfeldes
KM Ga6: kathod. Verdampfung in Luft bei 6A und 350 G für GaAs
KM Ga12: kathod. Verdampfung in Luft bei 12A und 150 G für GaAs
Liniencharakteristik siehe Tabelle II

beschriebene anodische Brennfleckaufspaltung im magnetfeldbeeinflußten Bogen ist deutlich im Fall der Lanthan-Äquidensitogramme zu erkennen.

Beim Vergleich der Abbildungen 2 und 7 ist außerdem zu sehen, daß sich das Maximum der Strahlungsintensität des Cyanradikals von der Anode zur Kathode verlagert hat. Daraus geht hervor, daß auch bei Anwendung

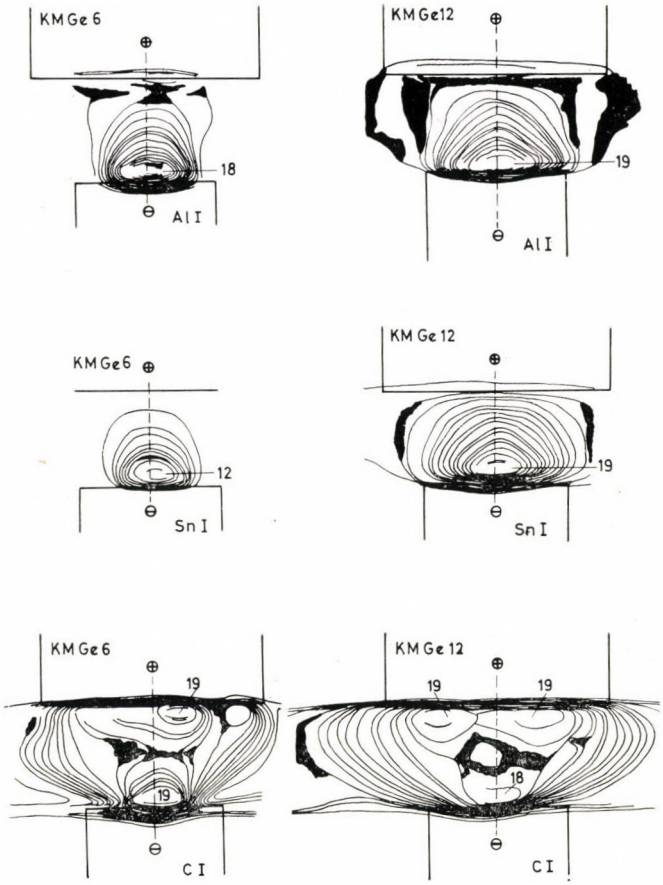

Abb. 9. Monochromatische Äquidensitogramme für die Nebenbestandteile Aluminium, Zinn und für Kohlenstoff (Matrix GeO_2) bei kathodischer Verdampfung in Luft in Gegenwart eines Magnetfeldes
KM Ge6: kathod. Verdampfung in Luft bei 6A und 350G Matrix GeO_2
KM Ge12: kathod. Verdampfung in Luft bei 12A und 150G Matrix GeO_2
Liniencharakteristik siehe Tabelle II

eines solchen Plasmas für analytische Bestimmungen der Einsatz von Inertgasen von Vorteil ist.

Auch in Gegenwart der Gallium- bzw. Germanium-Matrix wird eine typische Pinchkonfiguration des Bogens erhalten. Der Bogen verbreitert sich von der Kathode zur Anode. Er brennt stabil, die Rotation der Helix erreicht einige Umdrehungen pro Sekunde. Bei der gewählten Schaltung wirken die Konvektion und die magnetfeldbedingte Strömung in der gleichen Richtung, d. h. von der Kathode (unten) zu der Anode (oben). Die Pinchkonfiguration ist bei hoher Feldstärke (6 A, 350 Gauß) stärker ausgeprägt als bei niedriger Feldstärke (12 A, 150 Gauß). Die unterschiedliche magnetische Feldstärke mußte

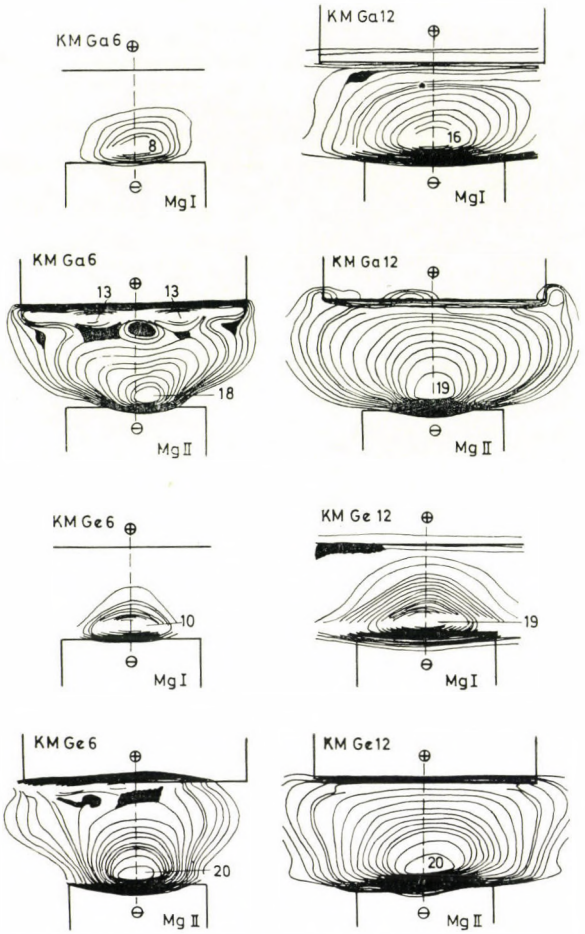

Abb. 10. Monochromatische Äquidensitogramme für Magnesiumatome und -ionen bei kathodischer Verdampfung in Gegenwart eines Magnetfeldes
KM Ga6: kathod. Verdampfung in Luft bei 6A und 350G Matrix GaAs
KM Ga12: kathod. Verdampfung in Luft bei 12A und 150G Matrix GaAs
KM Ge6: kathod. Verdampfung in Luft bei 6A und 350G Matrix GeO_2
KM Ge12: kathod. Verdampfung in Luft bei 12A und 150G Matrix GeO_2
Liniencharakteristik siehe Tabelle II

gewählt werden, da nur so ein stabiles Bogenplasma bei unterschiedlichen Stromstärken erhalten werden konnte. Das Äquidensitogramm des Kohlenstoff-Überganges zeigt außerdem mehrere Maxima vor der Anode. Diese werden durch die Rotation des anodischen Brennfleckes hervorgerufen.

Die schon bei der kathodischen Verdampfung ohne Magnetfeld beobachtete Anreicherung der Spurenelemente vor der Kathode ist auch in Gegenwart eines Magnetfeldes zu beobachten (vergleiche Abbildung 3 mit 8, 5 mit 9 und 6 mit 10). In den meisten Fällen ist die Volumenvergrößerung des magnet-

feldbeeinflußten Bogens zu erkennen. Wiederum sind Unterschiede in Abhängigkeit von der Matrix zu erkennen. Im Galliumarsenid-Plasma wird die Leuchtdichteverteilung der Nebenbestandteile kaum durch die Gegenwart des Magnetfeldes beeinflußt. Im Germaniumdioxid-Plasma ist für Aluminium und Zinn eine starke Vergrößerung des Strahlungsbereiches in axialer Richtung zu erkennen. Dies gilt ebenfalls für die Atom- und Ionenübergänge des Magnesiums in dieser Matrix.

Es ist bekannt, daß das Magnetfeld bei anodischer Verdampfung besonders dann einen linienintensität erhöhenden Einfluß ausübt, wenn die Matrix ein hohes Ionisationspotential besitzt, z. B. bei der Bestimmung von Spurenelementen in Graphit.

Auch bei der kathodischen Verdampfung hat offensichtlich das Ionisationspotential der Matrix einen entscheidenden Einfluß auf die Leuchtdichteverteilung der Nebenbestandteile in einem magnetfeldbeeinflußten Bogenplasma. So ist im leicht ionisierbaren Gallium kein und im schwerer ionisierbaren Germanium ein Einfluß des Magnetfeldes auf die Leuchtdichteverteilung erkennbar.

Die entsprechenden Verstärkungsfaktoren sind in der Tabelle VI zusammengefaßt.

Tabelle VI

Verstärkungsfaktoren der relativen Strahlungsintensitäten des kathodischen Raumes bezogen auf die Bogenmitte für die kathodische Verdampfung in Gegenwart eines Magnetfeldes

Stromstärke	6 A		12 A	
Magnetfeldstärke	350 Gauß		150 Gauß	
Matrix	GaAs	GeO_2	GaAs	GeO_2
Element	kathodische Verstärkungsfaktoren $VF_{kath.}$			
Al I	2,55	4,24	2,40	3,33
Sn I	1,79	2,35	2,21	2,12
Ge I	1,36	—	1,36	—
As I	1,17	—	1,33	—
C I	1,22	2,25	1,00	1,11
Mg I	1,64	1,96	2,00	3,75
Mg II	2,60	2,89	1,65	2,42

4. Allgemeine Schlußfolgerungen

Die kathodische Verdampfung der untersuchten Matrizes führt infolge des geringen Abbrandes je Zeiteinheit zu einer Veränderung der Bogenbedingungen. Durch die Umkehrung der Elektrodenpolung ändert sich die Richtung

des feldbedingten Transportes der Ionen. Die Ergebnisse zeigen die Möglichkeit einer gezielten analytischen Anwendung des Gleichstrombogens mit kathodischer Verdampfung für die untersuchten Matrizes auf. Dabei müßte der Bogenbereich erhöhter Leuchtdichte direkt auf dem Spalt abgebildet werden. Der Vorteil eines solchen Verfahrens läge nicht zuletzt darin, daß nur geringe Probemengen benötigt werden.

Die Anwendung eines Magnetfeldes auf ein solches Bogenplasma wird in den meisten Fällen keine zusätzliche Verbesserung der Intensität bringen. Genaue Aussagen über die Verbesserung von Nachweisgrenzen lassen sich mit dem vorliegenden Material nicht geben, da hierfür genaue Untersuchungen des Linie-Untergrund-Verhältnisses erforderlich sind.

Es kann jedoch festgestellt werden, daß die äquidensitometrische Auswertung von spektralen Photographien derartiger Plasmen gute qualitative Überblicke über die axiale Teilchenverteilung liefert.

*

Herrn W. Högner vom Zentralinstitut für Astrophysik der AdW der DDR, Karl-Schwarzschild-Observatorium Tautenburg danken wir hiermit für die Anfertigung der Äquidensiten.

LITERATUR

[1] Laqua, K., Waechter, H.: Proc. Coll. Spectrosc. Int., 14th, Debrecen (1967), 775
[2] Decker, R. J.: Spectrochim. Acta **28B** 339 (1973)
[3] Dittrich, K., Niebergall, K., Rössler, H.: Z. Chem. **13**, 231 (1973)
[4] Dittrich, K., Niebergall, K., Rössler, H.: Spectrochim. Acta (im Druck)
[5] Dittrich, K., Rössler, H., Niebergall, K.: Acta Chim. (Budapest) (im Druck)
[6] Leushacke, D. F.: Dissertation, Berichte der Kernforschungsanlage Jülich, Jül. — 732 — RW (1971)
[7] Bril, J., Duverneuil, G., Leushacke, D. F., Nickel, H.: Spectrochim. Acta **27B**, 35 (1972)

Klaus Dittrich
Knut Niebergall
Helmut Rößler

Sektion Chemie der Karl-Marx-Universität Leipzig, 701 Leipzig, Liebigstr. 18. DDR.

Acta Chimica Academiae Scientiarum Hungaricae, Tomus 89 (4), pp. 381–391 (1976)

ELECTRONIC ABSORPTION SPECTRA OF SOME DIARYLIDENECYCLOPENTANONES AND -CYCLOHEXANONES

R. M. Issa,* S. H. Etaiw,* I. M. Issa and A. K. El-Shafie

(Chemistry Department, Faculty of Science, Assiut University, A. R., Egypt)

Received March 20, 1975;
in revised form November 6, 1975

The electronic absorption spectra of some diarylidenecyclohexanones and cyclopentanones have been studied in organic solvents and buffer solutions. The spectral shifts are discussed in terms of solvent effects and in relation to the molecular structure. The acid dissociation constants of the compounds containing OH groups were determined from measurements in buffer solutions. The important bands in the IR spectra are assigned and discussed in relation to the molecular structure.

Introduction

Diarylidenecyclanones containing a hydroxyl or amino group are considered to function as acid-base indicators, owing to their ability to capture or release a proton [1, 2], however, the pK_a values of such compounds have not been determined. Some diarylidenecyclanones were found to exhibit some biological activities [3]. These properties attach interest to the chemistry of this class of compounds. The spectra of a series of diarylidenecyclanones were the subject of some investigations [4—7], however, few attempts have been made as far as band assignment and solvent effects are concerned.

In the present work, the electronic absorption spectra of some diarylidenecyclohexanones and cyclopentanones have been studied in organic solvents and buffer solutions with the aim to throw light on the spectral behaviour of these compounds. Also the important IR bands are assigned and discussed in relation to the molecular structure.

Experimental

The compounds used in the present investigation were prepared by the condensation of cyclohexanone or cyclopentanone with different aldehydes under suitable experimental conditions as given by other authors [6, 8]. The products obtained were crystallized from an appropriate solvent. The compounds had the following structures:

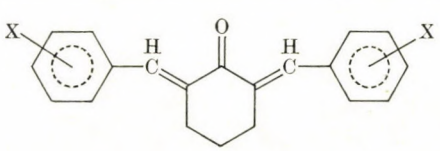

I

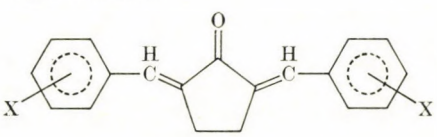

II

* Present adress: Chemistry Department, Faculty of Science, Tanta University, Tanta, Egypt

where X = H (*a*); *p*-OCH_3 (*b*); *p*-OH (*c*); *p*-$N(CH_3)_2$ (*d*); *p*-Cl (*e*); *m*-NO_2 (*f*); *o*-OH (*g*); *p*-OH-*m*-OCH_3 (*h*) and *o*-OH-*m*,*m*-diBr (*i*).

The solvents used were purified according to recommended procedures [9]; the buffer solutions were prepared as given by BRITTON [10].

The absorption spectra were recorded on a UNICAM SP 8000 spectrophotometer using 1 cm matched quartz cells. The PH measurements were carried out with the aid of a RADIOMETER pH-meter, Model 28.

Results and discussion

(A) *Spectra in organic solvents*

The absorption spectra in organic solvents (Tables I and II; Fig. 1) mostly display two bands. The shorter wavelength band within the range 215—270 nm is due to the $\pi - \pi^*$ transition of the aromatic system ($^1L_a \leftarrow {}^1A$), whereas

Table I

Results obtained in organic solvents for series **I**
λ_{max}(nm) and $\varepsilon_{max} \cdot 10^{-4}$ ($mole^{-1} \cdot cm^2$)

Compound	CCl_4		$CHCl_3$		Ether		Ethanol		Assignment
	λ_{max}	ε_{max}	λ_{max}	ε_{max}	λ_{max}	ε_{max}	λ_{max}	ε_{max}	
(*a*)					230	1.94	230	0.66	$\pi - \pi^{*(a)}$
	332	3.73	322	2.45	320	3.62	330	0.94	C.T.
(*b*)					238	1.61	243	2.35	$\pi - \pi^{*(a)}$
	350	3.94	332	1.45	347	3.01	364	4.12	C.T.
(*c*)					242	S	245	1.91	$\pi - \pi^{*(a)}$
	355	S	360	S	350	S	375	3.72	C.T.
(*d*)	268	1.92	272	1.59	270	S	270	1.06	$\pi - \pi^{*(a)}$
	320	0.77	320	0.40	325	S	330	0.21	$\pi - \pi^{*(b)}$
	410	4.09	435	2.97	407	S	447	3.9	C.T.
(*e*)					234	2.00	238	1.92	$\pi - \pi^{*(a)}$
	330	3.34	334	3.46	325	4.01	332	3.61	C.T.
(*f*)					220	S	225	2.11	$\pi - \pi^{*(a)}$
	270	2.18	275	1.98	272	S	278	1.82	$\pi - \pi^{*(b)}$
	313	3.86	314	3.12	310	S	315	2.77	C.T.
(*h*)					252	S	255	1.13	$\pi - \pi^{*(a)}$
	365	1.79	370	2.91	365	S	390	3.25	C.T.

S saturated solution used
(a) $^1L_a \leftarrow {}^1A$
(b) $^1L_b \leftarrow {}^1A$
C.T. = charge transfer band

Table II

Results obtained in organic solvents for series **II**
λ_{max}(nm) $\varepsilon_{max} \cdot 10^{-4}$ (mole$^{-1} \cdot$ cm^2)

Compound	CCl_4		$CHCl_3$		Ether		Ethanol		Assignment
	λ_{max}	ε_{max}	λ_{max}	ε_{max}	λ_{max}	ε_{max}	λ_{max}	ε_{max}	
(*a*)					230	2.39	230	1.66	$\pi - \pi^{*(a)}$
	343	4.17	350	3.59	338	4.65	354	4.38	C.T.
(*b*)					240	S	243	2.65	$\pi - \pi^{*(a)}$
	373	4.65			370	S	394	4.49	C.T.
(*c*)					235	S	245	8.98	$\pi - \pi^{*(a)}$
			385	S	375	S	395	2.83	C.T.
(*d*)					270	1.49	270	S	$\pi - \pi^{*(a)}$
					325	0.40	330	S	$\pi - \pi^{*(b)}$
					363	4.85	476	S	C.T.
(*e*)					237	1.53	238	1.84	$\pi - \pi^{*(a)}$
	348	3.35	355	7.13	345	3.39	358	4.32	C.T.
(*g*)					234	S	238	1.64	$\pi - \pi^{*(a)}$
					255	S	260	1.29	$\pi - \pi^{*(b)}$
	315	S	325	S	320	S	332	1.87	C.T.
	366	S	380	S	367	S	390	4.32	C.T.
(*h*)					250	S	248	1.61	$\pi - \pi^{*(a)}$
	390	S	395	S	395	S	410	4.72	C.T.
(*i*)					215	S	220	5.72	$\pi - \pi^{*(a)}$
					258	S	258	2.36	$\pi - \pi^{*(b)}$
	310	0.56	310	0.55	310	S	310	0.67	C.T.

For symbols, see Table I

the longer wavelength band is assigned to an intramolecular charge transfer. The charge transfer involves the transition of an electron from the highest filled energy level of the aromatic system to the lowest vacant level of the C=O group. The mesomeric shift, representing such a charge transfer can be formulated as follows:

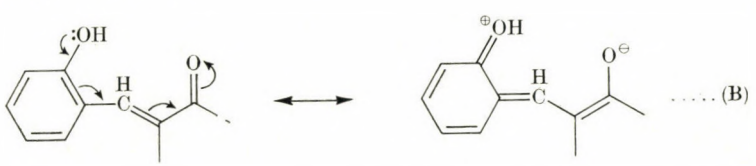

..... (B)

The charge transfer character of the electronic transition is supported by the high extinction and broadening of the band. It is also substantiated by the fact that the band position is markedly influenced by the nature of the substituents. The band is shifted towards red in the case of electron donor substituents, while electron acceptors cause a blue shift (Tables I and II). The plot of λ_{max}. *vs.* σ (Hammett constant of the substituent) reveals a more or less linear relation.

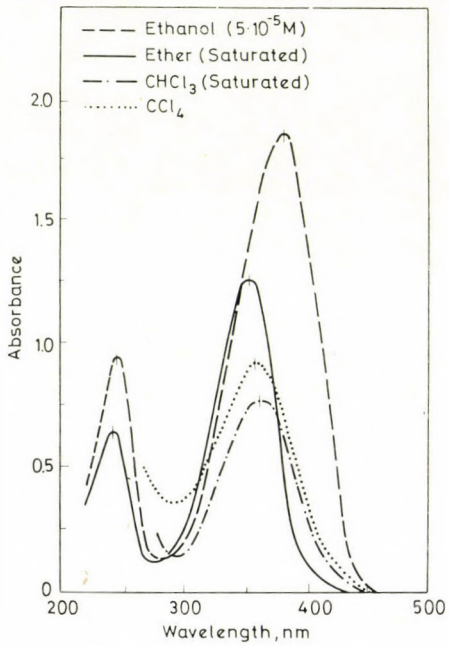

Fig. 1. Spectra of **Ic**

The charge transfer band shifts towards red with increasing solvent polarity in the order $CCl_4 \rightarrow CHCl_3 \rightarrow$ ethanol. In ether, however, the band is mostly blue-shifted in comparison to CCl_4, though the latter has lower polarity. The charge transfer band also shifts towards red on going from cyclohexanone derivatives to the cyclopentanone series. This is in accordance with the previous observation [11] that cyclopentanone derivatives absorb at longer wavelengths as compared with cyclohexanones.

The short-wavelength band exhibits no apparent shifts with solvent polarity, indicating that it is due to a localized transition. The shift towards red observed in some cases is of low magnitude in comparison with the charge transfer band.

The spectra of compounds $\mathbf{I}_d$, $\mathbf{I}_f$, $\mathbf{II}_d$, $\mathbf{II}_g$ and $\mathbf{II}_i$ show a small band within the 250—330 nm range, which can be assigned to the lowest energy transition of

the aromatic nucleus ($^1L_b \leftarrow {}^1A$). This band acquires a small red shift with increasing solvent polarity denoting that it corresponds to a $\pi - \pi^*$ transition.

The spectra of II_g are characterized by a broad band in the 330 nm region. The band exhibits the character of charge transfer bands as far as the solvent shift, band broadening and extinction are concerned. The appearance of two charge transfer bands in the spectra of this compound may be explained by the possibility of two intramolecular charge transfer interactions. The first originates from the phenyl ring, being enhanced by the substituent OH group

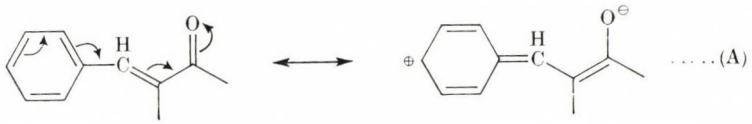

.....(A)

The second transition does not involve an interaction with the OH group, and recalls the case of the non-substituted compound, characterized by the mesomeric shift (A).

(B) *Spectra in mixed organic solvents*

The shift of the charge transfer band towards red in ethanol is much higher than corresponding to the change of solvent polarity. The application of the equation given by GATI and SZALAY [12]

$$\Delta\nu = \left\{\left(\frac{n^2-1}{2n^2+1}\right)(a-b)\right\} + b\left(\frac{D-1}{D+1}\right)$$

did not yield a linear relation between $\Delta\nu$ and $\left(\frac{D-1}{D+1}\right)$. The shift is thus due not only to changes in the dielectric constant of the medium or altered solvation energy, but also accounts for the possible hydrogen bond formation between the solute and solvent molecules. Hydrogen bonding occurs probably between the C=O group of the solute molecules and the protons of ethanol. This type of bonding lowers the charge density on the C=O group, hence increases its electron accepting character. The change in excitation energy on going from the low polarity solvent to ethanol amount to 2.5—3.7 kcal/mole (Table II).

The formation of intermolecular hydrogen bonding is supported by the spectra taken in low-polarity solvents containing increasing quantities of ethanol. The spectra represented in Fig. 2 reveal that the charge transfer band is generally shifted towards red with increasing ethanol concentration A clear isosbestic point is observed indicating that an equilibrium is attained in solution

between the molecules solvated by the low-polarity solvents and those bonded to ethanol through intermolecular hydrogen bonds, forming a sort of molecular complex.

$$S + nROH \rightleftharpoons (ROH)_n \ldots S$$

For this equilibrium reaction

$$K_f = \frac{[(ROH)_n \ldots S]}{[S]\,[ROH]^n}$$

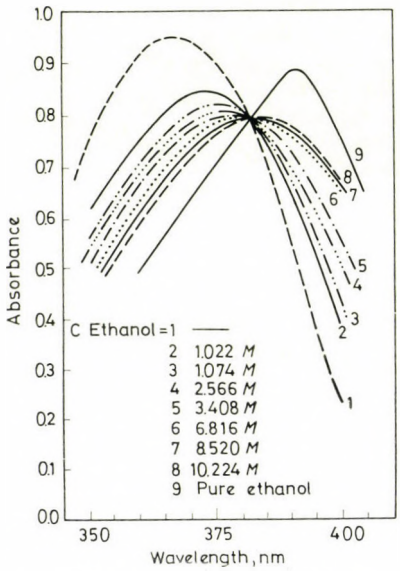

Fig. 2. Spectra of **II**g in ether–ethanol solvent mixtures

The value of K_f can be determined from the variation of absorbance with the ethanol concentration at a given wavelength. The equation used is that given before [13], namely

$$\log C_{ROH} = -\left(\frac{1}{n}\log K_f\right) + \frac{1}{n}\log\left(\frac{A - A_0}{A_l - A}\right)$$

where A_0 = absorbance in the low-polarity solvent,
A_l = limiting absorbance in the presence of excess ethanol,
A = absorbance in the mixed solvent.

The values of K_f, ΔG^*, n and ΔE obtained for some compounds are listed in Table III. The results indicate that the molecular complex is formed through a weak intermolecular hydrogen bond and has the stoichiometric ratio 1 : 1. The value of K_f is dependent on both the solute and the low-polarity solvent used. This is an accordance with previous observations [13].

Table III

Results obtained in mixed organic solvents

Compound	Solvent system	λ, nm	n	log K_f	K_f	ΔG^*, kcal/mole	ΔE, kcal/mole
Id	CCl_4–Ethanol	460	0.70	0.55	3.55	−0.74	3.58
Ig	CCl_4–Ethanol	370	0.62	0.17	1.48	−0.23	3.54
Ih	$CHCl_3$–Ethanol	390	0.66	0.31	2.04	−0.42	2.70
Ic	$CHCl_3$–Ethanol	385	0.70	0.17	1.48	−0.23	2.54
Ic	Ether–Ethanol	380	0.60	0.50	3.16	−0.67	3.70
IIg	Ether–Ethanol	390	0.55	0.45	2.82	−0.61	3.00

(C) *Spectra in buffer solutions*

The spectra of the compounds with OH-group were studied in buffer solutions containing 30% (by volume) ethanol. The addition of ethanol was necessary to increase the solubility of the compounds, permitting the recording of spectra with measurable absorbance, especially at low pH values, where the compounds exist as non-ionic species.

The spectra in buffer solutions, represented in Fig. 3, show the normal behaviour. Solutions of low pH display a band with λ_{max} at shorter wavelengths corresponding to the absorbance of the non-ionic form. With increasing pH, the absorbance of the band decreases, while another band is developed at a longer wavelength. The absorbance of this band is due to absorbtion by the ionic species, and it attains a more or less constant value at high pH. Commonly two isosbestic points are observed, within the pH ranges 2—8 and 8—12. In a few cases the second is not observed, but the spectra at higher pH deviate from the isosbestic point observed in the lower pH range. The absorbance *vs.* pH curves (Fig. 4) are typical dissociation curves with a small inflection on the rising part. This denotes that the two protons are dissociated in a stepwise manner from the solute molecule, leading to two equilibria

$$H_2B \rightleftharpoons H^+ + HB^-$$
$$HB^- \rightleftharpoons H^+ + B^{--}$$

This pH-titration of some compounds revealed that two moles of sodium hydroxide are consumed in the neutralization reaction. Also, the titration curve is characterized by two, but not well defined, inflections. Accordingly, it can be concluded that the two OH-groups are not simultaneously dissociated. The stepwise dissociation of the OH-groups indicate that the ionized part can hinder to some extent the intramolecular charge transfer from the non-ionized OH-group.

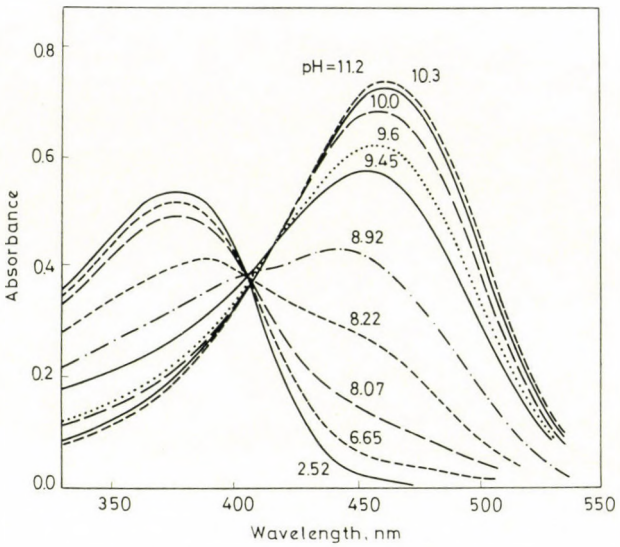

Fig. 3. Spectra of **Ic** in buffer solutions

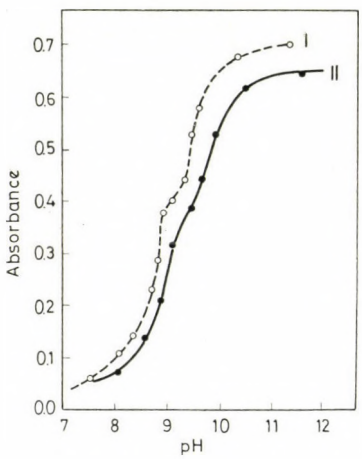

Fig. 4.

The dissociation constants of the compounds were determined applying the methods discussed previously; in the main they were the following:

(1) Half-height method [14].

(2) The limiting absorbance method as modified for stepwise equilibria [14].

(3) The Colleter [15] method modified for acid-base equilibria [14].

The results obtained are shown in Table IV. These values indicate that (*h*) has a higher pK_a than (*c*) due to the presence of the donor OCH_3 in the

Table IV

Results obtained in buffer solutions

Compound	Non-ionic form		Ionic form		pK_1				pK_2			
	λ_{max}	$\varepsilon_{max} \cdot 10^{-4}$	λ_{max}	$\varepsilon_{max} \cdot 10^{-4}$	1	2	3	Meam	1	2	3	Mean
Ic	357	4.28	460	3.66	8.75	8.75	8.65	8.72	9.50	9.50	9.45	9.47
Ih	395	3.58	490	5.45	8.90	8.92	8.85	8.89	9.80	9.97	9.70	9.82
IIc	405	4.02	495	5.26	8.60	8.55	8.52	8.56	9.40	9.35	9.45	9.40
IIg	395	3.09	490	3.19	8.95	8.97	9.00	8.98	9.95	9.95	10.05	9.98
IIh	410	4.13	505	5.44	8.60	8.65	8.70	8.65	9.58	9.66	9.70	9.65
IIi	310	4.23	405	4.73	7.60		7.80	7.70	8.75		8.30	8.27

former. Also (*g*) has a slightly pK_a value than (*c*), indicating a lower participation of the *o*-OH group in the intramolecular charge transfer. The presence of the two acceptor Br atoms in (*i*) lowers pK_a to a measurable extent.

(D) *Infrared absorption spectra*

The infrared spectra of the compounds under investigation were recorded in the 4000—400 cm^{-1} region in KBr pellets. The present discussion is primarily concerned with the bands influenced by the molecular structure, mainly the C=O bands (Table V). The bands corresponding to the OH stretch-

Table V

Solid state[(a)] *infrared spectral data*[(b)] *for series* **I** *and* **II**

Series	(*a*)	(*b*)	(*c*)	(*d*)	(*e*)	(*f*)	(*g*)	(*h*)	(*i*)	Band assignment
	—	—	3300	—	—	—	3450	3400	3420	νOH
	1665	1660	1657	1650	1670	1672	1660	1640	1700	νC=O
I	1612	1600	1600	1605	1610	1615	1605	1600	1610	νC=O
	1585	1575	1580	1580	1580	1580	1570	1580	1590	νC=C skeletal vibr.
	1500	1505	1520	1520	1495	1490	1485	1510	1490	νC=C skeletal vibr.
	1450	1450	1450	1450	—	1440	1450	1450	1460	νC=C skeletal vibr.
	—	—	3320	—	—	—	3300	3400	3440	νOH
	1686	1683	1680	1675	1690	1650	1650	1690	1660	νC=O
	1635	1625	1630	—	1630	1630	—	1620	1610	νC=C
II	1610	1600	1610	1590	1600	1610	1605	1600	1590	νC=C skeletal vibr.
	1500	1510	1520	1520	1480	1490	1490	1520	1480	νC=C skeletal vibr.
	1450	1450	1445	1440	1450	1452	1460	1450	1450	νC=C skeletal vibr.

(a) In KBr pellet
(b) Absorption band frequencies, cm^{-1}

ing frequency of compounds (*c*), (*h*), (*g*) and (*i*) are observed within the range 3300—3450 cm^{-1}. The low values indicates that the OH group is probably involved in an intermolecular hydrogen bonding. This band will shift to lower frequencies on going from $\mathbf{I}_g$ to $\mathbf{I}_i$, $\mathbf{I}_h$ and $\mathbf{I}_c$.

The band due to the stretching vibration of the C=O group appears in the 1700—1640 and 1690—1650 cm^{-1} regions for compounds of the series **I** and **II**, respectively. For one and the same series, the band is shifted to lower frequencies as compared with the parent compound when the aromatic system has an electron donor substituent, and it is shifted to higher frequencies when

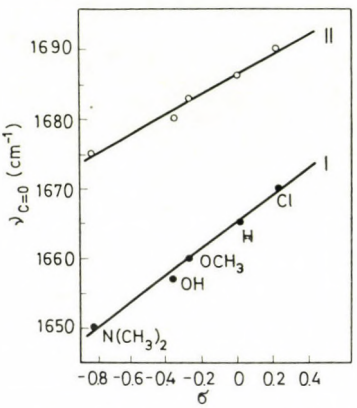

Fig. 5. ν_{C-O} (Hammett) plots

the substituent has electron acceptor character. Obviously, the electron donating groups favour the polarization of the carbonyl group through their enhancement of the charge transfer from the phenyl ring, while electron attracting groups oppose this polarization. The spectra of $\mathbf{I}_i$ and $\mathbf{II}_i$ show this band at 1700 and 1660 cm^{-1}, respectively. The band is thus shifted to a lower frequency compared with $\mathbf{I}_g$ and $\mathbf{II}_g$, *i.e.* the compounds without bromine substituents. This indicates a decreased polarization of the C=O band owing to the influence of the acceptor character of the bromine atoms.

Generally, it can be stated that the position of the carbonyl stretching frequency band is influenced by the charge transfer from the phenyl ring, *i.e.* by the nature of the substituent attached to the aromatic system, especially in the *para* position. The plots of νC=O as a function of σ (Hammett constant), (Fig. 5) show linear relations for each series.

The νC=O band of $\mathbf{II}_a$ is located at a higher frequency than that of $\mathbf{I}_a$. The red shift and the strengthening of the bond is due to the strain in the five-membered ring. It seems to be part of a general phenomenon which appears to have its basis in the *sp* hybridization ratio changes of the carbon σ valence orbitals, with the result that all bonds directly attached to a strained ring become stronger, whereas the bonds of the ring itself become weaker [16].

REFERENCES

[1] SAMDAHL, R.: J. Pharm. Chem., **7,** 162 (1929); **8,** 8 (1930)
[2] SAMDAHL, R., HAUSEN, B.: J. Pharm. Chem., **19,** 573 (1934)
[3] EUCKER, H.: Arch. Exptl. path. Pharmakol., **198,** 140 (1941)
[4] FRENCH, H. S., HOLDEN, M. G. T.: J. Am. Chem. Soc., **67,** 1239 (1945)
[5] HUITRIC, A. C., KUMLER, W. D.: J. Am. Chem. Soc., **78,** 614 (1956)
[6] RASANI, B. K., SUGDEN, J. K.: Chem. Ind. (London) **21,** 685 (1970)
[7] FARRELL, P. G.: Canad. J. Chem., **46,** 3684 (1968)
[8] MACCIONI, A., MARONGU, E.: Ann. Chim. (Rome), **49,** 1283 (1959)
[9] VOGEL, A. I.: "Practical Organic Chemistry", 4th Ed., p. 163, Longmans, London 1964
[10] BRITTON, H. T. S.: "Hydrogen Ions". 2nd Ed., p. 365 Chapman and Hall, London 1952
[11] CROMWELL and JOHNSON: J. Am. Chem. Soc., **65,** 316 (1943)
[12] GATI, L., SZALAY, L.: Acta Phys. Chem., **5,** 87 (1959)
[13] ISSA, I. M., ISSA, R. M., IDRIS, K. A., HAMMAM, A. M.: Egypt. J. Chem. (Special issue) 67 (1973)
[14] ISSA, R. M.: Z. Physik. Chem. N. F., **74,** 17 (1971); Egypt. J. Chem., **14,** 113 (1971)
[15] COLLETER, C. R.: Ann. Chim. (Paris), **5,** 415 (1960)
[16] COULSON, M., MOFFITT, F.: Phil. Mag. **40,** 1 (1949)

R. M. ISSA, S. H. ETAIW — Chemistry Department, Faculty of Science, Tanta University, Tanta, Egypt.

I. M. ISSA, A. K. EL-SHAFIE — Chemistry Department, Faculty of Science, Assiut University, A. R. Egypt.

Acta Chimica Academiae Scientiarum Hungaricae, Tomus 89 (4), pp. 393—404 (1976)

INVESTIGATION OF THE CHEMISTRY OF DIOLS AND CYCLIC ETHERS, XXXIX

MECHANISM OF DEHYDRATION OF DIOLS OVER COPPER CATALYSTS

Á. MOLNÁR and M. BARTÓK

(Department of Organic Chemistry, József A. University, Szeged)

Received April 17, 1975

Transformations of three deuterium-labelled diols, viz. 1,3-butanediol-[3-^{2}H] (**I**), 1,4-pentanediol-[4-^{2}H] (**II**) and 3-methyl-2,4-pentanediol-[O,O'-$^2H_2$] (**III**) have been studied over Cu/Al and Cu catalysts, at 200 and 205 °C in order to obtain a deeper insight into the mechanism of processes revealed earlier. The mechanism of the main processes represented by these three diols (dehydration into oxo compounds and oxacycloalkanes containing the same number of carbon atoms as the original diols, as well as fragmentation) have been elucidated and the importance of metal-catalyzed hydrogen transfer processes is demonstrated.

Introduction

Transformations of diols over metal catalysts have been reported in some of our earlier papers [1—3]. Raney copper (hereafter Cu/Al) induces the following reactions in various types of diols:

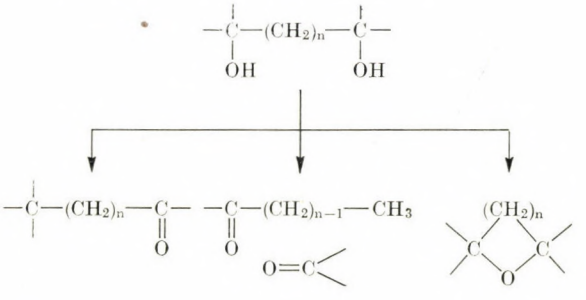

(1)

No reaction occurs when $n = 0$; if $n = 1$, oxo compounds as well as fragments are formed, whereas in the case of $n = 2$ or 3, dehydration into cyclic ethers can be observed.

The following suggestions can be put forward with respect to the mechanisms of the above transformations, considering literature data as well as other evidences.

Transformation into oxo compounds can be visualized as shown in Scheme (2) describing the reaction of 1,3-butanediol as an example. A direct transformation of diols can be assumed *via* hydrogen migration in a six-membered, cyclic transition state, with the participation of both hydroxyl groups:

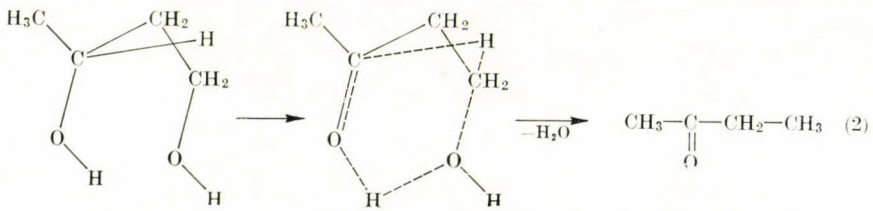

(2)

The formation of oxo compounds can, in principle, be interpreted in terms of further reactions of various primary products from diols:

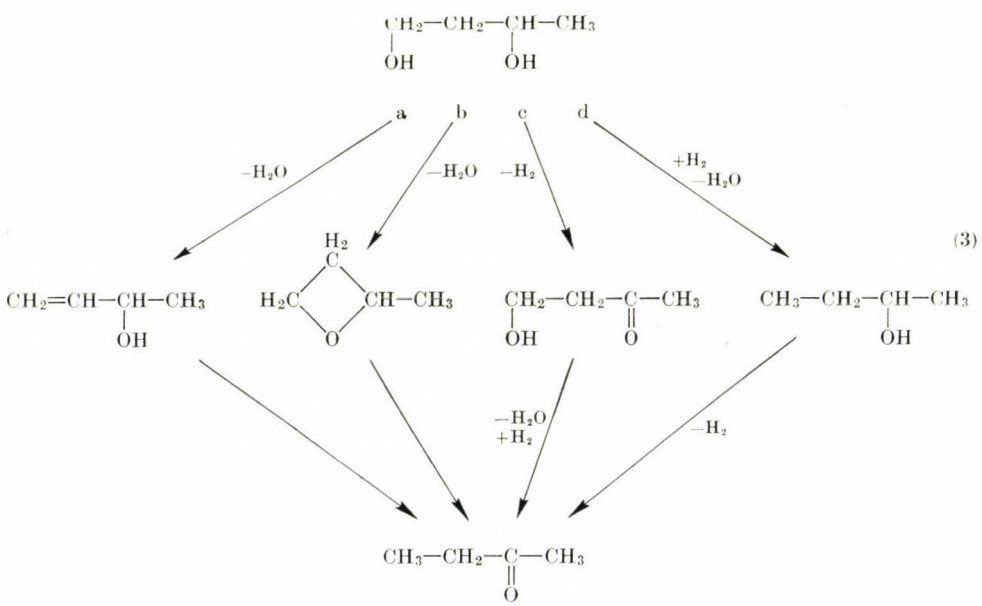

(3)

The following three possibilities can be presumed for diol fragmentation:

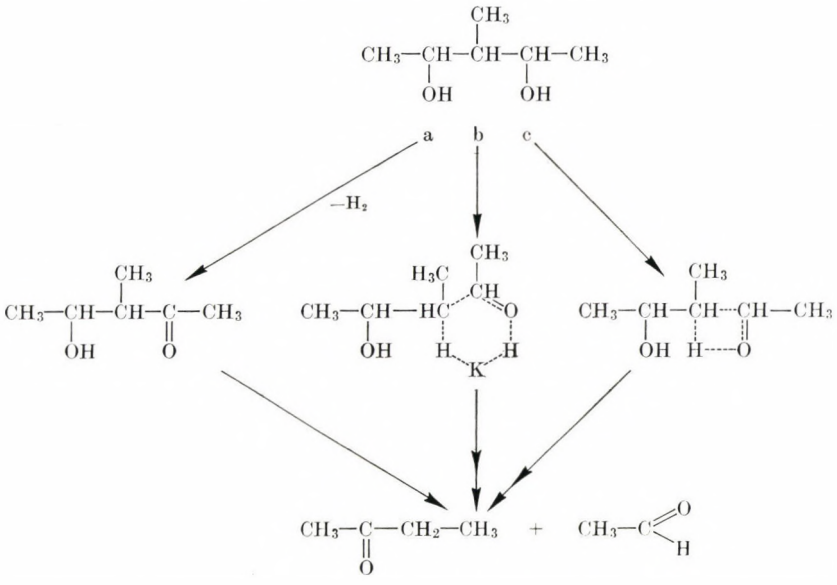

(4)

The formation of cyclic ethers may occur *via* a four-membered cyclic intermediate involving the two hydroxyl groups:

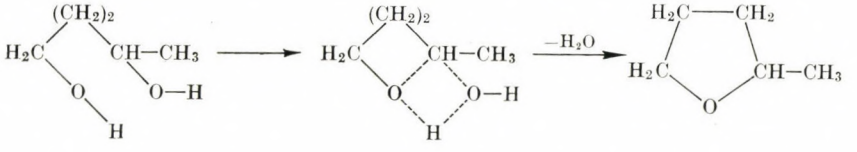

(5)

At the same time, another transition state is also conceivable, based on the concepts of BALANDIN *et al.* [4]:

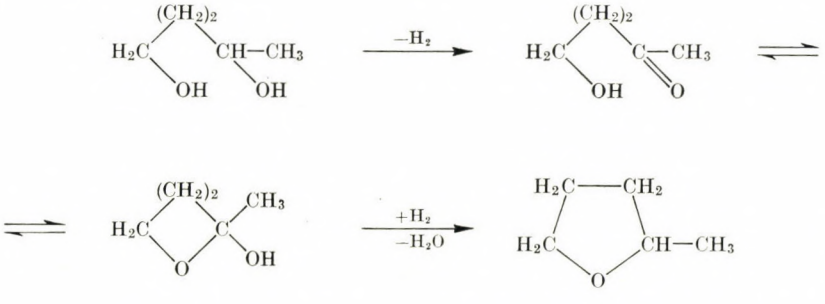

(6)

The actual probabilities of the various mechanisms will be discussed later.

In the present work, we report on a study of the mechanism of the above three processes by means of deuterated starting substances. The model com-

pounds were selected so as to ensure the predominance of one of the possible processes in each case. Thus, the characteristic reaction of 1,3-butanediol-[3-^{2}H] is transformation into an oxo compound, that of 1,4-pentanediol-[4-^{2}H] is production of a cyclic ether, whereas 3-methyl-2,4-pentanediol-[O,O'-$^2H_2$] gives mainly fragments. The interpretation of the mechanisms will be done considering our previous results, too.

Experimental

Syntheses of model compounds

1,3-*butanediol*-[3-^{2}H] (**I**) was synthesized by reacting 1-hydroxybutanone-3 with $LiAlD_4$. The product contained 90% of **I**, as shown by mass spectrometry.

1,4-*pentanediol*-[4-^{2}H] (**II**) was prepared by reducing 1-hydroxy-4-pentanone with $LiAlD_4$. The product contained 90% of **II**(determined mass spectrometrically).

3-*methyl*-2,4-*pentanediol*-[O,O'-$^2H_2$] (**III**) was prepared by means of deuterium exchange between 3-methyl-2,4-pentanediol and D_2O according to Ref. [5]. The product was analyzed by IR spectroscopy and contained 85% of **III**.

Ethanol-[O-^{2}H] was obtained from sodium ethylate and D_2O according to Ref. [6].

Methanol-[$^2H_4$] was a commercial product (BDH).

Catalysts

The Cu/Al *catalyst* was obtained according to Ref. [7], with the following modification. The fraction of a 1 : 1 Cu + Al alloy between grain sizes of 0.63 and 1 mm was treated with 25% KOH for 24 hrs (ice-cooled initially), then washed free of alkali. Bulk density after drying: 1.8 g cm^{-3}.

Cu *catalyst*. The 0.63—1 mm fraction of CuO obtained from "Merck" CuO powder by pressing, grinding and screening, was reduced by heating in a hydrogen stream of 60 ml min^{-1} up to 190 °C during 1 hr. The sample was kept at this temperature for 2 hrs, then at 200 °C for further two hours. This was followed by heating up to 250 °C (heating period 1 hr) and reduction for 2 hrs; the same procedure was repeated with 290 °C as the final temperature. The catalyst was stored in hydrogen after reducing and activated for 2 hrs before use in a hydrogen stream of 60 ml min^{-1}, at the temperature of the experiment. Bulk density: 2.2 g cm^{-3}.

Procedure

Experiments were carried out in a glass reactor tube at 200 and 205 °C. 12.5 cm^3 of the Cu/Al or 7.5 cm^3 of the Cu catalyst was placed into the reactor tube under a glass bead layer serving for evaporation. The temperature was controlled by a temperature regulator and measured by a thermocouple placed into a 3 mm I.D. pocket in the center of the reactor. The sensor was placed in at half height of the catalyst layer.

Diols were introduced into the reactor by a glass syringe driven by an electric clockwork. A feed rate of 2 cm^3 hr^{-1} of liquid was maintained for the Cu/Al catalyst, whereas this value was 1.2 cm^3 hr^{-1} for the Cu catalyst; these values gave identical space velocities in both cases (0.16 hr^{-1}). Since, apart from hydrogen, no gaseous products formed, evaluation, identification and calculation of the composition were carried out on the basis of the liquid products.

Investigation of deuterium exchange was carried out under conditions identical with those applied for diol reactions (200 °C, 2 ml hr^{-1} for Cu/Al and 205 °C, 1.2 ml hr^{-1} for Cu with both ethanol-[0-^{2}H] and methanol-[$^2H_4$] as starting materials). Reactions and sampling were carried out with the exclusion of air humidity.

The isotopic purity of starting materials was checked by mass spectrometry and IR spectroscopy; the deuterium content and distribution of products were measured by mass spectrometry. A FINNIGAN 1015 S/L GC + MS device served for the latter purpose.

In one case, an NMR spectrum was recorded on a JEOL C 60 HL spectrometer in order to determine the position of deuterium in deutero-2-methyltetrahydrofuran.

Products of catalytic reactions were identified by gas chromatography, using reference substances. The conditions of chromatography were as follows. Column: 2 m packed with 0.2—0.3 mm Merck Kieselguhr coated with 15% diphenylformamide; carrier gas: hydrogen, 40 cm^3 min^{-1}; temperature: 65 °C; detector current: 180 mA; apparatus Carlo Erba FRACTOVAP Model P. (For Fig. 5: stationary phase CARBOWAX 1500, flow rate 60 cm^3 min^{-1}, $t = 80$ °C).

Results

First, the activity of the catalyst in deuterium exchange was checked. Ethanol-[O-^{2}H] was used to study exchange in the O–D group and methanol-[$^2H_4$] exchange in the C–D group.

On the Cu/Al catalyst, ethanol-[O-^{2}H] transformed almost completely into "light" ethanol; at the same time the C–D bonds of methanol-[$^2H_4$] showed no reaction; consequently, deuterium in the hydroxyl group is exchanged rapidly over this catalyst, whereas that bonded to of carbon atom is not reactive. This is obviously due to the fact that part of the aluminium is transformed into Al_2O_3 during dissolution of the alloy and remains in the catalyst; this component brings about deuterium exchange. Consequently, this catalyst is not suitable for the study of 3-methyl-2,4-pentanediol-[O,O'-$^2H_2$] (*i.e.* the model substance for fragmentation); this was the reason why we prepared the other Cu catalyst causing no deuterium exchange in either the C–D or O–D bonds.

In order to determine the extent of deuterium exchange between the oxo compounds formed and the alcoholic hydroxyl group, 1 : 1 mixture of methyl ethyl ketone and ethanol-[O-^{2}H] was introduced onto the Cu catalyst and the deuterium content of methyl ethyl ketone determined. The latter value was about 10% and the deuterium contents of both alkyl groups were nearly equal. Since the effects observed during in the reactions were considerably larger than the extent of exchange, the latter was assumed not to influence significantly the correctness of the conclusions.

The two catalyst types were compared by determining the temperature dependence of the transformation of 1,3-butanediol on them. Figures 1 and 2 show at lower temperatures both catalysts are very similar, giving practically identical products in nearly identical amounts, presumably formed via identical mechanisms. Figure 3 shows the chromatograms of the products from 3-methyl-2,4-pentanediol formed on both catalysts. The conclusion may be similar to that drawn before, but fragmentation is even more selective on Cu. At the same time, no cyclic ether is formed on the Cu catalyst, instead, a lacton is produced; therefore, this compound could be investigated with respect to cyclic ether formation on the Cu/Al catalyst (Fig. 4).

The dehydrogenation of primary and secondary alcohols shows about the same yield over both catalysts at 200 °C; *e.g.* *n*-propanol gave about 10—15% of propionaldehyde and *i*-propanol about 50—60% of acetone. No dehydration could be observed on the Cu catalyst up to 290 °C in contrast

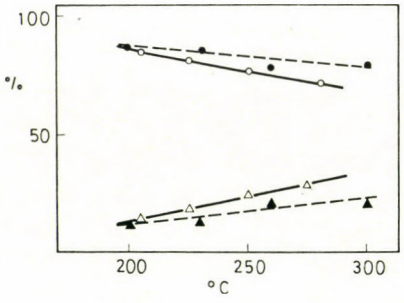

Fig. 1. Transformation of 1,3-butanediol as a function of the temperature, over Cu and Cu/Al catalysts (100% conversion in every case). – – – – transformation over Cu/Al catalyst, ——— transformation over Cu catalyst; ○● products with the same carbon number as the diol; △▲ fragmentation products

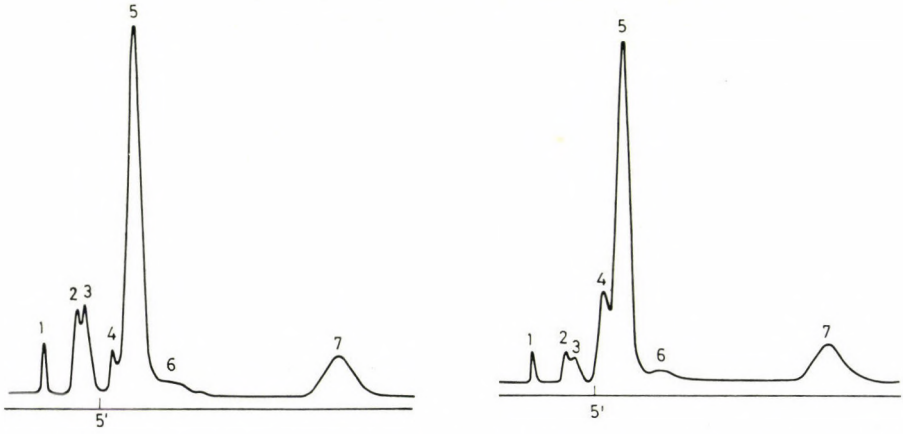

Fig. 2. Chromatogram of products obtained in the transformation of 1,3-butanediol; *a:* Cu/Al, 200 °C; *b:* Cu, 205 °C. *1* acetaldehyde; *2* acetone, *3* ethanol, *4* butyraldehyde, *5* methyl ethyl ketone, *6* 2-butanol, *7* 1-butanol

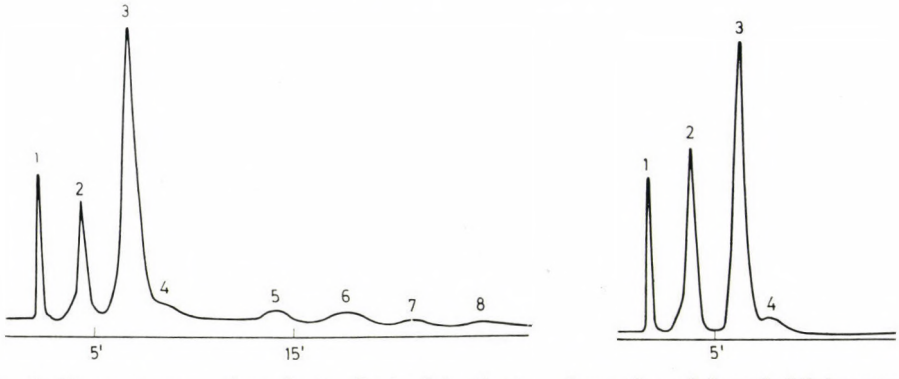

Fig. 3. Chromatogram of products obtained in the transformation of 3-methyl-2,4-pentanediol; *a:* Cu/Al, 200 °C; *b:* Cu, 205 °C. *1* acetaldehyde, *2* ethanol, *3* methyl ethyl ketone, *4* 2-butanol, *5*, *6*, *7*, *8* unidentified products

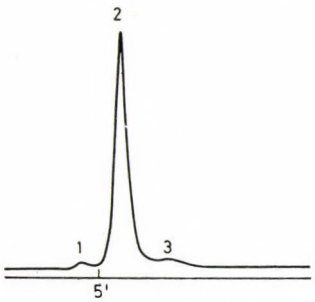

Fig. 4. Chromatogram of products obtained in the transformation of 1,4-pentanediol over a Cu/Al catalyst, at 200 °C. *2* 2-methyltetrahydrofuran, *1* and *3* unidentified products

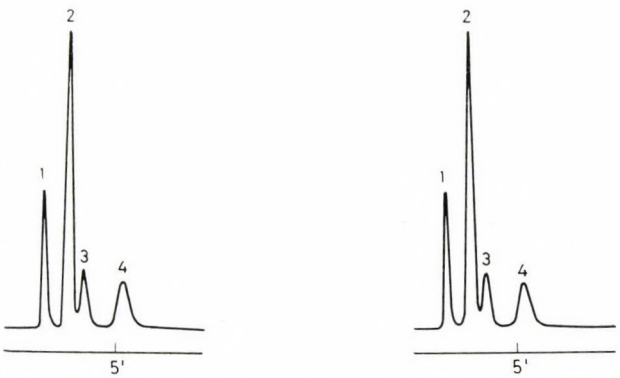

Fig. 5. Chromatogram of products formed in the reaction of a 1 : 1 mixture of methyl vinyl ketone and 1-propanol. *a:* Cu/Al, 200 °C; *b:* Cu, 205 °C. *1* propionaldehyd, *2* methyl ethyl ketone, *3* methyl vinyl ketone, *4* 1-propanol

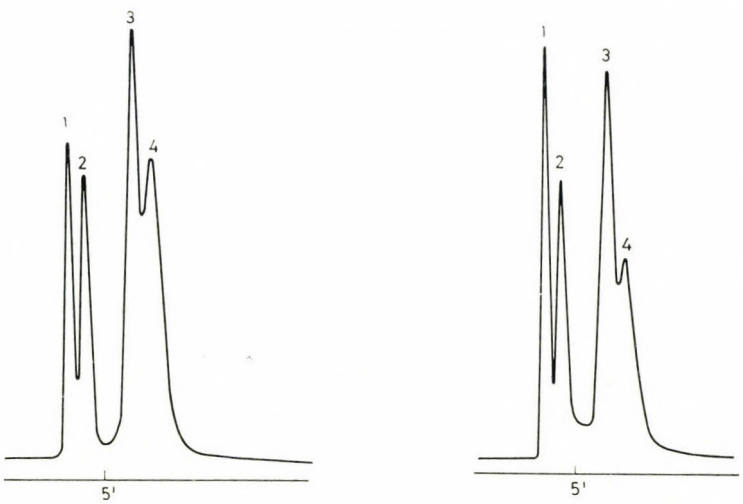

Fig. 6. Chromatogram of products formed in the reaction of methyl vinyl ketone and 2-propanol (1 : 1 mixture). *a:* Cu/Al, 200 °C; *b:* Cu, 205 °C. *1* acetone, *2* 2-propanol, *3* methyl ethyl ketone, *4* methyl vinyl ketone

with the results of TÉTÉNYI *et al.* [8] who have found dehydration of secondary alcohols over a Cu sample prepared similarly, *i.e.* by reduction of CuO.

The catalysts were observed to behave similarly in hydrogen transfer processes, too: different catalysts gave identical amounts of methyl ethyl ketone from methyl vinyl ketone in the presence of 1-propanol and 2-propanol (Figs. 5 and 6).

The results concerning deuterium-labelled compounds are summarized in Table I.

Discussion

On the basis of our previous [1, 2, 3] and present results, the following conclusions can be drawn with respect to the alternative mechanisms described in the Introduction.

Mechanism of oxocompound formation

With reference to Scheme (3), isomerization of the unsaturated alcohol (a) and dehydrogenation of the saturated alcohol (d) are rapid but the formation of these compounds is very slow, because the elimination of the primary hydroxyl group and its hydrogenolysis are both very slow. Thus, the highest overall probability can be attributed to process *b*, *i.e.* 1,3-rearrangement *via* a cyclic ether or a cyclic-ether-like transition state, as well as to reaction *c*, provided that the hydroxyoxo compound formed is consumed in a reaction whose activation energy is lower than that of the hydrogenolysis of the hydroxyl group, which is a slow process.

Both catalysts produced unlabelled methyl ethyl ketone but almost completely deuterated butyraldehyde; thus it can be concluded that process *c* is actually more likely to take place than process *b*. Had the reaction involved a cyclic ether as an intermediate, both compounds should have been labelled, since they would have formed *via* intramolecular deuterium transfer from the cyclic ether.

Consequently, the first step of the process is dehydrogenation, producing an unstable β-hydroxyoxo compound, which undergoes thermal decomposition, giving an unsaturated oxo compound by water elimination. This, in turn, gives an aldehyde or ketone in hydrogen transfer processes with the participation of the unreacted diol:

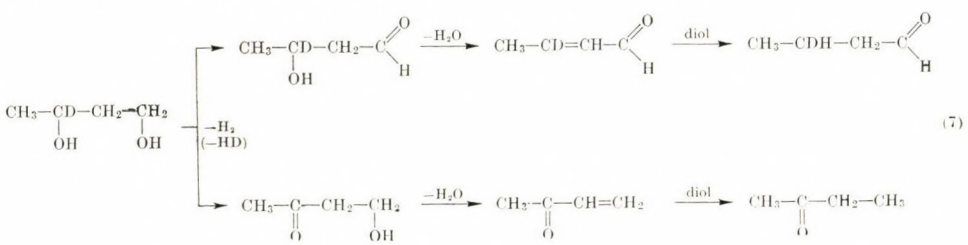

(7)

Table I

Labelled compounds produced during transformations of deuterated diols and their ratio to the corresponding unlabelled compounds

	Cu/Al catalyst	Cu catalyst
$CH_2CH_2-CD-CH_3$ OH OH	$CH_3-CHD-CH_2-C(=O)H$ 90 $CH_3CH_2-CH_2-C(=O(*))H$ 10	$CH_3-CHD-CH_2-C(=O)H$ 90 $CH_3-CH_2-CH_2-C(=O(*))H$ 10
$CH_3-CH(CH_3)CH(OD)-CH_3$ OD	no experiments due to rapid H—D exchange	$CH_3-C(=O)-CHD-CH_3$ 50 $CH_3-C(=O)-CH_2CH_3$ 50 $CH_3-CHD-OH(D)$ 30 $CH_3-CH_2-OH(D)$ 70
$CH_2CH_2CH_2CD-CH_3$ OH OH	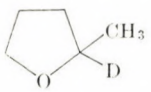 50 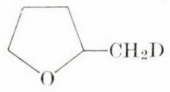 20 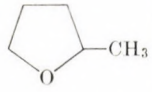 30	lacton formation

* No labelled methyl ethyl ketone produced

The primary step of the sequence — *i.e.* diol dehydrogenation — is initially a purely catalytic reaction, but, as it can be concluded from the facts mentioned, during further stages also unsaturated oxo compounds acquire some role, and saturated oxocompounds can be transformed into alcohols *via* hydrogen transfer. With respect to the last step, it is well known from the literature that α,β-unsaturated aldehydes can be converted into saturated aldehydes in the presence of alcohols over copper catalysts [9]. The mechanism of the process has been confirmed recently by an isotope technique in connection with the isomerization of unsaturated alcohols [10].

Other pieces of evidences in support of the above mechanism are as follows:

(i) the catalytic conversion of an equimolar mixture of methyl vinyl ketone and 1,3-butanediol gives 100% methyl ethyl ketone;

(ii) methyl vinyl ketone gives methyl ethyl ketone in the presence of both primary and secondary alcohols with simultaneous dehydrogenation of the alcohol;

(iii) when 1,3-butanediol is reacted at high space velocities, 1-hydroxy--3-butanone as well as methyl vinyl ketone are found among the products [2];

(iv) the ratio of the two oxo compounds formed is in good agreement with different reactivities of the two diol hydroxyl groups in the first step, *i.e.* dehydrogenation;

(v) this mechanism offers an explanation for the phenomenon that very low conversions can be observed for transformations of 1,2-diols — except for pinacoline — over metal catalysts [1]. Dehydrogenation of these diols gives α-hydroxyoxo compounds, the water elimination of which is much slower than that of the β-hydroxyoxo compounds produced from 1,3-diols.

The copper catalysts studied participate in the first and third step of the dehydration of diols into oxo compounds, *i.e.* in the dehydrogenation and hydrogen transfer processes, whereas, the dehydration step itself occurs — according to our opinion — without participation of the copper catalyst.

Mechanism of fragmentation

Of the mechanisms put forward in Scheme (4), process *a*, *i.e.* dealdolization of the β-hydroxyoxo intermediate can be regarded as the most likely explanation for fragmentation on the basis of our experiments. Process *b* has a low probability over copper since at temperatures similar to those in our experiments, no chemisorbed hydrogen should be present on copper [11].

The product composition observed is against mechanisms *b* and *c*. These latter processes should lead to 2-butanol and acetaldehyde; at the same time, nearly equal amounts of acetaldehyde and ethanol have been found, with only

traces of 2-butanol. Under the conditions applied, 2-butanol is dehydrogenated into methyl ethyl ketone with a conversion of about 50—60%, therefore, the ketone obviously cannot be formed via this route, neither can the presence of ethanol be explained by these mechanisms. Dealdolization cannot be responsible for ethanol formation either, indicating that even if the process involves a β-hydroxyoxo compound as an intermediate, the products must participate in secondary processes.

Based on experiments with 3-methyl-2,4-pentanediol-[O,O']-$^2H_2$], as well as on other observations, the following pathway can be suggested for fragmentation:

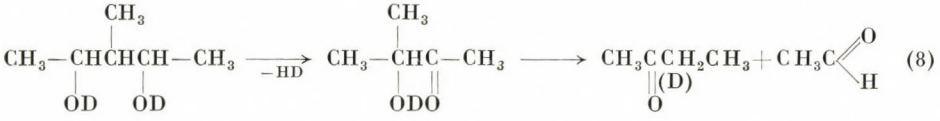

(8)

The first step is dehydrogenation into a β-hydroxyoxo compound, similarly to the transformation leading to the oxo compound. The subsequent reaction of this compound is the reverse process of aldolization (dealdolization), giving two oxo compounds. The detailed mechanism of this process still remains unknown, therefore, it is not clear how deuterium enters into the methyl ethyl ketone molecule. It is unlikely that deuterium in the hydroxyoxo compound could jump over to the neighbouring carbon atom, simultaneously with C–C bond fission. It would be more likely that H and D atoms produced on the catalyst surface during dehydrogenation participate in the process or, eventually, deuterium transfer from another diol molecule takes place.

The two oxo compounds produced may react with the diol in hydrogen transfer processes giving the corresponding alcohol.

Thus, it has been proved that the primary step of both the transformation into on oxo compound and the fragmentation involve the formation of a β-hydroxyoxo intermediate. The subsequent reaction is determined by the structure and reactivity of this intermediate. In cases when water elimination from the hydroxyoxo compound is hindered by the presence of substituents (in all probability, it is a thermal *cis*-elimination), the process manifests itself as dealdolization leading to two oxo compounds.

Mechanism of formation of cyclic ethers

Experiments have shown that the product formed from 1,4-pentanediol-[4-^{2}H] over the Cu/Al catalyst contains both deuterated and unlabelled 2-methyltetrahydrofuran; on this basis, one could conclude that both mechanisms suggested are actually involved in the cyclization into cyclic ethers (process (5) gives a deuterated, whereas process (6) an unlabelled product).

The fact, however, that 1-pentanol-4-one does not give a cyclic ether either with a primary or a secondary alcohol as hydrogen donor, contradicts this hypothesis and indicates that mechanism (6) is not likely. The lower deuterium content can be explained in terms of deuterium exchange of the product, supported also by the formation of two types of labelled ethers: in addition to 50% of 2-methyltetrahydrofuran-[2-^{2}H], 20% of methyl-deuterated cyclic ether has also been produced. At the same time, the elimination of deuterium in the following process observed with other diols is also possible, leading to unlabelled diol in the carbon chain:

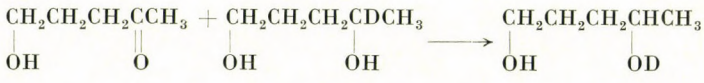

(9)

*

The authors wish to express their gratitude to Dr. István Szilágyi for kindly performing and evaluating the mass spectrometric measurements.

REFERENCES

[1] Bartók, M., Molnár, Á., Noteisz, F.: Acta Phys. et Chem. Szeged, **18,** 207 (1972)
[2] Bartók, M., Molnár, Á.: Acta Chim. (Budapest) **76,** 409 (1973)
[3] Bartók, M., Molnár, Á.: Acta Chim. (Budapest) **78,** 305 (1973)
[4] Balandin, A. A., Karpeiskaya, E. I., Tolstopyatova, A. A.: Dokl. Akad. Nauk. SSSR, **122,** 227 (1958)
[5] Iogansen, A. V., Rozenberg, M. Sh.: Zh. Prikl. Spektr., **9,** 1027 (1968)
[6] Jákli, Gy., Jancsó, G., Illy, J.: KFKI Közl., **13,** 235 (1965)
[7] Bartók, M., Kozma, B.: Acta Phys. et Chem. Szeged, **9,** 116 (1963)
[8] Tétényi, P., Schächter, K.: Acta Chim. Acad. Sci. Hung., **56,** 141 (1968)
[9] Satake, K., Akabori, S.: J. Chem. Soc. Japan, **70,** 84 (1949)
[10] Eadon, G., Shiekh, M. Y.: J. Amer. Chem. Soc., **96,** 2288 (1974)
[11] Babkova, P. B., Avetisov, A. K., Lyubarskii, G. D., Gelbstein, A. I.: Kinet. Katal., **11,** 1451 (1970)

Árpád Molnár
Mihály Bartók } H-6720 Szeged, Dóm tér 8.

Acta Chimica Academiae Scientiarum Hungaricae, Tomus 89 (4), pp. 405—410 (1976)

O-α-L-RHAMNOPYRANOSYL-(1 → 4)-O-α-L-RHAMNOPYRANOSYL-(1 → 6)-D-GALACTOPYRANOSE NONAACETATE

SYNTHESIS OF THE CARBOHYDRATE COMPONENT OF RHAMNAZIN-3-O-TRIOSIDE

H. WAGNER, A. LIPTÁK,* and P. NÁNÁSI*

(Institute of Pharmacy of the University Munich, G. F. R. and Institute of Biochemistry of the University Debrecen)*

Received September 1, 1975

A robinobiose derivate (**3**) was synthesized by way of condensation of 1,2,3,4-di-O-isopropylidene-α-D-galactopyranose (**1**) with 2,3,4-tri-O-acetyl-α-L-rhamnopyranosyl bromide (**2**) in benzene : nitromethane (1 : 1) solution, in the presence of $Hg(CN)_2$. The disaccharide was characterized as the crystalline robinobiose heptaacetate (**5**). The product (**3**) of the first condensation was deacetylated by ZEMPLÉN's method allowed to react with acetone to give **6**. The second condensation of **6** with **2** resulted in the protected trisaccharide derivate (**7**). The title compound (**8**) was obtained *via* deacetylation and hydrolysis of **7** followed by acetylation.

From the fruit of *Rhamnus petiolaris* (Bois) WAGNER *et al.* [1] isolated two flavone glycosides. One of these glycosides is a rhamnazin-3-O-trioside which — on the basis of chemical and spectroscopic evidence — proved to be rhamnazin-3-O-[α-L-rhamnopyranosyl-(1 → 4)-α-L-rhamnopyranosyl-(1 → → 6)]-β-D-galactopyranoside. The trisaccharide was called rhamninose. Glycosides of this trisaccharide were also found in the fruit of *Rhamnus tinctoria* and *Rhamnus infectorius* L. (xanthorhamnine) [2] and *Rhamnus catharticus* L. (catharticine) [3]. The structures of xanthorhamnine and catharticine were studied by SCHMIDT *et al.* [4], and on the basis of mass spectrometric investigations they postulated two alternative structures for rhamninose, namely, O-α-L-rhamnopyranosyl-(1 → 4)-O-α-L-rhamnopyranosyl-(1 → 6)-D-galactose or O-α-L-rhamnopyranosyl-(1 → 5)-O-α-L-rhamnofuranosyl-(1 → 6)-D-galactose. The isolation of robinobiose (O-α-L-rhamnopyranosyl-(1 → 6)-D-galactose) as a partial hydrolysis product of the rhamnazion-3-O-trioside seemed to make sure that rhamninose is O-α-L-rhamnopyranosyl-(1 → 4)-O-α-L-rhamnopyranosyl-(1 → 6)-D-galactose.

The subject of our recent work was the proof of the structure of this trisaccharide by synthesis. For that purpose it was necessary to prepare a suitable protected derivate of robinobiose as the starting material of the synthesis.

The first synthesis of robinobiose, reported by ZEMPLÉN *et al.* [5], did not provide a suitable starting compound for the synthesis of the trisaccharide, as it seemed impossible to obtain a product with selective protection containing free hydroxyl group only at the C_4 position of the rhamnose moiety.

Thus the choice fell on 1,2;3,4-di-O-isopropylidene-α-D-galactopyranose (**1**) [6] which was made to react with acetobromorhamnose (**2**) [7] in a mixture of benzene and nitromethane (1 : 1), in the presence of $Hg(CN)_2$ catalyst. Traces of the starting materials and the decomposition products of **2** were removed by short-column chromatography [8] and the disaccharide (**3**) was obtained in a yield of 76%.

The IR and NMR spectra of **3** unequivocally support the expected structure; the C_1-proton of the galactose moiety appears with a chemical shift of $\delta = 5.52$ ppm and with a coupling constant of $J = 5$ Hz, indicating its *quasi-equatorial* position (in $^4C_1$ (D) conformation) in the tricyclic ring system. At the same time, according to the data of the chemical shift ($\delta = 4.56$ ppm) and the coupling constant ($J = 1.5$ Hz) of the C_1 proton of the rhamnose moiety, the position of this proton must also be *equatorial* in the $_4C^1$ (L) conformation. A similar synthesis of **3**, under diverse reaction conditions, was previously reported by Japanese authors [9] in 38% yield, but the compound was not fully characterized.

By saponification of **3** using ZEMPLÉN's method, **4** was obtained, which contained free hydroxyl groups only in the rhamnose moiety, all the hydroxyl groups of the galactose moiety being protected. The structure of **4** was also supported by its IR spectrum. On the hydrolysis of **4** with 50% acetic acid free robinobiose was obtained, which was acetylated without isolation by means of acetic anhydride in pyridine to yield the know robinobiose heptaacetate (**5**).

The reaction of **4** with abs. acetone in the presence of sulphuric acid gave 1,2;3,4;2',3'-tri-O-isopropylidenerobinobiose (**6**). The analysis of the gas chromatogram [11] of the alditol acetate mixture — obtained by methylation of **6** using KUHN's method [10], followed by acid hydrolysis, reduction with $NaBH_4$ and subsequent acetylation — showed only the presence of 4-O-methylrhamnitol besides galactitol. Deacetylation of **5** followed by treatment with acetone — sulphuric acid gave also **6**. The reaction of **6** with **2** in a mixture of benzene–nitromethane (1 : 1) in the presence of $Hg(CN)_2$ catalyst resulted in **7** in a yield of 62%. The crude **7** was purified by short-column chromatography to obtain the pure product as a white amorphous powder.

In the case of **7** the anomeric configuration of the interglycosidic bond between the two rhamnose moieties was questionable. Calculations based on the optical activity made the α-L-configuration probable, which structure was then unequivocally supported by the NMR spectrum of **7**. The signals of the three anomeric protons appeared with the following chemical shifts and coupling constants: $\delta = 5.58$ ppm ($J = 5$ Hz); $\delta = 5.01$ ppm ($J = 1.5$ Hz) and $\delta = 4.63$ ppm ($J = 1.5$ Hz).

Compound **7** was deacetylated by ZEMPLÉN's method and the isopropylidene groups were hydrolyzed with 50% acetic acid. The free trisaccharide

obtained after evaporation of the hydrolyzate was acetylated with pyridine–acetic anhydride mixture to give the nonaacetate (**8**), which was isolated in crystalline form from 70% aqueous ethanol.

Experimental

M. p.'s were determined on a Kofler hot-stage apparatus and are uncorrected. Optical rotations were measured with a Polamat (Zeiss) automatic photoelectric polarimeter. NMR spectra were recorded on a Jeol MH-100 (100 MHz) instrument using TMS as internal standard. IR spectra were obtained with a Perkin—Elmer instrument, Model 700, in KBr discs.

1,2;3,4-Di-O-isopropylidene-6-O-(2,3,4-tri-O-acetyl-α-L-rhamnopyranosyl)-α-D-galactopyranose (3)

1,2;3,4-Di-O-isopropylidene-α-D-galactopyranose (5.20 g; 0.02 moles) (**1**) [6]and $Hg(CN)_2$ (5.10 g; 0.022 moles) were dissolved in a mixture of abs. benzene (70 ml) and nitromethane (70 ml) and the solution was concentrated at atmospheric pressure to about 60 ml. After cooling to 45 °C, 7.13 g (0.022 moles) of α-acetobromo-L-rhamnose (**2**) [7] was added, and the mixture was stirred in the absence of moisture. After 2 hrs TLC indicated the disappearance of the starting compounds. The mercury salts which precipitated were filtered off and the filtrate evaporated in vacuum. The residue was dissolved in chloroform (250 ml), filtered again and successively washed with 5% KI solution (5 × 20 ml) and water (3 × 100 ml). The neutral solution was dried over Na_2SO_4 and evaporated to dryness. The syrupy residue was purified by short-column chromatography on Kieselgel G (350 g) with 9 : 1 benzene–methanol as the eluant, to give a syrupy product which solidified to an amorphous mass after standing a few days (8.16 g; 76.6%). $[\alpha]_D$ −93.2° (c = 0.81, chloroform). R_f 0.60 (benzene–methanol, 9 : 1).

NMR (in $CDCl_3$): δ = 5.52 ppm (d, 1 H, C_1-H, J = 5 Hz); 5.35—3.50 (m, 10 H, skeleton protons); 4.56 (d, 1 H, C_1-H, J = 1.5 Hz); 2.15, 2.08, 1.99 (ss, 9 H, 3 Ac); 1.58—1.14 (m, 15 H, 2 $C(CH_3)_2$ and 1 CH_3).

$C_{24}H_{36}O_{13}$ (532.5). Calcd. C 54.12; H 6.81. Found C 55.10; H 7.02%.

1,2;3,4-Di-O-isopropylidene-6-O(α-L-rhamnopyranosyl)-α-D-galactopyranose (4)

A solution of **3** (0.50 g) in abs. methanol (20 ml) was deacetylated with 0.5 ml of 0.1 M $NaOCH_3$. After standing for 24 hrs at room temperature, the reaction mixture was neutralized with Dowex 50 (H^+) ion exchange resin, filtered and evaporated to give 0.32 g (84.2%) of syrupy **4**, which solidified to a pulverizable amorphous glassy product, $[\alpha]_D$ −70.5° (c = 1.39, pyridine). R_f 0.08 (benzene–methanol, 9 : 1).

$C_{18}H_{30}O_{10}$ (406.4). Calcd. C 53.19; H 7.44. Found C 53.90; H 7.60%.

Robinobiose heptaacetate (5)

Compound **4** (0.50 g) was dissolved in 50% aqueous acetic acid (25 ml) and heated at 85 °C (bath temperature) until the complete hydrolysis of the isopropylidene groups was attained. As checked by TLC (benzene–methanol, 9 : 1), the hydrolysis was complete after 6 hrs. The reaction mixture was evaporated in vacuum and the traces of water were removed by repeated addition and distillation of abs. benzene (5 × 20 ml). After drying over P_2O_5, the hydrolyzate was acetylated with a mixture of acetic anhydride (5 ml) and pyridine (5 ml) at room temperature for 24 hrs. The mixture was then evaporated to 3—4 ml, poured into crushed ice (25 g) and the product crystallized from 75% aqueous ethanol. The yield of the microcrystalline acetate was 0.70 g (92.1%), m. p. 80—82 °C (lit. [9] m. p. 84.5—85 °C); $[\alpha]_D$ −8.9° (c = = 0.9, chloroform). R_f 0.50 (benzene–methanol, 9 : 1).

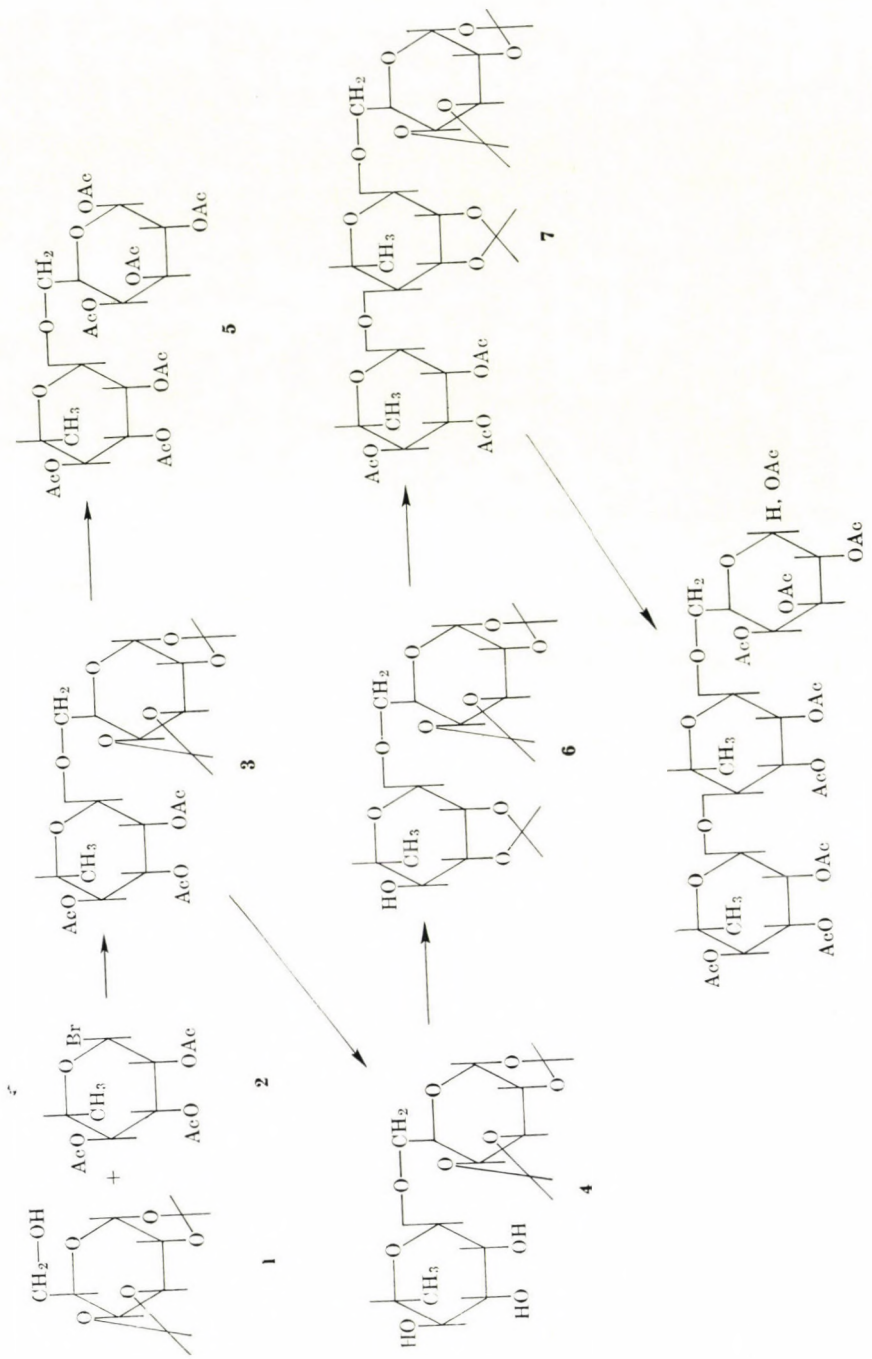

1,2;3,4-Di-0-isopropylidene-6-0-(2,3-0-isopropylidene-α-L-rhamnopyranosyl)α-D-galactopyranose (6)

Compound **4** (2.70 g) was dissolved in 90 ml of abs. acetone containing 0.27 ml of conc. sulphuric acid. After shaking for 2hrs, the reaction became nearly complete (~80%, as shown by TLC) and this ratio did not alter even on further shaking for 1 hr. The mixture was then neutralized with conc. NH_4OH, filtered and evaporated. The residue was dissolved in chloroform (100 ml) and then unreacted **4** was removed by extraction with water (3×20 ml). The organic layer was dried over $CaCl_2$ and evaporated to obtain 1.87 g (63.1%) of chromatographically homogeneous, pulverizable, glassy **6**; $[\alpha]_D$ −80.6° (c = 0.64, chloroform). R_f 0.34 (benzene–methanol, 9 : 1).

$C_{21}H_{34}O_{10}$ (446.5). Calcd. C 56.48; H 7.67. Found C 57.40; H 7.82%.

50 mg of **6** was methylated with methyl iodide (0.1 ml) and Ag_2O (0.1 g) according to Kuhn's procedure. The thin-layer chromatographically homogeneous syrup obtained after the methylation (R_f 0.52, benzene–methanol, 9 : 1) was directly hydrolyzed with 0.5 M H_2SO_4 (2 ml) at 100 °C for 6 hrs. After dilution with water (5 ml) the reaction mixture was neutralized with $BaCO_3$ and evaporated. The hydrolyzate contained an equimolar amount of D-galactose and 4-O-methyl-L-rhamnose (PC solvent: n-butanol–ethanol–water, 5 : 1 : 4, R_{TMG} 0.07 (galactose), 0.56 (4-O-methyl-L-rhamnose)).

10 mg of the hydrolyzate was reduced with $NaBH_4$ (30 mg) in water (2 ml) by letting the mixture to stand overnight. It was then neutralized with acetic acid and re-evaporated with methanol. The residue was acetylated with acetic anhydride (0.5 ml) and pyridine (0.5 ml) for 15 min at 100 °C. The alditol acetates formed were directly injected to a GC apparatus (R_T 8.2 min (4-O-methyl-L-rhamnitol), 44.6 min (galactitol)). The standard 4-O-methyl-L-rhamnose was prepared according to [12].

1,2,;3,4-Di-0-isopropylidene-6-0-[2,3-0-isopropylidene-4-0-(2,3,4-tri-0-acetyl-α-L-rhamnopyranosyl)-α-L-rhamnopyranosyl]-α-D-galactopyranose (7)

Compound **6** (1.80 g; $4 \cdot 10^{-3}$ moles) was dissolved in a mixture of benzene (50 ml and nitromethane (50 ml), and the solution was concentrated at atmospheric pressure to 35—40 ml. After cooling to 45 °C, $Hg(CN)_2$ (1.23 g; $4.2 \cdot 10^{-3}$ moles) and α-acetobromo-L-rhamnose (**2**) (1.48 g; $4.2 \cdot 10^{-3}$ moles) were added and resulting mixture was stirred for 8 hrs until the starting material disappeared. The reaction mixture was then cooled, filtered and evaporated. The residue was dissolved in chloroform, filtered, the filtrate was successively washed with 5% KI solution (3×30 ml) and water (4×20 ml), dried ($CaCl_2$) and evaporated to dryness. The syrupy **7** was purified by short-column chromatography on Kieselgel G (solvent system : benzene–methanol, 9 : 1). 1.78 g (61.5%) of amorphous **7** was obtained, $[\alpha]_D$ −94.5° (c = = 1.85, chloroform). R_f 0.66 (benzene–methanol, 9 : 1).

NMR (in $CDCl_3$): δ = 5.52 ppm (d, 1 H, C_1-H, J = 4.9 Hz); 5.40—3.40 (m, 16 H, 2 anomeric and 14 skeleton protons); 2.16, 2.07, 1.98 (ss, 9 H, 3 Ac); 1.60—1.12 (m, 24 H, 3 $C(CH_3)_2$ and 2 CH_3).

$C_{33}H_{50}O_{17}$(718.7). Calcd. C 55.14; H 701. Found C 55.82; H 6.83%.

4-0-[2,3,4-Tri-0-acetyl-α-L-rhamnopyranosyl]-(1→4)-[2,3-di-0-acetyl-α-L-rhamnopyranosyl]-(1 → 6)-1,2,3,4-tetra-0-acetyl-D-galactopyranose (8)

Compound **7** (1.26 g) was dissolved in 20 ml of abs. methanol and deacetylated with 1 M $NaOCH_3$ solution (0.2 ml). The reaction mixture was neutralized, evaporated, and the residue (R_f 0.46, benzene–methanol, 8 : 2) was hydrolyzed with 50% aqueous acetic acid (30 ml) at 80 °C for 36 hrs. The product obtained after the concentration of the hydrolyzate was dried and acetylated with acetic anhydride (5 ml) in pyridine (5 ml) at room temperature. The solution was poured into ice-water and the solid product which precipitated was crystallized from 70% aqueous ethanol to give 1.35 g (90.6%) of **8**, m. p. 82—84 °C. $[\alpha]_D$ −30.5° (c = 0.59, chloroform). R_f 0.40 (benzene–methanol, 9 : 1).

$C_{36}H_{50}O_{23}$ (850.8). Calcd. C 50.82; H 5.92. Found C 51.20; H 6.10%.

*

Thanks are due to the Alexander von Humboldt Foundation for the Perkin—Elmer 700 IR spectrophotometer presented to the Institute of Biochemistry, as well as to Dr. L. SZILÁGYI (Institute of Organic Chemistry, Kossuth L. University, Debrecen) for the 100 MHz NMR spectra.

REFERENCES

[1] WAGNER, H., ERTAN, M., SELIGMANN, O.: Phytochemistry **13,** 857 (1974)
[2] LIEBERMANN, C., HÖRMANN, O.: Ber., **11,** 952 (1878)
[3] PARIS, R. R., QUIRIN, M.: Compt. Rend. Acad. Sci., **256,** 2448 (1960)
[4] SCHMIDT, R. D., VARENNE, P., PARIS, R. R.: Tetrahedron, **28,** 5037 (1972)
[5] ZEMPLÉN, G., GERECS, Á., FLESCH, H.: Ber., **71,** 774 (1938)
[6] GRUNENBERG, H., BREDT, C., FREUDENBERG, W.: J. Am. Chem. Soc., **60,** 1507 (1938)
[7] FISCHER, E., BERGMANN, M., RABE, A.: Ber., **53,** 2362 (1920)
[8] HUNT, B. J., RIGBY, W.: Chem. and Ind., **1967,** 1868
[9] KAMIYA, S., ESAKI, S., HAMA, M.: Agr. Biol. Chem., **31,** 261 (1967)
[10] KUHN, R., TRISCHMAN, A., LÖW, I.: Angew. Chem., **67,** 32 (1955)
[11] BJÖRNDAL, H., HELLERQUIST, C. G., LINDBERG, B., SVENSSON, S.: Angew. Chem., **82,** 643 (1970)
[12] LIPTÁK, A., NÁNÁSI, P.: Submitted for publication

Hildebert WAGNER; D-8000 München 2, Karlstrasse 29, West Germany

András LIPTÁK, Pál NÁNÁSI } H-4010 Debrecen, Pf. 14.

RECENSIONES

Advances in Polymer Science

(Fortschritte der Hochpolymeren Forschung) Vol. 17

Springer Verlag, Berlin—Heidelberg—New York 1975, 103 pages

The volume contains the following review articles:

A. CASALE—R. S. PORTER: Mechanical synthesis of block and graft copolymers.

The paper of 71 pages is written in English. It contains 32 figures, 23 tables and 113 references.

Block and graft copolymers are manufactured and used today already on an industrial scale. In their preparation, the properties of the starting polymers can be modified within wide limits. One of the methods for their preparation is the mechanochemical approach. Concerning the mechanochemistry of polymers, several excellent monographs have been published, so that the authors of the present paper do not discuss the subject on the basis of the equipment used, but primarily on the basis of the physical state of the starting polymer. Thus, the preparation of block and graft copolymers by the mechanochemical route from solid polymer, polymer in rubber-elastic state, molten polymer and polymer in solution is described.

The survey is based primarily on the works of BARAMBOIN and his school, and SIMIONESCU and his school. Therefore, more than half (56.6%) of the references concerns the work of Soviet and Rumanian authors.

The material compiled is fairly known and rather old, which is indicated also by the fact that 69 references from before 1965, 34 papers cited were published between 1965 and 1969, and only 10 in 1970 or later.

The authors often use as source the first English edition of the book of BARAMBOIN (published in 1964, see: references [11]) though a second edition (in Russian) is also known since 1971.

It would have been more useful to survey the development in this field on the basis of publication appearing after 1970 and embracing an as wide as possible domain.

As concerns the lucidity of the compilation, its usability is made difficult and its value diminished by the inconsequent use of symbols (polymethyl methacrylate: PMMA or PMM, methyl methacrylate: MMA or MAM, acrylonitrile: AN or ACN, ethylene diamine: ED or ETDA, etc.), incomplete figures (Fig. 1: horizontal axis missing of dimension, Fig. 8: arbitrary curves, Fig. 15: PMM, Figs 27 and 28: incorrect coordinate indication, Fig. 31: arbitrary drawing of the curve, etc.), inexact formulas and citations (among the references, 15 were observed to be inexact or faulty).

The paper contains many missprints. These could have been eliminated by more careful proof reading.

W. H. SHARKEY: Polymerization through the carbon-sulfur double bond.

The paper of 31 pages is written in English. It contains 4 tables and 70 references.

The survey gives a clear picture on the preparation of compounds containing C–S group, liable to polymerization, and on their polymerization. Primarily, the following compounds are discussed: thioformaldehyde, thioacetophenone, 1-thioacyl aziridines, further thiocarbonyl fluoride, perfluorated thioacid halides and perfluoro thioketones. Among these compounds, polythioformaldehyde seemed to be promising, owing to its high melting point and crystallinity, but similarly to the other H-containing derivatives with substantially lower melting points, its stability is poor. Therefore, it is not used in practice. Fluorine-containing polymers are rubber-elastic. Since they possess a series of valuable properties, the present research is aimed at the preparation of a product, in which the disadvantageous properties (trend for recrystallization, etc.) are eliminated.

With the exception of a few missprints and inaccuracies (*e.g.* references 22 and 23 in the list of references are nowhere mentioned in the text, etc.), the paper gives a useful sum-

mary evaluation on the present state of our polymer chemical knowledge concerning thiocarbonyl compounds.

Beginning with the present Volume 17, the Publisher changed (enlarged) somewhat the format of the volume, owing to financial reasons. At the same time, to facilitate an easy survey, a cumulative author index of the volumes published so far (1—17) has been added to this volume.

I. GÉCZY

Topics in Current Chemistry, Vol. 57. *Cyclic Compounds*

Springer-Verlag, Berlin, Heidelberg, New York, 1975, 143 pages

The volume contains two monographs.

The first part is *Structure and Reactivity of Cyclopropenones and Triafulvenes* by T. EICHER and J. L. WEBER. Research into the macrocyclics, which is of increasing importance from both theoretical and preparative aspects, dates back barely more than ten years. As this excellent review shows, however, this short past has revealed many interesting features. After a brief introduction, the work (109 pages) discusses the chemistry of the cyclopropenones and triafulvenes in four chapters. These deal with the syntheses, structural and electron-structural characteristics, spectroscopic (UV, IR and NMR) and mass-spectro scopic investigations, and finally with their high reactivities. This illustrative and well-constructed work includes ample literature references (303).

The second review of the volume is *The Higher Annulenones* by M. V. SARGENT and T. M. CRESP. It deals with the structures of completely conjugated monocarbocyclic ketones, cyclic compounds the necessarily containing odd numbers of carbon atoms ($4n + 3$, $n = 2$; $4n + 1$, $n = 3$; $4n + 3$, $n = 3$; $4n + 1$, $n = 4$; $4n + 1$, $n = 5$), and annulenediones, and with studies of the diatropic and atropic properties of the rings, mainly based on NMR spectroscopy, together with the synthetic availability of the compounds (32 pages, 64 references). This valuable review demonstrates that numerous questions remain to be solved in this field.

Both parts of the volume comprise worthy contributions to this high-quality series. It is particularly praiseworthy that both monographs refer to publications appearing up to the middle of 1974. This volume is invaluable for both the organic chemist and the spectroscopist.

K. HIDEG

G. W. GIBSON: *Mastering Chemistry*

W. B. Saunders Co., Philadelphia, London, Toronto, 1975, 468 pages

The book is a collection of general chemical examples, containing more than 1000 examples in 20 chapters. The solution is given for every example, and in many cases the results are supplemented by a few words of explanation. The subject matter of the book embraces virtually the whole of general chemistry: it contains an abundance of examples for every topic, starting from the atom and proceeding via thermodynamics and solutions to complex ions and the various equilibria.

In the first two chapters one can find examples connected with the use of numbers and equations: after examples dealing with logarithms, powers, the normal forms of numbers, roots, etc., problems are given relating to the interconversion of various units and to the accuracy of data. The problems involving the accuracy of the starting data and the calculated results are particularly valuable. The chapter dealing with the atom contains examples connected with the elementary particles and electron configurations. The chapter on compounds deals with ionic and covalent bonds, the valence bond and molecular orbital theories, the geometries of molecules, hybridization, and terminology. This is the longest chapter of the book. The topics in chapter 5 are atomic weight, molecular weight, the concept of mole and chemical formulas. Chapter 6 contains problems connected with chemical equations and stoichiometry. The subsequent chapter features thermochemical equations and the calculation of reaction heats, followed by two chapters with problems on the first and second laws of thermodynamics.

Chapter 10 contains examples connected with the gas law. In chapter 11 we find problems relating to the heats of vaporization and boiling points of liquids, and the bonding forces in liquids. Chapter 12 discusses the solid state, and phase diagrams and changes of state feature among the problems. The chapter on solutions deals with the different concentration units, their interconversion, and the laws of dilute solutions. The chapter on reaction kinetics contains examples on reaction rates and rate constants. The subsequent chapters provide examples dealing with equilibria of gases, the solubility product, chemical equilibria of acids and bases, and pH calculations. The topics of chapter 18 include electrochemical redox processes, electrode potentials, galvanic cells, electromotive force, and electrolysis. Chapter 19 contains examples connected with complex ions. The theme of the final chapter is organic substances: 85 examples deal with organic processes, various reactions, isomerism, and nomenclature. The book is supplemented by an 8-page index.

To summarize, it may be stated that the book uses examples to treat most areas of general chemistry in a well surveyable form. In every chapter numerous problems are to be found which are provided with detailed explanations, while the processes of solving the problems are also described.

J. NAGY

Henry M. DREW: *Metal-based Lubricant Compositions*

The book of H. M. DREW on metal based lubricant compositions has been published in 1975 by Noyes Data Corp. in New Jersey and London. The book treats over 349 pages the relevant U. S. patent literature of recent times. The number of patents discussed is 257, beginning with registration number 3.265.621 and closing with number 3.853.772. The book contains 309 tables and 2 figures.

The selection of themes is based on the more important additive groups of lubricants, comprising the organometallic compounds and the metal soaps of organic acids.

The substances are discussed in three principal groups. The first group contains the metal based additives of lubricating oils, the second of cutting liquids, and the third of lubricating greases.

Among the lubricating oil additives, the metal phenates, sulphonates and carboxylates, and within these, mainly the calcium, magnesium and zinc derivatives are discussed. It is actually difficult to class the other groups of the lubricating oil additives discussed within the subject matter of the book, because their important part essentially does not contain a metal ion. This chapter deals with the succinimide derivatives, *i.e.* with the ash-free dispersant additives on nitrogen basis. For the sake of completeness, the so called low-ash dispersant additives, *e.g.* certain barium, calcium and zinc derivatives are also classed into this group.

In the third group of lubricating oil additives, oxidation and corrosion inhibitors, used primarily as additives of motor oils, first of all phosphorus and sulphur containing substances, such as zinc dialkyl dithiophosphoric acid derivatives and related compounds are discussed. Aluminium and lithium derivatives are also treated in this part, and surprisingly, ferrocene derivatives are also classed into this group.

The next part of the main chapter dealing with lubricating oils describes rather different products, *e.g.* copper powder, lead, zinc and nickel salts, further heat-carrying liquids, such as germano siloxane polymers and related compounds, which actually do not belong to the group of lubricants.

Finally, extreme pressure (EP) additives of lubricating oils are discussed. Among these, molybdenum derivatives are described, out of which molybdenum dithiophosphates and molybdenum naphthenates are novelties worth of attention. Novel types of lead compounds, considered already as classical, thus *e.g.* lead thiosulfates, further recent trends of developments in the field of the similarly classical zinc compounds are discussed. New types of EP additives of fundamental interest are gold salts, antimony salts, titanium complexes, but also such simple compounds as calcium nitrate, further alkali borate dispersions.

A separate chapter deals with the auxiliary substances of metal working. These are not grouped according to the type of the additive, but according to the character of the working process. Auxiliaries of metal working, cutting oils, forging lubricants and lubricants of continuous casting, quenching oils, hydraulic liquids, elastomer inhibitors, emulsion inhibitors are discussed here, further a few solid lubricants, which again do not fit closely in the topics of the book, *e.g.* sodium fluoride–graphite mixtures, boron nitride–sulfur mixtures, the mixtures of metal fluorides and aluminium phosphates, etc.

The third main chapter of the book discusses lubricating greases grouped according to the base. Primarily, the most widely used lubricating greases, lithium based greases are discussed, and as contrary to customary practice, here the gel forming component of the grease, soap, is also considered as additive. Thus, the process of lubricating grease manufacture proper is also discussed. Next, the additives increasing the film strength of lithium based greases are discussed, and the corrosion inhibitors of lithium based greases.

In accordance with their importance, the other types of lubricating greases are dealt with briefly. This involves aluminium and calcium based greases, and recent results achieved in the field of sodium based greases, on the way of becoming obsolate. This is followed by the description of development work concerning lubricating greases jellyfied with various gel formers, such as bentonite, polymers and similar substances. The main chapter on lubricating greases closes with the description of silicone greases, synthetic lubricating greases containing ester oil, and certain lubricating greases containing synthetic oils of other type.

This brief description of the contents of the book shows that the selection of the topics of the book is more or less arbitrary, but it is based anyway on a tribological concept. Accordingly, basic knowledge can hardly be gained from the book, moreover, the author assumes that the reader is already well versed in this field. The purpose of the book is to acquaint the reader with the newest pertinent patent literature, since, according to the opinion of the author, this is the largest and all-embracing collection of technical-scientific literature in the world. In this literature, more practical information is collected, than in all the other sources. In general, his information is not taken into consideration and missed by those, who rely only on literature in journals, though a precondition of the publication of this type of information is the very fact to contain something *new*. Therefore, patent literature is never of summarizing or repetitive character. Moreover, patent literature always gives very good ideas for the starting of further research.

In addition to the above considerations of the author, it has to be established that orientation in patent literatur is actually circumstantial, strenuous, time-consuming and difficult. Therefore, a periodic treatment of patent literature according to subject, facilitating greatly the information of those interested in the single topics, must be approved of. This is the chief merit of the book.

At the same time, both author and reader must be aware of the fact that an information source of this type becomes most quickly obsolete, because the predominant part of technical-scientific principles is more or less durable, while technical skill, *i.e.* practical technical knowledge becomes today very quickly obsolete. Thus, reviews of this kind furnish information of merit for 5, but at the most for 10 years.

Conform to several books published in the USA literature, a characteristic feature of the book is that it is not critical and does not take a stand. Patents of different importance are discussed and considered at equal length and without a critical comment on their true utility. However, an important advantage of the book, as compared to other similar works is that it gives a summary picture on the state of art in the discussion of the single patent groups, and ranges new knowledge within this frame.

A further limiting factor of the book is perhaps that it deals exclusively with U. S. patent literature, and limits thereby the usability of the book, particularly for Europeans, to a certain degree.

In summary, the book gives valuable technical information, without a claim to critical evaluation or fundamental scientific consideration, mainly for practical specialists, interested in process technology and application techniques.

E. VÁMOS

International Review of Science, Inorganic Chemistry, Series Two, Volume 4. Organometallic Derivatives of the Basic Group Elements

Edited by B. J. Aylett, Westfield College, University of London. Buttetworths. London, University Park Press Baltimore

The book is one of the complementary volumes of the series Inorganic Chemistry Series One, consisting of eleven volumes, terminated in 1972. The purpose of the volume is to give a review and a survey for universities and researchers on the results attained in organo-element chemistry in the period 1971—72.

The aim of the authors was to report those new results of the organic compounds of elements belonging to the main groups of the periodic system, which are of importance from the point of view of preparative chemistry, spectroscopy and molecular structure.

The book consists of eleven chapters. The chapters were written by world-wide known experts of the corresponding fields of organo-element chemistry.

The first chapter deals with the chemistry of organo-alkali metals. It describes primarily the preparation and use of organolithium compounds. A separate part covers spectroscopical studies. The possible reactions of various organic compounds with lithium and the further usability of the compounds formed are described in detail. Of particular interest is the description of organo-element compounds containing also lithium. Special attention is paid to the reactions of organolithium compounds and derivatives of the elements of the IV main group. The discussion of the organolithium compounds of transition metals is also noteworthy.

The second chapter deals with the organoboron compounds and their chemistry. A general description of organohydroborans and organohalogenborans is given and their preparation and structure are discussed.

Triorganoborans and organoboron chalcogen derivatives are treated in a separate part. Within this part, boron-sulfur and boron-selenium systems are also covered.

The main part of the chapter concerns with boron-nitrogen chemistry. A detailed description is given of the chemistry of borazines, of imine boranes and of organoboron nitrogen-containing heterocyclic molecules.

The author discusses anions of borate type, and a separate part deals with organoboron metal compounds.

The third part treats recent results of tin- and leadorganic chemistry.

The organotin and -lead compounds are described, and the decomposition reactions of the tin–carbon and lead–carbon bonds and organic tin and lead radicals are discussed.

Hydrides, halogenides and pseudo-halogenides, compounds formed with the elements of the VI/1 and V/1 groups, and the derivatives of tin and lead formed with the elements of other main groups and with transition metals are described, each in a separate part.

The fourth chapter discusses the organic compounds of aluminium, gallium, indium and thallium. In the first place, the compounds of aluminium are described, but the derivatives of the other elements of the III/1 group are also dealt with. After the introduction of structural problems, the preparation of the corresponding organo-elements, reactions with various compounds, and the description of compounds formed with other elements are covered.

The great number of publications, which appeared in recent times on organosilicon compounds justifies that in the present book two chapters are devoted to organosilicon compounds.

The fifth chapter concerns with silicon-carbon chemistry, various substituted silanes, siloxanes, cyclic compounds, their preparation and reactions, and discusses in detail the chemical properties of silyl-substituted carbon compounds and silacycloalkanes containing double and triple bonds.

The sixth chapter reports the results of physico-chemical investigations achieved in organosilicon chemistry, and discusses then compounds containing a silicon–nitrogen bond. In recent times the chemistry of silicon–nitrogen organocompounds underwent a rapid development, and this field of chemistry is covered in this chapter.

Silylazenes containing nitrogen–nitrogen double bond, silyltriazenes containing three nitrogen atoms next to each other, and organosilicon compounds containing phosphorus and arsenic are described. The author of the sixth chapter reports also on organosilicon peroxides and ozonides prepared very recently. Researches the organosilicon compounds of sulfur, selenium and tellur is also briefly discussed.

The next chapter deals with the chemistry of organogermanium compounds. After discussing the preparation and reactions of compounds containing germanium–carbon bond, the author describes the organo-element germanium-metal compounds, then the derivatives containing elements of the V/1 groups, and finally cyclic organogermanium compounds.

The eighth chapter reports on the present state of research in the field of organic zinc, cadmium and mercury derivatives. Of partieular interest are organomercury compounds, which steadily gain ground in modern organo-element chemistry. The author lists a wide range of organic compounds containing mercury, and discusses also their structural problems.

The ninth chapter reports on recent research and results attained in the field of the organic compounds of arsenic, antimony and bismuth, the tenth chapter on those of the organic compounds of beryllium, calcium, stroncium and barium. Both chapters discuss in detail the preparation, properties and reactions of the corresponding compounds, and even the compounds formed with other elements.

The last chapter deals with organomagnesium compounds. After the discussion of the

molecular structure and spectroscopic results, the applicability of Grignard reagents in almost all the fields of organic chemistry is shown.

The last chapter is followed by a subject index.

The book of 417 pages contains a total of 2764 references. With the aid of the index, this book which can be regarded as a handbook will be of particular value to all those who intend to obtain informations on recent development in organoelement chemistry.

J. NAGY

Transition Metal Chemistry

The importance of transition metals in various fields of chemistry is not of recent origin, but it increased in the last two-three decades abruptly, and presumably, this development will still increase in the future. They are widely used in inorganic, organic, organometallic, physical, polymer and biochemistry. Their application in the chemical industry stimulated the interest of scientists. The number of scientific publications increased in recent years almost explosively, and became more and more difficult to survey. This difficulty was further increased by the fact that the great number of papers has been published in the most various journals.

A newly published international journal

Transition Metal Chemistry

is intended to ease this situation.

The first issue of the English-language journal of nice presentation has been published in the care of Verlag Chemie, GmbH in Octobre 1975. The editors promised 5 issues for 1976, and following this, bimonthly publication.

In accordance with its title, *Transition Metal Chemistry* will publish papers dealing with the preparation of transition metal-based compounds, the determination of their structure, physical and chemical properties, the use of these metals in chemical syntheses, the study of their role in natural substances and their analytical determination. The field the new journal is designed to deal with is clearly determinad. This permits to hope that its aims will be satisfactorily attained, and scientists engaged in transition metal chemistry will be informed in the future in an easier way on the most important new results in their field.

B. HEIL

INDEX

ANALYTICAL CHEMYSTRY

PHYSICAL AND INORGANIC CHEMISTRY

ORGANIC CHEMISTRY

Printed in Hungary

A kiadásért felel az Akadémiai Kiadó igazgatója — Műszaki szerkesztő: Zacsik Annamária

A kézirat nyomdába érkezett: 1976. III. 25. — Terjedelem: 12,75 (A/5) ív, 78 ábra

76.2970 Akadémiai Nyomda, Budapest — Felelős vezető: Bernát György

ACTA CHIMICA

ТОМ 89 — ВЫП. 4

РЕЗЮМЕ

Применение метода гидропиролиза для определения содержания галогена в органических соединениях

Л. МАЗОР

Пары органических галоидных соединений или продукты пиролиза, насыщенные водяным паром, в потоке инертного газа при температуре 800—1100°С на платиновом катализаторе полностью разлагаются до галоидоводородных кислот и окислов углерода. Дистиллят содержит кислоты или галогенидные ионы в относительно небольшом объеме, свободно от других ионных помех, т. о., они могут быть количественно определены с помощью объемного или другого метода анализа.

Экстракция празеодима трибутилфосфатом из растворов, содержащих смеси минеральных солей

Л. ГЕНОВ и И. ДУКОВ

Исследована экстракция празеодима раствором трибутилфосфата в CCl_4 из водной фазы, содержащей смеси $NaClO_4$ и $NaNO_3$; $NaClO_4$ и NaSCN или $NaNO_3$ и NaSCN. Показано, что при наличи этих смесей экстракция празеодима увеличивается.

Обнаружено, что увеличение экстракции определяется увеличением коэффициентов активности, если в водной фазе находится $NaClO_4$ и $NaNO_3$, и образованием смешанных комплексов если в водной фазе находится $NaClO_4$ и NaSCN или $NaNO_3$ и NaSCN.

Калориметрическое исследование полимеризации цис-2,4-диметил-2,4,8,8, 10,1-гексафенил-спиро (5,5)-пентасилоксана

Т. СЕКЕЙ, М. ЛЕНДЬЕЛ, В. С. ПАПКОВ, А. В. ЗАЧЕРНЮК, А. А. ЖДАНОВ и К. А. АНДРИАНОВ

Следя за калорийными изменениями цис-2,4-диметил-2,4,8,8,10,10-гексафенил-спиро(5,5)-пентасилоксана с помощью ДСК микрокалориметра было установлено, что в ходе плавления протекает процесс перекристаллизации, т. к. исходная модификация превращается в модификацию, плавящуюся при более высокой температуре. Была исследована полимеризация вышеуказанного мономера в присутствии различных количеств катализатора КОН. Было установлено, что реакция является сложной и протекает на нескольких ступенях. Исходя из калориметрических кривых, были определены величины характеристических температур, а также теплоты плавления и полимеризации. С помощью приближенных методов была рассчитана энергия активации полимеризации, которая оказалась равной 30 ккал/моль.

Реакции соединений осмия (VIII) с аммиаком

Я. НИЛАШИ и П. ОРШОШ

В ходе реакции, протекающей между тетраокисью осмия и аммиаком в среде гидроокиси калия, образуется калийнитридо-осмат (VIII), содержание азота в котором нельзя измерить с помощью метода Кьельдаля, а оно может быть определено лишь после восстановления со сплавом Дьюара. Согласно нашим результатам, ионы нитридоосмата(VIII) проявляют каталитическое влияние на процесс разложения концентрированной серной кислотой, используемой при определении азота методом Кьельдаля, в случае применения сульфата калия как обычного агента, повышающего температуру кипения. В таких условиях аммиак окисляется до элементарного азота. Пока в системе находится аммиак, там может присутствовать и ион нитридоосмата(VIII), но более вероятно, образующееся из него соединение осмия с более низкой степенью окисления. Если, однако, аммиак полностью окислился до элементарного азота, то катализирующее соединение осмия удаляется из среды концентрированной серной кислоты в форме OSO_4. Степень окисления зависит от молярного соотношения $HSO_4^- : H_2SO_4$ и тогда становится максимальной, когда величина этого отношения равна 1. Тетраокись осмия не проявляет такого каталитического эффекта. Если, однако, перед разложением серной кислотой была возможность для образования нитридоосмата(VIII), то его присутствие в сильной мере мешает при определении азота по Кьельдалю, даже вообще последнее может и не удаться.

Свойства смесей спирт-амин, IX

Ф. РАТКОВИЧ и Л. ДОМОНКОШ

Дипольный момент вторичных аминов в случае жидких диэтил-, ди-н-пропил- и ди-н-бутиламинов уменьшается с увеличением температуры. Это явление объясняется на основе самоассоциации и параллельного расположения молекул в ассоциатах. Энтальпия образования водородных связей N—H . . . N, рассчитанная на основе модели типа Меке—Кемптер, равна 2 ккал/моль. Дипольный момент третичных аминов увеличивается с повышением температуры. Это явление указывает на сильное взаимодействие между молекулами в жидкой фазе, а также на то, что вследствие этого взаимодействия молекулы располагаются антипараллельно по отношению друг к другу.

Свойства смесей спирт-амин, X

Вязкость вторичных аминов

Ф. ПАТКОВИЧ и. Т- ШАЛАМОН

На основе измерений вязкости ди-н- пропил -и ди-н- бутиламилов в интервале температур —20—+80°С, были исследованы изменения средней степени ассоциации в зависимости от температуры. Было обнаружено, что с уменьшением температуры энтальпия активации ламинарного течения, а вмехте с нею и средняя степень ассоциации сильно возрастают. Это явление можно интерпретировать на основе модели Меке - Кемптера, исходящей из бесконечной цепи ассоциации. Энтальпия образования водородного мостика чассчитанная из данных измерений вязкости, равна—2,4 ккал/моль, что хорошо согласуется с расчетными величинами данных диелектрических измерений.

Расчет π-электронной структуры производных дизамещенного бензола, содержащих донорные и акцепторные группы, с помощью метода ППП—МО

А. КИШ и Й. СЁКЕ

π-Электронная структура и спектры производных дизамещенного бензола, содержащих электронодонорную и электроноакцепторную группы, были рассчитаны с помощью метода Паризер—Папп—Попла. В деталях обсуждается применимость одинаковой системы параметров к более широкому кругу производных бензола. Расчеты дают хорошие результаты для спектральных характеристик, плотностей заряда основного состояния и порядка связей. Приводятся сравнения с другими литературными расчетами π-электронной структуры.

Эквидензитометрия — метод определения структуры плзамы, IV

К. ДИТРИХ, К. НИБЕРГАЛ и Х. РЁССЛЕР

Описывается экспериментальная характеристика дуговых плазм постоянного тока для La_2O_3, GaAS и GeO_2. Был использован новый метод, объединяющий спектральную фотографию с фотографической эквидензитометрией. Удалось получить качественные результаты относительно аксиального распределения в плазме. Плазмы были генерированы испарением катода в присутствии или отсутствии магнитного поля.

Показано, что максимум радиации всегда находится перед катодом как в отсутствии, так и в присутствии магнитного поля. Величина катодного обогащения зависит от ионизационного потенциала матрицы и следов. Влияние магнитного поля проявляется в случае трудно ионизуемых матриц.

Эквидензитометрия — метод определения структуры плазмы, III

К. ДИТРИХ, Х. РЁССЛЕР и К. НИБЕРГАЛ

Описывается экспериментальная характеристика дуговых плазм постоянного тока для GaAS и GeO_2. Был использован новый метод, комбинирующий спектральную фотографию с фотографической эквидензитометрией. Удалось получить качественные данные относительно аксиального распределения элементов в плазме.

Было показано, что распределение элементов матрицы и следов зависит от ионизационного потенциала. Катод обогащается элементами с низким ионизационным потенциалом, а анод — элементами с высоким ионизационным потенциалом. Температура плазмы и матрицы влияет на распределение частиц. Результаты подробно обсуждаются.

Электронные спектры поглощения некоторых диарилиденов циклопентанона и циклогексанона

Р. М. ИССА, С. Х. ИТАИВ, И. М. ИССА и А. К. ИЛЬ-ШАФИ

Были сняты электронные спектры поглощения некоторых диарилиденов циклогексанона и циклопентанона в органических растворителях и буферных растворах. Спектральные сдвиги обсуждаются с точки зрения эффекта среды и молекулярной структуры. Кислотные константы диссоциации соединений, содержащих группы ОН, были определены на основе измерений в буферных растворах. Были ассигнованы важнейшие полосы поглощения ИК спектров. Последние обсуждаются с точки зрения молекулярной структуры.

Химия диолов и циклических эфиров, XXXIX

Механизм дегидратации диолов на медном катализаторе

А. МОЛЬНАР и М. БАРТОК

Были исследованы превращения трех, меченных дейтерием диолов (1,3-бутандиол -[3-H^2](I), 1,4-пентандиол-[4-H^2](II), 3-метил-2,4-пентандиол-[0,0'-H^2_2](III) на катализаторах Cu/Al и Cu при температурах 200 и 205°. Целью исследований было выяснение механизма уже ранее изученных процессов. Был установлен механизм основных процессов превращений (дегидрация с образованием оксосоединений и оксоциклоалканов с тем же самым числом углеродных атомов как и в диолах, и фрагментация), демонстрируемый на трех диолах, выделяя при этом определяющую роль процесса переноса водорода, катализированного металлом, в данных реакциях диолов.

Нонаацетат О-α-L-рамнопиранозил-(1→4)-О-α-L-(1→6)-D-галактопиранозы

Синтез карбогидратного компонента рамназин-3-О-триозида

Х. ВАГНЕР, А. ЛИПТАК и П. НАНАШИ

Производное робинобиозы (*3*) было синтезировано путем конденсации 1,2 : 3,4-ди-О--изопропилиден-α-D-галактопиранозы (*1*) с 2,3,4-три- О-ацетил-α-L-рамнопиранозилбромидом (*2*) в растворе смеси бензола с нитрометаном (1 : 1) и в присутствии $Hg(CN)_2$. Дисахарид был охарактеризован как кристаллический гептаацетат робинобиозы (*5*). Продукт первой конденсации (*3*) был деацитилирован методом Земплена и затем подвергнут взаимодействию с ацетоном, давая *6*. Вторая конденсация соединения *6* и *2* приводит к образованию защищенного производного трисахарида (*7*). Заглавное соединение (*8*) было получено через деацитилирование и гидролиз соединения *7* с последующим ацетилированием.

The Acta Chimica publish papers on chemistry, in English, German, French and Russian.

The Acta Chimica appear in volumes consisting of four parts of varying size, 4 volumes being published a year.

Manuscripts should be addressed to

Acta Chimica
H-1521 Budapest, Hungary

Correspondence with the editors should be sent to the same address.

The rate of subscription is $ 32,00 a volume.

Orders may be placed with "*Kultúra*" Foreign Trade Company for Books and Newspapers (1389 Budapest 62, P.O.B. 149 Account No. 218 10990) or with representatives abroad.

Les Acta Chimica paraissent en français, allemand, anglais et russe et publient des mémoires du domaine des sciences chimiques.

Les Acta Chimica sont publiés sous forme de fascicules. Quatre fascicules seront réunis en un volume (4 volumes par an).

On est prié d'envoyer les manuscrits destinés à la rédaction à l'adresse suivante:

Acta Chimica
H-1521 Budapest, Hungary

Toute correspondance doit être envoyée à cette même adresse.

Le prix de l'abonnement est de $ 32,00 par volume.

On peut s'abonner à l'Entreprise pour le Commerce Extérieur de Livres et Journaux «*Kultúra*» (1389 Budapest 62, P.O.B. 149 Compte-courant No. 218 10990) ou à l'étranger chez tous les représentants ou dépositaires.

«*Acta Chimica*» издают трактаты из области химической науки на русском, французском, английском и немецком языках.

«*Acta Chimica*» выходят отдельными выпусками разного объема. 4 выпуска составляют один том. 4 тома публикуются в год.

Предназначенные для публикации рукописи следует направлять по адресу:

Acta Chimica
H-1521 Budapest, BHP

По этому же адресу направлять всякую корреспонденцию для редакции.

Подписная цена — $ 32,00 за том.

Заказы принимает предприятие по внешней торговле книг и газет «*Kultúra*» (1389 Budapest 62, P.O.B. 149 Текущий счет № 218 10990) или его заграничные представительства и уполномоченные.

Reviews of the Hungarian Academy of Sciences are obtainable at the following addresses:

AUSTRALIA

C. B. D. Library and Subscription Service
Box 4886, G. P. O.
Sydney N. S. W. 2001

Cosmos Bookshop
145 Acland St.
St. Kilda 3182

AUSTRIA

Globus
Höchstädtplatz 3
A—1200 Wien XX

BELGIUM

Office International de Librairie
30 Avenue Marnix
1050-Bruxelles

Du Monde Entier
162 Rue du Midi
1000—Bruxelles

BULGARIA

Hemus
Bulvar Ruszki 6
Sofia

CANADA

Pannonia Books
P. O. Box 1017
Postal Station "B"
Toronto, Ont. M5T 2T8

CHINA

CNPICOR
Periodical Department
P. O. Box 50
Peking

CZECHOSLOVAKIA

Mad'arská Kultura
Národní třida 22
115 66 Praha

PNS Dovoz tisku
Vinohradská 46
Praha 2

PNS Dovoz tlače
Bratislava 2

DENMARK

Ejnar Munksgaard
Nörregade 6
DK—1165 Copenhagen K

FINLAND

Akateeminen Kirjakauppa
P. O. Box 128
SF-00101 Helsinki 10

FRANCE

Office International de Documentation et Librairie
48, Rue Gay-Lussac
Paris 5

Librairie Lavoisier
11 Rue Lavoisier
Paris 8

Européridiques S. A.
31 Avenue de Versailles
78170 La Celle St.-Cloud

GERMAN DEMOCRATIC REPUBLIC

Haus der Ungarischen Kultur
Karl-Liebknecht-Strasse 9
DDR—102 Berlin

Deutsche Post
Zeitungsvertriebsamt
Strasse der Pariser Kommüne 3—4
DDR-104 Berlin

GERMAN FEDERAL REPUBLIC

Kunst und Wissen
Erich Bieber
Postfach 46
7 Stuttgart s

GREAT BRITAIN

Blackwell's Periodicals
P. O. Box 40
Hythe Bridge Street
Oxford OX1 2EU

Collet's Holdings Ltd.
Denington Estate
London Road
Wellingborough Northants NN8 2QT

Bumpus Haldane and Maxwell Ltd.
5 Fitzroy Square
London W1P 5AH

Dawson and Sons Ltd.
Cannon House
Park Farm Road
Folkestone, Kent

HOLLAND

Swets and Zeitlinger
Heereweg 347b
Lisse

Martinus Nijhoff
Lange Voorhout 9
The Hague

INDIA

Hind Book House
66 Babar Road
New Delhi 1

India Book House
Subscription Agency
249 Dr. D. N. Road
Bombay

ITALY

Santo Vanasia
Via M. Macchi 71
20124 Milano

Libreria Commissionaria Sansoni
Via Lamarmora 45
50121 Firenze

JAPAN

Kinokuniya Book-Store Co. Ltd.
826 Tsunohazu 1-chome
Shinjuku-ku
Tokyo 160—91

Maruzen and Co. Ltd.
P. O. Box 5050
Tokyo International 100—31

Nauka Ltd.-Export Department
2—2 Kanda
Jinbocho
Chiyoda-ku
Tokyo 101

KOREA

Chulpanmul
Phenjan

NORWAY

Tanum-Cammermayer
Karl Johansgatan 41—43
Oslo 1

POLAND

Węgierski Instytut Kultury
Marszalkowska 80
Warszawa

BKWZ Ruch
ul. Wronia 23
00—840 Warszawa

ROUMANIA

D. E. P.
Bucureşti

Romlibri
Str. Biserica Amzei 7
Bucureşti

SOVIET UNION

Sojuzpechatj — Import
Moscow

and the post offices in each town
Mezhdunarodnaya Kniga
Moscow G—200

SWEDEN

Almqvist and Wiksell
Gamla Brogatan 26
S—101 20 Stockholm

A. B. Nordiska Bokhandeln
Kunstgatan 4
101 10 Stockholm 1 Fack

SWITZERLAND

Karger Libri AG.
Arnold-Böcklin-Str. 25
4000 Basel 11

USA

F. W. Faxon Co. Inc.
15 Southwest Park
Westwood, Mass. 02090

Stechert-Hafner Inc.
Serials Fulfillment
P. O. Box 900
Riverside N. J. 08075

Fam Book Service
69 Fifth Avenue
New York N. Y. 1003

Maxwell Scientific International Inc.
Fairview Park
Elmsford N. Y. 10523

Read More Publications Inc.
140 Cedar Street
New York N. Y. 10006

VIETNAM

Xunhasaba
32, Hai Ba Trung
Hanoi

YUGOSLAVIA

Jugoslavenska Knjiga
Terazije 27
Beograd

Forum
Vojvode Mišiča 1
21000 Novi Sad